

# **Chemoenzymatic synthesis of nitriles and lubricant esters**

Dissertation zur Erlangung des Doktorgrades der  
Naturwissenschaften (Dr. rer. nat)

vorgelegt von

M. Sc.

**Tobias Betke**

aus Lübbecke, Nordrhein-Westfalen

November 2018

# **Chemoenzymatische Synthese von Nitrilen und Schmierstoffestern**

Dissertation zur Erlangung des Doktorgrades der  
Naturwissenschaften (Dr. rer. nat)

vorgelegt von

M. Sc.

**Tobias Betke**

aus Lübbecke, Nordrhein-Westfalen

November 2018

Erstgutachter: Prof. Dr. Harald Gröger

Zweitgutachter: Prof. Dr. Norbert Sewald

Termin der Disputation: 20.12.2018

Ort: Bielefeld

Die vorliegende Arbeit wurde an der Fakultät für Chemie der Universität Bielefeld im Arbeitskreis Organische Chemie I im Zeitraum von Mai 2015 bis November 2018 angefertigt, sowie im Enzyme Laboratory des Biotechnology Research Center der Toyama Prefectural University, Toyama, Japan, vom Oktober 2017 bis Dezember 2017.

Die Betreuung der Doktorarbeit erfolgte durch Prof. Dr. Harald Gröger während des gesamten Zeitraums.

Diese Dissertation wurde selbstständig verfasst und hat weder in aktueller oder anderer Fassung einer anderen Fakultät oder Hochschule vorgelegen.

Lediglich die in dieser Arbeit aufgeführten Hilfsmittel wurden verwendet.

Bielefeld, den 07.11.2018

---

Tobias Betke

# Veröffentlichungen im Rahmen dieser Arbeit

## Publikationen

1. T. Betke, P. Rommelmann, K. Oike, Y. Asano, H. Gröger  
*Cyanide-Free and Broadly Applicable Enantioselective Synthetic Platform for Chiral Nitriles through a Biocatalytic Approach*, *Angew. Chem. Int. Ed.* **2017**, 56, 12361–12366; *Angew. Chem.* **2017**, 129, 12533–12538.
2. T. Betke, P. Rommelmann, K. Oike, Y. Asano, H. Gröger  
*Back-Cover Picture of the Angew. Chem. Int. Ed. Issue 40/2017*, *Angew. Chem. Int. Ed.* **2017**, 56, 12374; *Angew. Chem.* **2017**, 129, 12546.
3. P. Rommelmann, T. Betke, H. Gröger  
*Synthesis of Enantiomerically Pure N-Acyl Amino Nitriles via Catalytic Dehydration of Oximes and Application in a de novo-Synthesis of Vildagliptin*, *Org. Process Res. Dev.* **2017**, 21, 1521-1527.
4. T. Betke, J. Higuchi, P. Rommelmann, K. Oike, T. Nomura, Y. Kato, Y. Asano, H. Gröger  
*Biocatalytic Synthesis of Nitriles through Dehydration of Aldoximes: The Substrate Scope of Aldoxime Dehydratases*, *ChemBioChem* **2018**, 19, 768-779.
5. T. Betke, J. Higuchi, P. Rommelmann, K. Oike, T. Nomura, Y. Kato, Y. Asano, H. Gröger  
Cover Picture of *ChemBioChem* Issue 8/2018, *ChemBioChem* **2018**, 19, 766.
6. T. Betke, M. Maier, H. Gruber-Wölfler, H. Gröger  
*Biocatalytic production of adiponitrile and related aliphatic linear  $\alpha,\omega$ -dinitriles*, angenommen zur Veröffentlichung.
7. C. Plass, A. Hinzmann, M. Terhorst, W. Brauer, K. Oike, H. Yavuzer, Y. Asano, A. Vorholt, T. Betke, H. Gröger  
*Approaching bulk chemical nitrile from alkenes: A hydrogen cyanide-free approach through combination of hydroformylation and biocatalysis*, eingereicht zur Veröffentlichung.

## Patente

1. H. Gröger, T. Betke, P. Rommelmann, *Verfahren zur Herstellung chiraler Aminonitrile*, DE 102016116130.6, eingereicht am 30. August 2016; PCT/EP2017070820 eingereicht am 17. August 2017.
2. T. Betke, C. Plass, H. Gröger, D. Loderer, S. Seemeyer, T. Kilthau, L. Ma, *Neue Esterverbindungen, Verfahren zu ihrer Herstellung sowie ihre Verwendung*, DE 102018002891A1, eingereicht am 13.04.2017.
3. T. Betke, H. Gröger, *Verfahren zur Herstellung von aliphatischen linearen  $\alpha,\omega$ -Dinitrilen aus  $\alpha,\omega$ -Dialdehyddioxim-Vorstufen*, DE 102017112191.9, eingereicht am 02. Juni 2017.

## Vorträge

1. T. Betke, P. Rommelmann, H. Gröger, *New approach for important precursors of Gliptins*, Plenarvortrag, *BioVaria 2017* in München, 23.05.2017.
2. T. Betke, P. Rommelmann, K. Oike, Y. Asano, H. Gröger, *Aldoxime dehydratase catalysis: A cyanide-free and broadly applicable process platform for enantioselective nitrile synthesis*, Plenarvortrag, *Biotrans 2017* in Budapest, 09.-13.07.2017.
3. T. Betke, M. Maier, H. Gruber-Wölfler, H. Gröger, *Nitrile synthesis with aldoxime dehydratases*, Plenarvortrag, *SusChemSys 2.0 Meeting* in Dortmund, 25.08.2017.
4. T. Betke, M. Maier, H. Gruber-Wölfler, H. Gröger, *Biocatalytic production of adiponitrile and related aliphatic linear  $\alpha,\omega$ -dinitriles*, Plenarvortrag, 51. *Jahrestreffen Deutscher Katalytiker* in Weimar, 14.-16.03.2018.

## Posterpräsentationen

1. T. Betke, A. Lehmann, A. Liese, H. Gröger, *Towards less energy-intensive fatty alcohol production through combination of lipase-catalysis and metal-catalyzed hydrogenation*, 51. *Jahrestreffen Deutscher Katalytiker* in Weimar, 16.-18.03.2016.
2. T. Betke, P. Rommelmann, K. Oike, Y. Asano, H. Gröger, *Cyanide-free, enantioselective nitrile synthesis with aldoxime dehydratases – Synthetic potential of an unusual enzyme class*, *ORCHEM 2016* in Weimar, 05.-07.09.2016.
3. T. Betke, P. Rommelmann, K. Oike, Y. Asano, H. Gröger, *Cyanide-free, enantioselective nitrile synthesis with aldoxime dehydratases – Synthetic potential of an unusual enzyme class*, 5. Sitzung des wissenschaftlichen Beirats des CeBiTec in Bielefeld, 06.12.2016.
4. T. Betke, M. Maier, H. Gruber-Wölfler, H. Gröger, *Biocatalytic production of Nylon-precursor adiponitrile and related aliphatic linear  $\alpha,\omega$ -dinitriles*, *SusChemSys 2.0 Meeting* in Aachen, 06.04.2018.
5. T. Betke, M. Maier, H. Gruber-Wölfler, H. Gröger, *Biocatalytic production of Nylon-precursor adiponitrile and related aliphatic linear  $\alpha,\omega$ -dinitriles*, 1. *ICRC Biocascades Symposium* in Bielefeld, 09.-11.04.2018.



*Mein lieber Sohn, du tust mir leid.  
Dir mangelt die Enthaltbarkeit.  
Enthaltbarkeit ist das Vergnügen  
An Sachen, welche wir nicht kriegen.  
Drum lebe mäßig, denke klug.  
Wer nichts gebraucht, der hat genug!*

aus: Die Haarbeutel (1878) – Einleitung

Wilhelm Busch

*Weiß man, wie oft ein Herz brechen kann?  
Wie viel Sinne hat der Wahn?  
Lohnen sich Gefühle?  
Wie viele Tränen passen in einen Kanal?  
Leben wir noch mal?  
Warum wacht man auf?  
Was heilt die Zeit?*

*Ich bin dein 7. Sinn,  
Dein doppelter Boden,  
Dein zweites Gesicht.  
Du bist eine kluge Prognose,  
das Prinzip Hoffnung,  
ein Leuchtstreifen aus der Nacht.  
Irgendwann find und lieb ich dich ...*

aus: Demo (Letzter Tag) (2002)

Herbert Grönemeyer





## Danksagung

Als erstes möchte ich mich äußerst herzlich bei meinem Doktorvater Prof. Dr. Harald Gröger bedanken, der mich während der vergangenen Jahre nicht nur durch seine fachliche Expertise und intensive Gespräche bei der Anfertigung dieser Arbeit begleitet und angeleitet hat, sondern vor allem mir durch tiefgehendes Vertrauen und gegenseitigen Respekt in jeder Hinsicht eine außergewöhnliche Förderung und Entwicklung in menschlicher und beruflicher Hinsicht ermöglicht hat. Vielen herzlichen Dank!

Herrn Prof. Dr. Norbert Sewald danke ich ausdrücklich für die Übernahme des Zweitgutachtens und die schon frühe Förderung während des Studiums im Rahmen meiner Bachelorarbeit.

Ausdrücklichen Dank möchte ich zudem Herrn Prof. Yasuhisa Asano von der Toyama Prefectural University aussprechen. Zum einen für die stete Unterstützung in unserer nun schon knapp vierjährigen Kooperation bei der Erforschung der Aldoximdehydratasen, zum anderen aber habe ich vor allem durch ihn die Möglichkeit erhalten Japan, ein wunderschönes Land in jeglicher Hinsicht, sowohl beruflich als auch kulturell und kulinarisch näher kennenzulernen und wertzuschätzen. どうもありがとうございます (Dōmo arigatō gozaimasu!)

Zudem möchte ich Herrn Prof. Dr. Andreas Liese, Kim Schlipköter und Andrea Lehmann von der Technischen Universität Hamburg-Harburg für die langjährige, herzliche Kooperation bei Kombination von Bio- und Metallkatalyse für die Tetradecanolsynthese danken. Die gegenseitigen Besuche und Meetings haben mir immer sehr viel Freude bereitet. Vielen Dank!

Dr. Andreas Vorholt, Prof. Dr. Arno Behr und Michael Terhorst von der Technischen Universität Dortmund danke ich herzlich für die unglaubliche Unterstützung bei der Inbetriebnahme der Hochdruckreaktorenanlage für Hydroformylierungen hier in Bielefeld durch ihre Beratung und Anleitung. Außerdem freue ich mich herzlich über unsere Kooperation zur Kombination von Hydroformylierung und Aldoximdehydratasen-Katalyse. Außerdem schätze ich im höchsten Maße die ehrliche und kollegiale Art des Umgangs miteinander. Michael Terhorst danke ich zusätzlich für die gemeinsamen Momente im Rahmen des SusChemSys 2.0 Clusters.

Herrn Dr. Thomas Kiltthau und Herrn Dr. Ling Ma von der Klüber Lubrication München SE & Co.KG spreche ich meinen tiefen Dank aus für die wirklich offene und konstruktive Kooperation für die Synthese neuer Estolidverbindungen als Schmierstoffe aus erneuerbaren Rohstoffen. Vor allem die gegenseitigen Besuche und die ausführlichen Führungen durch ihre Räumlichkeiten in München haben mich sehr beeindruckt. Vielen Dank!

Frau Prof. Dr. Heidrun Gruber-Wölfler und Manuel Maier von der Technischen Universität Graz danke ich für die Löslichkeitsbestimmungen im Rahmen des Projekts der biokatalytischen Dinitrilsynthese.

Dr. Jürgen Walkenhorst, Prof. Dr. Frank Entschladen, Dr. Wolfram Schleich, Dr. Thorsten Schaefer und Dr. Andreas Wagener von der ProVendis GmbH danke ich herzlich für die Anmeldung und Vermarktung der zwei Patentanmeldungen für chirale Aminonitrile und die biokatalytische Dinitrilsynthese. Besonders bedanke ich mich zudem für die Möglichkeit auf ihre Einladung hin bei der BioVaria2017 in München unsere Patentanmeldung für die chiralen Aminonitrile vorzustellen. Vielen Dank!

Frau Dr. Inga Marin vom Dezernat Forschungsförderung & Transfer (FFT) der Universität Bielefeld danke ich für die unkomplizierte und freundliche Unterstützung beim Einreichen unserer Patentanmeldungen, sowie für ihre lehrreichen Seminare zum Patentwesen.

Herrn Dr. Aloys Hüttermann und Dr. Sonja Althausen von Michalski-Hüttermann & Partner, sowie Herrn Dipl.-Ing. Hartmut Hering von Berendt, Leyh & Hering danke für die Anfertigungen der Patentschriften.

Herrn Dr. Jens Sproß, Heinz-Werner Patruck und Sandra Heitkamp danke ich für die massenspektroskopischen Analysen, als auch die gemeinsamen Grillabende und Unterstützung bei IT-Fragen. Herrn Klaus-Peter Mester danke ich für die Vermessung mehrere hundert NMR-Proben. Herrn Manfred Hoffmann von der Mechanischen Werkstatt danke ich für diverse Anfertigungen für und Reparaturen an unserer Autoklavenstation.

Besonders Aem Nuylert, Daijun Zheng und Siriporn Chaikaew danke ich für die herzliche Aufnahme in Toyama und die vielen schönen Abende, die wir gemeinsam im Labor und in diversen Restaurants oder beim Karaoke verbracht haben. Akari Yagi, Yoshiki Yamamoto, Kiyoshi Yamaguchi, Masaki Fukutani, Risa Inoue, Sayaka Kamai und Tomoya Mori danke ich für ihre freundliche und herzenswarme Art im Labor, den Partys und den Karaoke-Abenden. Herrn Prof. Makoto Hibi, Prof. Daisuke Matsui und Frau Ai Kuchiki danke ich neben ihrer herzlichen Art vor allem für die Hilfe bei der Anreise, Appartementein- und auszug und die Erledigung vieler bürokratischer Formalitäten. Mina-san, dōmo arigatō gozaimasu! (皆さん、どうもありがとうございます。)

Ohne ein gutes Team ist jeder Einzelne nichts. Carmen Plass danke ich für ihre Unterstützung beim Klüberprojekt und ihren Einsatz beim Etablieren der Hydroformylierungsanlagen. Nadine, Jana, Ji Eun und Keiko (das Girls Lab) danke ich für ihr Engagement beim Finnbahnrennen 2016, die Einführung des Obstkorbs und vielen gemeinsamen Aktionen, die auf ihren Impuls hin organisiert wurden. Franziska danke ich für die vielen gemeinsamen Gespräche, die zahlreichen Andorabende, ihr großes Engagement bei der Neueinrichtung des Kafferraums, die schönen Tanzabende und super Feten. Dr. Anke Hummel, Dr. Daniel Bakonyi und Thomas Geisler danke ich für die herzliche Aufnahme in den Arbeitskreis und ihre Anleitung vor allem zu Beginn meiner Forschungstätigkeit. Thomas sei hiermit auch explizit für die schönen Feuerbowlenabende und seine Spendenaktionen für das Kolpingwerk gedankt, für die ich immer gerne und reichlich gespendet habe. Angelika Bendick danke ich für ihren Einsatz für uns Doktoranden durch unkomplizierte Erledigung administrativer Aufgaben und vor allem für das durch sie eingeleitete geerdete, heimische Klima im Arbeitskreis. Severin Wedde, Juraj Paris, Melissa Kracht und Dr. Yasunobu Yamashita danke ich für ihre gute Mitarbeit in den vergangenen Jahren. Prof. Dr. Dietmar Kuck und Wilko Greschner danke ich für ihre Anleitung während meines Forschungspraktikums und vor allem zu Beginn meiner Tätigkeit im Arbeitskreis, besonders bei organisch synthetischen Fragestellungen. Dr. Tina Reiß und Dr. Marc Biermann danke ich für ihre Hilfe und Unterstützung, als ich eines der jüngsten Mitglieder im Arbeitskreis war und wünsche ihnen alles Gute für die Zukunft. Jannis Nonnhoff und Niklas Adebar wünsche ich eine schöne Zeit während ihrer neuangefangenen Promotion.

Explizit hervorheben möchte ich hiermit noch meine drei Schicksalsgenossen des Labors F3-264. Zuerst Matthias Pieper, dem ich an dieser Stelle alles Gute für den familiären Nachwuchs wünsche. Matthias ging auf das gleiche Gymnasium wie ich und die Gespräche über alte Lehrer und Mitschüler waren immer eine schöne Erinnerung an die Jugend. Als nächstes Philipp Rommelmann, der zu unserem großen Glück sich zur Promotion in der Organischen Chemie I entschieden hat. Wir haben während der Promotion exzellent zusammengearbeitet. Vor allem sein künstlerisches Geschick und freundliches Wesen sind Dinge, die ich an ihm bewundere.

Dann wären da noch Florian Uthoff und seine Birte. Was wahrscheinlich nur wenige wissen ist, dass Florian eine unglaubliche Auffassungsgabe und beeindruckenden Einblick in nicht nur chemische Sachverhalte hat, sondern vor allem in die des alltäglichen Lebens. Ich habe es immer genossen tiefgehend miteinander zu diskutieren oder einfach mal die Seele zu Liedern über Körperteile von Primaten baumeln zu lassen. Besonders danke ich Florian und Birte aber für die schönen vielen Momente, die wir in den letzten Jahren zusammen verbracht haben, sowohl innerhalb als auch außerhalb der Universität, privat wie beruflich und dass noch viele weitere folgen mögen. Danke, Florian und Birte!

Anika Hegemann danke ich neben ihrer Unterstützung im Labor für all die Unterstützung, die sie mir als Mensch in den Jahren und besonders den letzten Monaten zuteil werden ließ. Dadurch konnte ich wieder das Lachen lernen. Danke, Anika!

Da ein Mensch bekanntlich nur zwei Hände hat, die Fülle der Forschung jedoch nur durch mehrere Hände ausreichend ausgeschöpft werden kann, möchte ich hiermit allen Forschungspraktikanten und Bacheloranten danken, die mich tatkräftig während der Promotion unterstützt haben. Danke an Clara Belu, Theresa Tabarelli, Jasmin Busch, Inna Brod, Hilmi Yavuzer und Daniel Ossadnik für ihre engagierte Arbeit im Rahmen ihrer Forschungspraktika. Danke auch an Jasmin Busch, Monja Jochmann, Waldemar Brauer und Salvador Martinez Rivadeneira für ihr Engagement im Rahmen ihrer Bachelorarbeiten. Ihre Arbeit hat viele der Ergebnisse dieser Dissertation erst ermöglicht.

Besonders dankbar bin ich auch für meine langjährigen Freunde aus Lübbecke, Lars und Kirsten, Max und Gesa, Patric und Aisha, Birk und die anderen, mit denen ich mittlerweile schon so viele wunderschöne Dinge erleben durfte und weiter erleben darf. Eure Freundschaft gibt mir jederzeit viel Halt und Glück.

Ohne meine Familie und ihre herzliche Liebe, sowie Unterstützung über mein ganzes Leben hinweg, wäre ich nicht in der Lage gewesen den Weg an die Universität zu finden und sogar eine Promotion anzustreben. Vor allem mein Vater Egon und meine Brüder Kilian-Philipp und Christoph haben mir ermöglicht so zu werden, wie ich bin. Meiner Mutter Heike danke ich für eine schöne Kindheit. Des Weiteren danke ich besonders meiner Oma Heidemarie Brinkmann und meinem Opa Heinrich Ernst Wilhelm Brinkmann für einfach alles und insbesondere in Hinblick auf das Studium für ihre mentale und finanzielle Unterstützung. Zusätzlich danke ich meinem früh verstorbenen Opa Alfred Betke und meiner Oma Ingeborg Betke. Außerdem danke ich herzlich meiner lieben Tante Ute Rosemarie Betke, meinen Cousins Timon und Mailo, meinem Onkel Urs und meiner Tante Lille. Herzlich danke ich auch meinem Großonkel und Großtante Karl-Heinz Bruning und Brigitta Bruning, die mir die USA näher gebracht haben in einer Art, in der es nicht erwartet hätte. Danke! Außerdem danke ich Kirsten, Wally, Joshua und Caleb Brown, sowie Eric und Kim Bruning für ihre Herzlichkeit während unserer USA-Reise 2016.

Des Weiteren danke ich besonders Ralf und Marion Hinzmann, Inge und Günter Leimkuhl, Irmgard und Herbert Hinzmann, Tobias, Fabian, Alica, Carina, Frauke, Thomas, Lenya, Charlotte, Andrea, Jannik, Jolene, Niklas, Kerstin und Luca für die herzliche Aufnahme in ihre Mitte und für wunderschöne zweieinhalb Jahre. Bleibt bitte gesund und so wie ihr seid. Ich wünsche euch alles Gute für die Zukunft! Ihr seid mir wie meine Familie ans Herz gewachsen.



# TABLE OF CONTENTS

<b>1 PPP of Biocatalysis: Potential, possibilities and perspectives .....</b>	<b>1</b>
<b>1.1 Potential and possibilities.....</b>	<b>1</b>
<b>1.2 Perspectives .....</b>	<b>4</b>
<b>2 Discovery and state of the art for utilization of aldoxime dehydratases for the biocatalytic nitrile-synthesis .....</b>	<b>12</b>
<b>2.1 Introduction .....</b>	<b>12</b>
<b>2.2 Properties, structures and mechanism of aldoxime dehydratases .....</b>	<b>19</b>
<b>2.3 Substrate scope of aldoxime dehydratases.....</b>	<b>22</b>
2.3.1 Arylaliphatic aldoximes .....	22
2.3.2 Aromatic aldoximes .....	24
2.3.3 Aliphatic aldoximes.....	27
2.3.4 Chiral aldoximes .....	30
<b>3 Cyanide free, biocatalytic synthesis of chiral nitriles .....</b>	<b>35</b>
<b>3.1 Motivation .....</b>	<b>35</b>
<b>3.2 Substrate selection and synthesis .....</b>	<b>36</b>
<b>3.3 Substrate scope study and lead structure identification .....</b>	<b>41</b>
3.3.1 Substrate overview and general activity study .....	41
3.3.2 Investigations on the enantioselective nitrile synthesis on analytical scale .....	43
3.3.3 Lead structure hypothesis and confirmation for the enantioselective nitrile synthesis.....	46
3.3.4 Enantioselective nitrile synthesis on preparative scale.....	51
3.3.5 Attempted biotransformations of O-methylated oximes.....	52
<b>3.4 Summary and outlook for the biocatalytic, enantioselective nitrile     synthesis .....</b>	<b>54</b>
<b>4 Biocatalytic synthesis of aliphatic linear <math>\alpha,\omega</math>-dinitriles .....</b>	<b>55</b>
<b>4.1 Relevance of aliphatic linear <math>\alpha,\omega</math>-dinitriles in industry and everyday life.</b>	<b>55</b>
<b>4.2 Substrate synthesis based on dialdehydes or their acetals.....</b>	<b>57</b>
<b>4.3 Proof of the biotransformation process .....</b>	<b>60</b>
<b>4.4 Bioprocess development for the adiponitrile synthesis.....</b>	<b>69</b>
<b>4.5 High cell-density fermentation .....</b>	<b>74</b>
<b>4.6 Immobilization of OxdB from <i>Bacillus sp.</i> OxB-1 by crosslinking with     glutaraldehyde to obtain CLEAs for process intensification of linear aliphatic     <math>\alpha,\omega</math>-dinitrile synthesis .....</b>	<b>79</b>
4.6.1 Overview of different enzyme immobilization strategies .....	79
4.6.1.1 Enzyme immobilization by carrier binding.....	80
4.6.1.2 Enzyme immobilization by entrapment.....	81

4.6.1.3 Enzyme immobilization by cross-linking .....	83
4.6.2 Expression and purification of OxdB(C <sub>His6</sub> ) by Ni-NTA affinity chromatography	84
4.6.3 CLEA formation and activity quantification in aqueous medium .....	85
4.6.4 Recycling study for long-term stability determination of OxdB-CLEAs in aqueous und organic medium .....	86
4.6.5 Adiponitrile synthesis in organic, aqueous and biphasic systems .....	88
<b>4.7 Outlook for the technical feasibility of the biocatalytic adiponitrile synthesis .....</b>	<b>89</b>
<b>5 Chiral <i>N</i>-acyl-<math>\alpha</math>-aminonitriles <i>via</i> Copper catalysis and incorporation into a <i>de novo</i> synthesis of Vildagliptin .....</b>	<b>91</b>
<b>5.1 Nitriles in the pharmaceutical industry.....</b>	<b>91</b>
<b>5.2 Copper-catalyzed dehydration of <i>N</i>-acyl <math>\alpha</math>-amino aldoximes and implementation into a <i>de novo</i> synthesis of Vildagliptin.....</b>	<b>94</b>
5.2.1 State of the art of the vildagliptin synthesis.....	94
5.2.2 Copper-catalyzed dehydration of <i>N</i> -acyl $\alpha$ -amino aldoximes .....	95
5.2.3 Discovery of the stereochemistry retention during aldoxime dehydration.....	98
5.2.4 Implementation of the copper-catalyzed dehydration into a <i>de novo</i> -synthesis of Vildagliptin by <i>Rommelmann</i> .....	100
<b>6 New lubricant ester structures based on renewable ressources .....</b>	<b>103</b>
<b>6.1 Estolides - Introducing sustainability in the lubricant industry .....</b>	<b>103</b>
<b>6.2 New lubricant ester structures – Synthesis and biodegradability .....</b>	<b>112</b>
<b>6.3 Summary and outlook for the estolide synthesis .....</b>	<b>122</b>
<b>7 Summary and Outlook .....</b>	<b>125</b>
<b>8 Zusammenfassung und Ausblick .....</b>	<b>129</b>
<b>9 Experimental procedures .....</b>	<b>133</b>
<b>9.1 General Information .....</b>	<b>133</b>
<b>9.2 Analytical methods .....</b>	<b>134</b>
<b>9.3 Cyanide-free, biocatalytic synthesis of chiral nitriles.....</b>	<b>135</b>
9.3.1 Synthesis of reference compounds .....	135
9.3.1.1 General procedure 1 (GP1): Nitroaldol condensation of aromatic aldehydes with Nitromethane.....	135
9.3.1.1.1 Synthesis of (E)-1-bromo-4-(2-nitrovinyl)benzene.....	135
9.3.1.1.2 Synthesis of (E)-1-bromo-4-(2-nitrovinyl)benzene.....	136
9.3.1.1.3 Synthesis of (E)-1-bromo-4-(2-nitrovinyl)benzene.....	136
9.3.1.2 General procedure 2 (GP2): Michael Addition of methylmagnesium bromide with Nitroalkenes .....	137
9.3.1.2.1 Synthesis of rac-1-bromo-4-(1-nitropropan-2-yl)benzene.....	137
9.3.1.2.2 Synthesis of rac-1-bromo-3-(1-nitropropan-2-yl)benzene.....	138

9.3.1.2.3 Synthesis of rac-1-bromo-2-(1-nitropropan-2-yl)benzene.....	138
9.3.1.3 General procedure 3 (GP3): Synthesis of racemic aldoximes <i>via</i> disproportionation of racemic nitroalkanes with benzyl bromide .....	139
9.3.1.3.1 Synthesis of rac-(E/Z)-2-(4-bromophenyl)propanal oxime .....	139
9.3.1.3.2 Synthesis of rac-(E/Z)-2-(3-bromophenyl)propanal oxime .....	140
9.3.1.3.3 Synthesis of rac-(E/Z)-2-(2-bromophenyl)propanal oxime .....	141
9.3.1.4 General procedure 4 (GP4): Synthesis of aldoximes by condensation of aldehydes with hydroxyl amine salts.....	143
9.3.1.4.1 (E/Z)-phenyl acetaldehyde oxime .....	143
9.3.1.4.2 rac-(E/Z)-3-cyclohexene-1-carboxaldehyde oxime.....	144
9.3.1.4.3 rac-(E/Z)-3-phenylbutyraldehyde oxime.....	145
9.3.1.4.4 rac-(E/Z)-2-methyl-3-(3,4-methylenedioxyphenyl)-propanal oxime .	145
9.3.1.4.5 rac-(E/Z)-2-methyl-3-(4-isopropylphenyl)propionaldehyde oxime....	146
9.3.1.5 General procedure 5 (GP5): Copper (II) catalyzed synthesis of racemic nitriles .....	148
9.3.1.5.1 Phenyl acetonitrile .....	148
9.3.1.5.2 rac-3-cyclohexene-1-carbonitrile .....	149
9.3.1.5.3 rac-3-phenylbutanenitrile .....	149
9.3.1.5.4 rac- $\alpha$ -methyl-1,3-benzodioxole-5-propanenitrile.....	150
9.3.1.5.5 rac- $\alpha$ -methyl-4-(1-methylethyl)-benzenepropanenitrile .....	150
9.3.1.5.6 rac-2-(4-bromophenyl)propanenitrile .....	151
9.3.1.5.7 rac-2-(3-bromophenyl)propanenitrile .....	151
9.3.1.5.8 rac-2-(2-bromophenyl)propanenitrile .....	152
9.3.2 Preparation of whole cell catalysts and biotransformations of aldoximes into nitriles .....	153
9.3.2.1 General procedure 6 (GP6): Expression and storage of the aldoxime dehydratases (Oxds) .....	153
9.3.2.2 General procedure 7 (GP7): Standard protocol for determination of Oxd activity .....	155
9.3.2.3 General procedure 8 (GP8): Enantioselective biotransformations of ( <i>E</i> )- and ( <i>Z</i> )-enriched racemic aldoximes into chiral nitriles on analytical scale .....	158
9.3.2.4 General procedure 9 (GP9): Enantioselective biotransformations of ( <i>E</i> )- and ( <i>Z</i> )-enriched racemic aldoximes into chiral nitriles on preparative scale.....	161
9.3.2.4.1 Synthesis of ( <i>S</i> )-2-(2-bromophenyl)propanenitrile.....	161
9.3.2.4.2 Synthesis of ( <i>R</i> )-2-(3-bromophenyl)propanenitrile.....	162
9.3.2.4.3 Synthesis of ( <i>S</i> )- $\alpha$ -methyl-1,3-benzodioxole-5-propanenitrile.....	162
9.3.3 Synthesis and attempted biotransformations of O-methylated aldoximes ....	162
9.3.3.1 General procedure 10 (GP10): O-methylated aldoxime synthesis by condensation of aldehydes with hydroxylamine hydrochloride.....	162
9.3.3.1.1 rac-(E/Z)-2-phenylpropionaldehyde O-methyloxime.....	163
9.3.3.1.2 rac-(E/Z)-cyclohex-3-enecarbaldehyde O-methyl oxime .....	163

9.3.3.1.3	rac-(E/Z)-2-methyl-3-(3,4-methylenedioxyphenyl)propanal O-methyloxime.....	164
9.3.3.1.4	rac-(E/Z)-3-phenylbutyraldehyde O-methyloxime.....	164
9.3.3.1.5	rac-(E/Z)-2-methyl-3-(4-isopropylphenyl)propionaldehyde O-methyloxime.....	165
9.3.3.1.6	(E/Z)-3-phenylpropionaldehyde O-methyloxime .....	165
9.3.3.2	Attempted biotransformations of O-methylated aldoximes.....	166
<b>9.4</b>	<b>Biocatalytic production of adiponitrile and related aliphatic linear <math>\alpha,\omega</math>-dinitriles .....</b>	<b>167</b>
9.4.1	Synthesis of reference compounds .....	167
9.4.1.1	General procedure 11 (GP11): Adipaldehyde synthesis by oxidation of trans-1,2-Cyclohexanediol .....	167
9.4.1.2	General procedure 12 (GP12): Synthesis of linear, aliphatic $\alpha,\omega$ -dialdehydes by oxidation of linear, aliphatic $\alpha,\omega$ -dialcohols with Bobbitt's salt (4-(Acetylamino)-2,2,6,6-tetramethyl-1-oxo-piperidinium tetrafluoroborate) .....	168
9.4.1.2.1	Heptanedial .....	168
9.4.1.2.2	Octanedial .....	169
9.4.1.2.3	Nonanedial .....	169
9.4.1.2.4	Decanedial.....	169
9.4.1.3	General procedure 13 (GP13): Synthesis of linear, aliphatic $\alpha,\omega$ -dioximes <i>via</i> condensation of Bis(dimethyl)acetals with hydroxylamine hydrochloride.....	171
9.4.1.3.1	Malonoaldehyde dioxime .....	171
9.4.1.3.2	Succinaldehyde dioxime .....	172
9.4.1.4	General procedure 14 (GP14): Synthesis of linear, aliphatic $\alpha,\omega$ -dioximes <i>via</i> condensation of linear, aliphatic $\alpha,\omega$ -dialdehydes with hydroxylamine hydrochloride .....	173
9.4.1.4.1	Glutaraldehyde dioxime.....	173
9.4.1.4.2	Adipaldehyde dioxime .....	174
9.4.1.4.3	Heptanedial dioxime .....	174
9.4.1.4.4	Octanedial dioxime .....	175
9.4.1.4.5	Nonanedial dioxime .....	175
9.4.1.4.6	Decanedial dioxime.....	176
9.4.2	Biotransformations for the biocatalytic production of aliphatic linear $\alpha,\omega$ -dinitriles.....	177
9.4.2.1	General procedure 15 (GP15): Activity assay for the biocatalytic dehydration of dioximes by OxdA and OxdB .....	177
9.4.2.2	General procedure 16 (GP16): Influence of water soluble cosolvents on the activity of Oxds (short term studies).....	178
9.4.2.3	General procedure 17 (GP17): Influence of water soluble cosolvents on the activity of OxdA und OxdB (long term studies).....	181
9.4.2.4	General procedure 18 (GP18): Preparative scale experiments for the biocatalytic synthesis of adiponitrile.....	183



9.4.2.5 Attempted biotransformation of succinaldehyde dioxime and glutaraldehyde dioxime.....	184
9.4.2.6 High cell-density fermentations of OxdB.....	184
9.4.3 Expression, Purification and Immobilization by crosslinking of his-tagged aldoxime dehydratase from <i>Bacillus sp.</i> OxB-1 (OxdB <sub>CHis6</sub> ) .....	185
9.4.3.1 Expression of OxdB(C <sub>His6</sub> ) in <i>E.Coli</i> BL21 (DE3) .....	185
9.4.3.2 Purification of OxdB(C <sub>His6</sub> ) by NiNTA affinity chromatography .....	186
9.4.3.3 Optimized of CLEA formation by crosslinking of purified OxdB(CHis6) with glutaraldehyde.....	186
9.4.3.3 Activity assays for determination of OxdB(C <sub>His6</sub> ) activity .....	187
9.4.3.3.1 Purified OxdB(C <sub>His6</sub> ).....	187
9.4.3.3.2 Crude extract of (C <sub>His6</sub> ), CLEA supernatant and washing fraction.....	187
9.4.3.3.3 OxdB(C <sub>His6</sub> ) CLEAs .....	188
9.4.3.4 General procedure 19 (GP19): Recycling study for the long-term stability of OxdB(C <sub>His6</sub> ) CLEAs in aqueous media .....	189
9.4.3.5 General procedure 20 (GP20): Recycling study for the long-term stability of OxdB(C <sub>His6</sub> ) CLEAs in organic media.....	190
9.4.3.6 Synthesis of adiponitrile in aqueous and organic media with OxdB(C <sub>His6</sub> ) CLEAs .....	190
9.4.3.7 Synthesis of adiponitrile in a biphasic system with OxdB(C <sub>His6</sub> ) CLEAs ....	191
<b>9.5 Chiral N-Acyl-<math>\alpha</math>-aminonitriles via Copper catalysis and incorporation into a de novo synthesis of Vildagliptin .....</b>	<b>192</b>
9.5.1 General procedure 21 (GP21): Condensation of Mono-aldehydes with hydroxylamine salts.....	192
9.5.1.1 ( <i>E/Z</i> )- <i>N</i> -Boc-D-phenylalaninal oxime.....	192
9.5.1.2 ( <i>E/Z</i> )- <i>N</i> -Boc-L-phenylalaninal oxime .....	193
9.5.2 General procedure 22 (GP22): Copper(ii) acetate catalyzed dehydration of $\alpha$ -Amino aldoximes .....	194
9.5.2.1 ( <i>R</i> )- <i>N</i> -Boc-Phenylalanine Nitrile.....	194
9.5.2.2 ( <i>S</i> )- <i>N</i> -Boc-phenylalanine Nitrile.....	195
<b>9.6 New lubricant ester structures based on renewable resources.....</b>	<b>196</b>
9.6.1 General procedure 23 (GP23): Biocatalytic synthesis of oleic acid esters by esterification of oleic acid with Guerbet alcohols .....	196
9.6.1.1 2-ethylhexyl oleate.....	196
9.6.1.2 2-butyloctyl oleate .....	197
9.6.1.3 2-hexyldecyl oleate .....	197
9.6.1.4 2-octyldodecyl oleate.....	198
9.6.1.5 General procedure 24 (GP24): Recycling of Novozym 435 for the synthesis of 2-ethylhexyl oleate in a SpinChem reactor.....	199
9.6.2 General operating procedure 25 (GP25): Ene reaction of oleic acid and oleic esters with paraformaldehyde and Lewis acids .....	200

9.6.2.1 ( <i>E</i> )-9+10-(hydroxymethyl)octadec-10+8-enoic acid .....	200
9.6.2.2 2-ethylhexyl ( <i>E</i> )-9+10-(hydroxymethyl)octadec-10+8-enoate .....	201
9.6.3 General working procedure 26 (GP26): Palladium catalyzed C=C-hydrogenation of oleic acid derivatives .....	202
9.6.3.1 9+10-(hydroxymethyl)octadecanoic acid.....	202
9.6.3.2 2-ethylhexyl 9+10-(hydroxymethyl)octadecanoate.....	203
9.6.3.3 2-ethylhexyl 9+10-((stearoyloxy)methyl)octadecanoate .....	204
9.6.4 General operating procedure 27 (GP27): Biocatalytic esterification of fatty acids with hydroxymethylated oleic acid derivates to estolide dimers .....	205
9.6.4.1 2-ethylhexyl 9+10-((stearoyloxy)methyl)octadecanoate .....	205
9.6.4.2 2-(8-((2-ethylhexyl)oxy)-8-oxooctyl)undecyl oleate and 11-((2- ethylhexyl)oxy)-2-octyl-11-oxoundecyl oleate .....	206
9.6.4.3 2-ethylhexyl 9 und 10-((stearoyloxy)methyl)octadec-8 und 10-enoate ..	207
9.6.5 Synthesis of 2-ethylhexyl 12-(stearoyloxy)octadecanoate starting from 12- hydroxystearic acid.....	208
9.6.5.1 2-ethylhexyl 12-hydroxyoctadecanoate.....	208
9.6.5.2 2-ethylhexyl 12-(stearoyloxy)octadecanoate .....	209
<b>10 List of abbreviations .....</b>	<b>211</b>
<b>11 References .....</b>	<b>215</b>
<b>12 Appendix.....</b>	<b>223</b>
<b>12.1 Sequences and Plasmids cards of the aldoxime dehydratases (Oxds) .</b>	<b>223</b>
12.1.1 Aldoxime dehydratase from <i>Pseudomonas chlororaphis</i> B23 (OxdA) .....	223
12.1.2 Aldoxime dehydratase from <i>Bacillus</i> sp. strain OxB-1 (OxdB) in pUC18..	223
12.1.3 Aldoxime dehydratase from <i>Bacillus</i> sp. strain OxB-1 (OxdB(C <sub>His6</sub> ), codon- optimized) in pET-22b.....	224
12.1.4 Aldoxime dehydratase from <i>Fusarium graminearum</i> MAFF305135 (OxdFG(N <sub>His6</sub> ), codon-optimized) in pET28a .....	225
12.1.5 Aldoxime dehydratase from <i>Rhodococccs erythropolis</i> ( <i>Rhodococccs</i> sp. N- 771, OxdRE(N <sub>His6</sub> ), codon-optimized) in pET28a .....	226
12.1.6 Aldoxime dehydratase from <i>Rhodococccs globerulus</i> A-4 (OxdRG(N <sub>His6</sub> ), codon-optimized) in pET28a .....	226





# 1 PPP OF BIOCATALYSIS: POTENTIAL, POSSIBILITIES AND PERSPECTIVES

## 1.1 POTENTIAL AND POSSIBILITIES

The expeditious depletion of the world's resources, which is especially true for noble metals, prompts us to rethink the production methods for many of today's chemical compounds. Furthermore, the rapidly increasing population of the earth and the increasing product demand in all segments of the chemical industry force us to develop reliable (and at the same time sustainable) production processes which can meet our needs now and in the future.

Catalysis is the key technology for enabling these processes and most promisingly its subarea biocatalysis (**Figure 1**).<sup>[1,2,3-5]</sup> Not only do biocatalytic processes perform under milder conditions than most conventional chemical processes and excel in selectivity, they also offer the opportunity of geopolitical independence. While transition metal catalyzed processes always depend on the current price and availability of the corresponding metal, biocatalysts can be simply produced by microorganisms starting from the simplest building blocks of life. Hence, biocatalysts can be generated everywhere in the world and do not require rare, depletable ore deposits. As a consequence, there can never be a shortage of biocatalysts. Additionally, the precious metals need to be efficiently recycled and have to be restricted in their exposition towards animals, humans and environment due to their high toxicity. Biocatalysts on the other hand are completely biodegradable and, under optimized cultivation procedures, cheaply produced.

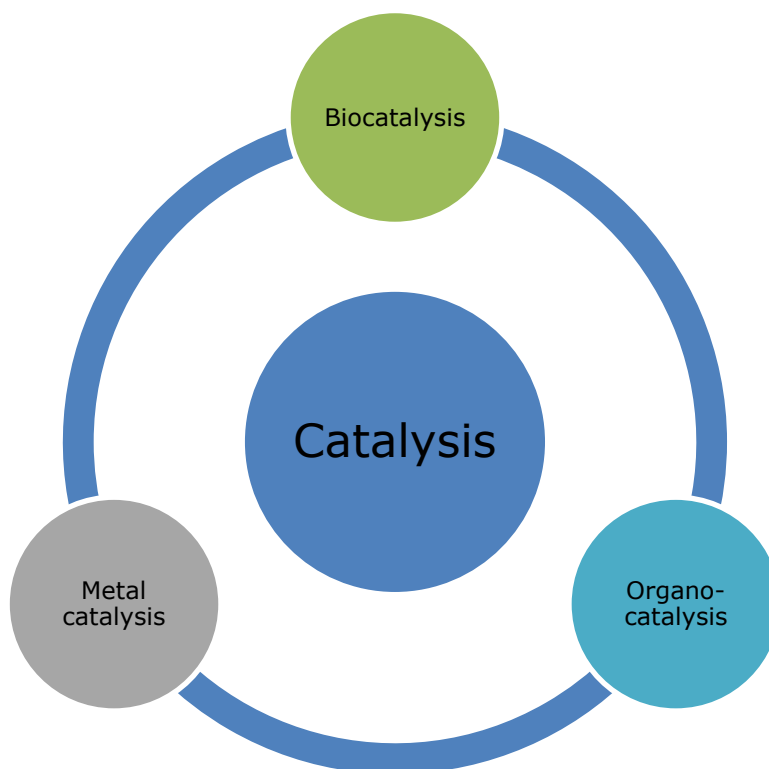


**Figure 1:** Classification of catalysis subareas.

However, biocatalysis has restrictions of its own. Enzymes may be deactivated by solvents or harsh reaction conditions, often require several months or even years before being used efficiently in a process and many chemical reactions are still not conductable (or at least efficiently) with biocatalysts. Hence, the successive implementation of biocatalytic processes into the chemical industry should always be regarded and used as an additional alternative to other catalytic processes, may they be homogeneous or heterogeneous.<sup>[6]</sup> This additional alternative should be viewed as a broadening of the chemical repertoire and not as the all-promising solution to every synthetic problem. New and fascinating possibilities open up by abiding these standpoints.

If one is not familiar with the history of biocatalysis, one may think that this technology is a rather new discipline. However, the beginnings of biocatalysis stretch way further back and its emerge in the last century is often described in the form of waves.<sup>[7]</sup> In the first wave, which began roughly 100 years ago, whole-cell catalysts like baker's yeast or the fungus *Rhizopus arrhizus* were used for hydrocyanation of aldehydes or hydroxylation of steroids (**Figure 2**).<sup>[6]</sup> The hydroxylation of progesterone by *Rhizopus arrhizus* decreased the number of synthesis steps drastically from 32 to 6, avoiding the generation of big amounts of waste and lowering the cost of cortisone from 200 to 6 \$/g of product.

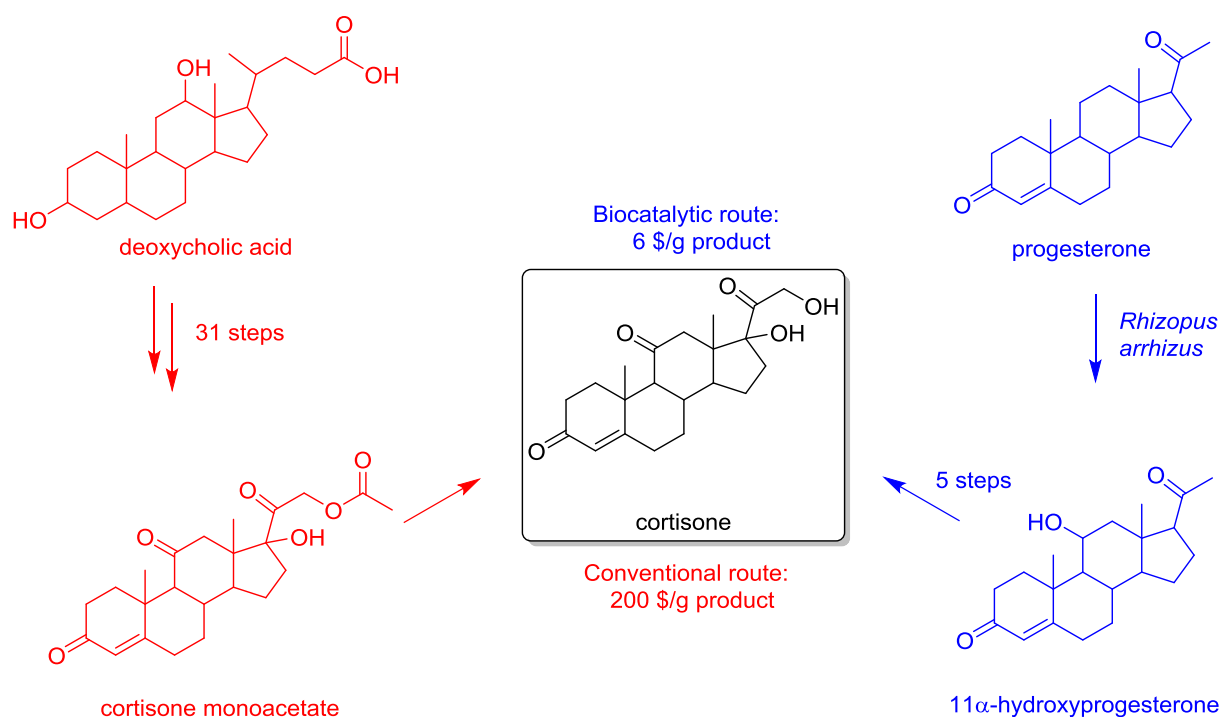
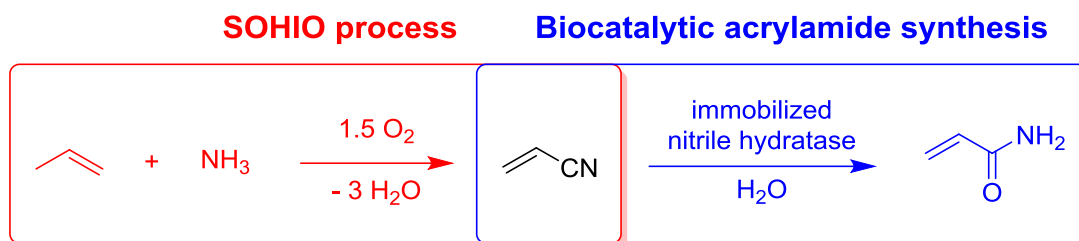


**Figure 2:** Influence of biocatalysis on the efficient synthesis of cortisone.<sup>[6]</sup>

In the second wave of biocatalysis which started roughly in the early 1980s, genetic engineering tools were developed which allowed for a site-directed mutation of enzymes. Furthermore, chemical modifications like immobilization methods<sup>[8]</sup> for reusing the enzymes were developed. As a consequence, new and unnatural substrates could be transformed by biocatalysts which were not recognized beforehand.<sup>[7]</sup> This led to the implementation of biocatalysis into the fine chemical industry, bulk chemical industry and pharmaceutical research since it was recognized as a part of the toolbox for organic chemistry.<sup>[9]</sup> Especially kinetic resolutions catalyzed by lipases (hydrolases) or asymmetric reductions with carbonyl reductases allowed access to enantiomerically pure alcohols and

esters. Another prominent example of the second wave is the development of the biocatalytic hydration of acrylonitrile to acrylamide, which is nowadays run at a scale of over 30000 tons per year with a constantly growing production volume (**Scheme 1**).<sup>[6,10]</sup> The required acrylonitrile for this process is produced by ammoxidation (SOHIO process).<sup>[11]</sup> Further examples of technical processes are the D-glucose isomerization to D-fructose with over 100000 tons per year, the kinetic resolution of phenylethylamines with lipases with 10000 tons per year or the hydrolysis of penicillin G to (+)-6-aminopenicillanic acid (6-APA) with 40000 tons per year. All of these processes are performed with immobilized biocatalysts.<sup>[10]</sup>



**Scheme 1:** Ammoxidation of propene and biocatalytic hydration of acrylonitrile.

The third wave of biocatalysis started in the early 1990s by great advances in the molecular biology field.<sup>[7]</sup> Especially further developments in molecular biology methods like error prone polymerase chain reactions opened the path to high-throughput screening of enzymes. The research results of *Arnold* and *Reetz* in the area of directed evolution by random mutagenesis or gene shuffling enabled one to improve wild-type enzymes. After a few rounds of mutations, drastically improved biocatalysts in terms of activity against substrates, solvent stability and enantioselectivity can be generated.<sup>[1,12]</sup> Hence, biocatalytic engineering became much more potent and coupled with improved protocols for gene expression and enzyme purification methods increased the value of biocatalysis drastically.<sup>[4,13]</sup>

Looking at the present, highly complex modelling programs, high-throughput screening methods, bioinformatic tools and other achievements start to develop a fourth wave of biocatalysis, in which novel enzymes classes may be discovered just by the deposited data in gene libraries.<sup>[14]</sup> These accomplishments allows one to close the speed gap needed e.g. in the pharmaceutical to develop process solutions in less time.<sup>[15]</sup> Furthermore, less screening effort results in lower development costs and coupled with efficient fermentation processes reduce the overall costs of biocatalysts to a more competitive level.<sup>[16]</sup>

As the above mentioned cortisone example shows impressively (**Figure 2**), biocatalysis is highly compatible with the principles of green chemistry, which were coined by *Anastas*.<sup>[3,17]</sup> Biocatalysis operates under mild conditions, avoids hazardous waste generation and is inherently safe. Additionally, it operated mostly in water or non-toxic solvents and the biocatalysts can be discarded as non-hazardous waste after sterilization or other denaturation.<sup>[18]</sup>

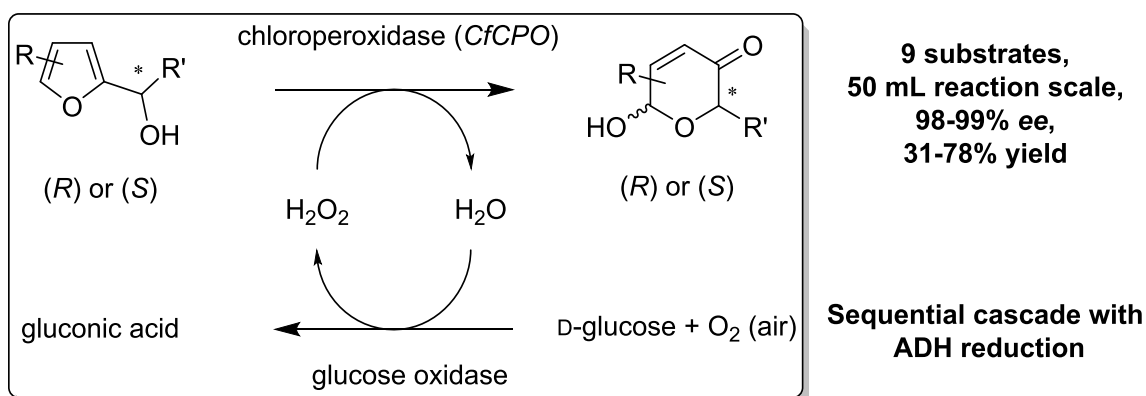
Lastly, biocatalysis has been successfully coupled with metal- or organocatalysis in several cascade reactions that allow one to skip work-up steps of intermediates.<sup>[19]</sup> These processes are becoming more and more efficient and represent one of the biggest growth field for the future apart from newly discovered reaction types catalyzed by enzymes (**Figure 1**).

## 1.2 PERSPECTIVES

Biocatalysis excels at selectivity, may it be chemo-, regio-, stereoselectivity. This property allows a chemist to plan complex synthesis steps without the need for protecting groups or enables one with the possibility to completely skip unnecessary steps.

The rapid progress of biocatalysis in this regard reveals itself best by visualizing a selection of the most impactful synthetic possibilities that were conquered in the last five years. While earlier advances in the biocatalytic repertoire mainly focused on rather straightforward reactions like ester formation, amide hydrolysis etc., the current advances are way more subtle. Especially the advances in the field of protein engineering enabled several new synthetic possibilities. The big potential and impact of protein engineering of enzymes was recently honored by awarding the Nobel prize for chemistry of 2018 to *Frances H. Arnold* by the Royal Swedish Academy of Sciences.

The basis of tomorrow's chemical industry will be based on renewable resources since crude oil is a limited resource. Especially compounds like furane derivatives that can be gained out of lignocellulose are potential gamechanger in this area. In 2014, *Deska et al.*<sup>[20]</sup> described a biocatalytic Achmatowicz reaction which represents a ring rearrangement reaction under utilization of racemic or enantiomeric pure furyl alcohols to yield the corresponding pyranons with defined stereochemistry. To this end, they used a combination of a glucose oxidase for oxygen activation ( $O_2$  to  $H_2O_2$ ) and conducted the rearrangement by usage of a chloroperoxidase (**Scheme 2**). Furthermore, access to the required enantiomerically pure furyl alcohols could be gained by reduction of the ketones with alcohol dehydrogenases (ADHs). A sequential cascade reaction (due to different pH optima of the enzymes) of the ADH-catalyzed reduction and Achmatowicz reaction could also be realized. This reaction may play a crucial role in an environmentally benign furane valorization, avoiding reagents like *m*-chloroperoxybenzoic acid. Two years later, in 2016, *Hollmann et al.*<sup>[21]</sup> expanded this synthetic method towards the Aza-Achmatowicz with nitrogen containing heterocycles.



Conditions: 10 mM substrate, 50 mM glucose, citrate buffer (45 mL, 0.1M, pH = 5.5), *t*BuOH (5 mL), room temperature

**Scheme 2:** Biocatalytic Achmatowicz reaction reported by *Deska et al.*<sup>[20]</sup>

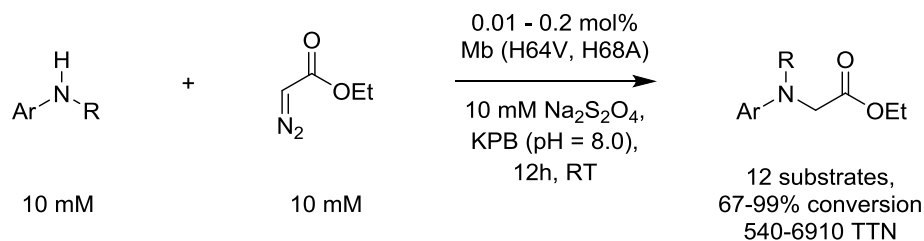
C-H functionalization is one of the most investigated topics in chemistry and catalysis in the last years. The groups of *Arnold* and *Fasan* have discovered excellent advancements in this field. From 2011-2016, *Fasan's* group developed a high throughput screening method they call the "fingerprinting method" to rapidly estimate the size and shape of an



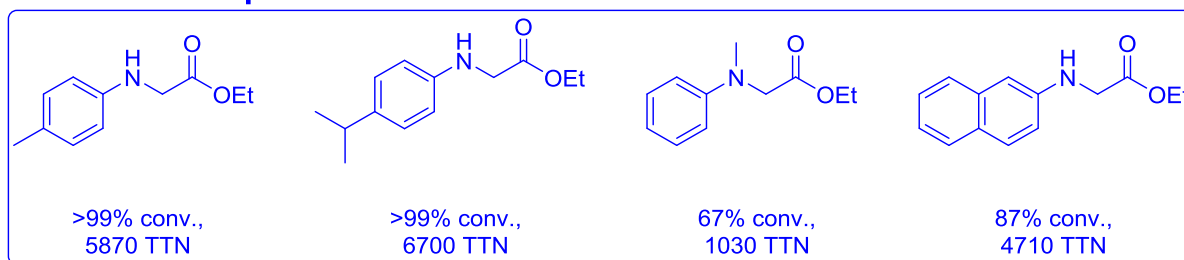
active site of CYP450 monooxygenases.<sup>[22]</sup> This allowed them to conduct high throughput screening for mutations of CYP450 monooxygenases, leading to selective hydroxylation of highly interesting synthetic structures like derivatives of the terpene-based anti-malaria drug Artemisinin.

Furthermore, *Fasan's* group discovered the possibility of intramolecular  $sp^3$  C-H amination with arylsulfonyl azide substrates. This C-H amination proceeds *via* elimination of  $N_2$  from the azide to bind the remaining nitrogen as nitrene to the iron atom of the heme group of a CYP450 monooxygenase.<sup>[23]</sup> Afterwards, the intramolecular addition to benzylic carbon atoms proceeded. They obtained nine different cyclic benzosulfonamides with this method, however with low yields and only moderate *ee*-values. Despite their initial success with this synthetic method, they deemed the CYP450 monooxygenases too labile, unproductive and complicated. Hence, they focused on a more stable and easier productable biocatalytic in their further studies: myoglobin (Mb) from sperm whale.<sup>[24]</sup> In 2014, they obtained first promising results by site-directed mutation of the Mb active site and could obtain cyclic benzosulfonamides with a total turnover number (TTN) of up to 200 and moderate *ee*-values. Additionally, they tried to enhance the catalytic performance by exchanging the metal centre of the heme group in Mb by exchanging it with cobalt and manganese. However, these attempts led to decreased catalytic activity.<sup>[24,25]</sup>

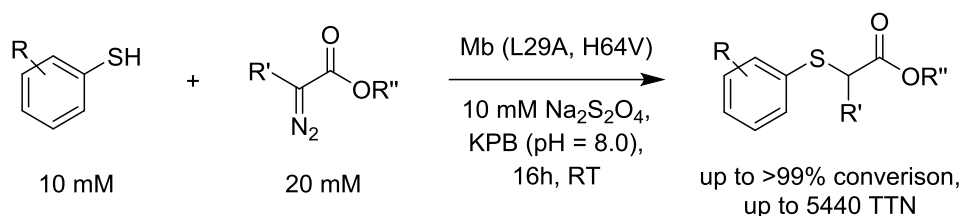
Inspired by their progress with the C-H bond functionalization by azide compounds, *Fasan's* group started to focus in 2015 on the insertion of carbenes into N-H and S-H bonds.<sup>[26-28]</sup> For this, they utilize  $\alpha$ -diazoesters which *in situ* eliminate  $N_2$  and the resulting carbene is directly bound to the iron atom of the heme group in Mb. During these studies, they discovered that two distinctive mutations in the active site of Mb led to drastically increased TTN and allowed them to conduct biotransformation with up to 6700 TTN at 10 mM substrate concentrations for the N-H insertion (**Scheme 3**). The S-H insertion was conducted on 10 mM scale with up to 5440 TTN. Additionally, first attempts of an enantioselective S-H carbene insertion have been conducted. One selected thioether was obtained with up to 49% *ee* at 4 °C, demonstrating the challenging enantioselective insertion of carbenes into S-H bonds (**Scheme 4**).



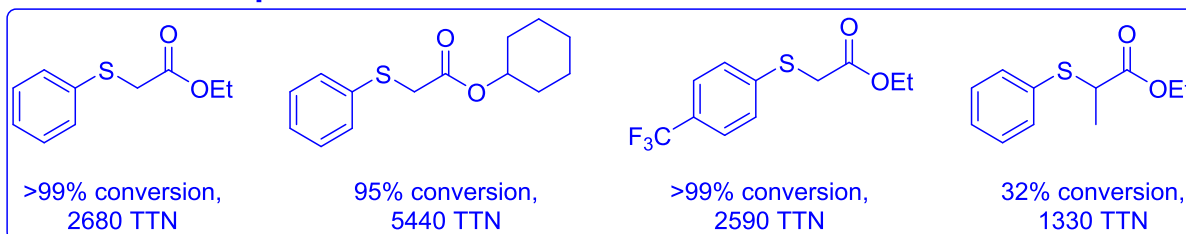
### Selected examples



**Scheme 3:** Biocatalytic N-H insertion of carbenes reported by *Fasan et al.*<sup>[26]</sup>

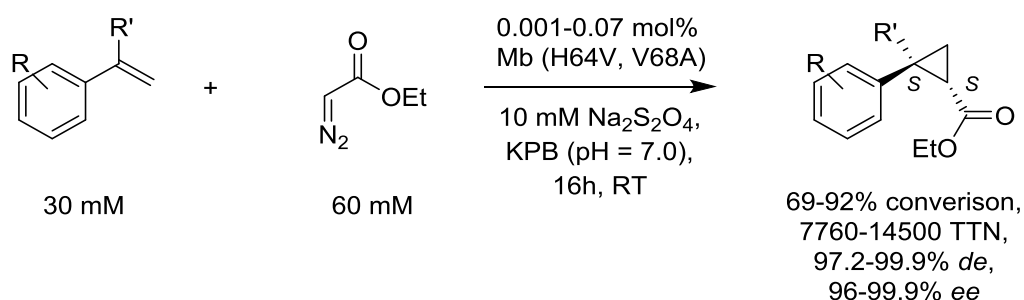


### Selected examples

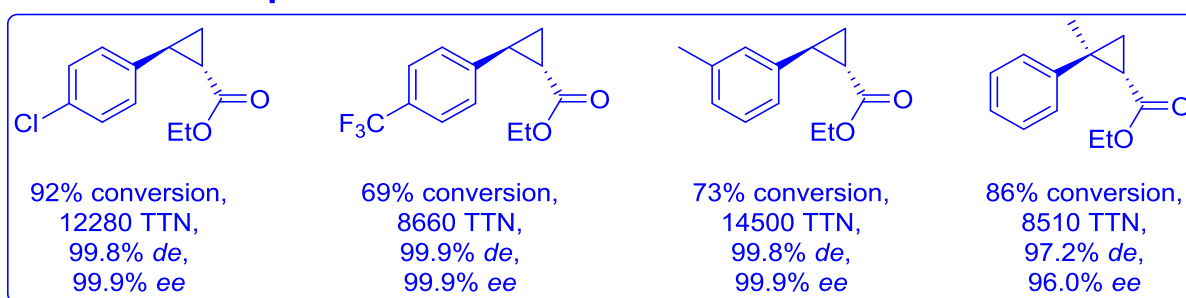


**Scheme 4:** Biocatalytic S-H insertion of carbenes reported by *Fasan et al.*<sup>[27]</sup>

The most impressive and synthetically potent discovery of *Fasan's* group in recent years has been the potential of their developed Mb platform to synthesize substituted cyclopropane rings out of olefins and carbenes in a highly stereoselective manner.<sup>[29-31]</sup> Starting in 2015, they conducted site-directed mutagenesis of the active site of Mb to obtain a double mutant (H64V, V68A) capable of transforming styrene with ethyl diazoacetate with 99.9% *de* for the *trans*-configured product and 99.9% *ee* for the (1*S*,2*S*) enantiomer, even at 200 mM substrate concentration. They reached turnover numbers (TON) of up to 46800 and could also synthesize several cyclopropane derivatives in the same manner with the same excellent stereoselectivity and TTN of up to 14500 and 30 mM scale (**Scheme 5**). The authors furthermore tried to rationalize the stereoselectivity of the reaction by modelling studies.

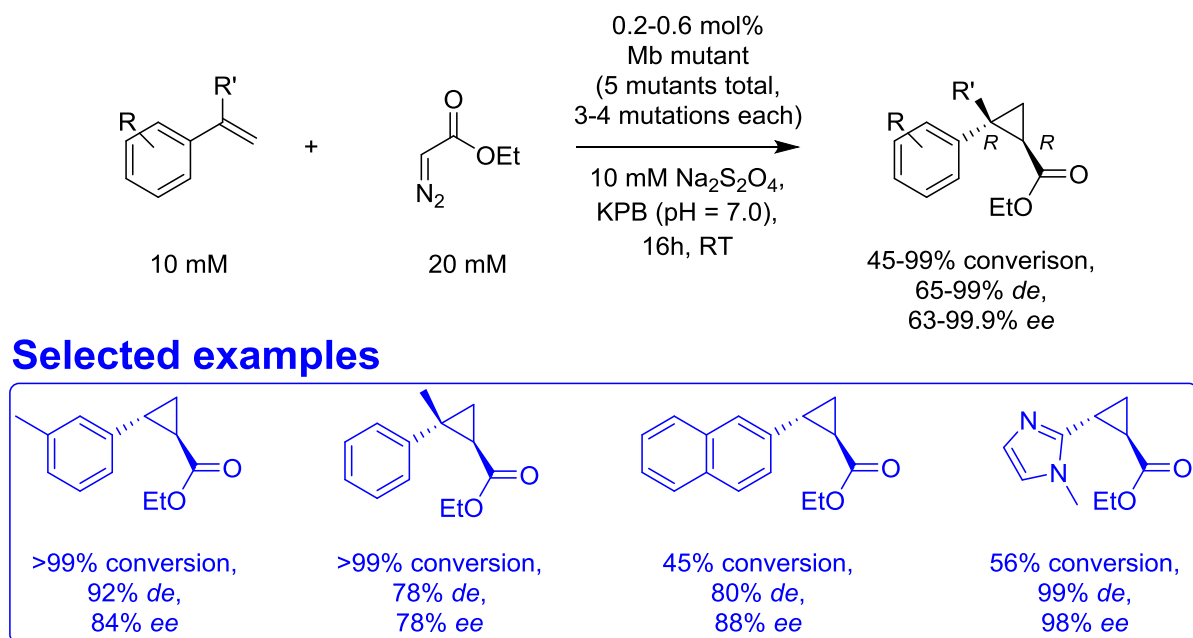


### Selected examples



**Scheme 5:** Substrate scope of the stereoselective cyclopropanation of styrene derivatives with ethyl diazoacetate.<sup>[29]</sup>

In 2016, *Fasan's* group extended this synthetic platform by saturated site-directed mutagenesis of four amino acid residues in the active site of Mb.<sup>[30]</sup> Some of the mutants (76 in total) led to a switch in enantioselectivity of the Mb in the cyclopropanation reaction, giving access to the (1*R*,2*R*)-configured cyclopropanes at 10 mM scale with 65-99% *de* and 63-99.9% *ee* (**Scheme 6**).



**Scheme 6:** Substrate scope for the saturated site-directed mutagenesis of Mb for switching the enantioselectivity of the cyclization reaction, reported by *Fasan et al.*<sup>[30]</sup>

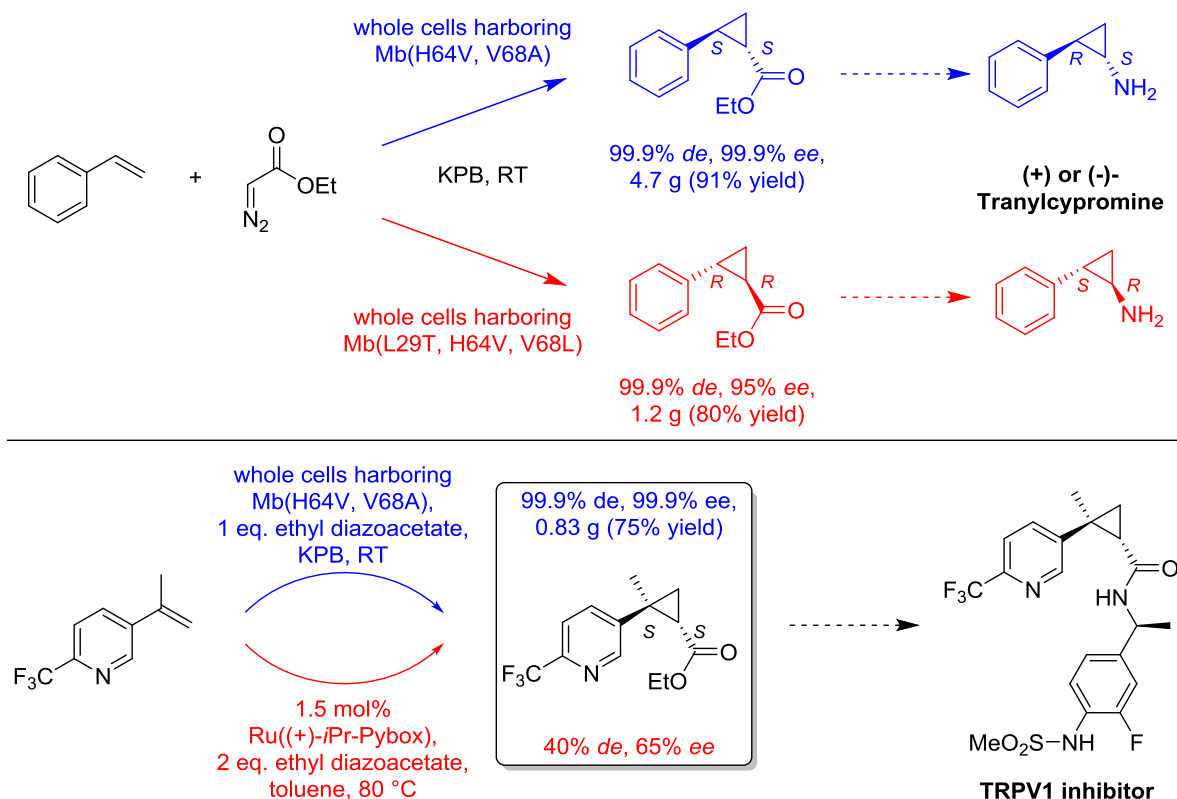
To prove the high value of this enzyme biocatalytic method, the authors furthermore conducted whole-cell biotransformations yielding precursors of four different pharmaceuticals with excellent selectivities and yields. These results exceeded literature reported protocols drastically and proved the already high value of this catalytic method, skipping transition metal catalysts and several synthetic steps (**Scheme 7**). As examples, the precursors for tranilcypropane (an antidepressant) and a TRPV1 inhibitor<sup>[32]</sup> (against chronic pain) were synthesized.

The latest advance in the biocatalytic, stereoselective cyclopropanation by *Fasan's* group is dealing with the issue of using different diazo reagents apart from ethyl diazoacetate. In 2017, they utilized 2-diazo-1,1,1-trifluoroethane (CF<sub>3</sub>CHN<sub>2</sub>) as diazo reagent and were able to obtain the corresponding cyclopropanes with excellent values of up to 99.9% *de* and 99.9% *ee* with whole-cell catalysts.<sup>[31]</sup>

Besides the crucial advances in carbon-carbon bond formation, *Arnold's* group has furthermore developed two more groundbreaking synthetic processes.<sup>[33,34]</sup>

The first breakthrough is the discovery of the carbon-silicon bond formation, catalyzed by cytochrome c.<sup>[33]</sup> Enzymes that catalyze carbon-silicon bond formation are unknown to nature and the biocatalytic formation of those bonds would broaden the chemical repertoire of biocatalysis drastically. While they discovered that also other heme containing enzymes

like CYP450 monooxygenases or myoglobin variants, cytochrome c showed aside from the general activity also excellent selectivity in the carbon-silicon bond formation (**Scheme 8**).



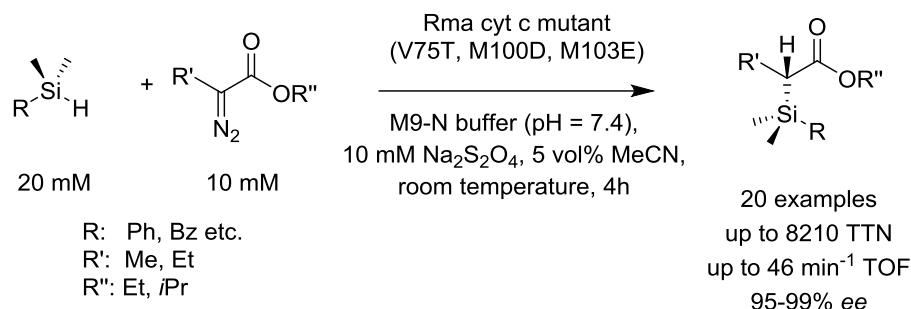
**Scheme 7:** Synthesis of important intermediates for pharmaceuticals by the biocatalytic, stereoselective cyclopropanation reported by *Fasan et al.*<sup>[30]</sup>

The mechanism of this reaction seems to be quite similar to the one they proposed in conjunction with carbon-carbon bond formation. The carbon-silicon bond formation is postulated to proceed *via* carbene insertion into the silicon-hydrogen bond. The required carbene is formed *via* N<sub>2</sub> elimination of the diazoester substrate, which is then coordinated to the iron atom in the heme group.

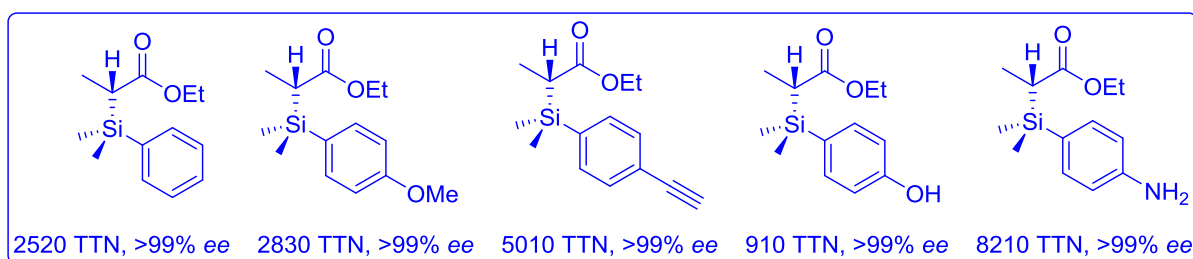
From a broad range of cytochrome c from different organisms, they selected the cytochrome c from *Rhodothermus marinus* (Rma cyt c) as a scaffold for directed evolution, since it showed the best initial enantioselectivity of all enzymes. The authors proposed that all reactions are (*R*)-selective, due to comparison with literature known retention times of the compounds in HPLC chromatograms.<sup>[33]</sup>

After saturated site-directed mutagenesis of three selected amino acid residues in the active site, they were able to transform 20 different silanes with the triple mutant of the cytochrome c with total turnover numbers (TTN) of up to 8210 and turnover frequencies (TOF) of 46 min<sup>-1</sup>. These values are up to 15 times higher than the best reported chemocatalytic methods, which rely on the usage of expensive transition metal complexes. Another advantage of this method is the high chemoselectivity of the silicon-carbon bond formation over other possible insertions like that of hydroxyl- or amino groups. The enantioselectivity of the reaction was excellent, reaching from 95-99% ee with most products being obtained with >99% ee. Lastly, preparative scale experiments were conducted on 0.1 mmol scale with an isolated yield of 70% and 98% ee utilizing *E.coli* whole cell catalysts, skipping the tedious enzyme purification steps. This discovery is a

powerful demonstration of the promiscuity that is inherent to biocatalysts. Although some possible reactions of biocatalysts do not appear in nature, scientist may alter and design an enzyme to perform these unnatural reactions.



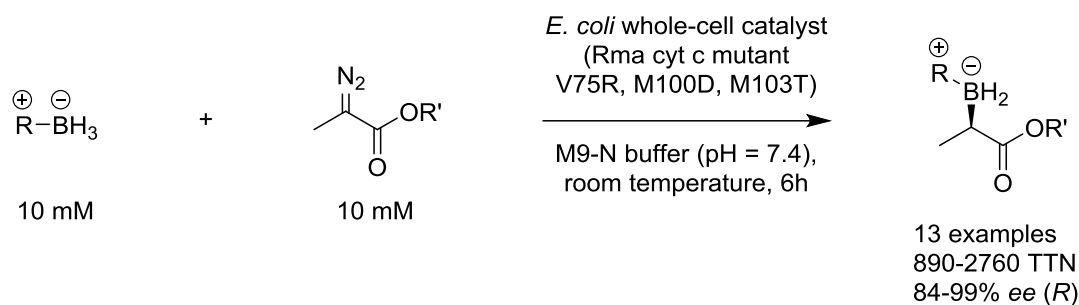
### Selected examples



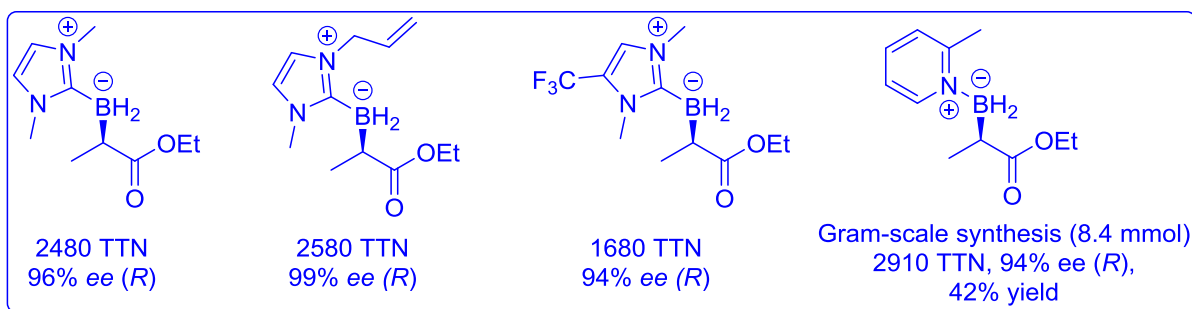
**Scheme 8:** Biocatalytic, enantioselective silicon-carbon bond formation reported by *Arnold et al.*<sup>[33]</sup>

Utilizing the same biocatalytic platform, cytochrome *c* from *Rhodotermus marinus* (Rma cyt *c*), *Arnold et al.* were able to perform the first reported organoborane synthesis just recently in 2017.<sup>[34]</sup> Strikingly, they were able to conduct all of their synthesis either with isolated enzymes or in *E. coli* whole-cell catalysts. The whole-cells proved to be more stable and hence more suitable for the organoborane synthesis, since they did not show any substrate or product inhibition in contrast to the isolated enzymes. Conducting saturated site-directed mutagenesis at three selected amino residues of Rma cyt *c*, they were able to obtain an optimized mutant that could synthesize the organoborane compounds with TTN of 890-2760 and ee-values of 84-99% for the (*R*)-configured product for 13 different examples (**Scheme 9**).

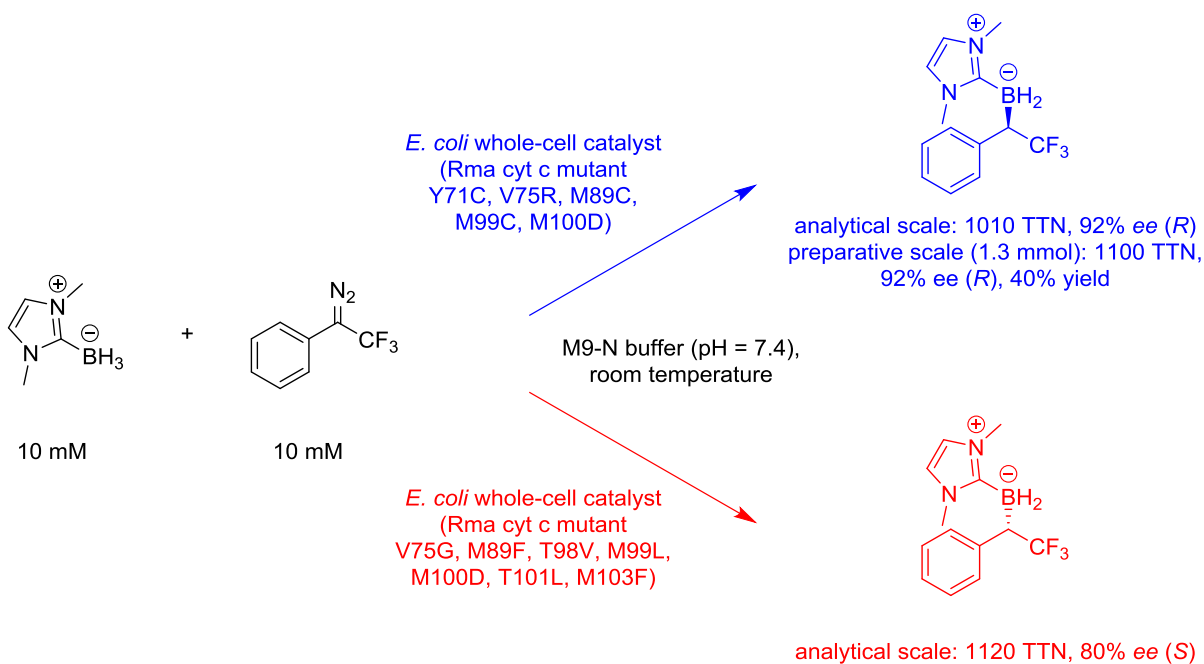
Additionally, they conducted preparative biotransformations on gram-scale to obtain one selected product with 92% ee and 42% isolated yield. Their results are drastically better than the so far reported methods for chiral organoborane synthesis, which mainly rely on transition metal catalysis and are only able to reach up to 32 TTN. Further findings in this work revolve around the continuing cell *viability* after organoborane synthesis, the possibility to switch the enantioselectivity towards the (*S*)-configured organoborane products and to be able to transform substrates bearing bulky substrates. Towards this end, they conducted further mutations and obtained the (*R*)- and (*S*)-configured products of a trifluorophenyl diazo compound with 1010 TTN and 92% ee for the (*R*)-product, while the (*S*)-product was obtained with 1120 TTN and 80% ee. In a preparative biotransformation on 1.3 mmol-scale, they obtained the (*R*)-product with 40% isolated yield with 1100 TTN and 92% ee (**Scheme 10**). In summary, they demonstrated powerfully the high potential of biocatalysis to claim enantioselective organoborane synthesis as one of the most impressive additions of the biocatalytic repertoire in recent years.



### Selected examples



**Scheme 9:** Biocatalytic, enantioselective organoborane synthesis reported by *Arnold et al.*<sup>[34]</sup>

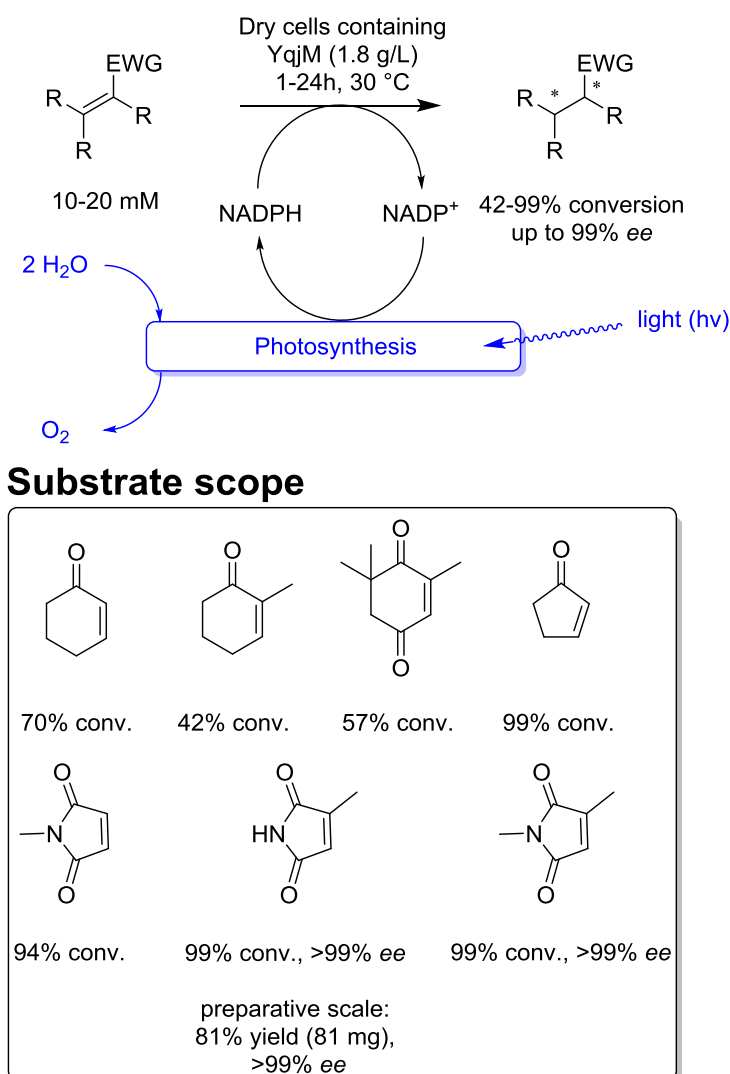


**Scheme 10:** Access to both enantiomers of organoboranes bearing bulky substituents.<sup>[34]</sup>

Apart from conquering new reactivities by biocatalysis, solving inherent problems of processes is equally important. The fundamental flaw of oxidoreductase catalysis is that one-step oxidation/reduction reactions are not redox-neutral and hence require a sacrificial substrate to regenerate the cofactor (e.g. NADH, NADPH, FADH<sub>2</sub>). While several possibilities to achieve the cofactor regeneration are sufficiently researched, including e.g. glucose oxidation *via* glucose dehydrogenase (GDH) or formate oxidation *via* formate

dehydrogenase (FDH), it does not solve the inherent problem of requiring the sacrificial substrate.

The best imaginable possibility to soothe this inherent problem is by utilizing  $O_2$  and  $H_2O$  as redox equivalents for cofactor regeneration. In 2016, *Kourist et al.* reported a biocatalytic reduction of activated Michael systems with ene-reductases that took place in cyanobacteria.<sup>[35]</sup> These cyanobacteria (*Synechocystis sp.* PCC 6803) were overexpressing the ene reductase YqjM from *Bacillus subtilis* by light induction. After successful overexpression, a set of seven different cyclic substrates were reduced towards the corresponding ketones or lactams with up to 99% ee at 10-20 mM substrate without the need for additional cofactor regeneration other than the photosynthesis of the cyanobacteria (**Scheme 11**). The authors proved the need for light by conducting control experiments in a dark environment which led to significantly reduced conversion of the substrates. The overall cell loading was quite acceptable with 1.8 g/L of dry cell weight and preparative scale synthesis of (*R*)-2-methylsuccinimide yielded the product with 80% isolated yield (81 mg) and excellent 99% ee. While this synthetic methodology is still at an early stage, further development of it is definitely recommendable given the drastic decrease in waste that could be obtained by this technology. Very recently, *Gröger et al.* could transfer this concept to reductive amination of aldehydes with microalgae.<sup>[36]</sup>



**Scheme 11:** Photocatalyzed reduction of activated C=C double bonds in cyanobacteria.<sup>[35]</sup>

## 2 DISCOVERY AND STATE OF THE ART FOR UTILIZATION OF ALDOXIME DEHYDRATASES FOR THE BIOCATALYTIC NITRILE-SYNTHESIS

### 2.1 INTRODUCTION

Parts of this chapter have already been published in alternative form as mini-review in the journal *ChemBioChem* by the author of this thesis and his co-authors.<sup>[37]</sup>

The advances in the biocatalytic synthesis of many compound classes like alcohols, amines, carboxylic acids have been quite great over the last decades (see **chapter 1**). However, the biocatalytic synthesis of nitriles had not been discovered until the late 1990s despite them being a product class that is mostly needed and produced by the chemical industry.<sup>[38,39]</sup> What makes nitriles particularly interesting is the fact that nitriles are omnipresent in all segments of the chemical industry, ranging from high-volume low-price products (bulk chemicals) to high-price compounds such as pharma drugs that are produced only in smaller volumes. Examples for this are the pharmaceuticals vildagliptin and saxagliptin.<sup>[38,39,40,41–46]</sup> Various nitriles of industrial interest jointly with their application area are shown in **Figure 3**. Acrylonitrile and adiponitrile are produced on million tons scale and are widely used in polymers or as their precursors<sup>[38,39]</sup> whereas, e.g., vildagliptin is a pharmaceutical against diabetes with sales of over one billion dollar in 2015.<sup>[47]</sup>

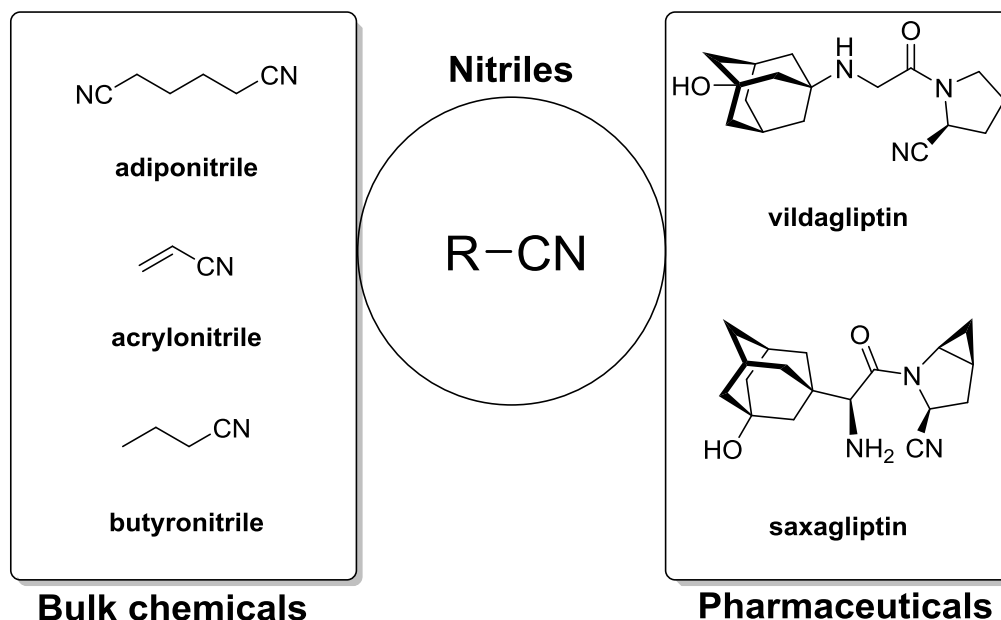


**Figure 3:** Overview over industrially relevant nitriles, either in the bulk chemical or pharmaceutical sector..

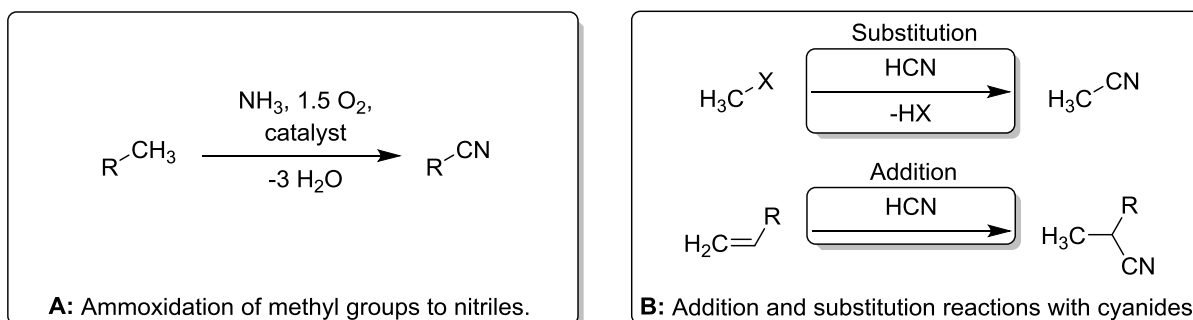
There are two main technologies for the synthesis of nitriles in the chemical industry. The first one is ammoxidation, which is a high temperature transformation in the gas phase (**Scheme 12**, A).<sup>[48]</sup> The other most used approach represents a substitution or addition reaction with hydrogen cyanide or a salt or other derivative thereof as the source for the



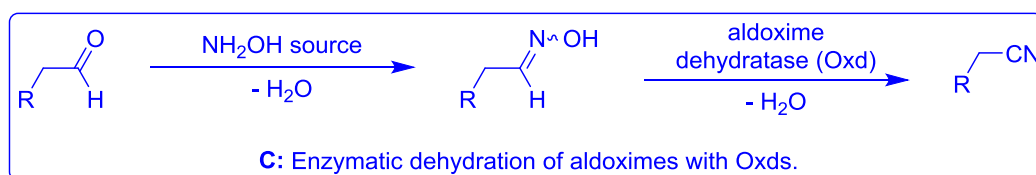
cyano functionality (**Scheme 12, B**).<sup>[5,49]</sup> This reaction is also mostly used in laboratories by organic chemists. But the major drawback and limitation of this approach is the very high toxicity of cyanide. Hence, a sustainable and inherently safe nitrile is still missing.

Most promisingly, nitriles are also formed in nature by an alternative biosynthetic pathway.<sup>[50–53]</sup> This enzymatic approach towards nitriles has been disclosed by the *Asano* group when identifying an enzyme class called aldoxime dehydratase (Oxd) in bacteria (**Scheme 12, C**).<sup>[50–53]</sup> Oxds transform an aldoxime *via* dehydration into nitriles and they co-exist with nitrile degrading enzymes, thus being catalyzing the so-called “aldoxime-nitrile pathway”.<sup>[52]</sup> Furthermore, the Aono and Asano groups jointly succeeded in obtaining the first protein structure for an Oxd enzymes, when solving this structure for the Oxd from *Rhodococcus* sp. N-771.<sup>[54]</sup> In a subsequent work, the Kobayashi group obtained a structure for the Oxd from *Pseudomonas chlororaphis* B23.<sup>[55]</sup> Such Oxd structures enabled to get a mechanistic insight into the course of this enzyme-catalyzed dehydration reaction which was found to have some similarities to CYP450 monooxygenases since Oxds are also heme containing enzymes (see **chapter 2.2**).<sup>[54,55]</sup> The *Asano* group also succeeded in disclosing and proving the biosynthetic formation of aldoximes when finding that in the Japanese apricot (*Prunus mume*) aldoxime formation occurs as a part of the amino acid metabolism, thus being synthesized by oxidation and decarboxylation of amino acids.<sup>[53]</sup> Thus, for nature (bio-)synthesis of aldoximes is rather tedious and complex, whereas chemically aldoximes can be easily prepared through a condensation reaction of an aldehyde with hydroxylamine.

### Industrial technologies for nitrile synthesis



### Newly discovered biocatalytic route



**Scheme 12:** Synthetic approaches towards nitriles based on ammoxidation, cyanide chemistry or biocatalytic dehydration.

Aldehydes are easily accessible substrates and are mainly synthesized on large scale by hydroformylation, the biggest homogeneously metal catalyzed process technology (>10 million tons).<sup>[56]</sup> The combination of the readily access towards aldehydes and the smooth biocatalytic dehydration (which runs in water) represents an attractive option to broaden the spectrum of methods for the synthesis of nitriles.

There is a broad variety of synthetic methods already available for the dehydration of oximes towards the corresponding nitriles. However, none of them is capable of converting a racemic oxime enantioselectively into the chiral nitrile.<sup>[57–65]</sup> Some selected methods for oxime dehydration include copper(II) catalysis<sup>[59,60]</sup>, which proceeds in acetonitrile smoothly and highly selectively (**Figure 4**). Further methods include iron(III) catalysis under acetonitrile-free conditions in toluene<sup>[61]</sup>, the preactivation of PPh<sub>3</sub> by oxalyl chloride and successive dehydration of the oxime<sup>[62]</sup> or the dehydration in presence of potassium phosphate (K<sub>3</sub>PO<sub>4</sub>) in xylene.<sup>[63]</sup> However, the listed methods are only an excerpt of a vast catalogue for oxime dehydration and one may find further methods more suitable for one's purposes.

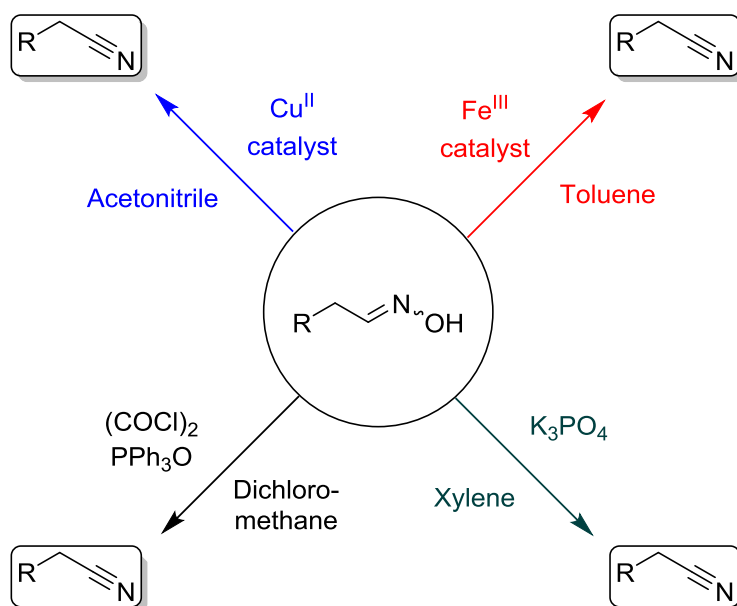
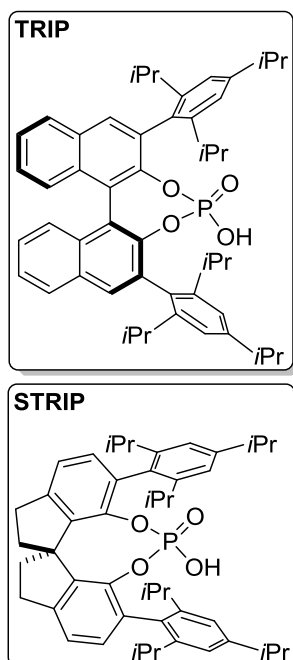
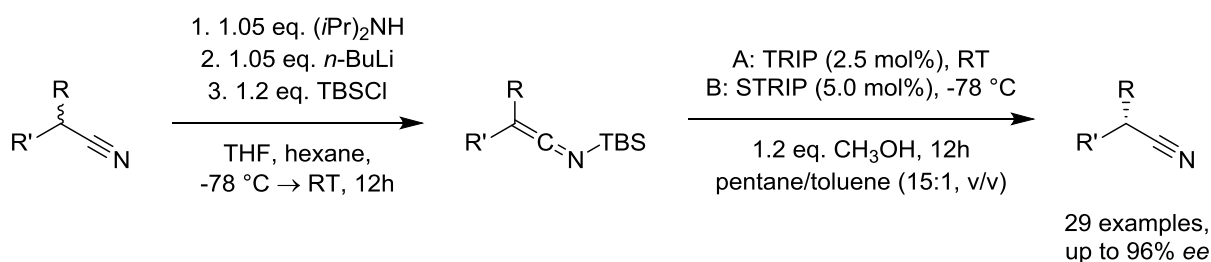


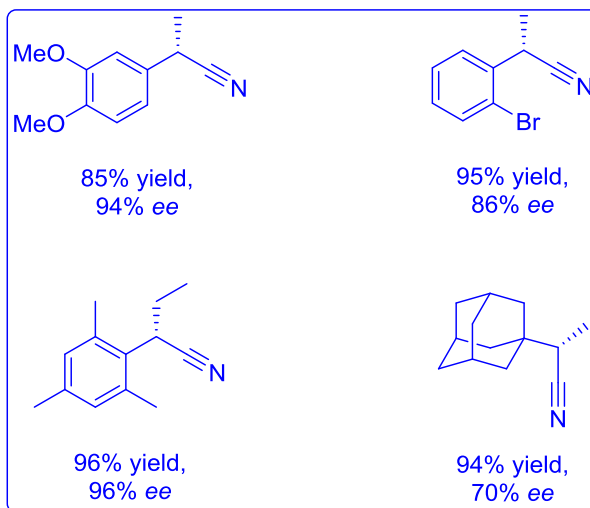
**Figure 4:** A selection of conventional approaches towards nitriles by means of aldoxime dehydration.

It should be added that there are also many possibilities to access (chiral) nitriles by synthetic methods other than dehydration of oximes. However, most of them require the usage of highly complex ligands and other auxiliaries and extreme reaction conditions, like the enantioselective *Strecker* reaction.<sup>[66]</sup> Some of the methods are presented in the following.

In 2013, *Guin et al.* developed chiral phosphoric acids to enantioselectively protonate silyl ketene imines towards their nitriles.<sup>[65]</sup> For this, they synthesized racemic, secondary nitriles by  $\alpha$ -alkylation of achiral, (aryl-)aliphatic nitriles at  $-78\text{ }^{\circ}\text{C}$ . The obtained racemic nitrile was afterwards converted into the corresponding silyl ketene imine by deprotonation with lithium diisopropylamide (LDA) in THF at  $-78\text{ }^{\circ}\text{C}$  and subsequent reaction with *tert*-butyldimethylsilyl chloride (TBSCl). The enantioselective protonation with methanol as proton source was afterwards either conducted at room temperature or  $-78\text{ }^{\circ}\text{C}$ , dependant on the utilized chiral phosphoric acid (2.5 or 5.0 mol%, **Scheme 13**). In total, 29 different silyl ketene imines were enantioselectively protonated, with most *ee*-values reaching from 80–96% *ee*. Although this method does indeed yield a broad range of chiral nitriles, the tedious synthesis of the silyl ketene imines at extreme reaction conditions under utilization of many, harmful reagents and the bad atom economy of the reaction sequence drastically diminishes the value of this method.



### Selected examples



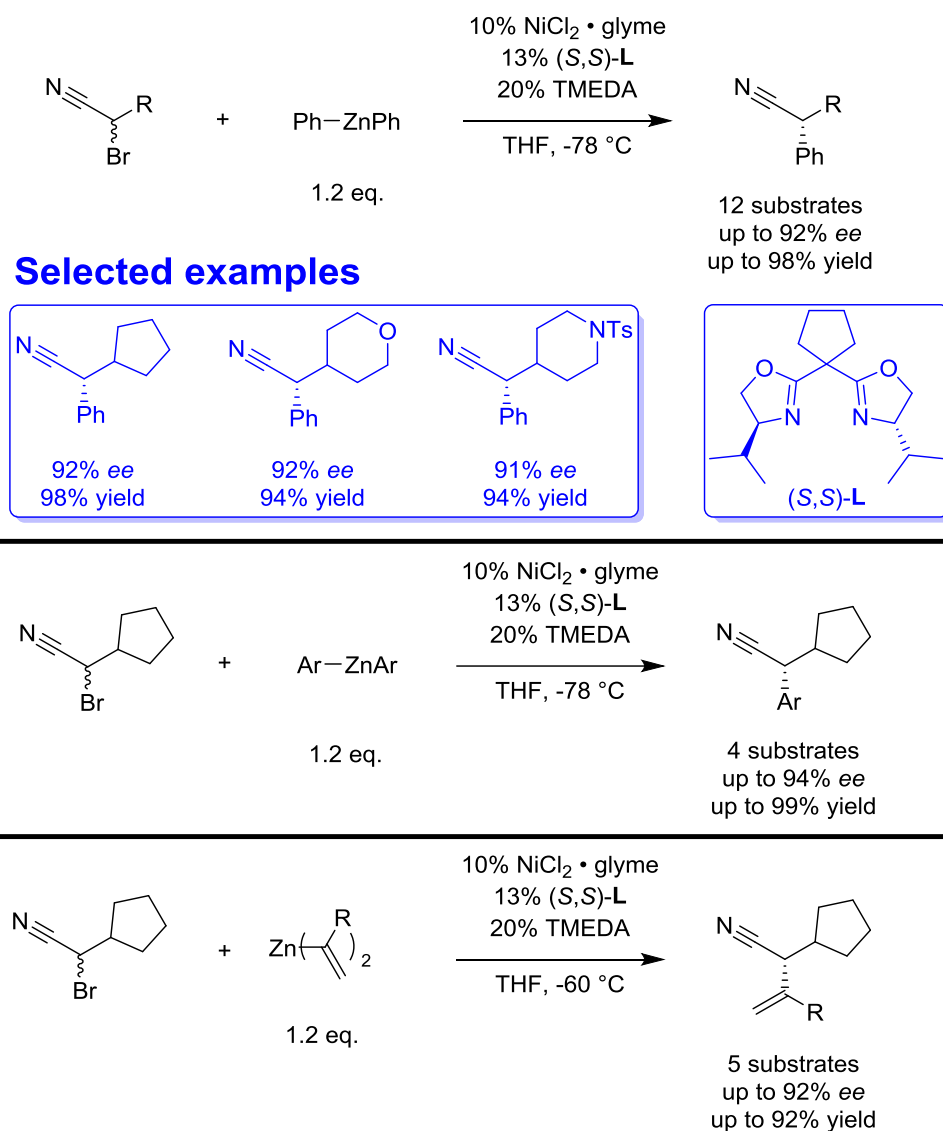
**Scheme 13:** Enantioselective protonation of silyl ketene imines, catalyzed by chiral phosphoric acids.<sup>[65]</sup>

Another possibility for the enantioselective nitrile synthesis is the stereoconvergent *Negishi* arylation and alkenylation of racemic  $\alpha$ -bromonitriles as an example for coupling chemistry, reported by *Choi et Fu* in 2012.<sup>[67]</sup> They optimized this transformation utilizing an enantiopure bidentate bis(oxazoline) as chiral ligand and could conduct the *Negishi* phenylation of racemic  $\alpha$ -bromonitriles for 12 different substrates with up to 92% ee and 98% yield. The *Negishi* arylations of the racemic  $\alpha$ -bromonitriles could be achieved for four different substrates with up to 94% ee and 99% yield. Lastly, the *Negishi* alkenylation of the racemic  $\alpha$ -bromonitriles was realized for five different substrates with up to 92% ee and 94% yield (**Scheme 14**).

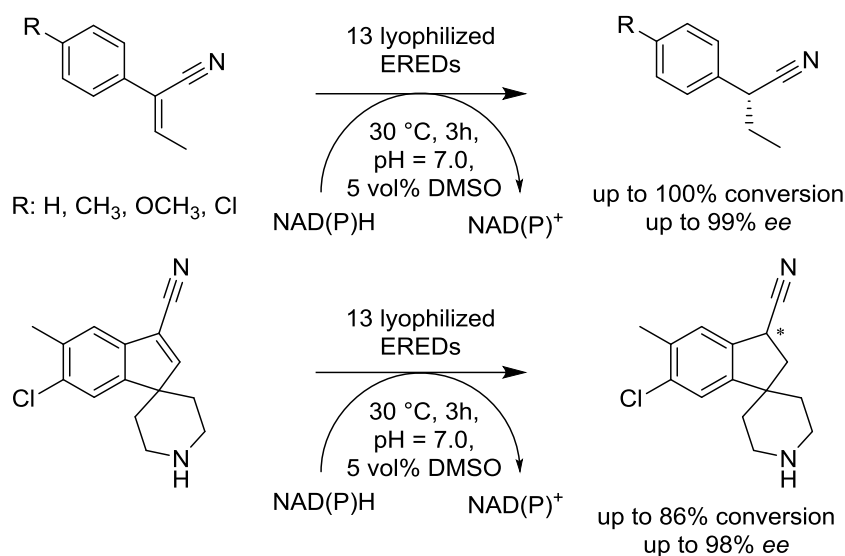
While this method shows a broad substrate spectrum and leads to overall good ee-values, the extreme reaction conditions, rather high catalyst loading and the requirement to synthesize the nitriles beforehand, including the  $\alpha$ -halogenation, make this method rather inconvenient for the enantioselective nitrile synthesis.

Regarding the biocatalytic access towards chiral nitriles, a few examples are also present in the literature. In 2008, *Kosjek et al.* utilized 13 different enoate reductases (EREDs) in isolated form to asymmetrically reduce the C-C double bond of  $\alpha,\beta$ -unsaturated nitriles. This study represents an early example for a biocatalytic approach and the results in the study were all obtained in analytical scale (0.5 mg substrate loading, 0.5 mL reaction volume). Nevertheless, all four initially investigated substrates were at least transformed by eight out of the 13 different EREDs with conversion of up to 100% and 99% ee,

underlining the high selectivity of this biocatalytic approach. Apart from this initial screening and evaluation of a substrate scope, they also reduced a pharmaceutical building block with up to 86% conversion and 98% ee, which is an outstanding result considering the fact that these were wild-type enoate reductases and the substrate is quite bulky (**Scheme 15**). However, one has to bear in mind that these results on analytical scale still have to be done on preparative scale to really quantify the scalability and robustness of this process.



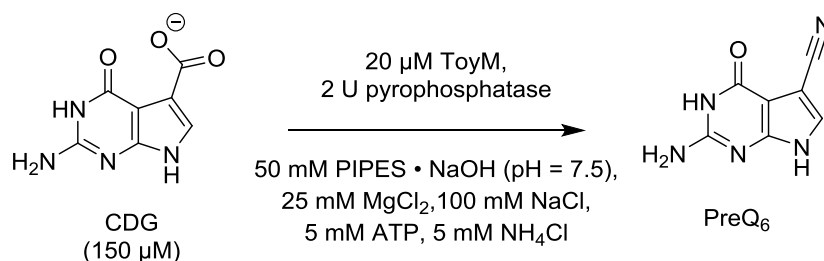
**Scheme 14:** Catalytic, asymmetric synthesis of secondary nitriles *via* stereoconvergent Negishi arylations and alkenylation, reported by *Choi et Fu*.<sup>[67]</sup>



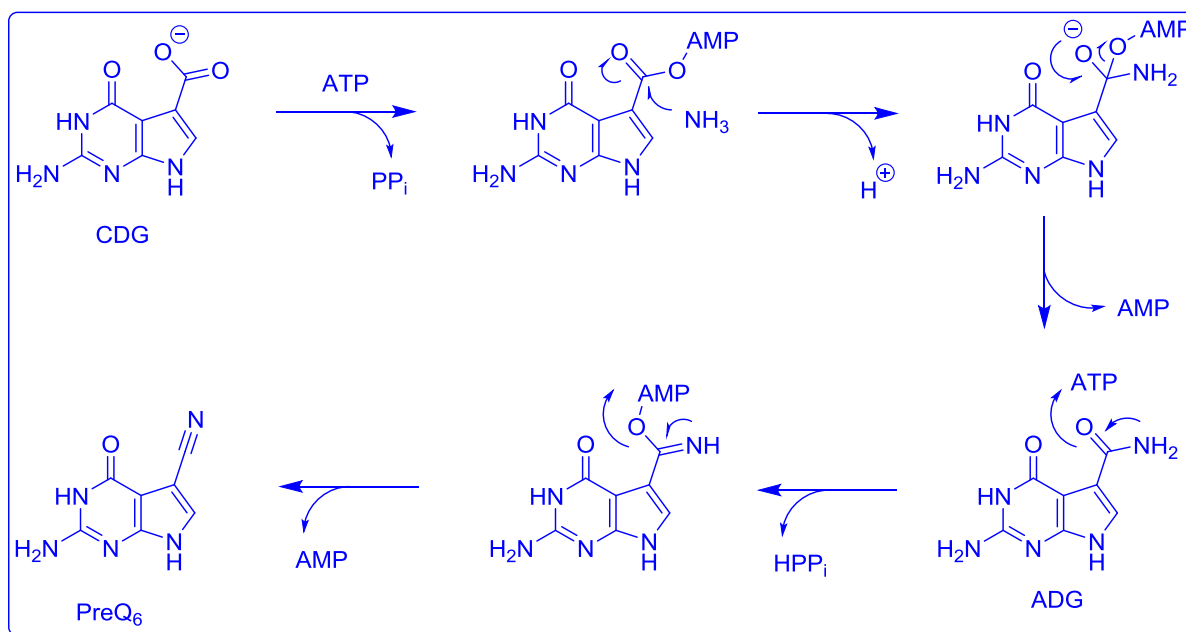
**Scheme 15:** Biocatalytic reduction of  $\alpha,\beta$ -unsaturated nitriles with EREDs.<sup>[64]</sup>

An impressive example for a direct, multistep transformation of a carboxylic acid into a nitrile has been recently reported by *Nelp et Bandarian* in 2015.<sup>[68]</sup> They utilized the ATP dependent nitrile synthetase ToyM, which is capable of transforming 7-carboxy-7-deazaguanine (CDG) into its corresponding nitrile, 7-cyano-7-deazaguanine (preQ<sub>6</sub>).

This transformation occurs according to the proposed mechanism of the authors *via* an amide intermediate (ADG), which means that ToyM is capable of activating two substrates, the carboxylic acid and its amide (**Scheme 16**). The authors propose that this promiscuity is the result of the evolution of a nitrile synthetase. While this process is quite remarkable, it is still in the proof-of-concept stage and is limited to one selected substrate and was only conducted in analytical scale (150  $\mu\text{M}$ ). While the conversion seemed quite complete after less than 30 minutes, no isolation of the product was done. Furthermore, the need for utilizing more than one equivalent of ATP as a reagent makes this process quite expensive. However, by employing metabolic engineering, this process may be transferred to fermentation processes in the future.



### Proposed mechanism



**Scheme 16:** Biocatalytic, one pot conversion of a carboxylic acid into its nitrile catalyzed by ToyM, reported by *Nelp et Bandarian*.<sup>[68]</sup>

In summary, a broad variety of methods for the enantioselective nitrile synthesis are already reported. However, they either rely on expensive metal catalysts, require harsh reaction conditions or are not yet in a state that could be efficiently utilized in bigger scale experiments. Most processes still rely on cyanation reactions<sup>[69]</sup>, which should be replaced by sustainable, cyanide-free processes in the future. This may be achieved by further developing the biocatalytic dehydration of aldoximes with aldoxime dehydratases (Oxds).

## 2.2 PROPERTIES, STRUCTURES AND MECHANISM OF ALDOXIME DEHYDRATASES

After the aldoxime dehydratase from *Bacillus* sp. OxB-1 (OxdB) was discovered by Asano's group in the late 1990s, several Oxd enzymes have been described (**Table 1**). In general, Oxds are enzymes with a molecular weight of approximately 40 kDa. Some of them exist as homodimer under native conditions and all of them contain heme b as a prosthetic group. Their optimum pH-values range from 5.5 to 8.0 and they are stable between pH values ranging from 5.5 to 9.5 in some cases. In general, all of them are highly active and stable under neutral conditions. Their temperature stability ranges from 30-45 °C and most of them have an optimal temperature of 30 °C.

**Table 1:** Properties of reported aldoxime dehydratases (Oxds).<sup>[37]</sup>

Property	OxdA <sup>[70]</sup>	OxdB <sup>a,[71,72]</sup>	OxdFG <sup>a,[73]</sup>	OxdRE <sup>a,[74,75]</sup>	OxdRG <sup>a,[76]</sup>	OxdK <sup>a,[77]</sup>
Molecular weight (Da)	76,400	42,000	34,100	80000	80000	85000
Native						
Sequence	40,129	40,972	44,070	44,794	44,817	44,511
Subunits	2	1	1	2	2	2
Soret peak (nm) ferric form	408	407	420	409	409	408
Ferrous form	428	432	431	428	428	428
Optimum pH <sup>b</sup>	5.5	7.0	5.5	8.0	8.0	7.0
Optimum temp. (°C) <sup>b</sup>	45	30	25	30	30	20
Stability pH	6.0-8.0	6.5-8.0	4.5-8.0	6.0-9.5	6.0-9.5	5.5-6.5
Stability temp. (°C) <sup>b</sup>	<40	<45	<20	<40	<40	<30

OxdA: aldoxime dehydratase 1 from *Pseudomonas chlororaphis* B23; OxdB: aldoxime dehydratase from *Bacillus* sp. OxB-1; OxdFG: aldoxime dehydratase from *Fusarium graminearum* MAFF305135; OxdRE: aldoxime dehydratase from *Rhodococcus* sp. N-771; OxdRG: aldoxime dehydratase from *Rhodococcus globerulus* A-4; OxdK: aldoxime dehydratase from *Pseudomonas* sp. K-9.

a) As His6-tagged form at the N-terminus; b) The effects of pH were measured in 0.1 M buffers at various pHs and the effect of temperature were investigated at various temperatures between 20 and 80 °C in 0.1 M KPB (pH 7.0) using (*Z*)-phenylacetaldehyde oxime ((*Z*)-PAOx) as substrate.

The heme b group contained in Oxds was first identified in 2000<sup>[71]</sup> and in the upcoming years it was shown that the iron atom in the heme b group needs to be in its ferrous ( $\text{Fe}^{\text{II}}$ ) state to effectively catalyze the dehydration of the oximes to nitriles.<sup>[70-72]</sup> The ferric state ( $\text{Fe}^{\text{III}}$ ) only showed strongly reduced or no residual activity. These studies were conducted *via* utilization of several reducing and oxidizing reagents in combination with UV/Vis-spectroscopy and EPR. Furthermore, the studies revealed that in contrast to other heme containing enzymes like CYP450 monooxygenases, the aldoxime substrates are directly bound *via* their N-atom to the iron ( $\text{Fe}^{\text{II}}$ ) atom in the heme b of aldoxime dehydratases.<sup>[72,75]</sup> However, oxidizing the iron to its ferric form lead to preferentially coordination of the substrate *via* its O-atom, leading to no dehydration activity.

The next advance in understanding the mechanism of aldoxime dehydratases was achieved by identifying crucial histidine residues that act as proximal ligand of the heme group and other histidine residues which act as a distal ligand that is crucial for catalytic activity.<sup>[54,55,78-83]</sup> This was achieved by mutagenesis of the respective histidine residues.

The mechanism of Oxds was finally disclosed by obtaining two crystal structures.<sup>[54,55]</sup> In 2009, the aldoxime dehydratase from *Rhodococcus* sp. N-771 (OxdRE) was reported, including a Michaelis complex of OxdRE with bound *n*-butyraldehyde oxime (**Figure 5, A**).<sup>[54]</sup> In 2013, the crystal structure of the aldoxime dehydratase from *Pseudomonas chlororaphis* B23 (OxdA) was reported (**Figure 5, B**).<sup>[55]</sup>

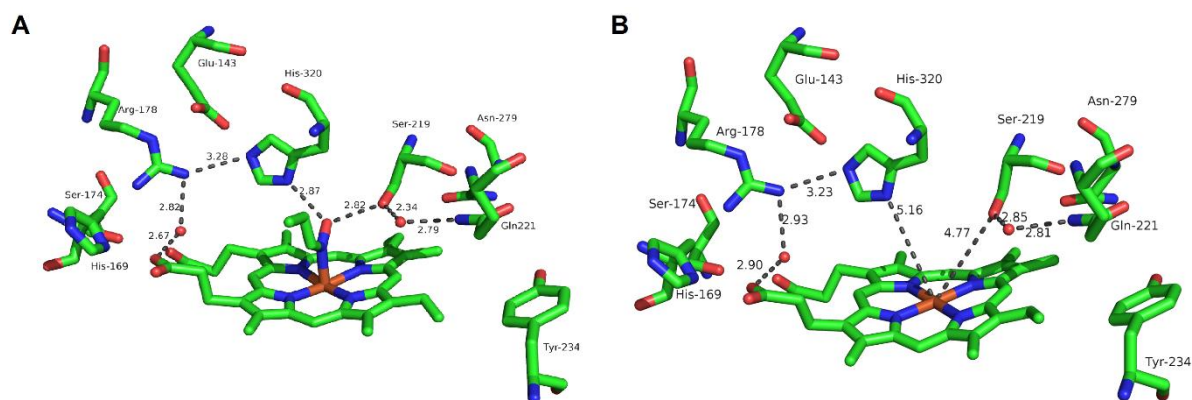


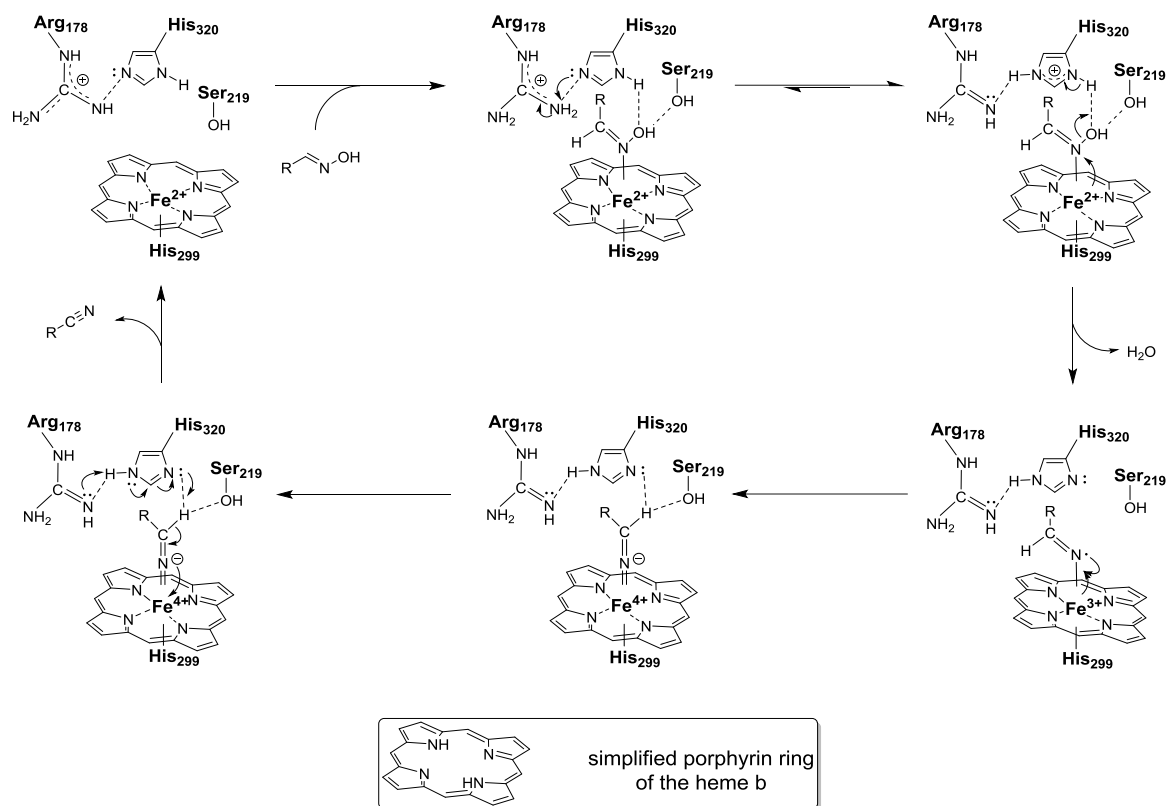
**Figure 5:** Active sites of OxdRE with bound *n*-butyraldehyde oxime (A) and substrate-free OxdA (B) obtained by X-ray crystal structures.<sup>[54,55]</sup> The catalytic triad and the heme b group are highlighted. The graphic was generated by the PyMOL software and visualized by Rommelmann.<sup>[84]</sup>

In both cases, mutagenesis studies were conducted after retrieving the crystal structures. These studies revealed that Oxds can be considered as a type of hybrid between monooxygenases and lipases, containing both a heme group and a catalytic triad. Especially the residues Arg178, His320 and Ser219 are crucial for catalytic activity and could be interpreted as a catalytic triad. This triad is highly conserved in the aldoxime dehydratases and only in OxdB the serine residue is substituted by a threonine residue. Furthermore, the Oxds possess a rather large, hydrophobic cavity in their active sides. This allows a broad range of substrates to enter it, thus being effectively dehydrated to the nitriles, as proven by the generally broad substrate scope of Oxds.

Based on earlier studies, which identified intermediates in the catalytic cycle of aldoxime dehydratases by utilization of resonance Raman spectroscopic analysis<sup>[78]</sup>, Fourier transform infrared (FTIR) spectroscopy<sup>[85]</sup> and quantum mechanics/molecular mechanics (QM/MM)



calculations<sup>[79,80]</sup> and all the above mentioned mutations to identify the crucial amino acid residues, a mechanism for OxDa (and in analogy for all other Oxds) was postulated (**Scheme 17**).



**Scheme 17:** Proposed mechanism for the catalytic dehydration of oximes to nitriles by aldoxime dehydratases.<sup>[54,55,78–80,85]</sup>

First, the aldoxime enters the active site and is coordinated *via* its N-atom to the Fe<sup>II</sup> atom of the heme b. Hydrogen bonds between the OH-group of the aldoxime and the serine and distal histidine residue increases the fixation of the substrate. Next, the histidine residue is protonated by the arginine residue, which increases the electrophilicity of the OH-group of the aldoxime. By elimination of water and double electron transfer from the Fe<sup>II</sup> to the N-atom of the aldoxime, the Fe<sup>IV</sup> intermediate is formed and the dehydrated aldoxime intermediate is now coordinating *via* its  $\alpha$ -hydrogen atom to the deprotonated histidine residue and the serine side chain. Lastly, by deprotonation of this intermediate and double electron transfer to the Fe<sup>IV</sup> species, the nitrile is released and the Fe<sup>II</sup> species is regenerated. Simultaneous re-protonation of the arginine residue closes the catalytic cycle. Interestingly, other enzyme classes like CYP450 monooxygenases and toluene dioxygenases seem to share this mechanism for the catalytic dehydration of oximes to nitriles.<sup>[81–83]</sup>

## 2.3 SUBSTRATE SCOPE OF ALDOXIME DEHYDRATASES

### 2.3.1 ARYLALIPHATIC ALDOXIMES

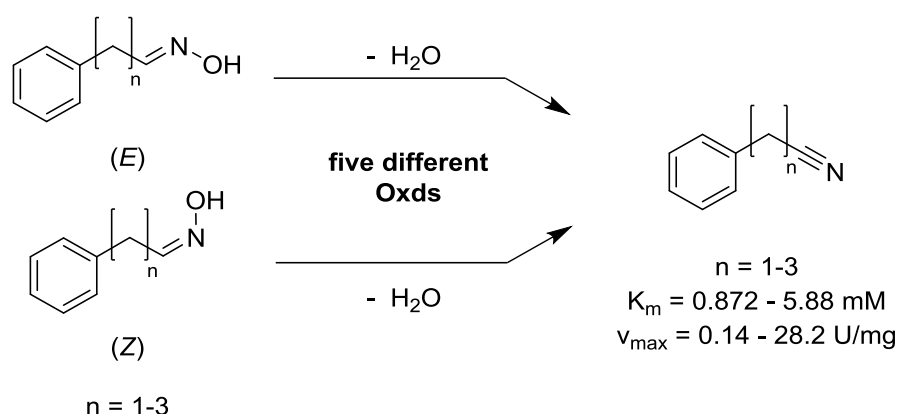
From the beginning of the discovery of this enzyme class on, arylaliphatic substrates have been one of the most investigated substrate classes for this new enzyme class. One substrate, (*Z*)-phenylacetaldoxime ((*Z*)-PAOx), is often described as the model substrate for most Oxd (**Table 2**, entries 1-5). This may stem from the circumstance that it is the metabolism product of phenylalanine in the above described aldome-nitrile pathway. A multitude of kinetic data for transformation of (*Z*)-PAOx with several Oxds has been reported by *Asano et al.*<sup>[52,53,71,73,74,76,77,86,87]</sup> Some of the most impressive results are the high specific activity of the Oxd from *Bacillus* sp. (OxdB) 19.5 U/mg in conjunction with examples in which 100% conversion and 89% isolated yield 0.5 M substrate concentration have been reported in preparative examples (**Table 2**, entry 1).<sup>[71,87]</sup> Among the other Oxds that were utilized for the transformation of (*Z*)-PAOx, the Oxd from *Fusarium graminearum* MAFF305135 (OxdFG) showed an extraordinary activity of 28.2 U/mg (**Table 2**, entry 4).<sup>[73]</sup>

Adding an additional methylene moiety to the substrate structure, one obtains the substrate 3-phenylpropanal oxime, which is quite similarly transformed by the Oxd enzymes as its homologue (*Z*)-PAOx. All Oxds except the one from *Rhodococcus* sp. YH3-3<sup>[86]</sup> accept it as a substrate, either as (*E/Z*)-mixture as in case of OxdB or as pure (*Z*)-isomer (**Table 2**, entries 6-11) with activity values ranging from 0.392 U/mg (OxdRG) up to 20.4 U/mg (OxdFG).<sup>[73]</sup> Preparative biotransformations with OxdB at 0.75 M substrate concentration led to 99.5%-100% conversion and 90% isolated yield, underlying the great synthetic potential (**Table 2**, entries 6 and 7).<sup>[71,87]</sup>

4-Phenylbutanaloxime (**Table 2**, entries 12-15) is the last homologue of the phenylalkylaldoximes that was investigated. Three Oxds, including OxdB, OxdFG and the Oxd from *Pseudomonas* sp. K-9 were capable of transforming 4-phenylbutanaloxime with activities ranging from 2.53 (Oxd from *Pseudomonas* sp. K-9) 14.1 U/mg (OxdFG) when starting from the (*E/Z*)-mixture. The  $K_m$ -values were higher than for the other substrates (e.g. 5.24 mM for OxdB), but these concentrations are still quite low and do not diminish the synthetic value in perspective of the already high concentrations of up to 0.75 M that were employed in the transformation of 3-phenylpropanal oxime.<sup>[71,87]</sup> Since Oxd enzymes can show different activity towards (*E*)- or (*Z*)-isomers of oximes, the  $K_m$  values for both isomers may differ.

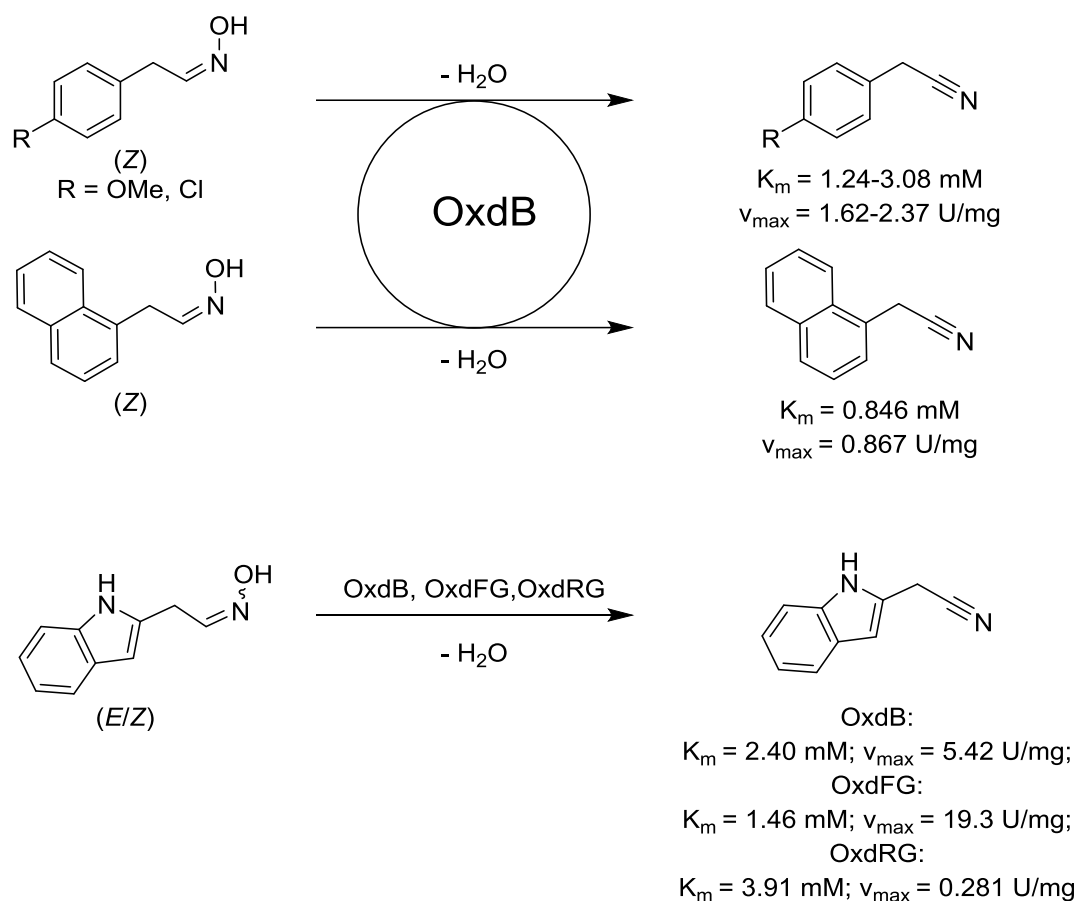
Methoxy- and chloro-substituted derivatives of phenylacetaldoxime have also been transformed by OxdB (**Scheme 18**). (*Z*)-2-(4-methoxyphenyl)acetaldehyde oxime was successfully converted with a maximum velocity of 2.37 U/mg<sup>[71]</sup> and (*Z*)-2-(4-chlorophenyl)-acetaldehyde oxime was converted by OxdB enzyme with 1.62 U/mg.<sup>[71]</sup> However, no other Oxd enzyme (OxdRG and Oxd from *Rhodococcus* sp. strain YH3-3) was capable of transforming these substrates.<sup>[76,86]</sup>

Lastly, aldoximes with a naphthyl or indolyl moiety were investigated as substrates (**Scheme 18**).<sup>[71,76]</sup> (*Z*)-naphthylacetaldoxime was transformed when using OxdB, which is the biocatalyst with broadest reported substrate scope for arylaliphatic substrates until now.<sup>[71]</sup> (*E/Z*)-indolacetaldoxime, on the other hand, was shown to be converted three Oxds, namely OxdB, OxdFG and OxdRG with up to 19.3 U/mg in case of OxdFG.<sup>[71,73,76]</sup> This broad spectrum already indicates the synthetic potential of Oxds to serve as a platform technology for the biocatalytic nitrile synthesis.

**Table 2:** Transformation of different achiral phenylalkylaldoximes with different methylene units by five different Oxds.<sup>[37]</sup>

Entry	n	Oxd	Stereoisomer	K <sub>m</sub> [mM]	V <sub>max</sub> [U/mg]	Conversion	ref.
						(Yield) [%]	
1	1	B <sup>a</sup>	Z	0.872	19.5	100 (89)	[71,87]
2	1	RG <sup>b</sup>	Z	1.40	0.14	-	[76]
3	1	RE <sup>c</sup>	Z	5.37	5.41	-	[74]
4	1	FG <sup>d</sup>	Z	3.52	28.2	-	[73]
5	1	<i>Pseudomonas</i> sp. K-9	Z	0.991	2.61	-	[77]
6	2	B <sup>a</sup>	Z	1.36	14.3	99.5 (90)	[71,87]
7	2	B <sup>a</sup>	E/Z	-	-	100	[87]
8	2	RG <sup>b</sup>	Z	2.31	0.392	-	[76]
9	2	RE <sup>c</sup>	Z	5.88	4.59	-	[74]
10	2	FG <sup>d</sup>	Z	2.76	20.4	-	[73]
11	2	<i>Pseudomonas</i> sp. K-9	Z	0.975	12.1	-	[77]
12	3	B <sup>a</sup>	E/Z	5.24	3.35	-	[71]
13	3	RG <sup>b</sup>	E/Z	n.d. <sup>e</sup>	n.d. <sup>e</sup>	-	[76]
14	3	FG <sup>d</sup>	E/Z	1.79	14.1	-	[73]
15	3	<i>Pseudomonas</i> sp. K-9	E/Z	0.882	2.53	-	[77]

a) OxdB: aldoxime dehydratase from *Bacillus* sp. OxB-1; b) OxDRG: aldoxime dehydratase from *Rhodococcus globerulus* A-4; c) Oxdre: aldoxime dehydratase from *Rhodococcus* sp. N-771; d) OxDFG: aldoxime dehydratase from *Fusarium graminearum* MAFF305135; e) n.d.: not determined.

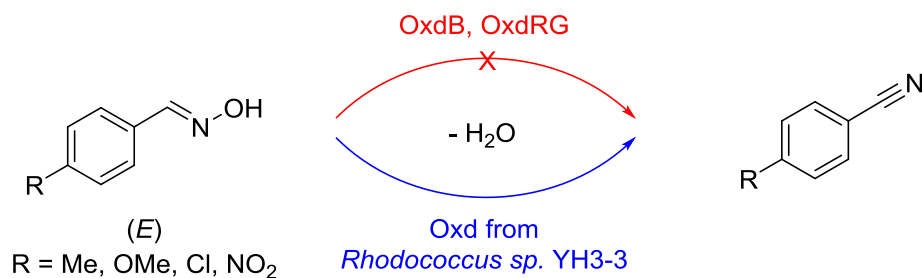


**Scheme 18:** (*E/Z*)- or (*Z*)-arylalkylaldoximes as substrates for OxdB, OxdFG and OxdRG.<sup>[71,73,76]</sup>

### 2.3.2 AROMATIC ALDOXIMES

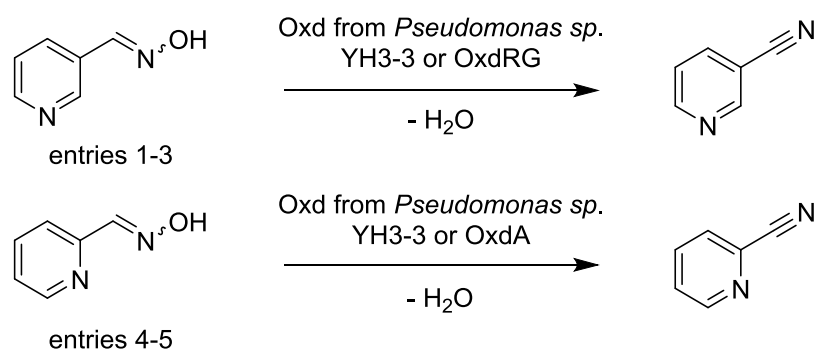
Aromatic aldoximes that bear the aldoxime moiety in the benzylic position have also been investigated as Oxd substrates in some studies so far.<sup>[71,76,86]</sup> However, only one aldoxime dehydratase, namely the Oxd from *Rhodococcus sp.* YH3-3, was capable of transforming four *para*-substituted (*E*)-benzaloximes with rather low conversions from 0.06% to 24% at best (**Table 3**). Neither OxdB and OxdRG were capable of transforming any of those substrates in other studies.<sup>[71,76]</sup> The difference in the acceptance of arylaliphatic and aromatic aldoximes is still not understood. Docking studies or QM-studies may provide answers in this regard.

Interestingly, heteroaromatic substrates with a pyridyl moiety were accepted as substrates by three different Oxds, namely OxdA, OxdRG and the Oxd from *Rhodococcus sp.* YH3-3 (**Table 4**).<sup>[70,71,74,76,86]</sup> The best accepted substrate was (*E*)-isomer of the *meta*-substituted pyridyl aldoxime with a high isolated yield of 98% when using the Oxd enzyme from *Rhodococcus sp.* strain YH3-3 (entry 1), but the (*Z*)-isomer of this substrate was also transformed by the same Oxd with 20% conversion (entry 2).<sup>[71,86]</sup> Kinetic data for the (*E*)-isomer are reported when using OxdRG with  $K_m = 20 \text{ mM}$  and  $v_{\max} = 0.065 \text{ U/mg}$  (entry 3). When the *ortho*-substituted pyridyl aldoxime was investigated as substrate (entries 4 and 5), the yield with the Oxd from *Rhodococcus sp.* strain YH3-3 was lower (30%) and only OxdA has been reported as the only other Oxd that accepts this substrate.<sup>[70,86]</sup>

**Table 3:** Substrate scope related to aromatic (*E*)-aldoximes derived from benzaldehydes and substituted derivatives thereof.<sup>[37,86]</sup>

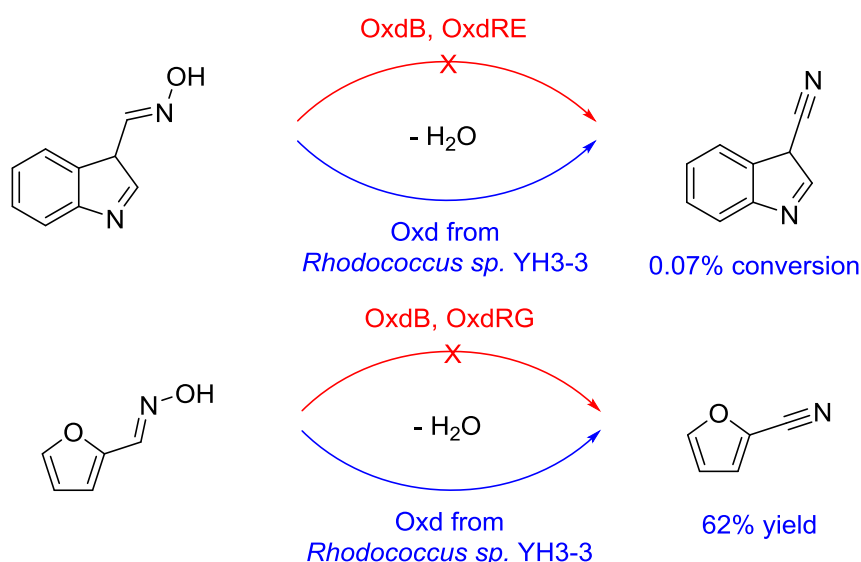
Entry	R	Oxd	K <sub>m</sub> [mM]	v <sub>max</sub> [U/mg]	Yield [%]
1	-Me	from <i>Rhodococcus</i> sp. YH3-3	n.d. <sup>a</sup>	n.d. <sup>a</sup>	(24) <sup>b</sup>
2	-OMe	from <i>Rhodococcus</i> sp. YH3-3	n.d. <sup>a</sup>	n.d. <sup>a</sup>	6
3	-Cl	from <i>Rhodococcus</i> sp. YH3-3	n.d. <sup>a</sup>	n.d. <sup>a</sup>	(7.2) <sup>b</sup>
4	-NO <sub>2</sub>	from <i>Rhodococcus</i> sp. YH3-3	n.d. <sup>a</sup>	n.d. <sup>a</sup>	(0.06) <sup>b</sup>

a) n.d.: not determined; b) Conversion according to HPLC-analysis.

**Table 4:** Substrate scope related to aldoximes derived from non-substituted heteroaromatic aldehydes with one heteroatom.<sup>[37]</sup>

Entry	Stereoisomer	Oxd	K <sub>m</sub> [mM]	v <sub>max</sub> [U/mg]	Yield [%]	ref.
1	<i>E</i>	from <i>Rhodococcus</i> sp. YH3-3	-	-	98	[86]
2	<i>Z</i>	from <i>Rhodococcus</i> sp. YH3-3	-	-	(20) <sup>d</sup>	[71]
3	<i>E</i>	RG <sup>a</sup>	20	0.065	-	[76]
4	<i>E/Z</i>	A <sup>b</sup>	3.4	(0.09) <sup>c</sup>	-	[70]
5	<i>E</i>	from <i>Rhodococcus</i> sp. YH3-3	-	-	30	[86]

a) OxdRG: aldoxime dehydratase from *Rhodococcus globerulus* A-4; b) OxdA: aldoxime dehydratase from *Pseudomonas chlororaphis* B23; c) The value given in parenthesis corresponds to the k<sub>cat</sub>-value in [min<sup>-1</sup>]; d) Conversion according to HPLC-analysis.

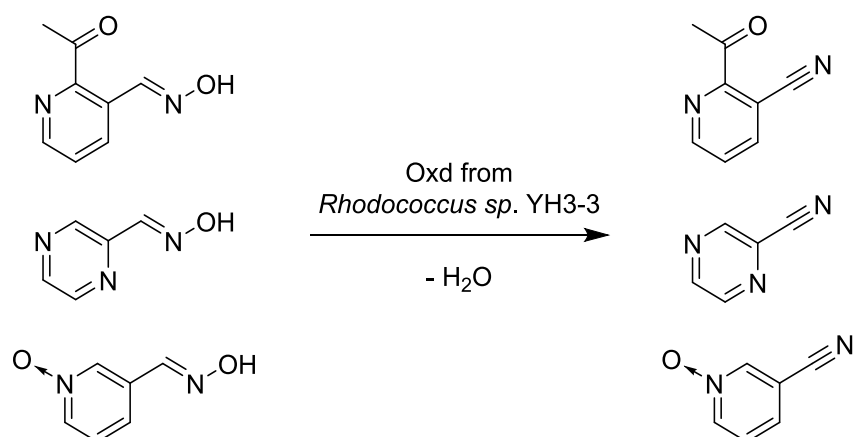


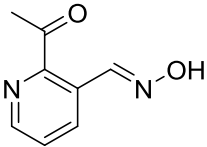
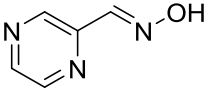
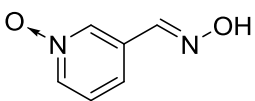
**Scheme 19:** Biotransformation of the indolyl- and furanyl substituted aldoximes by the Oxd from *Rhodococcus sp.* YH3-3 and attempted transformations with OxdB, OxdRE and OxdRG.<sup>[71,74,76,86]</sup>

Other heteroaromatic substrates like the (*E*)-isomers of an indolyl-substituted aldoxime or a furanyl substituted aldoxime were accepted only by the Oxd from *Rhodococcus sp.* YH3-3 as substrates, however the indolyl aldoxime only reached 0.07% conversion while the furanyl aldoxime was obtained with 62% yield (**Scheme 19**). Other aromatic substrates bearing a thiophene substituent were also reported to be converted with less 1%, which implies a strong dependency of the utilized heteroaromatic system to be serve as a substrate for Oxds.<sup>[86]</sup>

Further aldoxime substrates like a pyrazinealdoxime could also serve as a substrate for the Oxd from *Rhodococcus sp.* YH3-3, whose nitrile was obtained with 22% yield (**Table 5**, entry 1), while OxdB and OxdRE could not convert it.<sup>[71,74,86]</sup> Lastly, the Oxd from *Rhodococcus sp.* YH3-3 has been reported to transform an acyl substituted pyridinealdoxime with a conversion of 72% (entry 2) and an aromatic *N*-oxide aldoxime with 0.2% conversion (entry 3).<sup>[86]</sup> Putting all reported results for the transformation of aromatic aldoximes in perspective, only the Oxd from *Rhodococcus sp.* YH3-3 seems to be able to convert a multitude of substrates, especially when they bear heteroaromatic moieties.

**Table 5:** Transformation of further (*E*)-isomers of heteroaromatic aldoximes by the Oxd from *Rhodococcus sp.* YH3-3.<sup>[86]</sup>



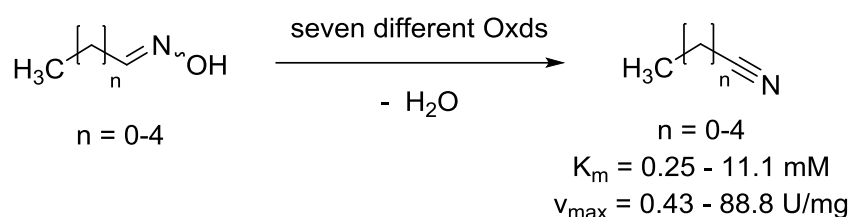
Entry	Substrate	Yield [%]
1		22
2		(73) <sup>a</sup>
3		(0.2) <sup>a</sup>

a) Conversion according to HPLC-analysis.

### 2.3.3 ALIPHATIC ALDOXIMES

Aliphatic aldoximes represent probably the most versatile substrate class that is converted by Oxds into the corresponding nitriles. Apart from several linear, non-branched aldoximes with a carbon chainlength from two up to six carbon atoms (**Table 6**), many aliphatic, linear branched aldoximes have been reported to be efficiently converted by several Oxds (**Table 7**).

Regarding the aliphatic linear chain-type aldoximes high yields were found independent of the chain length between C2 and C6 aldoximes (**Table 6**).<sup>[70,71,73,74,76,77,86,87]</sup> Even (*E/Z*)-acetoaldoxime, with a carbon chainlength of two carbon atoms, was converted into acetonitrile with 97% conversion at 100 mM substrate concentration (entry 2).<sup>[87]</sup> Its longer homologue propanonitrile (C3) was also obtained with 99.3% conversion (50 mM substrate concentration) and for *n*-butyronitrile (100 mM substrate concentration, C4) and *n*-pentanenitrile (250 mM substrate concentration, C5) quantitative conversions were observed. Lastly, *n*-capronitrile (C6) was converted with also converted quantitatively at elevated concentrations (300 mM) by OxdB (entries 3, 8, 14 and 19).<sup>[71,86,87]</sup> The kinetic data are quite diverse for this substrate class, but some data sets are quite astonishing. For example, (*E/Z*)-pentanal oxime was converted with  $v_{\max} = 88.8$  U/mg by OxDFG, which is the highest activity value reported for any substrate and Oxd (entry 15).

**Table 6:** Biotransformations and kinetic data of aliphatic linear, non-branched aldoximes.<sup>[37]</sup>

Entry	n	Stereoisomer	Oxd	K <sub>m</sub> [mM]	v <sub>max</sub> [U/mg]	Yield [%]	ref.
1	0	E/Z	A <sup>a</sup>	11	(5.6) <sup>f</sup>		[70]
2		E/Z	B <sup>b</sup>	-	-	(97) <sup>g</sup>	[87]
3	1	E/Z	B <sup>b</sup>	4.32	3.28	(99.3) <sup>g</sup>	[71,87]
4		E/Z	RG <sup>c</sup>	5.13	0.43		[76]
5		E/Z	RE <sup>d</sup>	2.17	5.78		[74]
6		E/Z	from <i>Pseudomonas</i> sp. K-9	0.778	2.90		[77]
7	2	E/Z	A <sup>a</sup>	0.25	(5.4) <sup>f</sup>		[70]
8		E/Z	B <sup>b</sup>	11.1	9.49	46 (100) <sup>g</sup>	[86,87]
9		E/Z	FG <sup>e</sup>	2.87	20.4		[73]
10		E/Z	RG <sup>c</sup>	1.73	0.689		[76]
11		E/Z	RE <sup>d</sup>	2.64	6.02		[74]
12		E/Z	from <i>Rhodococcus</i> sp. YH3-3	-	-	45	[71]
13		E/Z	from <i>Pseudomonas</i> sp. K-9	2.16	14.8		[77]
14	3	E/Z	B <sup>b</sup>	2.42	12.6	53 (100) <sup>g</sup>	[86,87]
15		E/Z	FG <sup>e</sup>	10.1	88.8		[73]
16		E/Z	RG <sup>c</sup>	1.13	1.64		[76]
17		E/Z	RE <sup>d</sup>	1.13	4.59		[74]
18		E/Z	from <i>Pseudomonas</i> sp. K-9	3.78	19.9		[77]
19	4	E/Z	B <sup>b</sup>	6.12	32.3	56 (99.5) <sup>g</sup>	[87]
20		E/Z	FG <sup>e</sup>	0.802	3.60		[73]
21		E/Z	RG <sup>c</sup>	2.94	1.66		[76]
22		E/Z	from <i>Pseudomonas</i> sp. K-9	3.12	15.3		[77]

a) OxdA: aldoxime dehydratase from *Pseudomonas chlororaphis* B23; b) OxdB: aldoxime dehydratase from *Bacillus* sp. OxB-1; c) OxdRG: aldoxime dehydratase from *Rhodococcus globerulus* A-4; d) OxdRE: aldoxime dehydratase from *Rhodococcus* sp. N-771B; e)

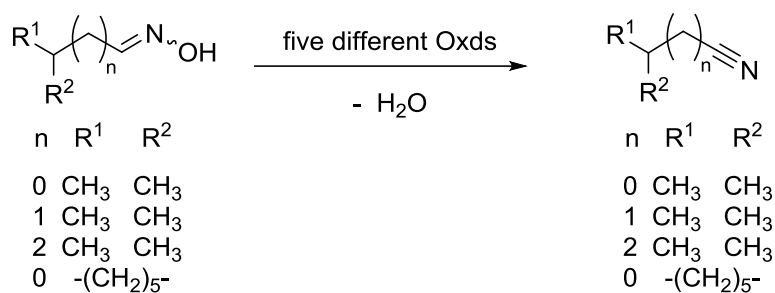


OxdFG: aldoxime dehydratase from *Fusarium graminearum* MAFF305135; f) The value given in parenthesis corresponds to the  $k_{cat}$ -value in  $[\text{min}^{-1}]$ ; g) Conversion according to gas chromatography (GC).

Aliphatic alkyl aldoximes can also have a branched aliphatic chain and still serve as substrates for several Oxds (**Table 7**)<sup>[71,73,74,76,77,86,87]</sup> For example, a high conversion of >99% (at 200 mM substrate concentration) was achieved for the dehydration of the (*E/Z*)-3-methylbutanal oxime (**Table 7**, entry 5).<sup>[86,87]</sup> Other aliphatic open-chain aldoximes, like (*E/Z*)-isobutyraldehyde oxime and (*E/Z*)-4-methylpentanal oxime, were also converted by several Oxd enzymes with quite comparable kinetic values as the non-branched homologues (entries 1-4, 10 and 11).<sup>[74,76,77,86,87]</sup> The only cyclic aliphatic aldoxime substrate, (*E/Z*)-cyclohexanecarbaldehyde oxime, was also transformed by three different Oxds (OxdRG, OxdRE and Oxd from *Pseudomonas sp.* K-9) into cyclohexyl nitrile, proving that also unsaturated carbon cycles may serve as a substrate motif (entries 11-14).<sup>[71,74,76,77]</sup>

While every reported aliphatic linear aldoxime could be transformed by at least one Oxd efficiently, it is important to note that none of the substrates had a carbon chainlength that exceeded six carbon atoms. However, substrates with a longer carbon chainlength would even more interesting since they may serve as precursors for the synthesis of fatty amines.

**Table 7:** Substrate scope related to aliphatic linear, branched (*E/Z*)-aldoximes.<sup>[37]</sup>



Entry	n	R	Stereoisomer	Oxd	$K_m$ [mM]	$v_{max}$ [U/mg]	Yield [%]	ref.
1	0	CH <sub>3</sub> /CH <sub>3</sub>	<i>E/Z</i>	B <sup>a</sup>	-	-	(35.3) <sup>f</sup> <sup>[86,87]</sup>	
2	0	CH <sub>3</sub> /CH <sub>3</sub>	<i>E/Z</i>	RG <sup>b</sup>	5.54	0.041	-	[76]
3	0	CH <sub>3</sub> /CH <sub>3</sub>	<i>E/Z</i>	RE <sup>c</sup>	1.41	8.33	-	[74]
4	0	CH <sub>3</sub> /CH <sub>3</sub>	<i>E/Z</i>	from <i>Pseudomonas sp.</i> K-9	0.538	5.87	-	[77]
5	1	CH <sub>3</sub> /CH <sub>3</sub>	<i>E/Z</i>	B <sup>a</sup>	3.58	7.72	50 (99.6) <sup>f</sup> <sup>[86,87]</sup>	
6	1	CH <sub>3</sub> /CH <sub>3</sub>	<i>E/Z</i>	FG <sup>d</sup>	2.66	23.1	-	[73]
7	1	CH <sub>3</sub> /CH <sub>3</sub>	<i>E/Z</i>	RG <sup>b</sup>	3.97	0.239	-	[76]
8	1	CH <sub>3</sub> /CH <sub>3</sub>	<i>E/Z</i>	RE <sup>c</sup>	2.43	5.71	-	[74]
9	1	CH <sub>3</sub> /CH <sub>3</sub>	<i>E/Z</i>	from <i>Pseudomonas sp.</i> K-9	1.33	35.1	-	[77]

Entry	n	R	Stereoisomer	Oxd	K <sub>m</sub> [mM]	v <sub>max</sub> [U/mg]	Yield [%]	ref.
10	2	CH <sub>3</sub> /CH <sub>3</sub>	<i>E/Z</i>	B <sup>a</sup>	2.98	10.1	-	[86]
11	2	CH <sub>3</sub> /CH <sub>3</sub>	<i>E/Z</i>	RG <sup>b</sup>	6.76	1.32	-	[76]
12	0	-(CH <sub>2</sub> ) <sub>5</sub> -	<i>E/Z</i>	RG <sup>b</sup>	1.13	0.386	-	[76]
13	0	-(CH <sub>2</sub> ) <sub>5</sub> -	<i>E/Z</i>	RE <sup>c</sup>	0.99	4.76	-	[74]
14	0	-(CH <sub>2</sub> ) <sub>5</sub> -	<i>E/Z</i>	from <i>Pseudomonas</i> sp. K-9	5.96	16.8	-	[77]

a) OxdB: aldoxime dehydratase from *Bacillus* sp. OxB-1; b) OxdRG: aldoxime dehydratase from *Rhodococcus globerulus* A-4; c) OxdRE: aldoxime dehydratase from *Rhodococcus* sp. N-771; d) OxDFG: aldoxime dehydratase from *Fusarium graminearum* MAFF305135; e) n.a.: not accepted as a substrate; f) Conversion according to gas chromatography (GC).

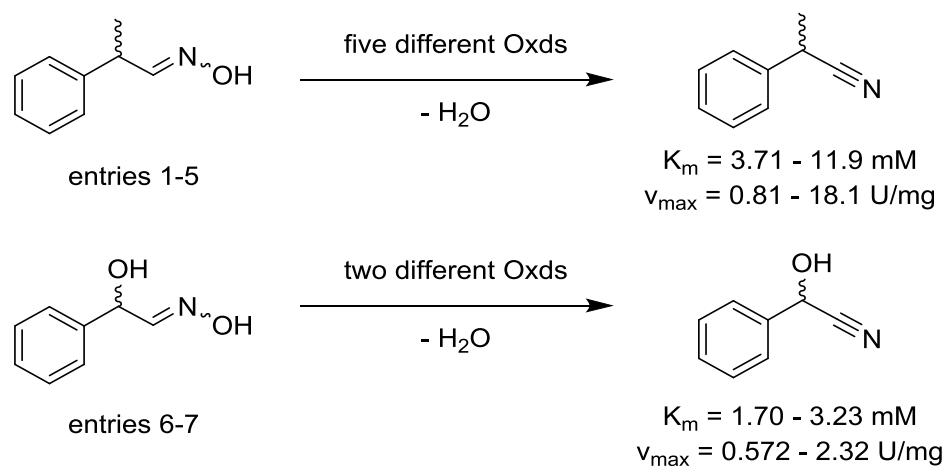
### 2.3.4 CHIRAL ALDOXIMES

Apart from the multitude of achiral aldoximes that can be converted by Oxds, may they be arylaliphatic, aromatic or aliphatic substrates, chiral aldoximes have also been reported to be suitable substrates for Oxds. Two different substrates bearing a stereogenic center, namely *rac*-(*E/Z*)-2-phenylpropionaldoxime and *rac*-(*E/Z*)-mandelaldoxime, were the first substrates that were investigated.<sup>[71,73,74,76,77,86,87]</sup> Both substrates are racemic  $\alpha$ -branched arylalkylaldoximes, but the stereochemical course of the reaction had initially not been investigated.

However, five different Oxds have been reported that accept *rac*-(*E/Z*)-2-phenylpropionaldoxime as a substrate: OxdB, OxDFG, OxdRG, OxdRE and the Oxd from *Pseudomonas* sp. K-9 (**Table 8**, entries 1-5), whereas no activity was observed for the Oxd from *Rhodococcus* sp. strain YH3-3 (entry 6).<sup>[73,74,76,77,86]</sup> The Oxd from *Rhodococcus* sp. strain YH3-3 seems to be more privileged to convert aromatic aldoximes (see **chapter 2.3.2**). Regarding the activity towards the substrates, up to v<sub>max</sub> = 18.1 U/mg with a K<sub>m</sub> = 3.71 mM was found for OxDFG, but OxdRE and the Oxd from *Pseudomonas* sp. K-9 also had impressive v<sub>max</sub> values of 6.93 and 7.93 U/mg (entries 4 and 5).

*rac*-(*E/Z*)-mandelaldoxime was the other investigated substrate (entries 6 and 7).<sup>[71,73,76]</sup> Only OxDFG and OxdRG were found to accept this substrate, while OxdB did not. Noteworthy, its kinetic data are in the same range as the ones of *rac*-(*E/Z*)-2-phenylpropionaldoxime with v<sub>max</sub> = 2.32 U/mg and K<sub>m</sub> = 1.70 mM for OxDFG and v<sub>max</sub> = 0.572 U/mg, K<sub>m</sub> = 3.23 mM for OxdRG. Unfortunately, the stereochemical reaction course for *rac*-(*E/Z*)-mandelaldoxime has so far not been investigated in the studies that followed the initial ones (see below), although this substrate is highly interesting since it contains a highly polar substituent (a hydroxy group) in the  $\alpha$ -position of the stereochemical center in contrast to all other chiral aldoximes that were investigated.

Recently, the synthesis of citronellyl nitrile (an terpene based aliphatic aldoxime with a stereocenter) and other compounds used in the fragrance industry by means of Oxds has been described in a patent application by BASF.<sup>[88]</sup> This result is quite interesting since the odors of compounds can also depend on their absolute configuration.

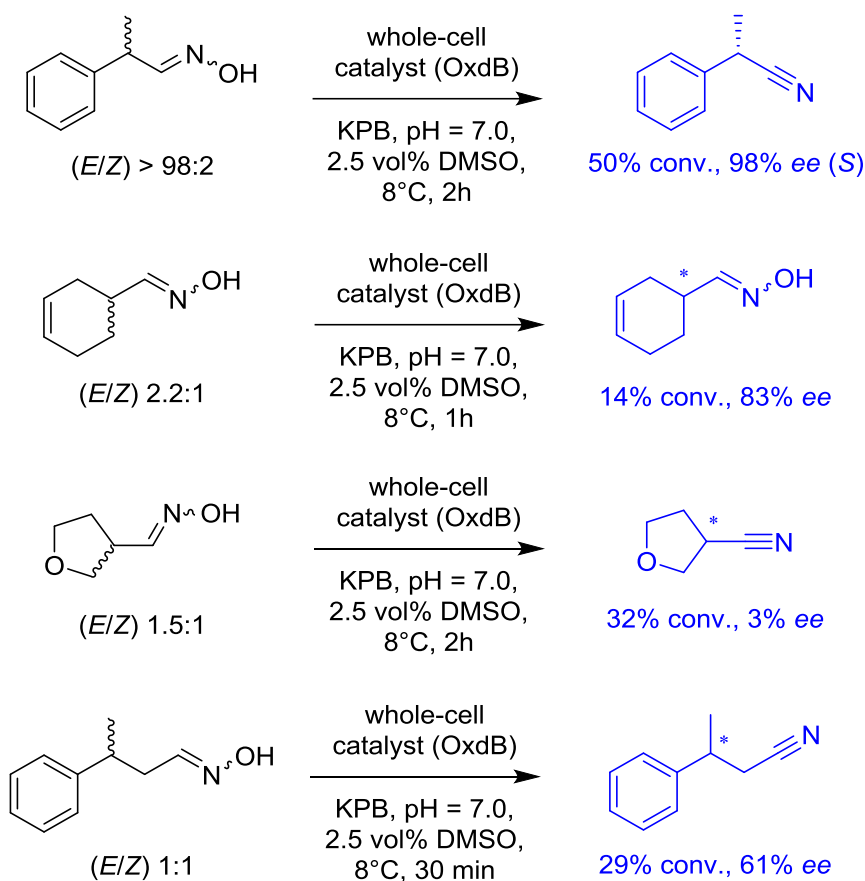
**Table 8:** Initial activity study of Oxd enzymes for branched chiral alkylaryldoximes.<sup>[37]</sup>

Entry	Oxd	Stereoisomer	$K_m$ [mM]	$v_{\max}$ [U/mg]	Conversion <sup>e</sup> [%]	ref.
1	B <sup>a</sup>	<i>E/Z</i>	-	-	37.1	[87]
2	FG <sup>b</sup>	<i>E/Z</i>	3.71	18.1	-	[73]
3	RG <sup>c</sup>	<i>E/Z</i>	11.9	0.81	-	[76]
4	RE <sup>d</sup>	<i>E/Z</i>	10	7.93	-	[74]
5	<i>Pseudomonas</i> sp. K-9	<i>E/Z</i>	4.07	6.93	-	[77]
6	FG <sup>b</sup>	<i>E/Z</i>	1.70	2.32	-	[73]
7	RG <sup>c</sup>	<i>E/Z</i>	3.23	0.572	-	[76]

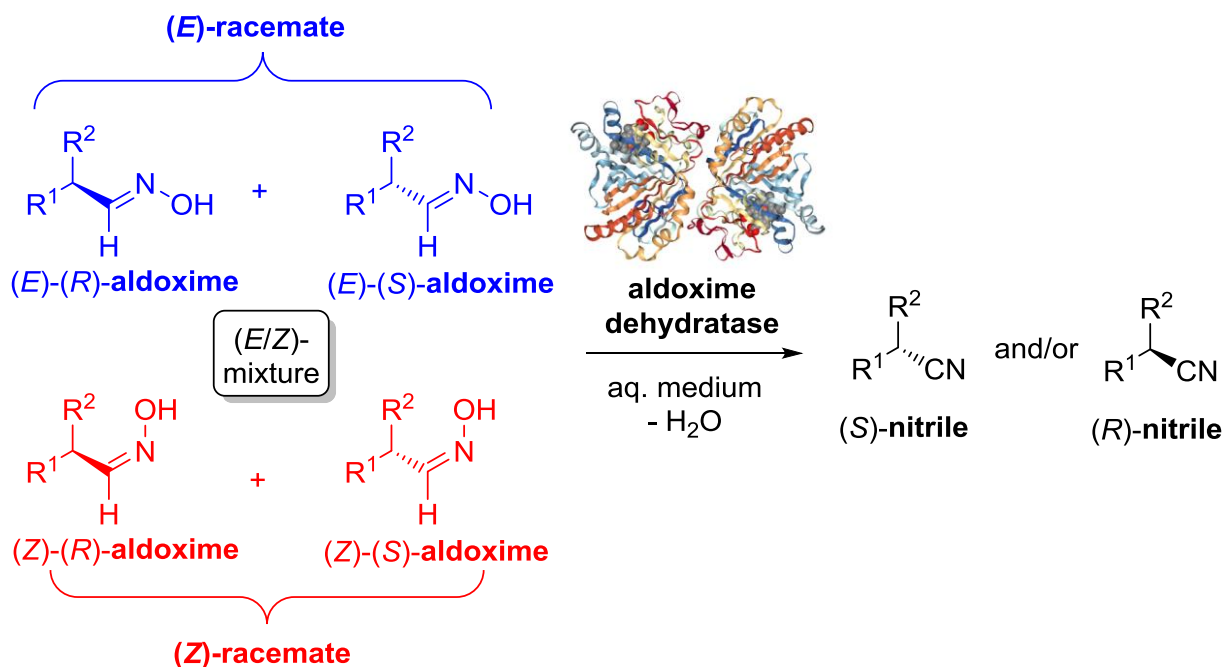
a) OxdB: aldoxime dehydratase from *Bacillus* sp. OxB-1; b) OxDFG: aldoxime dehydratase from *Fusarium graminearum* MAFF305135; c) OxDRG: aldoxime dehydratase from *Rhodococcus globerulus* A-4; d) Oxdre: aldoxime dehydratase from *Rhodococcus* sp. N-771; e) According to GC analysis.

In 2014, Metzner *et al.* conducted the first detailed study on the enantioselective nitrile synthesis utilizing OxdB (**Scheme 20**).<sup>[89,90]</sup>

Metzner discovered that the stereochemical course of the biocatalytic dehydration is heavily dependent on the reaction temperature and the ratio of the (*E/Z*)-isomers. When biotransformations at 30 °C were conducted for the substrate *rac*-(*E/Z*)-2-phenylpropionaldoxime (PPOx) with an (*E/Z*)-ratio of 4:1, a conversion of over 99% was observed. As a consequence, the formed 2-phenylpropionitrile was obtained as racemate. Once the reaction temperature was lowered to 8 °C, the conversion stopped at 60% and the nitrile was obtained with 65% ee (*S*). This conversion correlated to the complete conversion of both (*Z*)-enantiomers and one of the (*E*)-enantiomers. Since the racemic aldoxime consists of four stereoisomers due to the mixture of (*E/Z*)-isomers and (*R/S*)-enantiomers, this means that exclusively the (*E,R*)-stereoisomer is not transformed by OxdB (**Scheme 21**).



**Scheme 20:** First study on the enantioselective nitrile synthesis utilizing OxdB as whole-cell catalyst by Metzner *et al.*<sup>[89]</sup>



**Scheme 21:** Illustration of the four stereoisomers that are present in a *rac*-(*E/Z*) mixture of an aldoxime and their conversion into the corresponding nitrile enantiomers.

This hypothesis was proven when he converted the (*E*)-isomer enriched aldoxime (*E/Z* ratio 99:1) with 50% conversion towards the (*S*) nitrile with an *ee*-value of 98%. To broaden the scope of the Oxd catalyzed, enantioselective dehydration of racemic aldoximes, three further substrates were investigated, each belonging to a different substrate class. First off, *rac*-(*E/Z*)-3-cyclohexene-1-carbaldehyde oxime with an (*E/Z*) ratio of 2.2:1 was converted at 8 °C. The corresponding nitrile was obtained with 83% *ee* at 14% conversion after one hour. This substrate is quite challenging because the stereochemical information depends on the presence of a single carbon-carbon double bond in the ring. *rac*-(*E/Z*)-tetrahydrofuran-3-carbaldehyde oxime (*E/Z* 1.5:1), a heterocyclic substrate, was converted with 3% *ee* at 32% conversion. Lastly, conversion of *rac*-(*E/Z*)-3-phenylbutanal oxime (*E/Z* 1.5:1) led to 61% *ee* at 29% conversion. This substrate has its chiral center at the  $\beta$ -position to the oxime moiety in contrast to the other substrates (**Scheme 20**).

At first glance one can conclude from these results that especially substrates containing aromatic residues are privileged to yield the chiral nitrile in high enantiopurity. However, as has been seen in the study when different (*E/Z*) ratios of the aldoxime were used, the *ee*-values highly depend on the enrichment of one of the stereoisomers. Concordingly, one has also to consider if the separation of the (*E/Z*)-isomers is possible and the isomers should be investigated separately in the biotransformations. This is underlined by the fact that the biotransformation of a (*Z*)-enriched PPOx (*E/Z* ratio 1:11.5) led to the formation of the (*R*)-nitrile with 67% *ee* at 15% conversion. If the stereopreference of the Oxd differs for the (*E/Z*)-isomers, nitriles with low *ee*-values are obtained when one utilizes a substrate mixture with a low (*E/Z*)-ratio.



## 3 CYANIDE FREE, BIOCATALYTIC SYNTHESIS OF CHIRAL NITRILES

### 3.1 MOTIVATION

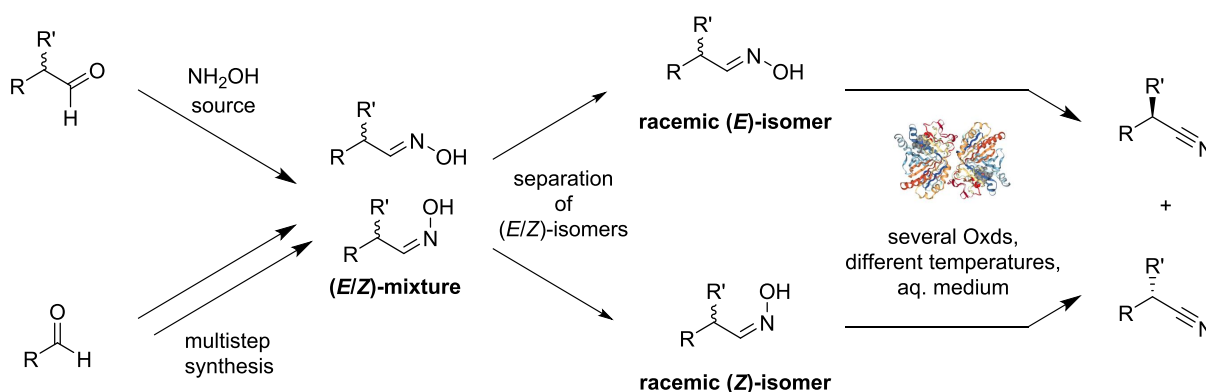
The former studies on the Oxd catalyzed synthesis of chiral nitriles suffer from a very narrow substrate scope. Furthermore, the stereochemical course of the enantioselective dehydration has only been investigated for OxdB. However, several Oxds have already been reported in the literature and their substrate scope, performance and selectivity in the enantioselective nitrile synthesis may differ greatly from OxdB.

Towards this end, commercially available racemic aldehydes and other precursors like benzaldehydes shall be converted into their racemic aldoximes. Following this conversion, an efficient method for the separation of the (*E/Z*)-isomers of the aldoximes shall be developed to enable a more detailed insight into the enantioselective nitrile synthesis in dependence of the configuration of the hydroxy group (**Scheme 22**).

The most important factor for the success of the enantioselective nitrile synthesis study is the control of the (*E/Z*) configuration during the biotransformation. This issue can be seen in the different conversions of PPOx at 30 °C and 8 °C (see **chapter 2.3.4**). The interconversion of the (*E/Z*)-isomers is thermally dependent because the inversion barrier of non-substituted aldoximes is quite low and proceeds willingly at temperatures like 30 °C.<sup>[91-96]</sup> The equilibrium ratio of the (*E/Z*)-isomers is also dependent on the sterical size of possible substituents that are close to the oxime moiety. The thermal isomerization at 30 °C of (*E/Z*)-PPOx was also proven by Metzner in his study.<sup>[89]</sup>

For the biocatalytic transformation of the (*E*)- or (*Z*)-enriched aldoximes, the literature reported Oxds are required as biocatalysts. To gain access towards them, expression methods for the Oxds in *E. coli* host cells have to be developed.

Since this substrate scope study should incorporate as many substrates as possible, the author conducted this study in close collaboration with Rommelmann<sup>[84]</sup> and Oike<sup>[84]</sup> by splitting the substrate synthesis and biotransformation of some substrates with them. Furthermore, some plasmids for Oxds were provided by Asano's group.

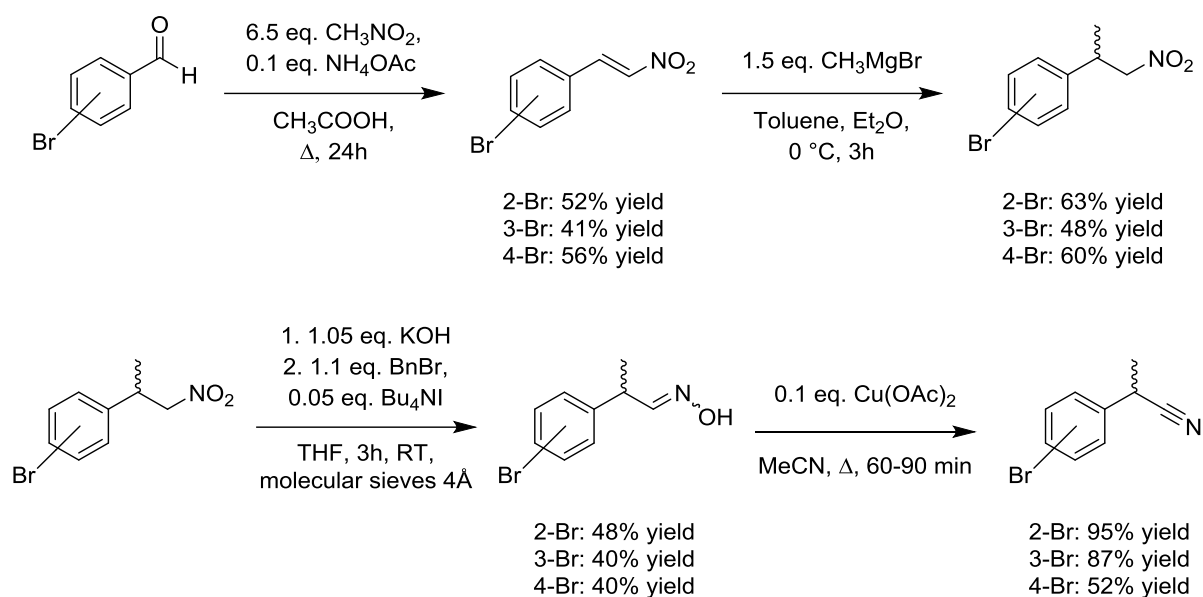


**Scheme 22:** Project plan for broadening the substrate scope of the Oxd catalyzed chiral nitrile synthesis.

### 3.2 SUBSTRATE SELECTION AND SYNTHESIS

The substrate scope of *Metzner's* preliminary study is quite narrow and he only utilized OxdB as catalyst for the enantioselective nitrile synthesis.<sup>[90]</sup> As a consequence, several new aldoxime substrates were synthesized to broaden the substrate scope, which shall be investigated with all five reported Oxds in a broad substrate scope study.

The first aspect that was deemed to be investigated was the influence of substituents on the phenyl moiety of the substrate *rac*-(*E/Z*)-2-phenylpropionaldoxime (PPOx). For this, a multi-step synthesis route was developed starting from cheap, commercially available bromobenzaldehydes (**Scheme 23**). Bromine is a highly versatile aromatic substituent, which allows for a broad range of cross-coupling reactions to be conducted.



**Scheme 23:** Multi-step synthesis route for the synthesis of bromo-substituted PPOx substrates and their nitriles as reference compounds.

In the first step, the bromobenzaldehydes were converted into their corresponding nitroalkenes in a nitroaldol condensation reaction with nitromethane. All three compounds could be isolated in multigram scale with moderate to good yields of 41-56% after recrystallization from ethanol. Next, a *Michael* addition of methylmagnesium bromide with all three nitroalkenes was successfully conducted to yield the racemic nitroalkanes with good yields of 48-63% after column chromatography purification.

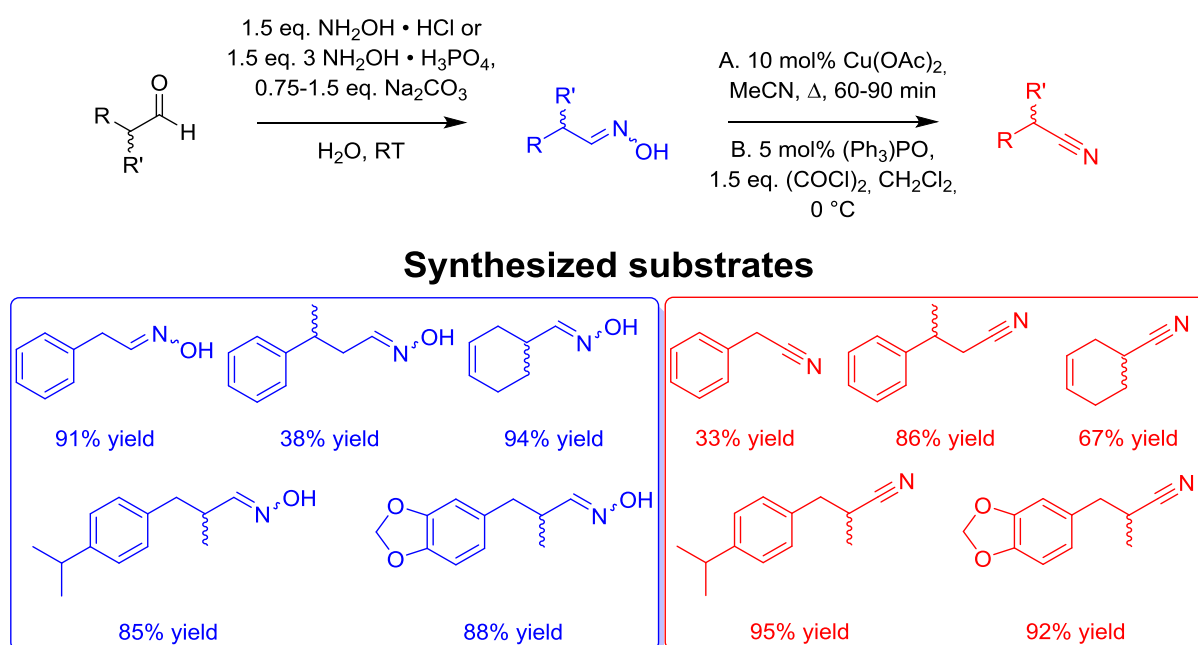
The crucial step in the substrate synthesis route was the disproportionation of the racemic nitroalkanes with benzyl bromide, which was conducted in analogy to the protocol reported by *Czekelius et Carreira* in 2005.<sup>[97]</sup> Careful conduction of the experimental procedure allowed to isolate the racemic, bromo-substituted PPOx-derivatives with isolated yields of 40-48% after column chromatography.

Lastly, a copper-catalyzed dehydration of the aldoximes in acetonitrile was conducted to obtain the corresponding nitrile as reference compound for HPLC analysis. All three nitriles could be obtained in good to excellent yields of 52-95% after column chromatography.



Hence, all three required, bromo-substituted substrates could be obtained successfully, including their corresponding nitriles for analytical purposes.

Apart from the bromo-PPOx derivatives, several other aldoximes were synthesized on gram-scale to broaden the substrate scope in terms of structure and sterical hinderance. Towards this end, previous investigated substrates like *rac*-3-cyclohexene-1-carboxaldehyde oxime as an example for a cyclic, non-aromatic substrate and *rac*-3-phenylbutyraldehyde oxime as an example for an aldoxime bearing its stereogenic center in  $\beta$ -position were synthesized from their commercially available aldehydes to investigate their conversion by the other Oxds (**Scheme 24**). Additionally, *rac*-2-methyl-3-(3,4-methylenedioxyphenyl)-propanal oxime and *rac*-2-methyl-3-(4-isopropylphenyl)propionaldehyde oxime were synthesized as examples for aldoximes with bigger substituents at their phenyl moiety. Their aldehydes are important fragrance compounds. However, nitriles are also important fragrance components due to their lower sensitivity against oxidation. Despite their general higher toxicity, several fragrance nitriles have been found to be non-genotoxic in *in vivo* and *in vitro* assays, increasing their attractiveness.<sup>[98]</sup> The last synthesized substrate was the non-chiral phenyl acetaldehyde oxime, which is the standard substrate for determining the activity of Oxds.



**Scheme 24:** Synthesized aldoxime substrates and nitrile reference compounds from commercially available aldehydes.

All aldoximes were isolated with high yields of 85-94% yields when they were synthesized with hydroxylamine hydrochloride as reagent. *rac*-3-phenylbutyraldehyde oxime, which was the only aldoxime synthesized utilizing the hydroxylamine phosphate salt, was obtained in 38% isolated yield. Regarding the reference nitriles, all nitriles were obtained with isolated yields of 33-95%, either by dehydration catalyzed by copper(II) acetate in acetonitrile as solvent or catalyzed by triphenylphosphine oxide and oxalyl chloride as activating reagent (**Scheme 24**).

Once all substrates were successfully synthesized, one crucial issue had to be considered before starting a substrate scope study for the enantioselective nitrile synthesis. As mentioned in **chapter 3.1**, aldoximes are prone to thermal isomerization of their (*E/Z*)-configuration dependent on the position of the hydroxyl group, even at ambient temperature.<sup>[91–96]</sup> However, the resulting *ee*-value of the aldoxime conversion by OxdB showed a strong dependency on the (*E/Z*)-ratio of the used substrate. As a consequence, an efficient separation of the isomers was necessary to verify the enantioselectivity of the biotransformation using Oxds against each isomer of the substrates. The most efficient methods for the separation of the isomers are column chromatography or fractional crystallization. Column chromatography was chosen as the method of choice for the separation since fractional crystallization requires tedious, time-consuming trial and error approaches for each compound.

While the chromatographic properties of the (*E/Z*)-isomers of an aldoxime are often different due to their different polarity, most (*E/Z*)-mixtures are hard to separate since the polarity differences are often rather low. Hence, manual column chromatography of larger amounts requires many hours to complete and hence is prone to time dependent isomerization while the aldoxime is dissolved in the eluent. Automatic flash column chromatography is nowadays superior to the manual method and allows due to highly sensitive UV or mass detectors a fast, real-time separation of the isomers in larger amounts in timespans of 15 minutes or less (**Figure 6**).

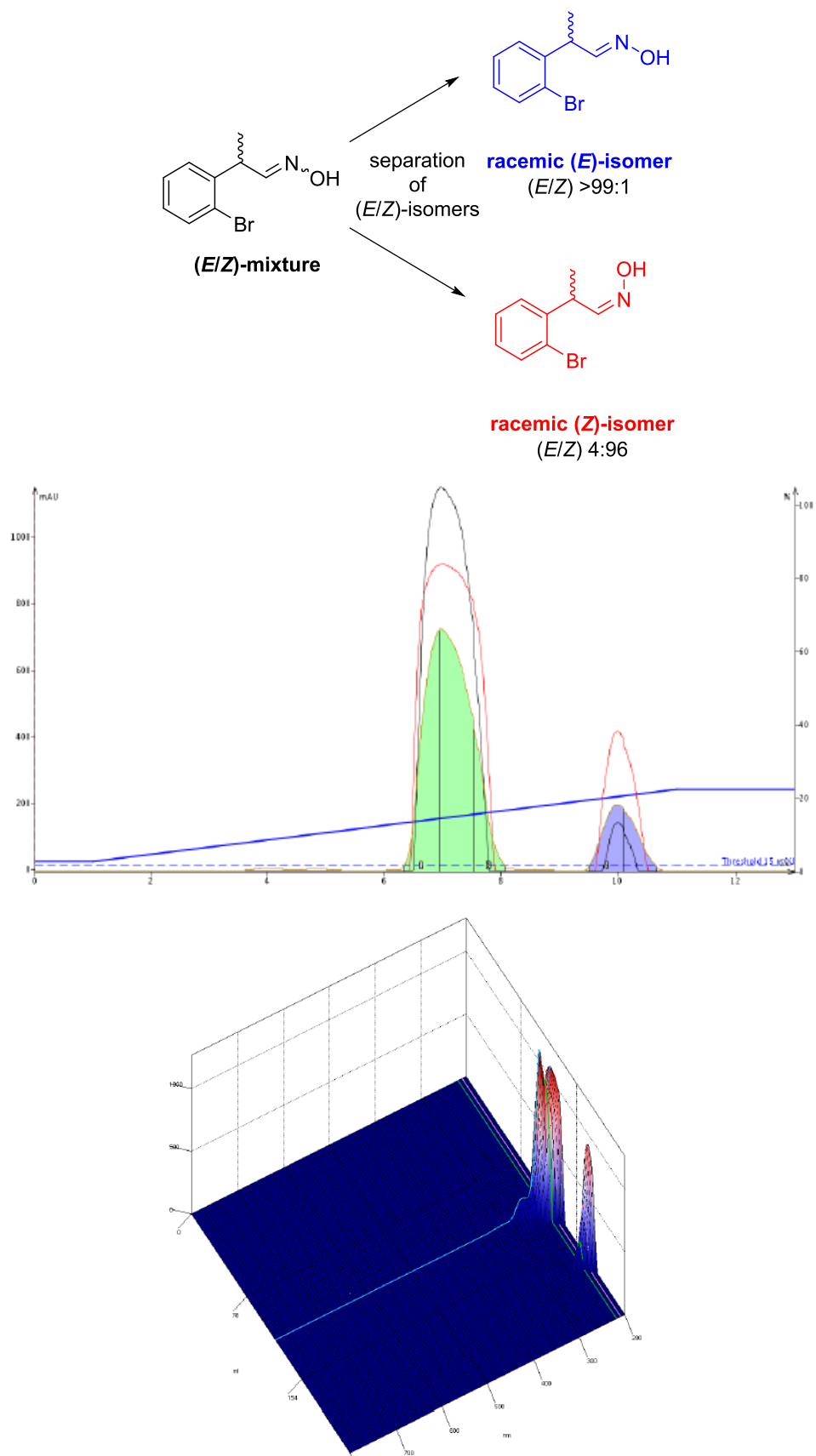


**Figure 6:** Separation of the *(E/Z)*-isomers of 2-Br-PPOx by automated flash chromatography (top). 2D (middle) and 3D (bottom) chromatogram, recorded by a Biotage Isolera One equipped with an UV detector.

The separation of the (*E/Z*)-isomers was successful for almost all substrates, yielding the isolated isomers in ratios of up to >99:1 (*E/Z*) or 5:95 (*E/Z*), respectively (**Figure 7**). Regarding the substrate *rac*-2-methyl-3-(4-isopropylphenyl)propionaldehyde oxime no separation was required because the substrate crystallized on its own as the pure (*E*)-isomer after storage at room temperature (*E/Z* 98:2). The same applies for the standard substrate phenyl acetaldehyde oxime, whose (*Z*)-isomer crystallized at room temperature. The only substrate which could not be separated efficiently into its isomers was the  $\beta$ -branched *rac*-3-phenylbutyraldehyde oxime. Even after successful separation *via* column chromatography, the isomers quickly isomerized even at 4 °C. This may result from the low inversion barrier since no substituent is present in the  $\alpha$ -position of the aldoxime. Noteworthy, many aldoximes were liquids or oils at room temperature as an (*E/Z*)-isomer mixture, while the separated isomers were often solids. This phenomenon also occurs in metal alloys or salt mixtures, which are eutectic systems.

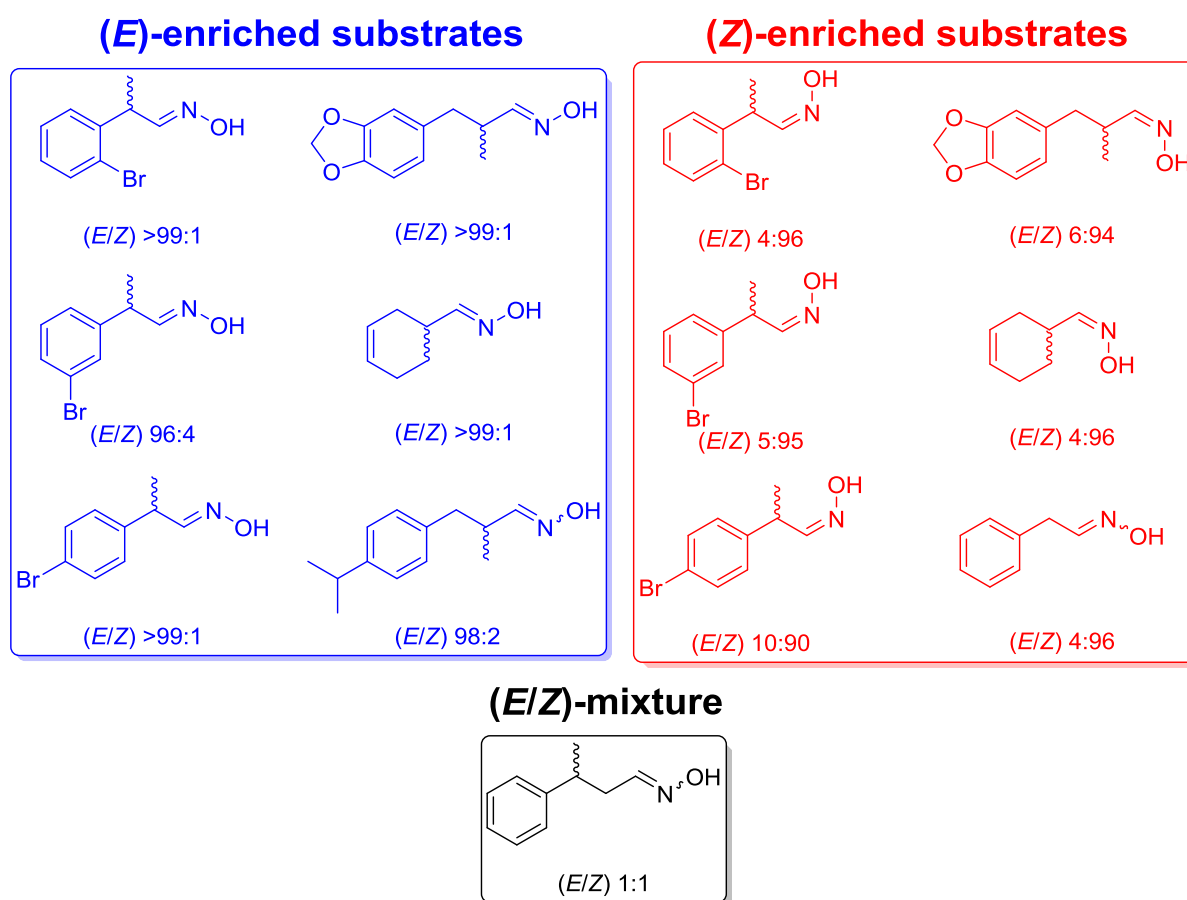
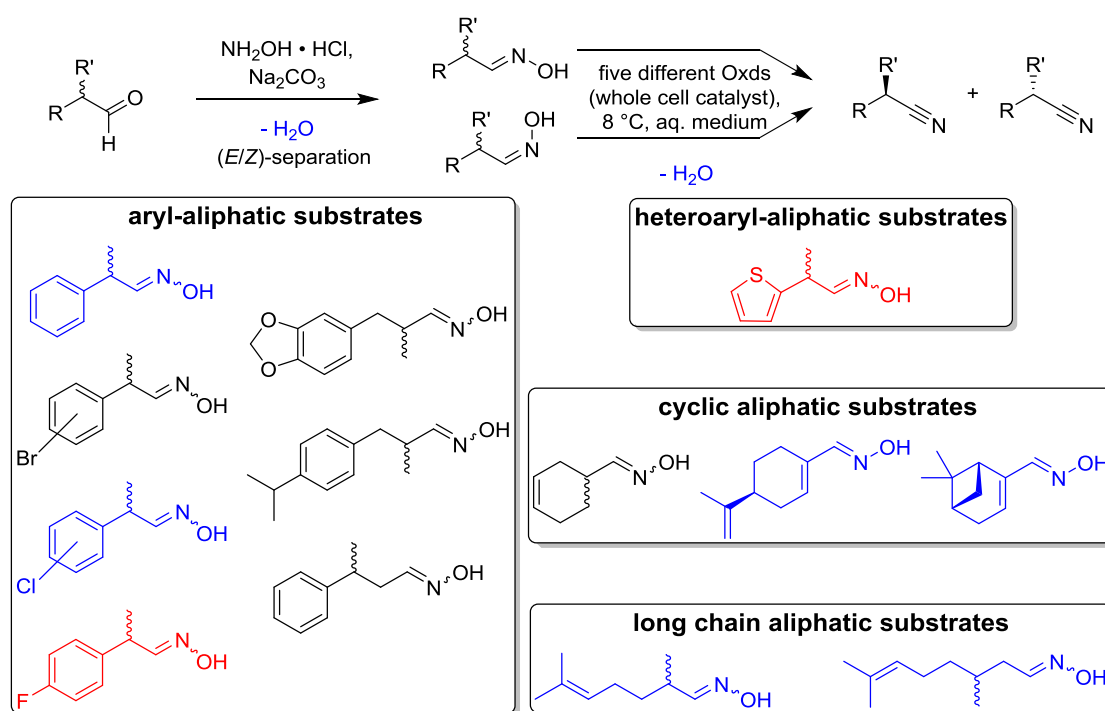


**Figure 7:** All successfully separated (*E*)- and (*Z*)-isomers that serve as substrate scope for the biocatalytic nitrile synthesis with five different Oxds.

### 3.3 SUBSTRATE SCOPE STUDY AND LEAD STRUCTURE IDENTIFICATION

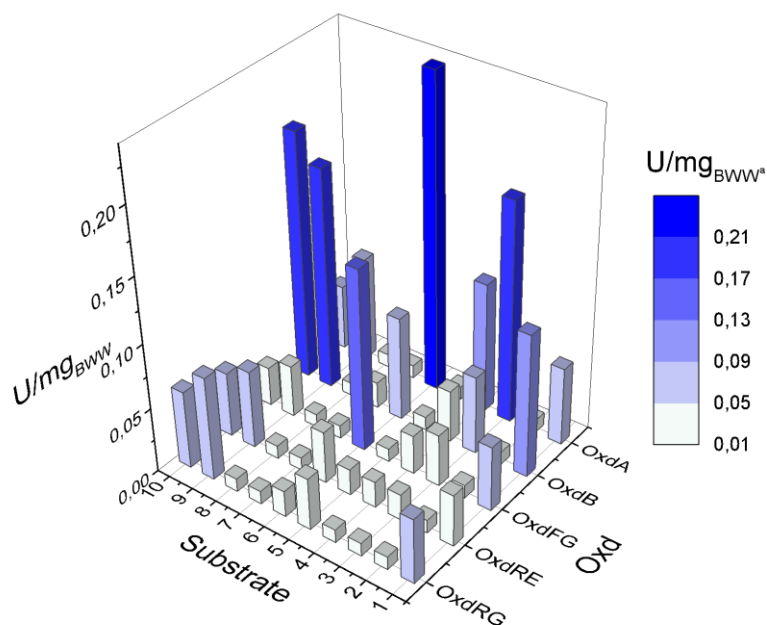
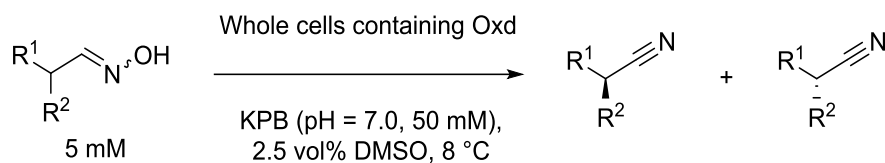
#### 3.3.1 SUBSTRATE OVERVIEW AND GENERAL ACTIVITY STUDY

After assembling a diverse range of substrates, including aryl-aliphatic, heteroaryl-aliphatic, cyclic aliphatic and long chain aliphatic ones and successfully separating their (*E/Z*)-isomers (**Scheme 25**), the five Oxds from *Pseudomonas chlororaphis* B23 (OxdA), *Bacillus sp.* OxB-1 (OxdB), *Fusarium graminearum* MAFF305135 (OxdFG), *Rhodococcus sp.* N-771 (OxdRE) and *Rhodococcus globerulus* A-4 (OxdRG, for further information on Oxds, see **chapter 2.2**) had to be heterogeneously expressed in *E. coli* host cells. After successful expression, initial conversion studies were conducted to estimate if the Oxds differ in their preferred substrate structures and overall activities.



**Scheme 25:** Overview of the substrate scope, including all investigated substrates. The substrate scope study was conducted in cooperation with Rommelmann<sup>[99]</sup> (blue substrates) and Oike<sup>[84]</sup> (red substrates).

Since the literature conditions for the optimal expression of the Oxds were inconveniently different for every single one of them, a general expression method that allowed a successful expression for all of them under the same conditions had to be evaluated. This was achieved by conducting the expression of the Oxds in terrific broth (TB) medium, which was mixed by the addition of glucose and lactose to control the expression of the Oxds by auto induction (AI). After consumption of the glucose, the expression starts by the induction of the promoter by the lactose. In contrast to induction by addition of e.g. IPTG, this allowed for a smoother expression. After a temperature screening from 15-30 °C, OxdA, OxdFG, OxdRE and OxdRG were all successfully expressed at 15 °C after 72 hours cultivation time (for details, see **chapter (8.3.2.1)**), with OxdB being the only Oxd that had to be expressed at 30 °C for optimal results.

**Table 9:** Activity values in U/mg<sub>BWW</sub> for five different Oxds in the initial substrate screening against all investigated substrates.

Entry	Substrate <sup>b</sup>	Entry	Substrate <sup>b</sup>
1 <sup>c</sup>	 E/Z 94:6	6	 E/Z 3:1
2	 E/Z 98:2	7 <sup>c</sup>	 E/Z 98:2
3	 E/Z 1:1	8 <sup>c</sup>	 E/Z 1:1
4	 E/Z 6:4	9 <sup>c</sup>	 E/Z = 1:1
5 <sup>c</sup>	 E/Z 70:30	10 <sup>c</sup>	 E/Z = 85:15

a) BWW = bio wet weight; b) (*E/Z*)-ratio was determined *via* <sup>1</sup>H-NMR spectroscopy; c) These substrates were synthesized and investigated by Rommelmann<sup>[99]</sup> and Oike<sup>[84]</sup>.

With all five Oxds in hand, an initial activity screening of all substrates (including the standard substrate PAOx) as (*E/Z*)-mixtures at 5 mM substrate concentration and 8 °C reaction temperature was conducted with all five Oxds as whole-cell catalysts (**Table 9**). Additionally, a neutral pH of 7.0 was chosen for the substrate screening since the optimal pH-value of the Oxds lies between pH = 5.5-8.0. Additionally, (*E/Z*)-isomerization may also be induced by base or acid catalysis, which is avoided at pH = 7.0. In accordance with the earlier studies of Metzner, the Oxds were utilized as whole-cell catalysts to protect the Oxds from oxidation and faster deactivation compared to the isolated enzymes.<sup>[89]</sup>

The amount of overexpression of all Oxds was quite comparable according to SDS-PAGE analysis (**chapter 9.3.2.1**). Since the enantioselective nitrile synthesis has to be conducted at 8 °C to prevent isomerization, overall activities of the whole-cell catalysts are drastically lower compared to their optimal temperatures, like 30 °C. Nevertheless, every single investigated substrate was recognized by at least one Oxd as a substrate with activity values of up to 0.26 U/mg<sub>BWW</sub>. If one considers that bio wet mass contains a lot of water, salt and other cell compartments beside the desired biocatalyst, these values are already quite remarkable. It is noteworthy nevertheless that substrates with bigger substituent residues (**Table 9**, entry 2, 7 and 8) showed the lowest activity values, not exceeding 0.01 U/mg<sub>BWW</sub>. However, these low values may also stem from their low solubility in aqueous media since only 2.5 vol% of DMSO as cosolvent may not be enough for a reasonable solubility above the  $K_m$  values of the Oxds.

### 3.3.2 INVESTIGATIONS ON THE ENANTIOSELECTIVE NITRILE SYNTHESIS ON ANALYTICAL SCALE

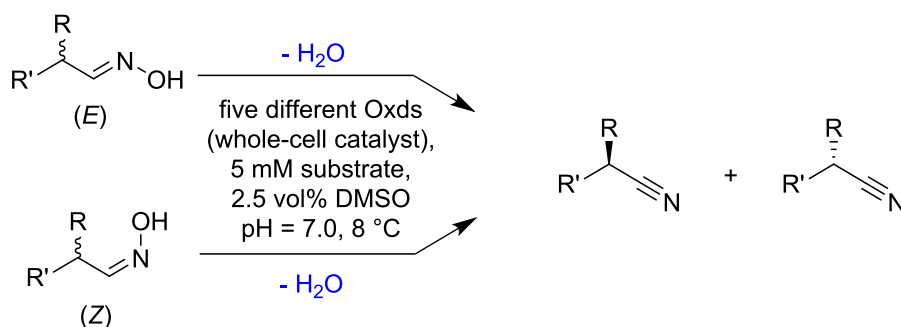
After proving that the substrate scope of the Oxds is indeed very broad, a detailed investigation on the enantioselectivity of all Oxds against the racemic (*E*)- or (*Z*)-isomers of all substrates was conducted. For this study, we utilized the same reaction conditions (5 mM substrate conc., 2.5 vol% DMSO, 8 °C, pH = 7.0) as we did for the initial activity study. The results of this study are listed in **Table 10** below.

First off, Rommelmann could prove that the previously investigated *rac*-(*E*)-2-phenylpropanal oxime is recognized by all Oxds as substrate and showed excellent enantioselectivity towards its nitrile by all of the Oxds when starting from a 94:6 enriched (*E/Z*)-mixture with 91-94% ee (*S*) at 25-26% conversion, identifying this substrate as a privileged one for the enantioselective nitrile synthesis.<sup>[84]</sup> Carrying on, Oike could demonstrate that the thiophene containing aldoxime (entry 2) is also converted with a certain degree of enantioselectivity by the Oxds, even though only a 70:30 (*E/Z*)-mixture could be utilized since the isomers could not be separated. The mediocre ee-values of 23-34% for four Oxds at 10-45% conversion may stem from a simultaneous transformation of both isomers with different enantiospecificity, as may be derived from the high ee-value of 90% at 7% conversion when utilizing OxdFG as catalyst. However, this hypothesis remains elusive until proven otherwise.

Next, the highly enriched (*E*)- and (*Z*)-isomers of the helional aldoxime (entries 3 and 4) were investigated. Surprisingly, a switch of enantiospecificity could be observed dependent on the used isomer. While OxdB converted the (*E*)-isomer (*E/Z* 99:1) with 70% ee at 40% conversion into the (*R*)-nitrile, the (*Z*)-isomer (*E/Z* 6:94) was converted with 36% ee at 71% conversion into the (*S*)-nitrile. Hence, with the usage of the same biocatalyst, one can obtain different enantiomers of the desired product just by utilization of the different

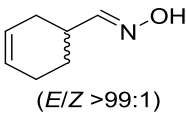
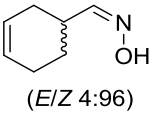
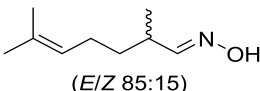
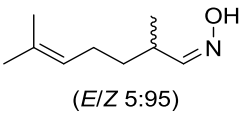
stereoisomers of the substrate without the need of developing or searching another catalyst! This switch in enantiospecificity was also observed with this substrate when using OxdA as catalyst.

**Table 10:** Study on the enantioselective dehydration of racemic (*E*)- or (*Z*)-enriched aldoximes with five different Oxds.



Entry	Substrate	Enzyme	Conv. [%] <sup>a</sup>	ee [%] <sup>b</sup>
1 <sup>c</sup>	 ( <i>E/Z</i> 94:6)	OxdA	26	91 ( <i>S</i> )
		OxdB	26	94 ( <i>S</i> )
		OxdFG	25	92 ( <i>S</i> )
		OxdRE	25	93 ( <i>S</i> )
		OxdRG	26	92 ( <i>S</i> )
2 <sup>c</sup>	 ( <i>E/Z</i> 70:30)	OxdA	18	34 (-)
		OxdB	10	23 (+)
		OxdFG	7	90 (+)
		OxdRE	28	27 (-)
		OxdRG	45	32 (-)
3	 ( <i>E/Z</i> >99:1)	OxdA	17	56 ( <i>S</i> ) <sup>d</sup>
		OxdB	40	70 ( <i>R</i> )
		OxdFG	52	83 ( <i>S</i> )
		OxdRE	20	35 ( <i>R</i> )
		OxdRG	25	27 ( <i>R</i> )
4	 ( <i>E/Z</i> 6:94)	OxdA	46	15 ( <i>R</i> )
		OxdB	71	36 ( <i>S</i> )
		OxdFG	72	8 ( <i>R</i> )
		OxdRE	21	18 ( <i>R</i> )
		OxdRG	34	15 ( <i>R</i> )



Entry	Substrate	Enzyme	Conv. [%] <sup>a</sup>	ee [%] <sup>b</sup>
5	 ( <i>E/Z</i> >99:1)	OxdA	54	4 (+)
		OxdB	29	71 (+)
		OxdFG	78	0
		OxdRE	52	13 (+)
		OxdRG	66	9 (+)
6	 ( <i>E/Z</i> 4:96)	OxdA	33	0
		OxdB	36	35 (+)
		OxdFG	30	0
		OxdRE	54	0
		OxdRG	67	0
7 <sup>c</sup>	 ( <i>E/Z</i> 85:15)	OxdA	38	43 (+)
		OxdB	11	22 (-)
		OxdFG	40	9 (+)
		OxdRE	42	22 (+)
		OxdRG	50	25 (+)
8 <sup>c</sup>	 ( <i>E/Z</i> 5:95)	OxdA	40	1 (-)
		OxdB	33	40 (-)
		OxdFG	11	19 (-)
		OxdRE	39	2 (+)
		OxdRG	30	3 (+)

[a] Absolute conversion (confirmed *via* calibration curves on RP-HPLC). [b] The symbols (+) and (-) refer to the first and second signals in chiral HPLC or GC chromatograms. [c] Investigated substrates by Rommelmann<sup>[99]</sup> and Oike<sup>[84]</sup>. [d] Absolute configuration was determined *via* comparison with literature data after a preparative scale experiment.<sup>[100]</sup>

Furthermore, the *rac*-(*E/Z*)-3-cyclohexene-1-carbaldehyde oxime (entries 5 and 6) was investigated as the next substrate. For the (*E*)-isomer (*E/Z* 99:1), only OxdB showed good enantioselectivity against this substrate with 71% ee at 29% conversion, while none of the other Oxds exceeded 13% ee at 52-66% conversion. OxdFG did not show any enantioselectivity at all. For the (*Z*)-isomer (*E/Z* 4:96, entry 6), this tendency was even more drastically. Only OxdB showed any enantioselectivity with 36% ee at 35% conversion, while the other Oxds always yielded racemic nitriles at 30-67% conversion. Noteworthy, the enantioselectivity was the same for both (*E*)- and (*Z*)-isomer.

Lastly, Rommelmann<sup>[99]</sup> could successfully separate the (*E/Z*)-isomers of melonal oxime (entries 7 and 8) and transform them with all five Oxds. The obtained ee-values for both isomers did not exceed 43% at 38% conversion for the (*E*)-isomer and 40% ee at 33% conversion for the (*Z*)-isomer.

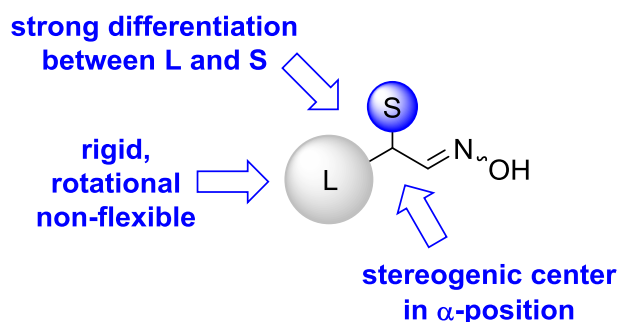
### 3.3.3 LEAD STRUCTURE HYPOTHESIS AND CONFIRMATION FOR THE ENANTIOSELECTIVE NITRILE SYNTHESIS

Taking into account the obtained *ee*-values of all products emerged from the different substrate stereoisomers (*E/Z*), a clear tendency for a privileged substrate structure could be identified that leads to high *ee*-values of over 90% even at elevated conversion rates of 25% or higher: *rac*-(*E*)-2-phenylpropanal oxime (**Table 10**, entry 1) represents this privileged substrate.

Key features of this proposed privileged substrate structure include the following elements (**Figure 8**):

1. There is a strong sterical differentiation between the substituents at the stereogenic center, like a methyl- and a phenyl-substituent.
2. The large substituent should be rather rigid and rotational non-flexible, as it is the case for the planar phenyl-substituent. By saturation of the benzene ring, its flexibility increases and potential n-n interactions get disrupted.
3. The stereogenic center should be positioned in the  $\alpha$ -position of the oxime moiety.

#### "privileged substrate structure" & key features



#### proven example:

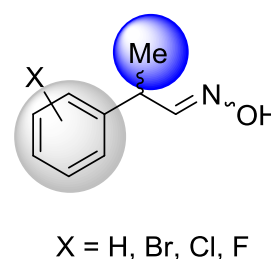


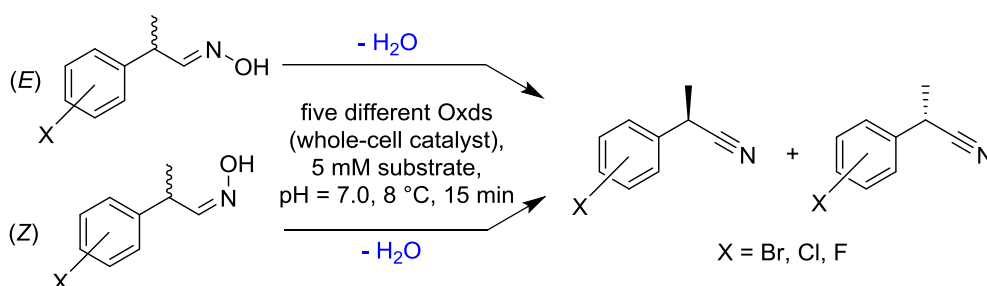
**Figure 8:** Identified lead structure for obtaining high enantioselectivities with all Oxd enzymes. L = large substituent, S = small substituent

These features are supported by the observation that the cyclic, aliphatic substrate *rac*-(*E/Z*)-3-cyclohexene-1-carbaldehyde oxime (entries 5 and 6) and the *rac*-(*E/Z*)-melonal oxime (entries 7 and 8) show generally quite low *ee*-values when transformed by all five Oxds. Although their stereogenic center is in the  $\alpha$ -position of the oxime moiety, their other aliphatic, flexible substituent lowers the enantioselectivity. The same accounts for the *rac*-(*E/Z*)-helional aldoxime (entries 3 and 4), whose phenyl-substituent is connected *via* a methylene bridge to the stereogenic center, increasing the flexibility and rotational freedom.

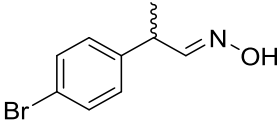
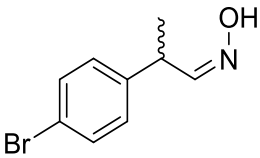
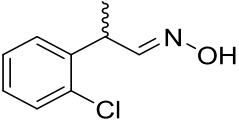
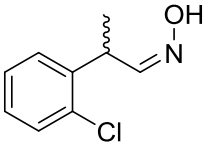
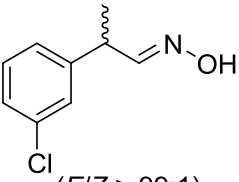
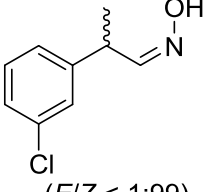
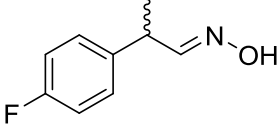
To confirm this hypothesis and to investigate the influence of substituents at the phenyl moiety of *rac*-(*E*)-2-phenylpropanal oxime derivatives, the Br-derivatives with the bromine atom in the *o*-, *m*- and *p*-position were synthesized according to **Scheme 23**. After successful separation of the (*E*)- and (*Z*)-isomers, all of the six substrates (**Table 11**,

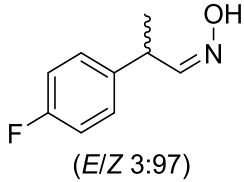
entry 1-6) were converted with the five different Oxds at the same conditions as the previous substrates (8 °C, pH = 7.0). Apart from the Br-derivatives, *Rommelmann*<sup>[99]</sup> and *Oike*<sup>[84]</sup> prepared the corresponding Cl- and F-derivatives and investigated their transformation in analogy (**Table 11**, entry 7-12). The Br- and Cl-derivatives would allow to access cross-coupling chemistry to broaden the accessible nitrile structures.<sup>[84]</sup>

**Table 11:** Enantioselective dehydration of (*E*)- and (*Z*)-isomer enriched, halogenated aldoximes.



Entry	Substrate	Enzyme	Conv. [%] <sup>a</sup>	ee [%] <sup>b</sup>
1	 (E/Z > 99:1)	OxdA	39	88 (S) <sup>d</sup>
		OxdB	7	9 (S)
		OxdFG	9	85 (S)
		OxdRE	21	91 (S)
		OxdRG	23	91 (S)
2	 (E/Z 4:96)	OxdA	-	-
		OxdB	-	-
		OxdFG	-	-
		OxdRE	-	-
		OxdRG	-	-
3	 (E/Z 96:4)	OxdA	-	-
		OxdB	-	-
		OxdFG	37	87 (S)
		OxdRE	-	-
		OxdRG	-	-
4	 (E/Z 5:95)	OxdA	38	94 (R) <sup>d</sup>
		OxdB	41	89 (R)
		OxdFG	51	88 (R)
		OxdRE	33	94 (R)
		OxdRG	46	90 (R)

Entry	Substrate	Enzyme	Conv. [%] <sup>a</sup>	ee [%] <sup>b</sup>
5	 ( <i>E/Z</i> > 99:1)	OxdA	-	-
		OxdB	15	99 (+)
		OxdFG	33	96 (+)
		OxdRE	-	-
		OxdRG	-	-
6	 ( <i>E/Z</i> 10:90)	OxdA	-	-
		OxdB	27	83 (-)
		OxdFG	46	84 (-)
		OxdRE	-	-
		OxdRG	-	-
7 <sup>c</sup>	 ( <i>E/Z</i> > 99:1)	OxdA	12	97 ( <i>S</i> ) <sup>d</sup>
		OxdB	2	87 ( <i>S</i> )
		OxdFG	12	91 ( <i>S</i> )
		OxdRE	33	97 ( <i>S</i> )
		OxdRG	16	99 ( <i>S</i> )
8 <sup>c</sup>	 ( <i>E/Z</i> < 1:99)	OxdA	5	2 ( <i>S</i> )
		OxdB	2	22 ( <i>S</i> )
		OxdFG	8	24 ( <i>R</i> )
		OxdRE	14	26 ( <i>R</i> )
		OxdRG	6	2 ( <i>R</i> )
9 <sup>c</sup>	 ( <i>E/Z</i> > 99:1)	OxdA	-	-
		OxdB	-	-
		OxdFG	14	51 ( <i>S</i> )
		OxdRE	-	-
		OxdRG	-	-
10 <sup>c</sup>	 ( <i>E/Z</i> < 1:99)	OxdA	10	93 ( <i>R</i> ) <sup>d</sup>
		OxdB	3	67 ( <i>R</i> )
		OxdFG	37	87 ( <i>R</i> )
		OxdRE	20	91 ( <i>R</i> )
		OxdRG	9	91 ( <i>R</i> )
11 <sup>c</sup>	 ( <i>E/Z</i> 92:8)	OxdA	14	97 (+)
		OxdB	7	73 (+)
		OxdFG	41	83 (+)

Entry	Substrate	Enzyme	Conv. [%] <sup>a</sup>	ee [%] <sup>b</sup>
12 <sup>c</sup>	 ( <i>E/Z</i> 3:97)	OxdRE	5	64 (+)
		OxdRG	6	67 (+)
		OxdA	6	52 (-)
		OxdB	10	93 (-)
		OxdFG	46	94 (-)
		OxdRE	3	71 (-)
		OxdRG	3	60 (-)

[a] Absolute conversion (confirmed *via* calibration curves on RP-HPLC), entry 1-4: 10 vol% DMSO, other entries: 2.5 vol% DMSO, entries 5-8: 3 h reaction time, entries 9+10: 4 h reaction time. "-" means no product detection below the detection limit of <2%. [b] The symbols (+) and (-) refer to the first and second signals in chiral HPLC or GC chromatograms. [c] Investigated substrates by Rommelmann<sup>[99]</sup> and Oike<sup>[84]</sup>. [d] Absolute configuration was determined *via* comparison with literature data after a preparative scale experiment.<sup>[65,101]</sup>

Strikingly, every single substrate was converted with at least 91% ee or even up to 99% ee by at least one of the Oxds, proving the hypothesized privileged substrate structures in an impressive manner. For the (*E*)-isomer of the *o*-Br-PPOx substrate (entry 1), good activities and high enantioselectivity were observed for all Oxds except OxdB, yielding the (*S*)-nitrile (determined by comparison with literature data<sup>[65]</sup>, see **chapter 3.3.4**) with 91% ee at 23% conversion when utilizing OxdRG. In contrast to this result, the (*Z*)-isomer was apparently not recognized as substrate by all five Oxds since no conversion was observed at all. This result emphasizes the importance and difference in recognition and selectivity of the (*E/Z*)-isomers when converted by Oxds.

Surprisingly, the opposite tendency could be observed when the *m*-Br-PPOx (entry 2) was utilized as substrate. Only OxdFG was capable of transforming the (*E*)-isomer with 87% ee at 37% conversion into the (*S*)-nitrile. The (*Z*)-isomer, however, was accepted by all five Oxds and exclusively transformed into the (*R*)-nitrile with up to 94% ee at 38% conversion by OxdA. This result is in agreement with the earlier observed switch in enantiospecificity with the helional oxime isomers (**Table 10**, entries 3 and 4).

The *p*-Br-PPOx substrate (entries 5 and 6) showed even another tendency than the previous *o*- and *m*-Br-PPOx substrates. While OxdA, OxdRE and OxdRG did neither recognize the (*E*)- or (*Z*)-isomer as substrate, OxdB and OxdFG transformed the (*E*)-isomer with excellent selectivity of 99% ee at 15% conversion (OxdB) or 96% ee at 33% conversion (OxdFG) into the nitrile. While the absolute configuration of the obtained nitrile could not be determined, the clear switch in enantiopreference could also be observed for the (*Z*)-isomer (entry 6). OxdB formed the nitrile with 83% ee at 27% conversion, while OxdFG transformed the (*Z*)-isomer with 84% ee at 46% conversion into the nitrile. Considering the fact that the (*Z*)-isomer was only available in an isomer ratio of (*E/Z* 10:90), one can conduct from the previous results of the (*E*)-isomer that the obtainable ee-value for the (*Z*)-isomer could be even higher for a higher (*Z*)-enriched substrate since the residual 10% of the (*E*)-isomer are also transformed into the nitrile with the opposite absolute configuration.

Since bromine is from a sterical standpoint the largest of the investigated halogen substituents, it was expected that the observed tendencies may also occur for the Cl- and F-PPOx derivatives, however in a less outstanding fashion. The Cl-PPOx substrates were investigated by Rommelmann<sup>[99]</sup> (entries 7-10), the F-PPOx substrates were investigated by Oike<sup>[84]</sup> (entries 11 and 12) and are discussed in the following. For the *o*-Cl-PPOx substrate (entries 7 and 8), the same tendency was observed as for the *o*-Br-PPOx substrate. The (*E*)-isomer was recognized by all five Oxds as substrate and exclusively transformed into the corresponding (*S*)-nitrile (determined by comparison with literature data<sup>[102]</sup>) with up to 99% ee at 16% conversion (OxdRG). Regarding the (*Z*)-isomer, it was apparent that this isomer is also recognized as substrate in contrast to the (*Z*)-isomer of the *o*-Br-PPOx. However, the switch in enantioselectivity is also observable in this case, but with lesser extent. OxdRE transformed the (*Z*)-isomer with 26% ee at 14% conversion into the (*R*)-nitrile. The *m*-Cl-PPOx substrate (entries 9 and 10) showed the same tendencies as the *m*-Br-PPOx substrate. The (*E*)-isomer was only recognized by OxdFG and transformed with 51% ee at 14% conversion into the (*S*)-nitrile. The (*Z*)-isomer, however, was recognized by all five Oxds as substrate and was exclusively transformed into the (*R*)-nitrile with up to 91% ee at 20% conversion (OxdRE). Lastly, the *p*-F-PPOx substrates investigated by Oike followed the observed tendencies of the *p*-Br-PPOx substrates. Although all Oxds seemed to be able to transform both the (*E*)- and (*Z*)-isomer of the substrate, especially OxdFG seemed to accept them very well since the (*E*)-isomer was transformed with 83% ee at 41% conversion into the corresponding nitrile, while the (*Z*)-isomer was transformed by OxdFG with 94% ee at 46% conversion into the nitrile with the other absolute configuration.

Summarizing the obtained results from the enantioselective dehydration of the halogenated PPOx-derivatives, one can state that the PPOx substrate platform represents indeed a privileged substrate structure for the enantioselective dehydration since all investigated substrates were at least transformed by one Oxd, including a high enantioselectivity of at least 91% ee, even reaching up to 99% ee.

Furthermore, the (*E*)-isomers showed a tendency to be transformed into the (*S*)-nitriles, while the (*Z*)-isomers were predominantly transformed into the (*R*)-nitriles. While the absolute configuration is not known for every obtained nitrile, the switch in enantioselectivity in dependence of the utilized (*E*)- or (*Z*)-isomers seems to be a reappearing tendency for these substrates. This may stem from the different orientation in the active site, especially since the aldoxime is bound *via* its N-atom to the Fe(II)-atom of the heme center (see **Scheme 17**, chapter 2). Moreover, in some cases only the (*E*)-isomer or (*Z*)-isomer of the substrate was accepted at all as substrate. This may result from different  $K_m$ -values of the substrates, but most reported  $K_m$ -values for aldoxime substrates lie between 1-11 mM (see chapter 2), which would lead at least to some conversion at a substrate concentration of 5 mM. Accordingly, it should be investigated in the future if in some cases (*E/Z*)-mixtures without the tedious isomer separation can be used as substrate at 8°C and still yield only the highly enantiomerically enriched nitrile. Strikingly, it should be mentioned that all of the investigated Oxds are indeed wildtype enzymes without any optimization by random mutagenesis or site-directed mutagenesis. The obtained results of ee-values up to 99% at high conversion rates underline the big potential of Oxds for the enantioselective nitrile synthesis. The mild reaction conditions without the need for hazardous auxiliaries or catalysts make this biocatalytic approach highly valuable and promising. Since two crystal structures of Oxds are already reported (OxdA and OxdRE), docking studies and followed-up mutagenesis studies may allow for an even greater differentiation of the Oxds between the (*E/Z*)-isomers, resulting in even better ee-values.

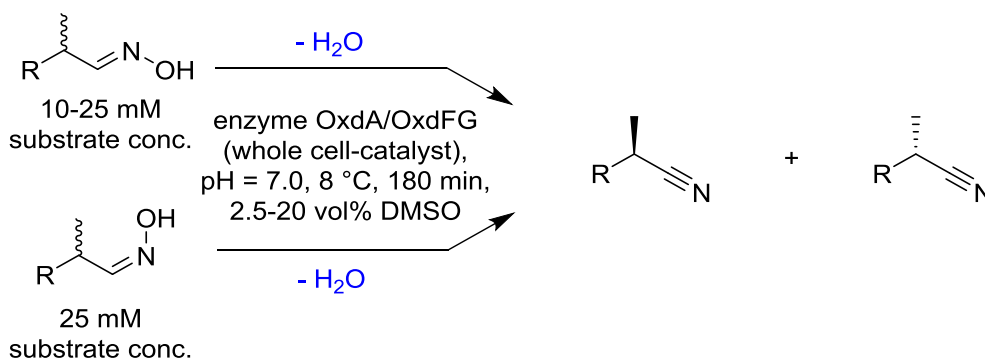
## 3.3.4 ENANTIOSELECTIVE NITRILE SYNTHESIS ON PREPARATIVE SCALE

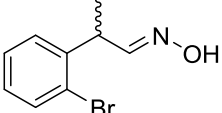
From the broad diversity of the investigated substrates some of the most promising substrates, which were converted highly enantioselectively into their nitriles in the analytical scale studies, were selected for preparative scale experiments (**Table 12**) to confirm the absolute configuration of the nitriles by comparison with their literature reported  $[\alpha]_D^{20}$  values.

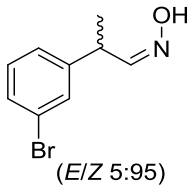
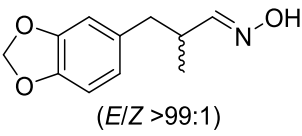
The substrate concentration was elevated to 10-25 mM for these experiments as a first intensification of this biocatalytic process. Additionally, 2.5 vol% of DMSO were chosen as cosolvent for OxdFG, while 20 vol% DMSO were used for the biotransformations with OxdA after confirming OxdA's stability against DMSO in a cosolvent study (chapter 4.3). Since OxdA performed very well for the Br-substituted PPOx derivatives, both the (*E*)-isomer of 2-Br-PPOx and the (*Z*)-isomer of 3-Br-PPOx were chosen as substrates for this scale-up experiment. Pleasingly, for (*E*)-2-Br-PPOx a conversion of 35% could be achieved and the corresponding nitrile, (*S*)-2-Br-PPN, was obtained with 98% ee and 21% (22 mg) isolated yield after column chromatography. Regarding (*Z*)-3-Br-PPOx, a conversion of 49% was observed and the corresponding nitrile, (*R*)-3-Br-PPN, was obtained with 87% ee and 23% (55 mg) isolated yield after column chromatography.

Lastly, the (*E*)-isomer of helional oxime could be transformed with OxdFG with 54% conversion after three hours, yielding the corresponding (*S*)-nitrile with 46% ee and an isolated yield of 28% (53 mg). Since the theoretical conversion of a kinetic resolution is capped at 50% as is the yield, the obtained results for all three substrates are already at an excellent level and represent a well-suited foundation for further process development steps, especially considering that the utilized Oxds were all wildtype enzymes and may be optimized in the future.

**Table 12:** Preparative scale biotransformations of selected substrates by Oxd whole-cell catalysts.



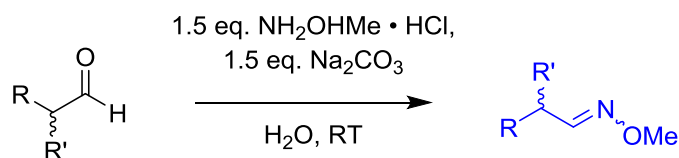
Entry	Substrate	Enzyme	Conv. [%] <sup>a</sup>	ee [%]	Yield [%]
1	 (E/Z > 99:1)	OxdA (72 mg <sub>BWW</sub> )	35	98 ( <i>S</i> ) <sup>b</sup>	21 (22 mg)

Entry	Substrate	Enzyme	Conv. [%] <sup>a</sup>	ee [%]	Yield [%]
2	 (E/Z 5:95)	OxdA (216 mg <sub>BWW</sub> )	49	87 (R) <sup>b</sup>	23 (55 mg)
3	 (E/Z >99:1)	OxdFG (928 mg <sub>BWW</sub> )	54	46 (S) <sup>b</sup>	28 (53 mg)

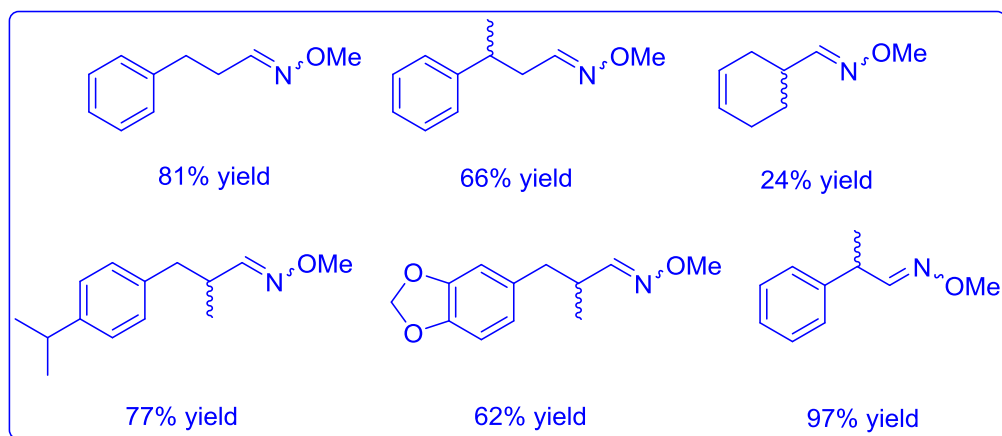
[a] Absolute conversion (confirmed *via* calibration curves on RP-HPLC); [b] Absolute configuration was determined *via* comparison with literature data.<sup>[65,100]</sup>

### 3.3.5 ATTEMPTED BIOTRANSFORMATIONS OF O-METHYLATED OXIMES

As the biocatalytic dehydration by Oxds is proposed to proceed *via* a protonation of the O-atom of the aldoxime group (chapter 2.3)<sup>[54,55,78–80,85]</sup>, one can envision O-methylated aldoximes as substrates for the biocatalytic nitrile synthesis. The resulting leaving group would be methanol and the O-methylated oximes can be as readily prepared as their non-methylated analoga (**Scheme 26**).



### Synthesized substrates



**Scheme 26:** Synthesis of the O-methylated aldoximes.

Once a selection of six different O-methylated oximes could be assembled, biotransformations with all six substrates using five different Oxds at analytical scale were



conducted at pH = 7.0 and 30 °C with a reaction time of 24 hours (**Table 13**). Unfortunately, none of the substrates were transformed by any of the Oxds. As a consequence, O-methylated aldoximes are seemingly not suitable substrates for the biocatalytic dehydration by Oxds. This phenomenon may be explained by docking studies in the future. Results from these docking studies may also allow the development of new synthetic possibilities with Oxds. Additionally, biotransformations with other aldoxime analogs should be investigated.

**Table 13:** Attempted biotransformations of O-methylated aldoximes with Oxds.

Entry	Substrate	Entry	Substrate
1	 (E/Z 70:30)	4	 (E/Z 67:33)
2	 (E/Z 75:25)	5	 (E/Z 33:67)
3	 (E/Z 50:50)	6	 (E/Z 50:50)

### 3.4 SUMMARY AND OUTLOOK FOR THE BIOCATALYTIC, ENANTIOSELECTIVE NITRILE SYNTHESIS

Starting from the preliminary study of Metzner *et al.*<sup>[89,90]</sup>, the author could identify with Rommelmann<sup>[99]</sup> and Oike<sup>[84]</sup> a privileged substrate structure for enantioselective nitrile synthesis with Oxds: 2-phenylpropanal oxime (**Figure 8**). This substrate was converted highly selectively by any of the five investigated Oxds with over 90% ee at conversion rates of at least 25%, sometimes even with up to 99% ee. This lead structure was identified after an initial, broad substrate scope study that proved the big substrate scope of Oxds since at least one of the Oxds was capable of recognizing the investigated compounds as substrate (**Table 9**).

Additionally, the separation of the (*E/Z*)-isomers of the aldoximes by automated column chromatography was crucial for the enantioselectivity study since it could be shown that dependent on either the (*E*)- or (*Z*)-configuration of the aldoxime, the enantiopreference of the Oxds may change from the (*S*)- to the (*R*)-nitrile and vice versa (**Table 10** and **Table 11**).<sup>[103]</sup> This observation holds especially true for 2-phenylpropanal oxime and should be investigated further in the future by docking studies to rationalize it. This phenomenon is highly exciting, since it allows the possibility to obtain two enantiomers of a compound with the same catalyst. Usually, one has to screen for enzymes with other enantiopreference in biocatalysis to be able to synthesize the other enantiomer of a compound. By skipping this screening effort, the efficiency of the Oxd catalyzed nitrile synthesis increases drastically.

The enantioselectivity study also revealed the influence of halogen substituents at 2-phenylpropanal oxime derivatives. The Br- and Cl-derivatives showed interesting results since in some cases only one of the isomers, either (*E*) or (*Z*), was recognized by some Oxds (**Table 11**). As a consequence, one can potentially skip the isomer separation in the future by transforming an isomer mixture, separating the product and then recycle the residual substrate by thermal isomerization.

Lastly, a first process development by increasing the substrate concentration to 25 mM and the conduction of preparative scale experiments has been successfully conducted. Three substrates were converted with up to 98% ee (*S*) and up to 28% yield (**Table 12**). The nitriles could be isolated in an amount that allowed the determination of the absolute configuration by comparison with literature data.<sup>[65,100]</sup>

Apart from the above mentioned docking studies to rationalize the enantiopreference of Oxds, more modifications of the substrate structure should be synthesized and investigated as potential substrates. Especially the methyl substituent in the  $\alpha$ -position of the oxime moiety has so far not been modified and it would be intriguing to investigate its influence both on substrate acceptance and enantiopreference.

Furthermore, the maximum yield of this biotransformation is limited to 50% since it represents a kinetic resolution. Hence, development of a dynamic kinetic resolution would be a nice asset since it would potentially increase the theoretical yield to 100%. Preliminary results for this and *in situ* (*E/Z*)-isomerization have been conducted by Yavuzer<sup>[104]</sup> and Brod<sup>[105]</sup> under supervision of the author of this thesis and are currently investigated deeper.

All in all, the obtained results represent a highly promising basis for further investigation in the Oxd-catalyzed, enantioselective nitrile synthesis.

## 4 BIOCATALYTIC SYNTHESIS OF ALIPHATIC LINEAR $\alpha,\omega$ -DINITRILES

### 4.1 RELEVANCE OF ALIPHATIC LINEAR $\alpha,\omega$ -DINITRILES IN INDUSTRY AND EVERYDAY LIFE

Linear  $\alpha,\omega$ -dinitriles are of very high importance as precursors for the polymer industry, especially for nylons and polyurethanes. The most prominent example is adiponitrile (1,6-hexanedinitrile) which is produced on an annual scale of over 1 million metric tons.<sup>[38,39]</sup> The main use of adiponitrile is the hydrogenation towards hexamethylenediamine<sup>[106]</sup> that is a key building block for the production of polyamides like Nylon 6.6.<sup>[38,39,107]</sup> The first approaches towards the synthesis of adiponitrile are based on chlorine chemistry, which are nowadays obsolete because of the tremendous amount of waste that was produced *via* this route and lacking sustainability.<sup>[39,108]</sup> The large waste amounts also severely hindered the economical profit. Today, there are two dominant production processes for adiponitrile.

The first one was developed by *Baizer* from the company Monsanto in the early 1960s and is based on the electro-hydromerization of two molecules of acrylonitrile (**Figure 9**).<sup>[109]</sup> While this process is still applied today, it has certain selectivity problems.

The second process, which is today the dominant one, was developed by DuPont and is based on the use of butadiene. Two molecules of hydrogen cyanide react in a terminal addition reaction to butadiene to directly yield adiponitrile (**Figure 9**).<sup>[110]</sup> While this process is nowadays successfully applied on large scale, it still has the major drawback of the high toxicity of hydrogen cyanide. Additionally, the regioselectivity of the addition reaction is somewhat problematic.

One of the biggest challenges in the field of future's chemicals product tree is the task to enable access to existing bulk chemicals by changing the raw material basis, replacing hazardous methodologies and reagents by more environmentally benign processes. For aliphatic, linear  $\alpha,\omega$ -dinitriles, several attempts have been investigated over the last years and decades in order to find new production processes (especially for adiponitrile). Some of the newly investigated approaches for green-chemistry based nitrile synthesis (especially adiponitrile) utilize heterogeneous catalysis like non-noble metal oxides-based nanocatalysts or homogeneous catalysis, utilizing an iron nitrate/TEMPO system.<sup>[111,112]</sup> While these approaches are quite elegant avoiding the use of cyanides and starting from readily available alcohols (like 1,6-hexanediol), some limitations exist. The heterogeneous approach suffers from high reaction temperatures ( $\geq 130$  °C) and runs at elevated pressure of five bar of pure molecular oxygen ( $O_2$ ), thus raising safety issues. The homogeneous approach runs at mild reaction conditions but high catalyst loading (5 mol%) and tedious separation of the used iron nitrate and TEMPO are drawbacks. On the other hand, nature provides unique opportunities for organic synthesis. Thus, it is worth to identify natural approaches towards the preparation of specific functional groups and adapt them to chemical synthesis.

Since Oxds showed great potential in the synthesis of several aliphatic mononitriles (see **chapter 2**) and chiral nitriles (see **chapter 3**), the broad investigation of Oxds' potential for the synthesis of the industrially important aliphatic, linear  $\alpha,\omega$ -dinitriles was deemed to be investigated.<sup>[52,70,74,76,77,86,87,89,103,113]</sup> In the following, the results of this biocatalytic production process that avoids the usage of cyanide are presented.

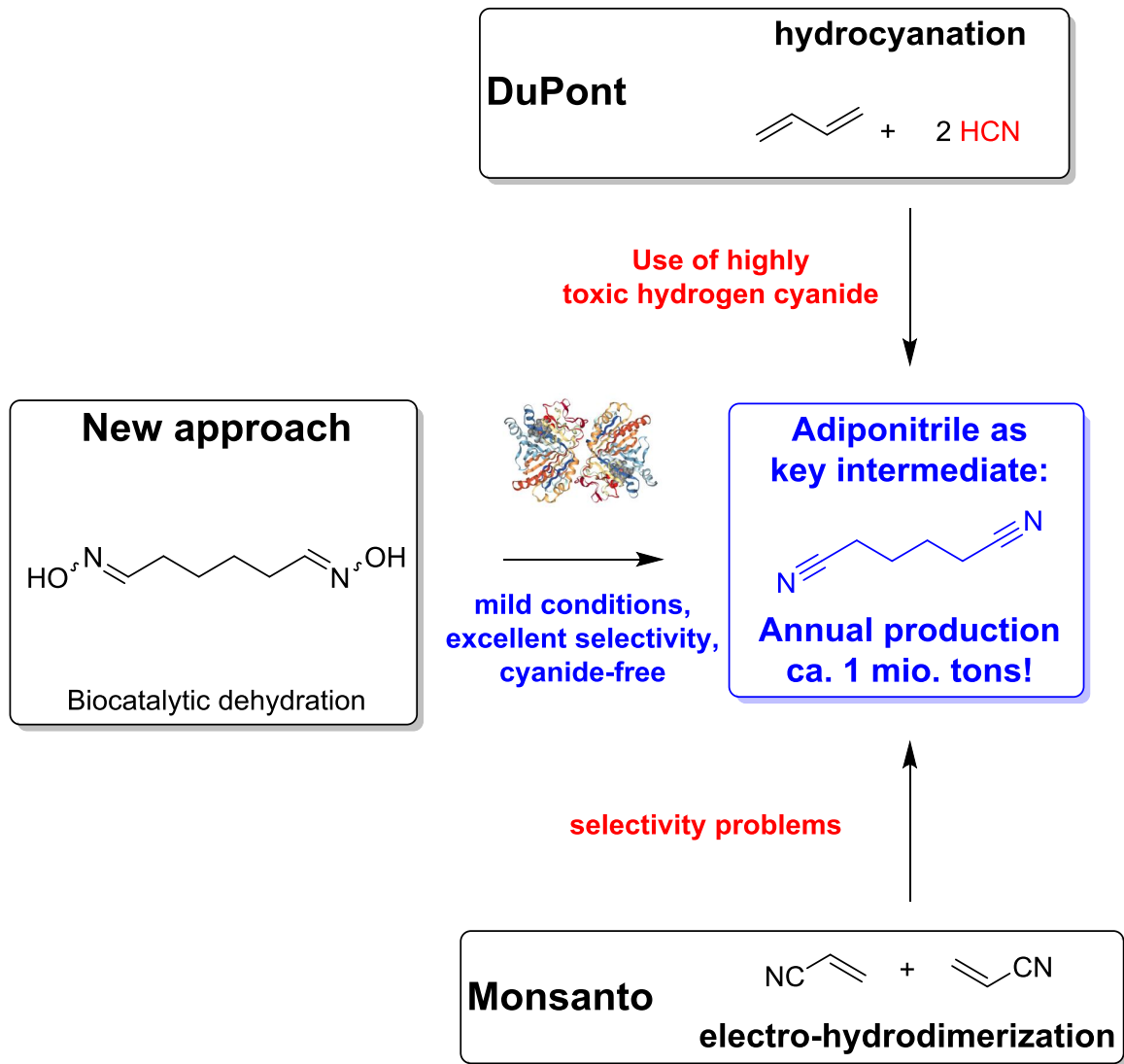
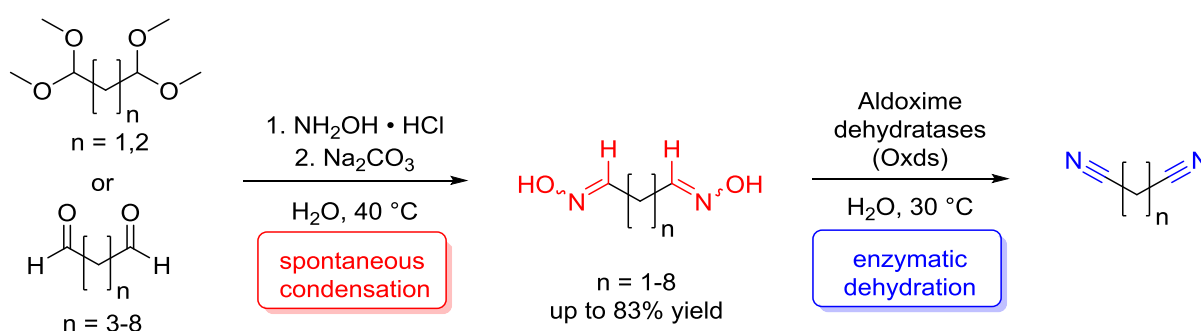


**Figure 9:** Today's production processes towards adiponitrile and the newly envisioned, biocatalytic production route *via* Oxd catalysis.

## 4.2 SUBSTRATE SYNTHESIS BASED ON DIALDEHYDES OR THEIR ACETALS

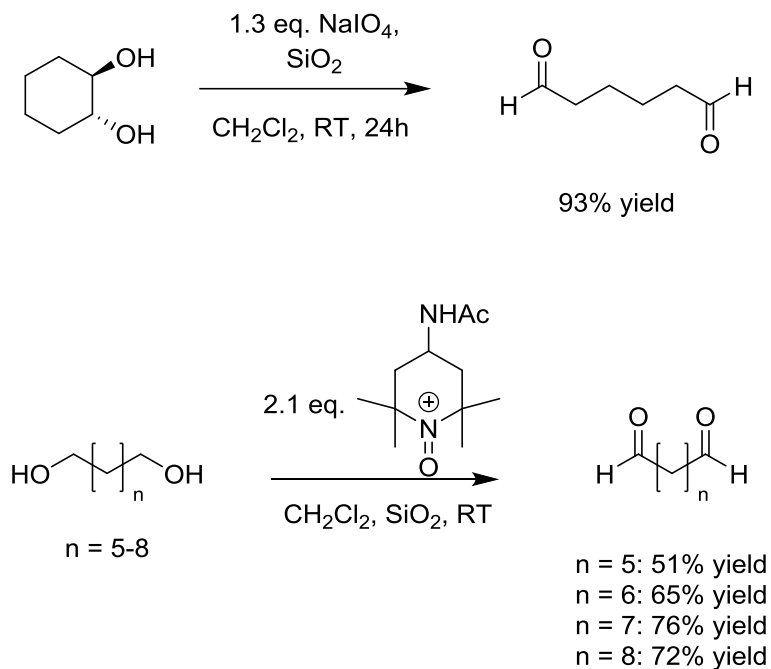
The new approach for the biocatalytic  $\alpha,\omega$ -dinitrile synthesis is based on the preparation of the dialdoximes as key intermediate, which is afterwards dehydrated twice by the aldoxime dehydratase to yield the dinitrile. As a consequence, the author had to synthesize the dialdoximes out of the corresponding  $\alpha,\omega$ -dialdehydes (**Scheme 27**). It was decided to investigate substrates with a carbon chain length of 3-10 carbon atoms since dinitriles of this chain length have a high relevance in the chemical industry. Due to their high reactivity, most  $\alpha,\omega$ -dialdehydes are only available in their protected form as acetals. One other  $\alpha,\omega$ -dialdehyde, glutaraldehyde (C5 dialdehyde), can be commercially purchased as aqueous solution. For the other  $\alpha,\omega$ -dialdehydes with a chain length of 6-10 carbon atoms, a synthetic approach had to be found which allowed access to bigger quantities of them. The availability of the dialdehydes is so low because the double,  $n$ -terminal hydroformylation of dienes like butadiene towards adipaldehyde has severe selectivity issues that are still object of research.<sup>[114-117]</sup> The best reported result reaches up to 73% selectivity for the double  $n$ -terminal hydroformylation of butadiene towards adipaldehyde. However, the formed adipaldehyde has to react *in situ* with two molecules of a dialcohol to form the stable bis-acetal. This additional protection step makes the process economically unattractive.<sup>[114]</sup>



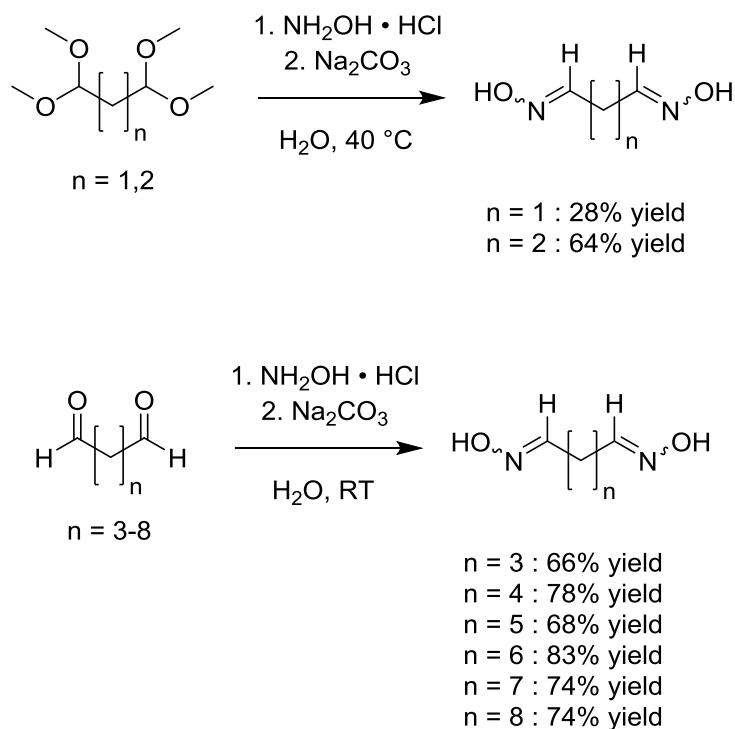
**Scheme 27:** Synthetic approach towards linear, aliphatic  $\alpha,\omega$ -dinitriles starting from dialdehydes or the acetals.

For the preparation of the C3 and C4-dialdoxime from their bis-dimethyl acetals they were *in situ* cleaved by addition of the hydrochloride salt of hydroxylamine to release the dialdehydes. After neutralization with sodium carbonate, the dialdoxime instantly starts to precipitate from the reaction solution. Glutaraldehyde (C5) was directly used for the dialdoxime synthesis from a commercial source. Adipaldehyde, the most intriguing substrate, had to be synthesized in larger quantities. For this, *trans*-1,2-cyclohexanediol was oxidized with sodium periodate ( $\text{NaIO}_4$ , **Scheme 28**). The largest reaction scale was 110 mmol of *trans*-1,2-cyclohexanediol, which had to be conducted in 2 liter round bottom flasks (**Figure 10**). Regarding the C7-C10 dialdehydes, a very recently reported protocol by *Bobbitt et al.* was utilized.<sup>[118]</sup> The reagent for this oxidation is called Bobbitt's salt and it represents a tetrafluoroborate salt of a 2,2,6,6-Tetramethylpiperidinyloxy (TEMPO) derivate (**Scheme 28**). Other approaches for the selective alcohol oxidation like the Dess-Martin periodinane and other ones have also been reported, but are way more complicated and restricted.<sup>[119]</sup> Both approaches yield the dialdehydes in very high yields and in multi gram scale, paving the way towards larger scale reactions.

Afterwards, the  $\alpha,\omega$ -dialdehydes were converted in analogy to the C3-C4 substrates by directly converting the  $\alpha,\omega$ -dialdehydes with hydroxylamine hydrochloride and sodium carbonate in aqueous solution, yielding the  $\alpha,\omega$ -dialdoximes with good yields (**Scheme 29**).



**Scheme 28:** Synthesis of the  $\alpha,\omega$ -dialdehydes with a chain length of 6-10 carbon atoms by oxidation of *trans*-1,2-cyclohexanediol or  $\alpha,\omega$ -dialcohols.



**Scheme 29:** Synthesis of the  $\alpha,\omega$ -dialdoximes by conversion with hydroxylamine hydrochloride and sodium carbonate in aqueous solution.

Interestingly, while the dialdoximes may appear as rather simple molecules, almost nothing is known about them in the literature or they have not been reported at all in many cases!<sup>[120,121]</sup> While monoaldoximes are often oils or solids that melt at rather low temperatures,  $\alpha,\omega$ -dialdoximes are very high melting solids that rather decompose at highly elevated temperatures than melting at all. These properties go hand in hand with the high stability of the  $\alpha,\omega$ -dialdoximes. While the  $\alpha,\omega$ -dialdehydes are highly reactive and prone to decomposition *via* oxidation, aldol reaction etc., the  $\alpha,\omega$ -dialdoximes showed no sign of deterioration when stored at room temperature for several months. This property might be helpful in technical applications since they eliminate the need for severe safety precautions to protect the substances from decomposition. The synthesized  $\alpha,\omega$ -dialdoximes can be simply purified *via* filtration and drying *in vacuo*, yielding them with purities of up to  $\geq 99\%$ .



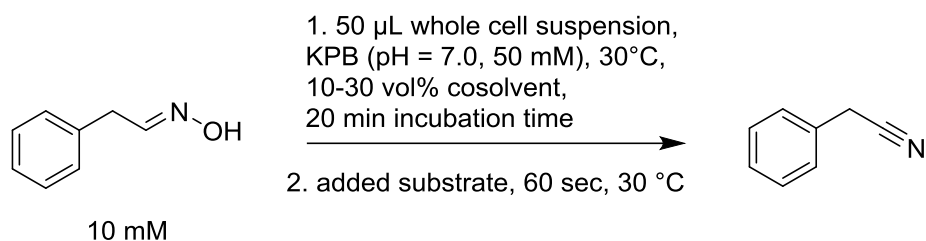
**Figure 10:** 2 liter scale reaction for the preparation of adipaldehyde starting from *trans*-1,2-cyclohexanediol.

Regarding the  $\alpha,\omega$ -dinitriles of interest, commercial reference compounds were purchased for establishing analytical methods to quantify the later conducted activity assays of the Oxds.

### 4.3 PROOF OF THE BIOTRANSFORMATION PROCESS

Once all  $\alpha,\omega$ -dialdoximes substrates with a chain length of 3-10 carbon atoms were assembled, the proof of concept for the biocatalytic dinitrile synthesis could be started. Towards this end the author decided to overexpress the same five aldoxime dehydratases (Oxds) in *E.coli* that we already utilized in the studies for the enantioselective, biocatalytic nitrile synthesis (**chapter 3**). This includes the following Oxds: OxdA from *Pseudomonas chlororaphis* B23, OxdB from *Bacillus* sp. OxB-1, OxdFG from *Fusarium graminearum* MAFF305135, OxdRE from *Rhodococcus* sp. N-771 and OxdRG from *Rhodococcus globerulus* A-4.

The overexpression was conducted *via* the described protocol in **chapter 9.3.2.1** and the overexpression was confirmed by SDS-PAGE (**Figure 36**). Before evaluating the activity of all five Oxds for the  $\alpha,\omega$ -dialdoximes substrates, a broad cosolvent study was conducted because the  $\alpha,\omega$ -dialdoximes substrates were empirically found to be hardly soluble in purely aqueous media. Since the reported  $K_m$ -values in the literature for linear, aliphatic monoaldoximes with chain lengths of two to six carbon atoms range from 0.25 – 11.1 mM, the addition of cosolvents was deemed necessary to avoid the issue of not reaching substrate concentrations that allow the enzymes to work a maximum velocity. For this, ten different water-soluble cosolvents were added to the activity assay of all five Oxds with the standard substrate phenylacetaldehyde oxime (PAOx). The assay was conducted at 500  $\mu$ L scale after a preincubation time of 20 minutes for each solvent to make a first selection among the cosolvents (**Figure 11, Figure 12, Figure 13, Figure 14, Figure 15**). The activities were calculated in relation to a reference activity assay in which 2.5 vol% of DMSO were used as cosolvent.



**Scheme 30:** Long-term stability study for five Oxds with ten different water-miscible cosolvents.



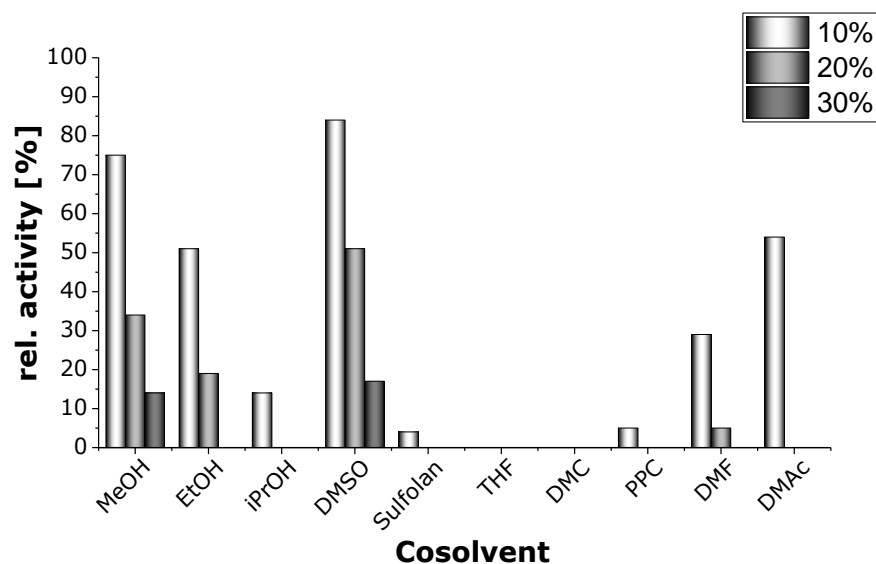


**Figure 11:** Relative activity of OxdA(C) in presence of water soluble cosolvents (for different volumetric percentages). The relative activity values correlate to a reference activity assay with 2.5 Vol% DMSO as cosolvent.

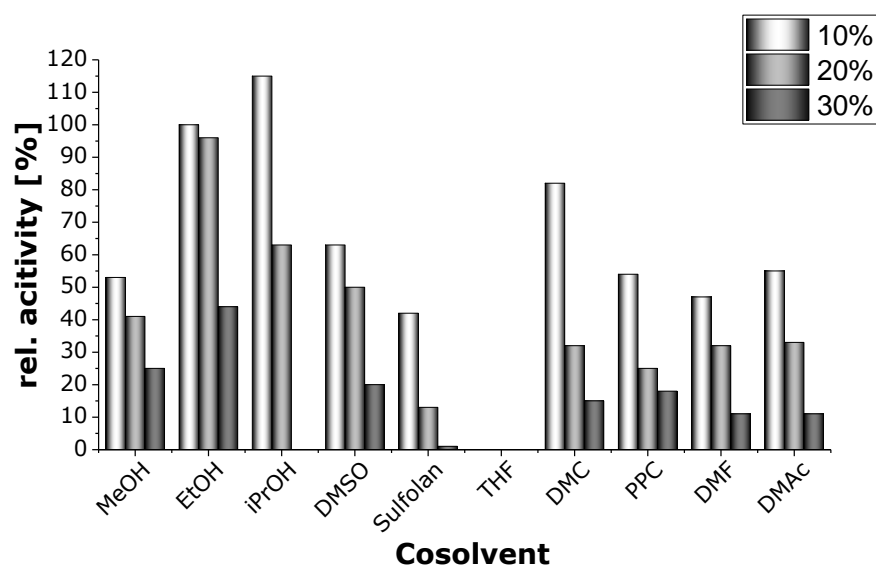


**Figure 12:** Relative activity of OxdB in presence of water soluble cosolvents (for different volumetric percentages). The relative activity values correlate to a reference activity assay with 2.5 Vol% DMSO as cosolvent.

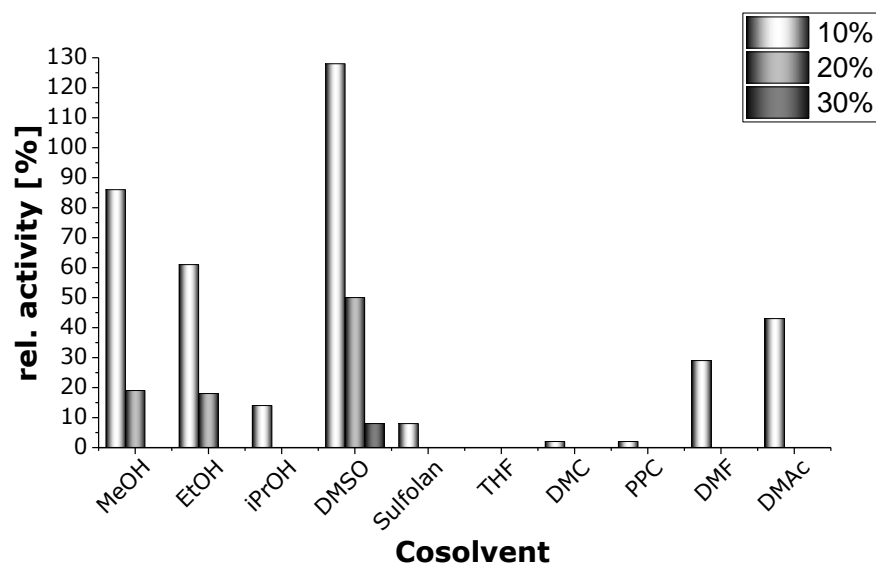


**Figure 13:** Relative activity of OxdFG(N) in presence of water soluble cosolvents (for different volumetric percentages). The relative activity values correlate to a reference activity assay with 2.5 Vol% DMSO as cosolvent.

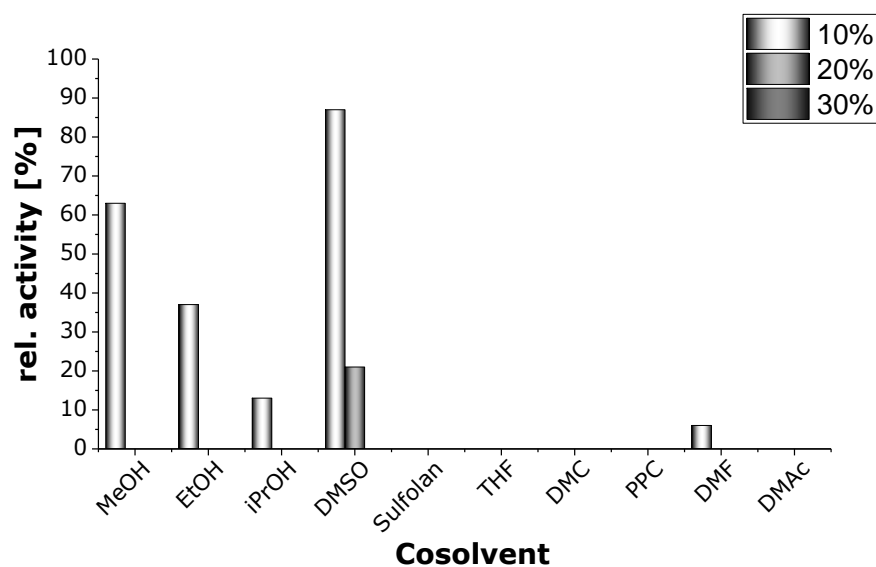


**Figure 14:** Relative activity of OxdRE(N) in presence of water soluble cosolvents (for different volumetric percentages). The relative activity values correlate to a reference activity assay with 2.5 Vol% DMSO as cosolvent.

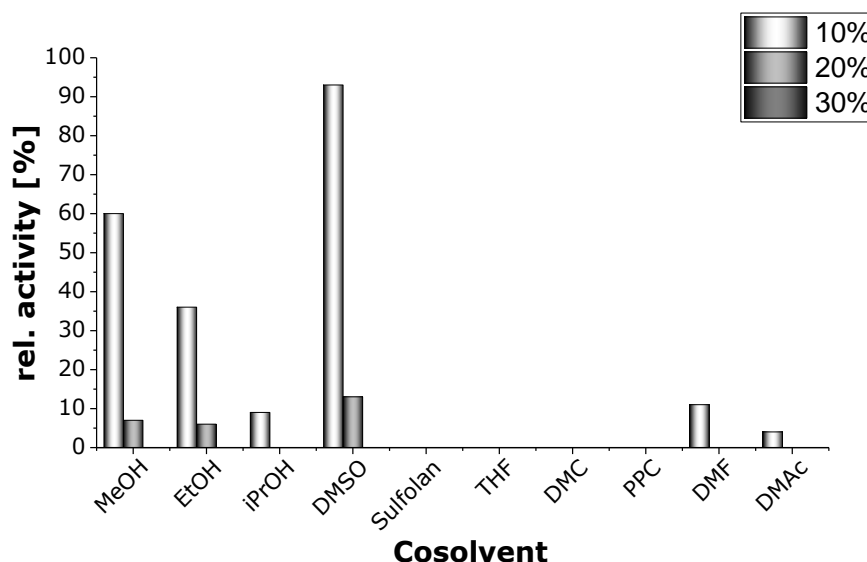
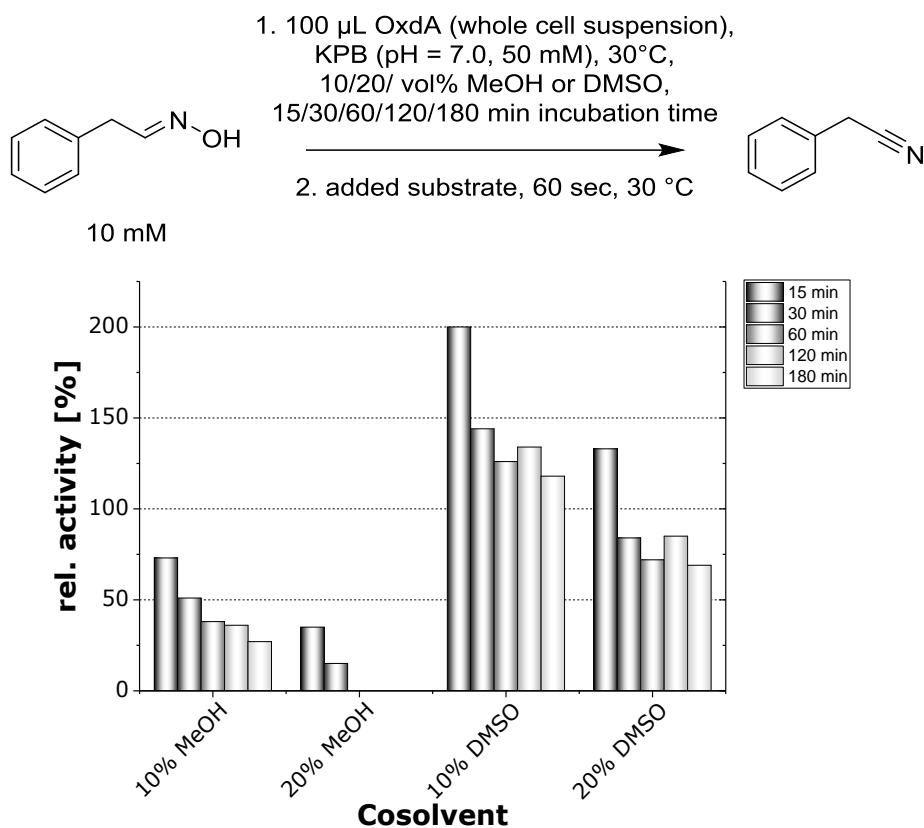


**Figure 15:** Relative activity of OxdRG(N) in presence of water soluble cosolvents (for different volumetric percentages). The relative activity values correlate to a reference activity assay with 2.5 Vol% DMSO as cosolvent.

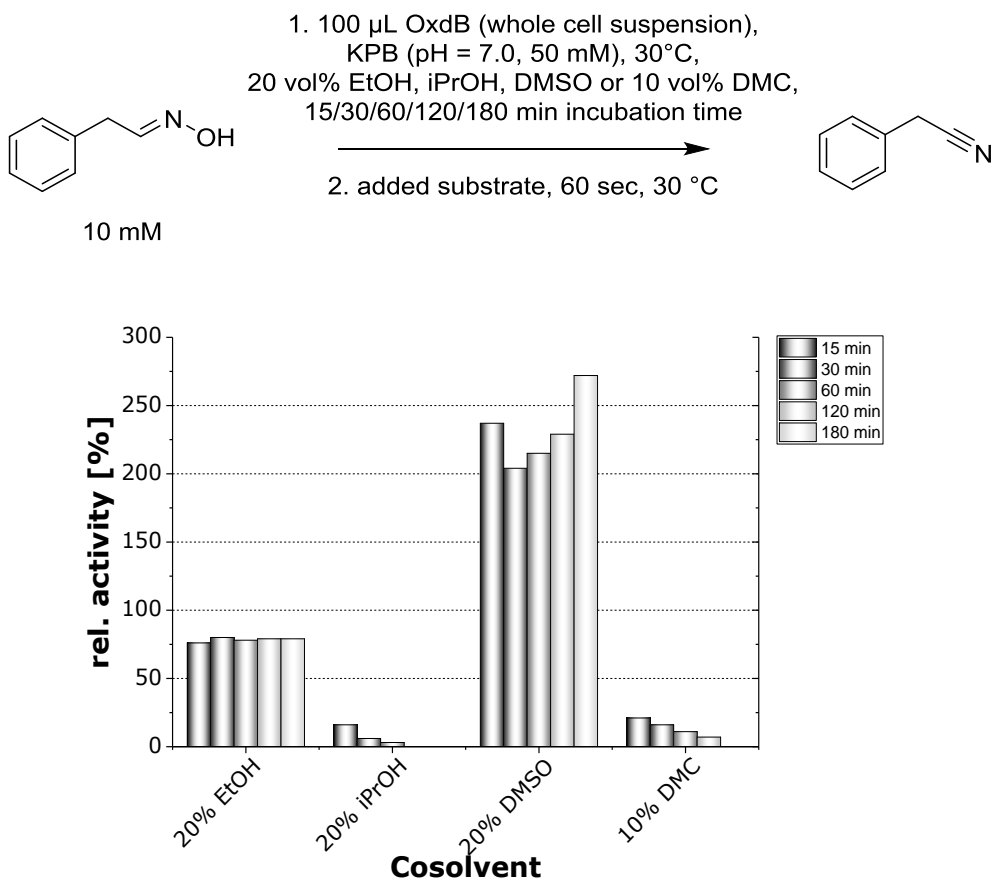
The selected ten cosolvents ranged from polar, protic solvents like methanol, ethanol and 2-propanol over to polar, non-protic solvents like dimethyl sulfoxide (DMSO), sulfolan, tetrahydrofuran (THF), dimethyl carbonate (DMC), propylene carbonate (PPC), dimethylformamide (DMF) and dimethylacetamide (DMAC). As one can depict from the figures above, especially the whole-cell catalysts containing OxdA and OxdB showed high short-time tolerance against a broad selection of the ten cosolvents. For OxdFG, OxdRE and OxdRG, they only showed some tolerance against DMSO at 10 vol% and almost no tolerance against the other five cosolvents.

For OxdA, especially methanol and DMSO were tolerated quite well with levels of up to 20 vol%. The most promising results were obtained for OxdB. Every cosolvent, expect for THF, is short-termed tolerated with up to 20 vol%. Especially ethanol, 2-propanol and DMSO showed high potential for further investigation. Additionally, DMC was deemed to be further investigated. Based on these results, only OxdA and OxdB were further investigated.

Since most biotransformations require several hours to complete, a long-term stability study for the stability of the whole-cell catalysts against the cosolvents was necessary. The long-term study was conducted with 10 or 20 vol% of methanol or DMSO for OxdA and with 20 vol% of ethanol, 2-propanol and DMSO for OxdB. Additionally, 10 vol% of DMC were investigated for OxdB. The whole-cell suspension was incubated with the cosolvent and the standard activity assay was started after incubation times of 15, 30, 60, 120 and 180 minutes (**Scheme 31**, **Scheme 32**). The obtained activity values were set in relation to a reference activity assay in which 2.5 Vol% DMSO were used as cosolvent.



Scheme 31: Long-term stability study for OxdA(C).



Scheme 32: Long-term stability study for OxdB.

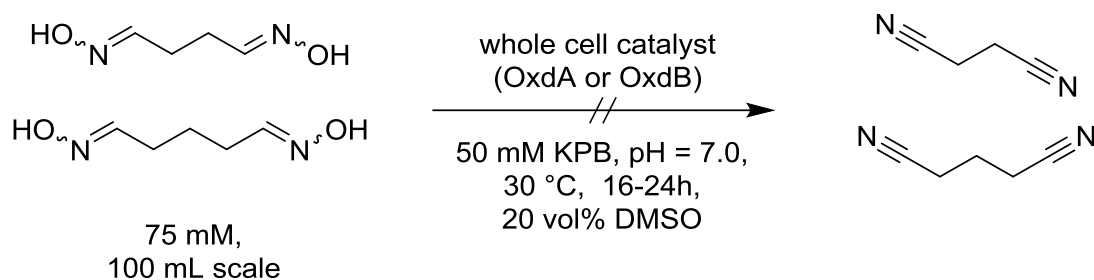
The results were highly intriguing. While for OxdA the relative activity (and also overall activity) decreased slowly with DMSO over three hours, methanol led to a stronger deactivation over three hours. Moreover, DMSO seemed to increase the activity of the whole-cell catalyst compared to a reference experiment without DMSO. This may result from higher permeability of the cell membrane because of DMSO. However, this hypothesis would have to be confirmed by further experiments. Nevertheless, OxdA was stable enough in the presence of 20 vol% DMSO to continue with the studies of the  $\alpha,\omega$ -dialdoxime conversion.

Regarding OxdB, even more promising results were obtained. While 2-propanol and DMC led to a rather fast deactivation of the whole-cell catalyst, ethanol seemed to be without any negative effect on the relative activity of the whole-cell catalyst. However, one has to carefully consider that this is relative activity in comparison to a reference experiment without any cosolvent. The absolute activity of the whole-cell catalyst slowly decreased during the three hours of the experiment. The best result was obtained with DMSO. DMSO activated the whole-cell catalyst, which is in agreement with the results for OxdA. Additionally, the relative activity of the whole-cell catalyst increased over time in the presence of DMSO: This correlates with a long-term stable, absolute activity. By reasons unknown, DMSO seems to stabilize the whole-cell catalyst.

Based on the encouraging results for the stability of the whole-cell catalyst harboring OxdA and OxdB in presence of DMSO, biotransformations on analytical scale with the eight different  $\alpha,\omega$ -dialdoxime substrates (C3-C10) were conducted (**Figure 17**). The concentrations of the substrates ranged from 3.0 mM to 75 mM in order to get an insight into the impact of substrate concentrations on the activity and reaction course. Due to the low solubility of the  $\alpha,\omega$ -dialdoximes in most all organic media, a solvent screening including correction factors for the extraction of the  $\alpha,\omega$ -dialdoximes and  $\alpha,\omega$ -dinitriles were determined. The most suitable solvent for extraction of both,  $\alpha,\omega$ -dialdoxime and  $\alpha,\omega$ -dinitrile, was found to be 2-methyltetrahydrofuran.

Interestingly, a very strong dependency on the carbon chain length of the substrate and the conversion by the Oxds could be observed. The C3-dialdoxime, whose dinitrile malononitrile is a well-researched compound that is broadly applied in the chemical industry<sup>[122]</sup>, was not accepted at all by OxdA or OxdB. This is in good agreement with the result of the attempted desymmetrization of a prochiral 1,3-dialdoxime in the investigation of the enantioselective, biocatalytic nitrile synthesis (**chapter 3**).

Regarding the C4 and C5-dioximes, both Oxds did only marginally produce the  $\alpha,\omega$ -dinitrile, but instead seemed to accumulate an unknown intermediate (**Scheme 33**, **Figure 16**). This tendency was also observed in the preparative scale experiments that were conducted with both OxdA and OxdB. The consumption of the substrate was accompanied by an increasing peak in the GC chromatograms that was located directly between the peaks of the  $\alpha,\omega$ -dialdoxime and the  $\alpha,\omega$ -dinitrile. Since the C6 dioxime and the higher analogues are converted towards the  $\alpha,\omega$ -dinitrile with the same appearing intermediate peak, we postulate that this unknown intermediate may indeed be the monodehydrated species that bears one aldoxime and one nitrile moiety. As a consequence, OxdA and OxdB only seem to be able to dehydrate  $\alpha,\omega$ -dialdoximes with a chainlength of up to five atoms only once. This phenomenon should be rationalized by docking studies in the near future.



**Scheme 33:** Attempted synthesis of succino- and glutaronitrile by biocatalytic dehydration.

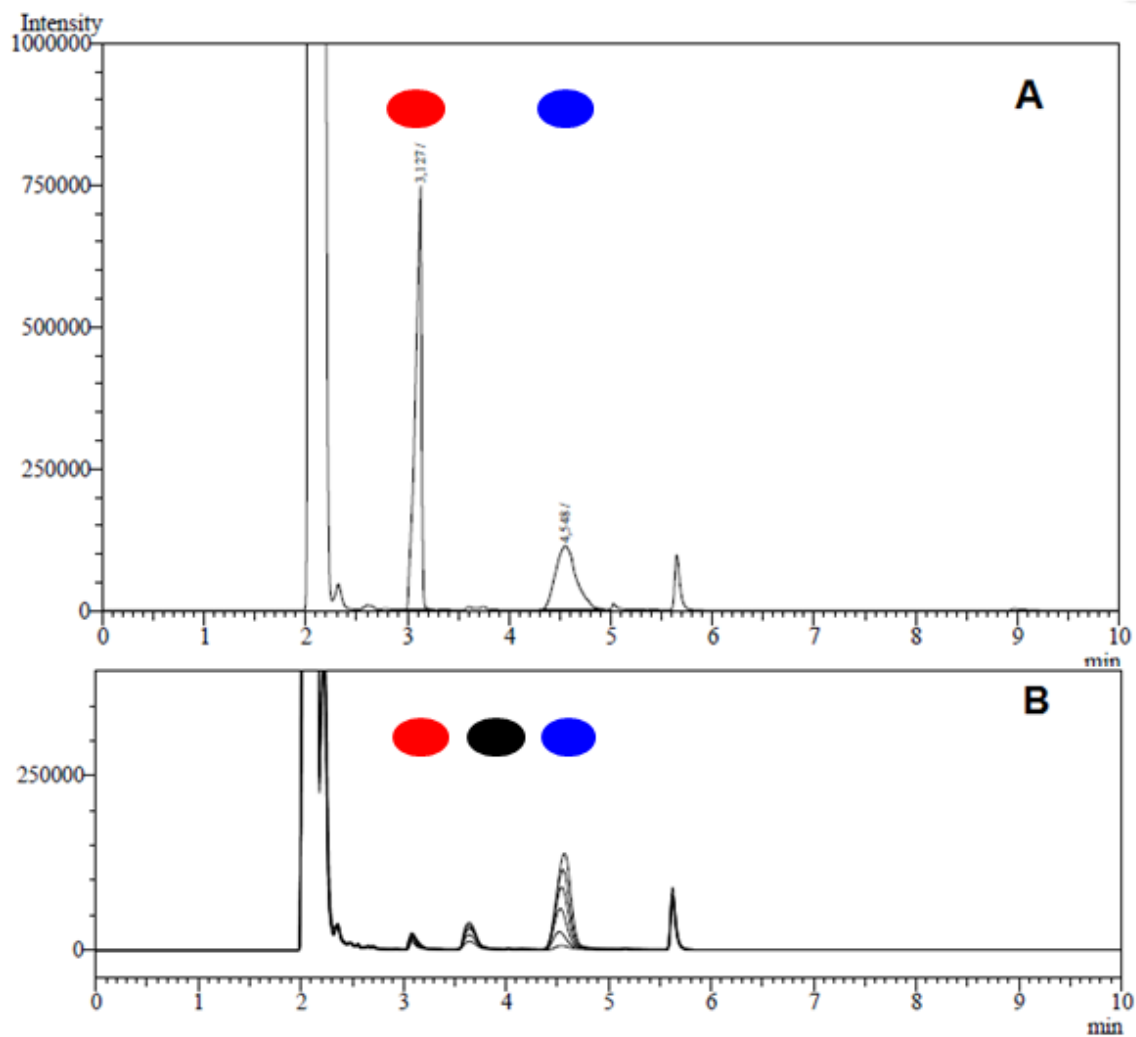
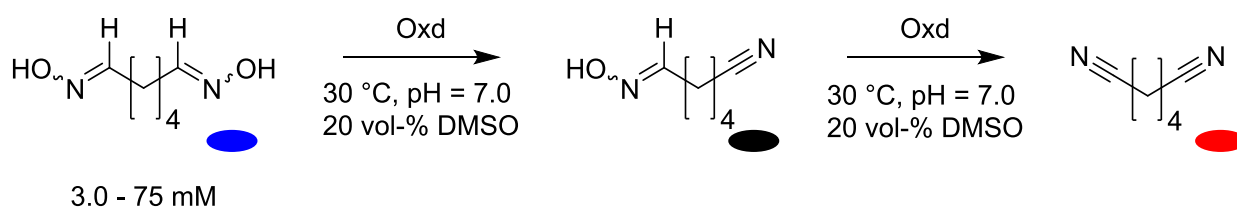


**Figure 16:** GC-chromatograms illustrating the formation of the postulated mononitrile-monoaldehyde intermediate in the biocatalytic dehydration of  $\alpha,\omega$ -dialdoximes. **A:** Reference chromatogram of pure adiponitrile and adipaldehyde dioxime; **B:** Overlay of GC-chromatograms in an activity assay.

The best results for the conversion of an  $\alpha,\omega$ -dialdoxime into its  $\alpha,\omega$ -dinitrile was obtained with the C6 dioxime, adipaldehyde dioxime. Both OxdA and OxdB showed the highest activity for this substrate, reaching up to 46 mU/mg<sub>BWW</sub> for OxdA and 169 mU/mg<sub>BWW</sub> for OxdB. It should be mentioned that the calculated activity values correspond to the formation of one molecule of  $\alpha,\omega$ -dinitrile out of one molecule of  $\alpha,\omega$ -dialdoxime, including two dehydration steps. The activity values peaked at substrate concentration of 12.5 mM and did only slight decrease at higher concentrations, showing great promise for preparative biotransformations with substrate concentrations of 75 mM and higher. To the great delight of the author, adipaldehyde dioxime is the most interesting substrate since its dinitrile adiponitrile is the precursor of hexamethylenediamine (HMDA), the most used  $\alpha,\omega$ -diamine for the synthesis of polyamides, in this case of Nylon 6,6.

Interestingly, the substrate preferences of the Oxds seemed to differ once the higher analogues of the  $\alpha,\omega$ -dialdoximes were investigated. While OxdB seemed to accept the C7 dioxime almost as good as the C6 dioxime, the activity values of the C8-C10 dioximes were drastically lower (**Figure 17**). In contrast to these results, OxdA seemed to have a higher affinity towards the  $\alpha,\omega$ -dialdoximes with longer carbon chains. The usage of the C7-C9 dioximes led to almost the same activity values of the C6 dioxime, but seemingly led to a mediocre substrate inhibition at elevated concentration. The C10 dioxime was the only  $\alpha,\omega$ -dialdoxime that led to increasing activity values even at 75 mM concentration. Noteworthy, the C7-C10 dioxime showed slight precipitation of the substrate at elevated concentrations, but this did not negatively impact the activity values. In its reported crystal structure, OxdA is known to have a very big hydrophobic pocket in its active site, which may be the reason why longer chain  $\alpha,\omega$ -dialdoximes are so well accepted. Unfortunately, no crystal structure has so far been reported for OxdB, which could help to understand the substrate preference of this enzyme.

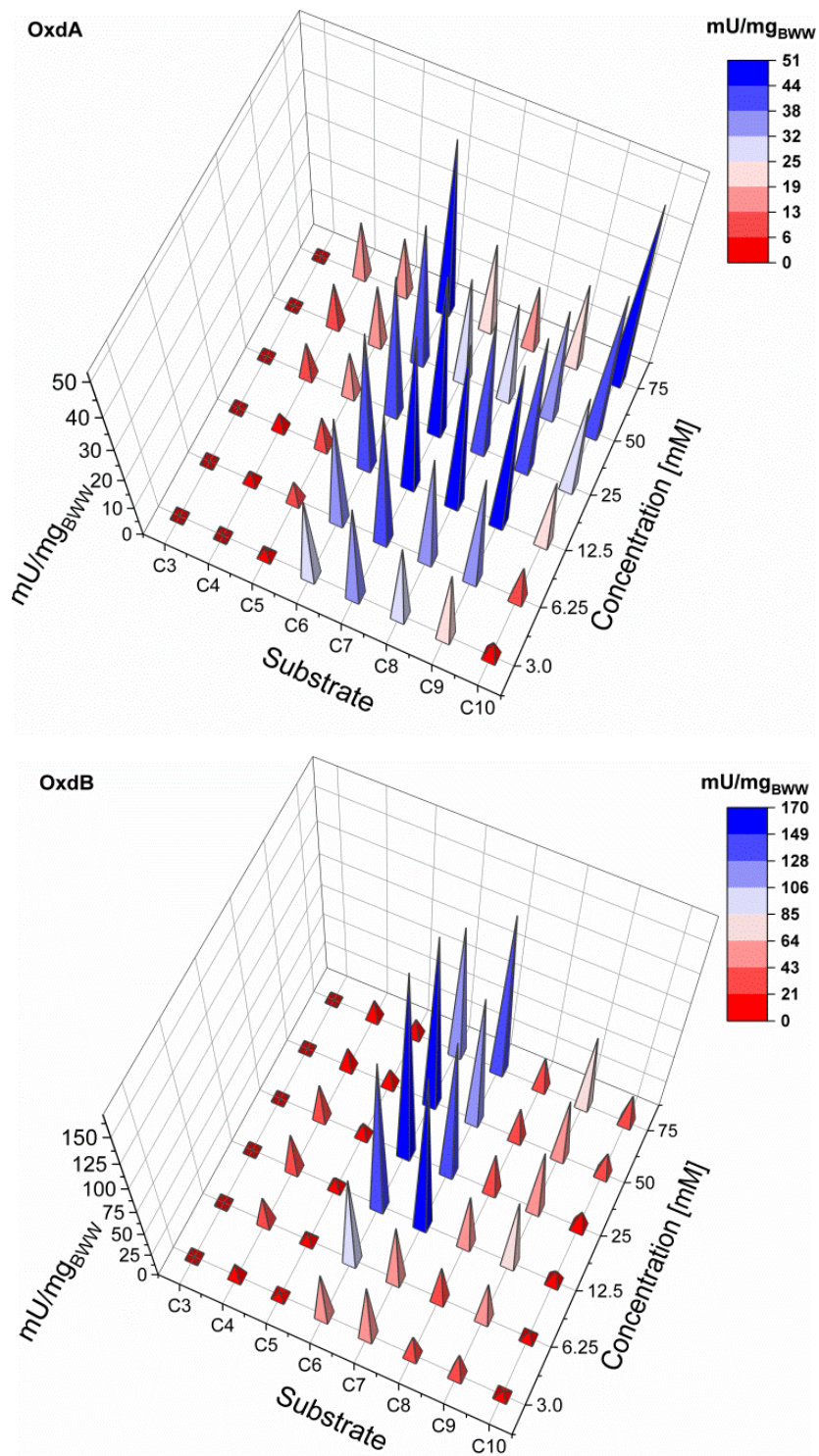
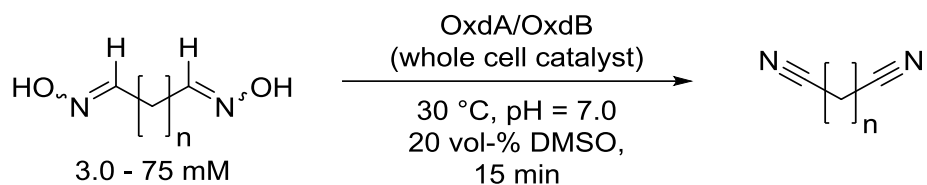


**Figure 17:** Activity values of OxdA and OxdB in mU/mg<sub>BWW</sub> for the C3-C10 dioximes. BWW = Bio wet weight; U-values calculated according to the conversion of one molecule of dioximes to one molecule of dinitrile.



## 4.4 BIOPROCESS DEVELOPMENT FOR THE ADIPONITRILE SYNTHESIS

Based on the obtained results of the substrate scope studies and due to its high industrial relevance, it was decided to conduct a bioprocess development for the adiponitrile synthesis to evaluate the synthetic potential of this process platform. For this upscaling, both OxdA and OxdB were chosen as whole-cell catalysts.

The process development was started by 10 g/L of substrate loading at 100 mL scale, which corresponds roughly to the 75 mM substrate concentration that was used in the analytical scale experiments. Importantly, all experiments were conducted in sealable shaking flasks and the air atmosphere was replaced by an argon atmosphere to push back the oxidation of the Fe<sup>II</sup> atom in the heme to Fe<sup>III</sup>. Since Oxds require iron in its ferrous state (Fe<sup>II</sup>) to be active, it is essential to push back this oxidation.<sup>[54,55,79,80]</sup>

The initial experiments with 10 g/L substrate loading proceeded smoothly and led to complete conversion towards adiponitrile, both with OxdA and OxdB as catalysts (**Table 14**, entry 1 and 3). The isolated yields also reached 75% and 55% and the chemical purity of the adiponitrile was determined *via* <sup>1</sup>H-NMR spectroscopy and GC analysis. To the author's great delight, the obtained adiponitrile was quantitatively pure, underlining the high chemoselectivity of this biocatalytic process. Since the substrate scope study revealed that concentrations of 12.5 mM are sufficient to reach the maximum velocity of both OxdA and OxdB, DMSO was excluded since this simplified the purification by extraction with an organic solvent drastically. No negative impact due to the absence of the organic solvent could be observed. Complete conversion was again achieved for both OxdA and OxdB with isolated yields of 59% and 70% on gram scale (**Table 14**, entry 2 and 4).

Since the substrate adipaldehyde dioxime is a colorless solid and the product adiponitrile is a liquid, one can track the conversion visually by the disappearing of the substrate (for photos, see **Scheme 34**). Due to the relatively high solubility of adiponitrile in water (~50 g/L)<sup>[38]</sup>, no organic phase is formed during the product formation.

Since the overall activity of OxdB against adipaldehyde dioxime is around three times as high compared to OxdA, the further process development was optimized using exclusively OxdB. Since substrate loadings of 10 g/l were easily converted completely to adiponitrile, an up-scaling to 50 g/L (347 mM) was conducted (**Table 14**, entry 5 and 6). Both experiments, with or without DMSO, led again to complete conversion towards adiponitrile with isolated yields of 67% and 80% (up to 2.9 g of pure adiponitrile). During these experiments, a slightly negative effect of DMSO on the long-term activity of OxdB was discovered since the biotransformation without DMSO was completed after 22 hours, whereas the biotransformation with DMSO required 87 hours to complete.

Increasing the substrate loading even further to 100 g/L led to a maximum conversion of 70-75% towards adiponitrile. Even after further biocatalyst was added to the biotransformation, no more conversion was observed. This may result from decreased stability of the enzyme under this high substrate and product loading. Another explanation could be the solubility limit of adiponitrile, which is reached at around 70-75% conversion of 100 g/L adipaldehyde dioxime. Studies by *Jochmann*<sup>[123]</sup> revealed that Oxd whole-cell catalysts are quite rapidly deactivated once a two-phase system is utilized for biotransformations with Oxds.

Nevertheless, complete conversion with 50 g/L substrate loading could already be realized.

**Table 14:** Preparative scale synthesis of adiponitrile with up to 100 g/L substrate loading.

Entry	Oxd	Substrate conc. [g/L]	Biomass [g <sub>BWW</sub> ] <sup>a</sup>	Time [h]	Conv. [%]	Yield [%]
1 <sup>b</sup>	OxdA/ 20% DMSO	<b>10</b>	0.58 (23 U)	96	<b>&gt;99</b>	75 (608 mg)
2 <sup>b</sup>	OxdA	<b>10</b>	1.16 (46 U)	64	<b>&gt;99</b>	59 (480 mg)
3 <sup>b</sup>	OxdB/ 20% DMSO	<b>10</b>	0.51 (57 U)	18	<b>&gt;99</b>	55 (446 mg)
4 <sup>b</sup>	OxdB	<b>10</b>	0.51 (57 U)	15	<b>&gt;99</b>	70 (570 mg)
5 <sup>b</sup>	OxdB /20% DMSO	<b>50</b>	1.50 (171 U)	87	<b>&gt;99</b>	67 (2.47 g)
6 <sup>b</sup>	OxdB	<b>50</b>	1.50 (171 U)	22	<b>&gt;99</b>	80 (2.91 g)
7 <sup>c</sup>	OxdB /20% DMSO	<b>100</b>	0.75 (86 U)	41	<b>70</b>	63 (1.18 g)
8 <sup>b</sup>	OxdB	<b>100</b>	4.00 (456 U)	41	<b>75</b>	63 (4.78 g)

[a] BWW = Bio wet weight, U = Unit, defined as  $\mu\text{mol}/\text{min}$  produced product; [b] 100 mL reaction volume; [c] 25 mL reaction volume.

Surprisingly, it was found during the bioprocess development that DMSO does not have a positive effect on performance of the biotransformation but rather seemed to be hindering the Oxds. Normally, water-miscible cosolvents are utilized to increase the soluble substrate concentration and are often mandatory assets when the substrate loading shall be increased in a process. As a consequence, the author hypothesizes that the solubility of adipaldehyde dioxime has to be sufficient to reach the maximum velocity of the Oxds because it lies significantly above the corresponding  $K_m$  values (or at least high enough to reach a good velocity). It was observed that concentrations of 12.5 mM to 25 mM led to the highest velocity with OxdB (**Figure 17**). These concentrations correlate to substrate loadings of 1.8 g/L to 3.6 g/L of adipaldehyde dioxime. To proof this hypothesis and to rationalize the impact of DMSO on the solubility of the substrate, detailed solubility measurements were conducted by *Gruber-Wölfler a Maier*<sup>[124]</sup> from the TU Graz. By controlled heating of a sample and measuring the transmission of light through it, clear points can be determined. At the clear point, the compound is completely dissolved and the sample is then slowly cooled to determine the cloud point. At the cloud point, precipitation of the compound initiates and the light is scattered stronger.

To simulate the reaction medium of the biotransformations, two different media were selected for the solubility measurements. The first one consisted of 50 mM potassium phosphate buffer (KPB) solution (pH = 7) and the second consisted of 50 mM KPB (pH = 7) with 20 vol% DMSO as cosolvent. These media are the exactly the ones that were used in the biotransformations. The obtained data points were fitted with van't Hoff type equations, whereby a good match was found (**Figure 18**).

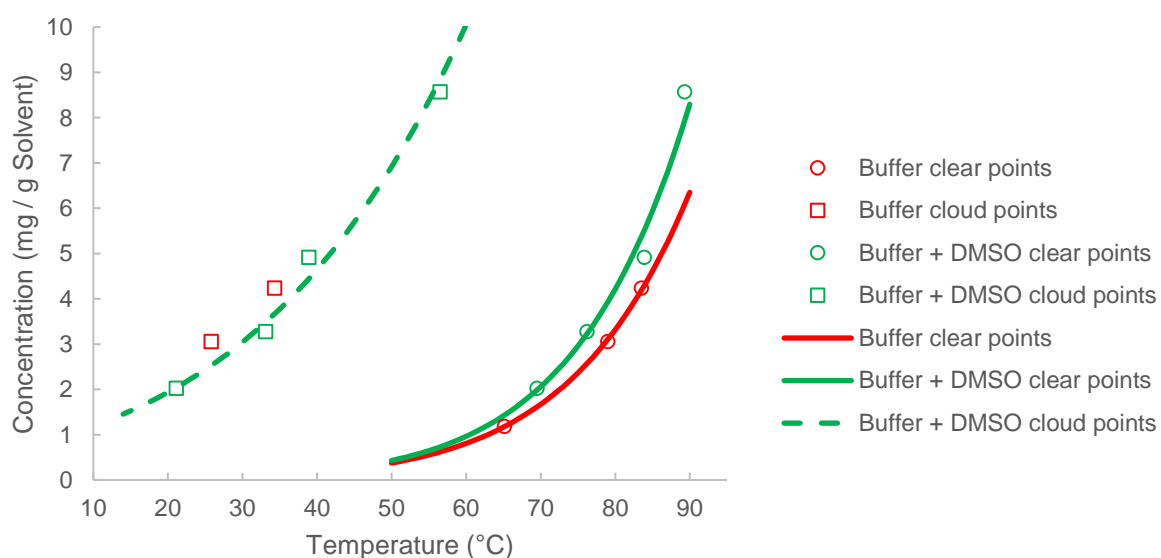


**Figure 18:** Determination of the solubility of adipaldehyde dioxime in presence or absence of DMSO in the reaction medium by *Gruber-Wölfler et Maier*.<sup>[124]</sup>

As one can depict from the data, the cloud points are around 3-4 g/kg substrate loading for both systems. The influence of DMSO on the solubility of adipaldehyde dioxime is only marginable, which explains the good results obtained in the biotransformation in which DMSO was excluded. With 3-4 g/kg of solvent, the active concentrations are in the range of the maximum velocity observed in the substrate scope study. Interestingly, the clear points lie in the range of <1 g/kg, which is below the required concentrations of at least

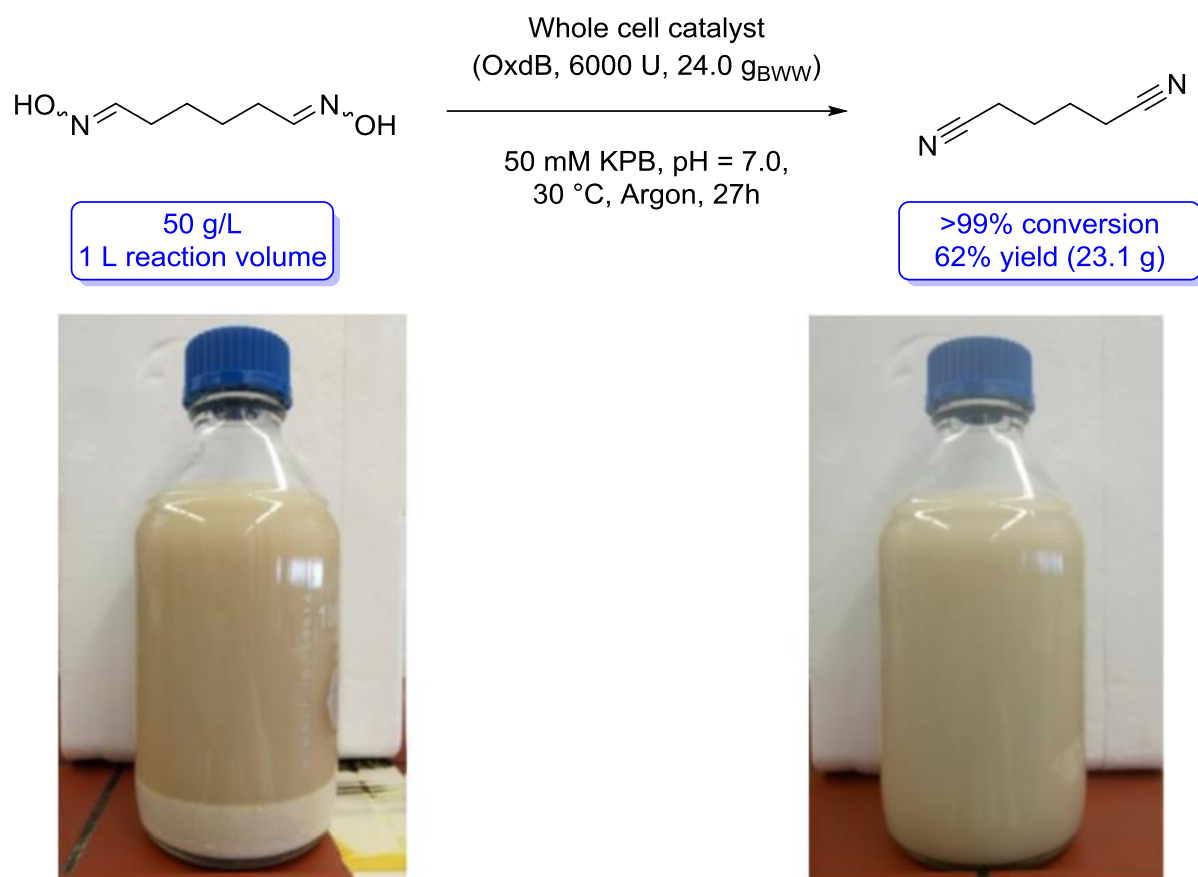
12.5 mM to reach a reasonable velocity. Since the substrate solution was not heated prior to a biotransformation, there are different explanations for the sufficient velocity of the biotransformation.

Since the loading of wet whole-cell catalysts in the biotransformation was in the range of 1-4 g/L, it may have a positive effect on the solubility of the substrate. Another explanation may be the very slow dissolving speed of the dioxime in aqueous media, since the crystal energy of oximes has been found to be very high and may in this case be kinetically or thermodynamically hindered.<sup>[125]</sup> Lastly, the increasing concentration of adiponitrile in the reaction medium may have a positive effect on the solubility of the dioxime since adiponitrile is highly soluble in water and may have a better effect as a cosolvent compared to DMSO.

Whichever explanation may be the case, the results from the substrate loading experiments demonstrate that even under exclusion of a water soluble co-solvent high substrate loadings of up to 50 g/L of adipaldehyd dioxime can be completely converted to adiponitrile with biocatalyst loading of roughly 1-4 wt%.

After rationalizing the influence of the cosolvent on the performance of the biotransformation and selecting the most promising results that were obtained on the 100 mL scale experiments, an experiment on liter scale was conducted to proof that the biocatalytic  $\alpha,\omega$ -dinitrile synthesis can already be easily scaled to bigger volumes. The selected scale was determined to be 1 L reaction volume and a substrate loading of 50 g/L Adipaldehyde dioxime (**Scheme 34**).

To the great delight of the author, an excellent conversion of >99% was observed after 27 hours of reaction time and adiponitrile could be isolated after aqueous extraction with MTBE with an isolated yield of 62% (23.1 g). The chemical purity was >98% according to GC analysis and <sup>1</sup>H-NMR spectroscopy, which demonstrates the high practicability, robustness and scalability of the developed biocatalytic  $\alpha,\omega$ -dinitrile synthesis. These results underline the potential of this Oxd catalyzed process technology for technical scale applications and is the first example of a cyanide-free, biocatalytic production method of this nylon precursor at ambient, neutral conditions in water and with an excellent chemoselectivity.



**Scheme 34:** Synthesis of adiponitrile at a substrate loading of 50 g/L on liter scale. The photos show the reaction mixtures at the start of the reaction (left) and after a reaction time of 27 hours (right).

## 4.5 HIGH CELL-DENSITY FERMENTATION

While the adiponitrile synthesis was very successful with complete conversion at 50 g/L substrate loading and liter scale, a decisive aspect for the technical feasibility of the chemoenzymatic dinitrile synthesis lies in the availability of the biocatalyst. At lab scale cultivation of microorganisms like *E. coli* can be sufficiently conducted in shaking flasks to obtain the cells with a biomass of a few grams per liter. However, for technical scale high biomass concentrations of several hundred grams per liter are necessary to decrease the cost per gram of biocatalyst drastically. In addition, cheap nutrition media should be utilized and the fermentation should be producing a high amount of biomass in a short period of time.

To successfully achieve high cell-density fermentations, one requires specialized equipment (**Figure 19**). In this case, the specialized equipment consists of custom designed glass fermenters of three liter capacity, which are connected to a broad diversity of electrical devices, probes and tubes. The oxygen saturation level, pH value and temperature are constantly measured and digitally controlled during the fermentation. The workgroup of *Friehs* provided this experimental setup and in cooperation with *Risse* a fed batch approach for the high cell-density fermentation by connecting a reservoir with feed medium to the fermenter was chosen. This feed medium contains high amounts of glycerol as a cheap carbon source and is slowly added to the main medium after the initial growth phase of the *E. coli* was completed.

Since OxdB contains a *heme b* group that has to be in its reduced, ferrous (Fe<sup>II</sup>) state to be active, the author decided to conduct two fermentation approaches with different amounts of oxygen saturation. In the first approach, the oxygen saturation was set to  $p = 5\text{-}20\%$  (low O<sub>2</sub>,  $p =$  saturation level). In the second approach, the oxygen saturation was set to  $p = 30\text{-}70\%$  (high O<sub>2</sub>). The oxygen saturation level is referenced to the oxygen content before beginning of the bacterial growth. The preset oxygen level were constantly monitored and controlled by selective addition of sterilized air to the fermentation broth.

Regarding the cultivation medium, the previously utilized autoinduction medium (AI medium), which has the advantage of not requiring an additional induction agent like IPTG was chosen. The autoinduction is started by lactose, which is added to the terrific broth (TB) medium together with glucose. Initially, the *E. coli* cells metabolize the glucose and after depletion of the glucose, expression of the OxdB is initiated by the remaining lactose which activates the *lac* operon.

The above mentioned feed medium also contained high amounts of magnesium sulfate to ensure a high cell growth rate. Both, the feed and AI medium, contained two antibiotics (34 µg/mL chloramphenicol, 100 µg/mL carbenicillin) to ensure that only cells harboring the plasmid containing the OxdB gene are able to grow.

The pH value was held constant by two control bottles that contained NaOH as base or H<sub>3</sub>PO<sub>4</sub> as acid, which were added to the culture medium if necessary. Lastly, a bottle containing an anti-foaming agent was attached to the fermenter to inhibit excessive foam formation during the fermentation (**Figure 20**).



**Figure 19:** High cell-density equipment utilized for the overexpression of OxdB in *E.coli* BL21 (DE3) Codon<sup>+</sup> RIL. Left fermenter: Low oxygen level (low O<sub>2</sub>), right fermenter: High oxygen level (high O<sub>2</sub>).



**Figure 20:** Bioreactor with external flasks containing feed medium (A), acid (B), base (C) and anti-foaming agent (D).

The high increase in biomass could very well be observed over the time by the formation of the light brown biomass, compared to the dark brown culture medium in the beginning (**Figure 21**).

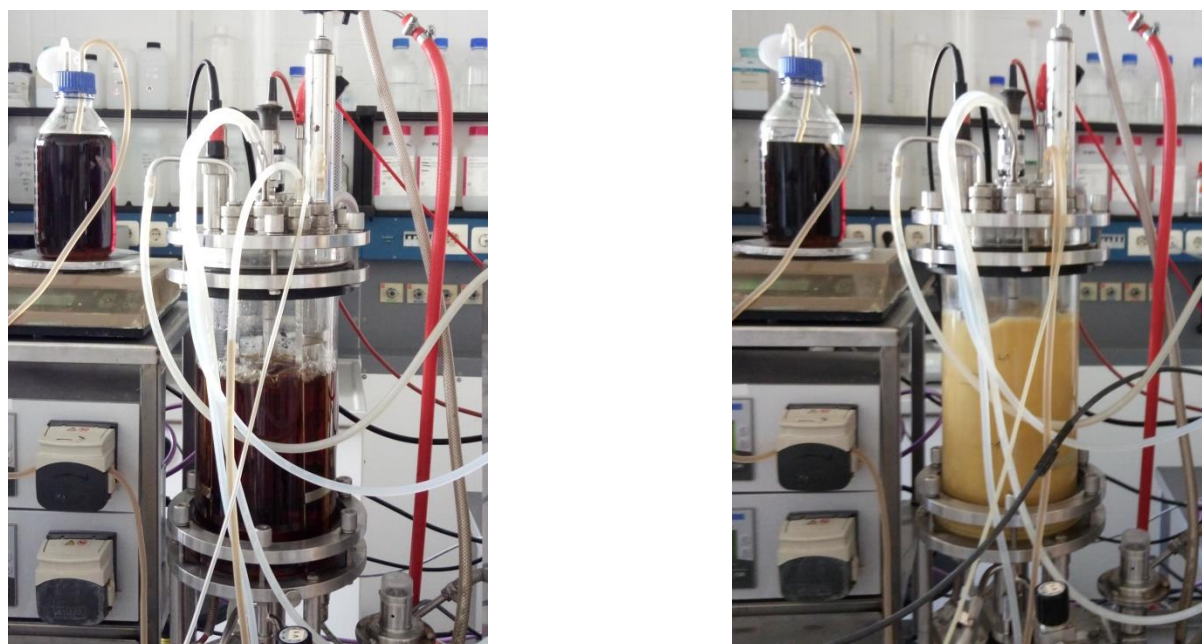


**Figure 21:** A fermentation in the bioreactor at the beginning (left) and after 24 hours (right).

After 72 hours, the feed medium was exhausted and the high cell-density fermentation was completed. After filtration and washing of the biomass, two pellets were obtained. From the low  $O_2$  fermentation, 375 g of wet biomass were obtained. From the high  $O_2$  fermentation, 260 g of wet biomass were obtained. As one can see from **Figure 22**, a slight difference in color can be observed for both pellets.

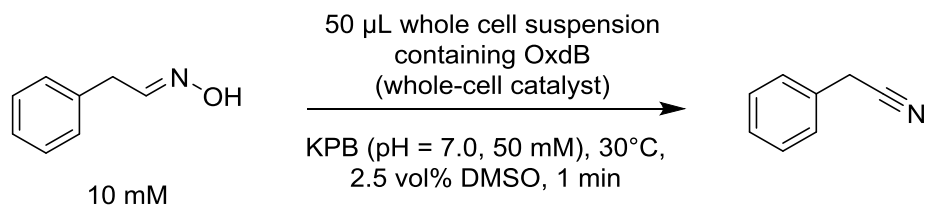


**Figure 22:** The obtained pellets (wet biomass) from the conducted high cell-density fermentations (left bag: Low  $O_2$ , right bag: High  $O_2$ ).



After the fermentation, the activity of the biocatalyst and the overexpression of the OxdB had to be verified (**Table 15**). For this, the standard activity assay for the conversion of phenylacetaldehyde oxime (PAOx) was conducted (for the reaction conditions, see chapter **9.3.2.2**).

**Table 15:** Determined activity values of the obtained wet biomass.



	OxdB (low O <sub>2</sub> )	OxdB (high O <sub>2</sub> )	OxdB (shaking flask)
protein conc. (mg/mL)	23.2	24.3	20.5
activity (PAOx) (mU/mg <sub>BWW</sub> )	57	51	2180 <sup>[103]</sup>

While the protein concentration of the crude extracts of the *E. coli* were quite in the same range, the overall activity of the *E. coli* cells from the high cell-density fermentations was drastically decreased in comparison to the ones from shaking flask cultivation. As a consequence, the overexpression of the OxdB was checked *via* SDS-PAGE (**Figure 23**). The OxdB was successfully expressed in all cultivations (40 kDa, red circle), but the expression was slightly better in the shaking flask cultivation compared to the high cell-density fermentation. Concordingly, it cannot be explained why the activity is so drastically lower (fourty times lower) for the high cell-density fermentations with only these analytical results.

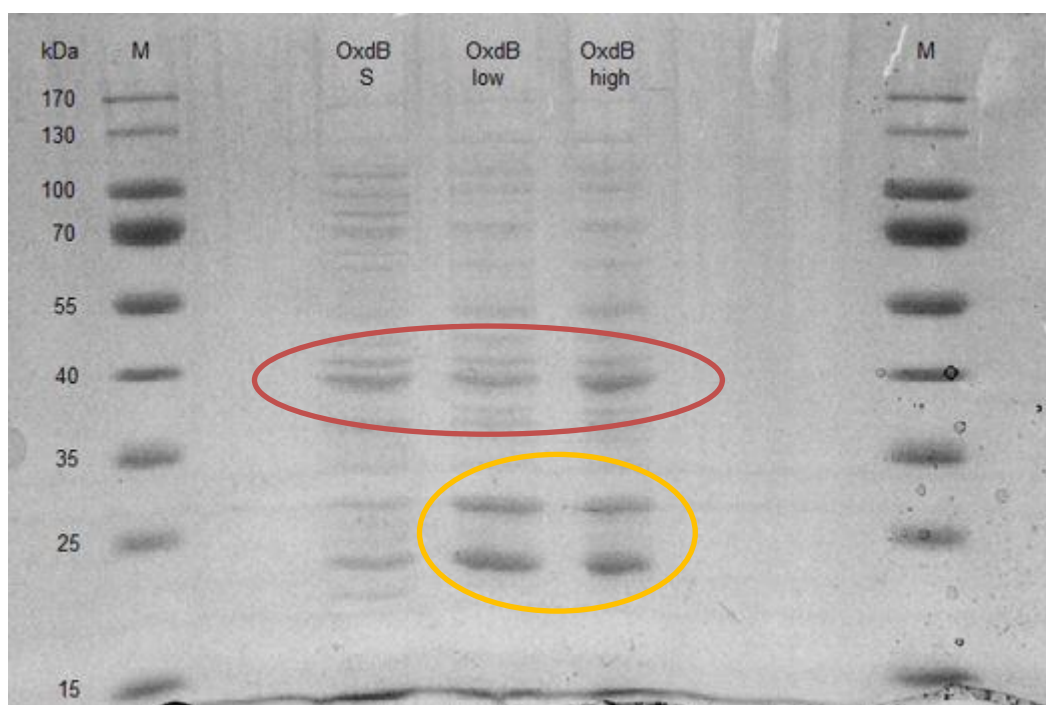


**Figure 23:** SDS-PAGE of the crude extracts containing OxdB. S = Shaking flask, low = low O<sub>2</sub>, high = high O<sub>2</sub>, M= Marker.

There are possible explanations for the drastically lower activity of the high cell-density fermentations that should be looked into in future experiments.

1. The iron atom is in its ferric form (Fe<sup>III</sup>) and not the required ferrous form (Fe<sup>II</sup>) inside the active site. This hypothesis could be proven by adding a reducing agent (like sodium dithionite) to the activity assay. If the activity is recovered, this hypothesis is confirmed.
2. The *E.coli* could not form enough *heme b* to incorporate it inside of the OxdB. This could be investigated by comparing the OxdB of shaking flask cultivation and high cell-density fermentation with mass spectrometry since OxdB without a *heme b* group has a lower molecular weight than one with a *heme b* group.
3. Due to iron depletion, other metals were incorporated into the active site of the OxdB. As a consequence, the OxdB would not be active.

In summary, first approaches towards the production of big quantities of Oxds have been conducted for the first time. Further steps, like analysis of the fermentation protocol, strain selection, medium selection and additive dosage are tasks for the future to establish a successful high cell-density fermentation protocol.

## 4.6 IMMOBILIZATION OF OXDB FROM *BACILLUS SP.* OXB-1 BY CROSSLINKING WITH GLUTARALDEHYDE TO OBTAIN CLEAS FOR PROCESS INTENSIFICATION OF LINEAR ALIPHATIC $\alpha,\omega$ -DINITRILE SYNTHESIS

### 4.6.1 OVERVIEW OF DIFFERENT ENZYME IMMOBILIZATION STRATEGIES

Although enzymes excel at chemo-, regio- and enantioselectivity and operate under very mild conditions in mainly aqueous media, they often lack long-term stability under process conditions.<sup>[8]</sup> As a consequence, efficient immobilization strategies had to be developed over the last decades to ensure the long-term stability of enzymes. This allows for efficient recycling of the biocatalyst, which lowers the overall cost of the process drastically because the expression, purification and optional immobilization of an enzyme are a very big cost factors. Additionally, immobilization of enzymes facilitates the easy separation of the biocatalyst from the reaction mixture which drastically simplifies workup procedures. As a consequence, enzyme leaching and hence residual levels of protein in the final product are nearly negligible. Since industrial production processes can differ drastically by terms of the reactor type and size, temperature, pressure or mechanical stress, one has to keep these parameters in mind when selecting a certain immobilization method.<sup>[8,126]</sup> Especially mechanical abrasion can lead to rapid decomposition of the immobilized catalyst.

To decide which immobilization one should select, the most prominent approaches shall be presented in the following (**Figure 24**).

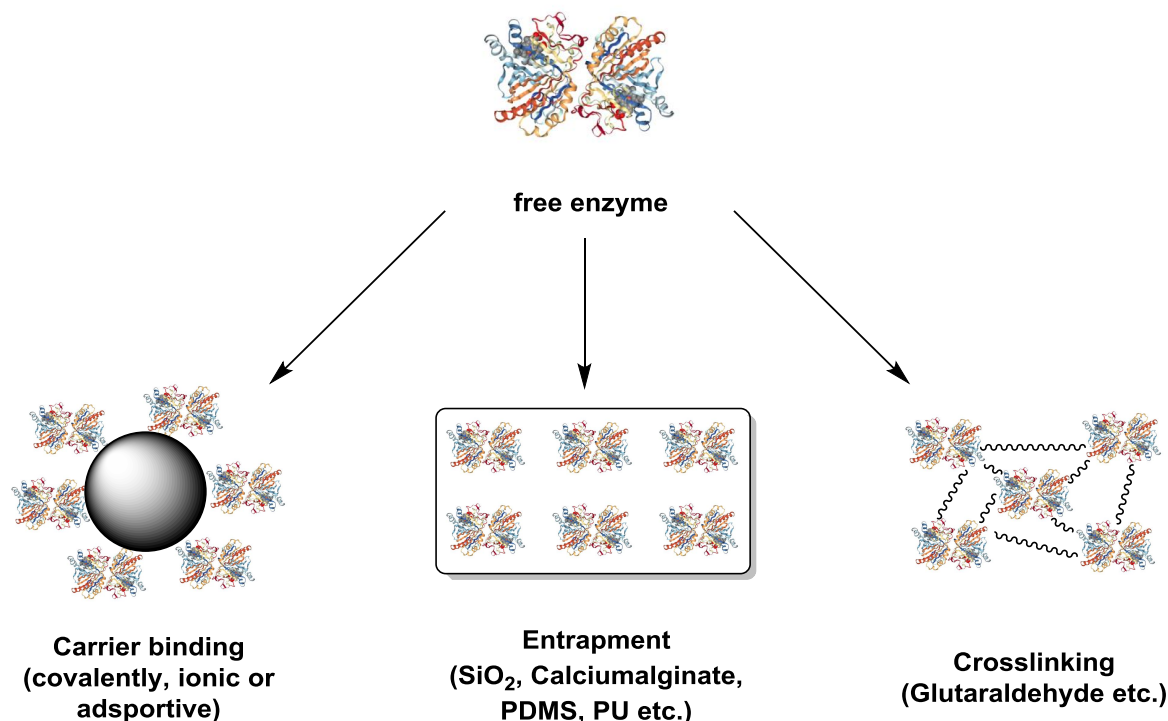


**Figure 24:** Different types of immobilization methods for enzymes.

In principal, one can divide the immobilization methods for enzyme immobilization into three categories:

1. Carrier binding, where the carrier mostly consists of a polymer bead that can optionally be chemically modified on its surface.
2. Entrapment of the enzyme either by an anorganic or organic matrix.
3. Crosslinking of the enzyme with itself by applying a crosslinking agent.

#### 4.6.1.1 Enzyme immobilization by carrier binding

Regarding carrier binding, this method is nowadays broadly applied due to the great variety of different available resins for immobilization. Some companies (Purolite, Resindion) have completely specialized themselves to the production of immobilization resins.<sup>[127,128]</sup> Most resins are made out of Poly(methyl methacrylate) (PMMA), styrene or copolymers of the former with other building blocks like divinylbenzene (DVB). The beads have a spherical shape and may be chemically modified to allow immobilization by different types of interaction between enzyme and carrier (**Figure 25**).

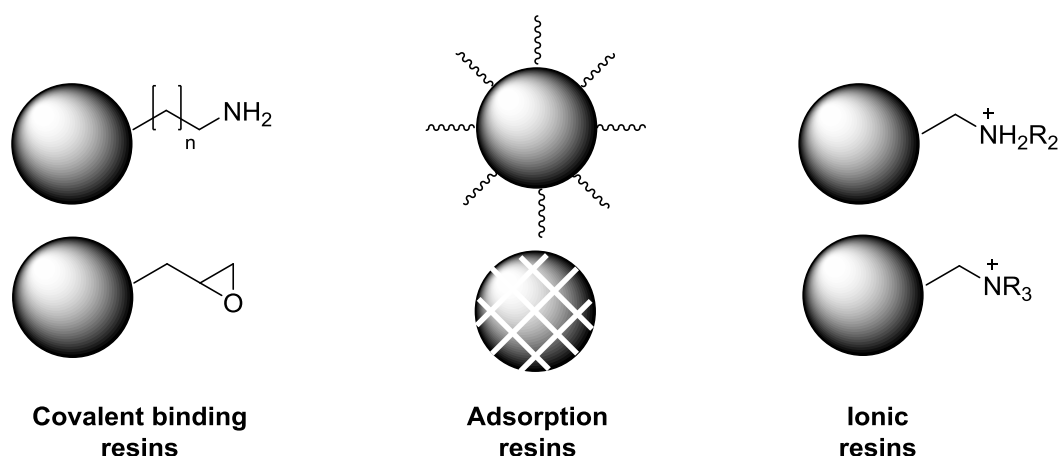


**Figure 25:** Chemically modified polymer beads (carriers) for enzyme immobilization with different modes of interaction.<sup>[127]</sup>

Modification of PMMA beads with short carbon linkers that contain a terminal amino or epoxy moiety results in resins that can bind enzymes by covalent binding. The epoxy ring can bind by nucleophilic attack of amino acid side chains like the ones of lysine, serine etc., while the amino spacers are preactivated with glutaraldehyde. After activation, the glutaraldehyde reacts with free amino side chains to form imino bridges between enzymes and carrier. However, the concrete binding mode is highly complex and the above mentioned description only represents a simplification.<sup>[129]</sup> As one can imagine, covalent binding represents a big interference in the complex interactions that determine the tertiary structure of an enzyme. As a result, major losses in enzyme activity are observed. However, covalent binding is the strongest possible interaction and leads to no or only negligible leaching of the enzyme off the carrier.

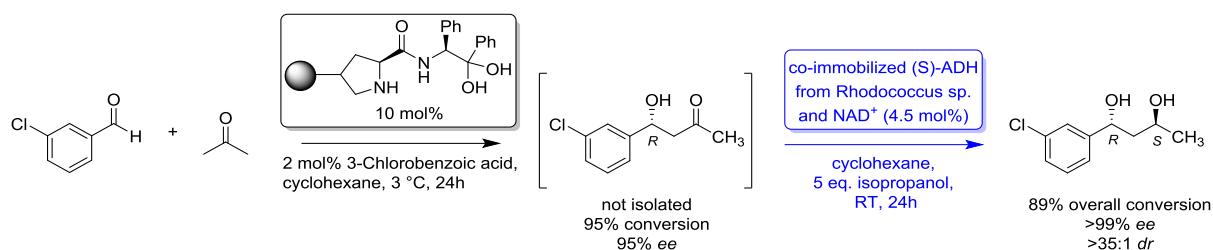
Other resins adsorb the enzymes by hydrophobic interaction. Most prominently, octadecyl groups are attached to the surface of the resins to increase the hydrophobicity of the carrier. Alternatively, enzymes can be adsorbed by highly porous styrene resins with big cavities. The enzyme wanders into the cavities, being surrounded by a hydrophobic environment. This method is milder than covalent binding, but may still lead to strong distortion of the enzyme structure because the hydrophobic areas of the enzyme will mainly try to interact with the carrier. Many enzymes however are mainly hydrophilic on the surface, turning the enzyme inside out and potentially deactivating it.

Lastly, one can attach substituted amino groups on the surface of a resin. These amino groups can either directly be positively charged (for quarternary amines) or be preactivated by acidic treatment (for tertiary amines). If the isoelectric point of an enzyme is known, adjustment of the pH above it turns the enzyme into a polyanion. As a result, it is strongly bound to the carrier by ionic interaction without distorting its tertiary structure.

#### 4.6.1.2 Enzyme immobilization by entrapment

Regarding the entrapment of an enzyme in an anorganic or organic matrix a broad variety of reported matrices exists, however only a small selection will be presented here. One of the oldest methods is the immobilization in calcium alginate beads. Due to the rather big pore size of the alginate beads, preferably whole cell catalysts are immobilized with this method. By dropping a suspension of whole cells and sodium alginate in a solution of calcium chloride, insoluble calcium alginate is formed and builds a protective barrier around the whole cells.<sup>[130]</sup> However, these beads are not very mechanically robust.

Another entrapment method is the immobilization in hydrogels. Hydrogels based on polyvinyl alcohol are already well established and utilized for industrial processes (Lentikats).<sup>[8,131]</sup> However, since these hydrogels represent an open polymer matrix, leaching of the enzyme can occur. As a consequence, mainly whole-cell catalysts are utilized for immobilization. Alternatively, prior crosslinking of the enzyme increases the size of the biocatalyst and reduces leaching as well.<sup>[131]</sup> A rather new approach is the immobilization of enzymes in hydrogels that are based on polyacrylic acid or polyacrylamide, so-called superabsorbers.<sup>[132]</sup> The superabsorbers provide an aqueous, natural environment for the enzyme, which is completely immobilized in the superabsorber. By applying a liquid, organic phase to the reaction, one can easily separate the immobilized enzyme and superabsorber by filtration. Hence, recycling of the immobilized biocatalyst is rather easily conducted. In 2014, *Gröger et al.* utilized the immobilization of an ADH in a superabsorber matrix for the combination of an organocatalytic, enantioselective aldol reaction followed up by a biocatalytic reduction with the immobilized ADH (**Scheme 35**).<sup>[132]</sup>



**Scheme 35:** Co-immobilization of a (*S*)-selective ADH from *Rhodococcus sp.* in superabsorber, reported by Gröger *et al.*<sup>[132]</sup>

Instead of using an open-pored prepolymerized organic matrix, one can also consider completely enclosing an enzyme in an impenetrable organic matrix by polymerizing the organic matrix *in situ* as a suspension with the enzyme. In this case, the enzyme is contained in an aqueous environment surrounded by a solid organic matrix. As an example, polydimethylsiloxane (PDMS) can be mixed with a pre-made enzyme solution and dropped into a solution of polyvinylalcohol in water. The formed droplets slowly polymerize, irreversibly trapping the enzyme inside in discrete aqueous droplets. Starting in 2005, *Ansorge-Schumacher's* group immobilized several lipases in PDMS beads for esterifications and dynamic kinetic resolutions.<sup>[133]</sup> They could impressively show the equally distributed aqueous droplets in the organic matrix, proving the native environment for the enzyme inside the PDMS beads.

In 2014, *Langermann et al.* expanded this method towards the biocatalytic, enantioselective cyanation of benzaldehyde with oxynitrilases utilizing commercially available Sylgard 184, the monomer of polydimethylsiloxane.<sup>[134]</sup> They stressed the point that the used organic phase for the reactions has to be saturated with water to prevent a slow extraction of the aqueous phase from the PDMS beads.

Drawbacks of this intriguing method are the rather long preparation time that can last several days because of the slow curing of PDMS at low temperature like room temperature. To decrease the curing time, one can increase the temperature. However, this may lead in conjunction with the curing time to strong inactivation of the biocatalyst. On top of that, a highly reproducible protocol for highly monodisperse PDMS is very difficult to establish, as *Rivadeneira* could show in his bachelor thesis under supervision of the author of this thesis.<sup>[135]</sup> In his work, the aldoxime dehydratase from *Bacillus sp.* OxB-1 (OxDB) was immobilized as crude extract and as whole cell-catalyst (in *E.coli*) in PDMS beads.

To circumvent the drawbacks of the long curing time and reproduction issues, *von Langermann et al.* changed the polymer matrix in 2017 towards polyurethanes.<sup>[136]</sup> By premixing of the enzyme with the polymer precursor, the same highly dispersed aqueous droplets are obtained as with the PDMS method. However, the polyurethane precursors rapidly and controllable polymerizes at ambient temperature once ultraviolet light is radiated upon him. Completely cured polyurethane is obtained in only five minutes, which drastically decreases the stress on the immobilized enzyme. The polyurethane is obtained as a solid plate that can be grinded to obtain it as small chips with a big surface area. As with the PDMS method, no or only negligible leaching can be observed.<sup>[136]</sup>

#### 4.6.1.3 Enzyme immobilization by cross-linking

The last category to immobilize an enzyme is by crosslinking it with a crosslinking agent like glutaraldehyde. While several crosslinking agents exist, the most prominent is glutaraldehyde (1,5-pentanedial). The crosslinking can then be applied to the corresponding enzyme formulation to crosslink it. One of the first methods was to crosslink crystallized enzymes to obtain crosslinked enzyme crystals (CLECs).<sup>[8]</sup> While these represent a good formulation, the biggest drawback is the often not achievable crystallization of the enzyme and the prior, expensive and time-intensive purification of the enzyme. Another approach lies in the easily achievable precipitation of an enzyme, followed by a crosslinking protocol. If one uses this approach, he obtains crosslinked enzyme aggregates (CLEAs). Instead of purified enzyme, one can simply utilize crude extract for the immobilization protocol. The precipitation acts as a purification step on itself, combining purification and immobilization in one step.

The benefit of CLEAs in comparison to free enzymes lies in the often improved operational stability in terms of tolerance against heat, organic solvents and autolysis. Additionally, the CLEAs show a low tendency of leaching and do not require an often rather expensive carrier to conduct the immobilization.<sup>[8]</sup> The crosslinking agent can also be mixed with other components that will help to finetune and optimize the immobilization, like amino containing sugars (chitosan) or siloxanes.<sup>[131]</sup> As with the immobilization on preactivated amino resins, the crosslinking of the enzymes in CLEA formation are rather complex and are not limited to imine formation.<sup>[129]</sup> As a consequence, further reduction with reagents as sodium hydroboride ( $\text{NaBH}_4$ ) may in principle be conducted but rarely shows any benefit. Especially the group of Sheldon has developed many contributions on the field of CLEA research, allowing a broad range of biotransformations with several enzyme classes to be conducted with CLEAs.<sup>[8,137,138,139]</sup>

Regarding Oxds, no investigations on immobilization have been conducted until today. Because of that, the author decided to pursue this challenging endeavor by choosing CLEAs as the first method for the immobilization of Oxds because of the well documented and rather straight-forward protocols in literature. Additionally, as mentioned earlier, the encapsulation of Oxds in PDMS beads was conducted by *Rivadeneira* under the supervision of the author.<sup>[135]</sup> However, the encapsulation attempt was not investigated further.

#### 4.6.2 EXPRESSION AND PURIFICATION OF OXDB(C<sub>HIS6</sub>) BY NI-NTA AFFINITY CHROMATOGRAPHY

Firstly, the aldoxime dehydratase from *Bacillus sp.* OxB-1 (OxDB) had to be heterogeneously expressed in *E. coli* BL21(DE3) cells. For simpler purification of the enzyme in later stages, the gene encoding for the OxDB harbored a sixfold C-terminal His-Tag (His<sub>6</sub>) and was located in a pET-22b(+) vector. The cultivation and overexpression was conducted on 500 mL scale in two different protocols. The first method for expression utilized TB-Medium and induction of expression by addition of IPTG. The other method utilized Auto-Induction medium (AI Medium), for which no additional reagents for expression are necessary.

Both protocols led to successful expression of the OxDB (**Figure 26**, Lane 1,6, 42 kDa).

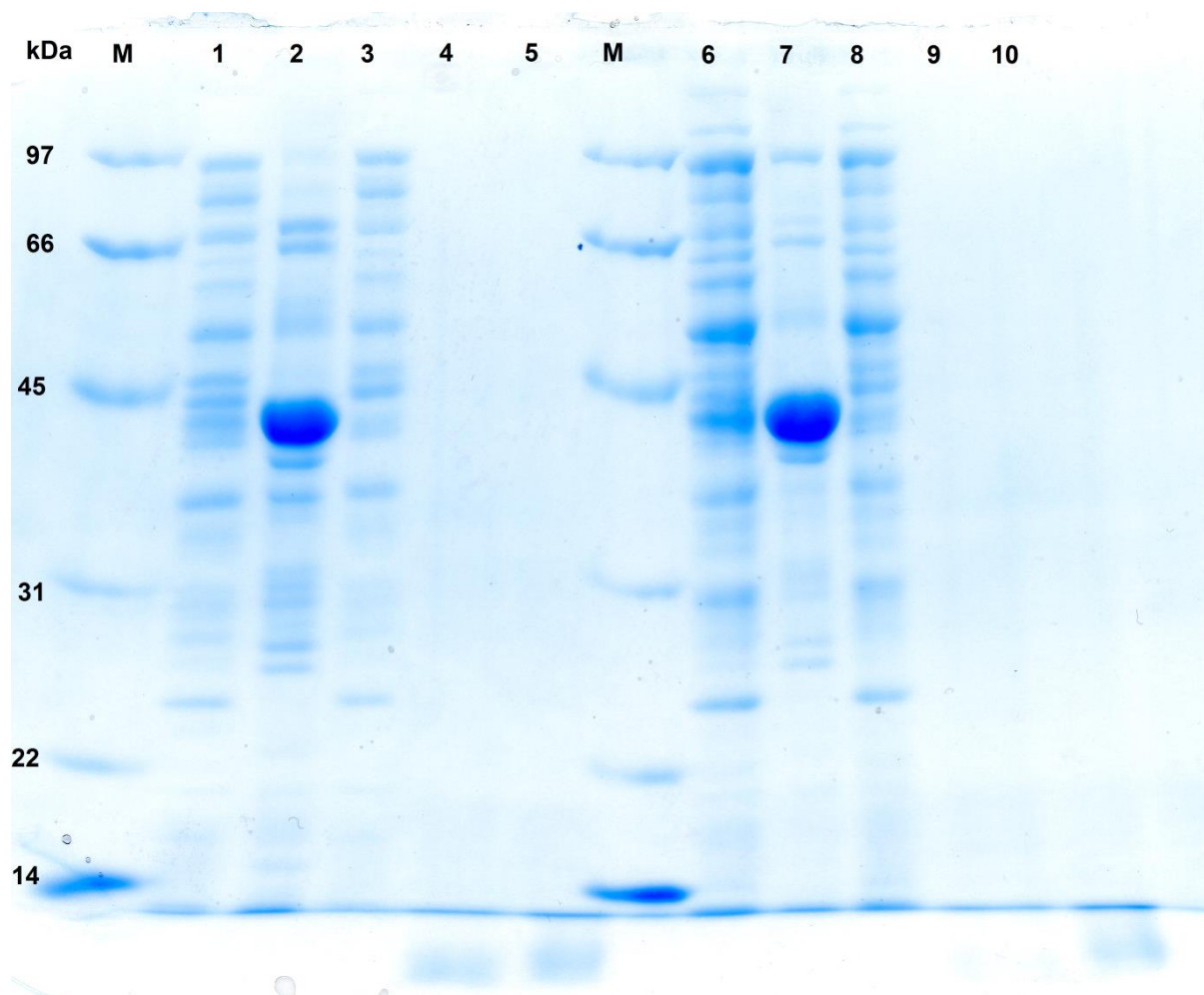


**Figure 26:** SDS-PAGE analysis of the OxDB(C) expression in *E. Coli* BL21 (DE3). Lanes: M = Marker, Lanes 1-5: Crude extract (AI protocol), purified OxDB, Ni-NTA-column elution, CLEA supernatant, Washing fraction; Lanes 6-10: Crude extract (TB protocol), purified OxDB, NiNTA-column elution, CLEA supernatant, Washing fraction.

The OxDB was purified by means of Ni-NTA affinity chromatography (**Figure 27**) yielding the OxDB in a high purity with only residual parts of other proteins remaining (**Figure 26**, Lane 2,7).



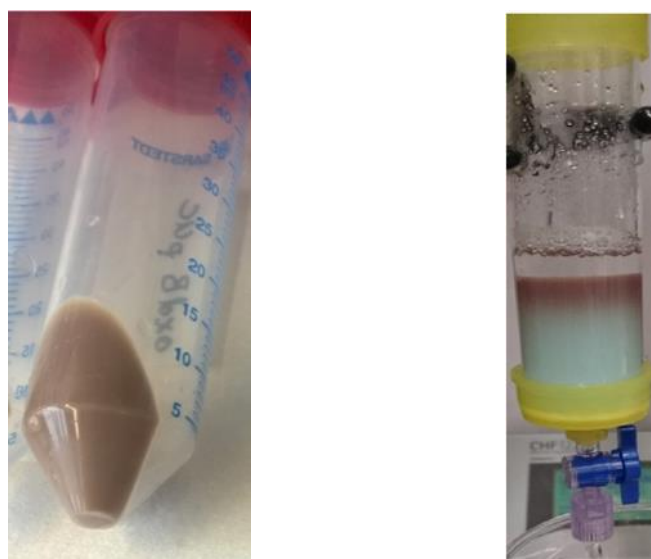


**Figure 27:** *E. coli* pellet (left) harboring OxdB(C<sub>His6</sub>) and purification via Ni-NTA affinity chromatography (right).<sup>[140]</sup>

#### 4.6.3 CLEA FORMATION AND ACTIVITY QUANTIFICATION IN AQUEOUS MEDIUM

The purified OxdB was subsequently immobilized by CLEA formation (**Table 16**). Since the crosslinking by glutaraldehyde represents a major incision in the conformation of enzyme, the resulting activity recovery is always below the level of the non-immobilized enzyme. Nevertheless, the CLEAs could be obtained with an activity recovery of up to 23% (**Table 17**). For the cross-linkings, 0.5-2.0 wt% of glutaraldehyde were utilized to investigate its influence on the CLEA formation.

**Table 16:** Activity of different OxdB(C<sub>His6</sub>) formulations including CLEAs (0.5-2.0 wt% glutaraldehyde).

Entry	Formulation	mg/mL	Activity (mU/mg)
1	Purified OxdB(C <sub>His6</sub> )	4.72	1630
2	Crude extract	7.02	4940 <sup>b</sup>
3	Supernatant CLEA 0.5-2.0	n.d.	0
4	Washing fraction 0.5-2.0	2.64-3.54	127-284
5	CLEA 0.5-2.0	700-800 µg <sup>a</sup>	336-372

a. dry weight; b. mU/mL; n.d. = not determinable

**Table 17:** Immobilization yield, efficiency and activity recovery of the obtained CLEAs (0.5-2.0 wt% glutaraldehyde).

CLEA	Immobilization yield [%]	Immobilization efficiency [%]	Activity recovery [%]
0.5	83	26	21
1.0	90	23	21
2.0	92	25	23

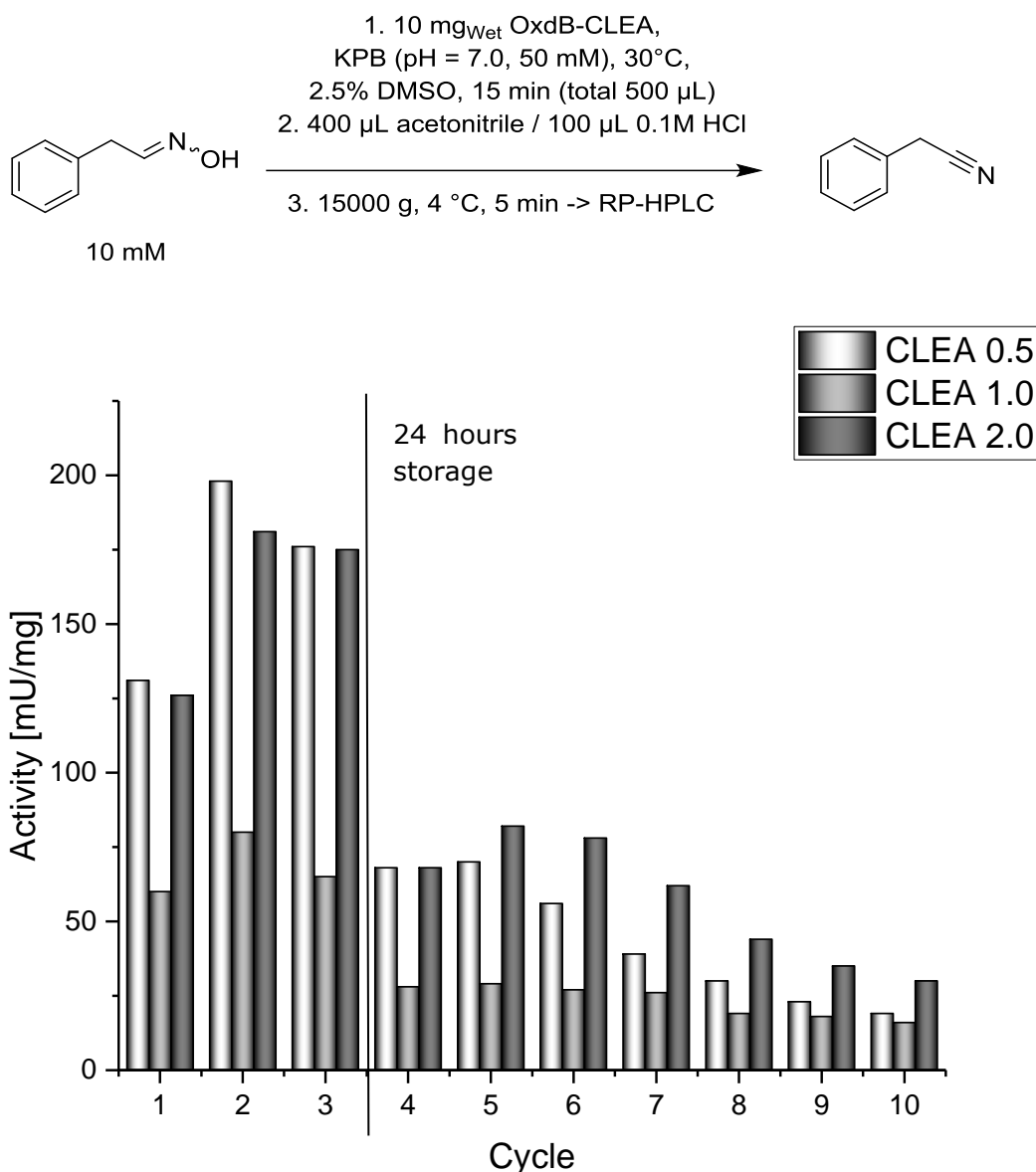
Due to interference of glutaraldehyde with the Bradford-Assay, which determines the protein concentration of solutions, no quantitative result could be obtained for the protein concentration of the CLEA supernatant.<sup>[129]</sup> Nevertheless, the SDS-PAGE (**Figure 26**) showed no detectable protein content and the results were promising for further experiments. The formed CLEAs were hence used for a recycling study in aqueous media.

#### 4.6.4 RECYCLING STUDY FOR LONG-TERM STABILITY DETERMINATION OF OXDB-CLEAS IN AQUEOUS UND ORGANIC MEDIUM

For 10 cycles, the CLEAs showed reappearing activity (**Scheme 36**). However, it decreased quite drastically with only ~20 mU/mg remaining activity at the 10<sup>th</sup> cycle. The reason for the declining activity has not been finally determined, since it may result from leaching of the enzyme out of the CLEAs, the inactivation of the enzyme by oxidation of the heme group or because of deactivating effects of the 50 vol% acetonitrile which was used to quench the activity assay. Compared to the cosolvent study from **chapter 4.3**, in which the highest amount of the cosolvents did not exceed 20 vol% because a higher amount deactivated the whole-cell catalysts very rapidly, 50 vol% is by far the highest achieved amount of water-miscible cosolvent investigated so far. Considering the whole amount of time that the Oxd was in contact with 50 vol-% acetonitrile, it would account for over three hours which was the longest time investigated in the prior stability study in **chapter 4.3**.

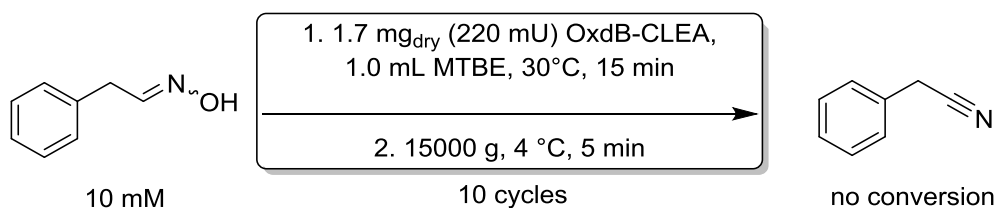
The obtained results show a potential stabilization of the OxdB by crosslinking since the CLEAs can be recycled for several cycles. However, the utilization of 50 vol% acetonitrile for quenching the activity assay may be the reason for the rather quick declining activity values. Interestingly, the initial activity of the CLEAs in the first reaction cycle is always lower than the subsequent ones. This may result from conformational changes due to freeze-drying and hence lower accessibility of the active sites in the beginning (**Scheme 36**, Cycle 1). Furthermore, the CLEAs retained around 40% of their activity after storing them for one day at room temperature after the first three reaction cycles. These intriguing results for the first ever approach to obtain long-term stability of aldoxime dehydratases is promising for further optimization.

The subsequent seven cycles (**Scheme 36**, Cycle 4-10) showed the same phenomenon with the rising activity after the first cycle and then slowly decreasing activity with only up to 20 mU/mg remaining activity after the 10<sup>th</sup> cycle.



**Scheme 36:** Results of the recycling study of the obtained CLEAs.

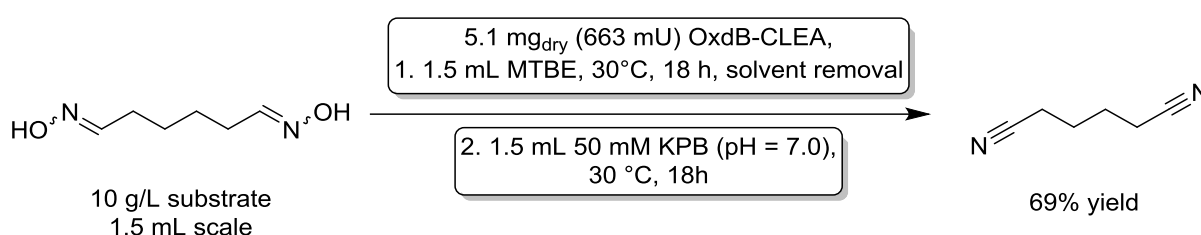
Beside the recycling study in aqueous medium, a further recycling study in organic medium (MTBE) with the freeze-dried CLEAs was conducted because earlier results of *Jochmann*<sup>[123]</sup> showed high tolerance of whole cells containing OxdB against MTBE. However, no conversion could be detected even after the first cycle (**Scheme 37**). This result indicates that Oxds either require an aqueous phase for the reaction or that the organic medium inactivates them.



**Scheme 37:** Recycling studies of OxdB(C<sub>His6</sub>)-CLEAs in organic medium.

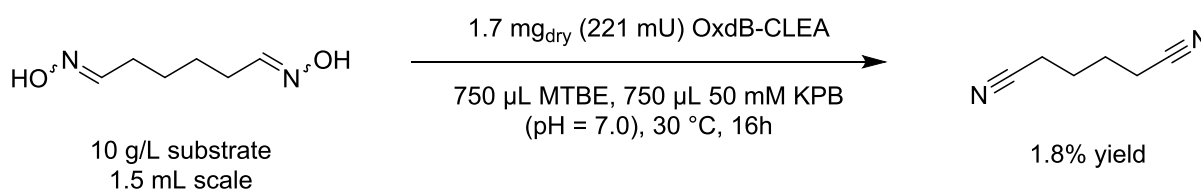
## 4.6.5 ADIPONITRILE SYNTHESIS IN ORGANIC, AQUEOUS AND BIPHASIC SYSTEMS

To validate the results of the long-term stability studies, a two-step experiment was conducted in which the biotransformation of (*E/Z*)-adipaldehyde oxime was conducted first in pure organic medium (MTBE). In accordance with the previous study, no product (adiponitrile) was detected *via*  $^1\text{H-NMR}$  analysis in the organic phase and hence no conversion was achieved. However, the remaining CLEAs and the product were after evaporation of the solvent mixed with KPB (50 mM, pH = 7.0) and the biotransformation in this aqueous medium yielded 69% of adiponitrile after 18 hours at 30 °C. This indicates that while the CLEAs may not be active in purely organic media, they are also stable and not strongly deactivated even after 18 hours remaining in the organic medium (**Scheme 38**).



**Scheme 38:** Adiponitrile synthesis with OxdB(C<sub>His6</sub>)-CLEAs in organic and aqueous medium.

Hence, a biotransformation with the same amount of (*E/Z*)-adipaldehyde oxime was conducted in a biphasic system consisting of 1:1 (v/v) MTBE/KPB (50 mM, pH = 7.0) (**Scheme 39**). Since (*E/Z*)-adipaldehyde oxime is almost insoluble in MTBE, the whole substrate remained in the aqueous phase, while the product adiponitrile is constantly extracted into the organic phase.



**Scheme 39:** Adiponitrile synthesis attempt in a biphasic system with OxdB-CLEAs.

According to  $^1\text{H-NMR}$  analysis, 1.8% yield of adiponitrile was obtained after 18 hours. This result indicates that the CLEAs may rather quickly be deactivated by the interface of the two phases.

In conclusion, further immobilization methods should be investigated in the near future. Especially polymer carriers seem to be promising since crosslinking by glutaraldehyde to form CLEAs also worked sufficiently. Especially free amino groups are used in the crosslinking and covalent binding to polymer carriers that are based on linking *via* epoxy groups. These carriers may also allow operating in biphasic systems.

## 4.7 OUTLOOK FOR THE TECHNICAL FEASIBILITY OF THE BIOCATALYTIC ADIPONITRILE SYNTHESIS

The overall progress for the biocatalytic synthesis of linear, aliphatic  $\alpha,\omega$ -dinitriles (especially for adiponitrile) in this work represents a very good foundation for the further development of an industrially feasible process. The already achieved high substrate loadings of 50 g/L, which can be quantitatively converted towards adiponitrile in liter scale prove the scalability of this process.

To increase the economical feasibility, first endeavors for the high cell-density fermentation of OxdB expressing *E. coli* have been conducted. The initial results allow, despite the low activity of the produced biomass, a further development in this field. Once optimized, Oxds will be available at a comparable cheap price. If improved mutants of the Oxds are developed in the future, one can already rely on the established high cell-density fermentation protocols to produce highly productive biocatalysts.

Additionally, first results for the immobilization of Oxds have been developed. Crosslinking with glutaraldehyde yielded CLEAs that showed reappearing activity for at least 10 cycles of activity assays. Additionally, the CLEAs tolerated 50 vol% of acetonitrile during the quenching and work-up procedures and could be stored for several days. Additionally, the activity recovery after the CLEA formation was quite high with 21%. In the future, further immobilization methods like binding to polymer carriers or immobilization of the crude extract or whole cells in a polymer matrix like PDMS beads or polyacrylic acids (superabsorber) should be looked into.

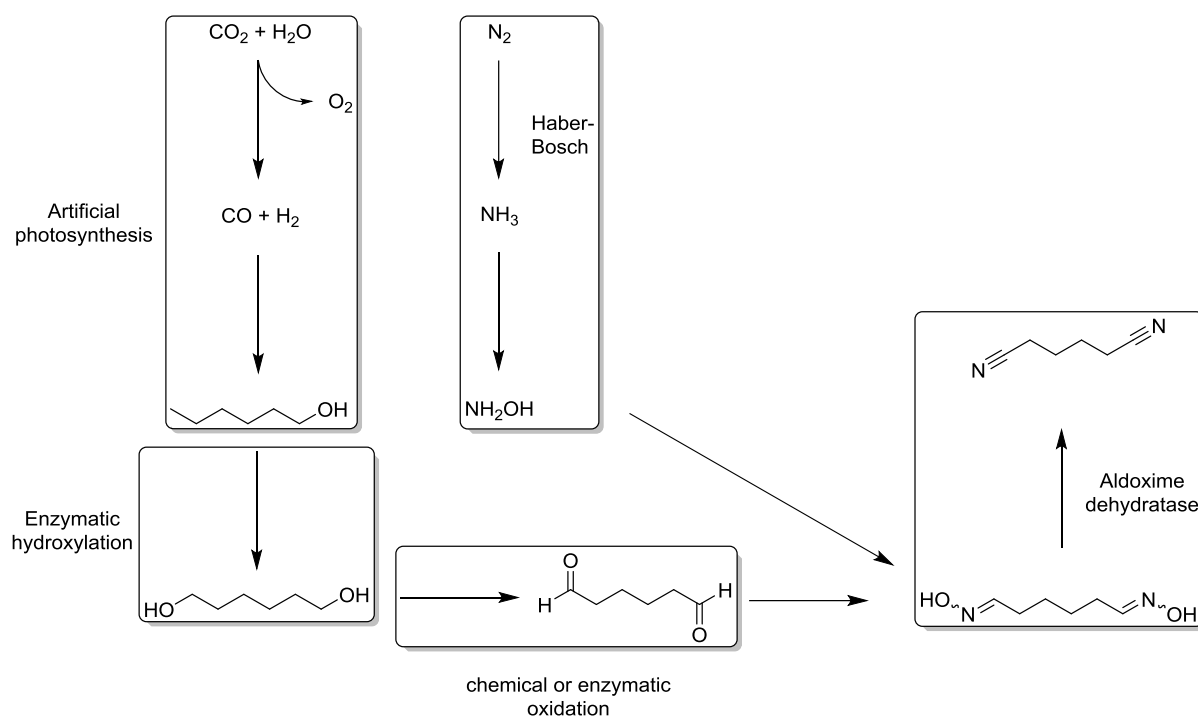
Apart from the optimization and availability of the biocatalyst, another part is even more crucial for the technical feasibility: The availability of the substrate is still not satisfying. As mentioned earlier, many attempts have been done to improve the double, *n*-terminal hydroformylation of butadiene towards adipaldehyde.<sup>[114-117]</sup> However, only marginable success has been achieved so far. The best reported result reaches up to 73% selectivity for the double *n*-terminal hydroformylation. However, the formed adipaldehyde has to react *in situ* with two molecules of a dialcohol to form the stable bis-acetal. This additional protection step makes the process economically unattractive.<sup>[114]</sup> A very intriguing possible alternative for the hydroformylation of alkenes is the usage of biocatalysts. Just recently, *Kamer et al.* modified a lipid-transport protein with a phosphine ligand that binds rhodium and catalyzes the hydroformylation of octene and longer olefins with high linear selectivity under very mild reaction conditions.<sup>[141]</sup> Furthermore, carboxylate reductases (CARs) are currently under intensive investigation for the reduction of carboxylic acids to aldehydes.<sup>[142]</sup>

A currently emerging alternative for the access of the substrate is based on artificial photosynthesis. Researchers from the companies *Evonik* and *Siemens* collaborate in the so-called "Rheticus" program. They combine solar powered electrochemical reduction of CO<sub>2</sub> and H<sub>2</sub>O to syngas (H<sub>2</sub> and CO) with a microbial fermentation to obtain aliphatic, linear alcohols like butan-1-ol or *n*-hexan-1-ol.<sup>[143]</sup> This approach opens up an access route towards adipaldehyde from completely renewable resources! The obtained *n*-hexan-1-ol from the artificial photosynthesis can be afterwards terminally hydroxylated *via* an enzymatic method developed by *Fujii et al.*<sup>[144]</sup> They utilized a CYP monooxygenase to terminally hydroxylate long chain alkanes and aliphatic monoalcohols towards the  $\alpha,\omega$ -dialcohols, with a carbon chain length of 5-16 carbon atoms. Especially mid-range substrates like the C6-C10 alkanes and monoalcohols were highly accepted substrates for

the terminal hydroxylation. This microbial terminal hydroxylation has also been conducted for the synthesis of  $\omega$ -aminolaurate.<sup>[145]</sup>

Once an  $\alpha,\omega$ -dialcohol has been synthesized, a multitude of methods exists to selectively oxidize the alcohol moieties into aldehydes. While some of them are conventional chemical methods, biocatalytic approaches for this also exist.<sup>[145]</sup> While this access towards adipaldehyde is still rather a vision than a reality, it opens up a very promising vision to solve this longstanding issue.

Once the adipaldehyde is produced, our approach with the formation of the dioxime by condensation with hydroxylamine and the highly selective, biocatalytic dehydration towards adiponitrile will be a highly valuable production route (**Scheme 40**).



**Scheme 40:** Envisioned access to adiponitrile starting from renewable resources.

In view of the author, this route is even more promising than the reductive amination of adipaldehyde towards hexamethylenediamine. First, adipaldehyde is a highly reactive compound that would undergo severe side reactions during the process of a reductive amination. Second, while this may seem trivial, the nitriles can be accessed *via* this route. These can always be easily converted into the amines, but the reverse reaction is way more complicated. Additionally, nitriles can also be used as intermediates for other functional groups, making the access towards several dinitriles (and not only adiponitrile) a valuable platform technology.

## 5 CHIRAL N-ACYL- $\alpha$ -AMINONITRILES VIA COPPER CATALYSIS AND INCORPORATION INTO A DE NOVO SYNTHESIS OF VILDAGLIPTIN

### 5.1 NITRILES IN THE PHARMACEUTICAL INDUSTRY

As of 2010, over 30 nitrile-containing pharmaceuticals were prescribed for a broad variety of medical indications and over 20 nitrile-containing lead structures were under clinical development.<sup>[44]</sup> Nitrile containing pharmaceuticals have been a staple of their own in the last decades with some representatives of them being one of the first choices for the treatment of severe diseases like breast cancer or angina (**Figure 28**). The most prominent compounds in this regard are:

1. Anastrozole, which is marketed as Arimidex by Astra-Zeneca and used against estrogen-dependent breast cancer.
2. Verapamil, which is a calcium channel antagonist and used against angina by relaxing blood vessels to allow easier pumping of the heart. Several attempts for the enantioselective synthesis of Verapamil have also been endeavored.<sup>[102,146]</sup>
3. Gallopamil, a methoxy derivative of Verapamil with a tenfold higher potency.

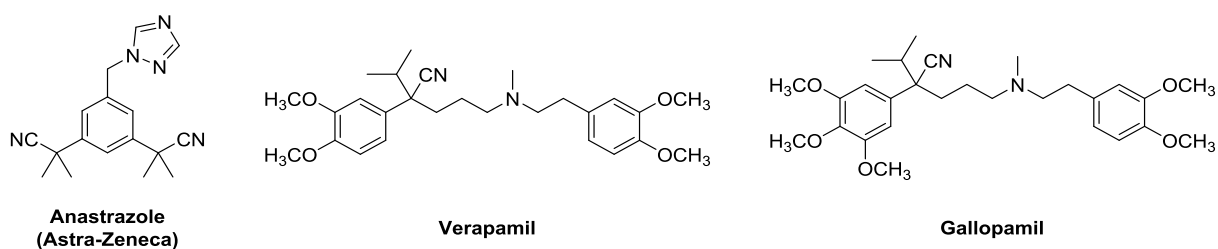


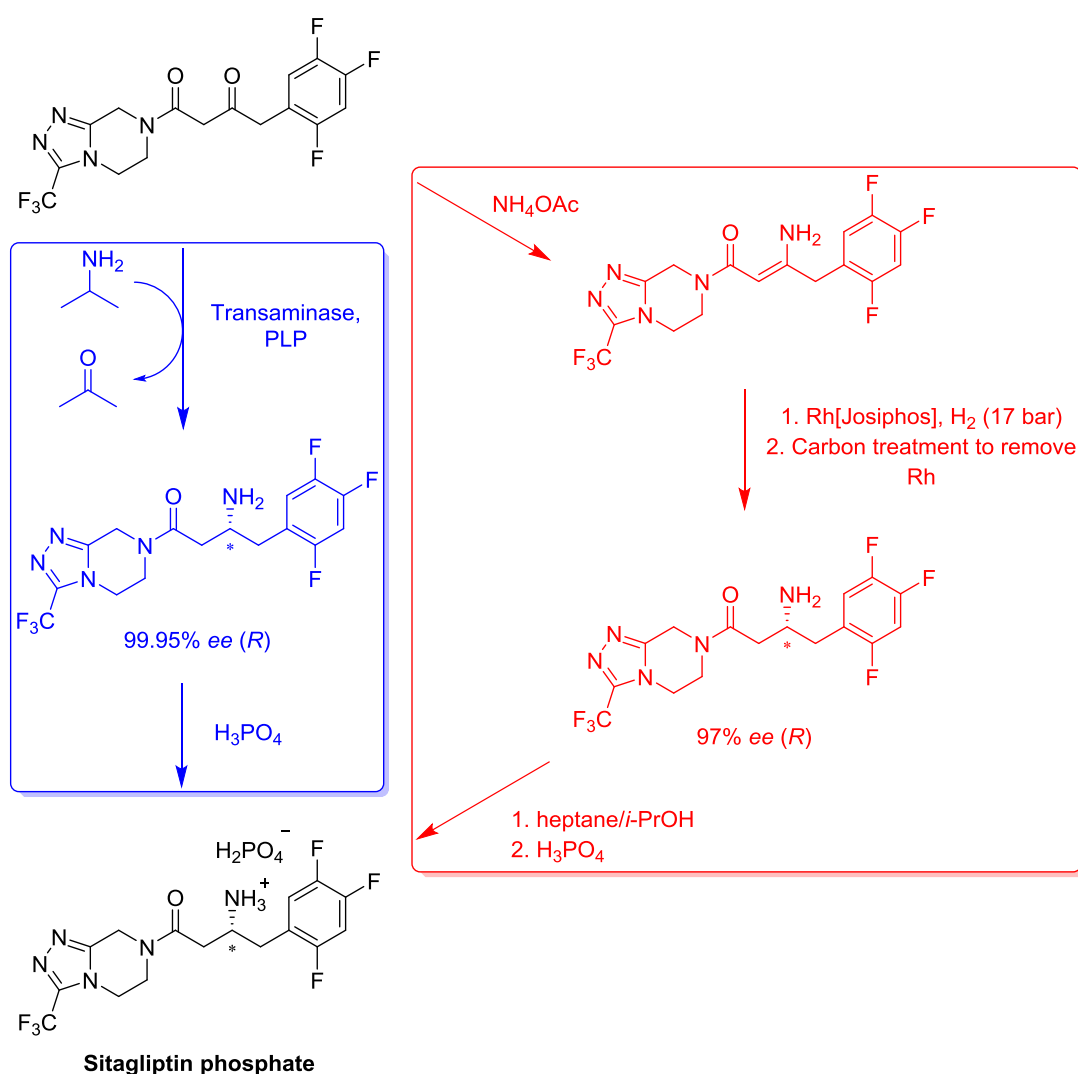
**Figure 28:** Nitrile-containing pharmaceuticals that are broadly prescribed.<sup>[44]</sup>

As one can already conclude from these pharmaceuticals, most of the nitrile-containing pharmaceuticals either contain an aromatic nitrile moiety or nitrile next to a quaternary carbon atom. The reason behind this structural preference lies in the potential oxidation of the  $\alpha$ -carbon atom next to the nitrile moiety, resulting in cyanhydrins. Cyanhydrins can decompose into the corresponding aldehyde and cyanide, which is highly toxic because it inhibits the aerobic production of ATP in cells.<sup>[44]</sup>

The nitrile moiety is a highly polar group that is relatively small and highly solubilized. It can act as a surrogate for carbonyl moieties and can form strong hydrogen bonds with hydrogen bond donors like carboxyl or hydroxyl groups that are present in several amino acid side chains. Additionally, like in the case of Verapamil, the nitrile moiety can form complexes with metal ions like calcium, potentially resulting in an inhibition or deactivation of a protein.<sup>[44]</sup> Furthermore, its small size allows it to reach even highly covered areas within proteins, which other substituents or motifs are not able to reach.

Despite the high concerns for cyanide release of nitrile-containing pharmaceuticals, several pharmaceuticals and lead structures have been developed, that are highly potent in e.g. the treatment of diabetes. Especially the advances in molecular modelling and docking studies have led to an increase of nitrile-containing molecules in the pharmaceutical industry since these tools allow a proper estimation of the function and potential metabolism of the pharmaceutical compound in the body.<sup>[44]</sup>

Since diabetes is an ever expanding disease in the industrial nations, the treatment of it is paramount. Regarding the diabetes mellitus type II, several pharmaceuticals have been developed over the last decades for efficient treatment of it. One class of the developed pharmaceuticals is called gliptins and they act as competitive inhibitors of the enzyme dipeptidyl peptidase IV (DPP-4), which is responsible for the degradation of incretins.<sup>[43,44,147]</sup> With low levels of incretins the glucose level in blood is increased, leading to the typical symptoms of diabetes. The first reported example of gliptins was the compound Sitagliptin in the year 2006, which is nowadays produced *via* a biocatalytic transamination and marketed by *Merck & Co.*<sup>[148]</sup> The development of this biocatalytic process is one of the most impressive industrial process examples of biocatalysis and has sparked a huge amount of attention back in 2010 (**Scheme 41**).



**Scheme 41:** Comparison of the biocatalytic and metal-catalyzed production of sitagliptin phosphate reported by *Savile et al.*<sup>[148]</sup>



Some of the gliptins contain a nitrile moiety and some of them have already been proven themselves as valuable compounds on the pharmaceutical market. A prominent example is Vildagliptin, which has been developed and marketed by Novartis (**Figure 29**).<sup>[41-43]</sup> With sales numbers of 1.14 billion dollars in 2015, it is ranked in the top 10 of the world's top selling diabetes drugs.<sup>[47]</sup> Another example for the high success of gliptins is Saxagliptin, which was developed jointly by Bristol-Myers Squibb (BMS) and Astra-Zeneca. Saxagliptin is now marketed by Astra-Zeneca and reached sales numbers of 786 million dollars in 2015.<sup>[45-47]</sup> Furthermore the compounds NVP-DPP-728 and Anagliptin have been developed. All of these compounds share the same backbone containing the nitrile moiety, which is derived from L-proline.

The nitrile-containing gliptins inhibit the DPP-4 by a nucleophilic attack of a serin side chain of the DPP-4 to the nitrile moiety. As a result, the serin side chain is reversibly, covalently bound to the gliptin (**Figure 6**).<sup>[44]</sup>

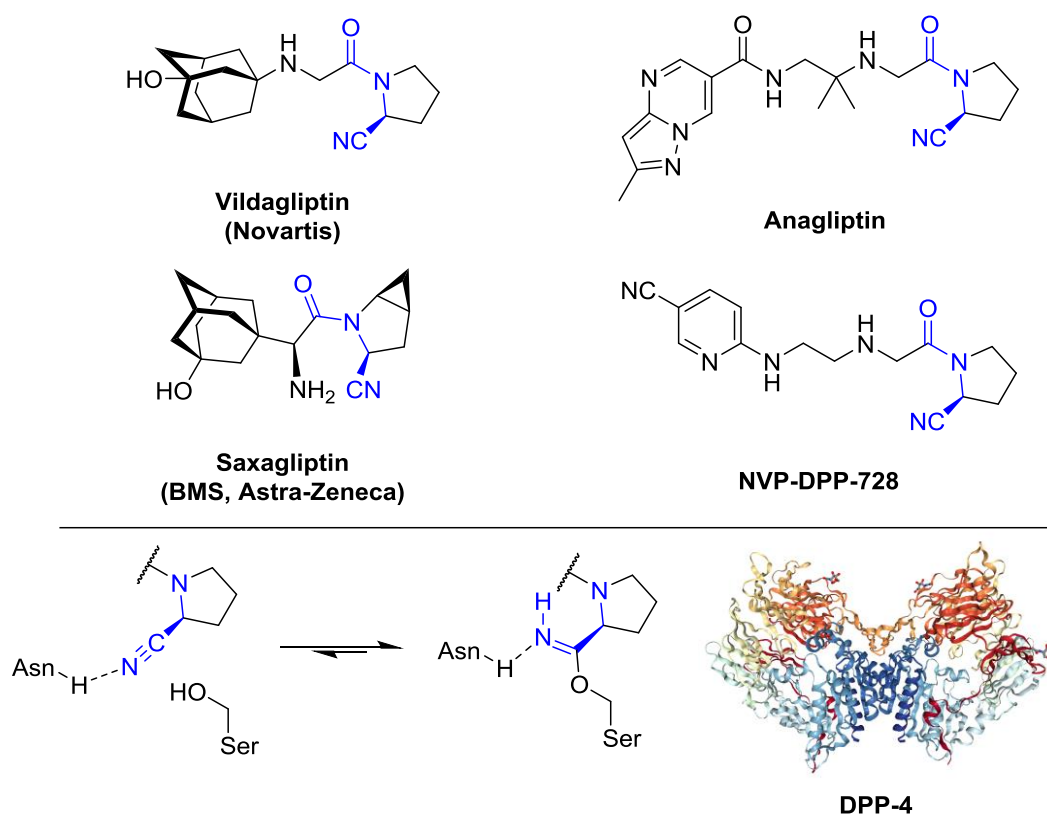


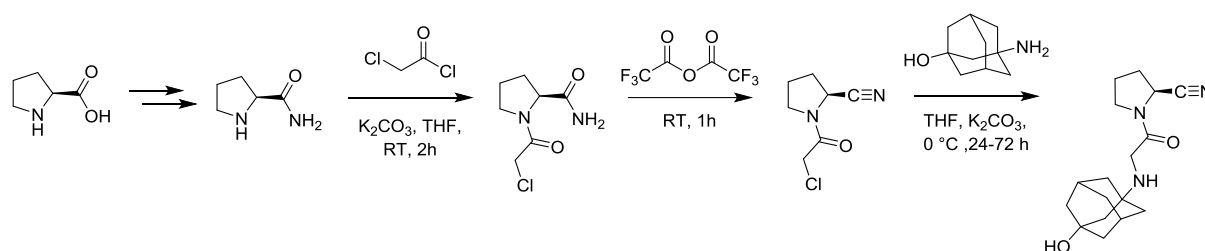
**Figure 29:** Nitrile-containing gliptins (top) and the inhibition of Dipeptidyl peptidase IV (DPP-4) by nitrile containing gliptins (bottom), including the X-ray crystal structure of DPP-4 (PDB-File: 1PFQ, visualized with NGI-Viewer).

Beside their high potential for the treatment of diabetes type II, gliptins have also proven themselves to treat osteoporosis in an efficient manner.<sup>[147,149]</sup> *Ambrosi et al.* could show in 2017 that treatment of elderly, obese animals with sitagliptin led to increased bone healing properties. The animals tended to produce bigger amounts of DPP-4, which led to decreased bone cell formation in their bone marrow. These results may allow for an efficient treatment of osteoporosis especially for obese, elderly people in the future.

## 5.2 COPPER-CATALYZED DEHYDRATION OF *N*-ACYL $\alpha$ -AMINO ALDOXIMES AND IMPLEMENTATION INTO A *DE NOVO* SYNTHESIS OF VILDAGLIPTIN

### 5.2.1 STATE OF THE ART OF THE VILDAGLIPTIN SYNTHESIS

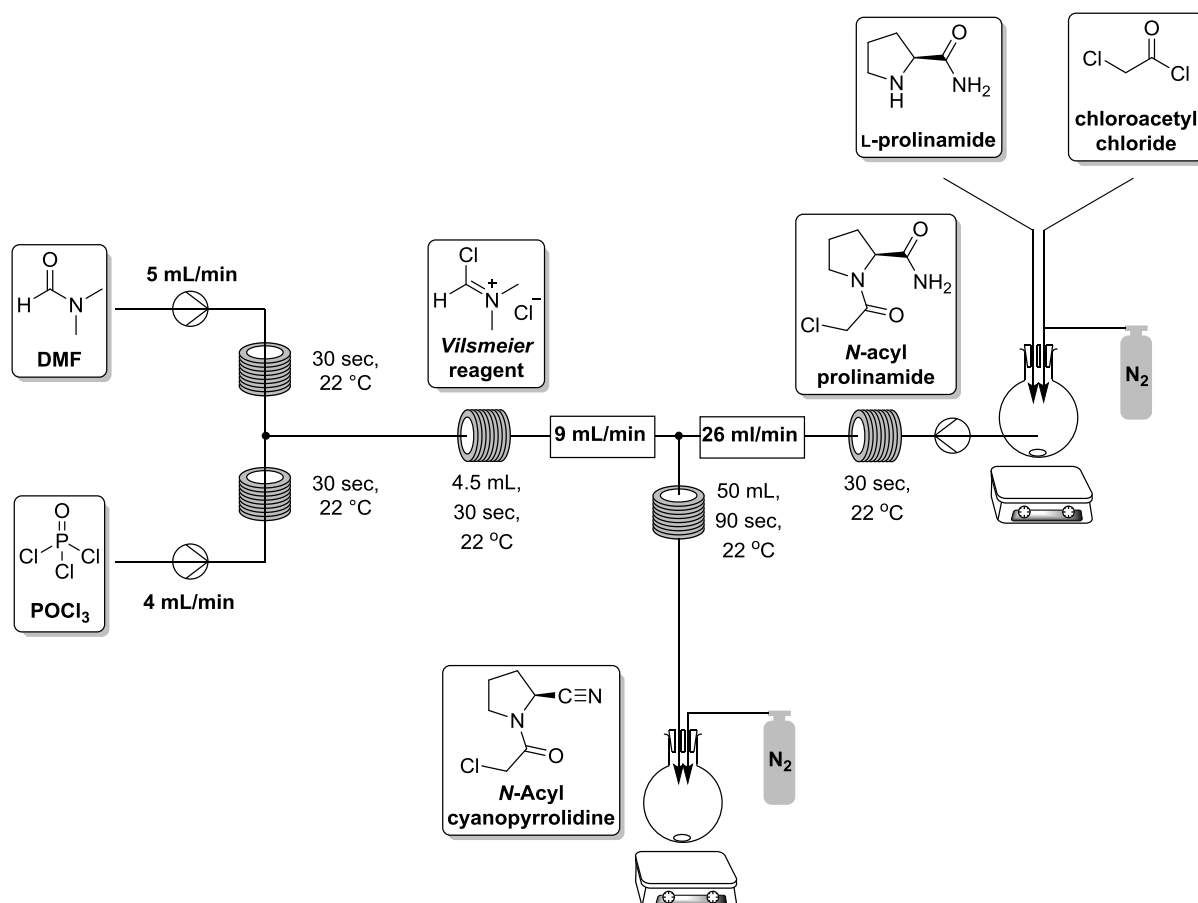
The current synthesis of nitrile-containing gliptins starts from L-proline, which is a cheap building block from the chiral pool with reported kilo prices in the range of 40 \$ per kilogram.<sup>[60,150]</sup> In case of the highest selling one, Vildagliptin, *Villhauer et al.* disclosed its synthesis in 1998 and 2003 (**Scheme 42**).<sup>[42,43]</sup>



**Scheme 42:** Synthesis of Vildagliptin reported by *Villhauer et al.*<sup>[42,43]</sup>

As one can depict from this synthetic sequence, a key step is the amidation of L-proline to yield L-prolinamide. While this transformation may seem trivial at first, direct amidation of carboxylic acids is not efficient and often requires a two-step sequence of acyl chloride formation and subsequent amidation. These steps are very waste intensive and increase the price of the process drastically. The secondary amine of L-prolinamide is afterwards protected by nucleophilic substitution with chloroacetyl chloride under presence of potassium carbonate in THF. Another critical step is then the dehydration of the primary amide group of the *N*-protected prolinamide. *Villhauer et al.* utilize trifluoroacetic anhydride for this, but its utilization leads to big amounts of acidic, fluorinated wastes. The final step involves a nucleophilic substitution of an amino derivative of adamantane to yield Vildagliptin.

As one can depict from this reaction sequence, especially the prolinamide formation and the subsequent dehydration with trifluoroacetic anhydride are critical steps that should be avoided. In 2015, *Pellegatti et Sedelmeier* tried to soothe these issues by implementing a dehydration of the *N*-acyl prolinamide with the Vilsmeier reagent in flow chemistry (**Scheme 43**).<sup>[41]</sup> The *Vilsmeier* reagent is formed by a reaction of *N,N*-dimethylformamide (DMF) with phosphoryl chloride ( $\text{POCl}_3$ ). Other reagents like oxalyl chloride ( $(\text{COCl})_2$ ) or thionyl chloride ( $\text{SOCl}_2$ ) were unfit for flow application due to gas formation and excessive heat formation. The flow application allowed to convert 2.34 mol of the *N*-acyl prolinamide ( $5.8 \text{ kg h}^{-1} \text{ L}^{-1}$ ) towards the *N*-acyl cyanopyrrolidine, demonstrating the big potential of flow chemistry.<sup>[41]</sup> Nevertheless, the excessive use of highly toxic DMF and  $\text{POCl}_3$  does not solve the hazard and waste issues of the Vildagliptin synthesis.



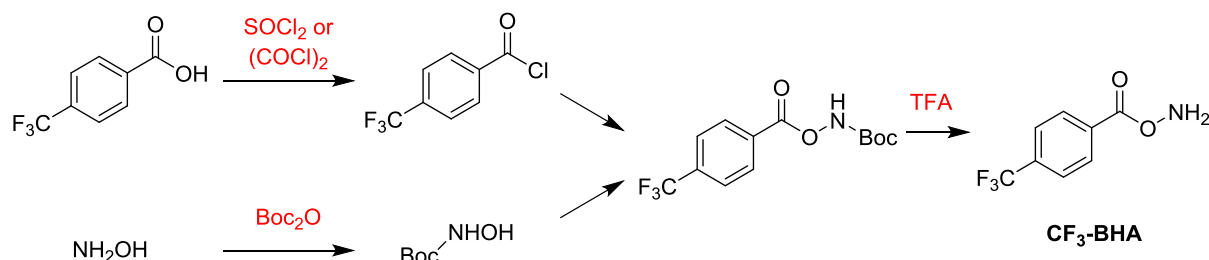
**Scheme 43:** Application of a *Vilsmeier* reagent dehydration in continuous flow by *Pellegatti et Sedelmeier*.<sup>[41]</sup>

### 5.2.2 COPPER-CATALYZED DEHYDRATION OF *N*-ACYL $\alpha$ -AMINO ALDOXIMES

To circumvent these issues, suitable reagents and reaction conditions had to be identified that would allow for a less waste intensive synthetic route towards Vildagliptin. It was decided to approach the synthesis of the key intermediate, the *N*-acyl pyrrolidine, *via* a two-step approach that started off from the *N*-acyl  $\alpha$ -amino aldehyde. By condensation with hydroxylamine, one can obtain the corresponding aldoxime that can subsequently be dehydrated towards the nitrile. The big advantage of this route compared to the amide dehydration is the fact that aldoximes can quite elegantly be dehydrated in comparison to the amides. There are plenty of possibilities for aldoxime dehydration; however one must carefully evaluate the practicability and economic impact of each route.

From the broad selection of methods for nitrile synthesis out of aldehydes over aldoximes, some of the inventions in this field have focused on one-pot strategies to skip workup procedures. While some of these approaches seem attractive at first glance, one has to evaluate the economical impact and workload to prepare the required reagents for these one-pot procedures. For example, *An et al.* reported in 2015 that they can convert 40 examples of aldehydes directly into the nitriles by employing the reagent *O*-(4-CF<sub>3</sub>-benzoyl)-hydroxylamine (CF<sub>3</sub>-BHA) and Brønsted acid catalysis at ambient conditions.<sup>[151]</sup> However, they did not discuss that the synthesis of their reagent requires four steps to be synthesized! These steps included acyl chloride formation with toxic thionyl chloride or oxalyl chloride, extremely atom inefficient protection of hydroxylamine with *Di-tert-*

butyldicarbonat ( $\text{Boc}_2\text{O}$ ), coupling of both compounds and final deprotection of the amine group by trifluoroacetic acid (**Scheme 44**).<sup>[152]</sup> Furthermore,  $\text{CF}_3$ -BHA is not recycled and has to be disposed as environmentally hazardous halogenated, organic waste. As a consequence, their proposed one-pot procedure for the nitrile synthesis is simply not practicable and is in reality not a one-pot procedure but rather a five step sequence.



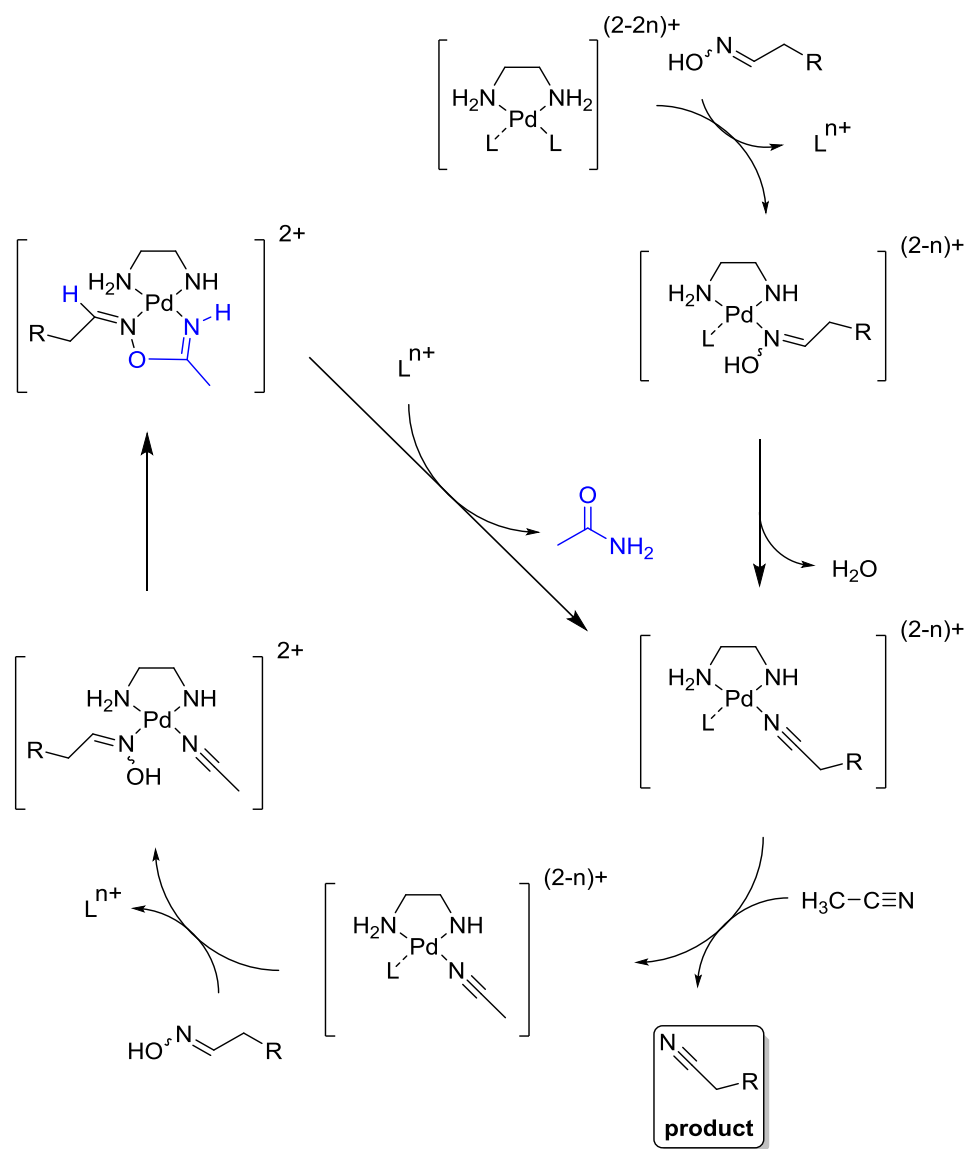
**Scheme 44:** Waste intensive synthesis of the reagent  $\text{CF}_3$ -BHA for the one-pot synthesis of nitriles out of aldehydes.<sup>[152]</sup>

While this example may seem drastic, the drawbacks of many reported one-pot procedures for the nitrile synthesis out of aldehydes are in the same range as the one discussed above, eliminating most approaches if environmental, cost and waste issues are considered. Examples of such procedures include the utilization of hexamethyldisilazane (HMDS)<sup>[153]</sup>, expensive derivatives of (2,2,6,6-tetramethylpiperidin-1-yl)oxyl (TEMPO) in stoichiometric amounts<sup>[154]</sup> or highly toxic ethyl dichlorophosphate.<sup>[155]</sup> Additionally, these procedures require excessive usage of Brønsted bases like DBU or pyridine.<sup>[154,155]</sup> Apart from one-pot procedures, many methods for the dehydration of oximes towards their nitriles have been disclosed. However, most of these methods lack the practicability like most of the one-pot procedures. For example, *Denton et al.* reported a method in 2012 that relies on activation of triphenylphosphine oxide ( $\text{Ph}_3\text{PO}$ ) by oxalyl chloride to dehydrate the aldoximes.<sup>[62]</sup> While this protocol is broadly applicable, oxalyl chloride is a highly toxic and corrosive compound. Furthermore, triphenylphosphine oxide ( $\text{Ph}_3\text{PO}$ ) is a highly unwanted side product, which is also one of the biggest concerns with *Wittig* olefinations up to this day. Another method reported by *Hendrickson et al.* in 1976 utilizes triflic anhydride, stoichiometric amounts of triethyl amine and operates at  $-78^\circ\text{C}$  to dehydrate the oximes.<sup>[156]</sup> This combination makes the method unattractive for further consideration. There are plenty of different methods to obtain the corresponding nitriles from aldoximes and if one wishes to delve deeper into this matter, several book chapters and reviews regarding this matter are present in the literature.<sup>[57,58,157]</sup> Additionally, a vast amplitude for the preparation of oximes, also out of other compound classes (like amines or nitro compounds) exists.<sup>[91,97,158,159]</sup> The same is true for nitriles.<sup>[63,160]</sup>

After critical assessment of this vast amplitude of synthetic possibilities, it was decided to investigate a copper-catalyzed dehydration of aldoximes into nitriles in acetonitrile as reaction medium for the synthesis of the required *N*-acyl  $\alpha$ -aminonitrile motif. In 1983, *Attanasi et al.* discovered that a wide variety of aliphatic and aromatic aldoximes was smoothly converted into their nitriles if they were treated with copper(II) acetate ( $\text{Cu}(\text{OAc})_2$ ) in boiling acetonitrile.<sup>[161]</sup> In their study, they used 5-10 mol% of  $\text{Cu}(\text{OAc})_2$  and obtained eight different nitriles with yields ranging from 85-98%. In 2013, *Ma et al.* extended this method to a broader substrate scope screening and identifying the transformation of the aldoxime into the corresponding amide if no acetonitrile is present.<sup>[159]</sup>

Additionally, they demonstrated the high tolerance against other functional groups of this method and conducted a parameter screening.

To rationalize the mechanism of the aldoxime dehydration in acetonitrile, *Tambara et Dan Pantoş* conducted a more detailed mechanistic study in 2013, when they investigated the palladium-catalyzed dehydration of aldoximes into nitriles (**Scheme 45**). They proposed that the aldoxime is coordinated to the metal center *via* its nitrogen atom and after coordination of a nitrile molecule to the metal center, an *in situ* H<sub>2</sub>O transfer takes place to yield the former nitrile as the corresponding amide and the former aldoxime as the nitrile. In case of the absence of acetonitrile, the H<sub>2</sub>O transfer is conducted between the already desired nitrile product and the substrate, which in the long run ends with complete conversion towards the unwanted amide product. By adding acetonitrile in an excessive amount, the equilibrium for the *in situ* H<sub>2</sub>O transfer is drastically shifted towards the hydration of acetonitrile, yielding one equivalent of acetamide as side product.



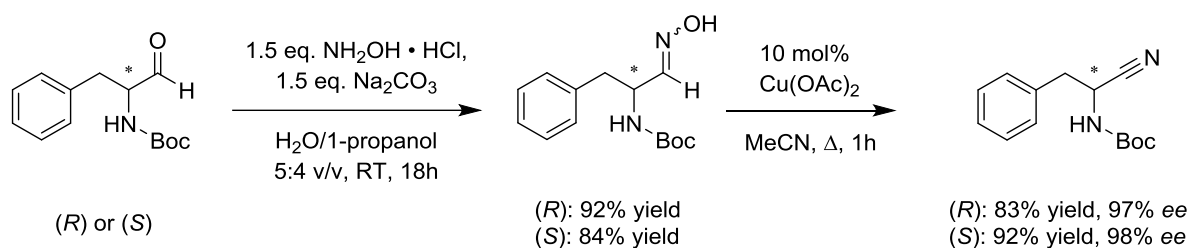
**Scheme 45:** Proposed mechanism for the metal-catalyzed dehydration of aldoxime to nitriles in the presence of acetonitrile, reported by *Tambara et Pantoş*.<sup>[162]</sup>

Due to the high polarity and boiling point of acetamide, its separation from the nitrile products *via* distillation or chromatography can be easily achieved. Additionally, acetamide can be recovered and reused since it is part of several industrial segments, e.g. as solvent or softener additive.

This method incorporates many aspects that allow for a less waste and hazard intensive approach to *N*-acyl  $\alpha$ -aminonitriles and was hence chosen for further investigation. The side product can be reused, the utilized metal catalyst is very cheap and relatively low toxic, the utilized solvent can be recycled for further reaction cycles and the separation of the product from the catalyst and side product is easily conducted. Apart from the chosen method, a later reported method in 2016 from *Hyodo et al.* utilizes Fe(III) catalysts in boiling toluene to dehydrate the aldoximes towards the nitriles without the need for acetonitrile.<sup>[61]</sup> The authors stated that they were inspired by the mechanism of aldoxime dehydratases, which shows the high value and impact of aldoxime dehydratase catalysis even among synthetic chemists that are not familiar with biocatalysis. A slight drawback of their method is, however, the rather low maximum substrate concentration of 50 mM to circumvent the amide formation, high temperature (refluxing toluene) and long reaction time of 24 hours.

### 5.2.3 DISCOVERY OF THE STEREOCHEMISTRY RETENTION DURING ALDOXIME DEHYDRATION

To investigate the potential of the copper-catalyzed dehydration of aldoximes for the synthesis of *N*-protected  $\alpha$ -aminonitriles, both enantiomers of the *N*-Boc protected phenylalaninal were commercially purchased and converted to the aldoximes by condensation with hydroxylamine in a mixture of H<sub>2</sub>O/1-propanol after 18 hours at room temperature. Both aldoximes were obtained with excellent isolated yields of 84% and 92% (**Scheme 46**).



**Scheme 46:** Two-step synthesis of *N*-Boc protected  $\alpha$ -aminonitriles of phenylalanine starting from the  $\alpha$ -aminoaldehyde.

Since  $\alpha$ -carbonyl compounds can form their corresponding enol and racemize in the process, it had to be clarified that neither in the aldoxime nor in the nitrile synthesis any or only marginable racemization occurs. For this, mixtures of the (*R*)-configured aldoxime and nitrile, as well as the (*S*)-configured ones were measured *via* chiral HPLC (**Figure 30**). These measurements revealed that indeed no or only marginable racemization occurs in the synthesis sequence. For the (*R*)-enantiomer of the nitrile, an *ee*-value of 97% was measured, while the (*S*)-enantiomer had an *ee*-value of 98%. While one might argue that these results imply that a slight racemization may occur, this may

indeed be not the case. Unfortunately, the commercial supplier of the *N*-Boc protected phenylalaninal did not give any specification regarding the optical purity of the aldehydes, only a purity percentage of 97%.<sup>[60]</sup> If the remaining 3% of the substrate consist of another compound or the other enantiomer remains illusive. Nevertheless, the copper-catalyzed dehydration to obtain *N*-acyl  $\alpha$ -aminonitriles proved its simplicity and practicability in the synthesis of the required products with easy conductable synthetic procedures and easy workups.

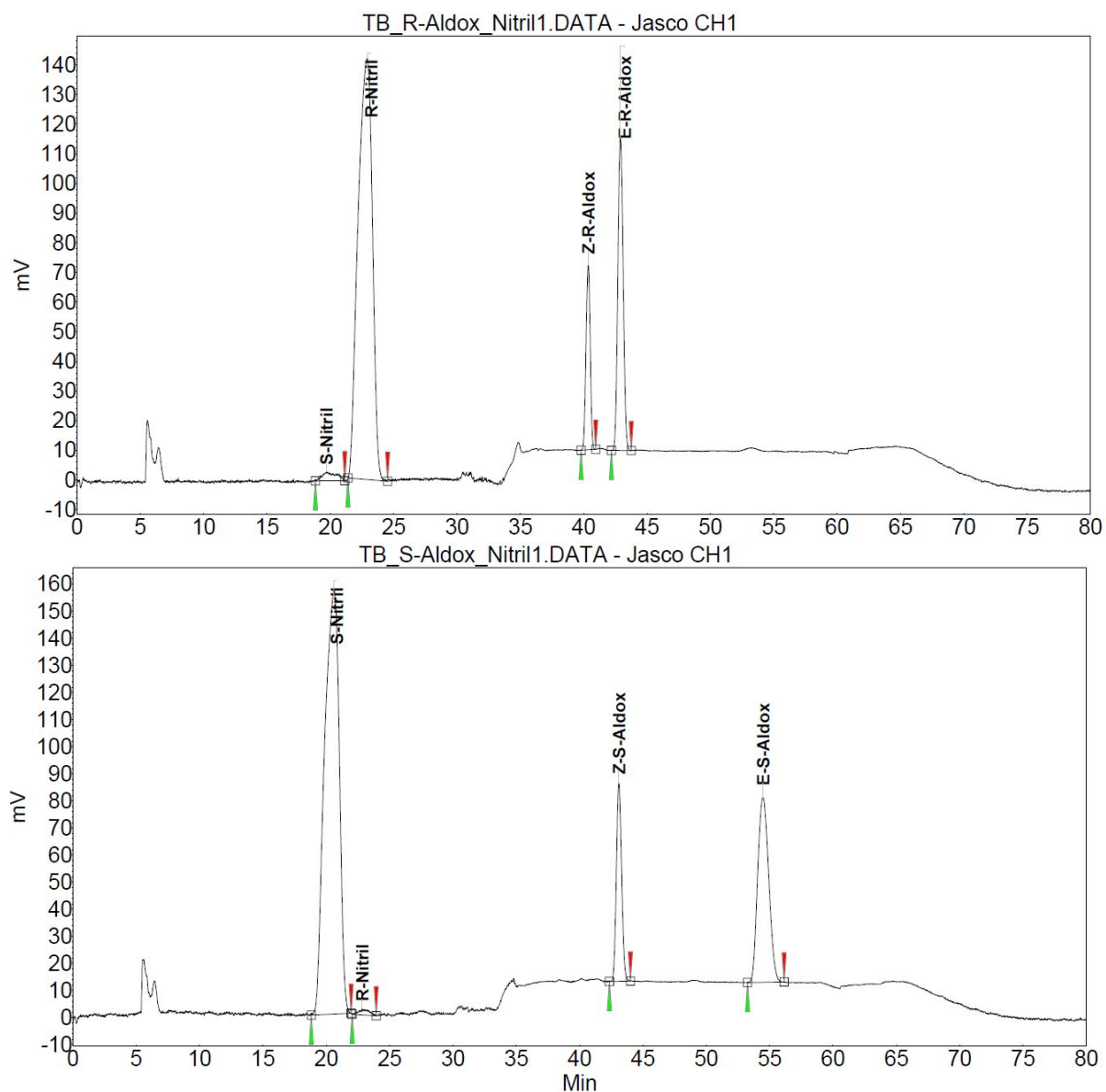


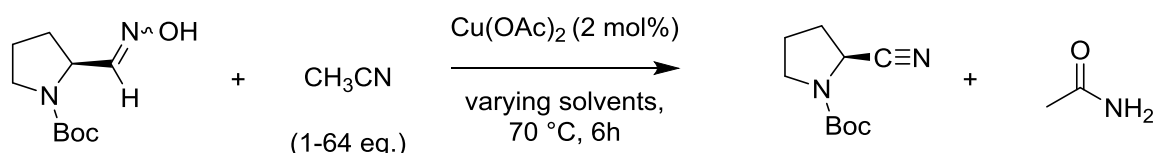
**Figure 30:** Chromatograms of the (*R*) and (*S*)-enantiomers for the aldoximes and nitriles of phenylalaninal on chiral HPLC.

### 5.2.4 IMPLEMENTATION OF THE COPPER-CATALYZED DEHYDRATION INTO A *DE NOVO*-SYNTHESIS OF VILDAGLIPTIN BY *ROMMELMANN*

Based on the gained insights into the mild and highly selective dehydration of the *N*-protected aldoximes without any observable racemization by the author, *Rommelmann*<sup>[99]</sup> transferred and optimized this procedure by several parameters and implemented it into a *de novo*-approach for the synthesis of Vildagliptin.

First, he evaluated the minimal amount of required acetonitrile for the dehydration reaction of the *N*-Boc proline aldoxime (**Table 18**). For this, varying amounts of acetonitrile were dissolved in ethyl acetate and the conversion towards the *N*-acyl cyanopyrrolidine was determined *via* <sup>1</sup>H-NMR measurements. This study revealed that the conversion towards the nitrile did not increase above 15 equivalents of acetonitrile and 10 equivalents of acetonitrile were the best compromise between conversion and a minimal used amount of acetonitrile as reagent/solvent.

**Table 18:** Solvent screening for the conversion of the *N*-Boc  $\alpha$ -amino aldoxime towards the *N*-acyl cyanopyrrolidine by *Rommelmann*.<sup>[60,99]</sup>

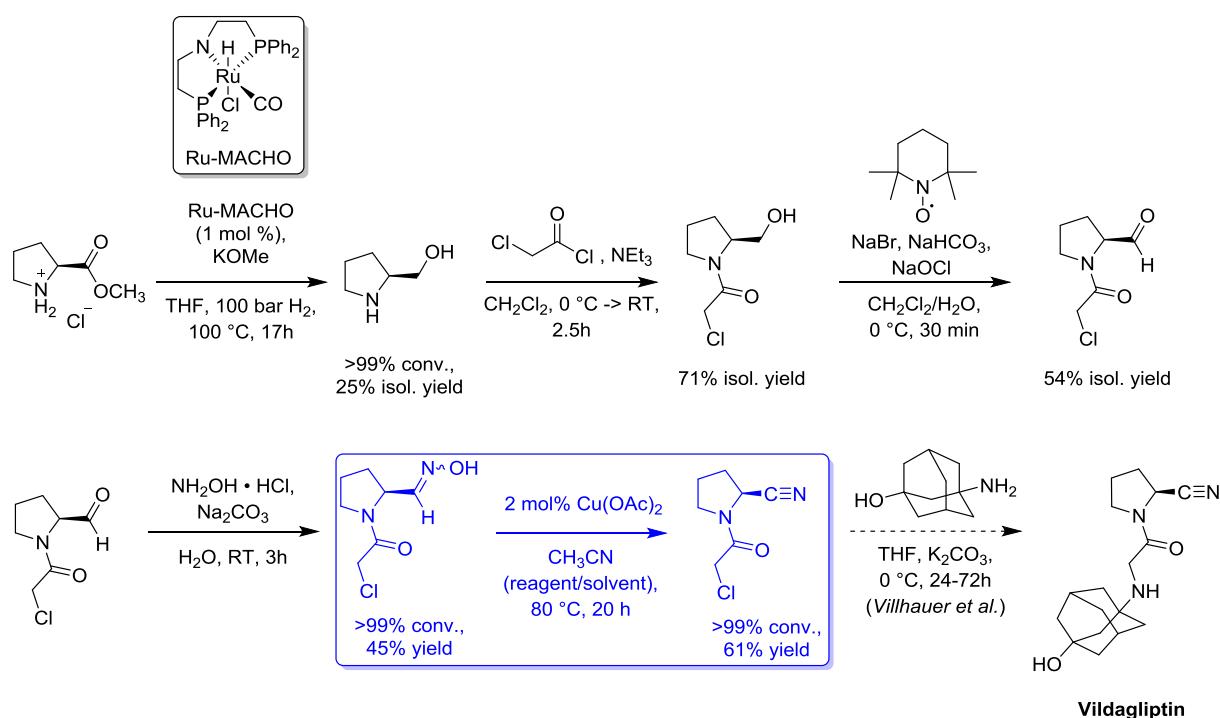


Entry	Solvent	Amount of acetonitrile (eq.)	Conversion (%)
1	ethyl acetate	1	54
2	ethyl acetate	2	57
3	ethyl acetate	4	71
4	ethyl acetate	6	74
5	ethyl acetate	8	78
6	ethyl acetate	10	81
7	ethyl acetate	15	92
8	ethyl acetate	20	92
9	acetonitrile	64	92
10	2-methyl THF	10	70
11	dimethyl carbonate	10	94
12	ethanol	10	80
13	methanol	10	74
14	water	10	46
15	cyclohexane	10	88
16	toluene	10	89



After this study, he compared the suitability of different solvents in conjunction with 10 equivalents of acetonitrile for the best conversion towards the cyanopyrrolidine (**Table 18**). While highly polar, protic solvents as methanol and ethanol resulted in a conversion of 74-80%, water led to a decreased conversion of only 46%. This circumstance was explained by the proposed mechanism of the dehydration, in which the *in situ* eliminated H<sub>2</sub>O from the aldoxime is transferred irreversibly to the acetonitrile to yield acetamide as side product and the other nitrile is released.<sup>[59,162]</sup> In the presence of water, the formed nitrile can also be hydrated again, resulting in the unwanted amide of the *N*-acyl cyanopyrrolidine as side product. Apolar, aprotic solvents like cyclohexane and toluene led to high conversions of 88-89%. The best results were obtained with the polar, aprotic solvent dimethyl carbonate with a conversion of 94%. Dimethyl carbonate is a green solvent and superior to other polar, aprotic solvents like ethyl acetate or 2-methyl tetrahydrofuran which only led to 70-81% conversion.

Afterwards, *Rommelmann* developed a *de novo*-approach towards vildagliptin starting from L-proline methyl ester hydrochloride (**Scheme 47**) and the results of this synthesis were jointly published with the results of the author of this thesis (see **chapter 5.2.3**).<sup>[60,99]</sup>



L-proline methyl ester hydrochloride was chosen by *Rommelmann* as starting material since the methyl ester of proline is easily produced directly from L-proline. To circumvent expensive reduction methods towards the L-prolinal, a ruthenium-catalyzed high-pressure hydrogenation towards L-prolinol was chosen. While the methyl ester was converted towards L-prolinol with complete conversion, the isolation of L-prolinol by extraction was difficult due to its high solubility in water. Hence, only 25% isolated yield were obtained. However, this problem can be easily solved by precipitation with hydrochloric acid (HCl) in future attempts. Afterwards, the L-prolinol was acylated with chloroacetyl chloride in dichloromethane and the *N*-acyl prolinol was obtained with 71% isolated yield. One could

also envision conducting the acylation step first, followed by the high-pressure hydrogenation. However, no conversion of the *N*-acylated proline methyl ester was observed under the same reaction conditions (100 °C, 100 bar H<sub>2</sub>).

For obtaining the *N*-acylated prolinal, a selective oxidation method of the alcohol towards the aldehyde is required. (2,2,6,6-tetramethylpiperidin-1-yl)oxyl (TEMPO) has proven itself as a selective catalyst to oxidize primary alcohols selectively towards aldehydes in two phase-systems under utilization of hypochlorite as stoichiometric oxidation reagent over the last decades. Employing this strategy led to 54% isolated yield of the *N*-acylated prolinal. Other oxidation methods like the well-known Swern oxidation, led to decomposition of the substrate.

Coming back to the earlier discovered two-step synthesis of the *N*-acylated cyanopyrrolidine, the obtained prolinal was converted with hydroxylamine hydrochloride towards the *N*-acylated prolinal aldoxime with complete conversion. However, *Rommelmann* reports that due to a non-optimized workup procedure, the isolated yield did not exceed 45%. Nevertheless, subsequent dehydration of the aldoxime yielded the *N*-acylated cyanopyrrolidine with complete conversion and 61% isolated yield. In concordance with the earlier results, no racemization of the starting material could be observed in the reaction sequence. The subsequent conversion towards Vildagliptin has already been described in the literature and was hence not conducted in the present study.

In summary, the newly developed *de novo*-approach towards Vildagliptin could be realized thanks to the jointly discovered non-racemizing two-step access route towards *N*-acylated  $\alpha$ -aminonitriles. This approach almost exclusively avoids usage of toxic reagents and operates under mild reaction conditions without the generation of big waste streams. As a result, a patent application has been filed for the two-step synthesis of *N*-acylated  $\alpha$ -aminonitriles in 2017 and the *de novo*-approach towards Vildagliptin was published in *Organic Process Research & Development* in 2017.<sup>[60]</sup>

## 6 NEW LUBRICANT ESTER STRUCTURES BASED ON RENEWABLE RESSOURCES

### 6.1 ESTOLIDES - INTRODUCING SUSTAINABILITY IN THE LUBRICANT INDUSTRY

Considering the growing impact of anthropogenous emissions on the ecosystem of the earth and the rapid depletion of fossil resources, one has to intensify and expand the production of high volume chemical compounds that are based on renewable resources. Furthermore, these compounds should be non-persistent and biodegradable.

However, newly developed compounds also have to fulfill economic standards (generating profit, reliable production processes etc.) to establish themselves on the market. Additionally, their performance should be equal if not superior compared to the already established products on the market.<sup>[163]</sup>

For the lubricant industry, most of today's products are based on petrochemical compounds which are obtained during the refining process of crude oil.<sup>[39,164]</sup> This resource stock opens up a broad selection basis of compounds. Thus, all required performance windows in terms of viscosity, product lifetime and material compatibility can be reached.<sup>[164]</sup> There exist a few tendencies/rules for the properties of lubricant base fluids.<sup>[163]</sup>

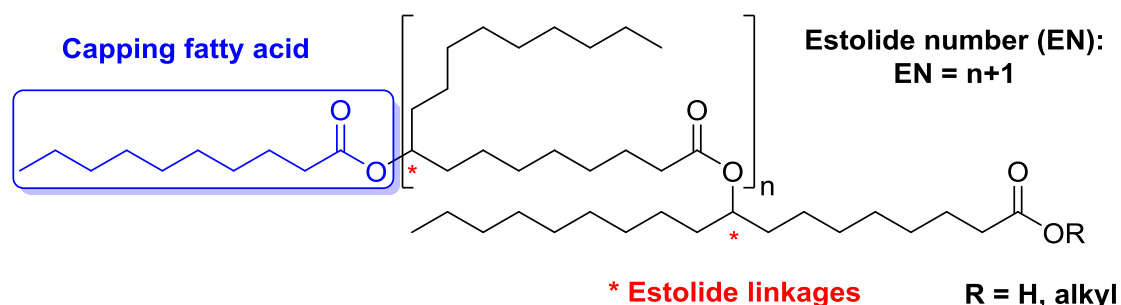
1. A high degree of branching of lubrication base fluids increases the low-temperature characteristics, leads to low viscosity indices and high hydrolytic stabilities.
2. High linearity leads to high viscosity indices and relatively poor low-temperature characteristics.
3. Low saturation leads to outstanding low-temperature characteristics, but on the other hand leads to limited oxidation stability.
4. High saturation leads to outstanding oxidation stability, but to poor low-temperature characteristics.

There are some properties that are often investigated and help to classify the performance of a lubricant. The pour point of a lubricant describes the minimum temperature at which the lubricant is still pouring. The viscosity describes the resistance of a lubricant against deformation. If a lubricant has a high viscosity index, the viscosity of it changes only marginally over a broad temperature range. Furthermore, the cloud point of a lubricant describes the temperature at which the crystallization of the oil components starts. In dependence of the charasteric profile of a lubricant, it may be privileged for different applications.

One of the most promising renewable feedstocks for the lubricant industry are vegetable oils. Especially soybean, sunflower and rapeseed oil is nowadays available with up to 85% of oleic acid ((9Z)-octadec-9-enoic acid) in their fat content. Oleic acid is due to its high availability and easily controlled chemical modification highly capable to serve as a platform molecule for a broad range of new lubricant structures.<sup>[164,165]</sup> However, also other fatty acids are highly interesting for the lubricant industry and various oils from different plants are currently under investigation for their potential as lubricant base oils, e.g. Cuphea, Lesquerella, Meadowfoam and Pennycress oils.<sup>[166]</sup>

In recent years, the focus on a certain product class based on fatty acids (especially oleic acid) has been intensified: Estolides. Estolides are esters of fatty acids either by esterification with e.g. diacids, dialcohols or with themselves as bifunctional fatty acids may be utilized as estolide building block. Estolides thereby incorporate a huge potential for diverse lubricant structures.<sup>[167,168]</sup>

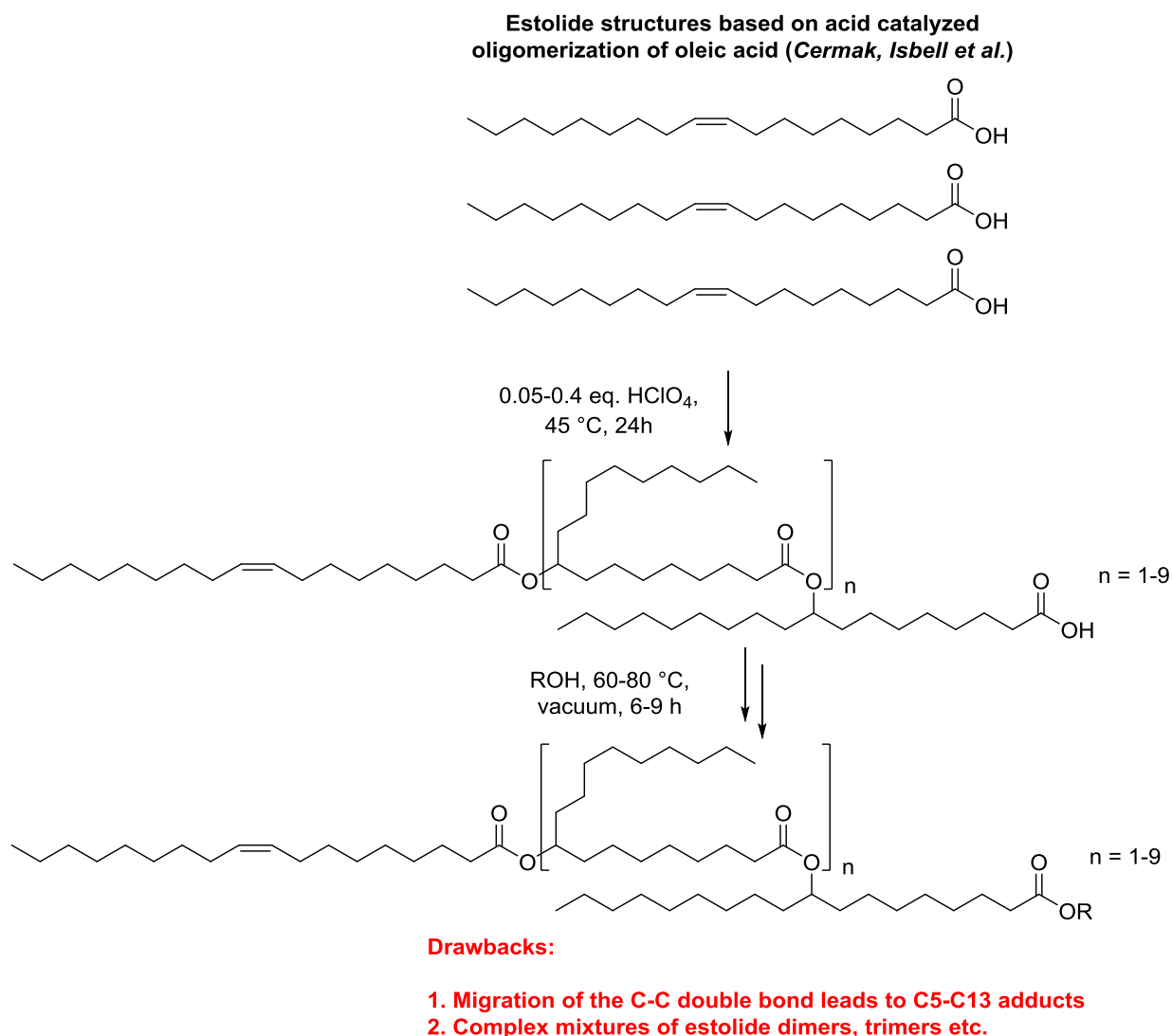
Estolides have a special nomenclature of their own, which is illustrated below in **Scheme 48**<sup>[167,168]</sup> This rather unconventional nomenclature is based on the number of branching fatty acid chains that are connected to the base fatty acid chain. If we look at the given example in **Scheme 48**, the case  $n = 1$  would be described as diestolide, since the estolide number (EN) would be 2 due to the formula  $EN = n+1$ . Hence, a diestolide represents a fatty acid trimer. The last branching fatty acid chain is also often referred to as capping fatty acid. The estolide linkage that connects the fatty acid chains often constitutes of a simple C-O-bond, but other linkages like C-C or C-N bonds are also possible.



**Scheme 48:** Estolide nomenclature explanation.<sup>[167]</sup>

Estolides may furthermore incorporate several unsaturated C-C double bonds, free OH-groups or other functionalities. The amount of functionalization of the estolide can be controlled by the choice of the base fatty acid (or a fatty acid mixture) which is used for the estolide synthesis and subsequent chemical modifications. Lastly, estolides can be optionally be esterified at the carboxyl group of the base fatty acid chain with a broad selection of alcohols which increases their structural diversity and physical/chemical properties.

The most promising and well investigated access route to estolides has been reported by *Cermak et al.* in 2013<sup>[169]</sup>, which is an improved process for an estolide production by oligomerization of oleic acid under presence of catalytic or stoichiometric amounts of HClO<sub>4</sub> (perchloric acid), which they initially described in 1994 and refined several times (**Scheme 49**).<sup>[169,170,171-175]</sup>



**Scheme 49:** Synthesis of oleic acid based estolide oligomers by HClO<sub>4</sub> catalysis.<sup>[169]</sup>

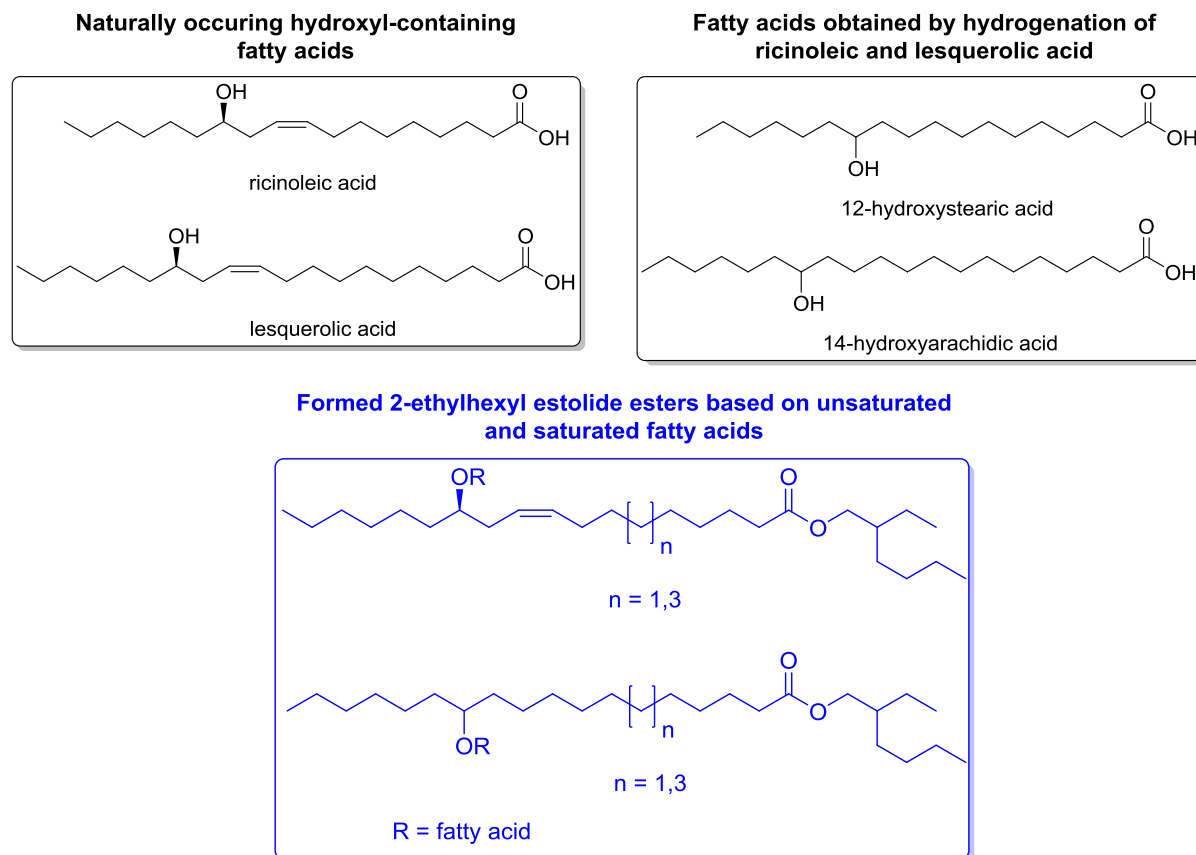
While this approach allows a rather straight-forward access to high performance estolides, it has several drawbacks.

1. The protonation of the C-C double bond by perchloric acid leads to migration of the C-C double bond by repeated protonation and elimination, before the addition of the lowly nucleophilic carboxyl group of another fatty acid chain binds to the carbocation. It was reported that the migration leads to mixtures of C5-C13 adduct mixtures of the obtained, increasing the complexity of the estolides.<sup>[168,171]</sup>
2. The amount of oligomerization is hard to control and the synthesized estolides are complex mixtures containing mono-, di-, tri- and higher branched estolides up to nonaestolides (EN = 10).<sup>[168]</sup> While some efforts have been undertaken to control the oligomerization degree of the obtained estolides by introducing saturated fatty acids (e.g. lauric acid) as stable capping chains<sup>[169,171]</sup>, the acid catalyzed route will always lead to a estolide mixture.

Another strategy for the synthesis of estolides beside the nucleophilic addition of a carboxyl group to a carbocation is based on naturally occurring fatty acids that contain a hydroxyl group like ricinoleic acid (from castor oil), 12-hydroxystearic acid or lesquerolic acid (from

lesquerella oil, **Table 19**). *Cermak et al.*<sup>[176]</sup> and *Teeter et al.*<sup>[177]</sup> investigated the 2-ethylhexylesters of these fatty acids and obtained excellent pour points, cloud points and low viscosity indices.

**Table 19:** Physical properties of several 2-ethylhexyl estolide esters.<sup>[167,176,177]</sup>



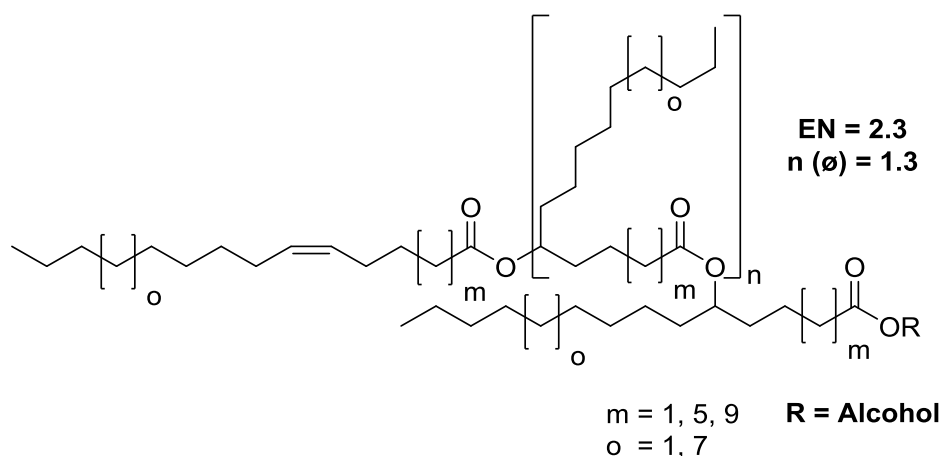
Base acid	Capping acid	Pour point (°C)	Cloud point (°C)	Viscosity at 40 °C (cSt)	Viscosity at 100 °C (cSt)
ricinoleic	oleic	-54	<-54	34.5	7.6
ricinoleic	2-ethylhexanoic	-51	<-51	70.6	11.8
ricinoleic	coco (C12-C16)	-36	-30	29.0	6.5
ricinoleic	stearic	3	23	41.7	8.6
lesquerolic	oleic	-48	-35	35.4	7.8
lesquerolic	2-ethylhexanoic	-54	<-54	51.1	10.1
lesquerolic	coco (C12-C16)	-24	<-24	40.4	8.4
lesquerolic	stearic	3	12	38.6	8.2
hydroxystearic	acetic	-63	n.d.	n.d.	n.d.
hydroxystearic	propanoic	-62	n.d.	n.d.	n.d.
hydroxystearic	butanoic	-31	n.d.	n.d.	n.d.
hydroxystearic	oleic	-36	<-36	68.3	12.2

Base acid	Capping acid	Pour point (°C)	Cloud point (°C)	Viscosity at 40 °C (cSt)	Viscosity at 100 °C (cSt)
hydroxystearic	stearic	6	25	43.6	8.7
hydroxyarachidic	oleic	-12	-6	37.0	7.9
hydroxyarachidic	stearic	6	31	45.7	9.1

n.d. = not determined

As one can depict from the data in **Table 19**, they are in excellent accordance with the rules/tendencies which were described earlier. The pour points and cloud points are the lowest for the unsaturated estolide esters and the highest for the saturated ones.

Beside the chosen base fatty acid for an estolide, the other important component that determines the physical properties of the estolide is the alcohol, which is used for esterification. In 2001, *Isbell et al.*<sup>[178]</sup> investigated the influence of the alcohol on the low-temperature properties and viscosities of estolides. Beside the oleic acid estolide they also investigated estolides based on crambe and meadowfoam oil<sup>[179]</sup>, which contain mainly erucic acid (crambe) or 5-eicosenoic acid (meadowfoam). They observed the best pour points for the oleic acid estolides which bear the estolide linkage in C9-position, while erucic acid estolides (C13 linkage) and 5-eicosenoic acid estolides (C5 linkage) lacked in low temperature performance. Especially Guerbet alcohols, e.g. 2-ethylhexanol, showed the best performance and properties when used for esterification with the estolides (**Table 20**). Furthermore, this study revealed that estolides with rather low EN numbers (EN = 1.1-1.5) have lower pour point as their analogues with higher EN numbers.

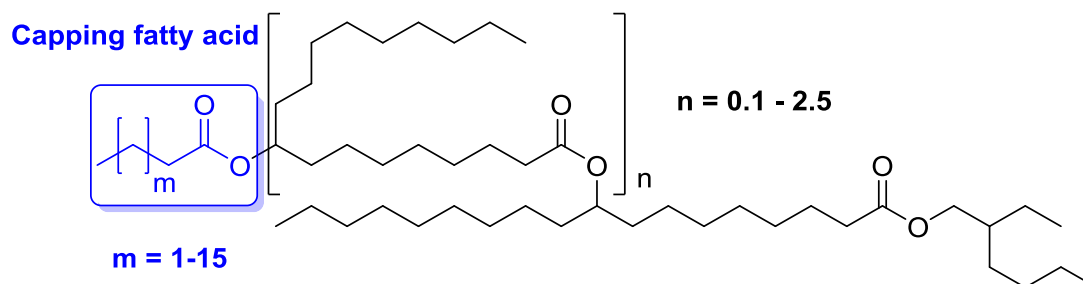
**Table 20:** Physical properties of oleic acid, erucic acid and 5-eicosenoic acid estolides, which are esterificated with different alcohols.<sup>[167,178]</sup>

Estolide	Melting point (°C)	Viscosity at 40 °C (cSt)	Viscosity at 100 °C (cSt)
erucic estolide	0	679.0	58.6
erucic estolide 2-ethylhexyl ester	-12	184.4	26.1
5-eicosenoic estolide	6	229.8	27.4
5-eicosenoic estolide 2-ethylhexyl ester	-1	104.2	16.5
oleic estolide	-31	404.9	40.0
oleic estolide methyl ester	-27	169.1	23.7
oleic estolide butyl ester	-27	238.4	30.3
oleic estolide decyl ester	-10	149.0	21.4
oleic estolide oleyl ester	-22	187.2	26.8
oleic estolide 2-methylpropyl ester	-32	200.7	26.7
oleic estolide 2-ethylhexyl ester	-34	161.2	22.5
oleic estolide C18 Guerbet ester	-43	206.6	27.4
oleic estolide C24 Guerbet ester	-32	169.4	24.3



Beside the base fatty acid chain and the alcohol used for esterification, the last important component for the physical properties of the estolide is the capping fatty acid. *Isbell et al.*<sup>[172]</sup> revealed that the pour point of oleic estolides capped with saturated fatty acids are lowest when they are capped with mid-sized linear fatty acids (C8 and C10, see **Table 21**) because they disrupt the alignment of the aliphatic chains best. This result was in good accordance with the observed properties of the estolides listed in **Table 20**, where the oleic estolides (C9 linkage) also showed the best low-temperature properties compared to C5- and C13-linked estolides.

**Table 21:** Influence of the capping acid on the properties of oleic estolides.<sup>[167,172]</sup>

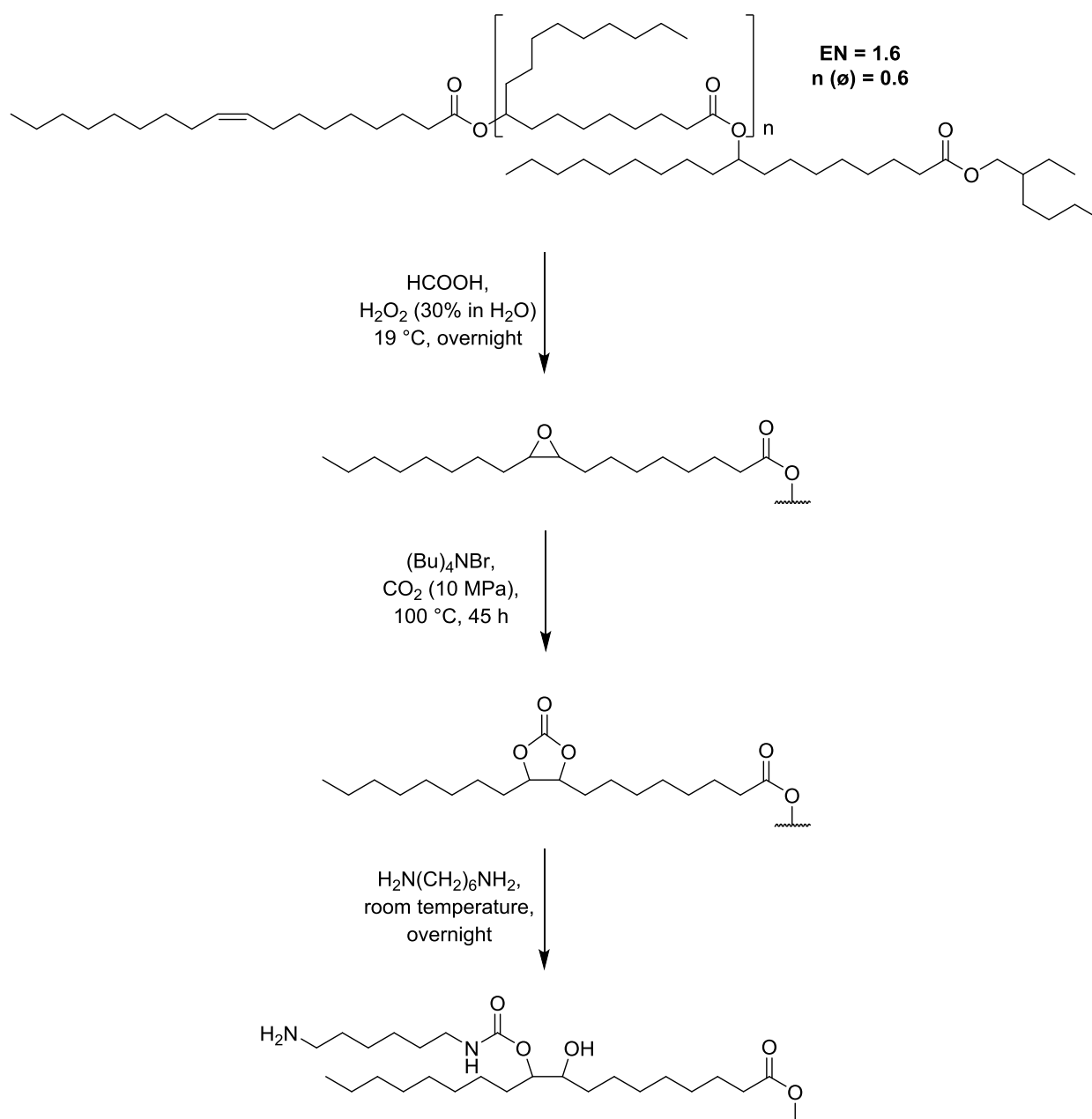


Capping fatty acid	EN <sup>a</sup>	Pour point (°C)	Cloud point (°C)	Viscosity at 40 °C (cSt)	Viscosity at 100 °C (cSt)
butyric (C4)	2.8	-30	-36	125.5	19.3
caproic (C6)	3.5	-30	-34	114.5	17.9
octanoic (C8)	3.0	-36	-41	104.4	16.8
decanoic (C10)	2.7	-39	n.d. <sup>b</sup>	93.8	15.5
lauric (C12)	2.2	-36	-32	73.9	13.0
myristic (C14)	2.0	-25	-22	80.5	13.9
palmitic (C16)	1.4	-12	-13	81.6	13.5
stearic (C18)	1.1	-5	-4	81.8	14.0

a. According to GC-analysis; b. n.d. = not determined

Importantly, the oleic estolides do not possess any unsaturated functionalities anymore, which is reflected in their excellent oxidative stability. *Cermak et al.*<sup>[173]</sup> could demonstrate that the oleic estolide have comparable oxidative stability over 240 minutes in the "Rotating Pressure Vessel Oxidation Stability Test" (RPVOT) like standard hydraulic fluids and aviation lubricants, when they are formulated with standard additives like butylated hydroxytoluene (BHT) or alkylated diphenylamines (ADA). This result underlines the high potential of estolide to compete with already established products in the lubricant market.

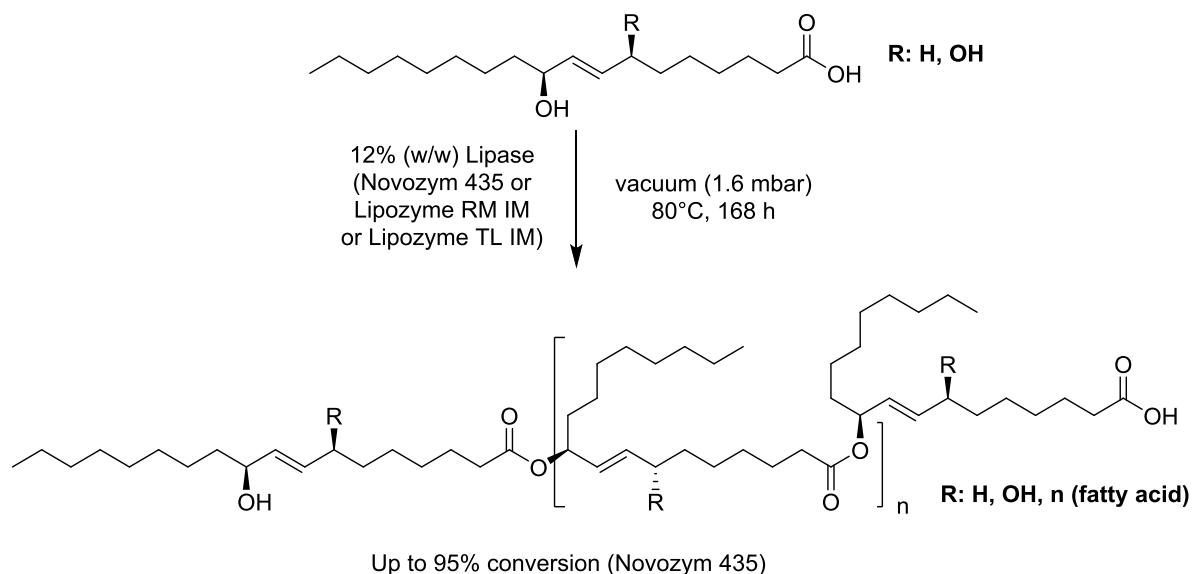
The newest developments in the estolide subject have dealt with disclosing new functionalities and properties. In 2016, *Doll et al.*<sup>[174,175]</sup> synthesized carbonated oleic estolide 2-ethylhexyl esters (**Scheme 50**), which were further functionalized with hexamethylenediamine ( $\text{H}_2\text{N}(\text{CH}_2)_6\text{NH}_2$ ) to yield carbamate containing estolides. They started with an epoxidation of the unsaturated C-C double bond of the capping oleic acid chain. Afterwards, high pressure addition of  $\text{CO}_2$  was conducted to yield the cyclic carbonate estolides. These were opened by hexamethylenediamine, which represents an isocyanate-free access route towards carbamates. Furthermore, they analyzed the C-C double bond geometry and other bond formations of the estolides *via* extensive NMR-studies. Earlier studies by *Lowery et al.*<sup>[180]</sup> and *Li et al.*<sup>[181]</sup> also dealt with further functionalization of epoxidized fatty acids for usage as lubricants.



**Scheme 50:** Synthesis of carbonated oleic estolide esters and functionalization with hexamethylenediamine.

Lastly, some chemo- and biocatalytic esterifications for the synthesis of various esters of fatty acids that are suitable as materials for estolide synthesis have been conducted.<sup>[182,183-188]</sup> Additionally, estolide synthesis by lipase catalyzed polymerization of fatty acids has also been conducted.

Most recently, *Martin-Arjol et al.*<sup>[189]</sup> used lipases to synthesize estolides. They started from the unsaturated fatty acids 10(*S*)-hydroxy-8(*E*)-octadecenoic acid and 7,10(*S,S*)-dihydroxy-8(*E*)-octadecenoic acid and polymerized them under neat conditions at 80 °C for 168 hours to obtain their unsaturated estolide esters (**Scheme 51**).



**Scheme 51:** Lipase-catalyzed estolide synthesis under neat conditions.<sup>[189]</sup>

However, several problems are inherent in this approach.

- 10(*S*)-hydroxy-8(*E*)-octadecenoic acid and 7,10(*S,S*)-dihydroxy-8(*E*)-octadecenoic acid have to be synthesized by fermentation of oleic acid with *Pseudomonas aeruginosa* 42A2, hence increasing the cost of the fatty acid tremendously.
- The lipases show relatively low activity towards the substrates, which is obvious regarding the high enzyme loading (12% (w/w)) and the incomplete conversions of up to 72% and 95%.
- The products are a broad mixture of oligomers (reaching up to decamers). This leads to hardly analyzable products.
- The unsaturation of the base fatty acid leads to low oxidative stability. Hydrogenation of the C-C double bond is preferable; however this is only achievable after tedious protection and successive deprotection of the OH-groups.
- The viscosities of the synthesized estolides are very high with 402-3235 cSt compared to other estolides which have been reported (e.g. 161 cSt at 40 °C for oleic acid 2-ethylhexyl ester, see **Table 20**).

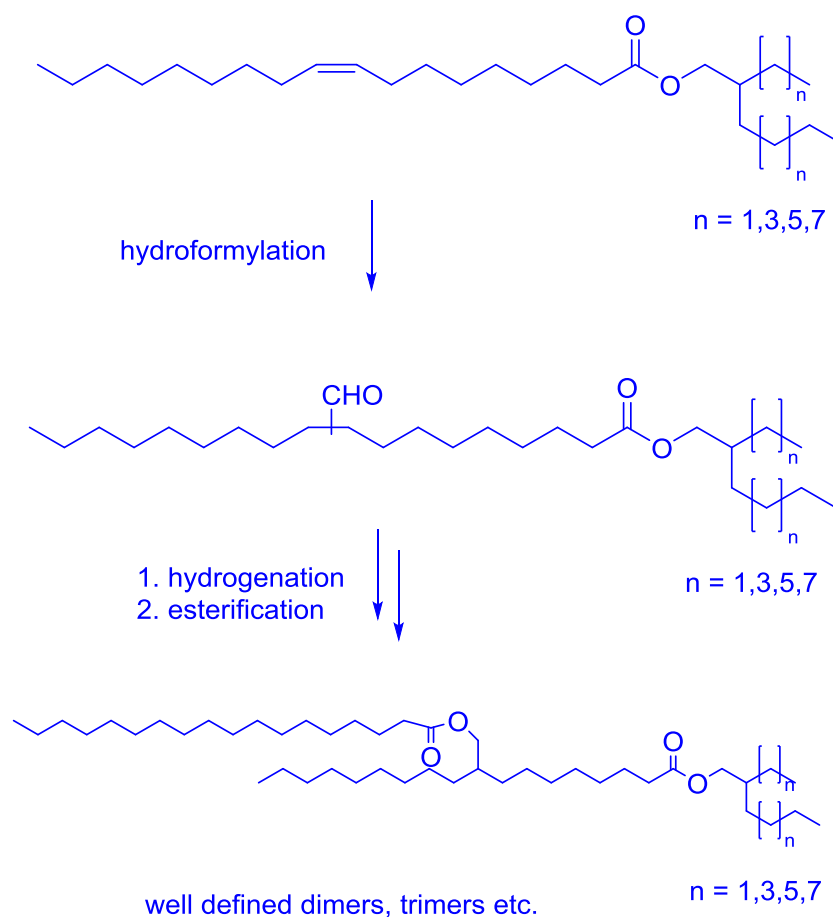
In summary, many pioneering works in the lubricant production out of renewable resources have been conducted in the last year, but the gap to commercial application has to be closed yet.

## 6.2 NEW LUBRICANT ESTER STRUCTURES – SYNTHESIS AND BIODEGRADABILITY

Our project started with the evaluation for an alternative approach for the controlled lubricant ester oligomer synthesis based on oleic acid. One possibility is the addition of a formyl fragment by hydroformylation (**Scheme 52**).<sup>[56,163,190]</sup> By subsequent hydrogenation of the aldehyde moiety, one obtains a hydroxylated fatty acid ester that can be esterified with a carboxylic acid (or its derivate) of choice.

As a starting point for the access of the new estolide structures *via* hydroformylation, one can consider the reported work of the *Börner*<sup>[191]</sup>, *Behr*<sup>[192]</sup> and *Hapiot*<sup>[193,194]</sup> groups on the hydroformylation of methyl oleate and triglycerides of unsaturated fatty acids.

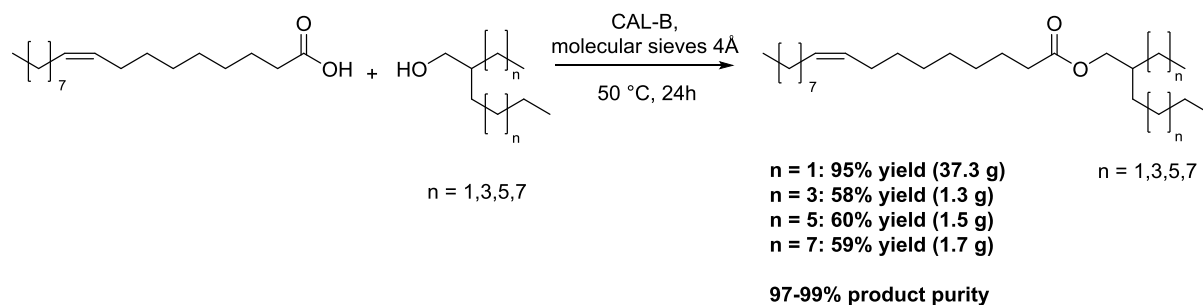
### Newly envisioned lubricant ester structures



**Scheme 52:** New, envisioned access route to estolide structures by modification at the C-C double bond of oleic acid.

However, the hydroformylation setup requires a lot of expertise and expensive hardware. Hence, an alternative route that could be conducted in lab scale had to be identified.

First, the esterification of oleic acid had to be optimized. In contrast to the conventional esterification that requires an excess of alcohol and Brønsted acid catalysis under reflux conditions, we decided to utilize the commercially available, immobilized lipase CAL-B (Novozym 435) for the esterification. In contrast to the conventional approach, only stoichiometric amounts of alcohol are required and the process can be run at lower temperatures (here 50 °C) and under neat conditions. To drive the reaction equilibrium towards complete conversion, we used molecular sieves (4 Å pore size) to bind the one equivalent of water that is formed during the esterification. Regarding the alcohol of choice for the esterification, we decided to use Guerbet alcohols. These alcohols are known for their excellent softener qualities and low viscosity levels and have already been proven to be the most promising alcohols to give estolides excellent viscosity properties (see **Table 20**). Furthermore, some earlier research had already been conducted for the synthesis of esters of fatty acids with Guerbet alcohol, including by means of biocatalytic esterification in up to 3000 L scale.<sup>[183–188]</sup> With this method, we were able to obtain the synthesized esters with 97–99% purity (according to GC analysis) on gram scale (**Scheme 53**). These esters were highly pure because of the mild reaction conditions of the lipase catalyzed esterification.



**Scheme 53:** Biocatalytic esterification of oleic acid with several Guerbet alcohols on gram scale.

Since the 2-ethylhexyl esters are privileged for low temperature applications due to their low melting points, we scaled up the synthesis for the 2-ethylhexyl oleate to 100 mmol scale and obtained 37.3 g (95% isolated yield) 2-ethylhexyl oleate.<sup>[167,178]</sup>

Due to the high cost of the biocatalyst, recycling of it for several production cycles is a requisite for its economic *viability*. As a consequence, we decided to conduct the biocatalytic esterification with an equipped catalyst container for heterogeneous catalysts (SpinChem-reactor), in which we deposited the immobilized biocatalyst and the molecular sieves (

Figure 31). Fortunately, we could not observe any deterioration of the biocatalyst activity after three production cycles. This proves the high practicability of the Novozym 435. More precisely, 96–98% conversion towards 2-ethylhexyl oleate was observed in all production batches (**Figure 32**). For better mixing of the components, we decided to use cyclohexane as a solvent in these experiments since it can easily be removed after esterification *in vacuo*. The high conversion values correlate very well with the batch production in a stirred flask.

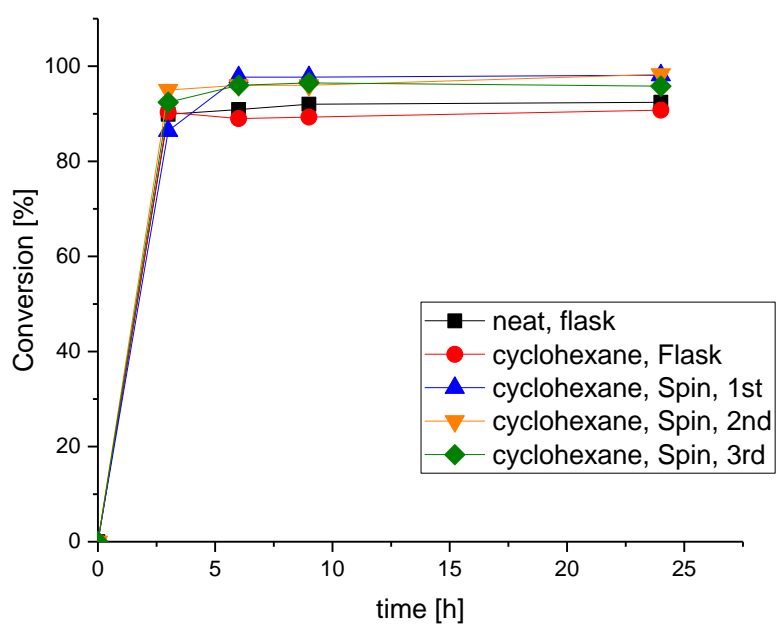
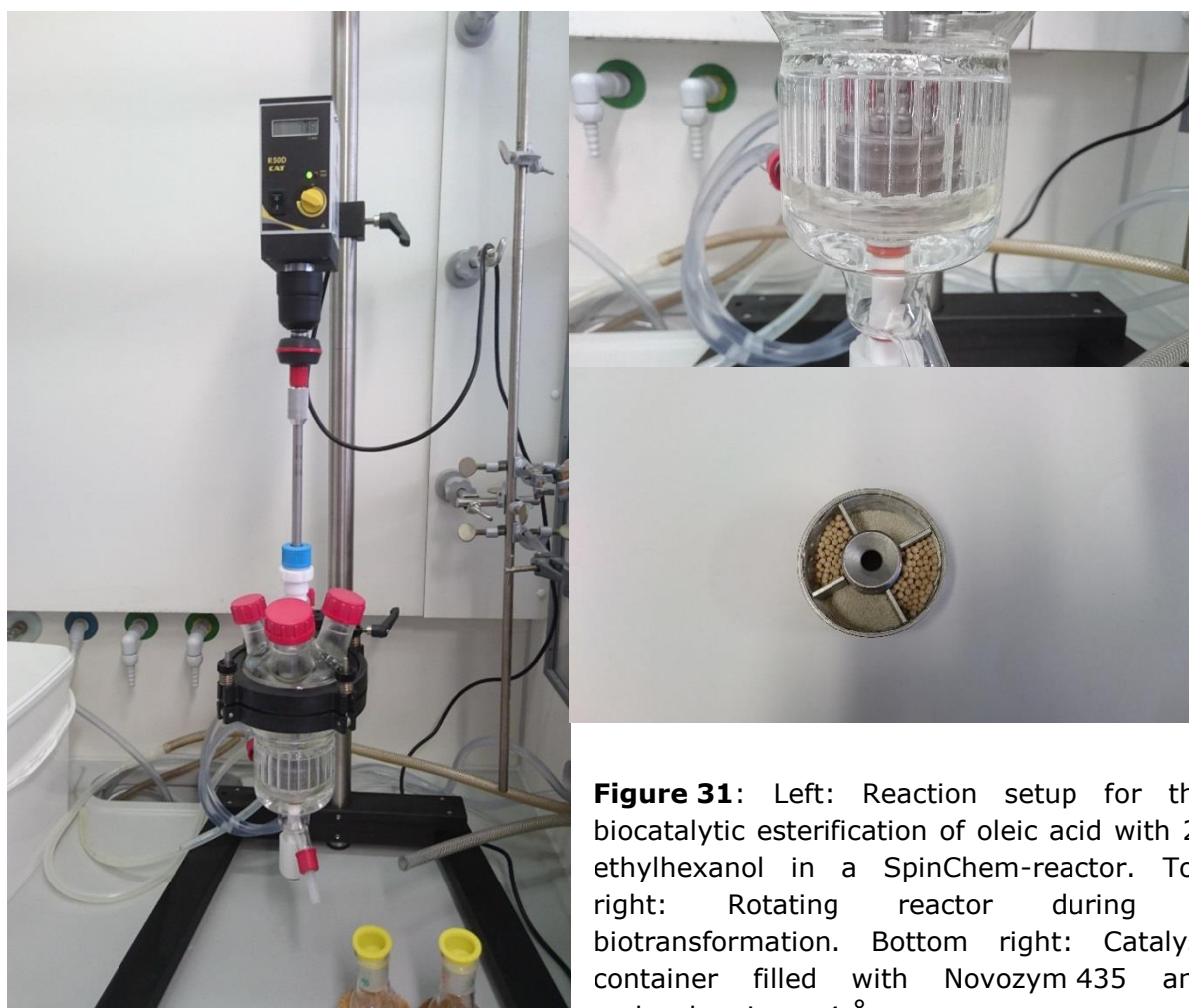
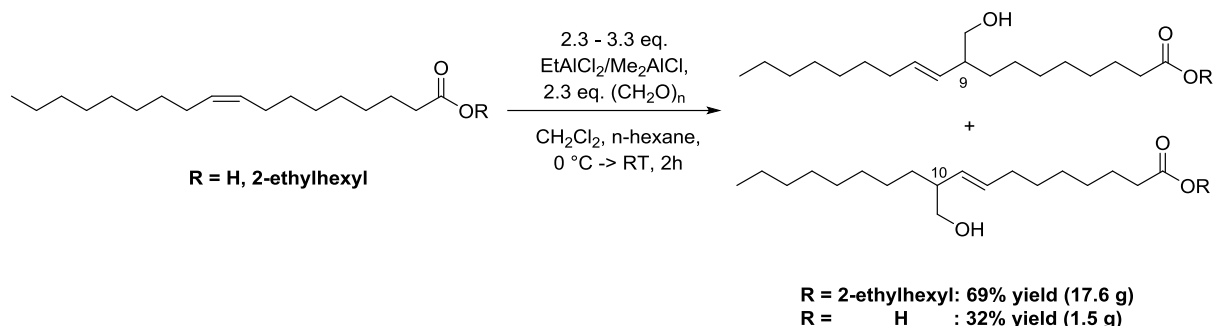


**Figure 32:** Time course for the conversion towards 2-ethylhexyl oleate.

For further upscaling of this esterification, *in vacuo* removal of the formed H<sub>2</sub>O in the reaction should be considered since molecular sieves are a major cost factor. The *in situ* removal of H<sub>2</sub>O for biocatalyzed estolide synthesis could already been shown by *Martin-Arjol et al.*<sup>[189]</sup> in 2015.

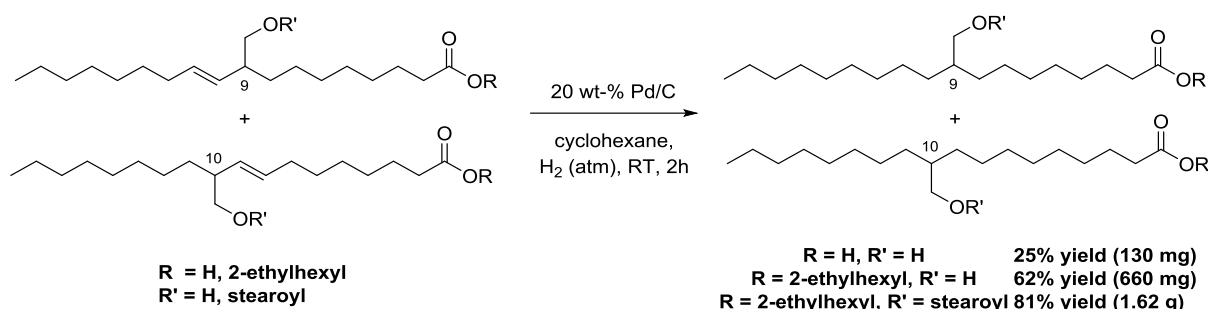
As an alternative to the hydroformylation of oleic acid esters exists a literature known approach *via* ene reaction with paraformaldehyde to introduce the required C1 fragment in one step as an hydroxy group. For this, either free oleic acid or its esters are treated with paraformaldehyde in dichloromethane in presence of aluminium Lewis acids (**Scheme 54**).<sup>[163,165,195–197]</sup> After several optimization experiments, it was decided to conduct the ene reaction only for the 2-ethylhexyl oleate instead of pure oleic acid since the overall yields were significantly higher. Under optimized conditions, the unsaturated, hydroxymethylated Guerbet ester could be obtained in up to 69% yield (17.6 g) after vacuum distillation. One of the advantages of this access route is the clearly defined position of the fatty acid chain modification. While the HClO<sub>4</sub>-catalyzed approach by *Cermak, Isbell et al.*<sup>[169]</sup> (see **Scheme 49**) leads to mixtures of C5-C13 adducts, this Lewis acid catalyzed ene reaction always leads to a 1:1 mixture of C9/C10 adducts. These positions have been proven to be the best ones for optimal properties of the estolides. A drawback of this synthesis is the required overstoichiometric amount (3.3 eq.) of aluminium Lewis acid and paraformaldehyde due to high waste generation. An alternative, catalytic approach would enhance the viability of this promising modification method for oleic acid and its derivatives. Additionally, Friedel-Crafts acylation of oleic acid derivates with acid chlorides followed up by hydrogenation of the obtained carbonyl moiety would open up the path to structures with higher branching and probably even better properties for use as lubricants.<sup>[165,198]</sup>



**Scheme 54:** Ene reaction of oleic acid or 2-ethylhexyl oleate.

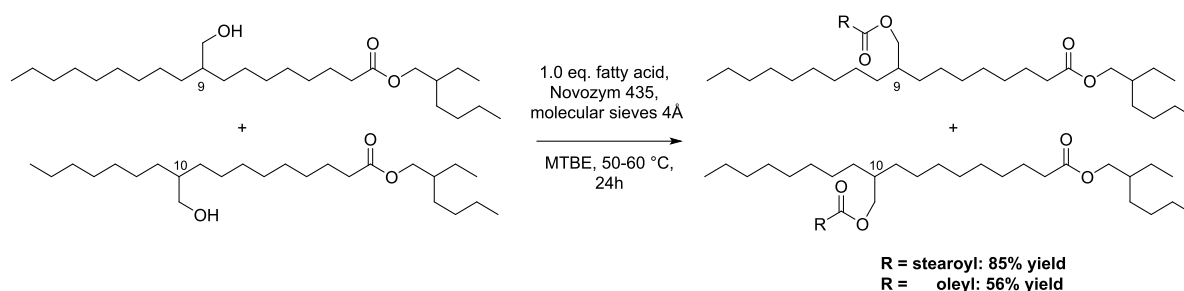
Once the hydroxymethylated oleic acid derivatives were obtained, hydrogenation of the C-C double bond was conducted with molecular hydrogen (H<sub>2</sub>) under atmospheric pressure, catalyzed by palladium immobilized on carbon (Pd/C) at room temperature. The hydrogenated, saturated alcohols could be obtained in 25% yield for the free acid derivative and 62% yield for the 2-ethylhexyl ester, respectively (**Scheme 55**). However, tedious work-up *via* column chromatography was necessary since hydrogenation of unprotected alcohols by Pd/C is accompanied by formation of side products by de-/hydrogenation of the OH-group. To avoid this drawback, the hydrogenation was conducted after esterification of the unsaturated, hydroxymethylated alcohol. In this case, hydrogenation was highly selective and yielded the saturated new dimer in high purity with

up to 81% yield (1.62 g). This hydrogenation could be conducted on bigger scale with similar yields.



**Scheme 55:** Hydrogenation of the C-C double bonds of the hydroxymethylated oleic acid derivatives by molecular hydrogen ( $\text{H}_2$ ).

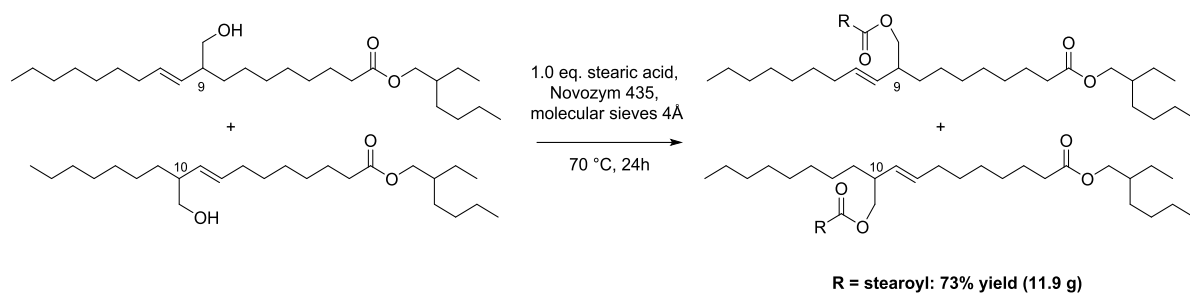
The selective esterification of the hydroxymethylated 2-ethylhexyl oleic acid esters was the next important step for the synthesis of the estolide dimers. Initially, we esterificated the saturated alcohol with the fatty acids in MTBE at 50-60 °C to obtain the dimer with 85% or 56% isolated yield (see **Scheme 56**).



**Scheme 56:** Biocatalytic esterification of the hydroxymethylated 2-ethylhexyl oleic acid ester with stearic acid or oleic acid.

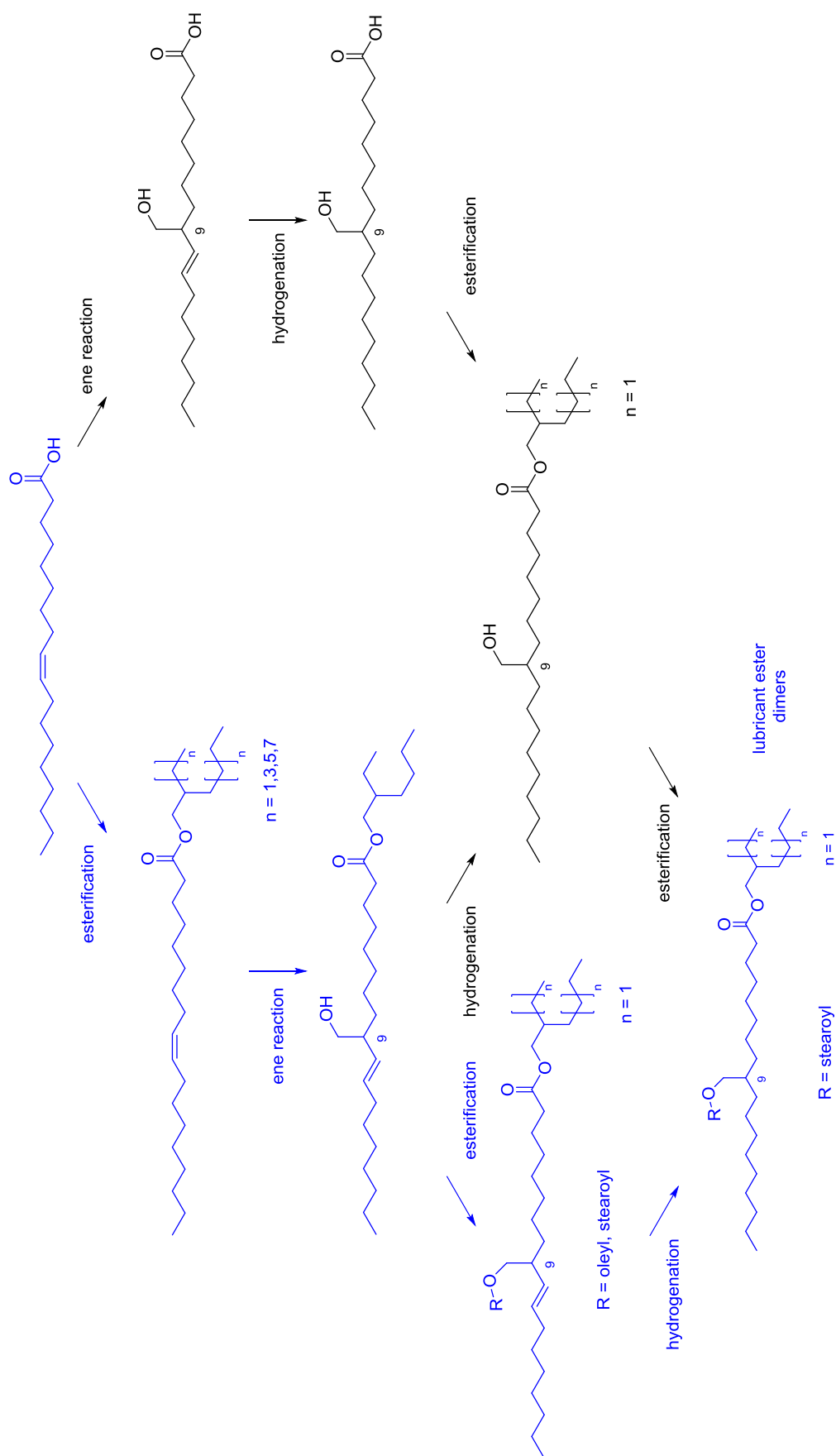
However, the above mentioned selectivity problems with the hydrogenation of non-protected alcohols prompted us to esterificate the unsaturated product of the ene reaction, 2-ethylhexyl (*E*)-9+10-(hydroxymethyl)octadec-10+8-enoate (C9/C10 adduct, 1:1 ratio), directly with stearic acid and conduct the hydrogenation with the formed estolide dimer (see **Scheme 55** and **Scheme 57**). After the desired dimer was filtrated over silica, it could be obtained with up to 73% yield (11.9 g) in high purity.





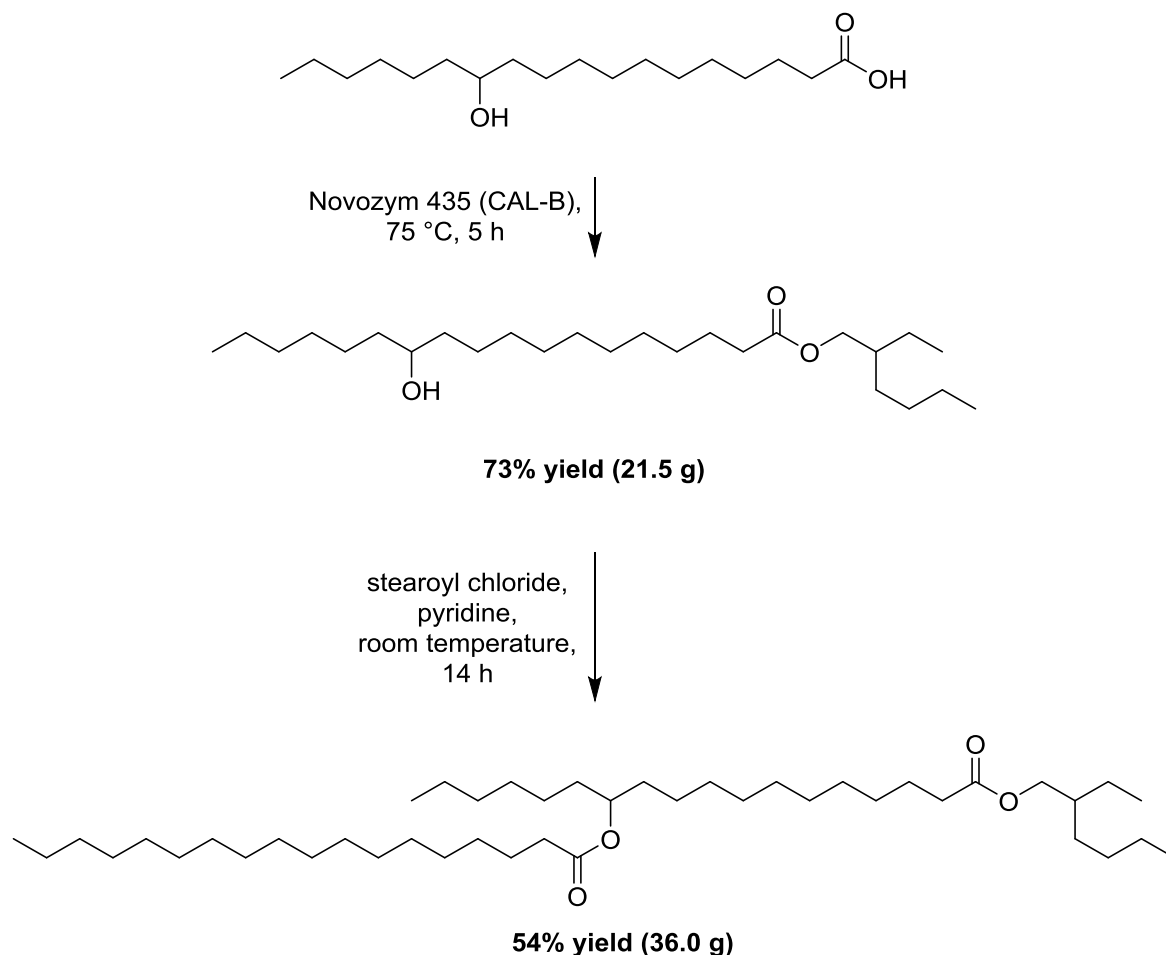
**Scheme 57:** Biocatalytic esterification of the unsaturated, hydroxymethylated alcohol with stearic acid.

There are different synthetic routes to obtain the new dimer structures. Based on the above mentioned results, the following one was chosen as the most promising one with respect to selectivity and yield: First, esterification of oleic acid with Guerbet alcohols is conducted. Second, ene reaction with paraformaldehyde of the Guerbet oleates is conducted. Third, esterification of fatty acids with the allyl alcohol derivate is conducted. Last, palladium catalyzed hydrogenation yields the saturated, new dimer (**Scheme 58**).



**Scheme 58:** Synthetic route overview for the synthesis of new lubricant esters. The preferred route is marked in blue. All reactions after the ene reaction include the C10-addition regioisomers (C9/C10 ratio: 1:1).

After successfully establishing an access towards the new estolide structures, the author decided to synthesize a reported estolide structure to get a direct comparison between the old and new structures in terms of their biodegradation. Towards this end, it was decided to synthesize a monoestolide 2-ethylhexyl ester derived from 12-hydroxystearic acid that is capped with stearic acid (**Scheme 59**). 12-Hydroxystearic acid is accessible by hydrogenation of ricinoleic acid from castor oil.<sup>[165,167]</sup>



**Scheme 59:** Synthesis of 2-ethylhexyl 12-(stearoyloxy)octadecanoate starting from 12-hydroxystearic acid.

The biocatalytic esterification of 2-ethylhexanol with 12-hydroxystearic acid was conducted with Novozym 435 (30 mg/mmol) at 75 °C for 5 hours and yielded the 2-ethylhexyl 12-hydroxyoctadecanoate with 73% yield after purification *via* vacuum distillation. Regarding the possible formation of 12-hydroxystearic acid oligomers by self-condensation, no amount of this side-product was detected *via* <sup>1</sup>H-NMR after five hours. This can be explained with the manifold faster catalyzed esterification of the primary hydroxy moiety with the carboxyl group through the Novozym 435. The slow reaction speed for the esterification of secondary esters with Novozym 435 was already shown by *Martin-Arjol et al.*<sup>[189]</sup> (see **Scheme 51**, chapter 6.1).

To avoid slow transesterification of the 2-ethylhexyl 12-hydroxyoctadecanoate with stearic acid, stearoyl chloride ( $n\text{-C}_{17}\text{H}_{35}\text{COCl}$ ) was used for the selective esterification to yield the monoestolide 2-ethylhexyl 12-(stearoyloxy)octadecanoate with a total yield of 54% (36.0 g) after column chromatography. For that synthetic step, products from four separate reactions on 10 g scale (referring oleic acid) were combined for the purification *via* column chromatography.

The most important criteria for the sustainability of a lubricant is its biodegradability, since every year huge amounts of lubricants are leaked into the environment, polluting huge amounts of water and ground. Hence, we decided to test the biodegradability of the newly synthesized estolides according to the OECD guideline 301 F. This guideline describes the biodegrading of a chemical compound in a closed-bottle test. For a successful biodegradation, over 60% of the investigated compound has to be decomposed after a defined time frame (28 days) under aerobic conditions.

To get a valuable comparison in terms of biodegradability, it was decided to test the newly synthesized lubricant ester, harboring a bridging methylene moiety, against the already reported estolide structure by *Cermak et al.*<sup>[176]</sup>, which is derived from 12-hydroxystearic acid (**Figure 33**).

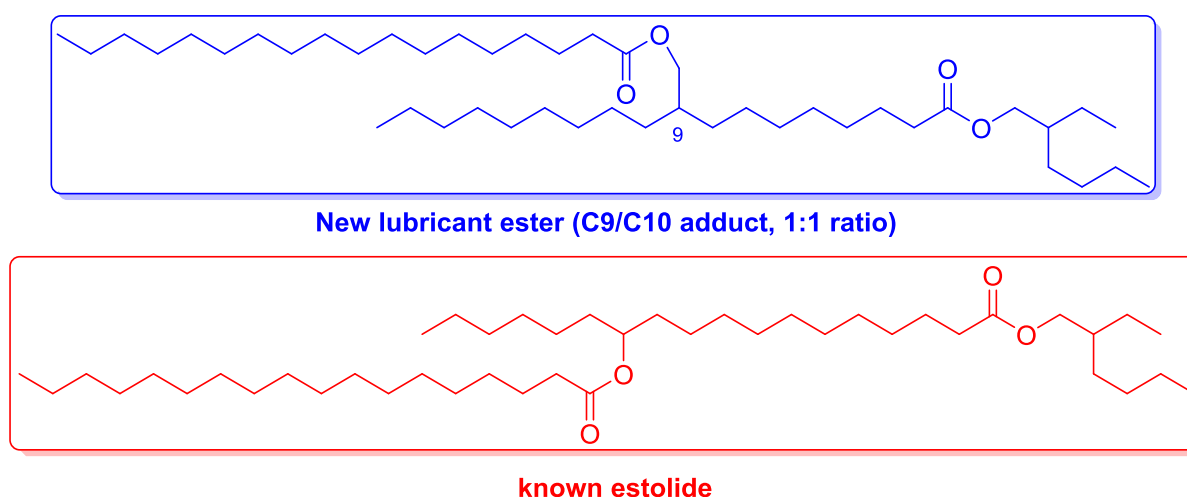


**Figure 33:** Structures of the investigated estolides for the biodegradability test according to guideline OECD 301 F (closed-bottle test).

Beside the minimum amount of 60% which have to be degraded, another criterion is the degradation of 50% of the compound in a time frame of 10 days once the first 10% have been degraded.

The closed-bottle test was conducted by *Klüber Lubrication* in Munich and the result is excellent.<sup>[199]</sup> After 28 days, 81.3% of the new lubricant ester have been degraded and the first 60% have been degraded after 8 days (**Figure 34**). These values prove the ready biodegradability of the new estolide and underline its potential as a sustainable alternative based on renewable resources. In comparison, the known estolide structure was also degraded to a total amount of 83.3% after 28 days, with the first 60% being degraded after 7 days (**Figure 35**). This result is very similar to the newly synthesized lubricant ester and demonstrates that the additional methylene moiety poses no threat to the biodegradability of a lubricant ester.

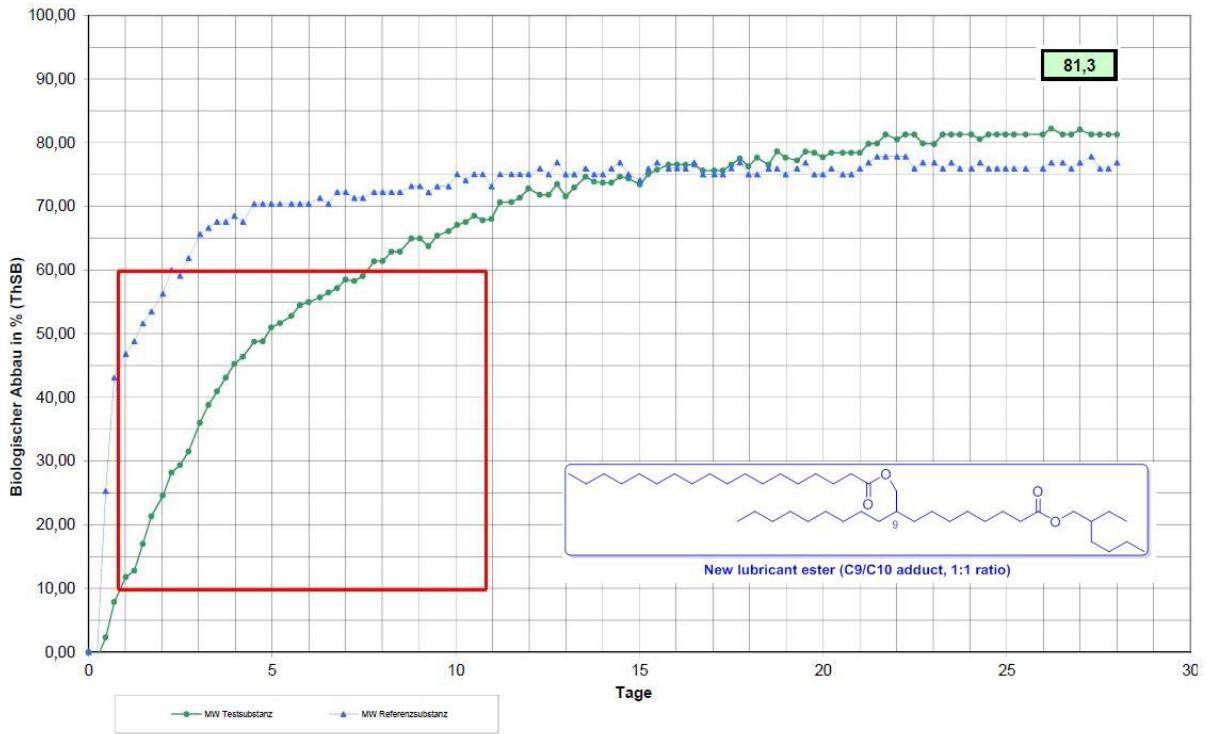


**Figure 34:** Biodegradability test according to OECD 301 F of the new lubricant ester, performed by and at *Klüber Lubrication*.<sup>[199]</sup>

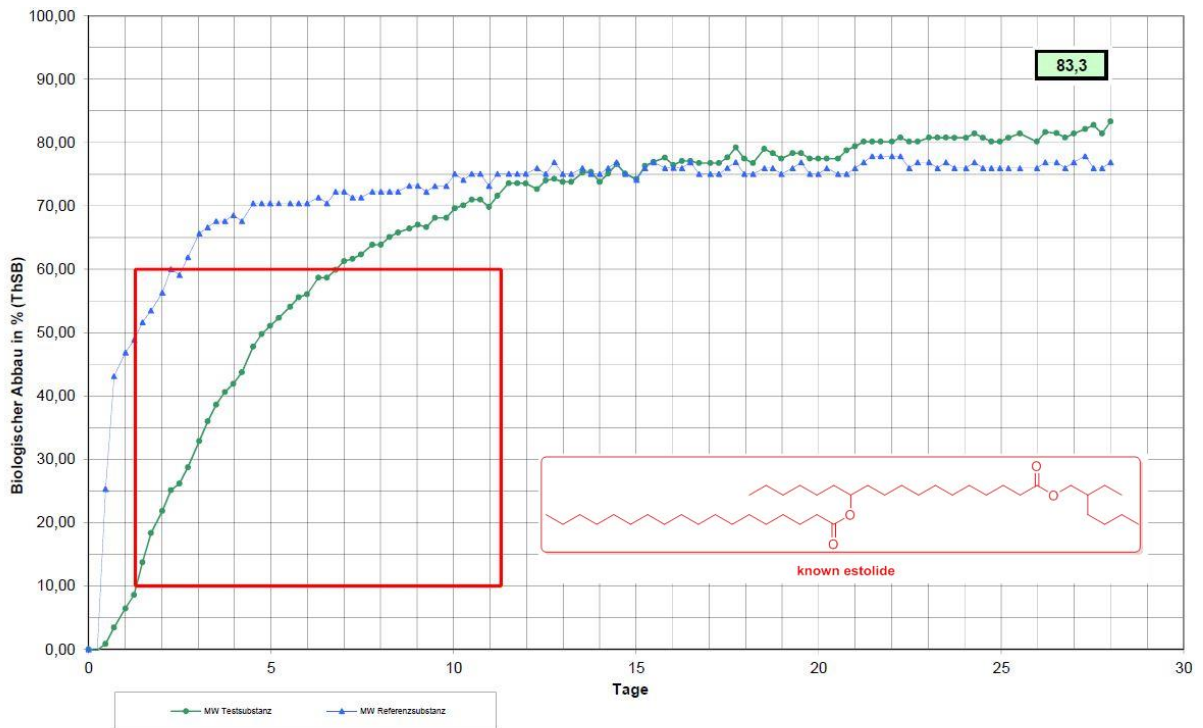


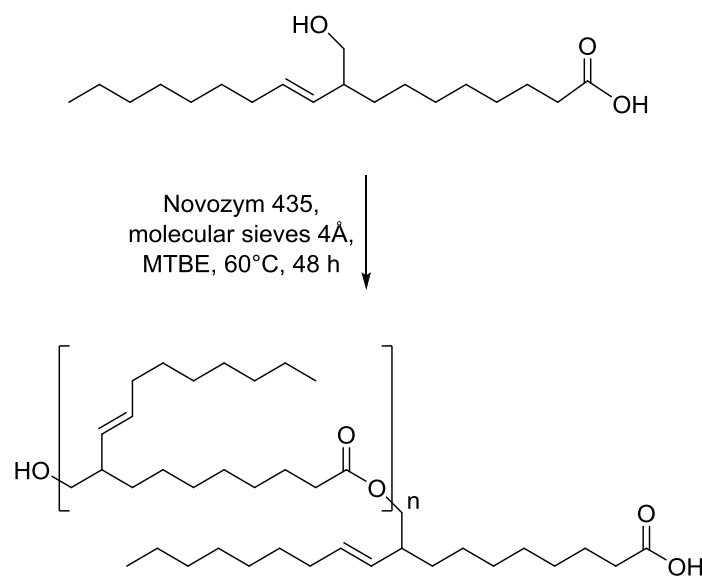
**Figure 35:** Biodegradability test according to OECD 301 F of the known estolide, performed by and at *Klüber Lubrication*.<sup>[199]</sup>

### 6.3 SUMMARY AND OUTLOOK FOR THE ESTOLIDE SYNTHESIS

The successful synthesis of new lubricant ester dimer structures, including the positive results for the biodegradability (see **Figure 34** and **Figure 35**), opens the path towards a highly attractive substrate motif for sustainable, environmentally friendly lubricants that are based on renewable resources. Synthesis of the dimers on multi-gram scale was successful and an access route *via* an ene reaction could be identified.

Another important milestone for the technical application of the new lubricant ester structures is the hydroformylation of the oleic acid esters in large scale. Based on the earlier works of the *Börner*<sup>[191]</sup>, *Behr*<sup>[192]</sup> and *Hapiot*<sup>[193,194]</sup> groups, this milestone should be feasible in a short-time period by implementing the know-how of a specialized company (e.g. OXEA).

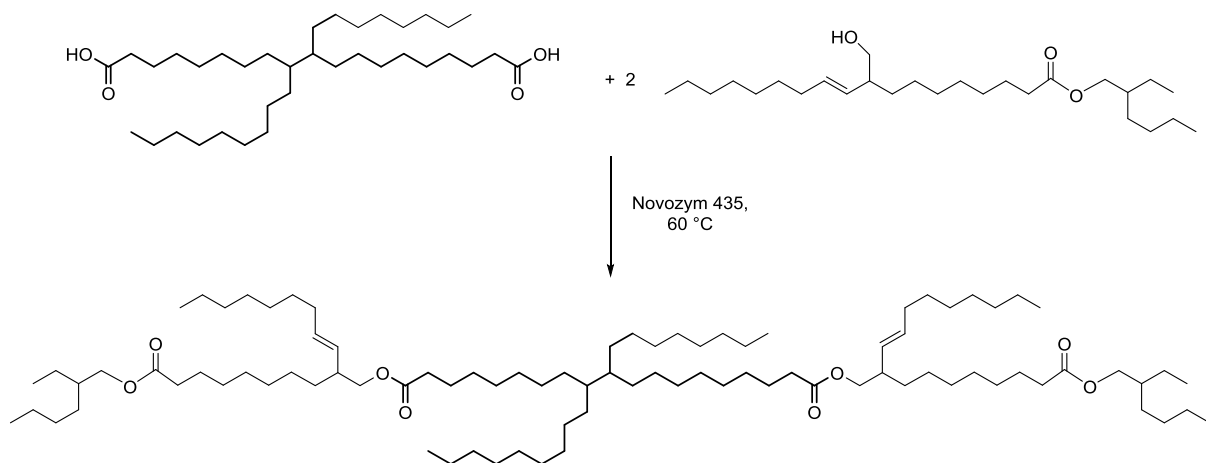
Beside the access towards lubricant ester dimers, the controlled access towards higher oligomers represents an important topic for this compound class. Currently, these investigations are on-going. In this approach, oligomerization of the unsaturated, hydroxymethylated oleic acid derivate by lipase catalysis is one of the possible access routes (**Scheme 60**).



**Scheme 60:** Lipase catalyzed oligomerization of 9+10-(hydroxymethyl)octadec-10+8-ene acid (C9/C10 mixture, 1:1 ratio).

Another possibility to gain access towards higher oligomers is represented by the esterification with the diacid PRIPOL 1013 (one of its possible constitutions is shown in **Scheme 61**). Further investigations are necessary to optimize this route.

Lastly, the ene reaction of oleic acid with formaldehyde is still far from an optimal state. Especially the large amounts of required Lewis acid are a drawback of this route. Maybe better reagents or catalysts exist that can be applied for a more efficient ene reaction, lowering to generated waste amount drastically.



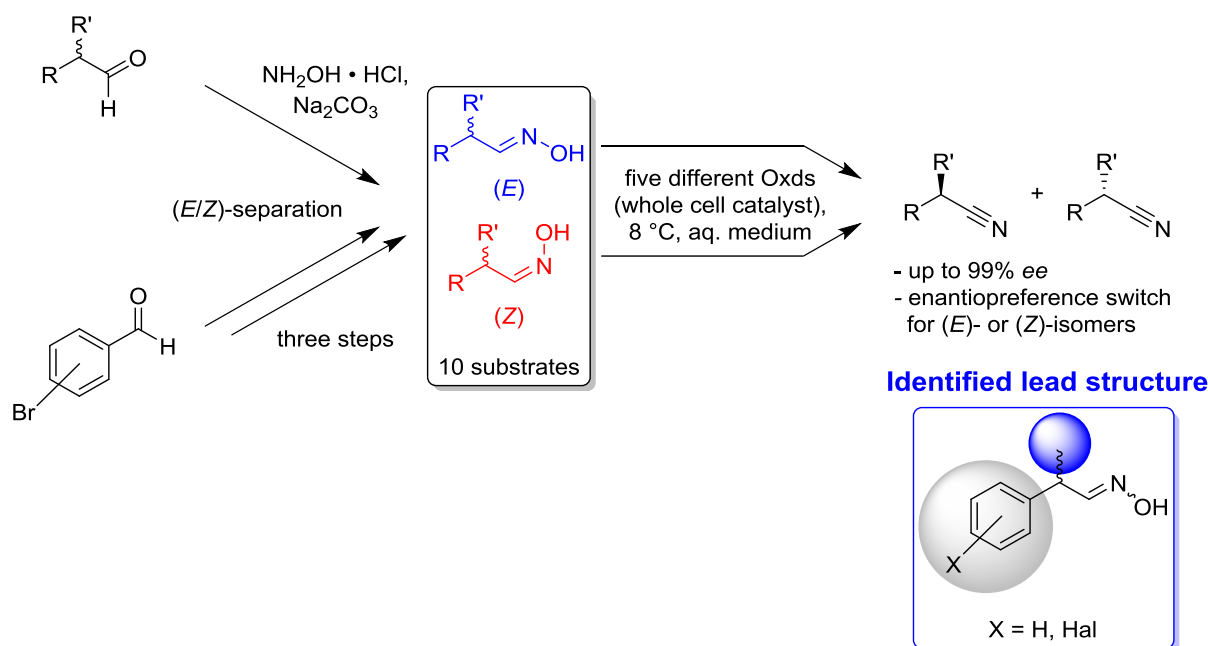
**Scheme 61:** Esterification of PRIPOL 1013 with the unsaturated alcohol derivative of oleic acid.





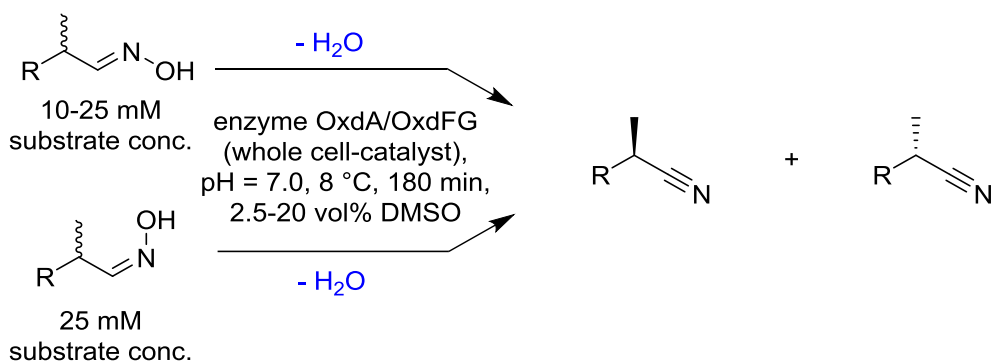
## 7 SUMMARY AND OUTLOOK

Several achievements could be realized in the course of this thesis. First off, the chiral nitrile synthesis with aldoxime dehydratases (Oxds) has been thoroughly investigated by transforming a broad range of arylaliphatic and aliphatic substrates, which were synthetically prepared, with five different Oxds as whole cell catalyst. Apart from the substrate scope broadening, a lead structure for obtaining high ee-values in the chiral nitrile synthesis has been identified: 2-phenylpropanal oxime (PPOx) and its derivatives. Transforming the racemic, brominated PPOx derivatives led to ee-values of at least 90% (and up to 99%) even at elevated conversion rates close to 50% in a kinetic resolution. Additionally, an impressive phenomenon could be observed when the in advance separated (*E*)- or (*Z*)-stereoisomers of the aldoximes were utilized as substrates: The enantioselectivity of the Oxds switched in dependence of the (*E/Z*)-configuration, yielding either the (*S*)-nitrile preferentially out of the (*E*)-isomers or the (*R*)-nitrile out of the (*Z*)-isomers. As a consequence, both enantiomers can be synthesized by the same biocatalyst without the need to screen for a new catalyst with different enantioselectivity (**Scheme 62**). This project was conducted in cooperation with Rommelmann<sup>[99]</sup>, Oike<sup>[84]</sup> and the Asano group from the Toyama Prefectural University.

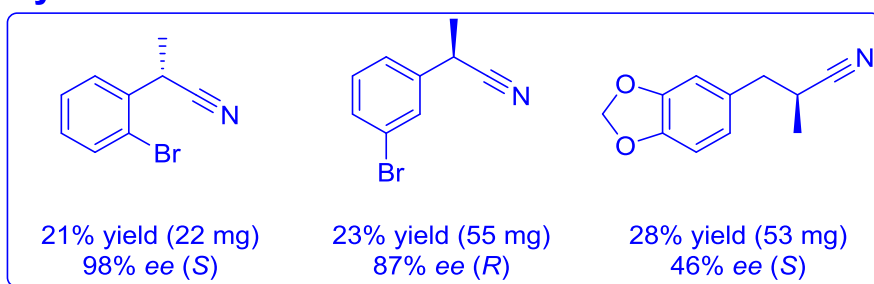


**Scheme 62:** Project overview of the enantioselective, biocatalytic nitrile synthesis.

Additionally, a first process development by conducting preparative scale experiments was successful (**Scheme 63**). Three substrates were transformed at 10–25 mM substrate concentration with isolated yields of up to 28% and ee-values with up to 98% (*S*).

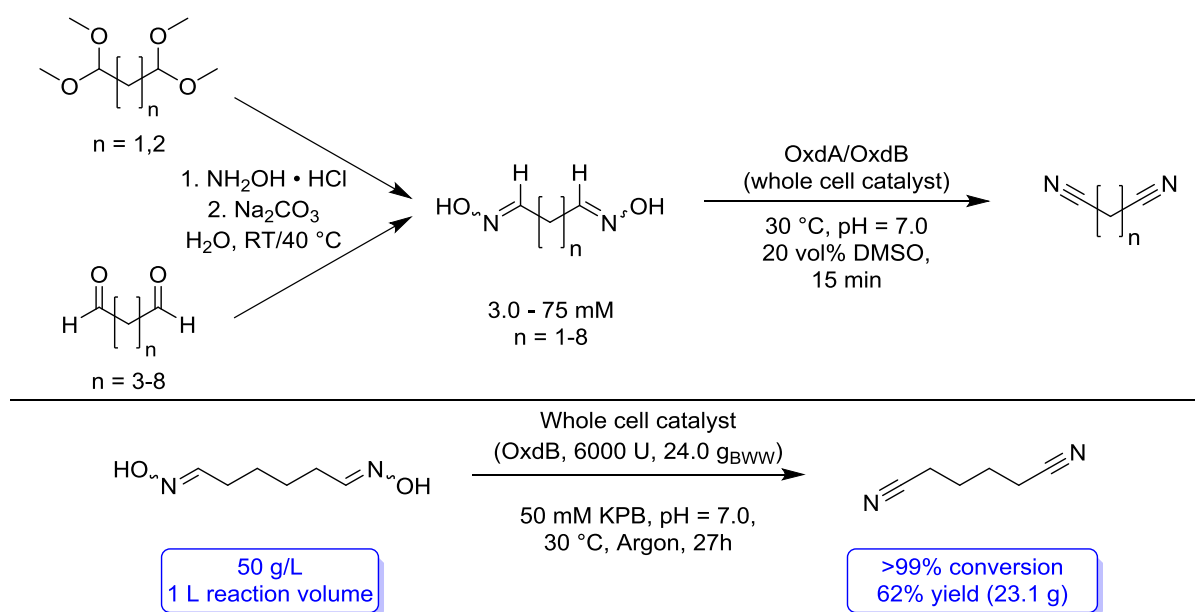


### Synthesized nitriles



**Scheme 63:** Biocatalytical synthesized chiral nitriles on preparative scale.

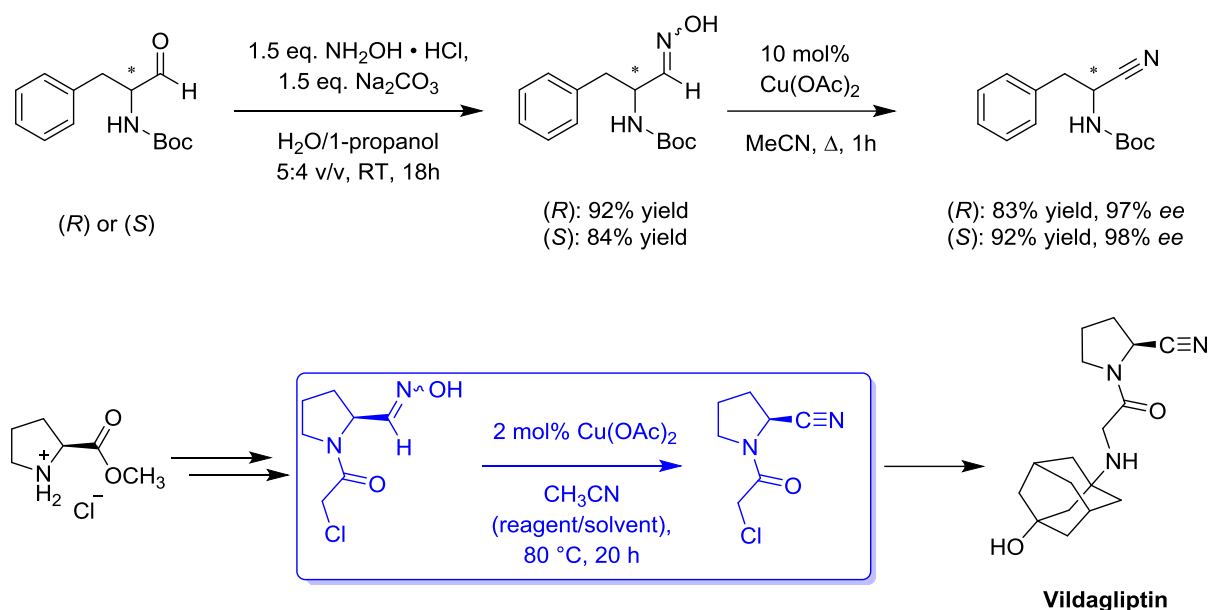
Apart from the achievements for the chiral nitrile synthesis with Oxds, the synthesis of dinitriles with Oxds could be shown for the first time (**Scheme 64**). Eight different dialdoximes, of which most were completely unknown in literature, with a chainlength from three to ten carbon atoms were synthesized and subsequently investigated for conversion by Oxds in a broad substrate scope study.



**Scheme 64:** Dialdoxime synthesis, substrate scope study and adiponitrile synthesis upscaling.

Especially adipaldehyde dioxime was identified as a privileged substrate. The synthesis of its dinitrile, the industrially highly important adiponitrile (precursor of hexamethylenediamine), was intensified in a process development study. Up to 50 g/L substrate loading could be completely converted into adiponitrile, even at liter scale (23.1 g isolated adiponitrile). This is the first example of an adiponitrile synthesis at ambient conditions in water without the generation of any waste except from two molecules of water and excellent chemoselectivity without any detectable side products. In cooperation with *Gruber-Wölfler* and *Maier* from the TU Graz the solubility of the adipaldehyde dioxime in the reaction medium could be rationalized.<sup>[124]</sup> Additionally, first results in the immobilization of Oxds were obtained and high cell-density fermentations were conducted to obtain larger amounts of Oxds in cooperation with the *Friehs* group.

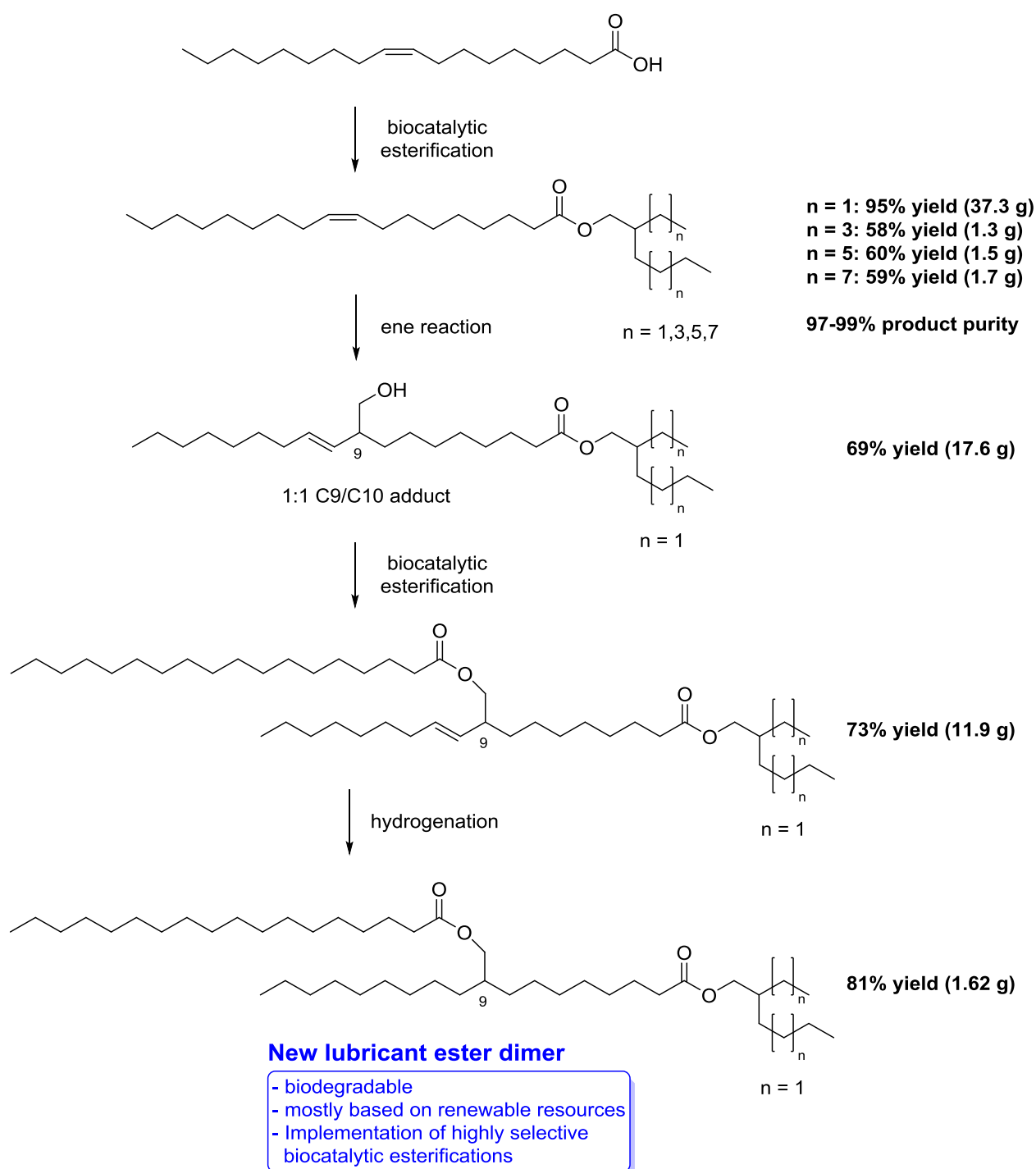
For the development of an alternative access route towards the anti-diabetic drug Vildagliptin, a two-step synthesis route for the synthesis of phenylalaninal nitrile starting from phenylalaninal was developed. Both enantiomers were separately converted into their aldoximes and subsequently dehydrated towards (*S*)- and (*R*)- nitrile in high yields (**Scheme 65**). Fortunately, no racemization of the phenylalaninal nitrile could be observed, which is paramount for the Vildagliptin synthesis. *Rommelmann*<sup>[99]</sup> implemented this method into a *de novo*-synthesis of Vildagliptin starting from L-proline methyl ester.



**Scheme 65:** Two-step, cyanide-free synthesis of the nitrile (top) out of phenylalaninal and implementation of the concept in the *de novo*-synthesis of Vildagliptin by *Rommelmann*<sup>[99]</sup> (bottom).

Lastly, new lubricant ester structures based on oleic acid as renewable resource have been synthesized in four steps after evaluating the most promising synthesis sequence in multi-gram scale (**Scheme 66**). First off, biocatalytic esterification of oleic acid with several Guerbet alcohols yielded the oleate esters with very high yields and purity (up to 95% yield and 99% purity). For implementation of a bridging methylene group, an ene reaction with formaldehyde and a Lewis acid led to hydroxymethylene derivate of the oleate with 69% yield. The unsaturated dimer was obtained after biocatalytic esterification with 73% yield and was successfully hydrogenated to the saturated dimer with 81% yield. This dimer represents a promising lubricant structure and has been proven to be biodegradable in a

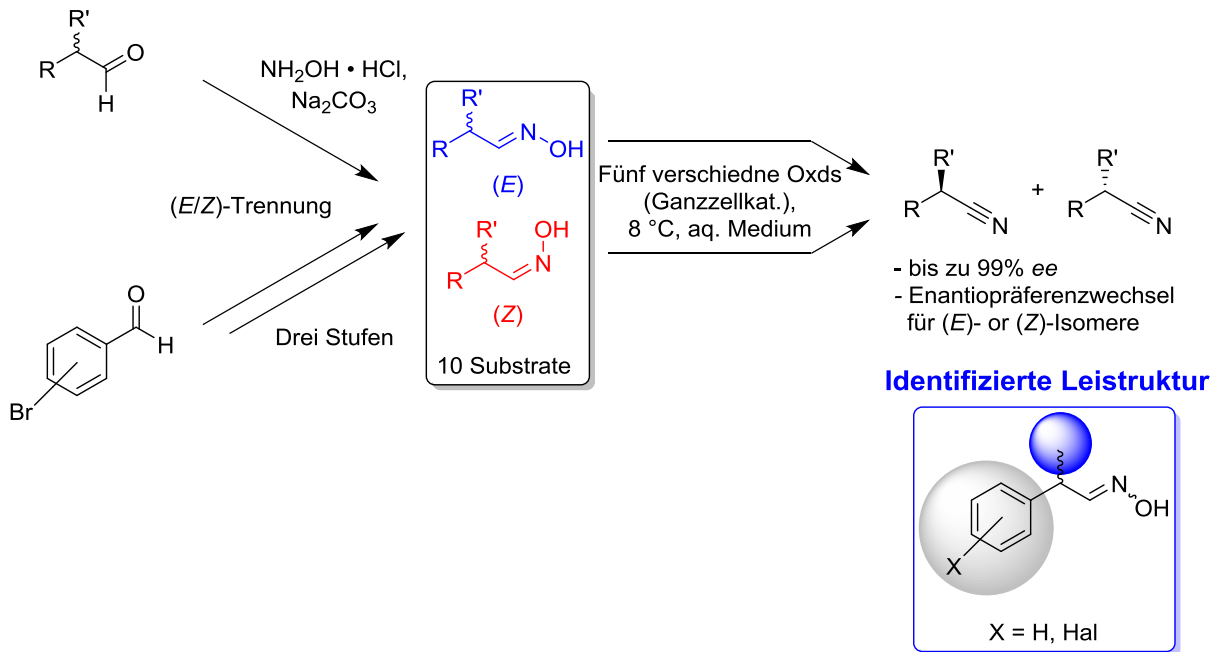
closed bottle test (according to OECD 301 F) at *Klüber Lubrication* in Munich.<sup>[199]</sup> After 28 days, 81.3% of the new lubricant ester dimer was completely degraded. This result is highly promising for the application of these lubricant esters in maritime environments, since it will not pollute the environment for a prolonged time span. Apart from the dimer, first functionalized derivatives of the dimer have been synthesized to gain access towards even higher oligomers of the lubricant esters, since these may even better perform at low temperatures due to lower melting point and lower viscosities.



**Scheme 66:** Multi-step synthesis of new lubricant ester dimer structures.

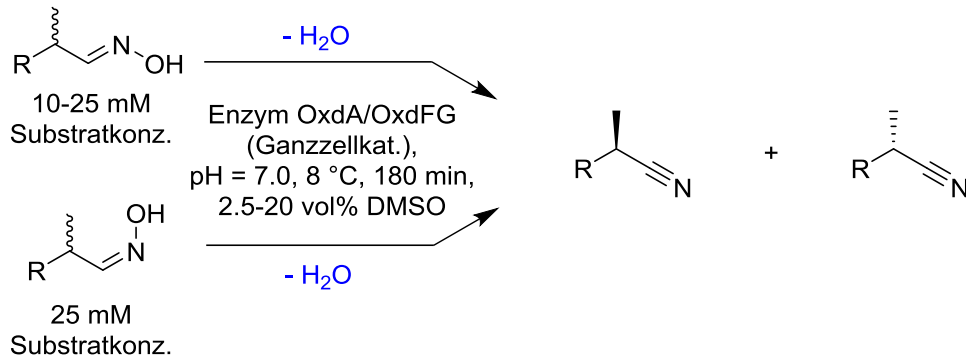
## 8 ZUSAMMENFASSUNG UND AUSBLICK

Verschiedene Errungenschaften konnten im Laufe dieser Arbeit realisiert werden. Zunächst wurde die chirale Nitrilsynthese mit Aldoximedehydratasen (Oxds) durchgängig untersucht, indem eine Bandbreite an synthetisierten arylaliphatischen und aliphatischen Aldoximsubstraten mit fünf verschiedenen Oxd-Ganzzellkatalysatoren umgesetzt wurde. Zusätzlich wurde neben dem Erweitern des Substratspektrums eine privilegierte Leitstruktur identifiziert, mit welcher hohe ee-Werte bei der chiralen Nitrilsynthese erzielt werden konnte: 2-Phenylpropionaldehydoxim (PPOx) und seine Derivate. Die Transformation der racemischen, bromierten PPOx-Derivate in einer kinetischen Racematspaltung führte zu ee-Werten von mindestens 90% (und sogar bis zu 99%) selbst bei höheren Umsatzraten nah an 50%. Darüber hinaus wurde ein beeindruckendes Phänomen beobachtet der Verwendung von zuvor getrennten (*E*)- oder (*Z*)-Stereoisomeren der Aldoxime als Substrate: Die Enantiopräferenz der Oxds wechselte in Abhängigkeit von der (*E/Z*)-Konfiguration, wobei entweder das (*S*)-Nitril bevorzugt aus den (*E*)-Isomeren oder das (*R*)-Nitril bevorzugt aus den (*Z*)-Isomeren gebildet wurde. Folglich können beide Enantiomere der Nitrile mit dem gleichen Biokatalysator zugänglich gemacht werden ohne nach weiteren Biokatalysatoren mit einer anderen Enantiopräferenz zu suchen (**Schema 1**). Dieses Projekt wurde in Kooperation mit *Rommelmann*<sup>[99]</sup>, *Oike*<sup>[84]</sup> und der *Asano*-Gruppe von der Toyama Prefectural University durchgeführt.

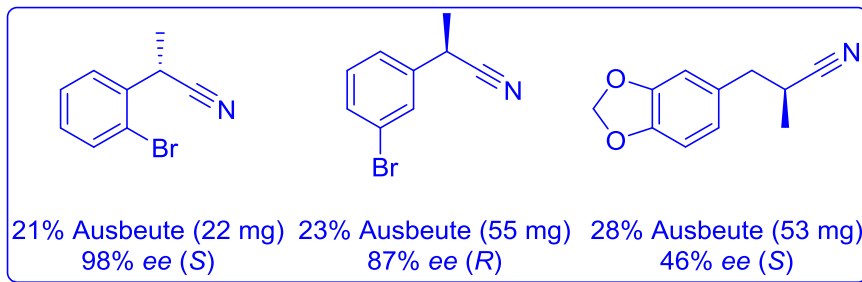


**Schema 1:** Projektübersicht der enantioselektiven, biokatalytischen Nitrilsynthese.

Desweiteren wurde hierfür eine erste Prozessentwicklung durchgeführt, indem Experimente im präparativen Maßstab erfolgreich durchgeführt werden konnten (**Schema 2**). Drei Substrate wurden bei 10-25 mM Substratkonzentration erfolgreich mit isolierten Ausbeute von bis zu 28% und ee-Werte von bis zu 98% (*S*) erhalten.

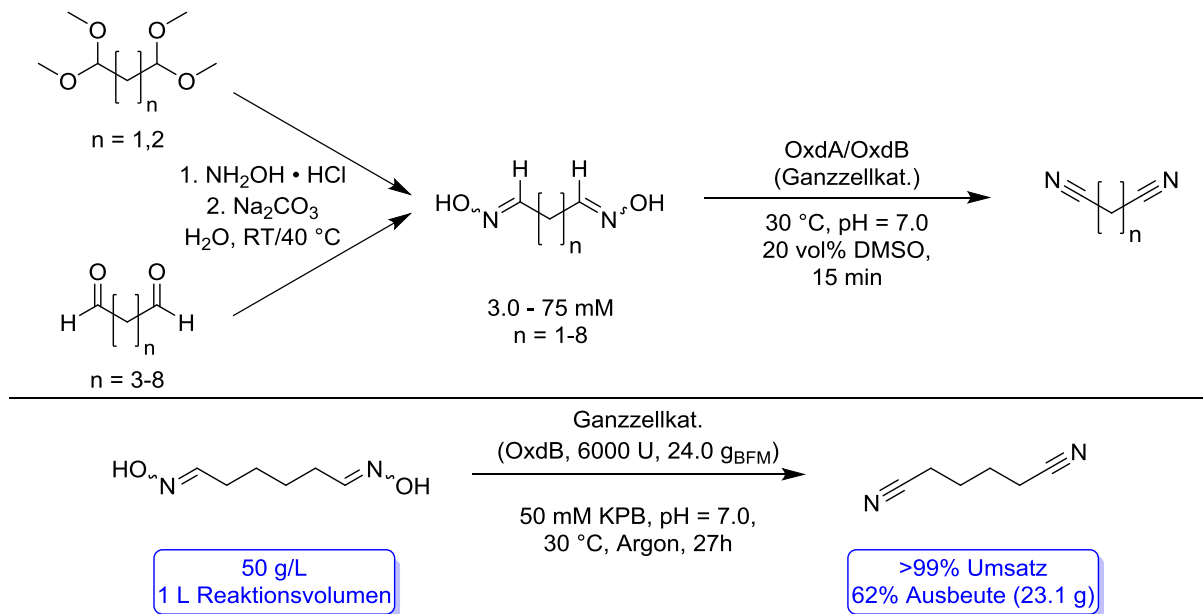


### Synthetisierte Nitrile



**Schema 2:** Biokatalytisch synthetisierte chirale Nitrile im präparativen Maßstab.

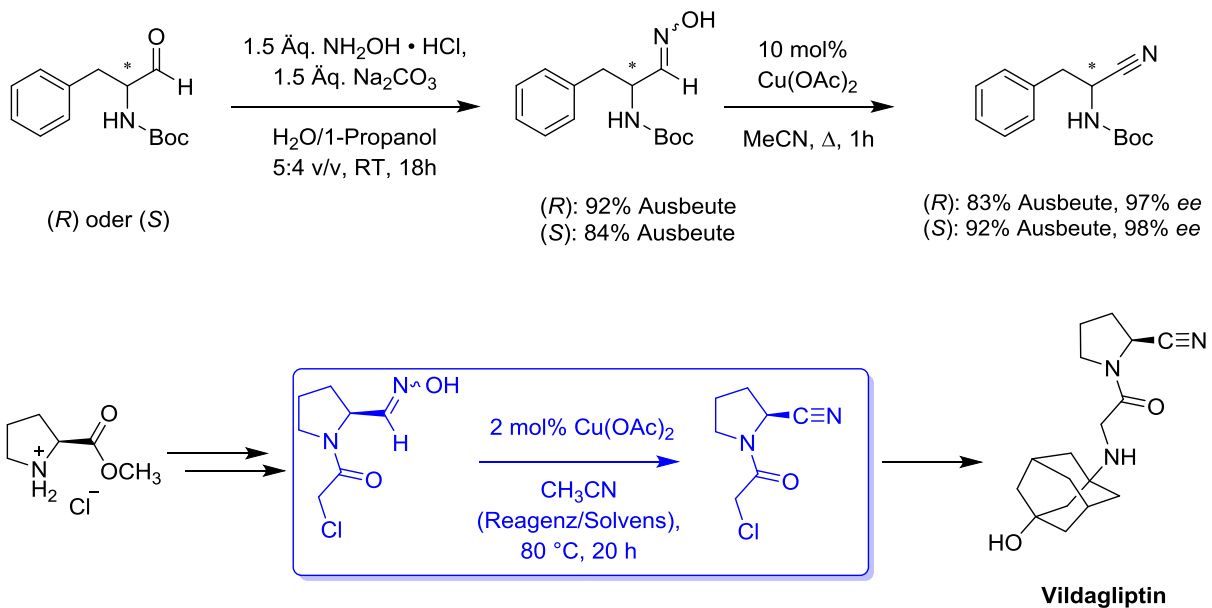
Neben den Errungenschaften in der chiralen Nitrilsynthese mit Oxds konnte auch erstmalig die Synthese von Dinitrilen mit Oxds demonstriert werden. (**Schema 3**). Acht verschiedene Dialdoxime mit einer Kettenlänge von drei bis zehn Kohlenstoffatomen, von denen die meisten komplett unbekannt in der Literatur waren, wurden synthetisiert und anschließend wurde ihre Umsetzung durch Oxds in einer breiten Substratspektrumsstudie untersucht.



**Schema 3:** Dialdoximsynthese, Substratspektrumsstudie und Hochskalierung der biokatalytischen Adiponitrilsynthese.

Als besonders privilegiertes Substrat konnte Adipaldehyddioxim identifiziert werden. Die Synthese dessen Dinitrils, des industriell höchst wichtigen Adiponitrils (Vorstufe von Hexamethyldiamin), wurde in einer Prozessentwicklungsstudie intensiviert. Bis zu 50 g/L an Substratmenge konnten komplett zu Adiponitril selbst im Litermaßstab umgesetzt werden (23.1 g isoliertes Adiponitril). Dies ist das erste Beispiel einer Adiponitrilsynthese bei Umgebungsbedingungen in Wasser ohne die Generierung von Abfall außer zwei Äquivalenten Wasser. Die Chemoselektivität war auch exzellent und es konnten keine detektierbaren Nebenprodukte festgestellt werden. In Kooperation mit *Gruber-Wölfler* und *Maier* von der TU Graz konnte die Löslichkeit von Adipaldehyddioxim im Reaktionsmedium rationalisiert werden.<sup>[124]</sup> Zusätzlich wurden erste Ergebnisse in der Immobilisierung von Oxds erhalten und Hochzelldichtefermentationen wurden in Kooperation mit der *Friebs*-Gruppe durchgeführt, um größere Mengen an Oxds zu erhalten.

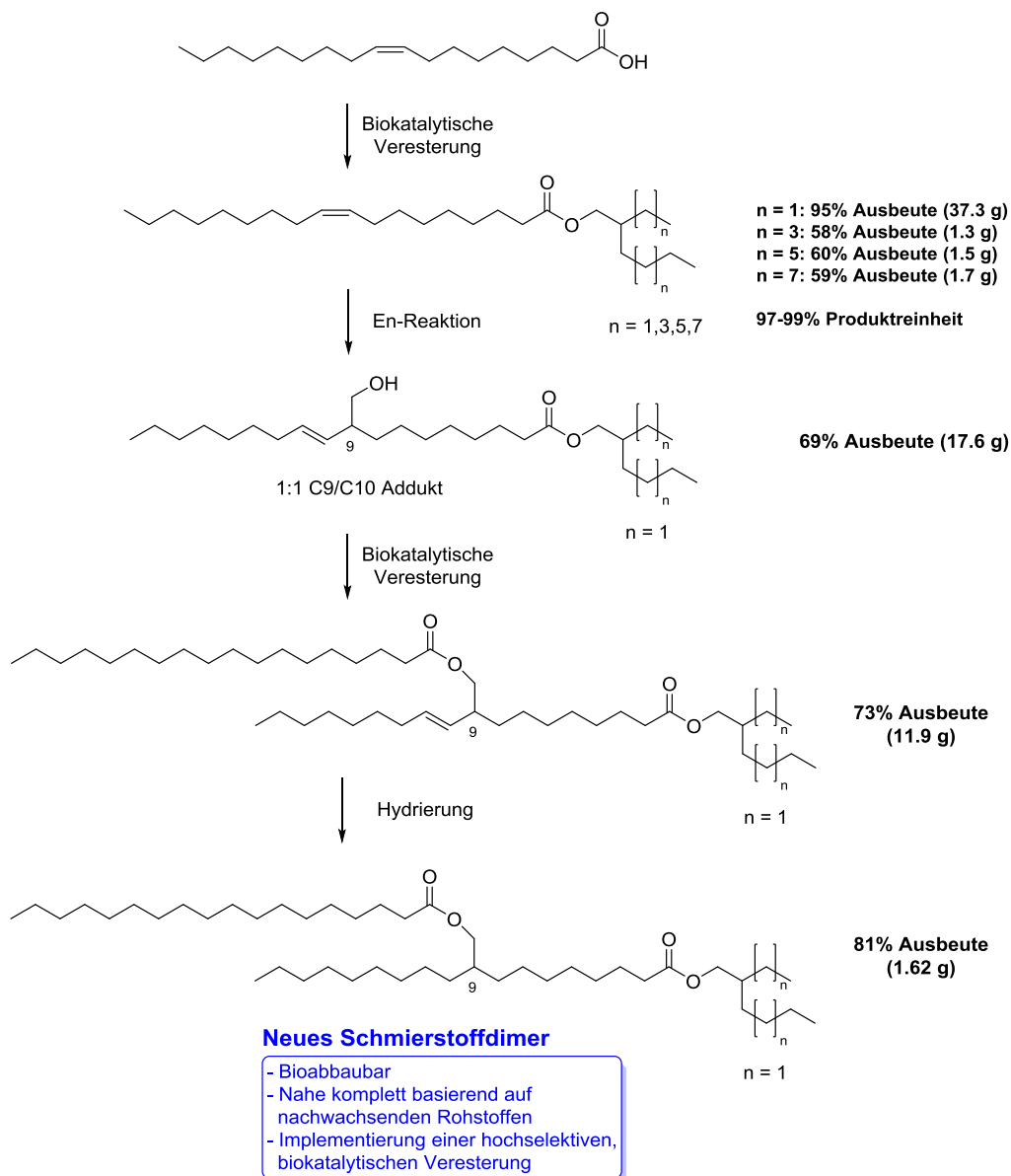
Bezüglich der Entwicklung einer alternativen Zugangsrute zu dem Antidiabetesmedikament Vildagliptin konnte eine zweistufige Syntheseroute für die Darstellung des Nitrils ausgehend von Phenylalaninal entwickelt werden. Beide Enantiomere dessen wurden getrennt voneinander in ihre entsprechenden Aldoxime umgewandelt und anschließend entweder zu (*S*)- oder (*R*)-Nitril in hohen Ausbeuten dehydratisiert (**Schema 4**). Bemerkenswerterweise wurde hierbei keine Racemisierung des Nitrils beobachtet werden, welches eine Grundvoraussetzung für eine erfolgreich Vildagliptinsynthese darstellt. *Rommelmann*<sup>[99]</sup> implizierte diese Methode erfolgreich in eine *de novo*-Synthese von Vildagliptin ausgehend von L-Prolinmethylester.



**Schema 4:** Zweistufige, cyanidfreie Synthese der Nitrile ausgehend von Phenylalaninal (oben) und Implementierung des Konzepts in eine *de novo*-Synthese von Vildagliptin durch *Rommelmann*<sup>[99]</sup> (unten).

Als letztes konnten neue Schmierstoffesterstrukturen basierend auf Ölsäure als erneuerbaren Rohstoff in vier Stufen und Multigrammmaßstab synthetisiert werden, nachdem die vielversprechendste Synthesesequenz identifiziert wurde (**Schema 5**). Als erstes lieferte die biokatalytische Veresterung von Ölsäure mit verschiedenen Guerbetalkoholen die Oleatester mit sehr hohen Ausbeuten und Reinheit (bis zu 95%

Ausbeute und 99% Reinheit). Zur Einführung einer verbrückenden Methylengruppe wurde eine En-Reaktion mit Formaldehyd in Anwesenheit einer Lewissäure durchgeführt, wodurch ein Hydroxymethylenderivat des Oleatesters mit 69% Ausbeute erhalten wurde. Das ungesättigte Dimer wurde erhalten nach biokatalytischer Veresterung mit 73% Ausbeute und wurde anschließend erfolgreich hydriert zum gesättigten Dimer mit 81% Ausbeute. Dieses Dimer stellt eine vielversprechende Schmierstoffstruktur dar und seine Bioabbaubarkeit konnte erfolgreich in einem manometrischen Respirationstest (nach OECD 301F) durch *Klüber Lubrication* in München nachgewiesen werden.<sup>[199]</sup> Nach 28 Tagen waren 81.3% des neuen Schmierstoffester-Dimers komplett abgebaut. Dieses Ergebnis ist vielversprechend für die Anwendung dieser Schmierstoffester im maritimen Bereich, da es die Umwelt nicht für einen längeren Zeitraum verschmutzen würde. Neben dem beschriebenen Dimer konnten erste funktionalisierte Derivate des Dimers synthetisiert werden, um Zugang zu höheren Oligomeren der Schmierstoffester zu erhalten. Diese könnten nämlich noch bessere Niedrigtemperatureigenschaften besitzen wie einen niedrigeren Schmelzpunkt oder niedrigere Viskositäten.



**Schema 5:** Mehrstufige Synthese von neuen Schmierstoffstrukturen.



## 9 EXPERIMENTAL PROCEDURES

### 9.1 GENERAL INFORMATION

All chemicals were purchased by commercial suppliers and used as received if not explicitly stated otherwise.

(*E/Z*)-isomer separation of the oximes was achieved by manual column chromatography with silica 60 (0.04-0.063  $\mu\text{m}$  particle size) or by utilization of the Biotage „Isolera One“ flash chromatography system with cyclohexane/ethyl acetate mixtures.

Evaporation of organic solvents was conducted at 20 °C bath temperature after (*E/Z*)-separation to suppress isomerization. Otherwise, 40 °C was used.

*E.coli* BL21-CodonPlus(DE3)-RIL cells were transformed with the corresponding plasmid containing the gene for each of the aldoxime dehydratases and stored at -80 °C as cryo culture in glycerol prior to use.

The gene for the aldoxime dehydratase from *Bacillus sp.* OxB-1 (OxdB) used for chiral nitrile synthesis was located on a pUC 18 vector.

The gene for the his-tagged aldoxime dehydratase from *Bacillus sp.* OxB-1 (OxdB<sub>CHis6</sub>) used in the immobilization studies was located on a pET22b vector.

The genes for the aldoxime dehydratases from *Pseudomonas chlororaphis* (OxdA), *Fusarium graminearum* (OxdFG), *Rhodococcus erythropolis* (OxdRE) and *Rhodococcus globerulus* (OxdRG) were purchased by GeneArt (Thermo Scientific) in their codon optimized form, located on pET28a or pET28b plasmids with an sixfold N- or C-terminal His-Tag (see Appendix).

OxdB<sub>(CHis6)</sub> was purified *via* NiNTA affinity chromatography with 1 mL His GraviTrap columns (GE Healthcare) according to the given protocol.

Cell lysis was conducted by sonification of cell suspension at 0 °C.

Bradford-Assays for protein concentration determinations were conducted with a standard protocol on 250  $\mu\text{L}$  scale.

SDS-PAGE analysis was conducted with 4% Polyacrylamide collection gels and 12% Polyacrylamide separation gels in a Mini-PROTEAN Electrophoresis cell (Bio-Rad Laboratories).

## 9.2 ANALYTICAL METHODS

Thin-layer chromatography (TLC) measurements were performed on Merck silica gel 60 F<sub>254</sub> plates. Oximes were visualized by UV light or staining with potassium permanganate solution. Nitriles were visualized by staining with Phosphomolybdic acid.

NMR spectra were recorded on a Bruker Avance III 500 at a frequency of 500 MHz (<sup>1</sup>H) or 125 MHz (<sup>13</sup>C). The chemical shift  $\delta$  is given in ppm and referenced to the corresponding solvent signal (CD<sub>2</sub>Cl<sub>2</sub> or CDCl<sub>3</sub>). Coupling constants are given in Hz.

CHN analysis was conducted by the CHN measurement service of the Bielefeld University.

IR spectra were measured on a Nicolet 380 of the Thermo Electron Corporation.

ESI Mass spectra were recorded on a Bruker Esquire 3000 in positive Ion mode.

Melting points were recorded on a Melting Point B-540 of the Büchi company.

Conversion of some biotransformations was determined by RP-HPLC measurements in comparison to a calibration curve. Measurements were conducted on a Macherey-Nagel Nucleodur C<sub>18</sub> HTec column at 40 °C with acetonitrile/water as mobile phase and UV detection at 210 or 220 nm.

Enantiomeric ratios were determined by Chiral HPLC measurements on the Daicel Chiracel OB-H, OJ-H and AD-H at 20 °C with supercritical CO<sub>2</sub>/isopropanol as mobile phase. Alternatively, enantiomeric ratios could also be determined on a chiral GC column BGB-174 (0.25 mm ID, 0.25  $\mu$ m film, 30 m) from the BGB Analytik AG company with N<sub>2</sub> as a carrier gas.

Optical rotations were measured on a Perkin Elmer Model 341 Polarimeter at 20 °C and 589 nm.

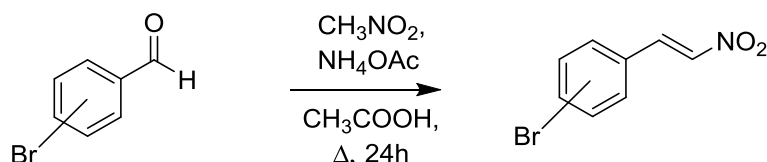
High resolution mass spectra are recorded using an Agilent 6220 time-of-flight mass spectrometer (Agilent Technologies, Santa Clara, CA, USA) in extended dynamic range mode equipped with a Dual-ESI source, operating with a spray voltage of 2.5 kV. Nitrogen served both as the nebulizer gas and the dry gas. Nitrogen was generated by a nitrogen generator NGM 11. Samples are introduced with a 1200 HPLC system consisting of an autosampler, degasser, binary pump, column oven and diode array detector (Agilent Technologies, Santa Clara, CA, USA) using a C18 Hypersil Gold column (length: 50 mm, diameter: 2.1 mm, particle size: 1,9  $\mu$ m) with a short gradient (in 4 min from 0% B to 98% B, back to 0% B in 0.2 min, total run time 7.5 min) at a flow rate of 250  $\mu$ L/min and column oven temperature of 40°C. HPLC solvent A consists of 94.9% water, 5% acetonitrile and 0.1% formic acid, solvent B of 5% water, 94.9% acetonitrile and 0.1% formic acid. The mass axis was externally calibrated with ESI-L Tuning Mix (Agilent Technologies, Santa Clara, CA, USA) as calibration standard.

Conversion of some biotransformations was determined by GC measurements in comparison to a calibration curve. GC-chromatograms were recorded on a Shimadzu GC-2010 using the column Phenomenex ZB-5MSi with different temperature programs and H<sub>2</sub> as carrier gas.

## 9.3 CYANIDE-FREE, BIOCATALYTIC SYNTHESIS OF CHIRAL NITRILES

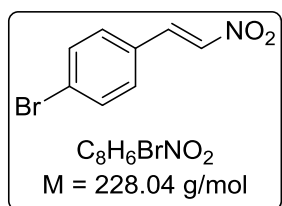
### 9.3.1 SYNTHESIS OF REFERENCE COMPOUNDS

#### 9.3.1.1 General procedure 1 (GP1): Nitroaldol condensation of aromatic aldehydes with Nitromethane



The synthesis was conducted in analogy to *Wong et al.*<sup>[200]</sup> The corresponding benzaldehyde (1.0 eq.), ammonium acetate (0.1 eq.) and nitromethane (6.5 eq.) were dissolved in acetic acid and heated to reflux for 24 hours. Afterwards, complete conversion was confirmed *via* TLC (cyclohexane/ethyl acetate). Water was added; the precipitate was filtered off and dried *in vacuo*. Recrystallization from ethanol yielded the corresponding *E*-nitroalkene as crystalline solid. The crude product could also be purified *via* column chromatography (cyclohexane/ethyl acetate).

##### 9.3.1.1.1 Synthesis of (*E*)-1-bromo-4-(2-nitrovinyl)benzene



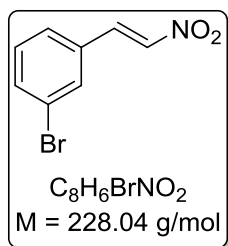
The synthesis was conducted according to GP1. 4-Bromobenzaldehyde (5.55 g, 30.0 mmol), ammonium acetate (231 mg, 3.00 mmol) and nitromethane (10.5 mL, 197 mmol) were dissolved in 15 mL acetic acid and refluxed for 24 hours. Recrystallization yielded the product as green, crystalline solid.

**Yield:** 3.86 g, 56%.

**<sup>1</sup>H-NMR** (500 MHz, CDCl<sub>3</sub>):  $\delta$  [ppm] = 7.93 (d, 1H, <sup>3</sup>J = 13.7 Hz, CH=CH), 7.59 (m, 2H, Ar-H), 7.58 (d, 1H, <sup>3</sup>J = 13.7 Hz, CH=CH), 7.42 (m, 2H, Ar-H).

**<sup>13</sup>C-NMR** (125 MHz, CDCl<sub>3</sub>):  $\delta$  [ppm] = 137.9, 137.6, 132.9, 130.5, 129.1, 126.9.

The analytical data correspond in analogy to the literature.<sup>[201]</sup>

9.3.1.1.2 Synthesis of (*E*)-1-bromo-4-(2-nitrovinyl)benzene

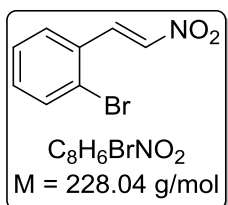
The synthesis was conducted according to GP1. Freshly distilled 3-Bromobenzaldehyde (2.33 mL, 20.0 mmol), ammonium acetate (154 mg, 2.00 mmol) and nitromethane (7.0 mL, 131 mmol) were dissolved in 10 mL acetic acid and refluxed for 24 hours. Recrystallization yielded the product as green, crystalline solid.

**Yield:** 1.85 g, 41%.

**$^1H$ -NMR** (500 MHz,  $CDCl_3$ ):  $\delta$  [ppm] = 7.92 (d, 1H,  $^3J = 13.7$  Hz, CH=CH), 7.70 (t, 1H,  $^4J = 1.8$  Hz, Ar-H), 7.62 (m, 1H, Ar-H), 7.56 (d, 1H,  $^3J = 13.7$  Hz, CH=CH), 7.47 (m, 1H, Ar-H), 7.34 (t, 1H,  $^3J = 8.0$  Hz, Ar-H).

**$^{13}C$ -NMR** (125 MHz,  $CDCl_3$ ):  $\delta$  [ppm] = 138.2, 137.5, 135.0, 132.2, 131.8, 131.0, 127.8, 123.6.

The analytical data corresponds to literature values.<sup>[202]</sup>

9.3.1.1.3 Synthesis of (*E*)-1-bromo-2-(2-nitrovinyl)benzene

The synthesis was conducted according to GP1. Freshly distilled 2-Bromobenzaldehyde (2.33 mL, 20.0 mmol), ammonium acetate (154 mg, 2.00 mmol) and nitromethane (7.0 mL, 131 mmol) were dissolved in 10 mL acetic acid and refluxed for 24 hours. Recrystallization yielded the product as bright yellow, crystalline solid.

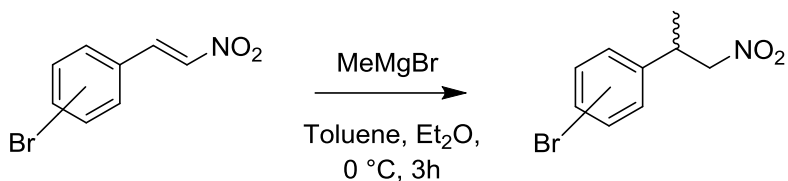
**Yield:** 2.36 g, 52%.

**$^1H$ -NMR** (500 MHz,  $CDCl_3$ ):  $\delta$  [ppm] = 8.38 (d, 1H,  $^3J = 13.7$  Hz, CH=CH), 7.69 (dd, 1H,  $^3J = 7.9$  Hz,  $^4J = 1.4$  Hz, Ar-H), 7.57 (dd, 1H,  $^3J = 7.7$  Hz,  $^4J = 1.8$  Hz, Ar-H), 7.53 (d, 1H,  $^3J = 13.7$  Hz, CH=CH), 7.39 (dt, 1H,  $^3J = 7.7$  Hz,  $^4J = 1.4$  Hz, Ar-H), 7.34 (dt, 1H,  $^3J = 7.9$  Hz,  $^4J = 1.8$  Hz, Ar-H).

**$^{13}C$ -NMR** (125 MHz,  $CDCl_3$ ):  $\delta$  [ppm] = 139.0, 137.7, 134.2, 133.1, 130.5, 128.6, 128.2, 126.5.

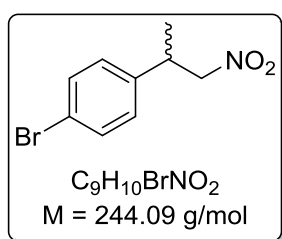
The analytical data corresponds to literature values.<sup>[203]</sup>

## 9.3.1.2 General procedure 2 (GP2): Michael Addition of methylmagnesium bromide with Nitroalkenes



The synthesis was carried out in a heat dried schlenk flask under argon. Dry toluene was filled into the flask and cooled to 0 °C. The nitroalkene (1.0 eq.) was dissolved and a 3.0 M solution of methylmagnesium bromide in diethyl ether (1.5 eq.) was slowly added to the solution under vigorous stirring. After three at 0 °C, complete conversion was achieved according to TLC (cyclohexane/ethyl acetate) and saturated  $\text{NH}_4\text{Cl}$ -solution (1:1, v/v) was added. The phases were separated and the aqueous phase was extracted three times with ethyl acetate (1:1, v/v). After washing of the organic phase with brine (1:3, v/v), it was dried over  $\text{MgSO}_4$  and the solvent was removed *in vacuo*. Column chromatography (cyclohexane/ethyl acetate 6:1 or 10:1, v/v) yielded the racemic nitroalkanes as oils.

## 9.3.1.2.1 Synthesis of rac-1-bromo-4-(1-nitropropan-2-yl)benzene



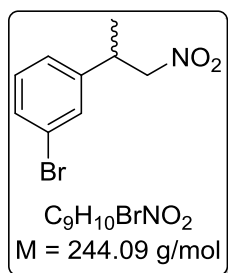
The synthesis was carried out according to GP2. (*E*)-1-bromo-4-(2-nitrovinyl)benzene (1.82 g, 8.00 mmol) was dissolved in 50 mL dry toluene at 0 °C and methylmagnesium bromide (4.00 mL, 12.0 mmol) was added. Work up yielded the product as yellow oil.

**Yield:** 1.10 g, 60%.

**$^1\text{H-NMR}$**  (500 MHz,  $\text{CDCl}_3$ ):  $\delta$  [ppm] = 7.46 (d, 1H,  $^3J = 8.4 \text{ Hz}$ , Ar-*H*), 7.11 (d, 1H,  $^3J = 8.4 \text{ Hz}$ , Ar-*H*), 4.51 (dd, 1H,  $^2J = 12.2 \text{ Hz}$ ,  $^3J = 7.7 \text{ Hz}$ ,  $\text{CHCH}_2\text{NO}_2$ ), 4.48 (dd, 1H,  $^2J = 12.2 \text{ Hz}$ ,  $^3J = 7.7 \text{ Hz}$ ,  $\text{CHCH}_2\text{NO}_2$ ), 3.62 (sx, 1H,  $^3J = 7.2 \text{ Hz}$ ,  $\text{CHCH}_2\text{NO}_2$ ), 1.37 (d, 3H,  $^3J = 7.1 \text{ Hz}$ ,  $\text{CH}_3$ ).

**$^{13}\text{C-NMR}$**  (125 MHz,  $\text{CDCl}_3$ ):  $\delta$  [ppm] = 140.0, 132.3, 128.8, 121.6, 81.6, 38.3, 18.8.

The analytical data corresponds with literature data.<sup>[204]</sup>

9.3.1.2.2 Synthesis of *rac*-1-bromo-3-(1-nitropropan-2-yl)benzene

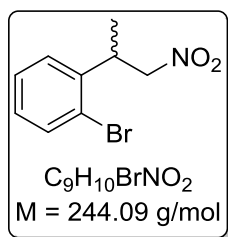
The synthesis was carried out according to GP2. (*E*)-1-bromo-3-(2-nitrovinyl)benzene (1.80 g, 7.90 mmol) was dissolved in 50 mL dry toluene at 0 °C and methylmagnesium bromide (4.00 mL, 12.0 mmol) was added. Work up yielded the product as yellow oil.

**Yield:** 928 mg, 48%.

**$^1H$ -NMR** (500 MHz,  $CDCl_3$ ):  $\delta$  [ppm] = 7.40 (d, 1H,  $^3J = 7.8$  Hz, Ar-*H*), 7.38 (s, 1H, Ar-*H*), 7.22 (t, 1H,  $^3J = 7.8$  Hz, Ar-*H*), 7.16 (d, 1H,  $^3J = 7.7$  Hz, Ar-*H*), 4.53 (dd, 1H,  $^2J = 12.2$  Hz,  $^3J = 7.8$  Hz,  $CHCH_2NO_2$ ), 4.48 (dd, 1H,  $^2J = 12.2$  Hz,  $^3J = 7.8$  Hz,  $CHCH_2NO_2$ ), 3.61 (sx, 1H,  $^3J = 7.2$  Hz,  $CHCH_2NO_2$ ), 1.37 (d, 3H,  $^3J = 7.1$  Hz,  $CH_3$ ).

**$^{13}C$ -NMR** (125 MHz,  $CDCl_3$ ):  $\delta$  [ppm] = 143.3, 130.9, 130.7, 130.2, 125.8, 123.1, 81.5, 38.4, 18.8.

The analytical data corresponds with literature data.<sup>[204]</sup>

9.3.1.2.3 Synthesis of *rac*-1-bromo-2-(1-nitropropan-2-yl)benzene

The synthesis was carried out according to GP2. (*E*)-1-bromo-2-(2-nitrovinyl)benzene (1.82 g, 8.00 mmol) was dissolved in 50 mL dry toluene at 0 °C and methylmagnesium bromide (4.00 mL, 12.0 mmol) was added. Work up yielded the product as yellow oil.

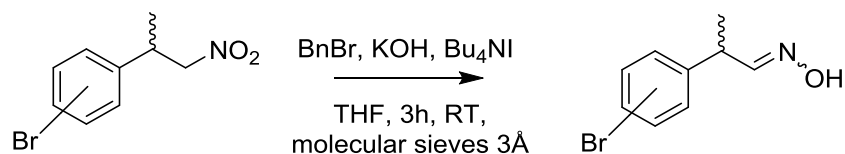
**Yield:** 1.15 g, 63%.

**$^1H$ -NMR** (500 MHz,  $CDCl_3$ ):  $\delta$  [ppm] = 7.59 (m, 1H, Ar-*H*), 7.32 (m, 1H, Ar-*H*), 7.24 (m, 1H, Ar-*H*), 7.14 (m, 1H, Ar-*H*), 4.66 (dd, 1H,  $^2J = 12.2$  Hz,  $^3J = 6.0$  Hz,  $CHCH_2NO_2$ ), 4.48 (dd, 1H,  $^2J = 12.2$  Hz,  $^3J = 8.8$  Hz,  $CHCH_2NO_2$ ), 4.16 (m, 1H,  $CHCH_2NO_2$ ), 1.40 (d, 3H,  $^3J = 7.0$  Hz,  $CH_3$ ).

**$^{13}C$ -NMR** (125 MHz,  $CDCl_3$ ):  $\delta$  [ppm] = 139.8, 133.7, 129.1, 128.2, 127.4, 124.6, 80.3, 37.4, 17.8.

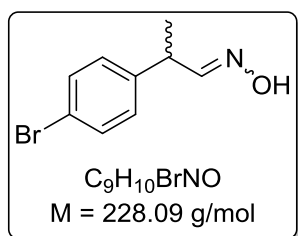
The analytical data corresponds with literature data.<sup>[205]</sup>

### 9.3.1.3 General procedure 3 (GP3): Synthesis of racemic aldoximes *via* disproportionation of racemic nitroalkanes with benzyl bromide



The syntheses were carried out in a heat dried schlenk flask under argon atmosphere in analogy to *Czekelius*.<sup>[97]</sup> Freshly distilled THF was given into the flask. KOH (85 wt% pellets, 1.05 eq.) and molecular sieves 4 Å were added and the suspension was stirred for one hour. Afterwards, benzyl bromide (1.1 eq.) and tetrabutylammonium iodide (TBAI, 0.05 eq.) were added. Lastly, the nitroalkane (1.0 eq.) was added over 5 min. The resulting suspension was stirred for three hours at room temperature and conversion was checked *via* TLC (cyclohexane/ethyl acetate). Water (1:1, v/v) was added, the phases were separated and the aqueous phase was extracted three times with ethyl acetate. Drying over MgSO<sub>4</sub> and removal of the solvent *in vacuo* yielded an oily crude product. Purification *via* automated column chromatography (cyclohexane/ethyl acetate) yielded the (*E*)- and (*Z*)- isomers as colorless solids or oils depending on percentage of isomeric excess.

#### 9.3.1.3.1 Synthesis of *rac*-(*E/Z*)-2-(4-bromophenyl)propanal oxime



The synthesis was carried out according to GP3. 10 mL THF were given into the schlenk flask, 85 wt% KOH (176 mg, 2.67 mmol) and molecular sieves 4 Å (150 mg) were added. Benzyl bromide (332 μL, 2.80 mmol) and TBAI (47.0 mg, 127 μmol) were added after an hour. *rac*-1-bromo-4-(1-nitropropan-2-yl)benzene (580 mg, 2.54 mmol) was added and the reaction mixture was stirred for three hours. Work up and purification *via* automated column chromatography (cyclohexane/ethyl acetate 6:1, v/v) yielded the (*E*)-isomer (>99% *E*) as pale yellow oil, which crystallized at -20 °C and the (*Z*)-isomer (89% *Z*) as colorless, crystalline solid.

**Combined yield:** 228 mg, 40%.

#### *rac*-(*E*)-2-(4-bromophenyl)propanal oxime:

**<sup>1</sup>H-NMR** (500 MHz, CD<sub>2</sub>Cl<sub>2</sub>): δ [ppm] = 7.47 (d, 1H, <sup>3</sup>J = 6.0 Hz, CHNOH), 7.46 (m, 2H, Ar-H), 7.13 (m, 2H, Ar-H), 7.12 (s, 1H, NOH), 3.63 (qi, 1H, <sup>3</sup>J = 6.8 Hz, Ph-CH), 1.41 (d, 3H, <sup>3</sup>J = 7.0 Hz, CH<sub>3</sub>).

**<sup>13</sup>C-NMR** (125 MHz, CD<sub>2</sub>Cl<sub>2</sub>): δ [ppm] = 154.8, 142.0, 132.2, 129.8, 121.1, 40.3, 19.1.

**IR** (neat) [cm<sup>-1</sup>]: 3241, 2965, 2924, 1486, 1447, 1402, 1369, 1300, 1074, 1008, 948, 933, 821, 716, 699, 533.

**RP-HPLC:** *Macherey-Nagel* Nucleodur C<sub>18</sub> HTec, water/acetonitrile 70:30, 1.5 mL/min, 40 °C, 210 nm, R<sub>t</sub> = 22.7 min.

**NP-HPLC:** *Daicel Chiracel* OB-H, CO<sub>2</sub>/isopropanol 98:2, 1.5 mL/min, 20 °C, 210 nm, R<sub>t1</sub> = 20.4 min, R<sub>t2</sub> = 23.9 min.

*rac*-(Z)-2-(4-bromophenyl)propanal oxime:

**<sup>1</sup>H-NMR** (500 MHz, CD<sub>2</sub>Cl<sub>2</sub>): δ [ppm] = 7.45 (m, 2H, Ar-H), 7.33 (s, 1H, NOH), 7.17 (m, 2H, Ar-H), 6.75 (d, 1H, <sup>3</sup>J = 7.3 Hz, CHNOH), 4.38 (qi, 1H, <sup>3</sup>J = 7.2 Hz, Ph-CH), 1.39 (d, 3H, <sup>3</sup>J = 7.2 Hz, CH<sub>3</sub>).

**<sup>13</sup>C-NMR** (125 MHz, CD<sub>2</sub>Cl<sub>2</sub>): δ [ppm] = 155.3, 142.3, 132.2, 129.6, 120.8, 34.9, 18.9.

**IR** (neat) [cm<sup>-1</sup>]: 3184, 3076, 2974, 2849, 1486, 1450, 1400, 1320, 1074, 1007, 928, 893, 881, 821, 696, 631, 613, 509.

**RP-HPLC:** *Macherey-Nagel* Nucleodur C<sub>18</sub> HTec, water/acetonitrile 70:30, 1.5 mL/min, 40 °C, 210 nm, R<sub>t</sub> = 26.3 min.

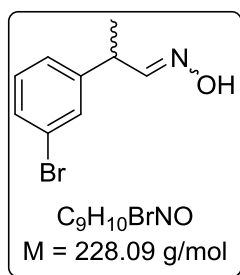
**NP-HPLC:** *Daicel Chiracel* OB-H, CO<sub>2</sub>/isopropanol 98:2, 1.5 mL/min, 20 °C, 210 nm, R<sub>t1</sub> = 25.1 min, R<sub>t2</sub> = 26.3 min.

*rac*-(E,Z)-2-(4-bromophenyl)propanal oxime:

**EA:** calcd for C<sub>9</sub>H<sub>10</sub>BrNO: C, 47.39; H, 4.42; N, 6.14. Found: C, 47.913; H, 4.63; N, 6.06.

**MS (ESI):** m/z = 228.1, 230.1 [M+H]<sup>+</sup>.

9.3.1.3.2 Synthesis of *rac*-(E/Z)-2-(3-bromophenyl)propanal oxime



The synthesis was carried out according to GP3. 20 mL THF were given into the schlenk flask, 85 wt% KOH (264 mg, 3.99 mmol) and molecular sieves 4 Å (230 mg) were added. Benzyl bromide (496 μL, 4.18 mmol) and TBAI (71.0 mg, 190 μmol) were added after an hour. *rac*-1-bromo-3-(1-nitropropan-2-yl)benzene (928 mg, 3.80 mmol) was added and the reaction mixture was stirred for three hours. Work up and purification *via* automated column chromatography (cyclohexane/ethyl acetate 8:1, v/v) yielded the (*E*)-isomer (96% *E*) as pale yellow oil and the (*Z*)-isomer (87% *Z*) as pale yellow oil.

**Combined yield:** 342 mg, 40%.

*rac*-(E)-2-(3-bromophenyl)propanal oxime:



**<sup>1</sup>H-NMR** (500 MHz, CD<sub>2</sub>Cl<sub>2</sub>): δ [ppm] = 7.48 (d, 1H, <sup>3</sup>J = 6.0 Hz, CHNOH), 7.39 (m, 2H, Ar-H), 7.21 (m, 2H, Ar-H), 7.06 (s, 1H, NOH), 3.64 (qi, 1H, <sup>3</sup>J = 6.8 Hz, Ph-CH), 1.42 (d, 3H, <sup>3</sup>J = 7.0 Hz, CH<sub>3</sub>).

**<sup>13</sup>C-NMR** (125 MHz, CD<sub>2</sub>Cl<sub>2</sub>): δ [ppm] = 154.7, 145.3, 131.1, 130.9, 130.5, 126.8, 123.1, 40.6, 19.1.

**IR** (neat) [cm<sup>-1</sup>]: 3253, 2971, 2930, 1592, 1566, 1474, 1449, 1424, 1299, 1073, 997, 929, 879, 781, 694, 669, 597.

**RP-HPLC**: *Macherey-Nagel* Nucleodur C<sub>18</sub> HTec, water/acetonitrile 70:30, 1.5 mL/min, 40 °C, 210 nm, R<sub>t</sub> = 21.3 min.

**NP-HPLC**: *Daicel Chiracel* OB-H, CO<sub>2</sub>/isopropanol 98:2, 1.5 mL/min, 20 °C, 210 nm, R<sub>t1+2</sub> = 16.6 min.

*rac-(Z)-2-(3-bromophenyl)propanal oxime:*

**<sup>1</sup>H-NMR** (500 MHz, CD<sub>2</sub>Cl<sub>2</sub>): δ [ppm] = 7.45 (m, 1H, Ar-H), 7.44 (s, 1H, NOH), 7.38 (m, 1H, Ar-H), 7.23 (m, 2H, Ar-H), 6.76 (d, 1H, <sup>3</sup>J = 7.3 Hz, CHNOH), 4.39 (qi, 1H, <sup>3</sup>J = 7.2 Hz, Ph-CH), 1.40 (d, 3H, <sup>3</sup>J = 7.2 Hz, CH<sub>3</sub>).

**<sup>13</sup>C-NMR** (125 MHz, CD<sub>2</sub>Cl<sub>2</sub>): δ [ppm] = 155.1, 145.5, 130.9, 130.8, 130.3, 126.6, 123.1, 35.2, 18.9.

**IR** (neat) [cm<sup>-1</sup>]: 3221, 3082, 2970, 2872, 1592, 1567, 1474, 1453, 1423, 1375, 1322, 1073, 1022, 928, 877, 816, 780, 691.

**RP-HPLC**: *Macherey-Nagel* Nucleodur C<sub>18</sub> HTec, water/acetonitrile 70:30, 1.5 mL/min, 40 °C, 210 nm, R<sub>t</sub> = 24.6 min.

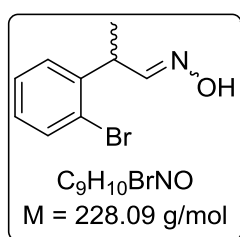
**NP-HPLC**: *Daicel Chiracel* OB-H, CO<sub>2</sub>/isopropanol 98:2, 1.5 mL/min, 20 °C, 210 nm, R<sub>t1</sub> = 19.6 min, R<sub>t2</sub> = 21.4 min.

*rac-(E,Z)-2-(3-bromophenyl)propanal oxime:*

**EA**: calcd for C<sub>9</sub>H<sub>10</sub>BrNO: C, 47.39; H, 4.42; N, 6.14. Found: C, 47.59; H, 4.52; N, 5.88.

**MS (ESI)**: m/z = 228.2, 230.1 [M+H]<sup>+</sup>.

9.3.1.3.3 *Synthesis of rac-(E/Z)-2-(2-bromophenyl)propanal oxime*



The synthesis was carried out according to GP3. 20 mL THF were given into the schlenk flask, 85 wt% KOH (348 mg, 5.25 mmol) and molecular sieves 4 Å (300 mg) were added. Benzyl bromide (653 μL, 5.50 mmol) and TBAI (93.0 mg, 250 μmol) were added after an hour. *rac*-1-bromo-2-(1-nitropropan-2-yl)benzene (1.14 g, 5.00 mmol) was added and the reaction mixture was stirred for three hours. Work up

and purification *via* automated column chromatography (cyclohexane/ethyl acetate 8:1, v/v) yielded the (*E*)-isomer (>99% *E*) and the (*Z*)-isomer (96% *Z*) as colorless solids.

**Combined yield:** 550 mg, 48%.

*rac*-(*E*)-2-(2-bromophenyl)propanal oxime:

**<sup>1</sup>H-NMR** (500 MHz, CD<sub>2</sub>Cl<sub>2</sub>): δ [ppm] = 7.57 (dd, 1H, <sup>3</sup>J = 8.0 Hz, <sup>4</sup>J = 1.2 Hz, Ar-*H*), 7.54 (d, 1H, <sup>3</sup>J = 5.0 Hz, CHNOH), 7.39 (s, 1H, NOH), 7.32 (dt, 1H, <sup>3</sup>J = 7.6 Hz, <sup>4</sup>J = 1.2 Hz, Ar-*H*), 7.25 (dd, 1H, <sup>3</sup>J = 7.8 Hz, <sup>4</sup>J = 1.8 Hz, Ar-*H*), 3.64 (dq, 1H, <sup>3</sup>J = 7.0, 5.0 Hz, Ph-CH), 1.42 (d, 3H, <sup>3</sup>J = 7.0 Hz, CH<sub>3</sub>).

**<sup>13</sup>C-NMR** (125 MHz, CD<sub>2</sub>Cl<sub>2</sub>): δ [ppm] = 154.0, 142.0, 133.6, 129.1, 129.0, 128.4, 124.7, 40.0, 18.3.

**IR** (neat) [cm<sup>-1</sup>]: 3268, 2973, 1469, 1432, 1369, 1287, 1248, 1023, 1009, 948, 935, 762, 751, 722, 661, 593, 546,

**RP-HPLC:** *Macherey-Nagel* Nucleodur C<sub>18</sub> HTec, water/acetonitrile 70:30, 1.5 mL/min, 40 °C, 210 nm, R<sub>t</sub> = 19.1 min.

**NP-HPLC:** *Daicel Chiracel* OB-H, CO<sub>2</sub>/isopropanol 98:2, 1.5 mL/min, 20 °C, 210 nm, R<sub>t1+2</sub> = 14.2 min.

*rac*-(*Z*)-2-(2-bromophenyl)propanal oxime:

**<sup>1</sup>H-NMR** (500 MHz, CD<sub>2</sub>Cl<sub>2</sub>): δ [ppm] = 7.96 (s, 1H, NOH), 7.56 (dd, 1H, <sup>3</sup>J = 8.0 Hz, <sup>4</sup>J = 1.0 Hz, Ar-*H*), 7.31 (m, 2H, Ar-*H*), 7.12 (ddd, 1H, <sup>3</sup>J = 9.0, 6.0 Hz, <sup>4</sup>J = 3.0 Hz, Ar-*H*), 6.87 (d, 1H, <sup>3</sup>J = 6.5 Hz, CHNOH), 4.66 (qi, 1H, <sup>3</sup>J = 7.0 Hz, Ph-CH), 1.42 (d, 3H, <sup>3</sup>J = 7.1 Hz, CH<sub>3</sub>).

**<sup>13</sup>C-NMR** (125 MHz, CD<sub>2</sub>Cl<sub>2</sub>): δ [ppm] = 154.8, 143.0, 133.6, 128.8, 128.6, 128.5, 124.5, 36.0, 18.8.

**IR** (neat) [cm<sup>-1</sup>]: 3180, 3059, 2858, 1469, 1458, 1436, 1309, 1056, 1019, 937, 903, 867, 818, 748, 699, 653, 567.

**RP-HPLC:** *Macherey-Nagel* Nucleodur C<sub>18</sub> HTec, water/acetonitrile 70:30, 1.5 mL/min, 40 °C, 210 nm, R<sub>t</sub> = 19.1 min.

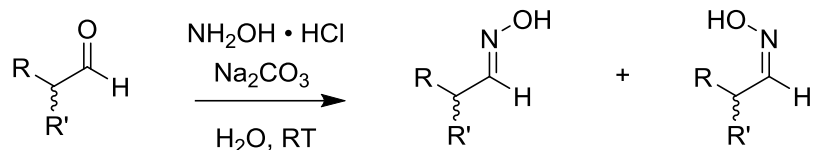
**NP-HPLC:** *Daicel Chiracel* OB-H, CO<sub>2</sub>/isopropanol 98:2, 1.5 mL/min, 20 °C, 210 nm, R<sub>t1+2</sub> = 19.7 min.

*rac*-(*E,Z*)-2-(3-bromophenyl)propanal oxime:

**EA:** calcd for C<sub>9</sub>H<sub>10</sub>BrNO: C, 47.39; H, 4.42; N, 6.14. Found: C, 47.61; H, 4.61; N, 6.13.

**MS (ESI):** m/z = 228.0, 230.0 [M+H]<sup>+</sup>.

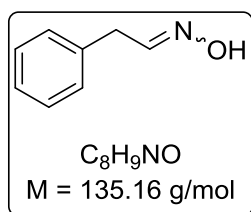
## 9.3.1.4 General procedure 4 (GP4): Synthesis of aldoximes by condensation of aldehydes with hydroxyl amine salts



R = Alkyl, Ph, etc.

R' = CH<sub>3</sub>, H, Alkyl

Hydroxylamine hydrochloride (1.5 eq.) and sodium carbonate (0.75 – 1.5 eq.) were dissolved in H<sub>2</sub>O at room temperature. Aldehyde was added to this solution and stirred vigorously until complete conversion according to TLC analysis (cyclohexane/ethyl acetate in different volumetric percentages) was achieved. The solution was extracted three times with ethyl acetate (1:1 v/v) and the combined organic phases were washed with H<sub>2</sub>O (1:3 v/v). Drying over MgSO<sub>4</sub> and evaporation of the solvent gave a crude product, which was purified by column chromatography if necessary. The (*E/Z*)-ratio of the product was determined by <sup>1</sup>H-NMR spectroscopy in CD<sub>2</sub>Cl<sub>2</sub>. The isomers were, if possible, separated *via* column chromatography or automated flash chromatography.

9.3.1.4.1 (*E/Z*)-phenyl acetaldehyde oxime

The synthesis was carried out according to GP4. Hydroxylamine hydrochloride (4.34 g, 62.4 mmol) and sodium carbonate (6.61 g, 62.4 mmol) were dissolved in 50 mL H<sub>2</sub>O at room temperature. After the addition of phenyl acetaldehyde (5.00 g, 41.6 mmol) the colorless suspension was stirred for 3 hours, upon which complete conversion was achieved according to TLC analysis (cyclohexane/ethyl acetate 1:1, v/v). The work up yielded the product as colorless solid, containing a mixture of (*E/Z*)-isomers (*E/Z* = 5:95).

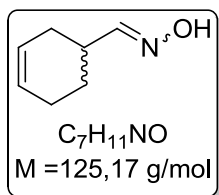
**Yield:** 5.06 g, 91%.

**<sup>1</sup>H-NMR** (500 MHz, CD<sub>2</sub>Cl<sub>2</sub>): δ [ppm] = 8.88 (s, 1H, CH=NOH), 8.33 (s, 1H, CH=NOH), 7.52 (t, 1H, <sup>3</sup>J = 6.3 Hz, CH=NOH), 7.35-7.21 (m, 5H, Ph-H), 6.88 (t, 1H, <sup>3</sup>J = 5.4 Hz, CH=NOH), 3.72 (d, 2H, <sup>3</sup>J = 5.4 Hz, CH<sub>2</sub>), 3.53 (d, 2H, <sup>3</sup>J = 6.3 Hz, CH<sub>2</sub>).

**<sup>13</sup>C-NMR** (125 MHz, CD<sub>2</sub>Cl<sub>2</sub>): δ [ppm] = 151.4, 151.22, 137.4, 136.9, 129.4, 129.3, 129.2, 129.2, 127.4, 127.2, 36.4, 32.1.

**RP-HPLC:** *Macherey-Nagel* Nucleodur C<sub>18</sub> HTec, Water/Acetonitrile 70:30, v/v, 1.0 mL/min, 40 °C, 210 nm, R<sub>t1</sub> = 7.2 min (*E*), R<sub>t2</sub> = 8.5 min (*Z*).

The data corresponds with literature data.<sup>[206]</sup>

9.3.1.4.2 *rac*-(*E/Z*)-3-cyclohexene-1-carboxaldehyde oxime

The synthesis was carried out according to GP4. Hydroxylamine hydrochloride (3.13 g, 45.0 mmol) and sodium carbonate (4.77 g, 45.0 mmol) were diluted in 50 mL H<sub>2</sub>O at RT. After the addition of *rac*-3-cyclohexene-1-carboxaldehyde (3.40 mL, 30.0 mmol) the colorless suspension was stirred for 3 hours, upon which complete conversion was achieved according to TLC analysis. The product was obtained as colorless oil after work up, which consisted of a 3:1 mixture of (*E/Z*)-isomers.

**Yield:** 3.54 g, 94%.

*rac*-(*E*)-3-cyclohexene-1-carboxaldehyde oxime:

**<sup>1</sup>H-NMR** (500 MHz, CD<sub>2</sub>Cl<sub>2</sub>): δ [ppm] = 7.39 (d, 1H, <sup>3</sup>J = 6.1 Hz, CH=NOH), 7.18 (s, 1H, CH=NOH), 5.69 (m, 2H, CH=CH), 2.49 (m, 1H, CH-CH-NOH), 2.16 (m, 1H), 2.09 (m, 2H), 2.02 (m, 1H), 1.85 (m, 1H), 1.52 (m, 1H).

**<sup>13</sup>C-NMR** (125 MHz, CD<sub>2</sub>Cl<sub>2</sub>): δ [ppm] = 155.8, 127.5, 125.7, 35.0, 29.1, 26.7, 24.7.

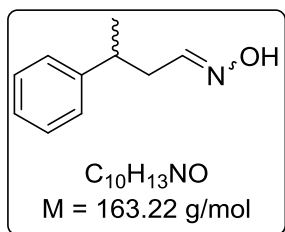
*rac*-(*Z*)-3-cyclohexene-1-carboxaldehyde oxime:

**<sup>1</sup>H-NMR** (500 MHz, CD<sub>2</sub>Cl<sub>2</sub>): δ [ppm] = 7.14 (s, 1H, CH=NOH), 6.60 (d, 1H, <sup>3</sup>J = 7.1 Hz, CH=NOH), 5.69 (m, 2H, CH=CH), 3.21 (m, 1H, CH-CH-NOH), 2.24 (m, 1H), 2.10 (m, 2H), 1.91 (m, 1H), 1.82 (m, 1H), 1.57 (m, 1H).

**<sup>13</sup>C-NMR** (125 MHz, CD<sub>2</sub>Cl<sub>2</sub>): δ [ppm] = 156.7, 127.6, 125.7, 30.3, 28.6, 25.8, 24.4.

**RP-HPLC:** *Macherey-Nagel* Nucleodur C<sub>18</sub> HTec, Water/Acetonitrile 70:30, v/v, 1.0 mL/min, 40 °C, 210 nm, R<sub>t1</sub> = 7.2 min (*E*), R<sub>t2</sub> = 8.1 min (*Z*).

The data corresponds with the literature.<sup>[89]</sup>

9.3.1.4.3 *rac*-(*E/Z*)-3-phenylbutyraldehyde oxime

Hydroxylamine phosphate (3.31 g, 16.8 mmol) und sodium acetate (3.67 g, 44.8 mmol) were suspended in 100 mL dest. H<sub>2</sub>O. After addition of *rac*-3-phenylbutyraldehyde (5.00 mL, 33.6 mmol) the colorless suspension was stirred for 3 hours, upon which complete conversion was achieved according to TLC analysis (cyclohexane/ethyl acetate, 2:1). The product was obtained as colorless oil after work up, which consisted of a 1:1 mixture of (*E/Z*)-isomers according to <sup>1</sup>H-NMR analysis.

**Yield:** 2.10 g, 38%.

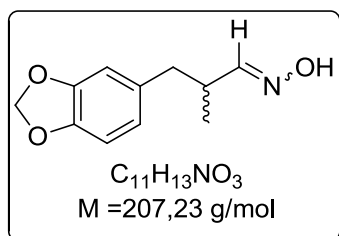
**<sup>1</sup>H-NMR** (500 MHz, CD<sub>2</sub>Cl<sub>2</sub>): δ [ppm] = 7.31-7.19 (m, 5H, Ph-*H*), 7.28 (m, 1H, CH=NOH), 6.62 (t, 1H, <sup>3</sup>J = 5.3 Hz, CH=NOH), 2.98 (sx, 1H, <sup>3</sup>J = 7.0 Hz, Ph-CH-CH<sub>3</sub>), 2.96 (sx, 1H, <sup>3</sup>J = 7.0 Hz, Ph-CH-CH<sub>3</sub>), 2.65 (m, 2H, Ph-CH-CH<sub>2</sub>), 2.46 (m, 2H, Ph-CH-CH<sub>2</sub>), 1.29 (d, 3H, <sup>3</sup>J = 7.0 Hz, CH<sub>3</sub>), 1.28 (d, 3H, <sup>3</sup>J = 7.0 Hz, CH<sub>3</sub>).

**<sup>13</sup>C-NMR** (125 MHz, CD<sub>2</sub>Cl<sub>2</sub>): δ [ppm] = 151.9, 151.5, 146.6, 146.4, 129.1, 129.0, 127.4, 127.4, 126.9, 126.9, 38.5, 38.2, 37.8, 33.4, 22.6, 22.2.

**RP-HPLC:** *Macherey-Nagel* Nucleodur C<sub>18</sub> HTec, Water/Acetonitrile 70:30, v/v, 1.0 mL/min, 40 °C, 210 nm, R<sub>t1</sub> = 22.6 min (*E*), R<sub>t2</sub> = 26.5 min (*Z*).

**NP-HPLC:** *Daicel* Chiracel OD-H, CO<sub>2</sub>/Isopropanol 98:2, v/v, 30 min, 0.7 mL/min; 60 min 98:2 to 90:10, v/v, 20 °C, 210 nm, R<sub>t1</sub> = 45.0 min, R<sub>t2</sub> = 47.5 min, R<sub>t3</sub> = 57.7 min, R<sub>t4</sub> = 64.3 min.

The data corresponds with literature data.<sup>[89]</sup>

9.3.1.4.4 *rac*-(*E/Z*)-2-methyl-3-(3,4-methylenedioxyphenyl)-propanal oxime

The synthesis was carried out according to GP4. Hydroxylamine hydrochloride (2.71 g, 39.0 mmol) and sodium carbonate (4.13 g, 39.0 mmol) were dissolved in 50 mL H<sub>2</sub>O at room temperature. *rac*-2-methyl-3-(3,4-methylenedioxyphenyl)propanal (**3**, 4.30 mL, 26.0 mmol) was added to the solution, upon which a pale yellow suspension was obtained. After two hours complete conversion was achieved according to TLC analysis (cyclohexane:ethyl acetate 3:1, v/v). The work up yielded the product as yellow oil, containing a mixture of (*E/Z*)-isomers (62:38).

**Yield:** 4.75 g, 88%.

*rac*-(*E*)-2-methyl-3-(3,4-methylenedioxyphenyl)propanal oxime:

**<sup>1</sup>H-NMR** (500 MHz, CD<sub>2</sub>Cl<sub>2</sub>): δ [ppm] = 7.55 (s, 1H, CHNOH), 7.33 (d, 1H, <sup>3</sup>J = 6.2 Hz, CHNOH), 6.74-6.60 (m, 3H, Ph-H), 5.92 (s, 2H, OCH<sub>2</sub>O), 2.75-2.52 (m, 2H, PhCH<sub>2</sub>), 2.60 (m, 1H, CH<sub>3</sub>CH), 1.04 (d, 3H, <sup>3</sup>J = 6.7 Hz, CH<sub>3</sub>CH).

**<sup>13</sup>C-NMR** (125 MHz, CD<sub>2</sub>Cl<sub>2</sub>): δ [ppm] = 156.2, 148.2, 146.5, 133.8, 122.6, 109.9, 108.5, 101.6, 41.0, 36.9, 17.8.

*rac*-(*Z*)-2-methyl-3-(3,4-methylenedioxyphenyl)propanal oxime:

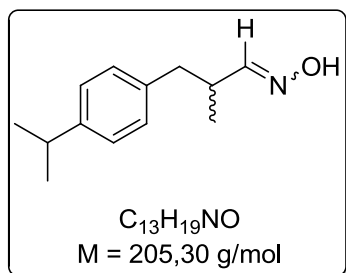
**<sup>1</sup>H-NMR** (500 MHz, CD<sub>2</sub>Cl<sub>2</sub>): δ [ppm] = 7.91 (s, 1H, NOH), 6.74-6.60 (m, 3H, Ph-H), 6.54 (d, 1H, <sup>3</sup>J = 7.4 Hz, CHNOH), 5.91 (s, 2H, OCH<sub>2</sub>O), 3.34 (sept, 1H, <sup>3</sup>J = 7.2 Hz, CH<sub>3</sub>CH), 2.75-2.52 (m, 2H, PhCH<sub>2</sub>), 1.02 (d, 3H, <sup>3</sup>J = 7.0 Hz, CH<sub>3</sub>CH).

**<sup>13</sup>C-NMR** (125 MHz, CD<sub>2</sub>Cl<sub>2</sub>): δ [ppm] = 157.1, 148.1, 146.5, 133.9, 122.4, 109.8, 108.4, 101.6, 40.5, 31.9, 17.3.

**RP-HPLC:** *Macherey-Nagel* Nucleodur C<sub>18</sub> HTec, Water/Acetonitrile 70:30, v/v, 1.0 mL/min, 40 °C, 220 nm, R<sub>t1</sub> = 15.3 min, R<sub>t2</sub> = 17.2 min.

**NP-HPLC:** *Daicel* Chiracel OD-H, CO<sub>2</sub>/Isopropanol 99:1, v/v, 1.0 mL/min, 20 °C, 210 nm, 30 min to CO<sub>2</sub>/Isopropanol 95:5, v/v, 1.2 mL/min, 20 °C, 210 nm, 30 min; R<sub>tE1</sub> = 41.7 min, R<sub>t2</sub> = 43.0 min, R<sub>tZ1</sub> = 48.3 min, R<sub>tZ2</sub> = 48.3 min.

The data corresponds with literature data.<sup>[159]</sup>

9.3.1.4.5 *rac*-(*E/Z*)-2-methyl-3-(4-isopropylphenyl)propionaldehyde oxime

The synthesis was carried out according to GP4. Hydroxylamine hydrochloride (2.74 g, 39.4 mmol) and sodium carbonate (4.18 g, 39.4 mmol) were dissolved in 50 mL H<sub>2</sub>O at room temperature. The addition of *rac*-2-methyl-3-(4-isopropylphenyl)propionaldehyde (5.26 mL, 26.3 mmol) led to formation of a colorless suspension. Complete conversion was achieved after four hours according to TLC analysis (cyclohexane:ethyl acetate 3:1, v/v). Work up yielded the product as colorless oil, which crystallized overnight as colorless solid. The (*E/Z*)-ratio was 98:2 according to <sup>1</sup>H-NMR analysis.

**Yield:** 4.61 g, 85%.

*rac*-(*E*)-2-methyl-3-(4-isopropylphenyl)propionaldehyde oxime:

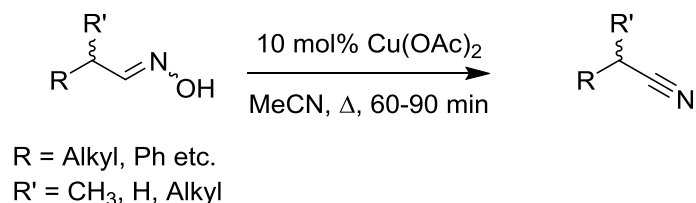
**<sup>1</sup>H-NMR** (500 MHz, CD<sub>2</sub>Cl<sub>2</sub>): δ [ppm] = 7.35 (d, 1H, <sup>3</sup>J = 6.1 Hz, CHNOH), 7.25 (s, 1H, CHNOH), 7.17-7.06 (m, 4H, Ph-H), 2.92-2.57 (m, 2H, PhCH<sub>2</sub>), 2.65 (m, 1H, (CH<sub>3</sub>)<sub>2</sub>CH), 1.24 (d, 6H, <sup>3</sup>J = 6.9 Hz, (CH<sub>3</sub>)<sub>2</sub>CH), 1.04 (d, 3H, <sup>3</sup>J = 6.7 Hz, CH<sub>3</sub>CH).

**<sup>13</sup>C-NMR** (125 MHz, CD<sub>2</sub>Cl<sub>2</sub>): δ [ppm] = 156.4, 147.4, 137.3, 129.6, 126.9, 40.9, 36.8, 34.3, 24.4, 17.9.

**RP-HPLC:** *Macherey-Nagel* Nucleodur C<sub>18</sub> HTec, Water/Acetonitrile 50:50, v/v, 1.0 mL/min, 40 °C, 220 nm, R<sub>t1</sub> = 13.2 min.

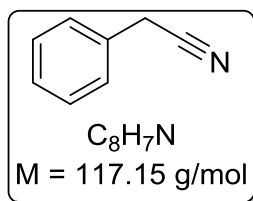
**NP-HPLC:** *Daicel* Chiracel OD-H, CO<sub>2</sub>/Isopropanol 98:2, v/v, 1.0 mL/min, 20 °C, 210 nm, R<sub>t1</sub> = 24.4 min, R<sub>t2</sub> = 29.0 min.

## 9.3.1.5 General procedure 5 (GP5): Copper (II) catalyzed synthesis of racemic nitriles



The syntheses were carried out in analogy to *Ma et al.*<sup>[15]</sup> Copper(II) acetate (2-10 mol-%) was dissolved in acetonitrile at room temperature. The corresponding aldoxime (1.0 eq.) was added and the solution was heated to reflux for 60 to 90 minutes. Complete conversion was determined *via* TLC (cyclohexane/ethyl acetate) and the solvent was removed *in vacuo*. The crude product was suspended in cyclohexane/ethyl acetate and filtered over a short plug of silica to yield the product as oil. Alternatively, vacuum distillation could be used for purification.

## 9.3.1.5.1 Phenyl acetonitrile



The synthesis was carried out according to GP5. Copper(II) acetate (74 mg, 407 μmol) was dissolved in 10 mL acetonitrile. Phenyl acetaldehyde (541 mg, 4.00 mmol) was added to the solution. After refluxing for 60 minutes, work up was conducted (cyclohexane/ethyl acetate 2:1, v/v) and yielded the product as pale yellow oil.

**Yield:** 153 mg, 33%.

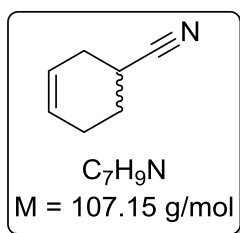
**<sup>1</sup>H-NMR** (500 MHz, CDCl<sub>3</sub>): δ [ppm] = 7.39 (m, 2H, Ph-*H*), 7.34 (m, 3H, Ph-*H*), 3.76 (s, 2H, CH<sub>2</sub>).

**<sup>13</sup>C-NMR** (125 MHz, CDCl<sub>3</sub>): δ [ppm] = 130.0, 129.3, 128.2, 128.1, 118.0, 23.8.

**RP-HPLC:** *Macherey-Nagel* Nucleodur C<sub>18</sub> HTec, Water/Acetonitrile 70:30, v/v, 1.0 mL/min, 40 °C, 210 nm, R<sub>t</sub> = 11.3 min.

The analytical data corresponds with the literature.<sup>[207]</sup>



9.3.1.5.2 *rac*-3-cyclohexene-1-carbonitrile

The synthesis was carried out according to GP5. Copper(II) acetate (143 mg, 827  $\mu$ mol) was dissolved in 20 mL acetonitrile. (*E/Z*)-*rac*-3-cyclohexene-1-carbaldehydoxime (1.02 g, 8.16 mmol) was added to the solution. After refluxing for 90 minutes, work up was conducted (cyclohexane/ethyl acetate 2:1, v/v) and yielded the product as yellow oil.

**Yield:** 590 mg, 67%.

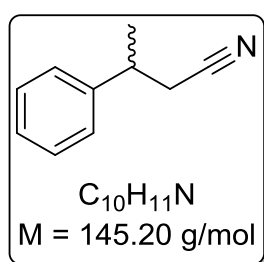
**$^1H$ -NMR** (500 MHz,  $CDCl_3$ ):  $\delta$  [ppm] = 5.75 (m, 1H, CH=CH-CH<sub>2</sub>-CH), 5.64 (m, 1H, CH=CH-CH<sub>2</sub>-CH), 2.81 (m, 1H, CH-CN), 2.38 (m, 1H, CH=CH-CH<sub>2</sub>-CH), 2.33 (m, 1H, CH=CH-CH<sub>2</sub>-CH), 2.22 (m, 1H, CH=CH-CH<sub>2</sub>-CH<sub>2</sub>), 2.12 (m, 1H, CH=CH-CH<sub>2</sub>-CH<sub>2</sub>), 1.98 (m, 1H, CH=CH-CH<sub>2</sub>-CH<sub>2</sub>), 1.89 (m, 1H, CH=CH-CH<sub>2</sub>-CH<sub>2</sub>).

**$^{13}C$ -NMR** (125 MHz,  $CD_2Cl_2$ ):  $\delta$  [ppm] = 127.13 (CH=CH-CH<sub>2</sub>-CH), 123.4 (CH=CH-CH<sub>2</sub>-CH), 122.61 (CN), 28.31 (CH=CH-CH<sub>2</sub>-CH), 25.47 (CH=CH-CH<sub>2</sub>-CH<sub>2</sub>), 24.78 (CH-CN), 23.06 (CH=CH-CH<sub>2</sub>-CH<sub>2</sub>).

**RP-HPLC:** *Macherey-Nagel* Nucleodur C<sub>18</sub> HTec, Water/Acetonitrile 70:30, v/v, 1.0 mL/min, 40 °C, 210 nm,  $R_t$  = 10.1 min.

**Chiral GC** (FID): BGB-174 (0.25 ID x 30m, 0.25  $\mu$ m film), 120 °C (isocratic),  $R_{t1}$  = 8.3 min,  $R_{t2}$  = 8.5 min.

The analytical data corresponds with the literature.<sup>[89]</sup>

9.3.1.5.3 *rac*-3-phenylbutanenitrile

Dry  $CH_2Cl_2$  (30 mL) was added to a heat dried schlenk flask and cooled to 0 °C. Triphenylphosphine oxide (44.8 mg, 150  $\mu$ mol) and oxalyl chloride (370  $\mu$ L, 4.59 mmol) were added. *rac*-(*E/Z*)-3-phenylbutyraldehyde oxime (500 mg, 3.06 mmol) was dissolved in 7 mL  $CH_2Cl_2$  and added dropwise. The reaction mixture was brought to room temperature and complete conversion was confirmed *via* TLC (MTBE). Saturated  $NaHCO_3$  was added and the aqueous phase was extracted three times with  $CH_2Cl_2$  (1:1, v/v). The combined extracts were washed with brine, dried over  $MgSO_4$  and the solvent was removed *in vacuo*. Filtration over a short plug of silica (MTBE) yielded the product as yellow oil.

**Yield:** 382 mg, 86%.

**$^1H$ -NMR** (500 MHz,  $CDCl_3$ ):  $\delta$  [ppm] = 7.35 (m, 2H, Ph-H *m*), 7.26 (m, 3H, Ph-H *o, p*), 3.16 (sx, 1H,  $^3J$  = 7.0 Hz, CH), 2.61 (dd, 1H,  $^2J$  = 16.6 Hz,  $^3J$  = 6.4 Hz, CH<sub>2</sub>), 2.57 (dd, 1H,  $^2J$  = 16.6 Hz,  $^3J$  = 6.4 Hz, CH<sub>2</sub>), 1.46 (d, 3H,  $^3J$  = 7.0 Hz, CH<sub>3</sub>).

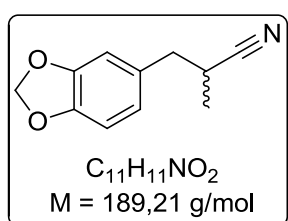
**$^{13}\text{C-NMR}$**  (125 MHz,  $\text{CDCl}_3$ ):  $\delta$  [ppm] = 143.3, 129.0, 127.5, 126.7, 118.7, 36.7, 26.5, 20.8.

**RP-HPLC:** *Macherey-Nagel* Nucleodur  $\text{C}_{18}$  HTec, Water/Acetonitrile 70:30, v/v, 1.0 mL/min, 40 °C, 210 nm,  $R_t$  = 26.0 min.

**NP-HPLC:** *Daicel* Chiracel OD-H,  $\text{CO}_2$ /Isopropanol 98:2, v/v, 30 min, 0.7 mL/min, 20 °C, 210 nm,  $R_{t1}$  = 21.5 min,  $R_{t2}$  = 23.6 min.

The analytical data corresponds with the literature.<sup>[89]</sup>

#### 9.3.1.5.4 *rac-a-methyl-1,3-benzodioxole-5-propanenitrile*



The synthesis was carried out according to GP5. Copper(II) acetate (32.6 mg, 179  $\mu\text{mol}$ ) was dissolved in 6.0 mL acetonitrile. *rac*-(*E/Z*)-2-methyl-3-(3,4-methylenedioxyphenyl)-propanal oxime (372 mg, 1.80 mmol) was added to the solution. After refluxing for 90 minutes, work up was conducted (cyclohexane/ethyl acetate 2:1, v/v) and yielded the product as pale yellow oil. Alternatively to NMR, conversion could be measured *via* RP-HPLC.

**Yield:** 313 mg, 92%.

**$^1\text{H-NMR}$**  (500 MHz,  $\text{CDCl}_3$ ):  $\delta$  [ppm] = 6.76 (d, 1H,  $^3J$  = 7.9 Hz, O-C=CH=CH), 6.70 (d, 1H,  $^4J$  = 1.6 Hz, O-C=CH=C), 6.68 (dd, 1H,  $^3J$  = 7.9 Hz,  $^4J$  = 1.6 Hz, O-CH=CH), 5.94 (s, 2H, O- $\text{CH}_2$ -O), 2.78 (m, 3H,  $\text{PhCH}_2$ ,  $\text{CHCN}$ ), 1.32 (d, 3H,  $^3J$  = 6.6 Hz,  $\text{CH}_3$ ).

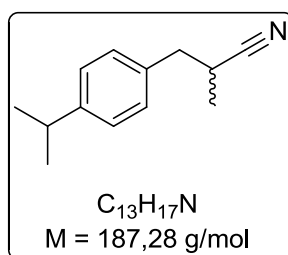
**$^{13}\text{C-NMR}$**  (125 MHz,  $\text{CDCl}_3$ ):  $\delta$  [ppm] = 147.9, 146.9, 130.6, 122.6, 122.3, 109.4, 108.5, 101.2, 39.8, 27.9, 17.6.

**RP-HPLC:** *Macherey-Nagel* Nucleodur  $\text{C}_{18}$  HTec, Water/Acetonitrile 70:30, v/v, 1.0 mL/min, 40 °C, 220 nm,  $R_t$  = 23.6 min,

**NP-HPLC:** *Daicel* Chiracel OD-H,  $\text{CO}_2$ /Isopropanol 99:1, v/v, 1.0 mL/min, 20 °C, 210 nm, 30 min to  $\text{CO}_2$ /Isopropanol 95:5, v/v, 1.2 mL/min, 20 °C, 210 nm, 30 min;  $R_{t(S)}$  = 23.5 min,  $R_{t(R)}$  = 24.5 min.

The analytical data corresponds with the literature.<sup>[100]</sup>

#### 9.3.1.5.5 *rac-a-methyl-4-(1-methylethyl)-benzenepropanenitrile*



The synthesis was carried out according to GP5. Copper(II) acetate (26.5 mg, 146  $\mu\text{mol}$ ) was dissolved in 5.0 mL acetonitrile. *rac*-(*E/Z*)-2-methyl-3-(4-isopropylphenyl)propionaldehyde oxime (300 mg, 1.46 mmol) was added to the solution. After refluxing for two hours, work up was conducted (cyclohexane/ethyl acetate 6:1, v/v) and yielded the product as pale greenish oil. Alternatively to NMR, conversion could be measured *via* RP-HPLC.

**Yield:** 260 mg, 95%.

**<sup>1</sup>H-NMR** (500 MHz, CDCl<sub>3</sub>): δ [ppm] = 7.19 (m, 4H, Ph-H), 2.94-2.76 (m, 4H, (CH<sub>3</sub>)<sub>2</sub>CH, PhCH<sub>2</sub>, CHCN), 1.32 (d, 3H, <sup>3</sup>J = 6.8 Hz, CH<sub>3</sub>CHCN), 1.25 (d, 6H, <sup>3</sup>J = 6.9 Hz, (CH<sub>3</sub>)<sub>2</sub>CH).

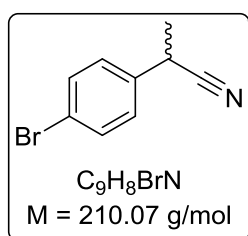
**<sup>13</sup>C-NMR** (125 MHz, CDCl<sub>3</sub>): δ [ppm] = 148.0, 134.3, 129.1, 126.9, 122.8, 39.8, 33.9, 27.7, 24.1, 17.8.

**RP-HPLC:** *Macherey-Nagel* Nucleodur C<sub>18</sub> HTec, Water/Acetonitrile 50:50, v/v, 1.0 mL/min, 40 °C, 220 nm, R<sub>t</sub> = 19.1 min.

**NP-HPLC:** *Daicel* Chiracel OD-H, CO<sub>2</sub>/Isopropanol 98:2, v/v, 1.0 mL/min, 20 °C, 210 nm, R<sub>t1</sub> = 11.0 min, R<sub>t2</sub> = 11.8 min.

The analytical data corresponds with the literature.<sup>[63]</sup>

#### 9.3.1.5.6 *rac*-2-(4-bromophenyl)propanenitrile



The synthesis was carried out according to GP5. Copper(II) acetate (16 mg, 88 μmol) was dissolved in 5 mL acetonitrile. *rac*-(*E/Z*)-2-(4-bromophenyl)propanal oxime (200 mg, 877 μmol) was added and the reaction mixture was heated to reflux for 90 minutes. The crude product was purified *via* vacuum distillation (10<sup>-3</sup> mbar, 150 °C) to yield the product as colorless oil.

**Yield:** 97 mg, 52%.

**<sup>1</sup>H-NMR** (500 MHz, CDCl<sub>3</sub>): δ [ppm] = 7.52 (d, 2H, <sup>3</sup>J = 8.3 Hz, Ar-H), 7.23 (d, 2H, <sup>3</sup>J = 8.3 Hz, Ar-H), 3.87 (q, 1H, <sup>3</sup>J = 7.3 Hz, Ph-CH), 1.62 (d, 3H, <sup>3</sup>J = 7.3 Hz, CH<sub>3</sub>).

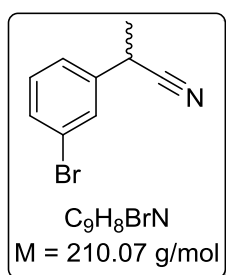
**<sup>13</sup>C-NMR** (125 MHz, CDCl<sub>3</sub>): δ [ppm] = 136.2, 132.5, 128.6, 122.3, 121.2, 31.0, 21.5.

**RP-HPLC:** *Macherey-Nagel* Nucleodur C<sub>18</sub> HTec, water/acetonitrile 70:30, 1.5 mL/min, 40 °C, 210 nm, R<sub>t</sub> = 37.1 min.

**NP-HPLC:** *Daicel* Chiracel OB-H, CO<sub>2</sub>/isopropanol 98:2, 1.5 mL/min, 20 °C, 210 nm, R<sub>t1</sub> = 10.1 min, R<sub>t2</sub> = 11.7 min.

The analytical data corresponds with literature data.<sup>[208]</sup>

#### 9.3.1.5.7 *rac*-2-(3-bromophenyl)propanenitrile



The synthesis was carried out according to GP5. Copper(II) acetate (8.2 mg, 45 μmol) was dissolved in 5 mL acetonitrile. *rac*-(*E/Z*)-2-(3-bromophenyl)propanal oxime (103 mg, 452 μmol) was added and the reaction mixture was heated to reflux for 90 minutes. The crude product was purified by filtration over silica (cyclohexane/ethyl acetate 8:1, v/v) to yield the product as pale green oil.

**Yield:** 83 mg, 87%.

**<sup>1</sup>H-NMR** (500 MHz, CDCl<sub>3</sub>): δ [ppm] = 7.51 (m, 1H, Ar-H), 7.48 (m, 1H, Ar-H), 7.30 (m, 1H, Ar-H), 7.27 (t, 1H, <sup>3</sup>J = 7.8 Hz, Ar-H), 3.87 (q, 1H, <sup>3</sup>J = 7.3 Hz, Ph-CH), 1.65 (d, 3H, <sup>3</sup>J = 7.3 Hz, CH<sub>3</sub>).

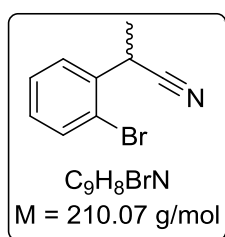
**<sup>13</sup>C-NMR** (125 MHz, CDCl<sub>3</sub>): δ [ppm] = 139.3, 131.5, 130.9, 130.1, 125.6, 123.3, 31.1, 21.5.

**RP-HPLC:** *Macherey-Nagel* Nucleodur C<sub>18</sub> HTec, water/acetonitrile 70:30, 1.5 mL/min, 40 °C, 210 nm, R<sub>t</sub> = 35.0 min.

**NP-HPLC:** *Daicel Chiracel* OB-H, CO<sub>2</sub>/isopropanol 98:2, 1.5 mL/min, 20 °C, 210 nm, R<sub>t(S)</sub> = 9.0 min, R<sub>t(R)</sub> = 11.2 min.

The analytical data corresponds with literature data.<sup>[208]</sup>

#### 9.3.1.5.8 *rac*-2-(2-bromophenyl)propanenitrile



The synthesis was carried out according to GP5. Copper(II) acetate (5.7 mg, 32 μmol) was dissolved in 5 mL acetonitrile. *rac*-(*E/Z*)-2-(2-bromophenyl)propanal oxime (72 mg, 32 μmol) was added and the reaction mixture was heated to reflux for 90 minutes. The crude product was purified by filtration over silica (cyclohexane/ethyl acetate 8:1, v/v) to yield the product as pale yellow oil.

**Yield:** 63 mg, 95%.

**<sup>1</sup>H-NMR** (500 MHz, CDCl<sub>3</sub>): δ [ppm] = 7.59 (m, 2H, Ar-H), 7.39 (m, 1H, Ar-H), 7.30 (m, 1H, Ar-H), 7.20 (dt, 1H, <sup>3</sup>J = 7.7 Hz, <sup>4</sup>J = 1.5 Hz, Ar-H), 4.36 (q, 1H, <sup>3</sup>J = 7.2 Hz, Ph-CH), 1.62 (d, 3H, <sup>3</sup>J = 7.2 Hz, CH<sub>3</sub>).

**<sup>13</sup>C-NMR** (125 MHz, CDCl<sub>3</sub>): δ [ppm] = 136.7, 133.5, 129.9, 128.6, 128.5, 122.8, 121.2, 31.6, 20.4.

**RP-HPLC:** *Macherey-Nagel* Nucleodur C<sub>18</sub> HTec, water/acetonitrile 70:30, 1.5 mL/min, 40 °C, 210 nm, R<sub>t</sub> = 34.2 min.

**NP-HPLC:** *Daicel Chiracel* OB-H, CO<sub>2</sub>/isopropanol 98:2, 1.5 mL/min, 20 °C, 210 nm, R<sub>t(S)</sub> = 6.3 min, R<sub>t(R)</sub> = 7.6 min.

The analytical data corresponds with literature data.<sup>[209]</sup>

### 9.3.2 PREPARATION OF WHOLE CELL CATALYSTS AND BIOTRANSFORMATIONS OF ALDOXIMES INTO NITRILES

#### 9.3.2.1 General procedure 6 (GP6): Expression and storage of the aldoxime dehydratases (Oxds)

Pre-culture: 10 mL LB-medium in a 100 mL Erlenmeyer flask containing 50 µg/mL kanamycin or 100 µg/mL carbenicillin and 34 µg/mL chloramphenicol were inoculated with an *E. coli* clone and incubated at 37 °C and 180 rpm for 24 hours.

Main culture: 100-450 mL (in 100-500 mL Erlenmeyer flasks) auto-induction medium (Recipe for 1L: 890 mL TB-Medium (pH = 7.0), 10 mL 50 g/L glucose and 100 mL 20 g/L lactose) was inoculated with 1.0 Vol.-% of the pre-culture, followed by addition of 50 µg/mL kanamycin or 100 µg/mL carbenicillin and 34 µg/mL chloramphenicol. The culture was incubated for one hour at 37 °C and 180 rpm, followed by incubation at 15 °C (OxdA, OxdFG, OxdRE, OxdRG) or 30 °C (OxdB) for 72 hours.

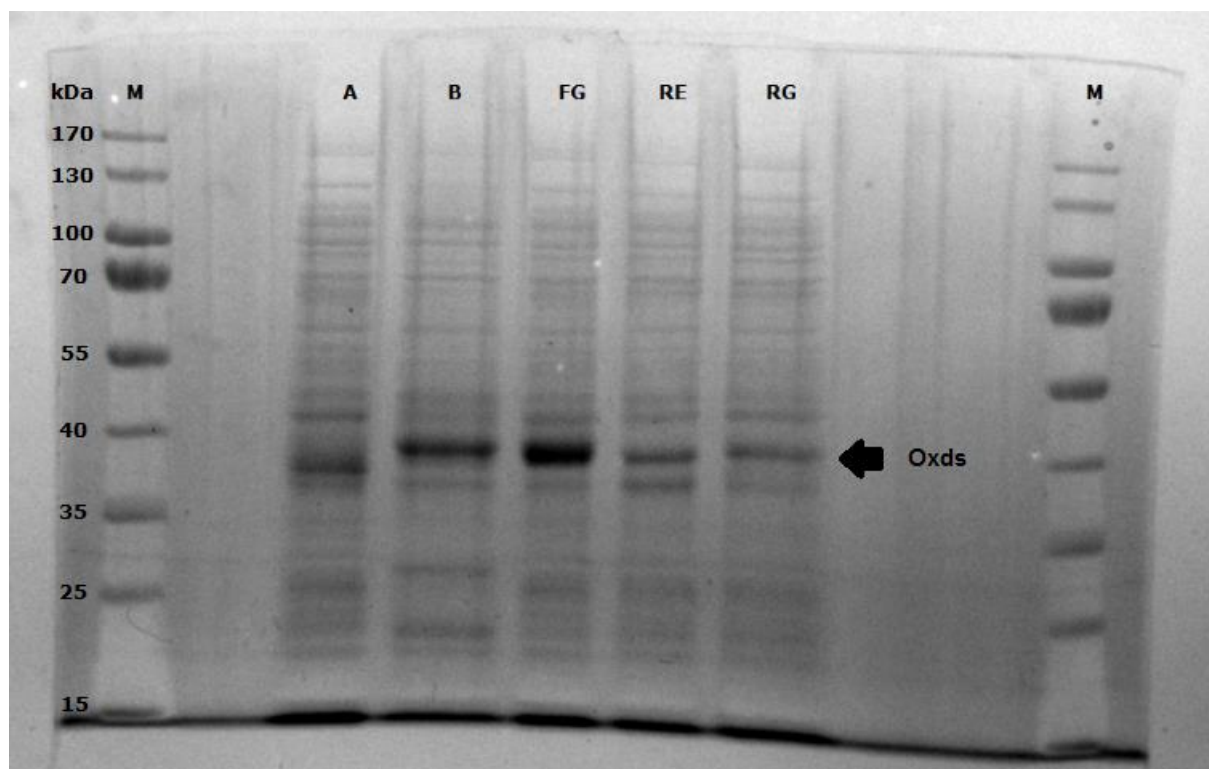
The cells were harvested by centrifugation (4000 g, 4 °C, 15 min). The supernatant was discarded and the pellets were washed twice with 50 mM potassium phosphate buffer (pH = 7.0). After repeated centrifugation (4000 g, 4 °C, 15 min) and weighing of the pellets (bio wet weight, BWW), they were suspended in 50 mM potassium phosphate buffer (50-fold concentrated, pH = 7.0), optionally overlaid with argon and stored at 4 °C as resting cell suspension (typically 25-35 wt%).

**Table 22:** Used plasmids for the transformation of *E. coli*.

Entry	Vector/plasmid	Source organism	Aldoxime dehydratase	Provider	Resistance
1	pET28_OxdA(C)	<i>Pseudomonas chlororaphis</i> B23	OxdA	Asano group	Kanamycin
3	pUC19_OxdB	<i>Bacillus</i> sp. OxB-1	OxdB	Asano group	Carbenicillin
4	pET28_OxdFG(N)	<i>Fusarium graminearum</i>	OxdFG	Thermo Fisher Scientific	Kanamycin
5	pET28_OxdRE(N)	<i>Rhodococcus erythropolis</i>	OxdRE	Thermo Fisher Scientific	Kanamycin
6	pET28_OxdRG(N)	<i>Rhodococcus globerulus</i> A-4	OxdRG	Thermo Fisher Scientific	Kanamycin

Overexpression of the aldoxime dehydratases was checked *via* SDS-PAGE. A 25 wt% cell suspension was disrupted by ultrasound sonification (*Sonoplus HD 2070*, 5 x 2 min, 10% power) on ice. Insoluble cell components were separated *via* centrifugation (21500 g, 4 °C,

15 min). 10  $\mu$ L of the diluted crude extract (1 mg protein/mL) were pipetted into the collection gel and analyzed *via* SDS-PAGE (12% separation gel).

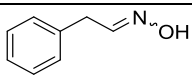
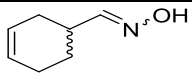
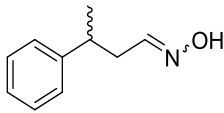


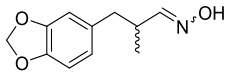
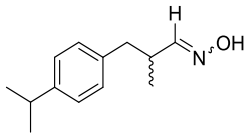
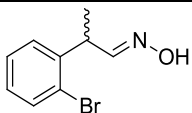
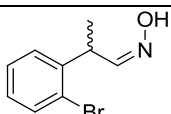
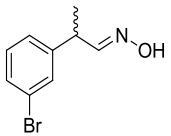
**Figure 36:** SDS-PAGE of all five crude extracts for OxdA (A), OxdB (B), OxdFG (FG), OxdRE (RE), OxdRG (RG). The molecular weight of the Oxds is in good agreement with the literature data. <sup>[70,71,73,74,76,113,210]</sup>

## 9.3.2.2 General procedure 7 (GP7): Standard protocol for determination of Oxd activity

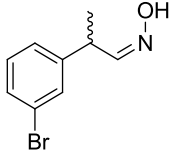
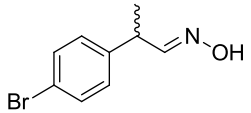
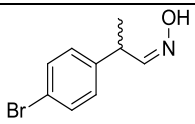
The corresponding aldoxime was dissolved in DMSO (200 mM). The reaction volume of 500  $\mu\text{L}$  in a 1.5 mL micro reaction tube with shaking of 1400 rpm at 8  $^{\circ}\text{C}$  or 30  $^{\circ}\text{C}$  consisted of varying amounts of 50 mM KPB (pH = 7.0) and resting cell suspension (total volume 487.5  $\mu\text{L}$ , typically 2-6  $\text{mg}_{\text{BWW}}$ ). The assay was started by addition of 12.5  $\mu\text{L}$  substrate (final concentration of 5 mM). 100  $\mu\text{L}$  0.1 M HCl and 400  $\mu\text{L}$  acetonitrile were added after 60 seconds to quench the reaction. 800  $\mu\text{L}$  of the supernatant after centrifugation (15000 g, 4  $^{\circ}\text{C}$ , 5 min) were transferred into a vial and measured on RP-HPLC for conversion. The activity was calculated in U/ $\text{mg}_{\text{BWW}}$  (Units are defined as  $\mu\text{mol}/\text{min}$ ).

**Table 23:** Calculated activities for different whole cell catalysts.

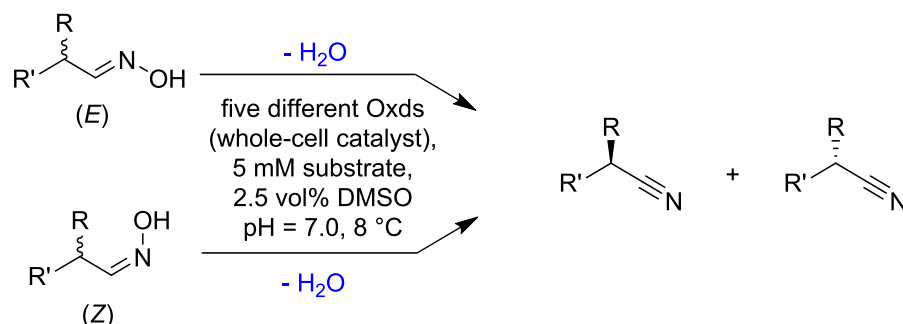
Entry	Substrate	Aldoxime dehydratase	Storage time [days] <sup>a</sup>	Temperature [ $^{\circ}\text{C}$ ]	U/ $\text{mg}_{\text{BWW}}$
1a		OxdA(C)	3	30	0.60
1b	(E/Z 1:19)	OxdB	3	30	2.18
1c		OxdFG(N)	3	30	0.46
1d		OxdRE(N)	3	30	1.69
1e		OxdRG(N)	3	30	0.65
2a		OxdA(C)	3	8	0.24
2b	(E/Z 3:1)	OxdB	3	8	0.08
2c		OxdFG(N)	3	8	0.14
2d		OxdRE(N)	3	8	0.04
2e		OxdRG(N)	3	8	0.02
3a		OxdA(C)	3	8	0.17
3b	(E/Z 1:1)	OxdB	3	8	0.06
3c		OxdFG(N)	3	8	0.04
3d		OxdRE(N)	3	8	0.02
3e		OxdRG(N)	3	8	0.01

Entry	Substrate	Aldoxime dehydratase	Storage time [days] <sup>a</sup>	Temperature [°C]	U/mg <sub>BWW</sub>
4a		OxdA(C)	3	8	0.10
4b	(E/Z 6:4)	OxdB	3	8	0.04
4c		OxdFG(N)	3	8	0.03
4d		OxdRE(N)	5	8	0.02
4e		OxdRG(N)	5	8	0.01
5a <sup>b</sup>		OxdA(C)	7	8	<0.01
5b <sup>b</sup>	(E/Z 98:2)	OxdB(N)	7	8	<0.01
5c <sup>b</sup>		OxdFG(N)	7	8	<0.01
5d <sup>b</sup>		OxdRE(N)	4	8	<0.01
5e <sup>b</sup>		OxdRG(N)	4	8	<0.01
6a		OxdA(C)	3	8	0.01
6b	(E/Z > 99:1)	OxdB	3	8	<0.01
6c		OxdFG(N)	3	8	<0.01
6d		OxdRE(N)	3	8	0.02
6e		OxdRG(N)	3	8	0.01
7a		OxdA(C)	3	8	- <sup>c</sup>
7b	(E/Z = 4:96)	OxdB	3	8	- <sup>c</sup>
7c		OxdFG(N)	3	8	- <sup>c</sup>
7d		OxdRE(N)	3	8	- <sup>c</sup>
7e		OxdRG(N)	3	8	- <sup>c</sup>
8a		OxdA(C)	3	8	- <sup>c</sup>
8b	(E/Z = 96:4)	OxdB	3	8	- <sup>c</sup>



Entry	Substrate	Aldoxime dehydratase	Storage time [days] <sup>a</sup>	Temperature [°C]	U/mg <sub>BWW</sub>
8c		OxdFG(N)	3	8	0.02
8d		OxdRE(N)	3	8	- <sup>c</sup>
8e		OxdRG(N)	3	8	- <sup>c</sup>
9a		OxdA(C)	3	8	0.01
9b	( <i>E/Z</i> = 5:95)	OxdB	3	8	0.03
9c		OxdFG(N)	3	8	0.02
9d		OxdRE(N)	3	8	0.02
9e		OxdRG(N)	3	8	0.01
10a		OxdA(C)	3	8	- <sup>c</sup>
10b	( <i>E/Z</i> > 99:1)	OxdB	3	8	0.01
10c		OxdFG(N)	3	8	0.02
10d		OxdRE(N)	3	8	- <sup>c</sup>
10e		OxdRG(N)	3	8	- <sup>c</sup>
10a		OxdA(C)	3	8	- <sup>c</sup>
10b	( <i>E/Z</i> = 10:90)	OxdB	3	8	0.02
10c		OxdFG(N)	3	8	0.02
10d		OxdRE(N)	3	8	- <sup>c</sup>
<b>10e</b>		OxdRG(N)	3	8	- <sup>c</sup>

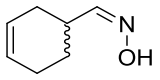
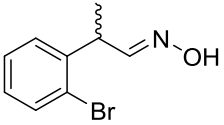
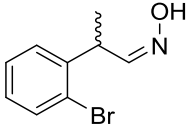
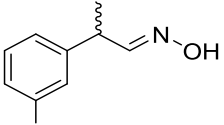
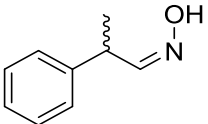
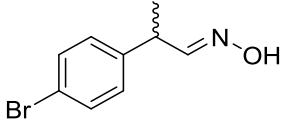
<sup>a</sup> time span between harvest of cells and activity assay, <sup>b</sup> after 2 hours, <sup>c</sup> no conversion detected.

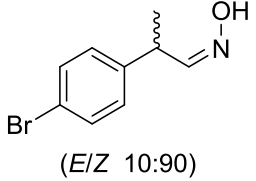
9.3.2.3 General procedure 8 (GP8): Enantioselective biotransformations of (*E*)- and (*Z*)-enriched racemic aldoximes into chiral nitriles on analytical scale

The corresponding aldoxime was dissolved in DMSO or a DMSO/H<sub>2</sub>O mixture (50-200 mM). This stock solution was stored at -20 °C prior to usage. The reaction volume of 500 μL in a 1.5 mL micro reaction tube with shaking of 1400 rpm at 8 °C consisted of varying amounts of 50 mM KPB (pH = 7.0) and resting cell suspension (total volume 450-487.5 μL, typically 2.6 mg<sub>BWW</sub>). The assay was started by addition of the substrate DMSO stock solution (12.5 μL-50 μL, final concentration of 5 mM). 100 μL 0.1 M HCl and 400 μL acetonitrile were added after 15 minutes to quench the reaction. 800 μL of the supernatant after centrifugation (15000 g, 4 °C, 5 min) were transferred into a vial and measured on RP-HPLC for conversion. The activity was calculated in U/mg<sub>BWW</sub> (Units are defined as μmol/min). Afterwards, the 500 μL of the sample were extracted with MTBE (1:1, v/v) by vortexing for 60 seconds. The organic phase was washed once with brine (1:1, v/v) and subsequently analyzed by chiral HPLC to determine the ee-value of the obtained nitrile.

**Table 24:** Conversions and ee-values of the enantioselective nitrile synthesis with five different Oxds on analytical scale.

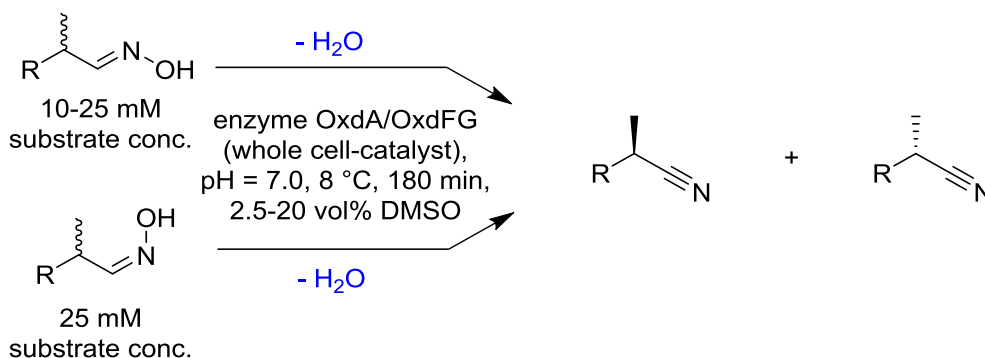
Entry	Substrate	Enzyme	Conv. [%] <sup>a</sup>	ee [%] <sup>b</sup>
1	 ( <i>E/Z</i> >99:1)	OxdA	17	56 ( <i>S</i> ) <sup>c</sup>
		OxdB	40	70 ( <i>R</i> )
		OxdFG	52	83 ( <i>S</i> )
		OxdRE	20	35 ( <i>R</i> )
		OxdRG	25	27 ( <i>R</i> )
2	 ( <i>E/Z</i> 6:94)	OxdA	46	15 ( <i>R</i> )
		OxdB	71	36 ( <i>S</i> )
		OxdFG	72	8 ( <i>R</i> )
		OxdRE	21	18 ( <i>R</i> )
		OxdRG	34	15 ( <i>R</i> )
3	 ( <i>E/Z</i> >99:1)	OxdA	54	4 (+)
		OxdB	29	71 (+)

Entry	Substrate	Enzyme	Conv. [%] <sup>a</sup>	ee [%] <sup>b</sup>
4	 <i>(E/Z 4:96)</i>	OxdFG	78	0
		OxdRE	52	13 (+)
		OxdRG	66	9 (+)
		OxdA	33	0
		OxdB	36	35 (+)
		OxdFG	30	0
5 <sup>d</sup>	 <i>(E/Z &gt; 99:1)</i>	OxdA	39	88 (S) <sup>c</sup>
		OxdB	7	9 (S)
		OxdFG	9	85 (S)
		OxdRE	21	91 (S)
		OxdRG	23	91 (S)
6 <sup>d</sup>	 <i>(E/Z 4:96)</i>	OxdA	-	-
		OxdB	-	-
		OxdFG	-	-
		OxdRE	-	-
		OxdRG	-	-
7	 <i>(E/Z 96:4)</i>	OxdA	-	-
		OxdB	-	-
		OxdFG	37	87 (S)
		OxdRE	-	-
		OxdRG	-	-
8	 <i>(E/Z 5:95)</i>	OxdA	38	94 (R) <sup>c</sup>
		OxdB	41	89 (R)
		OxdFG	51	88 (R)
		OxdRE	33	94 (R)
		OxdRG	46	90 (R)
9	 <i>(E/Z &gt; 99:1)</i>	OxdA	-	-
		OxdB	15	99 (+)
		OxdFG	33	96 (+)
		OxdRE	-	-
		OxdRG	-	-

Entry	Substrate	Enzyme	Conv. [%] <sup>a</sup>	ee [%] <sup>b</sup>
10	 ( <i>E/Z</i> 10:90)	OxdA	-	-
		OxdB	27	83 (-)
		OxdFG	46	84 (-)
		OxdRE	-	-
		OxdRG	-	-

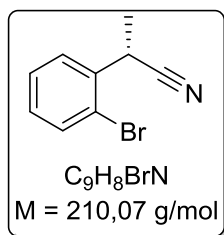
[a] Absolute conversion (confirmed *via* calibration curves on RP-HPLC), entry 1-4: 2.5 vol% DMSO, entry 5-10: 10 vol% DMSO, entries 5-8: 3 h reaction time, entries 9+10: 4 h reaction time. "-" means no product detection below the detection limit of <2%. [b] The symbols (+) and (-) refer to the first and second signals in chiral HPLC or GC chromatograms. [c] Absolute configuration was determined *via* comparison with literature data after a preparative scale experiment.<sup>[65,101]</sup>

### 9.3.2.4 General procedure 9 (GP9): Enantioselective biotransformations of (*E*)- and (*Z*)-enriched racemic aldoximes into chiral nitriles on preparative scale



Into a flask under argon atmosphere at 8 °C with stirring of 300 rpm were given 50 mM potassium phosphate buffer (KPB, pH = 7.0) and the resting cell suspension containing OxdA or OxdFG. The substrate stock solution in DMSO was added (final substrate concentration of 25 mM, 20 vol% DMSO) and the reaction mixture was stirred for three hours. A 500  $\mu$ L aliquot was taken out of the reaction mixture and treated with 100  $\mu$ L 0.1 M HCl and 400  $\mu$ L acetonitrile to quench the reaction. 800  $\mu$ L of the supernatant after centrifugation (15000 g, 4 °C, 5 min) were transferred into a vial and measured on RP-HPLC for conversion. The rest of the reaction mixture was extracted three times with MTBE (1:1, v/v), washed with brine (1:3, v/v) and the combined extracts were dried over MgSO<sub>4</sub>. Removal of the solvent under reduced pressure yielded the crude product as oil which was purified *via* column chromatography (cyclohexane/ethyl acetate). Enantiomeric excess was measured on chiral HPLC with the methods listed in chapter 4 and the absolute configuration was determined *via* the optical rotation of the compounds in reference to literature data.

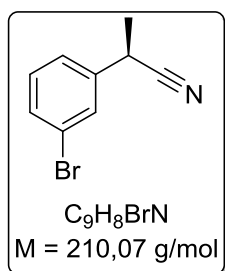
#### 9.3.2.4.1 Synthesis of (*S*)-2-(2-bromophenyl)propanenitrile



The synthesis was carried out according to GP9. KPB (4.00 mL) and resting cell suspension containing OxdA (12.0 mL, 72 mg cells, 2.8 U) were mixed with a DMSO substrate solution (125 mM, 4.00 mL, final concentration 25 mM). Conversion was 35% after three hours according to RP-HPLC. Work up (cyclohexane/ethyl acetate 7:1, v/v) yielded the product as pale yellow oil (98% ee according to chiral HPLC).

**Yield:** 22 mg, 21%.

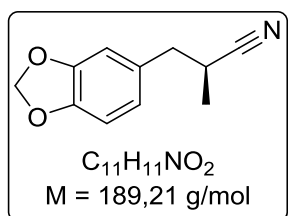
**[ $\alpha$ ]<sub>D</sub><sup>20</sup>:** -38 (c = 1.0, CH<sub>2</sub>Cl<sub>2</sub>).<sup>[65]</sup>

9.3.2.4.2 Synthesis of (*R*)-2-(3-bromophenyl)propanenitrile

The synthesis was carried out according to GP9. KPB (9.00 mL) and resting cell suspension containing OxdA (27.0 mL, 216 mg cells, 3.50 U) were mixed with a DMSO substrate solution (125 mM, 9.00 mL, final concentration 25 mM). Conversion was 49% after three hours according to RP-HPLC. Work up (cyclohexane/ethyl acetate 8:1, v/v) yielded the product as pale yellow oil (87% ee according to chiral HPLC).

**Yield:** 55 mg, 23%.

**[ $\alpha$ ]<sub>D</sub><sup>20</sup>:** +18 ( $c = 1.1$ ,  $CH_2Cl_2$ ).<sup>[65]</sup>

9.3.2.4.3 Synthesis of (*S*)-*a*-methyl-1,3-benzodioxole-5-propanenitrile

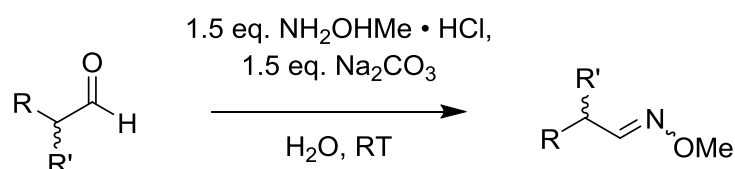
The synthesis was carried out in analogy to GP9. KPB (96.0 mL) and resting cell suspension containing OxdFG (1.50 mL, 928 mg cells, 17.0 U) were mixed with a DMSO substrate solution (400 mM, 2.50 mL, final concentration 10 mM). Conversion was 54% after three hours according to RP-HPLC. Work up (cyclohexane/ethyl acetate 6:1, v/v) yielded the product as pale yellow oil (46% ee according to chiral HPLC).

**Yield:** 53 mg, 28%.

**[ $\alpha$ ]<sub>D</sub><sup>20</sup>:** +18 ( $c = 1.3$ ,  $CHCl_3$ ).<sup>[100]</sup>

## 9.3.3 SYNTHESIS AND ATTEMPTED BIOTRANSFORMATIONS OF O-METHYLATED ALDOXIMES

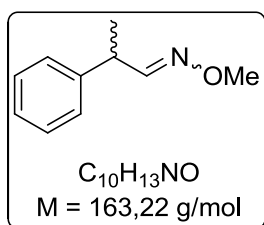
## 9.3.3.1 General procedure 10 (GP10): O-methylated aldoxime synthesis by condensation of aldehydes with hydroxylamine hydrochloride



O-methylhydroxylamine hydrochloride (1.5 eq.) and sodium carbonate (1.5 eq.) were dissolved in H<sub>2</sub>O at room temperature. Aldehyde (1.0 eq.) was added to this solution and stirred vigorously until complete conversion according to TLC analysis (cyclohexane/ethyl acetate in different volumetric percentages) was achieved. The solution was extracted three times with ethyl acetate (1:1 v/v) and the combined organic phases were washed

with H<sub>2</sub>O (1:3 v/v). Drying over MgSO<sub>4</sub> and evaporation of the solvent gave a crude product, which was purified by column chromatography if necessary. The (*E/Z*)-ratio of the product was determined by <sup>1</sup>H-NMR spectroscopy in CD<sub>2</sub>Cl<sub>2</sub>.

#### 9.3.3.1.1 *rac*-(*E/Z*)-2-phenylpropionaldehyde *O*-methyloxime



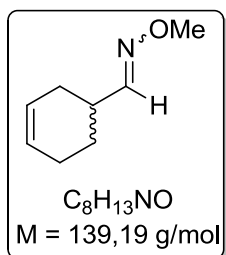
The synthesis was carried out according to GP10. *O*-methylhydroxylamine hydrochloride (933 mg, 11.2 mmol) and sodium carbonate (1.18 g, 11.2 mmol) were dissolved in 20 mL H<sub>2</sub>O at room temperature. After the addition of *RAC*-2-phenylpropionaldehyde (1.00 g, 7.45 mmol) stirring of the solution was conducted for 24 hours. The work up yielded the product as colorless oil. The (*E/Z*)-ratio was 1:1 according to <sup>1</sup>H-NMR analysis.

**Yield:** 1.09 g, 97%.

**<sup>1</sup>H-NMR** (500 MHz, CD<sub>2</sub>Cl<sub>2</sub>): δ [ppm] = 7.45 (d, 1H, <sup>3</sup>J = 6.5 Hz, CHNOCH<sub>3</sub>), 7.42-7.22 (m, 5H, Ar-H), 6.73 (d, 1H, <sup>3</sup>J = 7.4 Hz, CHNOCH<sub>3</sub>), 4.33 (quint, 1H, <sup>3</sup>J = 7.4 Hz, PhCHCH<sub>3</sub>), 3.86 (s, 3H, CHNOCH<sub>3</sub>), 3.82 (s, 3H, CHNOCH<sub>3</sub>), 3.65 (quint, 1H, <sup>3</sup>J = 6.8 Hz, PhCHCH<sub>3</sub>), 1.43 (d, 3H, <sup>3</sup>J = 7.0 Hz, CHCH<sub>3</sub>) 1.38 (d, 3H, <sup>3</sup>J = 7.2 Hz, CHCH<sub>3</sub>).

**RP-HPLC:** *Macherey-Nagel* Nucleodur C<sub>18</sub> HTec, water/acetonitrile 50:50, 1.0 mL/min, 40 °C, 210 nm, R<sub>t</sub> = 10.5 min.

#### 9.3.3.1.2 *rac*-(*E/Z*)-cyclohex-3-enecarbaldehyde *O*-methyl oxime



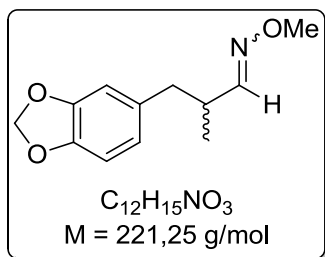
The synthesis was carried out according to GP10. *O*-methylhydroxylamine hydrochloride (1.14 g, 13.6 mmol) and sodium carbonate (1.44 g, 13.6 mmol) were dissolved in 15 mL H<sub>2</sub>O at room temperature. The addition of *rac*-3-cyclohexene carboxaldehyde (1.03 mL, 9.08 mmol) led to formation of a colorless suspension. Complete conversion was achieved after 22 hours according to TLC analysis (cyclohexane:ethyl acetate 30:1, v/v). Work up and column chromatography (pure cyclohexane) yielded the product as colorless oil.

The (*E/Z*)-ratio was 3:1 according to <sup>1</sup>H-NMR analysis.

**Yield:** 305 mg, 24%.

**<sup>1</sup>H-NMR** (500 MHz, CD<sub>2</sub>Cl<sub>2</sub>): δ [ppm] = 7.31 (d, 1H, <sup>3</sup>J = 6.3 Hz, CHNOCH<sub>3</sub>), 6.51 (d, 1H, <sup>3</sup>J = 7.2 Hz, CHNOCH<sub>3</sub>), 5.69 (m, 2H, CH=CH), 3.81 (s, 3H, OCH<sub>3</sub>), 3.77 (s, 3H, OCH<sub>3</sub>), 3.10 (m, 1H, CHCHNOCH<sub>3</sub>), 2.46 (m, 1H, CHCHNOCH<sub>3</sub>), 2.22-1.73 (m, 6H), 1.53-1.48 (m, 1H).

**RP-HPLC:** *Macherey-Nagel* Nucleodur C<sub>18</sub> HTec, water/acetonitrile 50:50, 1.0 mL/min, 40 °C, 210 nm, R<sub>t</sub> = 9.3 min.

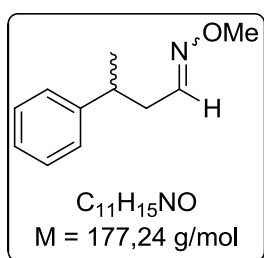
9.3.3.1.3 *rac*-(*E/Z*)-2-methyl-3-(3,4-methylenedioxyphenyl)propanal *O*-methyloxime

The synthesis was carried out according to GP10. *O*-methylhydroxylamine hydrochloride (651 mg, 7.80 mmol) and sodium carbonate (827 mg, 7.80 mmol) were dissolved in 15 mL H<sub>2</sub>O at room temperature. *rac*-2-methyl-3-(3,4-methylenedioxyphenyl)propanal (1.00 mL, 5.20 mmol) was added to the solution, upon which an orange solution was obtained. After 20 hours complete conversion was achieved according to TLC analysis (cyclohexane:ethyl acetate 30:1, v/v). The work up yielded the product as orange liquid. The (*E/Z*)-ratio was 2:1 according to <sup>1</sup>H-NMR analysis.

**Yield:** 710 mg, 62%.

**<sup>1</sup>H-NMR** (500 MHz, CD<sub>2</sub>Cl<sub>2</sub>): δ [ppm] = 7.25 (d, 1H, <sup>3</sup>J = 6.4 Hz, CHNOCH<sub>3</sub>), 6.74-6.59 (m, 3H, Ar-*H*), 6.45 (d, 1H, <sup>3</sup>J = 7.4 Hz, CHNOCH<sub>3</sub>), 5.92 (s, 2H, OCH<sub>2</sub>O), 5.91 (s, 2H, OCH<sub>2</sub>O), 3.78 (s, 3H, CHNOCH<sub>3</sub>), 3.74 (s, 3H, CHNOCH<sub>3</sub>), 3.23 (sept, 1H, <sup>3</sup>J = 7.1 Hz, CHCH<sub>3</sub>), 2.75-2.49 (m, 2H, Ar-CH<sub>2</sub>CH), 2.57 (m, 1H, CHCH<sub>3</sub>), 1.04 (d, 3H, <sup>3</sup>J = 6.6 Hz, CHCH<sub>3</sub>), 0.98 (d, 3H, <sup>3</sup>J = 7.0 Hz, CHCH<sub>3</sub>).

**RP-HPLC:** *Macherey-Nagel* Nucleodur C<sub>18</sub> HTec, water/acetonitrile 50:50, 1.0 mL/min, 40 °C, 210 nm, R<sub>t</sub> = 10.7 min.

9.3.3.1.4 *rac*-(*E/Z*)-3-phenylbutyraldehyde *O*-methyloxime

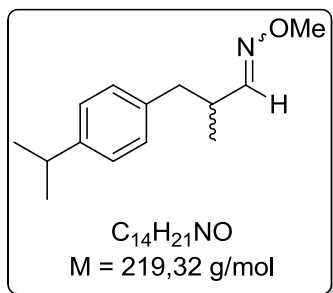
The synthesis was carried out according to GP10. *O*-methylhydroxylamine hydrochloride (845 mg, 10.1 mmol) and sodium carbonate (1.07 g, 10.1 mmol) were dissolved in 15 mL H<sub>2</sub>O at room temperature. The addition of *rac*-3-phenylbutyraldehyde (1.00 g, 6.75 mmol) led to formation of a colorless suspension. Complete conversion was achieved after 20 hours according to TLC analysis (cyclohexane:ethyl acetate 3:1, v/v). Work up yielded the product as colorless oil. The (*E/Z*)-ratio was 1:1 according to <sup>1</sup>H-NMR analysis.

**Yield:** 795 mg, 66%.

**<sup>1</sup>H-NMR** (500 MHz, CD<sub>2</sub>Cl<sub>2</sub>): δ [ppm] = 7.32-7.18 (m, 5H, Ar-*H*), 7.24 (m, 1H, CHNOCH<sub>3</sub>), 6.52 (t, 1H, <sup>3</sup>J = 5.4 Hz, CHNOCH<sub>3</sub>), 3.80 (s, 3H, CHNOCH<sub>3</sub>), 3.74 (s, 3H, CHNOCH<sub>3</sub>), 2.94 (m, 1H, PhCHCH<sub>3</sub>), 2.66-2.53 (m, 2H, PhCHCH<sub>2</sub>), 2.49-2.39 (m, 2H, PhCHCH<sub>2</sub>), 1.29 (d, 3H, <sup>3</sup>J = 6.9 Hz, PhCHCH<sub>3</sub>), 1.28 (d, 3H, <sup>3</sup>J = 6.9 Hz, PhCHCH<sub>3</sub>).

**RP-HPLC:** *Macherey-Nagel* Nucleodur C<sub>18</sub> HTec, water/acetonitrile 50:50, 1.0 mL/min, 40 °C, 210 nm, R<sub>t1</sub> = 12.1 min, R<sub>t2</sub> = 13.0 min.



9.3.3.1.5 *rac*-(*E/Z*)-2-methyl-3-(4-isopropylphenyl)propionaldehyde *O*-methyloxime

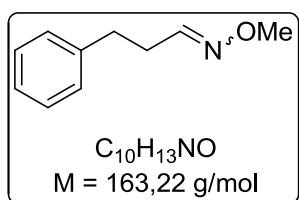
The synthesis was carried out according to GP10. *O*-methylhydroxylamine hydrochloride (659 mg, 7.89 mmol) and sodium carbonate (836 mg, 7.89 mmol) were dissolved in 15 mL H<sub>2</sub>O at room temperature. The addition of *rac*-2-methyl-3-(4-isopropylphenyl)propionaldehyde (1.00 g, 5.26 mmol) led to formation of a colorless suspension. Complete conversion was achieved after 22 hours according to TLC analysis (cyclohexane:ethyl acetate 3:1, v/v). Work up yielded the product as colorless liquid. The (*E/Z*)-ratio was 1:2 according

to <sup>1</sup>H-NMR analysis.

**Yield:** 890 mg, 77%.

**<sup>1</sup>H-NMR** (500 MHz, CD<sub>2</sub>Cl<sub>2</sub>): δ [ppm] = 7.28 (d, 1H, <sup>3</sup>J = 6.4 Hz, CHNOCH<sub>3</sub>), 7.17-7.06 (m, 4H, Ar-*H*), 6.47 (d, 1H, <sup>3</sup>J = 7.4 Hz, CHNOCH<sub>3</sub>), 3.76 (s, 3H, CHNOCH<sub>3</sub>), 3.74 (s, 3H, CHNOCH<sub>3</sub>), 3.27 (sept, 1H, <sup>3</sup>J = 7.1 Hz CH<sub>2</sub>CHCH<sub>3</sub>), 2.88 (sept, 1H, <sup>3</sup>J = 7.0 Hz, (CH<sub>3</sub>)<sub>2</sub>CH), 2.87 (sept, 1H, <sup>3</sup>J = 7.0 Hz, (CH<sub>3</sub>)<sub>2</sub>CH), 2.79-2.53 (m, 2H, PhCH<sub>2</sub>), 2.61 (sept, 1H, <sup>3</sup>J = 7.1 Hz CH<sub>2</sub>CHCH<sub>3</sub>), 1.23 (d, 6H, <sup>3</sup>J = 6.9 Hz, (CH<sub>3</sub>)<sub>2</sub>CH), 1.22 (d, 6H, <sup>3</sup>J = 7.0 Hz, (CH<sub>3</sub>)<sub>2</sub>CH), 1.05 (d, 3H, <sup>3</sup>J = 6.6 Hz, CH<sub>2</sub>CHCH<sub>3</sub>), 1.00 (d, 3H, <sup>3</sup>J = 6.8 Hz, CH<sub>2</sub>CHCH<sub>3</sub>).

**RP-HPLC:** *Macherey-Nagel* Nucleodur C<sub>18</sub> HTec, water/acetonitrile 50:50, 1.0 mL/min, 40 °C, 210 nm, R<sub>t</sub> = 49.0 min.

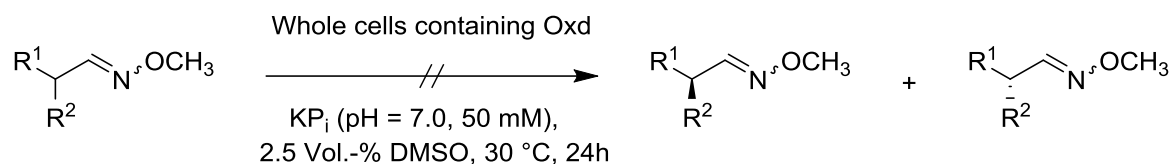
9.3.3.1.6 (*E/Z*)-3-phenylpropionaldehyde *O*-methyloxime

The synthesis was carried out according to GP10. *O*-methylhydroxylamine hydrochloride (1.01 g, 11.3 mmol) and sodium carbonate (1.20 g, 11.3 mmol) were dissolved in 15 mL H<sub>2</sub>O at room temperature. The addition of freshly distilled 3-phenylpropionaldehyde (1.00 mL, 7.53 mmol) led to formation of a colorless suspension. Complete conversion was achieved after 19 hours according to TLC analysis (cyclohexane:ethyl acetate 3:1, v/v). Work up yielded the product as colorless liquid. The (*E/Z*)-ratio was 7:3 according to <sup>1</sup>H-NMR analysis.

**Yield:** 990 mg, 81%.

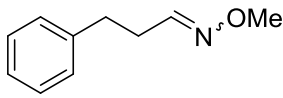
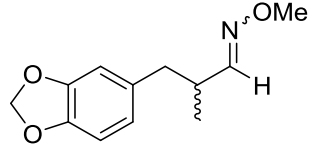
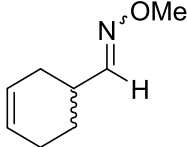
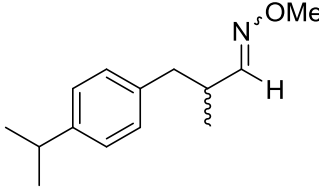
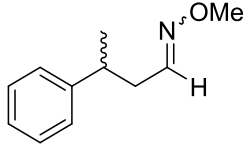
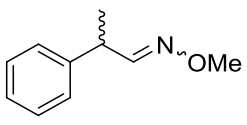
**<sup>1</sup>H-NMR** (500 MHz, CD<sub>2</sub>Cl<sub>2</sub>): δ [ppm] = 7.38 (t, 1H, <sup>3</sup>J = 5.9 Hz, CHNOCH<sub>3</sub>), 7.32-7.18 (m, 5H, Ar-*H*), 6.64 (t, 1H, <sup>3</sup>J = 5.3 Hz, CHNOCH<sub>3</sub>), 3.83 (s, 3H, CHNOCH<sub>3</sub>), 3.77 (s, 3H, CHNOCH<sub>3</sub>), 2.81 (t, 2H, <sup>3</sup>J = 7.7 Hz PhCH<sub>2</sub>CH<sub>2</sub>), 2.79 (t, 2H, <sup>3</sup>J = 8.0 Hz PhCH<sub>2</sub>CH<sub>2</sub>), 2.62 (dt, 2H, <sup>3</sup>J = 7.9 Hz, 5.3 Hz, PhCH<sub>2</sub>CH<sub>2</sub>), 2.49 (dt, 2H, <sup>3</sup>J = 8.1 Hz, 6.1 Hz, PhCH<sub>2</sub>CH<sub>2</sub>).

## 9.3.3.2 Attempted biotransformations of O-methylated aldoximes



The corresponding aldoxime was dissolved in DMSO (200 mM). The reaction volume of 500  $\mu\text{L}$  in a 1.5 mL micro reaction tube with shaking of 1400 rpm at 30  $^\circ\text{C}$  consisted of varying amounts of 50 mM KPB (pH = 7.0) and resting cell suspension (total volume 487.5  $\mu\text{L}$ , typically 2-6  $\text{mg}_{\text{BWW}}$ ). The assay was started by addition of 12.5  $\mu\text{L}$  substrate (final concentration of 5 mM). 500  $\mu\text{L}$  acetonitrile were added after 24 hours to quench the reaction. 800  $\mu\text{L}$  of the supernatant after centrifugation (15000 g, 4  $^\circ\text{C}$ , 5 min) were transferred into a vial and measured on RP-HPLC for conversion. However, none of the investigated substrates was transformed by any of the five Oxds.

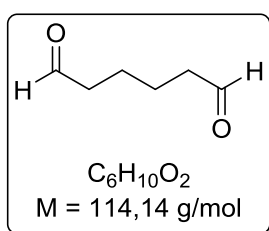
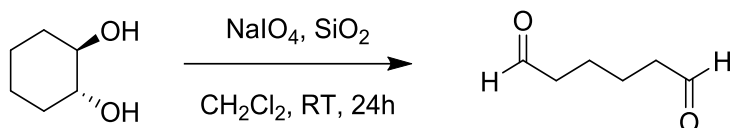
**Table 25:** Investigated O-methylated aldoximes for the biocatalytic nitrile synthesis.

Entry	Substrate	Entry	Substrate
1	 (E/Z 70:30)	4	 (E/Z 67:33)
2	 (E/Z 75:25)	5	 (E/Z 33:67)
3	 (E/Z 50:50)	6	 (E/Z 50:50)

## 9.4 BIOCATALYTIC PRODUCTION OF ADIPONITRILE AND RELATED ALIPHATIC LINEAR $\alpha,\omega$ -DINITRILES

### 9.4.1 SYNTHESIS OF REFERENCE COMPOUNDS

#### 9.4.1.1 General procedure 11 (GP11): Adipaldehyde synthesis by oxidation of *trans*-1,2-Cyclohexanediol



Silica (275 g) was suspended in 900 mL  $CH_2Cl_2$  in a 2 L three-necked flask equipped with two 500 mL dropping funnels. Afterwards, the apparatus was flushed with argon and a solution of  $NaIO_4$  (38.0 g, 178 mmol) in 250 mL  $H_2O$  was added dropwise. *trans*-1,2-cyclohexanediol (15.8 g, 136 mmol) was dissolved in 500 mL  $CH_2Cl_2$  and also added dropwise to the suspension. After stirring for 24 hours at room temperature, the solid was filtered off and washed with  $CH_2Cl_2$ . The solvent of the filtrate was evaporated *in vacuo* to yield Adipaldehyde as pale yellow liquid.

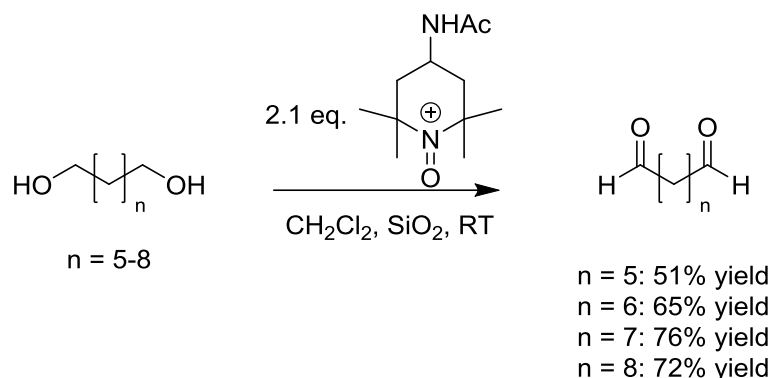
**Yield:** 14.4 g, 93%.

**$^1H$ -NMR** (500 MHz,  $CDCl_3$ ):  $\delta$  [ppm] = 9.75 (m, 2H,  $CH_2CH_2CHO$ ), 2.46 (m, 4H,  $CH_2CH_2CHO$ ), 1.65 (m, 4H,  $CH_2CH_2CHO$ ).

**$^{13}C$ -NMR** (125 MHz,  $CDCl_3$ ):  $\delta$  [ppm] = 202.03, 43.66, 21.57.

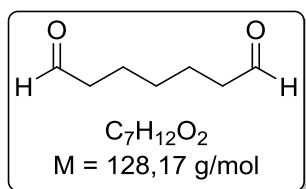
The analytical data corresponds with the literature.<sup>[211,212]</sup>

9.4.1.2 General procedure 12 (GP12): Synthesis of linear, aliphatic  $\alpha,\omega$ -dialdehydes by oxidation of linear, aliphatic  $\alpha,\omega$ -dialcohols with Bobbitt's salt (4-(Acetylamino)-2,2,6,6-tetramethyl-1-oxo-piperidinium tetrafluoroborate)



The syntheses were carried out according to *Miller et al.*<sup>[118]</sup> To a heat dried round bottom flask was added dialcohol (1.0 eq.) and 100 mL dichloromethane under an inert gas atmosphere. After stirring for five minutes at room temperature, silica (2 mass eq. to substrate) and Bobbitt's salt (2.1 eq.) were added, resulting in a yellow suspension. After stirring for 120 hours, filtration of the slurry through a 3 cm thick pad of silica was conducted. The residue was washed with dichloromethane and the filtrate was freed from the solvent *in vacuo* to yield the  $\alpha,\omega$ -dialdehydes as pale yellow liquids.

9.4.1.2.1 Heptanedial



The synthesis was carried out according to GP12. 1,7-Heptanediol (1.32 g, 10.0 mmol) was dissolved in 100 mL dichloromethane. Bobbitt's salt (6.30 g, 21.0 mmol) and silica (2.64 g) were added. Work-up yielded heptanedial as pale yellow liquid.

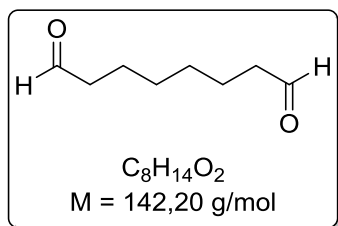
**Yield:** 650 mg, 51%.

**$^1\text{H-NMR}$**  (500 MHz,  $\text{CDCl}_3$ ):  $\delta$  [ppm] = 9.75 (m, 2H,  $\text{CH}_2\text{COH}$ ), 2.44 (t, 4H,  $^3J = 7.3 \text{ Hz}$ ,  $\text{CH}_2\text{COH}$ ), 1.64 (qi, 4H,  $^3J = 7.4 \text{ Hz}$ ,  $\text{CH}_2\text{CH}_2\text{COH}$ ), 1.35 (m, 2H,  $\text{CH}_2\text{CH}_2\text{CH}_2\text{COH}$ ).

**$^{13}\text{C-NMR}$**  (125 MHz,  $\text{CDCl}_3$ ):  $\delta$  [ppm] = 202.41, 43.72, 28.70, 21.86.

The analytical data corresponds with the literature.<sup>[118]</sup>

## 9.4.1.2.2 Octanedial



The synthesis was carried out according to GP12. 1,8-Octanediol (1.46 g, 10.0 mmol) was dissolved in 100 mL dichloromethane. Bobbit's salt (6.30 g, 21.0 mmol) and silica (2.64 g) were added. Work-up yielded octanedial as pale yellow liquid.

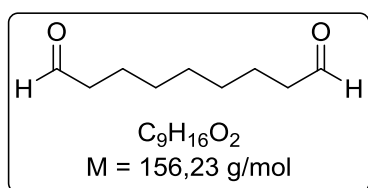
**Yield:** 925 mg, 65%.

**$^1\text{H-NMR}$**  (500 MHz,  $\text{CDCl}_3$ ):  $\delta$  [ppm] = 9.75 (m, 2H,  $\text{CH}_2\text{COH}$ ), 2.42 (t, 4H,  $^3J = 7.3 \text{ Hz}$ ,  $\text{CH}_2\text{COH}$ ), 1.62 (qi, 4H,  $^3J = 7.0 \text{ Hz}$ ,  $\text{CH}_2\text{CH}_2\text{COH}$ ), 1.34 (m, 4H,  $\text{CH}_2\text{CH}_2\text{CH}_2\text{COH}$ ).

**$^{13}\text{C-NMR}$**  (125 MHz,  $\text{CDCl}_3$ ):  $\delta$  [ppm] = 202.68, 43.87, 28.97, 21.91.

The analytical data corresponds with the literature.<sup>[118,211]</sup>

## 9.4.1.2.3 Nonanedial



The synthesis was carried out according to GP12. 1,9-Nonanediol (1.60 g, 10.0 mmol) was dissolved in 100 mL dichloromethane. Bobbit's salt (6.30 g, 21.0 mmol) and silica (2.64 g) were added. Work-up yielded nonanedial as pale yellow liquid.

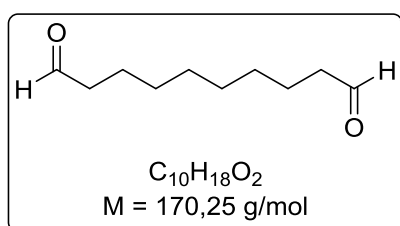
**Yield:** 1.18 g, 76%.

**$^1\text{H-NMR}$**  (500 MHz,  $\text{CDCl}_3$ ):  $\delta$  [ppm] = 9.75 (m, 2H,  $\text{CH}_2\text{COH}$ ), 2.41 (t, 4H,  $^3J = 7.3 \text{ Hz}$ ,  $\text{CH}_2\text{COH}$ ), 1.61 (qi, 4H,  $^3J = 7.1 \text{ Hz}$ ,  $\text{CH}_2\text{CH}_2\text{COH}$ ), 1.32 (m, 6H,  $\text{CH}_2\text{CH}_2\text{CH}_2\text{CH}_2\text{COH}$ ).

**$^{13}\text{C-NMR}$**  (125 MHz,  $\text{CDCl}_3$ ):  $\delta$  [ppm] = 202.83, 43.95, 29.20, 29.03, 22.06.

The analytical data corresponds with the literature.<sup>[118]</sup>

## 9.4.1.2.4 Decanedial



The synthesis was carried out according to GP12. 1,10-Decanediol (1.74 g, 10.0 mmol) was dissolved in 100 mL dichloromethane. Bobbit's salt (6.30 g, 21.0 mmol) and silica (2.64 g) were added. Work-up yielded decanedial as pale yellow liquid.

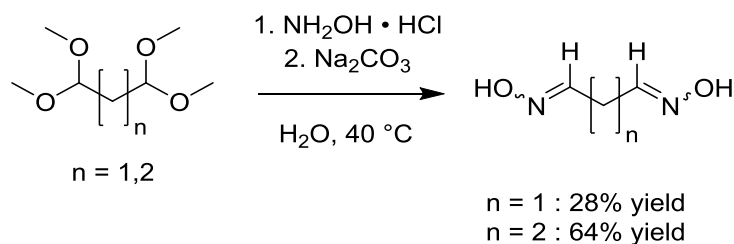
**Yield:** 1.22 g, 72%.

**<sup>1</sup>H-NMR** (500 MHz, CDCl<sub>3</sub>): δ [ppm] = 9.73 (m, 2H, CH<sub>2</sub>COH), 2.39 (t, 4H, <sup>3</sup>J = 7.1 Hz, CH<sub>2</sub>COH), 1.59 (qi, 4H, <sup>3</sup>J = 6.9 Hz, CH<sub>2</sub>CH<sub>2</sub>COH), 1.28 (m, 8H, CH<sub>2</sub>CH<sub>2</sub>CH<sub>2</sub>CH<sub>2</sub>COH).

**<sup>13</sup>C-NMR** (125 MHz, CDCl<sub>3</sub>): δ [ppm] = 202.88, 43.93, 29.19, 29.11, 22.07.

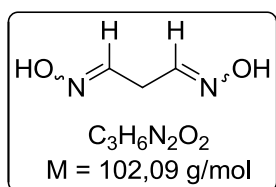
The analytical data corresponds with the literature.<sup>[118]</sup>

### 9.4.1.3 General procedure 13 (GP13): Synthesis of linear, aliphatic $\alpha,\omega$ -dioximes *via* condensation of Bis(dimethyl)acetals with hydroxylamine hydrochloride



Hydroxylamine hydrochloride (3.0 eq.) was dissolved in H<sub>2</sub>O at room temperature. The solution was degassed under vacuum, followed by flushing with argon to establish an inert atmosphere. The corresponding bis(dimethylacetal) was added to the solution and the suspension was heated to 40 °C, at which the reaction mixture became a clear solution. After 5 minutes sodium carbonate (1.5 eq.) was added, upon which a colorless solid precipitated. The suspension was cooled to 0 °C for 24 hours, upon which more solid precipitated. The solid was filtered off, washed with water and dried *in vacuo*. The dioximes had predominately *Z,Z*-configuration.

#### 9.4.1.3.1 Malonoaldehyde dioxime



The synthesis was carried out according to GP13. 1,1,3,3-Tetramethoxypropane (5.00 mL, 30.4 mmol) was given to a solution of hydroxylamine hydrochloride (6.34 g, 91.2 mmol) in 20 mL H<sub>2</sub>O. Heating to 40 °C resulted in a yellow solution, into which sodium carbonate (4.83 g, 45.6 mmol) was added. Work up yielded the product as colorless solid. (*E/Z*)-ratio (including both oxime groups) was 1:99 according to <sup>1</sup>H-NMR.

**Yield:** 744 mg, 28%.

**<sup>1</sup>H-NMR** (500 MHz, DMSO):  $\delta$  [ppm] = 11.03 (s, 2H, CH<sub>2</sub>(CHNOH)<sub>2</sub>), 6.78 (t, 2H, <sup>3</sup>J = 5.3 Hz, CH<sub>2</sub>(CHNOH)<sub>2</sub>), 3.19 (t, 2H, <sup>3</sup>J = 5.3 Hz, CH<sub>2</sub>(CHNOH)<sub>2</sub>).

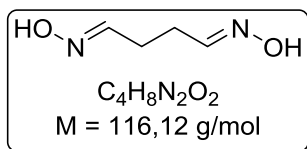
**<sup>13</sup>C-NMR** (125 MHz, DMSO):  $\delta$  [ppm] = 144.94, 22.63.

**GC (FID):** Phenomenex ZB-5MSi, 1.03 ml/min (H<sub>2</sub>), Inj. Temp.: 300 °C, Det. Temp.: 350 °C; 100 °C -> 125 °C (5 °C/min), 125 °C -> 205 °C (40 °C/min); R<sub>t</sub> dinitrile = 2.36 min, R<sub>t</sub> dioxime = 4.04 min.

**HRMS** (ESI): calcd for C<sub>3</sub>H<sub>7</sub>N<sub>2</sub>O<sub>2</sub> [M+H]<sup>+</sup> : 103.0502, found: 103.0508.

**IR** (neat) [cm<sup>-1</sup>]: 3081, 3041, 2809, 1660, 1434, 1399, 1320, 1252, 946, 927, 860, 782, 746, 676.

## 9.4.1.3.2 Succinaldehyde dioxime



The synthesis was carried out according to GP13. Succinaldehyde bis(dimethylacetal) (2.65 mL, 15.0 mmol) was given to a solution of hydroxylamine hydrochloride (3.13 g, 45.0 mmol) in 10 mL H<sub>2</sub>O. The phase separation disappeared at room temperature, upon which sodium carbonate (2.38 g, 22.5 mmol) was added. Work up yielded the product as colorless solid. (*E/Z*)-ratio (including both oxime groups) was 8:92 according to <sup>1</sup>H-NMR.

**Yield:** 1.12 g, 64%.

**<sup>1</sup>H-NMR** (500 MHz, DMSO): δ [ppm] = 10.86 (s, 2H, CH<sub>2</sub>(CHNOH)<sub>2</sub>), 6.66 (m, 2H, CH<sub>2</sub>(CHNOH)<sub>2</sub>), 2.38 (m, 2H, CH<sub>2</sub>(CHNOH)<sub>2</sub>).

**<sup>13</sup>C-NMR** (125 MHz, DMSO): δ [ppm] = 149.37, 21.55.

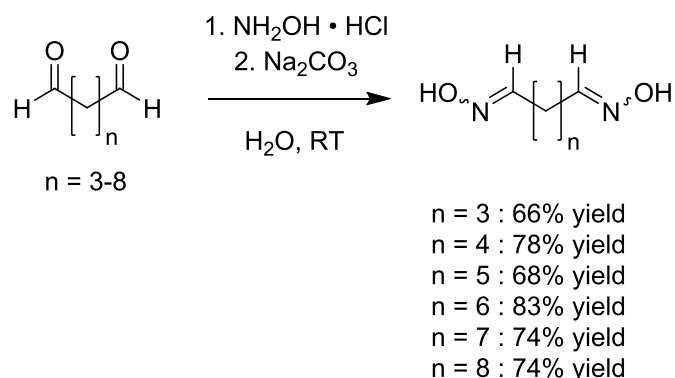
**GC (FID):** Phenomenex ZB-5MSi, 1.03 ml/min (H<sub>2</sub>), Inj. Temp.: 300 °C, Det. Temp.: 350 °C; 100 °C -> 135 °C (5 °C/min), 135 °C -> 215 °C (40 °C/min); R<sub>t</sub> dinitrile = 3.04 min, R<sub>t</sub> dioxime = 5.30 min.

**HRMS** (ESI): calcd for C<sub>4</sub>H<sub>9</sub>N<sub>2</sub>O<sub>2</sub> [M+H]<sup>+</sup> : 117.0659, found: 145.0669.

**IR** (neat) [cm<sup>-1</sup>]: 3085, 3043, 2868, 2810, 1671, 1448, 1420, 1328, 1234, 1037, 935, 918, 879, 807, 774, 753, 717.

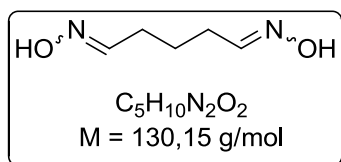


#### 9.4.1.4 General procedure 14 (GP14): Synthesis of linear, aliphatic $\alpha,\omega$ -dioximes *via* condensation of linear, aliphatic $\alpha,\omega$ -dialdehydes with hydroxylamine hydrochloride



Hydroxylamine hydrochloride (3.0 eq.) was diluted in H<sub>2</sub>O (optionally 20 vol% methanol were added) at room temperature. The corresponding dialdehyde was added to the solution and the suspension was stirred at room temperature. After 5 minutes sodium carbonate (1.5-3.0 eq.) was added, upon which a colorless solid precipitated. The suspension was further stirred at room temperature for 4-24 hours. The solid was filtered off, washed with water and dried *in vacuo*. The product was obtained as colorless solid. The dioximes had predominately *Z,Z*-configuration.

##### 9.4.1.4.1 Glutaraldehyde dioxime



The synthesis was conducted in analogy to GP14. A 50wt% solution of glutaraldehyde (2.00 mL, 11.2 mmol) was given to a solution of hydroxylamine hydrochloride (2.34 g, 33.6 mmol) and sodium carbonate (3.56 g, 33.6 mmol) in 50 mL H<sub>2</sub>O. After 30 min the solution turned into a colorless suspension.

After two hours complete conversion was achieved according to TLC. The purity of the crude product after extraction with ethyl acetate was satisfactory for further syntheses. The (*E/Z*)-ratio (including both oxime groups) was 8:92 according to <sup>1</sup>H-NMR.

**Yield:** 960 mg, 66%.

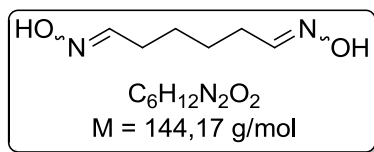
**<sup>1</sup>H-NMR** (500 MHz, DMSO):  $\delta$  [ppm] = 10.77 (s, 2H, *Z*, CHNOH), 10.41 (s, 2H, *E*, CHNOH), 7.30 (t, 2H, *E*, <sup>3</sup>*J* = 5.8 Hz, CHNOH), 6.65 (t, 2H, *Z*, <sup>3</sup>*J* = 5.4 Hz, CHNOH), 2.23 (m, 4H, *Z*, CH<sub>2</sub>CHNOH), 2.11 (m, 4H, *E*, CH<sub>2</sub>CHNOH), 1.55 (m, 2H, *E/Z*, CH<sub>2</sub>).

**<sup>13</sup>C-NMR** (125 MHz, DMSO):  $\delta$  [ppm] = 149.81 (*Z*), 149.11 (*E*), 24.43 (*Z*), 24.16 (*E*), 22.94 (*E*), 22.38 (*Z*).

**GC (FID):** Phenomenex ZB-5MSi, 0.87 ml/min (H<sub>2</sub>), Inj. Temp.: 300 °C, Det. Temp.: 350 °C; 140 °C → 190 °C (5 °C/min); *R*<sub>t</sub> dinitrile = 2.61 min, *R*<sub>t</sub> dioxime = 3.63 min.

The analytical data corresponds with the literature.<sup>[121]</sup>

## 9.4.1.4.2 Adipaldehyde dioxime



The synthesis was carried out according to GP14. Adipaldehyde (14.1 g, 124 mmol) was dissolved in 100 mL H<sub>2</sub>O and 25 mL methanol. Hydroxylamine hydrochloride (25.9 g, 372 mmol) was added and afterwards sodium carbonate (19.7 g, 186 mmol). Work up yielded the product as colorless solid. (*E/Z*)-ratio (including both oxime groups) was 7:93 according to <sup>1</sup>H-NMR.

**Yield:** 12.6 g, 70%.

**<sup>1</sup>H-NMR** (500 MHz, DMSO):  $\delta$  [ppm] = 10.73 (s, 2H, *Z*, CHNOH), 10.36 (s, 2H, *E*, CHNOH), 7.29 (t, 2H, *E*, <sup>3</sup>*J* = 5.9 Hz, CHNOH), 6.63 (t, 2H, *Z*, <sup>3</sup>*J* = 5.3 Hz, CHNOH), 2.24 (m, 4H, *Z*, CH<sub>2</sub>CHNOH), 2.10 (m, 4H, *E*, CH<sub>2</sub>CHNOH), 1.42 (m, 4H, *E/Z*, CH<sub>2</sub>).

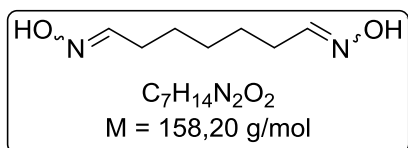
**<sup>13</sup>C-NMR** (125 MHz, DMSO):  $\delta$  [ppm] = 150.16, 150.14, 149.39, 149.37, 28.72, 28.71, 26.03, 25.71, 25.47, 25.16, 24.33.

**GC (FID):** Phenomenex ZB-5MSi, 0.87 ml/min (H<sub>2</sub>), Inj. Temp.: 300 °C, Det. Temp.: 350 °C; 140 °C -> 190 °C (5 °C/min);  $R_{t \text{ dinitrile}} = 3.08 \text{ min}$ ,  $R_{t \text{ dioxime}} = 4.52 \text{ min}$ .

**HRMS** (ESI): calcd for C<sub>6</sub>H<sub>13</sub>N<sub>2</sub>O<sub>2</sub> [M+H]<sup>+</sup> : 145.0972, found: 145.0972.

**IR** (neat) [cm<sup>-1</sup>]: 3182, 3084, 3039, 2934, 2865, 2810, 1664, 1451, 1415, 1345, 1322, 1058, 924, 826, 803, 733, 721, 705.

## 9.4.1.4.2 Heptanedial dioxime



The synthesis was conducted in analogy to GP14. Hydroxylamine hydrochloride (1.02 g, 14.7 mmol) was dissolved in 10 mL H<sub>2</sub>O and 2.5 mL methanol. Heptanedial (630 mg, 4.92 mmol) was added, followed by sodium carbonate (782 mg, 7.38 mmol). Work up yielded the product as colorless solid. (*E/Z*)-ratio (including both oxime groups) was 14:86 according to <sup>1</sup>H-NMR.

**Yield:** 532 mg, 68% yield.

**<sup>1</sup>H-NMR** (500 MHz, DMSO):  $\delta$  [ppm] = 10.71 (s, 2H, *Z*, CHNOH), 10.36 (s, 2H, *E*, CHNOH), 7.28 (t, 2H, *E*, <sup>3</sup>*J* = 5.9 Hz, CHNOH), 6.63 (t, 2H, *Z*, <sup>3</sup>*J* = 5.3 Hz, CHNOH), 2.21 (m, 4H, *Z*, CH<sub>2</sub>CHNOH), 2.08 (m, 4H, *E*, CH<sub>2</sub>CHNOH), 1.41 (m, 4H, *E/Z*, CH<sub>2</sub>CH<sub>2</sub>CHNOH), 1.29 (m, 2H, *E/Z*, CH<sub>2</sub>CH<sub>2</sub>CH<sub>2</sub>CHNOH).

**<sup>13</sup>C-NMR** (125 MHz, DMSO):  $\delta$  [ppm] = 150.29, 149.49, 28.86, 28.66, 28.37, 25.97, 25.35, 24.45.

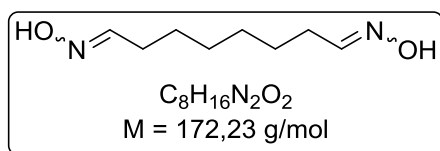
**GC (FID):** Phenomenex ZB-5MSi, 0.87 ml/min (H<sub>2</sub>), Inj. Temp.: 300 °C, Det. Temp.: 350 °C; 140 °C -> 190 °C (5 °C/min);  $R_{t \text{ dinitrile}} = 4.02 \text{ min}$ ,  $R_{t \text{ dioxime}} = 4.78+5.95 \text{ min}$ .

**MS** (ESI):  $m/z = 159.0$  [M+H]<sup>+</sup>.

**HRMS** (ESI): calcd for  $C_7H_{15}N_2O_2$   $[M+H]^+$  : 159.1128, found: 159.1131.

**IR** (neat)  $[cm^{-1}]$ : 3180, 3078, 3033, 2928, 2859, 1456, 1438, 1417, 1313, 1059, 920, 886, 814, 769, 722.

#### 9.4.1.4.3 Octanedial dioxime



The synthesis was conducted in analogy to GP14. Hydroxylamine hydrochloride (1.32 g, 19.0 mmol) was dissolved in 16 mL  $H_2O$  and 4 mL methanol. Octanedial (900 mg, 6.33 mmol) was added, followed by sodium carbonate (1.01 g, 9.49 mmol). Work up yielded the product as colorless solid. (*E/Z*)-ratio (including both oxime groups) was 40:60 according to  $^1H$ -NMR.

**Yield:** 900 mg, 83% yield.

**$^1H$ -NMR** (500 MHz, DMSO):  $\delta$  [ppm] = 10.70 (s, 2H, *Z*, CHNOH), 10.34 (s, 2H, *E*, CHNOH), 7.28 (t, 2H, *E*,  $^3J = 5.9$  Hz, CHNOH), 6.62 (t, 2H, *Z*,  $^3J = 5.3$  Hz, CHNOH), 2.21 (m, 4H, *Z*,  $CH_2$ CHNOH), 2.08 (m, 4H, *E*,  $CH_2$ CHNOH), 1.40 (m, 4H, *E/Z*,  $CH_2CH_2$ CHNOH), 1.28 (m, 4H, *E/Z*,  $CH_2CH_2CH_2$ CHNOH).

**$^{13}C$ -NMR** (125 MHz, DMSO):  $\delta$  [ppm] = 150.32, 149.53, 28.93, 28.60, 28.29, 26.15, 25.53, 24.52.

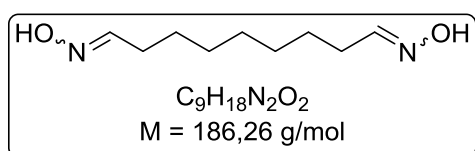
**GC (FID):** Phenomenex ZB-5MSi, 0.87 ml/min ( $H_2$ ), Inj. Temp.: 300 °C, Det. Temp.: 350 °C; 140 °C  $\rightarrow$  190 °C (5 °C/min);  $R_t$  dinitrile = 4.89 min,  $R_t$  dioxime = 5.90+7.37 min.

**MS** (ESI):  $m/z = 173.0$   $[M+H]^+$ .

**HRMS** (ESI): calcd for  $C_8H_{17}N_2O_2$   $[M+H]^+$  : 173.1285, found: 173.1284.

**IR** (neat)  $[cm^{-1}]$ : 3177, 3085, 3038, 2925, 2851, 1464, 1450, 1417, 1329, 1071, 918, 861, 813, 737, 719, 711.

#### 9.4.1.4.4 Nonanedial dioxime



The synthesis was conducted in analogy to GP14. Hydroxylamine hydrochloride (1.55 g, 22.3 mmol) was dissolved in 16 mL  $H_2O$  and 4 mL methanol. Nonanedial (1.16 g, 7.42 mmol) was added, followed by sodium carbonate (1.18 g, 11.1 mmol). Work up yielded the product as colorless solid. (*E/Z*)-ratio (including both oxime groups) was 9:91 according to  $^1H$ -NMR.

**Yield:** 1.02 g, 74% yield.

**<sup>1</sup>H-NMR** (500 MHz, DMSO):  $\delta$  [ppm] = 10.71 (s, 2H, *Z*, CHNOH), 10.35 (s, 2H, *E*, CHNOH), 7.27 (t, 2H, *E*,  $^3J = 5.9$  Hz, CHNOH), 6.61 (t, 2H, *Z*,  $^3J = 5.3$  Hz, CHNOH), 2.20 (m, 4H, *Z*, CH<sub>2</sub>CHNOH), 2.07 (m, 4H, *E*, CH<sub>2</sub>CHNOH), 1.40 (m, 4H, *E/Z*, CH<sub>2</sub>CH<sub>2</sub>CHNOH), 1.27 (m, 6H, *E/Z*, CH<sub>2</sub>CH<sub>2</sub>CH<sub>2</sub>CH<sub>2</sub>CHNOH).

**<sup>13</sup>C-NMR** (125 MHz, DMSO):  $\delta$  [ppm] = 150.30, 149.50, 28.97, 28.80, 28.53, 28.48, 26.25, 25.63, 25.51, 24.55.

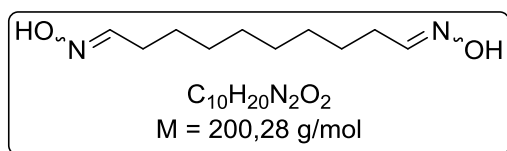
**GC (FID)**: Phenomenex ZB-5MSi, 0.87 ml/min (H<sub>2</sub>), Inj. Temp.: 300 °C, Det. Temp.: 350 °C; 150 °C -> 200 °C (5 °C/min);  $R_{t \text{ dinitrile}} = 5.18$  min,  $R_{t \text{ dioxime}} = 6.18+7.61$  min.

**MS** (ESI):  $m/z = 187.0$  [M+H]<sup>+</sup>.

**HRMS** (ESI): calcd for C<sub>9</sub>H<sub>19</sub>N<sub>2</sub>O<sub>2</sub> [M+H]<sup>+</sup> : 187.1441, found: 187.1446.

**IR** (neat) [cm<sup>-1</sup>]: 3194, 3085, 2923, 2848, 1463, 1440, 1416, 1329, 1308, 916, 840, 814, 749, 737, 712.

#### 9.4.1.4.5 Decanedial dioxime



The synthesis was conducted in analogy to GP14. Hydroxylamine hydrochloride (1.72 g, 24.7 mmol) was dissolved in 20 mL H<sub>2</sub>O and 5 mL methanol. Decanedial (1.40 g, 8.22 mmol) was added, followed by sodium carbonate (1.31 g,

12.3 mmol). Work up yielded the product as colorless solid. (*E/Z*)-ratio (including both oxime groups) was 43:57 according to <sup>1</sup>H-NMR.

**Yield**: 1.22 g, 74% yield.

**<sup>1</sup>H-NMR** (500 MHz, DMSO):  $\delta$  [ppm] = 10.69 (s, 2H, *Z*, CHNOH), 10.33 (s, 2H, *E*, CHNOH), 7.28 (t, 2H, *E*,  $^3J = 5.9$  Hz, CHNOH), 6.62 (t, 2H, *Z*,  $^3J = 5.3$  Hz, CHNOH), 2.20 (m, 4H, *Z*, CH<sub>2</sub>CHNOH), 2.07 (m, 4H, *E*, CH<sub>2</sub>CHNOH), 1.39 (m, 4H, *E/Z*, CH<sub>2</sub>CH<sub>2</sub>CHNOH), 1.26 (m, 8H, *E/Z*, CH<sub>2</sub>CH<sub>2</sub>CH<sub>2</sub>CH<sub>2</sub>CHNOH).

**<sup>13</sup>C-NMR** (125 MHz, DMSO):  $\delta$  [ppm] = 150.32, 149.51, 28.95, 28.85, 28.69, 28.54, 26.25, 25.63, 24.54.

**GC (FID)**: Phenomenex ZB-5MSi, 0.87 ml/min (H<sub>2</sub>), Inj. Temp.: 300 °C, Det. Temp.: 350 °C; 150 °C -> 200 °C (5 °C/min);  $R_{t \text{ dinitrile}} = 6.32$  min,  $R_{t \text{ dioxime}} = 7.58+9.13$  min.

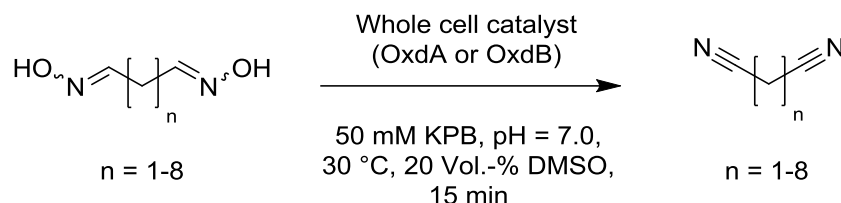
**MS** (ESI):  $m/z = 201.1$  [M+H]<sup>+</sup>.

**HRMS** (ESI): calcd for C<sub>10</sub>H<sub>21</sub>N<sub>2</sub>O<sub>2</sub> [M+H]<sup>+</sup> : 201.1598, found: 201.1595.

**IR** (neat) [cm<sup>-1</sup>]: 3184, 3080, 2923, 2849, 1465, 1446, 1323, 918, 884, 816, 745, 718.

## 9.4.2 BIOTRANSFORMATIONS FOR THE BIOCATALYTIC PRODUCTION OF ALIPHATIC LINEAR $\alpha,\omega$ -DINITRILES

### 9.4.2.1 General procedure 15 (GP15): Activity assay for the biocatalytic dehydration of dioximes by OxdA and OxdB



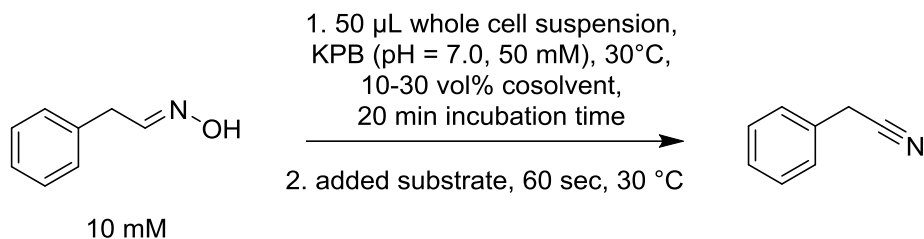
800  $\mu\text{L}$  of a whole cell catalyst suspension in 50 mM KPB, pH = 7.0 (2.0  $\text{mg}_{\text{BWW}}$ , containing OxdA or OxdB) was mixed with 0-192  $\mu\text{L}$  DMSO and incubated for five minutes at 30  $^\circ\text{C}$  and vigorous shaking. The assay was started by adding 8-200  $\mu\text{L}$  of a 375 mM stock solution of the substrate in DMSO. The assay was stopped by addition of 1.0 mL 2-Me-THF and immediate extraction of the substrate by vortexing for 60 seconds. After centrifugation (4  $^\circ\text{C}$ , 15000 g, 5 min), the supernatant (800  $\mu\text{L}$ ) was transferred into a GC-vial and analyzed by gas chromatography. The conversion was determined by calibration curves, including a correction factor accounting for incomplete extraction of the substrate and product.

**Table 26:** Activity values for OxdA and OxdB in  $\text{mU}/\text{mg}_{\text{BWW}}$ .

Substrate <sup>a</sup> / Conc.	3.0 mM	6.25 mM	12.5 mM	25 mM	50 mM	75 mM
C4 (OxdA)	n.d.	3.3 $\pm$ 0.1	4.7 $\pm$ 1.3	10.2 $\pm$ 0.4	12.3 $\pm$ 1.2	15.1 <sup>b</sup> $\pm$ 0.5
C5 (OxdA)	2.7 $\pm$ 0.1	6.6 $\pm$ 0.0	9.7 $\pm$ 0.1	13.0 $\pm$ 0.2	16.9 <sup>b</sup> $\pm$ 0.2	15.6 <sup>b</sup> $\pm$ 0.1
C6 (OxdA)	27.8 $\pm$ 0.9	34.6 $\pm$ 0.3	41.4 $\pm$ 0.4	40.4 <sup>b</sup> $\pm$ 3.2	38.7 <sup>b</sup> $\pm$ 0.4	45.6 <sup>b</sup> $\pm$ 5.0
C7 (OxdA)	32.7 $\pm$ 0.3	42.4 $\pm$ 0.4	46.3 <sup>b</sup> $\pm$ 0.3	45.9 <sup>b</sup> $\pm$ 0.3	29.8 <sup>b</sup> $\pm$ 0.3	24.2 <sup>b</sup> $\pm$ 0.1
C8 (OxdA)	26.6 $\pm$ 0.2	35.4 <sup>b</sup> $\pm$ 0.8	50.1 <sup>b</sup> $\pm$ 0.2	39.6 <sup>b</sup> $\pm$ 0.2	28.3 <sup>b</sup> $\pm$ 0.1	17.5 <sup>b</sup> $\pm$ 0.3
C9 (OxdA)	24.8 $\pm$ 0.7	36.1 <sup>b</sup> $\pm$ 0.3	50.6 <sup>b</sup> $\pm$ 0.7	40.9 <sup>b</sup> $\pm$ 0.4	32.0 <sup>b</sup> $\pm$ 0.0	23.6 <sup>b</sup> $\pm$ 0.5
C10 (OxdA)	6.1 $\pm$ 0.1	12.3 <sup>b</sup> $\pm$ 0.3	21.7 <sup>b</sup> $\pm$ 0.2	29.6 <sup>b</sup> $\pm$ 0.1	41.7 <sup>b</sup> $\pm$ 0.1	49.4 <sup>b</sup> $\pm$ 1.7
C4 (OxdB)	15.2 $\pm$ 0.4	28.1 $\pm$ 0.9	37.3 $\pm$ 0.5	33.6 $\pm$ 0.8	18.5 $\pm$ 0.1	16.6 <sup>b</sup> $\pm$ 1.6
C5 (OxdB)	4.9 $\pm$ 0.1	7.9 $\pm$ 0.0	10.1 $\pm$ 0.1	12.3 $\pm$ 0.4	15.0 <sup>b</sup> $\pm$ 0.0	15.0 <sup>b</sup> $\pm$ 0.7
C6 (OxdB)	51.5 $\pm$ 0.2	91.8 $\pm$ 0.4	145 $\pm$ 0.3	169 <sup>b</sup> $\pm$ 0.9	151 <sup>b</sup> $\pm$ 0.6	114 <sup>b</sup> $\pm$ 0.1
C7 (OxdB)	61.4 $\pm$ 0.3	62.0 $\pm$ 0.1	151 <sup>b</sup> $\pm$ 0.9	129 <sup>b</sup> $\pm$ 0.7	117 <sup>b</sup> $\pm$ 0.1	139 <sup>b</sup> $\pm$ 0.2
C8 (OxdB)	25.1 $\pm$ 0.5	38.9 <sup>b</sup> $\pm$ 0.5	54.5 <sup>b</sup> $\pm$ 0.3	39.2 <sup>b</sup> $\pm$ 0.1	30.8 <sup>b</sup> $\pm$ 0.2	29.6 <sup>b</sup> $\pm$ 0.1
C9 (OxdB)	28.7 $\pm$ 0.4	43.9 <sup>b</sup> $\pm$ 0.6	70.3 <sup>b</sup> $\pm$ 0.1	62.1 <sup>b</sup> $\pm$ 0.3	58.2 <sup>b</sup> $\pm$ 0.2	67.2 <sup>b</sup> $\pm$ 0.5
C10 (OxdB)	7.0 $\pm$ 0.2	9.1 <sup>b</sup> $\pm$ 0.1	13.5 <sup>b</sup> $\pm$ 0.0	17.7 <sup>b</sup> $\pm$ 0.2	22.9 <sup>b</sup> $\pm$ 0.1	27.9 <sup>b</sup> $\pm$ 0.5

a) no conversion detected for the C3-dioxime; b) partial precipitation of the substrate.

### 9.4.2.2 General procedure 16 (GP16): Influence of water soluble cosolvents on the activity of Oxds (short term studies)



Into a 1.5 mL micro reaction tube with shaking of 1400 rpm at 30 °C were given 400/350/300 µL 50 mM KPB (pH = 7.0) and 50 µL resting cell suspension. Afterwards a water-soluble cosolvent (37.5/87.5/137.5 µL) was added. The suspension was incubated for 20 minutes and the assay was started by addition of 12.5 µL phenylacetaldehyde oxime (400 mM, final concentration of 10 mM), dissolved in the corresponding cosolvent. 100 µL 0.1 M HCl and 400 µL acetonitrile were added after 60 seconds to quench the reaction. 800 µL of the supernatant after centrifugation (15000 g, 4 °C, 5 min) were transferred into a vial and measured on RP-HPLC for conversion according to a calibration curve. The relative activity was determined by comparison with a reference experiment, in which no cosolvent was added during the incubation time.

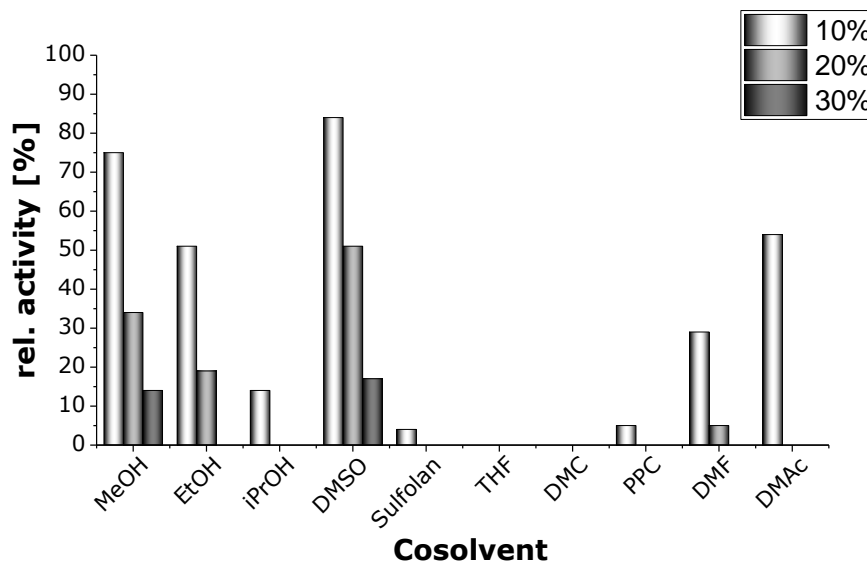


**Figure 37:** Relative activity of Oxda(C) in presence of water soluble cosolvents (for different volumetric percentages).

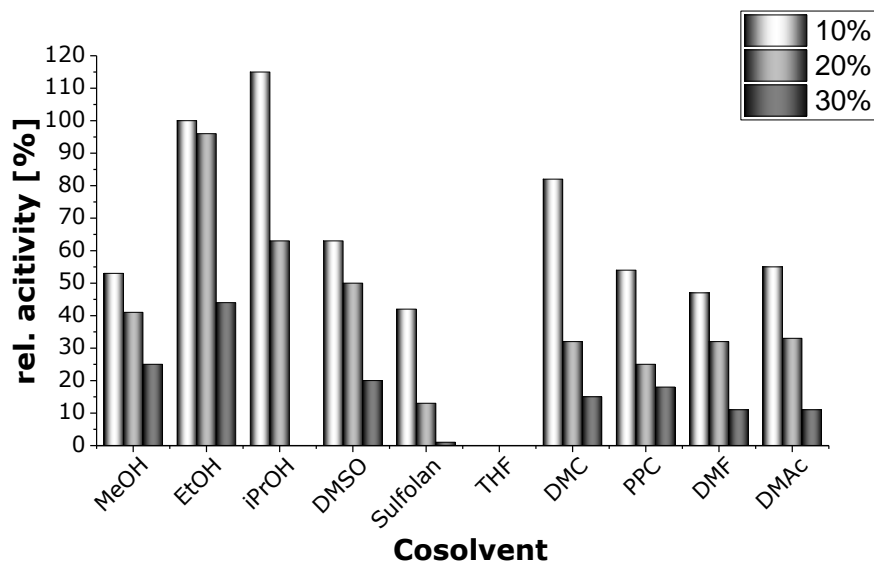


**Figure 38:** Relative activity of OxdB in presence of water soluble cosolvents (for different volumetric percentages).

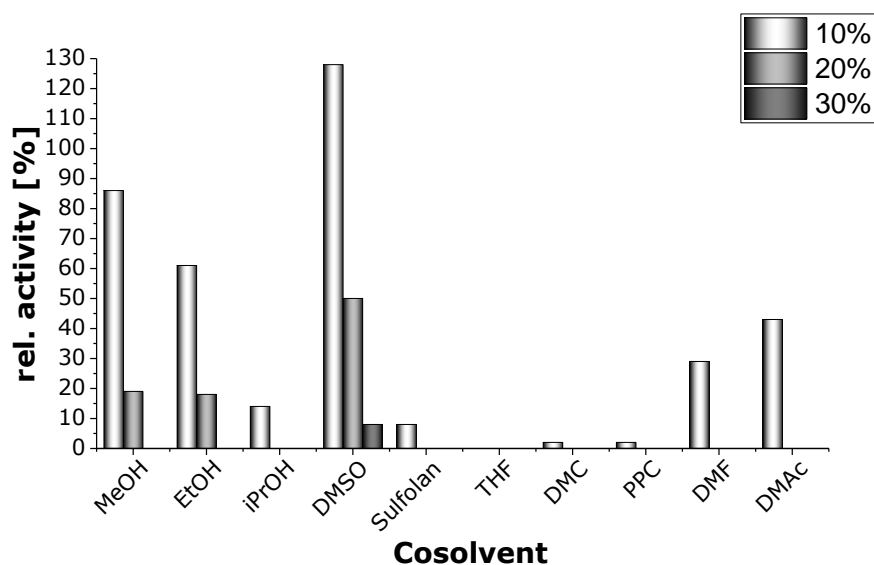


**Figure 39:** Relative activity of OxdFG(N) in presence of water soluble cosolvents (for different volumetric percentages).

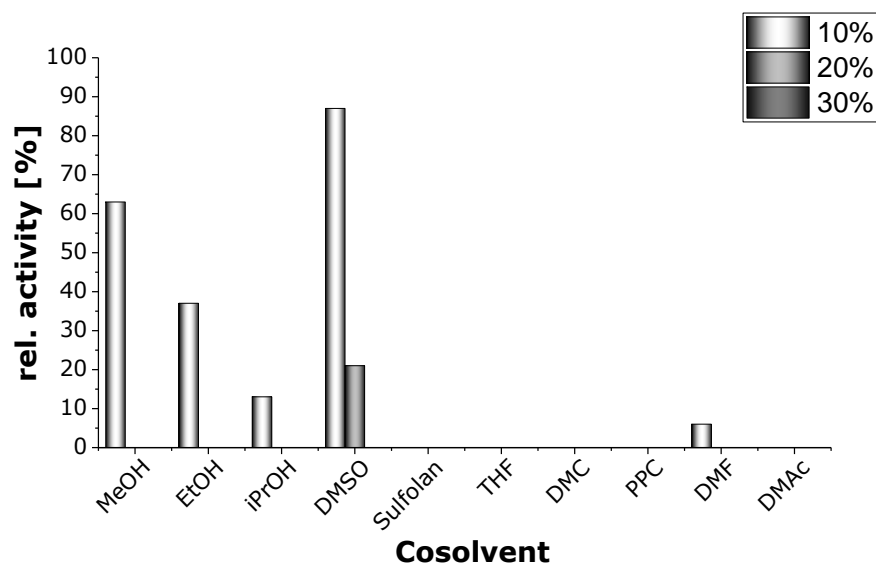


**Figure 40:** Relative activity of OxdRE(N) in presence of water soluble cosolvents (for different volumetric percentages).

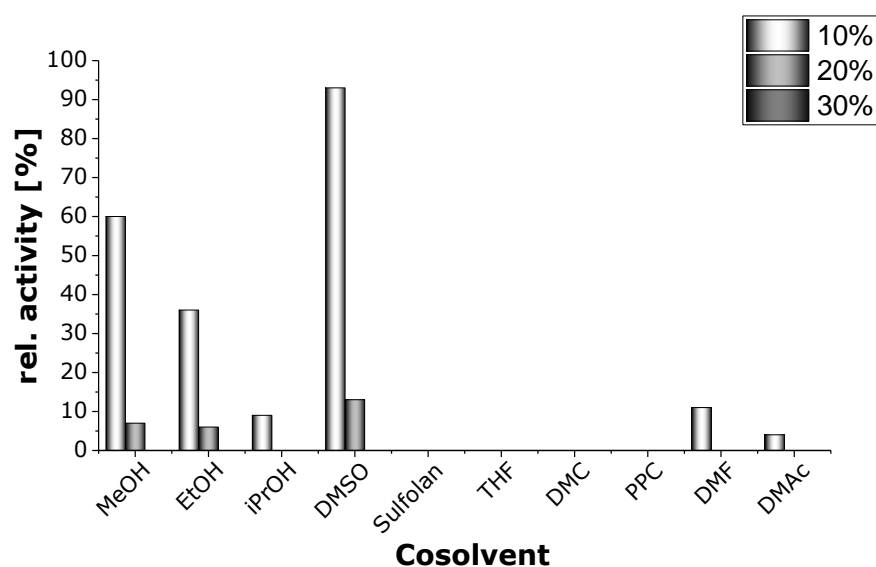
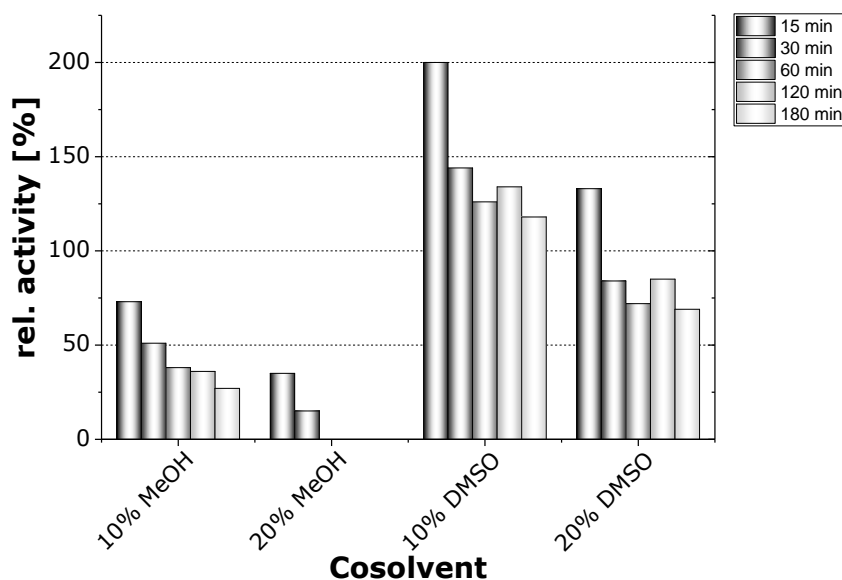
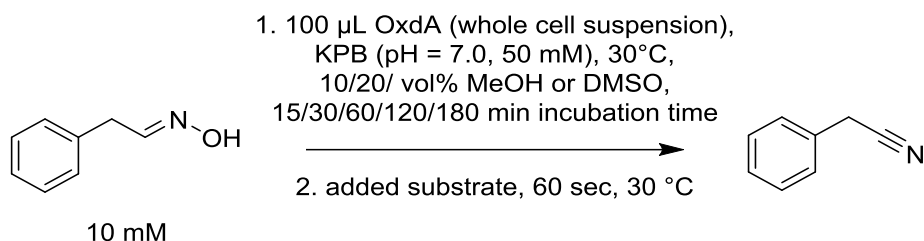


**Figure 41:** Relative activity of OxdRG(N) in presence of water soluble cosolvents (for different volumetric percentages).

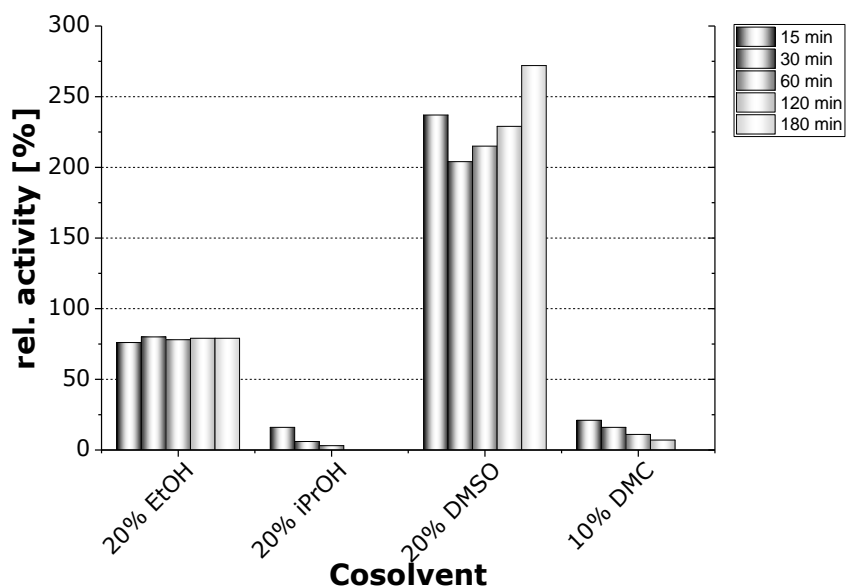
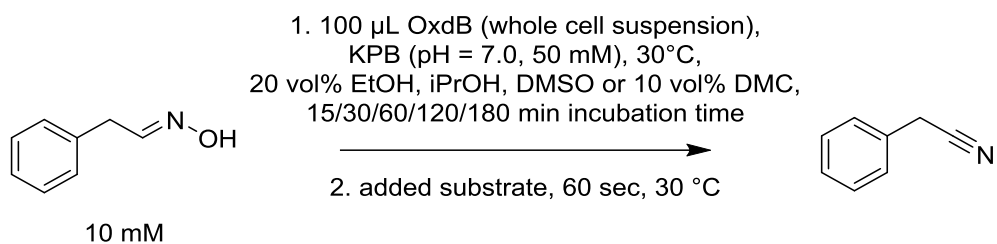


### 9.4.2.3 General procedure 17 (GP17): Influence of water soluble cosolvents on the activity of OxdA und OxdB (long term studies)

Into a 1.5 mL micro reaction tube with shaking of 1400 rpm at 30 °C were given 350/300  $\mu\text{L}$  50 mM KPB (pH = 7.0) and 100  $\mu\text{L}$  resting cell suspension. Afterwards were added 37.5/87.5  $\mu\text{L}$  of MeOH/DMSO (for OxdA) or 37.5/87.5  $\mu\text{L}$  EtOH/iPrOH/DMSO/DMC (for OxdB). The suspension was incubated for 15/30/60/120/180 minutes and the assay was started by addition of 12.5  $\mu\text{L}$  substrate (400 mM, final concentration of 10 mM), dissolved in the corresponding cosolvent. 100  $\mu\text{L}$  0.1 M HCl and 400  $\mu\text{L}$  acetonitrile were added after 60 seconds to quench the reaction. 800  $\mu\text{L}$  of the supernatant after centrifugation (15000 g, 4 °C, 5 min) were transferred into a vial and measured on RP-HPLC for conversion. The relative activity was determined by comparison with a reference experiment, in which no cosolvent was added during the incubation time.

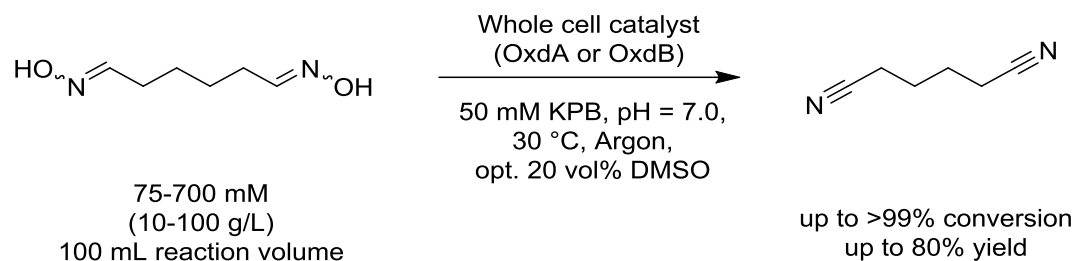


**Scheme 67:** Long-term stability study for OxdA(C).



**Scheme 68:** Long-term stability study for OxdB.

## 9.4.2.4 General procedure 18 (GP18): Preparative scale experiments for the biocatalytic synthesis of adiponitrile



A 100 mL reaction mixture consisting of whole cell catalyst suspension in 50 mM KPB, pH = 7.0 (0.6-4.0 wt%<sub>BWW</sub>, containing OxdA or OxdB) and the solid adipaldehyde oxime (1.0-10 g) were mixed in a sealable glass flask. Argon was flushed through the flask and it was sealed afterwards. The mixture was stirred at 180 rpm at 30 °C. In case of using DMSO as a cosolvent, the reaction mixture consisted of 80 mL cell suspension and 20 mL DMSO. An aliquot of 1.0 mL was taken several times to determine the conversion *via* gas chromatography (GC). For this, the aliquot was mixed with 1.0 mL 2-Me-THF and extracted for 1 minute. The supernatant was taken off and injected into the GC apparatus. The conversion was determined according to calibration curves.

After complete conversion to adiponitrile, the reaction mixture was extracted three times with MTBE (1:1, v/v). In case of using DMSO as cosolvent, the combined extracts were washed once with brine (1:3, v/v). Subsequently, the extracts were dried over MgSO<sub>4</sub>, filtered and the solvent was removed *in vacuo* to yield adiponitrile as pale yellow liquid with 98-99% purity. The purity of the product was determined *via* <sup>1</sup>H-NMR- and GC-analysis.

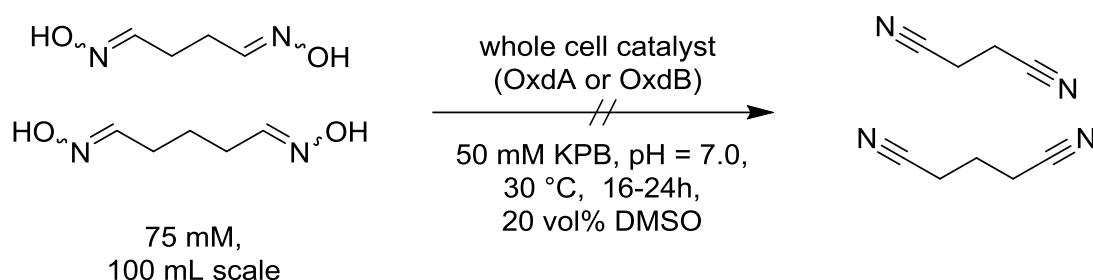
**Table 27:** Preparative scale synthesis with 10-100 g/L substrate concentration.

Entry	Oxd	Substrate conc. [g/L]	Biomass [g <sub>BWW</sub> ] <sup>a</sup>	Time [h]	Conv. [%]	Yield [%]
1	OxdA/ 20% DMSO	10	0.58 (23 U)	96	>99	75 (608 mg)
2	OxdA	10	1.16 (46 U)	64	>99	59 (480 mg)
3	OxdB/ 20% DMSO	10	0.51 (57 U)	18	>99	55 (446 mg)
4	OxdB	10	0.51 (57 U)	15	>99	70 (570 mg)
5	OxdB /20% DMSO	50	1.50 (171 U)	87	>99	67 (2.47 g)

6	OxdB	50	1.50 (171 U)	22	>99	80 (2.91 g)
7 <sup>b</sup>	OxdB	50	24.0 (6000 U)	27	>99	62 (23.1 g)
8 <sup>c</sup>	OxdB /20% DMSO	100	0.75 (86 U)	41	70	63 (1.18 g)
9	OxdB	100	4.00 (456 U)	41	75	63 (4.78 g)

[a] BWW = Bio wet weight, U = Unit, defined as  $\mu\text{mol}/\text{min}$  produced product; [b] 1000 mL reaction volume; [c] 25 mL reaction scale.

#### 9.4.2.5 Attempted biotransformation of succinaldehyde dioxime and glutaraldehyde dioxime



A 100 mL reaction mixture consisting of 80 mL whole cell catalyst suspension in 50 mM KPB, pH = 7.0 (0.5-0.6 wt%<sub>BWW</sub>, containing OxdA or OxdB) and 20 mL DMSO containing the dissolved succinaldehyde dioxime/glutaraldehyde dioxime (375 mM, final concentration 75 mM) were mixed in a sealable glass flask. Argon was flushed through the flask and it was sealed afterwards. The mixture was stirred at 180 rpm at 30 °C. An aliquot of 1.0 mL was taken several times to determine the conversion *via* gas chromatography (GC). For this, the aliquot was mixed with 1.0 mL 2-Me-THF and extracted for 1 minute. The supernatant was taken off and injected into the GC apparatus. The conversion was determined according to calibration curves. However, only marginable amounts of dinitrile were detected apart from unquantifiable amounts of an unknown intermediate.

#### 9.4.2.6 High cell-density fermentations of OxdB

For further information regarding the medium composition and antibiotic dosage, see **chapter 9.3.2.1**. A preculture (50 mL LB-medium, containing chloramphenicol and carbenicillin) was inoculated with an *E. coli* clone and incubated at 30 °C for 16 hours.

2 x 2 liter of AI-medium were prepared and treated with carbenicillin and chloramphenicol. Additionally, the feed medium was prepared.

Recipe for feed medium: Glycerol (527 g) and yeast extract (90 g) were mixed with distilled H<sub>2</sub>O to a total volume of 900 mL. Furthermore, MgSO<sub>4</sub> • 7 H<sub>2</sub>O (20 g) and lactose (20 g) were dissolved in 100 mL distilled H<sub>2</sub>O. After autoclaving, both solutions were combined to give 1 liter of feed medium.

Two liters of AI-medium were given into a fermenter each and the feed medium was connected to the fermenter. The main culture was inoculated with the previously prepared preculture (20 mL, 1%) and the fermentation process was started. The oxygen saturation level ( $p$ ) was set to  $p = 5\text{-}20\%$  (low O<sub>2</sub>) or  $30\text{-}70\%$  (high O<sub>2</sub>). Reservoirs with base, acid and anti-foaming agent were connected to the apparatus. During the fermentation, feed medium was constantly added to the main culture. The feed medium also contained chloramphenicol and carbenicillin. The fermentation was stopped after 72 hours and 375 g (low O<sub>2</sub>) and 260 g (high O<sub>2</sub>) of wet biomass were obtained.

### 9.4.3 EXPRESSION, PURIFICATION AND IMMOBILIZATION BY CROSSLINKING OF HIS-TAGGED ALDOXIME DEHYDRATASE FROM *BACILLUS SP.* OXB-1 (OXDBC<sub>HIS6</sub>)

#### 9.4.3.1 Expression of OxdB(C<sub>HIS6</sub>) in *E.Coli* BL21 (DE3)

Pre-culture: 5 mL LB-medium containing 50 µg/mL ampicillin were inoculated with an *E. coli* BL21 (DE3) clone harboring the OxdB(C<sub>HIS6</sub>) gene on a pET22b vector. Afterwards, the pre-culture was incubated at 37 °C and 180 rpm for 24 hours.

Main culture:

Variant A: 500 mL (in a 500 mL Erlenmeyer flask) of Auto-induction medium (Recipe for 500 mL: 410 mL Terrific-broth medium containing 12.0 g Yeast extract, 6.0 g polypeptone, 4.0 g glycerol, mixed with 50 mL potassium phosphate buffer (4.7 g K<sub>2</sub>HPO<sub>4</sub> and 1.1 g KH<sub>2</sub>PO<sub>4</sub>) and 10 mL of 60% glycerol solution, 5 mL of 10% glucose solution and 25 mL of 8% lactose solution) was inoculated with 5 mL (1.0 vol%) of the pre-culture, followed by addition of 100 µg/mL Ampicillin. The culture was incubated for one hour at 37 °C and 180 rpm, followed by incubation at 30 °C for 72 hours.

Variant B: A: 500 mL (in a 500 mL Erlenmeyer flask) of Terrific broth medium (Recipe for 500 mL: 450 mL H<sub>2</sub>O containing 12.0 g yeast extract, 6.0 g polypeptone, 4.0 g glycerol, mixed with 50 mL potassium phosphate buffer (4.7 g K<sub>2</sub>HPO<sub>4</sub> and 1.1 g KH<sub>2</sub>PO<sub>4</sub>)) was inoculated with 5 mL (1.0 vol%) of the pre-culture, followed by addition of 100 µg/mL ampicillin. The culture was incubated at 37 °C and 180 rpm until OD<sub>600</sub> reached 0.5-0.7, upon which IPTG (final conc. 1 mM) was added. The main culture was then incubated at 30 °C for 48 hours.

The cells were harvested by centrifugation (4000 g, 4 °C, 15 min). The supernatant was discarded and the pellets were washed twice with 50 mM potassium phosphate buffer (KPB, pH = 7.0). After repeated centrifugation (4000 g, 4 °C, 15 min) and weighing of the pellets (bio wet weight, BWW), they were stored at -20 °C until further use.

#### 9.4.3.2 Purification of OxdB(C<sub>His6</sub>) by NiNTA affinity chromatography

The harvested cell pellet was thawed and suspended in 20 mM TRIS-HCl buffer (pH = 8.0) containing 10 mM imidazole and 300 mM NaCl (binding buffer, usually 25-35 wt%). The cells were disrupted by ultrasound at 0 °C and the cell debris was centrifuged off (21500 g, 4 °C, 30 min).

The NiNTA column was equilibrated with 10 column volumina (CV) of binding buffer (see above) and the crude extract was given onto the column at room temperature. After flow through of the crude extract, the column was washed with 10 CV of binding buffer and the retained OxdB(C<sub>His6</sub>) was eluted with 5 mL elution buffer (20 mM TRIS-HCl, 150 mM Imidazole, 300 mM NaCl, pH = 8.0).

The obtained OxdB(C<sub>His6</sub>) was re-buffered to 50 mM KPB (pH = 7.0) *via* ultrafiltration and its purity confirmed *via* SDS-PAGE. The flow through of the NiNTA column did not contain any residual OxdB(C<sub>His6</sub>). OxdB(C<sub>His6</sub>) was stored at -20 °C until further use.

#### 9.4.3.3 Optimized of CLEA formation by crosslinking of purified OxdB(CHis6) with glutaraldehyde

150 µL of purified OxdB(C<sub>His6</sub>) (700 µg) was treated with 96 mg of (NH<sub>4</sub>)<sub>2</sub>SO<sub>4</sub> at 0 °C (85% saturation rate). The suspension was slowly shaken at 0 °C for 60 minutes to complete the precipitation. Afterwards, glutaraldehyde solution (final concentration of 0.5, 1.0, 2.0 wt%) was added and the suspension was slowly shaken for two hours at 0 °C. Afterwards, the formed CLEAs were centrifuged off (10000 g, 4 °C, 30 min). The supernatant was taken off and the CLEAs were washed with 150 µL KPB (50 mM, pH = 7.0). This washing fraction was collected and the CLEAs were either dried *in vacuo* at room temperature or freeze-dried at -50 °C *in vacuo*. The obtained CLEAs (~800 µg) were stored at 4 °C until further use. The activity of the CLEAs was determined according to the assay described in the next chapter and the results are summarized in **Table 28**.

Furthermore, the immobilization yield, activity recovery and immobilization efficiency were determined according to the following equations.<sup>[8,138,139]</sup>

$$\text{Immobilization yield (\%)} = 100 \times \frac{\text{immobilized activity}}{\text{starting activity}} = 100 \times \frac{A_{\text{pure}} - A_{\text{supernatant}} - A_{\text{washing}}}{A_{\text{pure}}}$$

$$\text{Immobilization efficiency (\%)} = 100 \times \frac{\text{observed activity}}{\text{immobilized activity}} = 100 \times \frac{A_{\text{CLEAs}}}{A_{\text{pure}} - A_{\text{supernatant}} - A_{\text{washing}}}$$

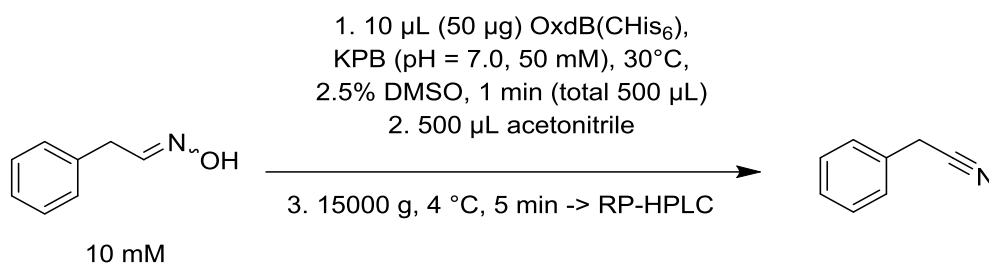
$$\text{Activity recovery (\%)} = 100 \times \frac{\text{observed activity}}{\text{starting activity}} = 100 \times \frac{A_{\text{CLEAs}}}{A_{\text{pure}}}$$

**Table 28:** Immobilization yield, efficiency and activity recovery for the obtained CLEAs.

CLEA	Immobilization yield [%]	Immobilization efficiency [%]	Activity recovery [%]
0.5	83	26	21
1.0	90	23	21
2.0	92	25	23

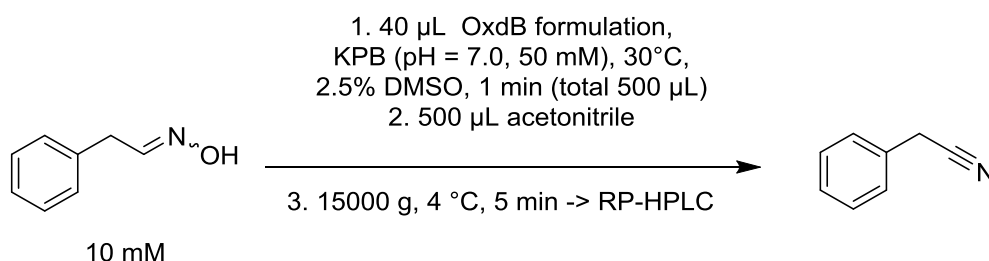
### 9.4.3.3 Activity assays for determination of OxdB(C<sub>His6</sub>) activity

#### 9.4.3.3.1 Purified OxdB(C<sub>His6</sub>)

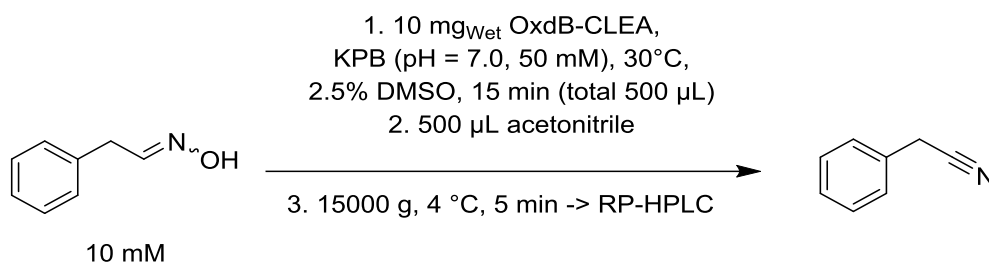


10  $\mu$ L (~50  $\mu$ g) purified OxdB(C<sub>His6</sub>) was dissolved in 477.5  $\mu$ L KPB (50 mM, pH = 7.0) and incubated for 5 minutes at 30 °C. The assay was started by adding 12.5  $\mu$ L of a 400 mM stock solution of (*E/Z*)-phenylacetaldehyde oxime (final concentration 10 mM). After 60 seconds at 30 °C and 1400 rpm shaking, 500  $\mu$ L acetonitrile was added. The solution was centrifuged (15000 g, 4 °C, 5min) and 800  $\mu$ L were transferred into a HPLC vial. The conversion was determined *via* RP-HPLC. The activity values are summarized in **Table 29**.

#### 9.4.3.3.2 Crude extract of (C<sub>His6</sub>), CLEA supernatant and washing fraction



40  $\mu$ L of crude extract, supernatant of the CLEA formation or the washing fraction of CLEA formation containing OxdB(C<sub>His6</sub>) was dissolved in 447.5  $\mu$ L KPB (50 mM, pH = 7.0) and incubated for 5 minutes at 30 °C. The assay was started by adding 12.5  $\mu$ L of a 400 mM stock solution of (*E/Z*)-phenylacetaldehyde oxime (final concentration 10 mM). After 60 seconds at 30 °C and 1400 rpm shaking, 500  $\mu$ L Acetonitrile was added. The solution was centrifuged (15000 g, 4 °C, 5min) and 800  $\mu$ L were transferred into a HPLC vial. The conversion was determined *via* RP-HPLC. The activity values are summarized in **Table 29**.

9.4.3.3.3 OxdB(C<sub>His6</sub>) CLEAs

Freeze dried OxdB(C<sub>His6</sub>)-CLEA (800-1700 µg) was suspended in 487.5 µL KPB (50 mM, pH = 7.0) and incubated for 5 minutes at 30 °C. The assay was started by adding 12.5 µL of a 400 mM stock solution of (*E/Z*)-phenylacetaldehyde oxime (final concentration 10 mM). After 15 minutes at 30 °C and 1400 rpm shaking, 500 µL acetonitrile was added. The suspension was centrifuged (15000 g, 4 °C, 5min) and 800 µL were transferred into a HPLC vial. The conversion was determined *via* RP-HPLC. The activity values are summarized in **Table 29**.

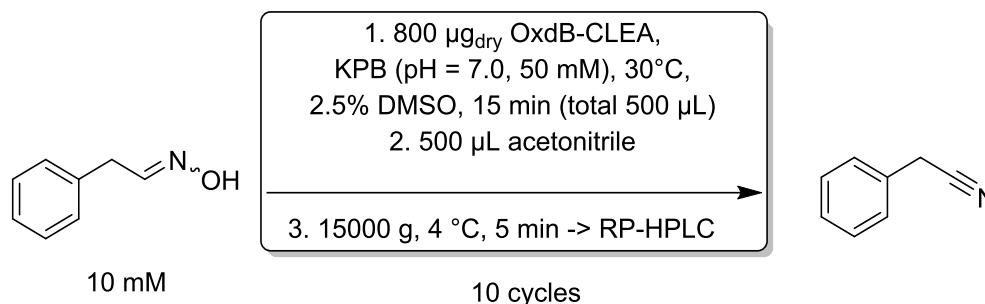
**Table 29:** Summary of the activities of different OxdB(C<sub>His6</sub>) formulations including CLEAs.

Entry	Formulation	mg/mL	Activity (mU/mg)
1	Purified OxdB(C <sub>His6</sub> )	4.72	1630
2	Crude extract	7.02	4940 <sup>b</sup>
3	Supernatant CLEA 0.5-2.0	n.d.	0
4	Washing fraction 0.5-2.0	2.64-3.54	127-284
5	CLEA 0.5-2.0	700-800 µg <sup>a</sup>	336-372

a. dry weight; b. mU/mL; n.d. = not determinable



#### 9.4.3.4 General procedure 19 (GP19): Recycling study for the long-term stability of OxdB(C<sub>His6</sub>) CLEAs in aqueous media



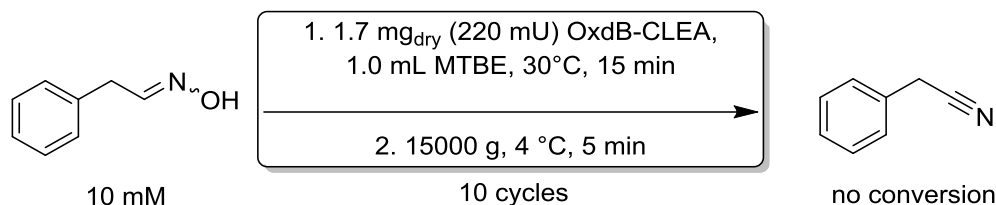
Freeze dried OxdB(C<sub>His6</sub>)-CLEAs (800 µg) were stored for two days at 4 °C in KPB (50 mM, pH = 7.0) prior to use. The CLEAs were suspended in 487.5 µL KPB (50 mM, pH = 7.0). The assay was started by adding 12.5 µL of a 400 mM stock solution of (*E/Z*)-phenylacetaldehyde oxime (final concentration 10 mM). After 15 minutes at 30 °C and 1400 rpm shaking, 500 µL acetonitrile was added. The suspension was centrifuged (15000 g, 4 °C, 5 min) and the supernatant was taken off for RP-HPLC analysis. The CLEAs were washed with 500 µL KPB (50 mM, pH = 7.0) and centrifuged off again (15000 g, 4 °C, 5 min). Afterwards, new 487.5 µL of KPB (50 mM, pH = 7.0) were added and the procedure started again for a total of ten cycles. The activity values are listed in **Table 30**.

**Table 30:** Activity (in mU/mg) of freeze dried OxdB(C<sub>His6</sub>)-CLEAs in aqueous media for 10 cycles.

	Cycle	1	2	3	4 <sup>a</sup>	5 <sup>a</sup>	6 <sup>a</sup>	7 <sup>a</sup>	8 <sup>a</sup>	9 <sup>a</sup>	10 <sup>a</sup>
<b>CLEA</b>	0.5%	131	198	176	68	70	56	39	30	23	19
	Glutaraldehyde										
	1.0%	60	80	65	28	29	27	26	19	18	16
	Glutaraldehyde										
	2.0%	126	181	175	68	82	78	62	44	35	30
	Glutaraldehyde										

a. Cycles conducted after 24 hour storage of the CLEAs at room temperature in KPB (50 mM, pH = 7.0)

### 9.4.3.5 General procedure 20 (GP20): Recycling study for the long-term stability of OxdB(C<sub>His6</sub>) CLEAs in organic media

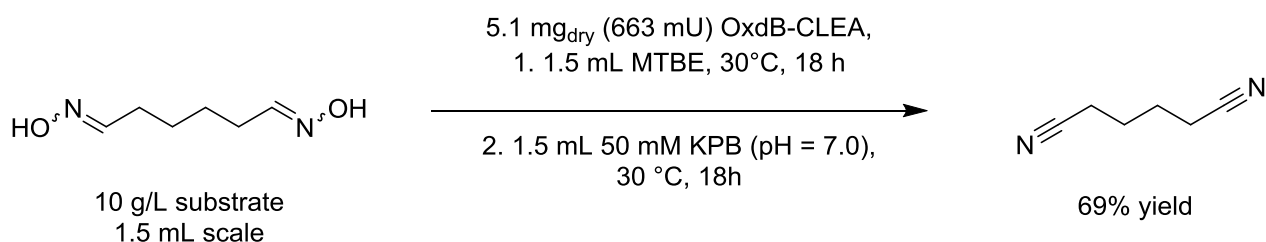


Freeze dried OxdB(C<sub>His6</sub>)-CLEA (1.7 mg, 220 mU) was mixed at 30 °C with 1.0 mL MTBE containing 10 mM (*E/Z*)-phenylacetaldehyde oxime in a 1.5 mL micro reaction tube. The suspension was shaken for 15 min at 30 °C and afterwards the CLEAs were centrifuged off (15000 g, 4 °C, 5 min) and the supernatant was freed from the solvent *in vacuo* and the conversion was determined according to <sup>1</sup>H-NMR analysis (in CDCl<sub>3</sub>). This procedure was repeated for 10 cycles.

**Table 31:** Observed conversion of (*E/Z*)-PAOx in organic media with OxdB-CLEAs.

Cycle	1	2	3	4	5	6	7	8	9	10
Conv. [%]	0	0	0	0	0	0	0	0	0	0
Activity [U/mg]	-	-	-	-	-	-	-	-	-	-

### 9.4.3.6 Synthesis of adiponitrile in aqueous and organic media with OxdB(C<sub>His6</sub>) CLEAs



Freeze dried OxdB(C<sub>His6</sub>)-CLEA (5.1 mg, 663 mU) was mixed at 30 °C with 1.5 mL MTBE and (*E/Z*)-adipaldehyde dioxime (15 mg, 104 μmol) in a 1.5 mL micro reaction tube. The suspension was vigorously shaken for 18 h at 30 °C and afterwards the CLEAs were centrifuged off (15000 g, 4 °C, 5 min) and the supernatant was freed from the solvent *in vacuo* and the conversion was determined according to <sup>1</sup>H-NMR analysis (in CDCl<sub>3</sub>). No product and hence conversion could be detected.

The residue in the micro reaction tube containing the OxdB(C<sub>His6</sub>)-CLEA and (*E/Z*)-adipaldehyde dioxime was mixed with 1.5 mL of 50 mM KPB (pH = 7.0) and the reaction mixture was vigorously shaken for 18 hours at 30 °C. The CLEAs were centrifuged off

(15000 g, 4 °C, 5 min) and the supernatant was extracted three times with 1.5 mL each. The solvent was removed *in vacuo* and the yield of adiponitrile was determined *via*  $^1\text{H-NMR}$  analysis ( $\text{CDCl}_3$  with TMS (0.03 v/v) as internal standard).

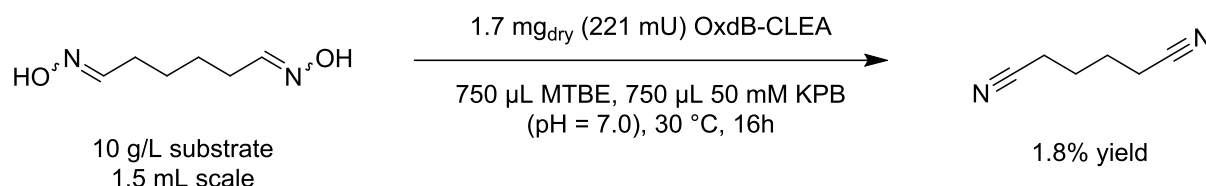
**Yield:** 6.9 mg, 62%.

**$^1\text{H-NMR}$**  (500 MHz,  $\text{CDCl}_3$ ):  $\delta$  [ppm] = 2.43 (m, 4H,  $\text{CH}_2\text{CH}_2\text{CN}$ ), 1.83 (m, 4H,  $\text{CH}_2\text{CH}_2\text{CN}$ ).

**$^{13}\text{C-NMR}$**  (125 MHz,  $\text{CDCl}_3$ ):  $\delta$  [ppm] = 118.80, 24.36, 16.76.

The analytical data corresponds with the literature.<sup>[112]</sup>

#### 9.4.3.7 Synthesis of adiponitrile in a biphasic system with OxdB( $\text{C}_{\text{His}6}$ ) CLEAs



Freeze dried OxdB( $\text{C}_{\text{His}6}$ )-CLEA (1.7 mg, 221 mU) was mixed with 750  $\mu\text{L}$  MTBE, 750  $\mu\text{L}$  50 mM KPb (pH = 7.0) and (*E/Z*)-adipaldehyde dioxime (15 mg, 104  $\mu\text{mol}$ ) in a 1.5 mL micro reaction tube. The suspension was vigorously shaken for 16 h at 30 °C and afterwards the CLEAs were centrifuged off (15000 g, 4 °C, 5 min). The phases were separated and the organic phase was freed from the solvent *in vacuo* and the conversion was determined according to  $^1\text{H-NMR}$  analysis (in  $\text{CDCl}_3$  TMS, 0.03 v/v, as internal standard).

**Yield:** 205  $\mu\text{g}$ , 1.8%.

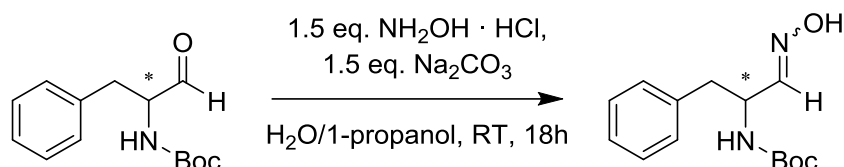
**$^1\text{H-NMR}$**  (500 MHz,  $\text{CDCl}_3$ ):  $\delta$  [ppm] = 2.43 (m, 4H,  $\text{CH}_2\text{CH}_2\text{CN}$ ), 1.83 (m, 4H,  $\text{CH}_2\text{CH}_2\text{CN}$ ).

**$^{13}\text{C-NMR}$**  (125 MHz,  $\text{CDCl}_3$ ):  $\delta$  [ppm] = 118.80, 24.36, 16.76.

The analytical data corresponds with the literature.<sup>[112]</sup>

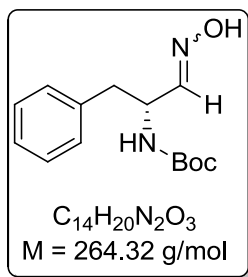
## 9.5 CHIRAL N-ACYL- $\alpha$ -AMINONITRILES VIA COPPER CATALYSIS AND INCORPORATION INTO A *DE NOVO* SYNTHESIS OF VILDAGLIPTIN

### 9.5.1 GENERAL PROCEDURE 21 (GP21): CONDENSATION OF MONO-ALDEHYDES WITH HYDROXYLAMINE SALTS



Hydroxylamine hydrochloride (1.5 eq.) and sodium carbonate (1.5 eq.) were dissolved in a mixture of H<sub>2</sub>O and 1-propanol at room temperature. Aldehyde was added to this solution and stirred vigorously until complete conversion according to TLC analysis (cyclohexane/ethyl acetate 3:1, v/v) was achieved. The solution was extracted three times with ethyl acetate (1:1 v/v) and the combined organic phases were washed with H<sub>2</sub>O (1:3 v/v). Drying over MgSO<sub>4</sub> and evaporation of the solvent gave a crude product, which was purified by silica column chromatography if desired. The (*E/Z*)-ratio of the product was determined by <sup>1</sup>H-NMR spectroscopy in CD<sub>2</sub>Cl<sub>2</sub>.

#### 9.5.1.1 (*E/Z*)-*N*-Boc-D-phenylalanyl oxime



The synthesis was carried out according to GP21. Hydroxylamine hydrochloride (146 mg, 2.11 mmol) and sodium carbonate (223 mg, 2.11 mmol) were dissolved in 5 mL H<sub>2</sub>O and 4 mL 1-propanol at RT. After the addition of *N*-Boc-D-phenylalanyl aldehyde (350 mg, 1.40 mmol) the resulting solution was stirred for 18 hours, upon which complete conversion was achieved according to TLC analysis. The work up yielded the product as colorless solid. The isomers were separated by column chromatography (cyclohexane:ethyl acetate 3:1, v/v), freed from the solvent at room temperature and obtained as colorless solids.

#### (*E*)-*N*-Boc-D-phenylalanyl oxime:

**Yield:** 200 mg, 54%.

**<sup>1</sup>H-NMR** (500 MHz, CD<sub>2</sub>Cl<sub>2</sub>):  $\delta$  [ppm] = 10.50 (s, 1H, NOH), 7.65 (s, 1H, NH), 7.42 (br s, 1H, CHNOH), 7.31 (m, 2H, Ar-H), 7.23 (m, 1H, Ar-H), 7.18 (m, 2H, Ar-H), 4.98 (s, 1H, CH<sub>2</sub>CHNH), 4.52 (m, 1H, CH<sub>2</sub>CHNH), 2.96 (m, 2H, CH<sub>2</sub>), 1.38 (s, 9H, Boc-H).

#### (*Z*)-*N*-Boc-D-phenylalanyl oxime:

**Yield:** 142 mg, 38%.

**<sup>1</sup>H-NMR** (500 MHz, CD<sub>2</sub>Cl<sub>2</sub>): δ [ppm] = 7.75 (s, 1H, NOH), 7.32 (m, 2H, Ar-H), 7.24 (m, 3H, Ar-H), 6.68 (d, 1H, <sup>3</sup>J = 6.1 Hz, CHNOH), 4.93 (m, 1H, CH<sub>2</sub>CHNH), 4.79 (s, 1H, NH), 3.03 (dd, 1H, <sup>2</sup>J = 13.9 Hz, <sup>3</sup>J = 5.4 Hz, CH<sub>2</sub>), 2.94 (m, 1H, CH<sub>2</sub>), 1.38 (s, 9H, Boc-H).

(E/Z)-N-Boc-D-phenylalaninal oxime:

**<sup>13</sup>C-NMR** (125 MHz, CD<sub>2</sub>Cl<sub>2</sub>): δ [ppm] = 156.8, 155.8, 155.5, 153.0, 151.0, 149.2, 137.6, 137.3, 130.15, 129.9, 19.0, 127.2, 81.6, 80.2, 51.7, 48.3, 41.8, 39.9, 37.9, 28.6.

**MS** (ESI): *m/z* = 265.1 ([M+H]<sup>+</sup>), 287.2 ([M+Na]<sup>+</sup>), 551.3 ([2M+Na]<sup>+</sup>).

**IR** [cm<sup>-1</sup>]: 3349, 1690, 1518, 1245, 1165, 698.

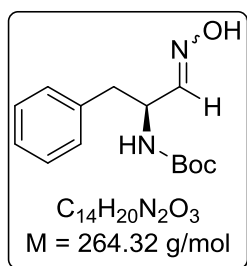
**MP**: 125 °C.

**RP-HPLC**: *Macherey-Nagel* Nucleodur C<sub>18</sub> HTec, Water/Acetonitrile 50:50, v/v, 1.0 mL/min, 40 °C, 220 nm, R<sub>t</sub> = 5.4 min.

**NP-HPLC**: *Daicel* Chiracel AD-H, CO<sub>2</sub>/Isopropanol 95:5, v/v, 0.75 mL/min, 30 min → 90:10, 2.00 mL/min, 30 min, 20 °C, 210 nm, R<sub>tZ</sub> = 40.6 min, R<sub>tE</sub> = 43.5 min.

The analytical data corresponds in analogy with the literature.<sup>[213]</sup>

#### 9.5.1.2 (E/Z)-N-Boc-L-phenylalaninal oxime



The synthesis was carried out according to GP21. Hydroxylamine hydrochloride (100 mg, 1.43 mmol) and sodium carbonate (152 mg, 1.43 mmol) were dissolved in 5 mL H<sub>2</sub>O and 4 mL 1-propanol at RT. After the addition of *N*-Boc-L-phenylalaninal (238 mg, 955 μmol) the colorless suspension was stirred for 18 hours, upon which complete conversion was achieved according to TLC analysis. The work up yielded the product as colorless solid.

**Yield**: 212 mg, 84%.

(E/Z)-N-Boc-L-phenylalaninal oxime:

**<sup>1</sup>H-NMR** (500 MHz, CD<sub>2</sub>Cl<sub>2</sub>): δ [ppm] = 10.02 (s, 1H, NOH), 7.86 (s, 1H, NOH), 7.54 (s, 1H, NH), 7.42 (br s, 1H, CHNOH), 7.33-7.18 (m, 5H, Ar-H), 6.68 (d, 1H, <sup>3</sup>J = 6.1 Hz, CHNOH), 5.71 (br s, 1H), 4.95 (s, 1H, CH<sub>2</sub>CHNH), 4.81 (s, 1H, NH), 4.52 (m, 1H, CH<sub>2</sub>CHNH), 3.03 (dd, 1H, <sup>2</sup>J = 13.9 Hz, <sup>3</sup>J = 5.4 Hz, CH<sub>2</sub>), 2.96 (m, 2H, CH<sub>2</sub>), 1.38 (s, 9H, Boc-H).

**<sup>13</sup>C-NMR** (125 MHz, CD<sub>2</sub>Cl<sub>2</sub>): δ [ppm] = 156.7, 155.7, 155.4, 153.1, 151.2, 149.4, 137.6, 137.3, 130.2, 129.9, 129.1, 129.0, 127.3, 127.2, 81.5, 80.1, 51.7, 41.7, 39.9, 28.5.

**IR** [cm<sup>-1</sup>]: 3349, 1690, 1518, 1245, 1165, 699.

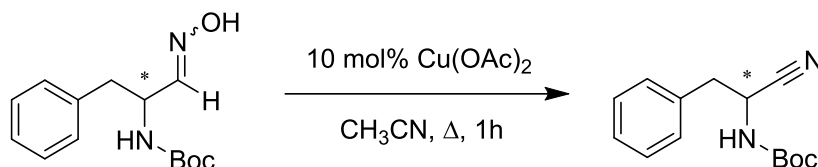
**MP**: 127 °C.

**RP-HPLC**: *Macherey-Nagel* Nucleodur C<sub>18</sub> HTec, Water/Acetonitrile 50:50, v/v, 1.0 mL/min, 40 °C, 220 nm, R<sub>t</sub> = 5.4 min.

**NP-HPLC:** *Daicel* Chiracel AD-H, CO<sub>2</sub>/Isopropanol 95:5, v/v, 0.75 mL/min, 30 min -> 90:10, 2.00 mL/min, 30 min, 20 °C, 210 nm, R<sub>tZ</sub> = 43.5 min, R<sub>tE</sub> = 55.1 min.

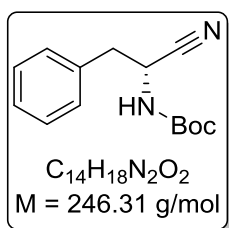
The analytical data corresponds with the literature.<sup>[213]</sup>

### 9.5.2 GENERAL PROCEDURE 22 (GP22): COPPER(II) ACETATE CATALYZED DEHYDRATION OF $\alpha$ -AMINO ALDOXIMES



Copper(II) acetate (10 mol-%) was dissolved in acetonitrile. Upon addition of the aldoxime, a rapid change in color from cyan to deep green was observed. The resulting suspension was heated to reflux for 60 minutes. After removal of the acetonitrile *in vacuo*, complete conversion was determined *via* TLC analysis (cyclohexane/ethyl acetate 2:1, v/v). The crude product, containing one equivalent of acetamide, was dissolved in cyclohexane/ethyl acetate (2:1, v/v) and filtered over a small silica column (4 cm), effectively removing acetamide and residual copper(II) acetate. Removal of the solvent yielded the desired nitrile. To determine the retention of absolute configuration, the product was analyzed by chiral HPLC. Alternatively to NMR, conversion could be measured *via* RP-HPLC.

#### 9.5.2.1 (*R*)-*N*-Boc-Phenylalanine Nitrile



The synthesis was carried out according to GP22. Copper(II) acetate (10.3 mg, 56.7  $\mu$ mol) was dissolved in 1.5 mL acetonitrile. (*E/Z*)-*N*-Boc-D-phenylalanyl oxime (150 mg, 567  $\mu$ mol) was added and the reaction mixture was heated to reflux for 60 min. The work up yielded the product as a colorless solid.

**Yield:** 116 mg, 83%.

**<sup>1</sup>H-NMR** (500 MHz, CDCl<sub>3</sub>):  $\delta$  [ppm] = 7.33 (m, 5H, Ar-*H*), 4.84 (br s, 2H, CH and NH), 3.09 (m, 2H, PhCH<sub>2</sub>), 1.44 (s, 9H, Boc-*H*).

**MS** (ESI): *m/z* = 269.1 ([M+Na]<sup>+</sup>), 515.2 ([2M+Na]<sup>+</sup>).

**IR** [cm<sup>-1</sup>]: 3350, 2922, 1688, 1518, 700.

**MP:** 115 °C.

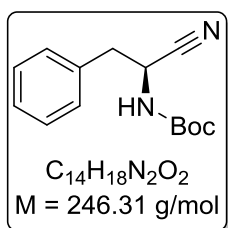
**[ $\alpha$ ]<sup>20D</sup>:** + 16 (c 0.98 dioxane).

**RP-HPLC:** *Macherey-Nagel* Nucleodur C<sub>18</sub> HTec, Water/Acetonitrile 50:50, v/v, 1.0 mL/min, 40 °C, 220 nm, R<sub>t</sub> = 9.0 min.

**NP-HPLC:** *Daicel* Chiracel AD-H, CO<sub>2</sub>/Isopropanol 95:5, v/v, 0.75 mL/min, 30 min -> 90:10, 2.00 mL/min, 30 min, 20 °C, 210 nm, R<sub>t</sub> = 23.3 min.

The analytical data corresponds in analogy with literature data.<sup>[66,214]</sup>

#### 9.5.2.2 (S)-N-Boc-phenylalanine Nitrile



The synthesis was carried out according to GP22. Copper(II) acetate (7.3 mg, 40.2 μmol) was dissolved in 1.0 mL acetonitrile. (*E/Z*)-N-Boc-L-phenylalaninal oxime (85.0 mg, 322 μmol) was added and the reaction mixture was heated to reflux for 60 min. The work up yielded the product as a colorless solid.

**Yield:** 73 mg, 92%.

**<sup>1</sup>H-NMR** (500 MHz, CDCl<sub>3</sub>): δ [ppm] = 7.33 (m, 5H, Ar-H), 4.84 (br s, 2H, CH and NH), 3.09 (m, 2H, PhCH<sub>2</sub>), 1.44 (s, 9H, Boc-H).

**IR** [cm<sup>-1</sup>]: 3351, 2923, 1688, 1518, 700.

**MP:** 115 °C.

**[α]<sup>20</sup><sub>D</sub>:** - 16 (c 0.98 dioxane).

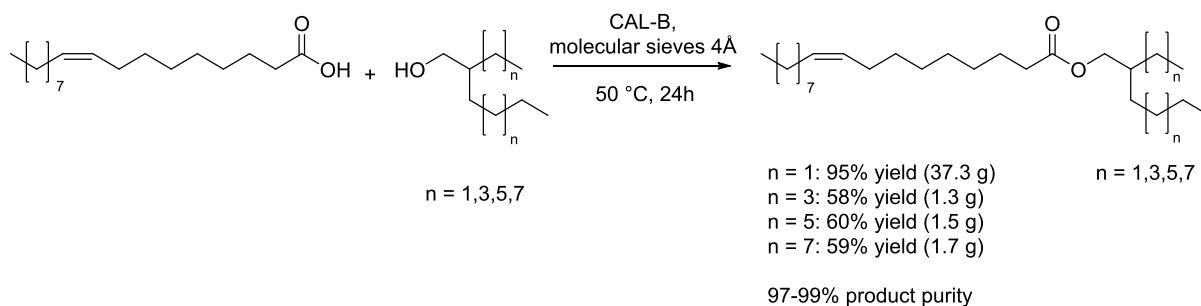
**RP-HPLC:** *Macherey-Nagel* Nucleodur C<sub>18</sub> HTec, Water/Acetonitrile 50:50, v/v, 1.0 mL/min, 40 °C, 220 nm, R<sub>t</sub> = 9.0 min.

**NP-HPLC:** *Daicel* Chiracel AD-H, CO<sub>2</sub>/Isopropanol 95:5, v/v, 0.75 mL/min, 30 min -> 90:10, 2.00 mL/min, 30min, 20 °C, 210 nm, R<sub>t</sub> = 20.9 min.

The analytical data corresponds with literature data.<sup>[66,214]</sup>

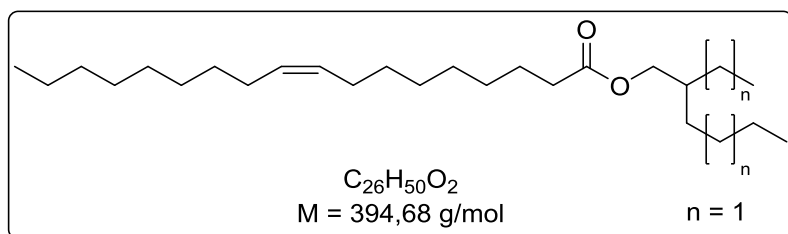
## 9.6 NEW LUBRICANT ESTER STRUCTURES BASED ON RENEWABLE RESOURCES

## 9.6.1 GENERAL PROCEDURE 23 (GP23): BIOCATALYTIC SYNTHESIS OF OLEIC ACID ESTERS BY ESTERIFICATION OF OLEIC ACID WITH GUERBET ALCOHOLS



Oleic acid (1.0 eq.) and Guerbet alcohol (1.0 eq.) were mixed with CAL-B (Novozym 435, 30 mg/mmol Substrate) and molecular sieves 4Å (120 mg/mmol). The reaction mixture was stirred at 50 °C for 24 hours and afterwards filtered through a 0.2 μM PTFE-Filter. The corresponding oleic acid ester was obtained in 97-99% purity.

## 9.6.1.1 2-ethylhexyl oleate



The synthesis was carried out according to GP23. Oleic acid (31.6 mL, 100 mmol) and 2-ethylhexanol (15.6 mL, 100 mmol) were mixed with Novozym 435 (3.00 g) and molecular sieves 4Å (12.0 g). 2-ethylhexyl oleate (99% purity) was obtained as colorless liquid.

**Yield:** 37.3 g, 95%.

**<sup>1</sup>H-NMR** (500 MHz, CDCl<sub>3</sub>): δ [ppm] = 5.34 (m, 2H, CH=CH), 3.98 (dd, 2H, <sup>2</sup>J = 5.8 Hz, <sup>3</sup>J = 2.4 Hz, OCH<sub>2</sub>), 2.29 (t, 2H, <sup>3</sup>J = 7.5 Hz, CH<sub>2</sub>CH<sub>2</sub>COOR), 2.01 (m, 4H, CH<sub>2</sub>CH=CHCH<sub>2</sub>), 1.61 (qi, 2H, <sup>3</sup>J = 7.3 Hz, CH<sub>2</sub>CH<sub>2</sub>COOR), 1.56 (sept, 1H, <sup>3</sup>J = 6.0 Hz, OCH<sub>2</sub>CH), 1.28 (m, 28H), 0.88 (m, 9H, CH<sub>3</sub>).

**<sup>13</sup>C-NMR** (125 MHz, CDCl<sub>3</sub>): δ [ppm] = 174.21, 130.11, 129.87, 66.76, 38.90, 34.58, 32.05, 30.57, 29.91, 29.84, 29.67, 29.47, 29.33, 29.29, 29.26, 29.07, 27.36, 27.31, 25.19, 23.95, 23.12, 22.83, 14.25, 14.18.

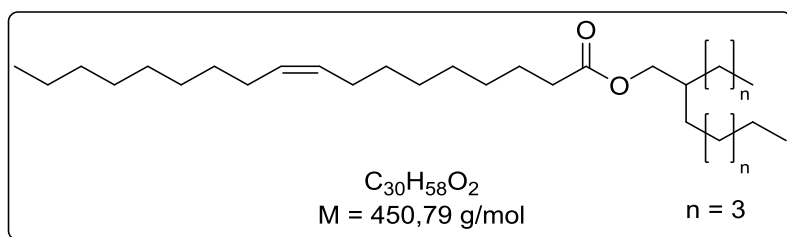
**GC (FID):** Phenomenex ZB-5MSi, 0.5 ml/min (H<sub>2</sub>), Inj. Temp.: 300 °C, Det. Temp.: 350 °C; 300 °C -> 350 °C (5 °C/min), 350 °C for 5 min, R<sub>t</sub> = 3.51 min.

**HRMS** (ESI): calcd for C<sub>26</sub>H<sub>50</sub>O<sub>2</sub>Na [M+Na]<sup>+</sup>: 417.3703, found: 417.3699.



**IR** (neat) [ $\text{cm}^{-1}$ ]: 2956, 2922, 2853, 1736, 1461, 1240, 1171, 724.

### 9.6.1.2 2-butylloctyl oleate



The synthesis was carried out according to GP23. Oleic acid (1.59 mL, 5.00 mmol) and 2-butylloctanol (1.12 mL, 5.00 mmol) were mixed with Novozym 435 (150 mg) and molecular sieves 4Å (600 mg). 2-butylloctyl oleate (97% purity) was obtained as colorless liquid.

**Yield:** 1.30 g, 58%.

**$^1\text{H-NMR}$**  (500 MHz,  $\text{CDCl}_3$ ):  $\delta$  [ppm] = 5.34 (m, 2H,  $\text{CH}=\text{CH}$ ), 3.96 (d, 2H,  $^2J = 5.8$  Hz,  $\text{OCH}_2$ ), 2.29 (t, 2H,  $^3J = 7.5$  Hz,  $\text{CH}_2\text{CH}_2\text{COOR}$ ), 2.01 (m, 4H,  $\text{CH}_2\text{CH}=\text{CHCH}_2$ ), 1.61 (m, 2H,  $\text{CH}_2\text{CH}_2\text{COOR}$ ), 1.60 (m, 1H,  $\text{OCH}_2\text{CH}$ ), 1.28 (m, 36H), 0.88 (m, 9H,  $\text{CH}_3$ ).

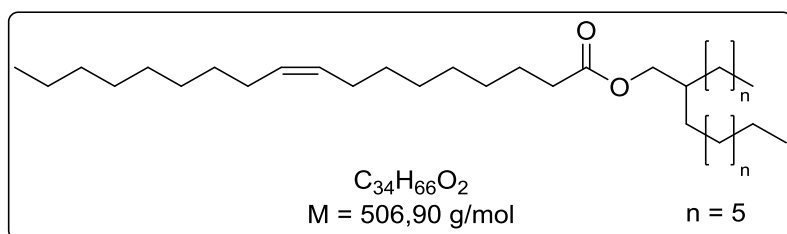
**$^{13}\text{C-NMR}$**  (125 MHz,  $\text{CDCl}_3$ ):  $\delta$  [ppm] = 174.21, 130.11, 129.87, 67.16, 37.43, 34.60, 32.06, 31.97, 31.44, 31.11, 29.92, 29.86, 29.78, 29.68, 29.47, 29.35, 29.31, 29.28, 29.07, 27.36, 27.32, 26.82, 25.21, 23.14, 22.83, 22.81, 14.25, 14.24, 14.19.

**GC (FID):** Phenomenex ZB-5MSi, 0.5 ml/min ( $\text{H}_2$ ), Inj. Temp.: 300 °C, Det. Temp.: 350 °C; 300 °C  $\rightarrow$  350 °C (5 °C/min), 350 °C for 5 min;  $R_t = 4.27$  min.

**HRMS** (ESI): calcd for  $\text{C}_{30}\text{H}_{58}\text{O}_2\text{Na}$  [ $\text{M}+\text{Na}$ ] $^+$ : 473.4329, found: 473.4324.

**IR** (neat) [ $\text{cm}^{-1}$ ]: 2954, 2922, 2853, 1737, 1457, 1241, 1169, 723.

### 9.6.1.3 2-hexyldecyl oleate



The synthesis was carried out according to GP23. Oleic acid (1.59 mL, 5.00 mmol) and 2-hexyldecanol (1.44 mL, 5.00 mmol) were mixed with Novozym 435 (150 mg) and molecular sieves 4Å (600 mg). 2-hexyldecyl oleate (97% purity) was obtained as colorless liquid.

**Yield:** 1.51 g, 60%.

**<sup>1</sup>H-NMR** (500 MHz, CDCl<sub>3</sub>): δ [ppm] = 5.34 (m, 2H, CH=CH), 3.97 (d, 2H, <sup>2</sup>J = 5.8 Hz, OCH<sub>2</sub>), 2.29 (t, 2H, <sup>3</sup>J = 7.5 Hz, CH<sub>2</sub>CH<sub>2</sub>COOR), 2.01 (m, 4H, CH<sub>2</sub>CH=CHCH<sub>2</sub>), 1.61 (m, 2H, CH<sub>2</sub>CH<sub>2</sub>COOR), 1.60 (m, 1H, OCH<sub>2</sub>CH), 1.28 (m, 44H), 0.88 (m, 9H, CH<sub>3</sub>).

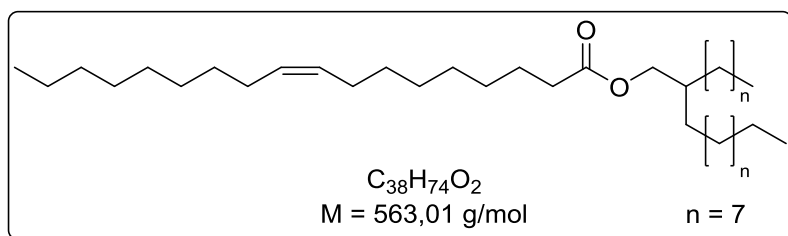
**<sup>13</sup>C-NMR** (125 MHz, CDCl<sub>3</sub>): δ [ppm] = 174.22, 130.12, 129.87, 67.18, 37.45, 34.61, 32.06, 31.97, 31.44, 30.12, 29.92, 29.86, 29.78, 29.72, 29.68, 29.48, 29.36, 29.32, 29.29, 27.37, 27.32, 26.86, 26.82, 25.21, 22.84, 22.81, 14.26, 14.25.

**GC (FID):** Phenomenex ZB-5MSi, 0.5 ml/min (H<sub>2</sub>), Inj. Temp.: 300 °C, Det. Temp.: 350 °C; 300 °C -> 350 °C (5 °C/min), 350 °C for 5 min; R<sub>t</sub> = 5.65 min.

**HRMS** (ESI): calcd for C<sub>34</sub>H<sub>66</sub>O<sub>2</sub>Na [M+Na]<sup>+</sup>: 529.4955, found: 529.4951.

**IR** (neat) [cm<sup>-1</sup>]: 2921, 2852, 1737, 1464, 1169, 722.

#### 9.6.1.4 2-octyldodecyl oleate



The synthesis was carried out according to GP23. Oleic acid (1.59 mL, 5.00 mmol) and 2-octyldodecanol (1.78 mL, 5.00 mmol) were mixed with Novozym 435 (150 mg) and molecular sieves 4Å (600 mg). 2-octyldodecyl oleate (98% purity) was obtained as colorless liquid.

**Yield:** 1.67 g, 59%.

**<sup>1</sup>H-NMR** (500 MHz, CDCl<sub>3</sub>): δ [ppm] = 5.34 (m, 2H, CH=CH), 3.97 (d, 2H, <sup>2</sup>J = 5.8 Hz, OCH<sub>2</sub>), 2.29 (t, 2H, <sup>3</sup>J = 7.5 Hz, CH<sub>2</sub>CH<sub>2</sub>COOR), 2.01 (m, 4H, CH<sub>2</sub>CH=CHCH<sub>2</sub>), 1.61 (m, 2H, CH<sub>2</sub>CH<sub>2</sub>COOR), 1.60 (m, 1H, OCH<sub>2</sub>CH), 1.28 (m, 52H), 0.88 (m, 9H, CH<sub>3</sub>).

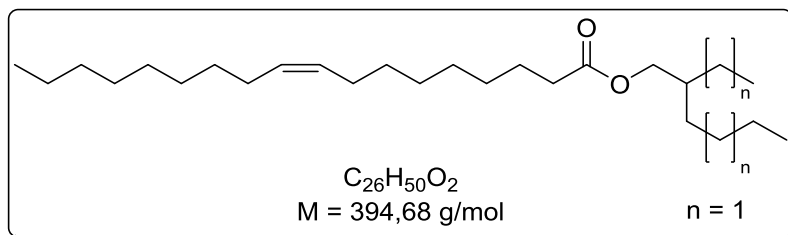
**<sup>13</sup>C-NMR** (125 MHz, CDCl<sub>3</sub>): δ [ppm] = 174.22, 130.12, 129.87, 67.19, 37.43, 34.61, 32.08, 32.07, 31.42, 30.12, 29.92, 29.87, 29.82, 29.81, 29.77, 29.72, 29.69, 29.52, 29.48, 29.36, 29.32, 29.29, 27.37, 27.32, 26.85, 25.21, 22.84, 14.27.

**GC (FID):** Phenomenex ZB-5MSi, 0.5 ml/min (H<sub>2</sub>), Inj. Temp.: 300 °C, Det. Temp.: 350 °C; 300 °C -> 350 °C (5 °C/min), 350 °C for 5 min; R<sub>t</sub> = 7.70 min.

**HRMS** (ESI): calcd for C<sub>34</sub>H<sub>66</sub>O<sub>2</sub>Na [M+Na]<sup>+</sup>: 585.5581, found: 585.5568.

**IR** (neat) [cm<sup>-1</sup>]: 2920, 2852, 1737, 1464, 1170, 722.

## 9.6.1.5 General procedure 24 (GP24): Recycling of Novozym 435 for the synthesis of 2-ethylhexyl oleate in a SpinChem reactor



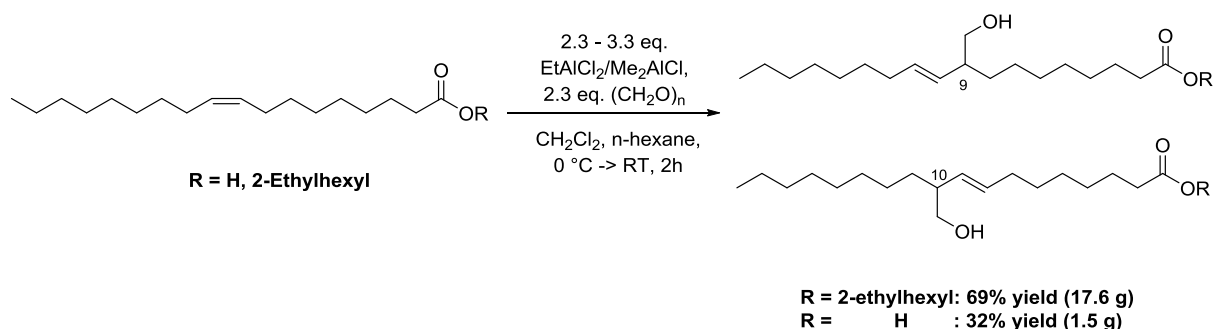
Oleic acid (18.9 mL, 60.0 mmol) and 2-ethylhexanol (9.4 mL, 60.0 mmol) were dissolved in 100 mL cyclohexane in a 200 mL SpinChem Vessel V2. Novozym 435 (1.80 g) and molecular sieves 4Å (7.4 g) were separately given into a SpinChem RBR S2 rotating bed reactor and the bed reactor was sealed. The reaction solution was stirred at 700 rpm for 24 hours at 50 °C. The conversion was determined after 3, 6, 9 and 24 hours by <sup>1</sup>H-NMR analysis. After 24 hours reaction time yielded removal of the solvent *in vacuo* 2-ethylhexyl oleate (98% purity) as colorless liquid.

**Yield:** 22.5 g, 95%.

**Table 32:** Observed conversions in the recycling of Novozym 435.

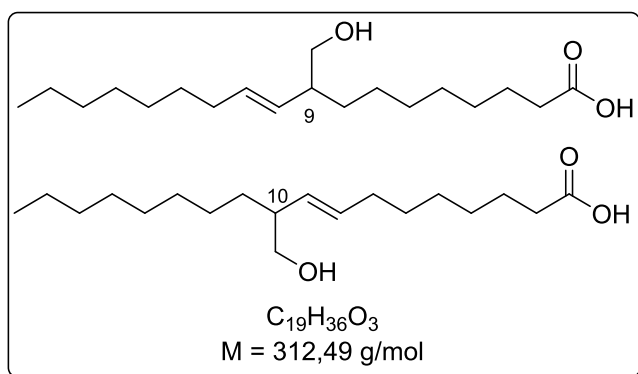
Time (h)	First cycle conversion (%)	Second cycle conversion (%)	Third cycle conversion (%)
3	86	95	92
6	98	96	96
9	98	96	96
24	98	98	96

### 9.6.2 GENERAL OPERATING PROCEDURE 25 (GP25): ENE REACTION OF OLEIC ACID AND OLEIC ESTERS WITH PARA-FORMALDEHYDE AND LEWIS ACIDS



In reference to *Metzger et Biermann*<sup>[195,196]</sup>: Oleic acid (1.0 eq.) oder its 2-ethylhexylester (1.0 eq.) and paraformaldehyde (2.3 eq.) were mixed under argon in dry dichloromethane and cooled to 0 °C. EtAlCl<sub>2</sub> or Me<sub>2</sub>AlCl (2.3 - 3.3 eq., 1.0 M in *n*-hexane) were added dropwise and the reaction mixture was stirred at room temperature for two hours. Water (1:1 v/v) was added and the pH adjusted to 1 with 4 M HCl. The organic and aqueous phase were separated and the aqueous one was extracted three times with diethyl ether (1:1 v/v). The combined organic phases were dried with MgSO<sub>4</sub> and freed from the solvent *in vacuo*. The products were obtained as colorless oils after column chromatography. The products were obtained as 1:1 mixture of the C9 and C10-adducts.

#### 9.6.2.1 (*E*)-9+10-(hydroxymethyl)octadec-10+8-enoic acid



The synthesis was carried out according to GP25. Oleic acid (4.73 mL, 15 mmol) and Paraformaldehyde (1.04 g, 34.5 mmol) were treated with Me<sub>2</sub>AlCl (34.5 mL, 34.5 mmol). Work-up and column chromatography (cyclohexane/ethyl acetate 7:3, v/v) yielded the product as colorless liquid.

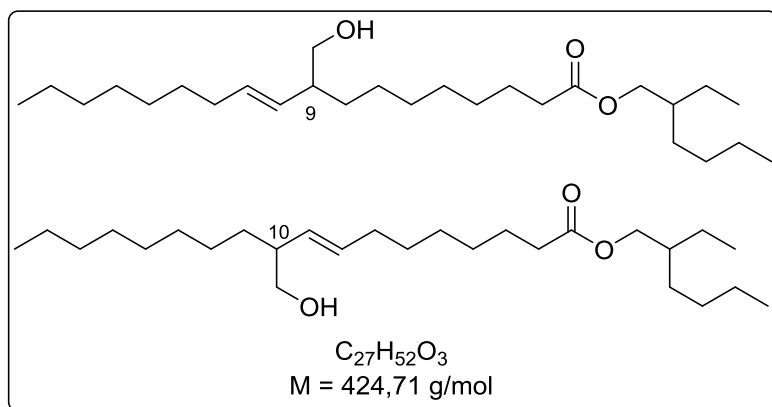
**Yield:** 1.50 g, 32%.

**<sup>1</sup>H-NMR** (500 MHz, CDCl<sub>3</sub>):  $\delta$  [ppm] = 5.52 (m, 1H, CH=CHCH), 5.13 (m, 1H, CH=CHCH), 3.52 (m, 1H, CH<sub>2</sub>OH), 3.33 (m, 1H, CH<sub>2</sub>OH), 2.34 (2 t, 2H, <sup>3</sup>J = 7.5 Hz, CH<sub>2</sub>COO), 2.15 (m, 1H, CH=CHCH), 2.04 (m, 2H, CH<sub>2</sub>CH=CH), 1.64 (m, 2H, CH<sub>2</sub>CH<sub>2</sub>COO), 1.27 (m, 22H), 0.88 (2 t, 3H, CH<sub>3</sub>).

**$^{13}\text{C-NMR}$**  (125 MHz,  $\text{CDCl}_3$ ):  $\delta$  [ppm] = 179.15, 179.07, 134.33, 133.88, 131.64, 131.30, 66.15, 66.10, 46.06, 34.01, 34.01, 32.82, 32.68, 32.03, 32.01, 31.27, 31.21, 29.82, 29.69, 29.68, 29.57, 29.45, 29.37, 29.29, 29.28, 29.26, 29.16, 28.99, 28.79, 27.24, 27.15, 27.07, 24.80, 24.75, 22.82, 22.81, 14.25.

The analytical data corresponds with literature data.<sup>[195]</sup>

#### 9.6.2.2 2-ethylhexyl (*E*)-9+10-(hydroxymethyl)octadec-10+8-enoate



The synthesis was carried out according to GP25. Oleic acid ester (23.7 g, 60 mmol) and paraformaldehyde (4.14 g, 138 mmol) were treated with  $\text{EtAlCl}_2$  (198 mL, 198 mmol). Work-up by vacuum distillation (at  $10^{-3}$  mbar) yielded the product as colorless liquid.

**Yield:** 17.6 g, 69%.

**$^1\text{H-NMR}$**  (500 MHz,  $\text{CDCl}_3$ ):  $\delta$  [ppm] = 5.51 (m, 1H,  $\text{CH}=\text{CHCH}$ ), 5.12 (m, 1H,  $\text{CH}=\text{CHCH}$ ), 3.98 (m, 2H,  $\text{COOCH}_2$ ), 3.51 (m, 1H,  $\text{CH}_2\text{OH}$ ) 3.32 (m, 1H,  $\text{CH}_2\text{OH}$ ), 2.29 (2 t, 2H,  $^3J = 7.5$  Hz,  $\text{CH}_2\text{COO}$ ), 2.12 (m, 1H,  $\text{CH}=\text{CHCH}$ ), 2.02 (m, 2H,  $\text{CH}_2\text{CH}=\text{CH}$ ), 1.61 (m, 2H,  $\text{CH}_2\text{CH}_2\text{COO}$ ), 1.56 (m, 1H,  $\text{OCH}_2\text{CH}$ ), 1.27 (m, 28H), 0.88 (3 t, 9H,  $\text{CH}_3$ ).

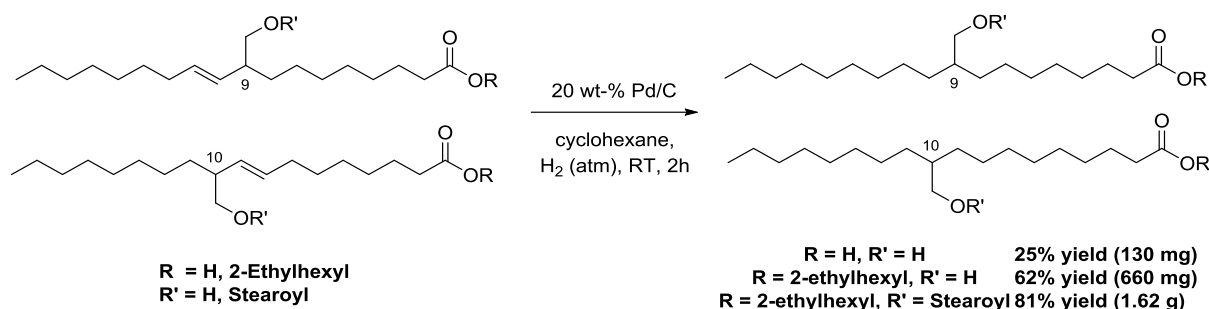
**$^{13}\text{C-NMR}$**  (125 MHz,  $\text{CDCl}_3$ ):  $\delta$  [ppm] = 174.21, 174.18, 134.27, 133.90, 131.58, 131.33, 66.79, 66.77, 66.12, 66.09, 46.09, 38.88, 34.56, 34.54, 32.81, 32.72, 32.02, 31.99, 31.25, 31.23, 30.56, 29.81, 29.67, 29.67, 29.64, 29.46, 29.44, 29.34, 29.28, 29.24, 29.10, 29.06, 28.90, 27.23, 27.18, 25.16, 25.12, 23.93, 23.12, 22.81, 22.80, 14.25, 14.24, 14.19, 11.13.

**GC (FID):** Phenomenex ZB-5MSi, 0.5 ml/min ( $\text{H}_2$ ), Inj. Temp.: 300 °C, Det. Temp.: 350 °C; 300 °C  $\rightarrow$  350 °C (5 °C/min), 350 °C for 5 min;  $R_t = 4.29, 4.53$  min.

**HRMS (ESI):** calcd for  $\text{C}_{27}\text{H}_{52}\text{O}_3\text{Na}$  [ $\text{M}+\text{Na}$ ] $^+$ : 447.3809, found: 447.3813.

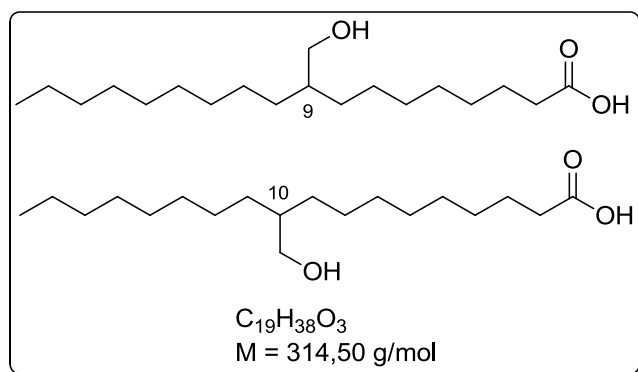
**IR (neat)** [ $\text{cm}^{-1}$ ]: 2923, 2854, 1733, 1462, 1379, 1171, 1032, 969.

### 9.6.3 GENERAL WORKING PROCEDURE 26 (GP26): PALLADIUM CATALYZED C=C-HYDROGENATION OF OLEIC ACID DERIVATIVES



The unsaturated acid (1.0 eq.) or 2-ethylhexylester (1.0 eq.) of the oleic acid derivatives was dissolved in cyclohexane under a  $\text{H}_2$ -atmosphere. Palladium on carbon (Pd/C, 10% Pd, 20 wt.-%) was added. The reaction mixture was stirred at room temperature for two hours and afterwards filtered through a 0.2  $\mu\text{m}$  PTFE-Filter. Column chromatography yielded the product as colorless oil.

#### 9.6.3.1 9+10-(hydroxymethyl)octadecanoic acid



The synthesis was carried out according to GP26. (*E*)-9+10-(hydroxymethyl)octadec-10+8-enoic acid (450 mg, 1.44 mmol) was dissolved in 25 mL cyclohexane under  $\text{H}_2$  atmosphere. Pd/C (90 mg) was added. Work-up and column chromatography (cyclohexane/ethyl acetate 1:2, v/v) yielded the product as colorless oil.

**Yield:** 130 mg, 25%.

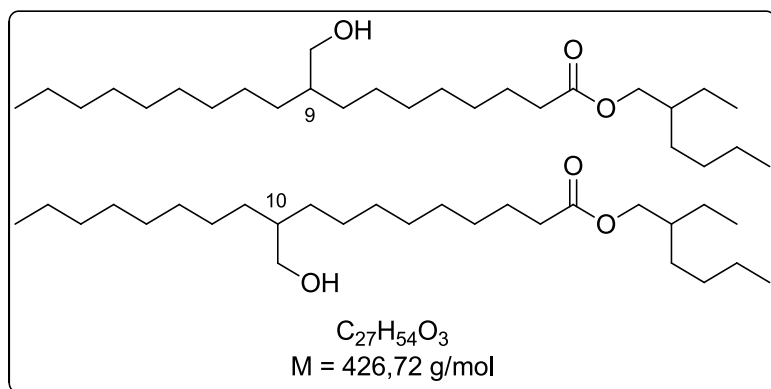
**$^1\text{H-NMR}$**  (500 MHz,  $\text{CDCl}_3$ ):  $\delta$  [ppm] = 3.53 (d, 2H,  $^3J = 5.5 \text{ Hz}$   $\text{CH}_2\text{OH}$ ), 2.35 (t, 2H,  $^3J = 7.5 \text{ Hz}$ ,  $\text{CH}_2\text{COO}$ ), 1.63 (qi, 2H,  $^3J = 7.3 \text{ Hz}$ ,  $\text{CH}_2\text{CH}_2\text{COO}$ ), 1.45 (m, 1H,  $\text{HOCH}_2\text{CH}$ ), 1.27 (m, 36H), 0.88 (t, 3H,  $^3J = 6.9 \text{ Hz}$ ,  $\text{CH}_3$ ).

**$^{13}\text{C-NMR}$**  (125 MHz,  $\text{CDCl}_3$ ):  $\delta$  [ppm] = 179.62, 65.81, 65.79, 40.59, 34.15, 34.14, 32.05, 31.07, 31.02, 30.99, 30.22, 30.05, 29.91, 29.80, 29.78, 29.76, 29.49, 29.30, 29.15, 29.13, 27.04, 26.92, 26.88, 24.80, 22.83, 14.27.

**HRMS** (ESI): calcd for  $\text{C}_{19}\text{H}_{38}\text{O}_3\text{Na}$  [ $\text{M}+\text{Na}$ ] $^+$ : 337.2713, found: 337.2717.

**IR** (neat) [ $\text{cm}^{-1}$ ]: 2913, 2848, 1699, 1469, 1185, 972, 719.

## 9.6.3.2 2-ethylhexyl 9+10-(hydroxymethyl)octadecanoate



The synthesis was carried out according to GP26. 2-ethylhexyl (*E*)-9+10-(hydroxymethyl)octadec-10+8-enoate (1.06 g, 2.50 mmol) was dissolved in 50 mL cyclohexane under  $H_2$  atmosphere. Pd/C (212 mg) was added. Work-up and column chromatography (cyclohexane/ethyl acetate 7:1, v/v) yielded the product as colorless oil.

**Yield:** 660 mg, 62%.

**$^1H$ -NMR** (500 MHz,  $CDCl_3$ ):  $\delta$  [ppm] = 3.97 (m, 2H,  $COOCH_2$ ), 3.54 (d, 2H,  $^3J = 5.5 \text{ Hz}$   $CH_2OH$ ), 2.29 (t, 2H,  $^3J = 7.5 \text{ Hz}$ ,  $CH_2COO$ ), 1.61 (m, 2H,  $CH_2CH_2COO$ ), 1.56 (m, 1H,  $OCH_2CH$ ), 1.27 (m, 36H), 0.89 (3 t, 9H,  $CH_3$ ).

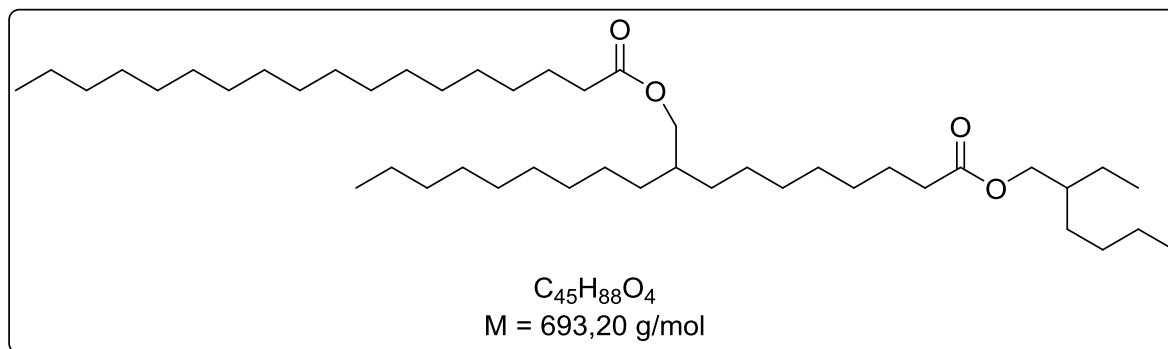
**$^{13}C$ -NMR** (125 MHz,  $CDCl_3$ ):  $\delta$  [ppm] = 174.27, 174.26, 66.79, 65.85, 65.83, 40.67, 38.90, 34.60, 34.58, 32.05, 31.08, 31.07, 31.05, 30.57, 30.22, 30.14, 30.02, 29.81, 29.78, 29.76, 29.59, 29.49, 29.41, 29.40, 29.30, 29.07, 27.05, 27.01, 26.97, 25.19, 23.95, 23.13, 22.83, 14.27, 14.20, 11.15.

**GC (FID):** Phenomenex ZB-5MSi, 0.5 ml/min ( $H_2$ ), Inj. Temp.: 300 °C, Det. Temp.: 350 °C; 300 °C  $\rightarrow$  350 °C (5 °C/min), 350 °C for 5 min;  $R_t = 4.61 \text{ min}$ .

**HRMS** (ESI): calcd for  $C_{27}H_{54}O_3Na$   $[M+Na]^+$ : 449.3965, found: 449.3975.

**IR** (neat)  $[cm^{-1}]$ : 2921, 2853, 1736, 1459, 1171, 1031.

## 9.6.3.3 2-ethylhexyl 9+10-((stearoyloxy)methyl)octadecanoate



The synthesis was carried out according to GP26. 2-ethylhexyl (*E*)-9-((stearoyloxy)methyl)octadec-10-enoate (2.00 g, 2.9 mmol) was dissolved in 50 mL cyclohexane under  $H_2$  atmosphere. Pd/C (400 mg) was added. Work-up and column chromatography (cyclohexane/ethyl acetate 15:1, v/v) yielded the product as colorless oil.

**Yield:** 1.62 g, 81%.

**$^1H$ -NMR** (500 MHz,  $CDCl_3$ ):  $\delta$  [ppm] = 3.97 (m, 4H,  $COOCH_2$ ), 2.28 (t, 4H,  $^3J = 7.5 \text{ Hz}$ ,  $CH_2COO$ ), 1.61 (m, 6H,  $CH_2CH_2COO$ ), 1.25 (m, 62H), 0.89 (m, 12H,  $CH_3$ ).

**$^{13}C$ -NMR** (125 MHz,  $CDCl_3$ ):  $\delta$  [ppm] = 174.22, 174.16, 67.13, 66.75, 38.91, 37.46, 34.60, 34.58, 32.07, 31.42, 30.58, 30.12, 30.06, 29.94, 29.85, 29.81, 29.76, 29.71, 29.65, 29.63, 29.58, 29.46, 29.43, 29.39, 29.34, 29.32, 29.07, 26.85, 25.21, 23.95, 23.12, 22.84, 14.25, 14.18, 11.13.

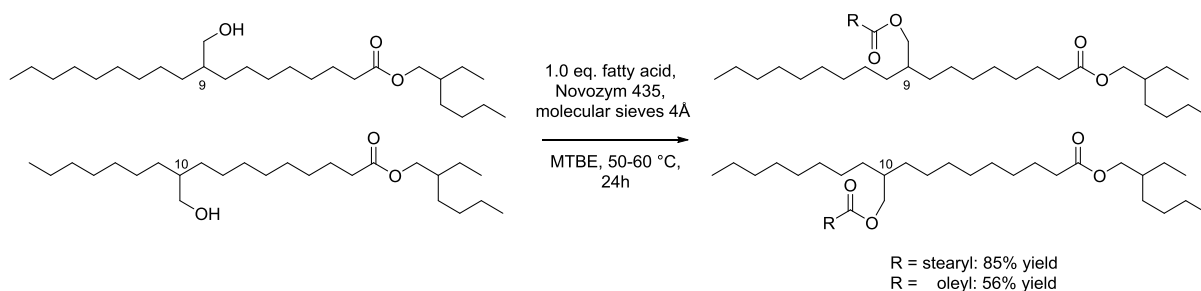
**GC (FID):** Phenomenex ZB-5MSi, 0.5 ml/min ( $H_2$ ), Inj. Temp.: 300 °C, Det. Temp.: 350 °C; 300 °C  $\rightarrow$  350 °C (5 °C/min), 350 °C for 5 min;  $R_t = 14.4 \text{ min}$ .

**HRMS** (ESI): calcd for  $C_{45}H_{88}O_4Na$  [ $M+Na$ ] $^+$ : 715.6575, found: 715.6573.

**IR** (neat) [ $cm^{-1}$ ]: 2921, 2852, 1736, 1463, 1169.

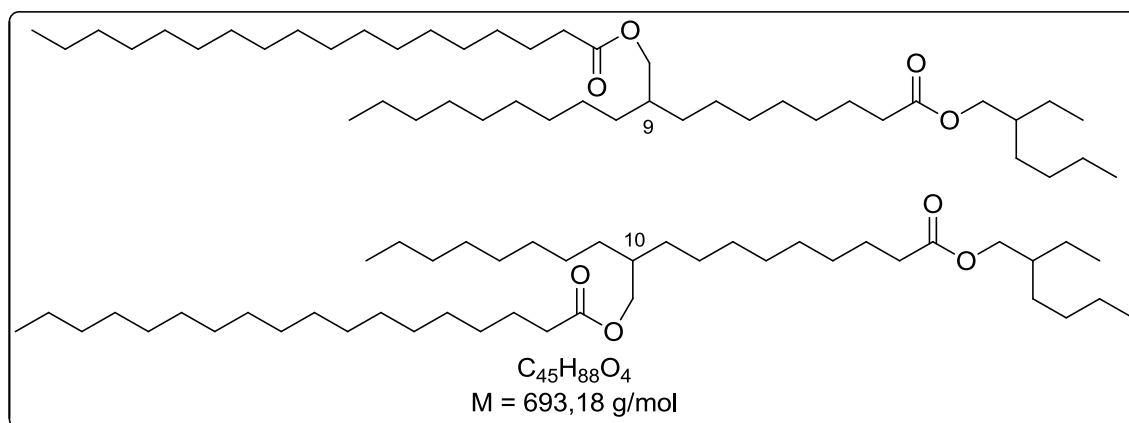


### 9.6.4 GENERAL OPERATING PROCEDURE 27 (GP27): BIOCATALYTIC ESTERIFICATION OF FATTY ACIDS WITH HYDROXYMETHYLATED OLEIC ACID DERIVATES TO ESTOLIDE DIMERS



The hydroxymethylated 2-Ethylhexyl oleate (1.0 eq.) was mixed with a fatty acid (1.0 eq.) and dissolved in MTBE. Novozym 435 (CAL-B, 30 mg/mmol) and molecular sieves 4Å (120 mg/mmol) were added. The reaction mixture was stirred for 24 hours at 50 or 60 °C. Filtration through a 0.2 µM PTFE-Filter was conducted afterwards. Removing the solvent *in vacuo* yielded the product as colorless oil.

#### 9.6.4.1 2-ethylhexyl 9+10-((stearoyloxy)methyl)octadecanoate



The synthesis was carried out according to GP27. 2-ethylhexyl 9+10-(hydroxymethyl)octadecanoate (51.7 mg, 100 µmol) and stearic acid (28.4 mg, 100 µmol) were dissolved in 50 µL MTBE. Novozym 435 (3 mg) and molecular sieves 4Å (12 mg) were added at 50 °C. Work-up yielded the product as colorless oil.

**Yield:** 58 mg, 85%.

**<sup>1</sup>H-NMR** (500 MHz, CDCl<sub>3</sub>): δ [ppm] = 3.97 (m, 4H, COOCH<sub>2</sub>), 2.28 (t, 4H, <sup>3</sup>J = 7.5 Hz, CH<sub>2</sub>COO), 1.61 (m, 6H, CH<sub>2</sub>CH<sub>2</sub>COO), 1.25 (m, 62H), 0.89 (m, 12H, CH<sub>3</sub>).

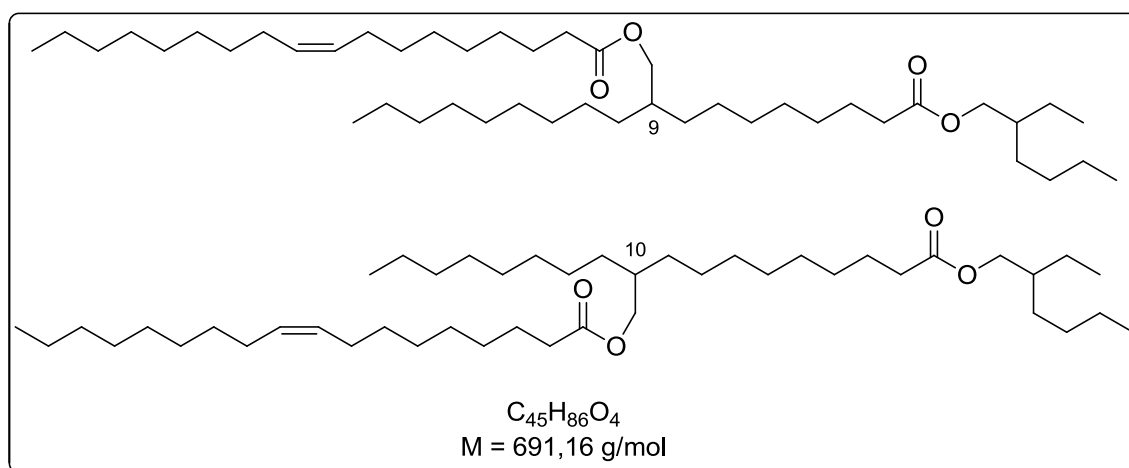
**<sup>13</sup>C-NMR** (125 MHz, CDCl<sub>3</sub>): δ [ppm] = 174.22, 174.16, 67.13, 66.75, 38.91, 37.46, 34.60, 34.58, 32.07, 31.42, 30.58, 30.12, 30.06, 29.94, 29.85, 29.81, 29.76, 29.71, 29.65, 29.63, 29.58, 29.46, 29.43, 29.39, 29.34, 29.32, 29.07, 26.85, 25.21, 23.95, 23.12, 22.84, 14.25, 14.18, 11.13.

**GC (FID):** Phenomenex ZB-5MSi, 0.5 ml/min (H<sub>2</sub>), Inj. Temp.: 300 °C, Det. Temp.: 350 °C; 300 °C -> 350 °C (5 °C/min), 350 °C for 5 min; R<sub>t</sub> = 14.4 min.

**HRMS** (ESI): calcd for  $C_{45}H_{88}O_4Na$   $[M+Na]^+$ : 715.6575, found: 715.6573.

**IR** (neat)  $[cm^{-1}]$ : 2921, 2852, 1736, 1463, 1169.

#### 9.6.4.2 2-(8-((2-ethylhexyl)oxy)-8-oxooctyl)undecyl oleate and 11-((2-ethylhexyl)oxy)-2-octyl-11-oxoundecyl oleate



The synthesis was carried out according to GP27. 2-ethylhexyl 9+10-(hydroxymethyl)octadecanoate (51.7 mg, 100  $\mu$ mol) and oleic acid (28.2 mg, 100  $\mu$ mol) were mixed with Novozym 435 (3 mg) and molecular sieves 4 $\text{\AA}$  (12 mg) and stirred at 60  $^{\circ}C$ . Work-up yielded the product as colorless oil.

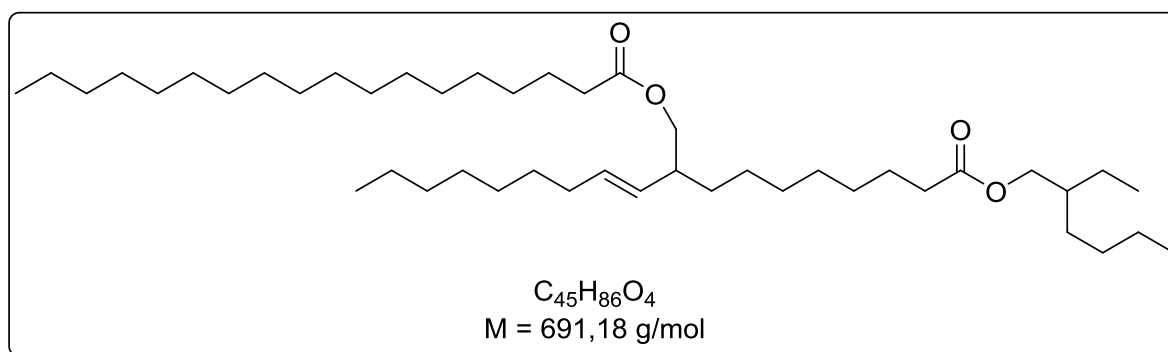
**Yield:** 39 mg, 56%.

**$^1H$ -NMR** (500 MHz,  $CDCl_3$ ):  $\delta$  [ppm] = 5.34 (m, 2H,  $CH=CH$ ), 3.98 (m, 2H,  $COOCH_2$ ), 3.95 (m, 2H,  $COOCH_2$ ), 2.29 (2 t, 4H,  $^3J = 7.4$  Hz,  $CH_2COO$ ), 1.61 (m, 4H,  $CH_2CH_2COO$ ), 1.56 (m, 2H,  $OCH_2CH$ ), 1.27 (m, 58H), 0.89 (4 t, 12H,  $CH_3$ ).

**MS (ESI):**  $m/z = 691.5$   $[M+H]^+$ .

**IR** (neat)  $[cm^{-1}]$ : 2959, 2926, 2856, 1736, 1257, 1011, 865, 790, 700.

## 9.6.4.3 2-ethylhexyl 9 und 10-((stearoyloxy)methyl)octadec-8 und 10-enoate



2-ethylhexyl (*E*)-9+10-(hydroxymethyl)octadec-10+8-enoate (10.0 g, 23.5 mmol) was mixed with a stearic acid (6.70 g, 23.5 mmol) and heated to 70 °C, upon which the stearic acid melted. Novozym 435 (CAL-B, 706 mg, 30 mg/mmol) and molecular sieves 4Å (3.3 g, 120 mg/mmol) were added. The reaction mixture was stirred for 24 hours at 70 °C. Filtration through a 0.2 µm PTFE-Filter was conducted afterwards. Removing the solvent *in vacuo* and filtration of silica (cyclohexane/ethyl acetate 15:1, v/v) yielded the product as colorless oil.

**Yield:** 11.9 g, 73%.

**<sup>1</sup>H-NMR** (500 MHz, CDCl<sub>3</sub>): δ [ppm] = 5.40 (m, 1H, CH=CH), 5.14 (m, 1H, CH=CH), 3.98 (m, 3H, COOCH<sub>2</sub>), 2.29 (m, 4H, CH<sub>2</sub>COO), 1.97 (m, 2H, CHCH<sub>2</sub>) 1.61 (m, 5H, CH<sub>2</sub>CH<sub>2</sub>COO + OCH<sub>2</sub>CH), 1.27 (m, 60H), 0.88 (4 t, 12H, CH<sub>3</sub>).

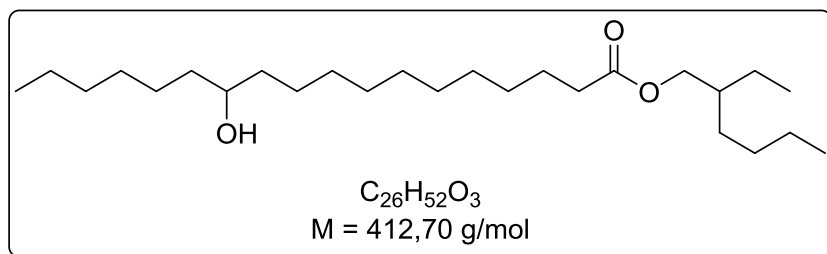
**GC (FID):** Phenomenex ZB-5MSi, 0.5 ml/min (H<sub>2</sub>), Inj. Temp.: 300 °C, Det. Temp.: 350 °C; 300 °C -> 350 °C (5 °C/min), 350 °C for 5 min; R<sub>t</sub> = 14.1 min.

**HRMS** (ESI): calcd for C<sub>45</sub>H<sub>86</sub>O<sub>4</sub>Na [M+Na]<sup>+</sup>: 713.6418, found: 713.6419.

**IR** (neat) [cm<sup>-1</sup>]: 2959, 2926, 2856, 1736, 1257, 1011, 865, 790, 700.

## 9.6.5 SYNTHESIS OF 2-ETHYLHEXYL 12-(STEAROYLOXY)OCTADECANOATE STARTING FROM 12-HYDROXYSTEARIC ACID

### 9.6.5.1 2-ethylhexyl 12-hydroxyoctadecanoate



12-hydroxystearic acid (21.3 g, 70.9 mmol) was mixed with 2-ethylhexanol (11.1 mL, 70.9 mmol) and the reaction mixture was heated to 75 °C, at which 12-hydroxystearic acid melted. Afterwards, Novozym 435 (2.13 g, 30 mg/mmol Substrate) and molecular sieves 4Å (8.51 g) were added and the reaction mixture was stirred for five hours at 75 °C. The reaction mixture was diluted with cyclohexane and filtered over a 0.2 µm PTFE membrane, yielding the crude product as colorless oil. The crude product was purified *via* vacuum distillation ( $10^{-2}$  mbar) to yield 2-ethylhexyl 12-hydroxyoctadecanoate as colorless oil.

**Yield:** 21.5 g, 73%.

**<sup>1</sup>H-NMR** (500 MHz, CDCl<sub>3</sub>): δ [ppm] = 3.98 (m, 2H, COOCH<sub>2</sub>), 3.57 (m, 1H, OH), 2.28 (t, 2H, <sup>3</sup>J = 7.4 Hz, CH<sub>2</sub>COO), 1.61 (m, 2H, CH<sub>2</sub>CH<sub>2</sub>COO), 1.56 (m, 1H, OCH<sub>2</sub>CH), 1.28 (m, 36H), 0.88 (4 t, 9H, CH<sub>3</sub>).

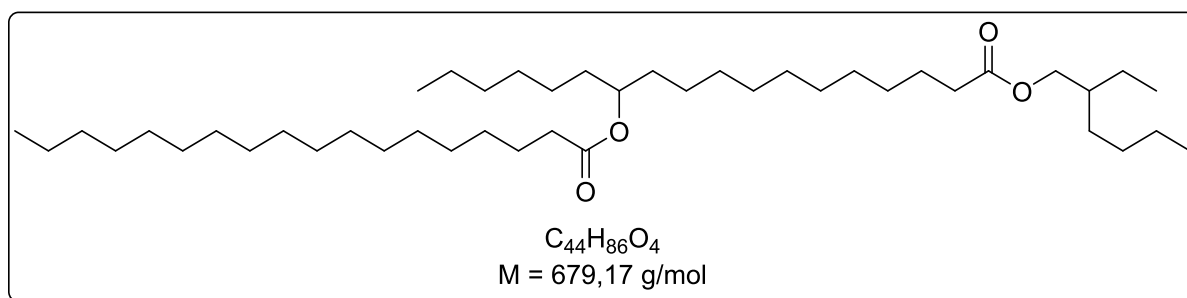
**<sup>13</sup>C-NMR** (125 MHz, CDCl<sub>3</sub>): δ [ppm] = 174.24, 72.12, 66.77, 38.90, 37.64, 37.63, 34.59, 31.99, 30.57, 29.83, 29.73, 29.66, 29.58, 29.53, 29.40, 29.30, 29.07, 25.79, 25.76, 25.19, 23.94, 23.12, 22.76.

**GC (FID):** Phenomenex ZB-5MSi, 0.5 ml/min (H<sub>2</sub>), Inj. Temp.: 300 °C, Det. Temp.: 350 °C; 300 °C -> 350 °C (5 °C/min), 350 °C for 5 min; R<sub>t</sub> = 3.56 min.

**HRMS** (ESI): calcd for C<sub>26</sub>H<sub>52</sub>O<sub>3</sub>Na [M+Na]<sup>+</sup>: 435.3809, found: 435.3800.

**IR** (neat) [cm<sup>-1</sup>]: 2922, 2853, 1736, 1463, 1246, 1172.

## 9.6.5.2 2-ethylhexyl 12-(stearoyloxy)octadecanoate



2-ethylhexyl 12-hydroxyoctadecanoate (39.3 g, 96.7 mmol, distributed into four equal parts) was dissolved in 100 mL pyridine each. Stearoyl chloride (33.7 mL, 99.8 mmol, distributed into four equal parts) was slowly added and the resulting orange reaction mixture was stirred at room temperature for 14 hours. Afterwards, two reactions were combined and were treated with 100 mL H<sub>2</sub>O and 100 mL concentrated HCl each. After washing of the organic phase, the phases were separated and the aqueous phase was extracted additional two times with 100 mL cyclohexane each. The combined extracts were carefully washed with 100 mL saturated sodium bicarbonate solution and the organic phases were dried over MgSO<sub>4</sub>. and freed from the solvent *in vacuo*. The crude product was purified *via* column chromatography (cyclohexane/ethyl acetate 15:1, v/v) to yield the product as pale yellow oil.

**Yield:** 36.0 g, 54%.

**<sup>1</sup>H-NMR** (500 MHz, CDCl<sub>3</sub>): δ [ppm] = 4.86 (qi, 1H, <sup>3</sup>J = 6.1 Hz CH<sub>2</sub>CHOOCCH<sub>2</sub>), 3.98 (m, 2H, COOCH<sub>2</sub>), 2.29 (2t, 4H, <sup>3</sup>J = 7.6 Hz, CH<sub>2</sub>COO), 1.61 (m, 4H, CH<sub>2</sub>CH<sub>2</sub>COO), 1.56 (m, 1H, OCH<sub>2</sub>CH), 1.49 (m, 4H, CH<sub>2</sub>CH(O)CH<sub>2</sub>), 1.28 (m, 58H), 0.88 (m, 12H, CH<sub>3</sub>).

**<sup>13</sup>C-NMR** (125 MHz, CDCl<sub>3</sub>): δ [ppm] = 174.23, 173.83, 74.19, 66.77, 38.91, 34.90, 34.60, 34.32, 32.08, 31.91, 30.58, 29.85, 29.81, 29.78, 29.69, 29.68, 29.61, 29.52, 29.47, 29.43, 29.36, 29.35, 29.33, 29.08, 25.48, 25.43, 25.34, 25.21, 23.96, 23.13, 22.84, 22.73, 14.27, 14.21, 14.19, 11.14.

**GC (FID):** Phenomenex ZB-5MSi, 0.5 ml/min (H<sub>2</sub>), Inj. Temp.: 300 °C, Det. Temp.: 350 °C; 300 °C -> 350 °C (5 °C/min), 350 °C for 5 min; R<sub>t</sub> = 13.1 min.

**HRMS** (ESI): calcd for C<sub>44</sub>H<sub>86</sub>O<sub>4</sub>Na [M+Na]<sup>+</sup>: 701.6418, found: 701.6423.

**IR** (neat) [cm<sup>-1</sup>]: 2921, 2852, 1733, 1463, 1172.



## 10 LIST OF ABBREVIATIONS

2-Me-THF = 2-methyltetrahydrofuran

6-APA = (+)-6-aminopenicillanic acid

ADA = Alkylated diphenylamines

ADH = Alcohol dehydrogenase

AI = Auto induction

ATP = Adenosine triphosphate

BHT = Butylated hydroxytoluene

Bn = Benzyl

Boc<sub>2</sub>O = Di-*tert*-butyl dicarbonate

BWW = Bio wet weight

CAL-B = *Candida Antarctica* Lipase B

CDG = 7-carboxy-7-deazaguanine

CHN analysis = Elemental analysis

CLEAs = Crosslinked enzyme aggregates

CLECs = Crosslinked enzyme crystals

CV = Column volume

CYP450 = Cytochrome P450

d = doublet

DBU = 1,8-Diazabicyclo[5.4.0]undec-7-ene

*de* = Diastereomeric excess

DMAc = Dimethylacetamide

DMC = Dimethyl carbonate

DMF = Dimethylformamide

DMSO = Dimethyl sulfoxide

DPP-4 = Dipeptidyl peptidase IV

DVB = Divinylbenzene

*E. coli* = Escherichia coli

EA = Elemental analysis

*ee* = Enantiomeric excess

EN = Estolide number

EPR = Electron paramagnetic resonance

ERED = Ene reductase

ESI = Electrospray ionization

EtOH = Ethanol  
FID = Flame ionization detector  
FTIR = Fourier-transform infrared  
GC = Gas chromatography  
GDH = Glucose dehydrogenase  
HMDA = Hexamethylenediamine  
HMDS = Hexamethyldisilazane  
HPLC = High-performance liquid chromatography  
HRMS = High-resolution mass spectrometry  
*i*PrOH = 2-Propanol  
IPTG = Isopropyl  $\beta$ -D-1-thiogalactopyranoside  
IR = Infrared  
*J* = Coupling constant [Hz]  
 $k_{\text{cat}}$  = Catalytic rate  
 $K_{\text{m}}$  = Michaelis constant  
KPB = Potassium phosphate buffer  
LB = Lysogeny broth  
LDA = Lithium diisopropylamide  
*m* = Multiplet  
Mb = Myoglobin  
MeCN = Acetonitrile  
MeOH = Methanol  
MM = Molecular mechanics  
MP = Melting point  
MS = Mass spectrometry  
MTBE = Methyl *tert*-butyl ether  
NAD(P) / NAD(P)H = Nicotinamide adenine dinucleotide (phosphate)  
NiNTA = Nickel nitrilotriacetic acid  
NMR = Nuclear magnetic resonance  
NP-HPLC = Normal phase high-performance liquid chromatography  
OD<sub>600</sub> = Optical density at 600 nm  
OECD = Organisation for Economic Co-operation and Development  
Oxd = Aldoxime dehydratase  
OxdA = Aldoxime dehydratase from *Pseudomonas chlororaphis* B23  
OxdB = Aldoxime dehydratase from *Bacillus sp.* OxB-1  
OxdFG = Aldoxime dehydratase from *Fusarium graminearum* MAFF305135



OxdK = Aldoxime dehydratase from *Pseudomonas sp.* K-9  
OxdRE = Aldoxime dehydratase from *Rhodococcus sp.* N-771  
OxdRG = Aldoxime dehydratase from *Rhodococcus globerulus* A-4  
 $p$  = Saturation level  
PAOx = Phenylacetaldehyde oxime  
PDMS = Polydimethylsiloxane  
PLP = Pyridoxal phosphate  
PMMA = Poly(methyl methacrylate)  
PPC = Propylene carbonate  
ppm = Parts per million  
PPOx = 2-phenylpropionaldoxime  
preQ<sub>6</sub> = 7-cyano-7-deazaguanine  
PTFE = Polytetrafluoroethylene  
PU = Polyurethane  
 $q$  = Quartet  
 $q_i$  = Quintet  
QM = Quantum mechanics  
RP-HPLC = Reversed phase high-performance liquid chromatography  
RPVOT = Rotating Pressure Vessel Oxidation Stability Test  
 $R_t$  = Retention time  
RT = Room temperature  
 $s$  = Singulet  
SDS-PAGE = Sodium dodecyl sulfate–polyacrylamide gel electrophoresis  
sept = Septet  
sx = Sextet  
 $t$  = Triplet  
TB = Terrific broth  
TBAI = Tetrabutylammonium iodide  
TBSCl = *tert*-butyldimethylsilyl chloride  
TEMPO = (2,2,6,6-Tetramethylpiperidin-1-yl)oxyl  
THF = Tetrahydrofuran  
TLC = Thin-layer chromatography  
TMEDA = Tetramethylethylenediamine  
TOF = Turnover frequency  
TON = Turnover number  
ToyM = Nitrile synthetase from *Streptomyces risomus*

TRIS = Tris(hydroxymethyl)aminomethane

TTN = Total turnover number

U = Unit (enzyme activity)

UV = Ultraviolet radiation/light

v/v = Volume ratio

Vis = Visible radiation/light

$v_{\text{Max}}$  = Maximum reaction rate

YgjM = Ene reductase from *Bacillus subtilis*

$\delta$  = Chemical shift (in ppm)

# 11 REFERENCES

- [1] M. T. Reetz, *J. Am. Chem. Soc.* **2013**, *135*, 12480.
- [2] a) U. T. Bornscheuer, *Angew. Chem. Int. Ed.* **2016**, *55*, 4372; b) M. Hönig, P. Sondermann, N. J. Turner, E. M. Carreira, *Angew. Chem. Int. Ed.* **2017**, *56*, 8942.
- [3] P. J. Dunn, *Chem. Soc. Rev.* **2012**, *41*, 1452.
- [4] G. A. Strohmeier, H. Pichler, O. May, M. Gruber-Khadjawi, *Chem. Rev.* **2011**, *111*, 4141.
- [5] H. Gröger, K. Drauz, O. May (Eds.) *Enzyme catalysis in organic synthesis*, Wiley-VCH, Weinheim, New York, **2012**.
- [6] R. Yuryev, A. Liese, *ChemCatChem* **2010**, *2*, 103.
- [7] L. Poppe, B. G. Vértessy, *ChemBioChem* **2018**, *19*, 284.
- [8] R. A. Sheldon, S. van Pelt, *Chem. Soc. Rev.* **2013**, *42*, 6223.
- [9] C. M. Clouthier, J. N. Pelletier, *Chem. Soc. Rev.* **2012**, *41*, 1585.
- [10] R. D. Schmid, R. Hammelehle, *Taschenatlas der Biotechnologie und Gentechnik*, Wiley-VCH, Weinheim, **2006**.
- [11] C. Elschenbroich, *Organometallchemie*, Vieweg+Teubner Verlag / GWV Fachverlage GmbH Wiesbaden, Wiesbaden, **2008**.
- [12] a) F. H. Arnold, *Angew. Chem. Int. Ed.* **2018**, *57*, 4143; b) J. L. Porter, R. A. Rusli, D. L. Ollis, *ChemBioChem* **2016**, *17*, 197.
- [13] R. A. Sheldon, P. C. Pereira, *Chem. Soc. Rev.* **2017**, *46*, 2678.
- [14] H.-J. Joosten, "Bio-Product", can be found under <https://3dm.bio-product.nl/>.
- [15] M. D. Truppo, *ACS Med. Chem. Lett.* **2017**, *8*, 476.
- [16] P. Tufvesson, J. Lima-Ramos, M. Nordblad, J. M. Woodley, *Org. Process Res. Dev.* **2011**, *15*, 266.
- [17] a) R. A. Sheldon, J. M. Woodley, *Chem. Rev.* **2018**, *118*, 801; b) R. A. Sheldon, *Green Chem* **2017**, *19*, 18; c) P. Anastas, N. Eghbali, *Chem. Soc. Rev.* **2010**, *39*, 301.
- [18] a) D. Prat, A. Wells, J. Hayler, H. Sneddon, C. R. McElroy, S. Abou-Shehada, P. J. Dunn, *Green Chem* **2016**, *18*, 288; b) C. J. Clarke, W.-C. Tu, O. Levers, A. Bröhl, J. P. Hallett, *Chem. Rev.* **2018**, *118*, 747.
- [19] a) J. H. Schrittwieser, S. Velikogne, M. Hall, W. Kroutil, *Chem. Rev.* **2017**; b) F. Rudroff, M. D. Mihovilovic, H. Gröger, R. Snajdrova, H. Iding, U. T. Bornscheuer, *Nat Catal* **2018**, *1*, 12; c) H. Groger, W. Hummel, *Curr Opin Chem Biol* **2014**, *19*, 171.
- [20] D. Thiel, D. Doknić, J. Deska, *Nat. Commun.* **2014**, *5*, 5278.
- [21] E. Fernández-Fueyo, S. H. H. Younes, S. van Rootselaar, R. W. M. Aben, R. Renirie, R. Wever, D. Holtmann, Rutjes, Floris P. J. T., F. Hollmann, *ACS Catal.* **2016**, *6*, 5904.
- [22] a) K. Zhang, S. El Damaty, R. Fasan, *J. Am. Chem. Soc.* **2011**, *133*, 3242; b) R. Fasan, *ACS Catal.* **2012**, *2*, 647; c) K. Zhang, B. M. Shafer, M. D. Demars, H. A. Stern, R. Fasan, *J. Am. Chem. Soc.* **2012**, *134*, 18695; d) J. N. Kolev, K. M. O'Dwyer, C. T. Jordan, R. Fasan, *ACS Chem. Biol.* **2014**, *9*, 164; e) V. Tyagi, H. Alwaseem, K. M. O'Dwyer, J. Ponder, Q. Y. Li, C. T. Jordan, R. Fasan, *Bioorg. Med. Chem.* **2016**, *24*, 3876.
- [23] R. Singh, M. Bordeaux, R. Fasan, *ACS Catal.* **2014**, *4*, 546.
- [24] M. Bordeaux, R. Singh, R. Fasan, *Bioorg. Med. Chem.* **2014**, *22*, 5697.
- [25] G. Sreenilayam, E. J. Moore, V. Steck, R. Fasan, *Adv. Synth. Catal.* **2017**, *359*, 2076.
- [26] G. Sreenilayam, R. Fasan, *Chem. Commun.* **2015**, *51*, 1532.
- [27] V. Tyagi, R. B. Bonn, R. Fasan, *Chem. Sci.* **2015**, *6*, 2488.

- [28] V. Tyagi, G. Sreenilayam, P. Bajaj, A. Tinoco, R. Fasan, *Angew. Chem. Int. Ed.* **2016**, *55*, 13562.
- [29] M. Bordeaux, V. Tyagi, R. Fasan, *Angew. Chem. Int. Ed.* **2015**, *54*, 1744.
- [30] P. Bajaj, G. Sreenilayam, V. Tyagi, R. Fasan, *Angew. Chem. Int. Ed.* **2016**, *55*, 16110.
- [31] A. Tinoco, V. Steck, V. Tyagi, R. Fasan, *J. Am. Chem. Soc.* **2017**, *139*, 5293.
- [32] K. J. Butcher, S. M. Denton, S. E. Field, A. T. Gillmore, G. W. Harbottle, R. M. Howard, D. A. Laity, C. J. Ngono, B. A. Pibworth, *Org. Process Res. Dev.* **2011**, *15*, 1192.
- [33] S. B. J. Kan, R. D. Lewis, K. Chen, F. H. Arnold, *Science* **2016**, *354*, 1048.
- [34] S. B. J. Kan, X. Huang, Y. Gumulya, K. Chen, F. H. Arnold, *Nature* **2017**, *552*, 132.
- [35] K. Köninger, Á. Gómez Baraibar, C. Mügge, C. E. Paul, F. Hollmann, M. M. Nowaczyk, R. Kourist, *Angew. Chem. Int. Ed.* **2016**, *55*, 5582.
- [36] J. Löwe, A. Siewert, A.-C. Scholpp, L. Wobbe, H. Gröger, *Sci. Rep.* **2018**, *8*, 10436.
- [37] T. Betke, J. Higuchi, P. Rommelmann, K. Oike, T. Nomura, Y. Kato, Y. Asano, H. Gröger, *ChemBioChem* **2018**, *19*, 768.
- [38] B. Elvers, F. Ullmann (Eds.) *Ullmann's encyclopedia of industrial chemistry*, Wiley-VCH, Weinheim, **2011**.
- [39] H.-J. Arpe, *Industrielle organische Chemie. Bedeutende Vor- und Zwischenprodukte*, Wiley-VCH, Weinheim, **2007**.
- [40] a) E. D. Villhauer **2000**; b) N. Kato, M. Oka, T. Murase, M. Yoshida, M. Sakairi, M. Yakufu, S. Yamashita, Y. Yasuda, A. Yoshikawa, Y. Hayashi et al., *Org. Med. Chem. Lett.* **2011**, *1*, 7.
- [41] L. Pellegatti, J. Sedelmeier, *Org. Process Res. Dev.* **2015**, *19*, 551.
- [42] E. B. Villhauer, J. A. Brinkman, G. B. Naderi, B. F. Burkey, B. E. Dunning, K. Prasad, B. L. Mangold, M. E. Russell, T. E. Hughes, *J. Med. Chem.* **2003**, *46*, 2774.
- [43] E. B. Villhauer, WO0034241 (A1), **1999**.
- [44] F. F. Fleming, L. Yao, P. C. Ravikumar, L. Funk, B. C. Shook, *J. Med. Chem.* **2010**, *53*, 7902.
- [45] T. C. Vu, D. B. Brzozowski, R. Fox, J. D. Godfrey, JR, R. L. Hanson, S. V. Kolotuchin, J. A. Mazzullo, JR, R. N. Patel, J. Wang, K. Wong et al., WO2004052850 (A2), **2003**.
- [46] S. A. Savage, G. S. Jones, S. Kolotuchin, S. A. Ramrattan, T. Vu, R. E. Waltermire, *Org. Process Res. Dev.* **2009**, *13*, 1169.
- [47] Pharmaceutical Technology, "The world's top selling diabetes drugs", can be found under <http://www.pharmaceutical-technology.com/features/featurethe-worlds-top-selling-diabetes-drugs-4852441/>, **2016**.
- [48] K. V. Raghavan, B. M. Reddy (Eds.) *Industrial catalysis and separations. Innovations for process intensification*, Apple Academic Press, Toronto, New Jersey, **2015**.
- [49] a) H. Gröger, *Chem. Rev.* **2003**, *103*, 2795; b) E. N. Jacobsen (Ed.) *Comprehensive asymmetric catalysis*, Springer, Berlin, **1999**.
- [50] L. Martíková, A. Stolz, F. van Rantwijk, N. D'Antona, D. Brady, L. G. Otten in *Cascade Biocatalysis Integrating Stereoselective and Environmentally Friendly Reactions* (Eds.: S. Riva, W.-D. Fessner), Wiley, Hoboken, **2014**, pp. 249–270.
- [51] L. Martinkova, V. Vejvoda, V. Kren, *Journal of Biotechnology* **2008**, *133*, 318.
- [52] Y. Kato, R. Ooi, Y. Asano, *Appl. Environ. Microbiol.* **2000**, *66*, 2290.
- [53] Y. Asano, Y. Kato, *FEMS Microbiol Lett* **1998**, *158*, 185.

- [54] H. Sawai, H. Sugimoto, Y. Kato, Y. Asano, Y. Shiro, S. Aono, *J. Biol. Chem.* **2009**, *284*, 32089.
- [55] J. Nomura, H. Hashimoto, T. Ohta, Y. Hashimoto, K. Wada, Y. Naruta, K.-I. Oinuma, M. Kobayashi, *Proc. Natl. Acad. Sci. U.S.A.* **2013**, *110*, 2810.
- [56] A. Börner, R. Franke, *Hydroformylation. Fundamentals, processes, and applications in organic synthesis*, Wiley-VCH Verlag GmbH & Co, Weinheim, **2016**.
- [57] D. S. Bolotin, N. A. Bokach, M. Y. Demakova, V. Y. Kukushkin, *Chem. Rev.* **2017**, *117*, 13039.
- [58] J. F. Liebman, Z. Rappoport, *The chemistry of hydroxylamines, oximes and hydroxamic acids*, Wiley, Chichester [u.a.], **2009**.
- [59] X.-Y. Ma, Y. He, T.-T. Lu, M. Lu, *Tetrahedron* **2013**, *69*, 2560.
- [60] P. Rommelmann, T. Betke, H. Gröger, *Org. Process Res. Dev.* **2017**, *21*, 1521.
- [61] K. Hyodo, S. Kitagawa, M. Yamazaki, K. Uchida, *Chem. Asian J.* **2016**, *11*, 1348.
- [62] R. M. Denton, J. An, P. Lindovska, W. Lewis, *Tetrahedron* **2012**, *68*, 2899.
- [63] K. Yagi, K. Ishida, EP2853526 (A1), **2013**.
- [64] B. Kosjek, F. J. Fleitz, P. G. Dormer, J. T. Kuethe, P. N. Devine, *Tetrahedron: Asymmetry* **2008**, *19*, 1403.
- [65] J. Guin, G. Varseev, B. List, *J. Am. Chem. Soc.* **2013**, *135*, 2100.
- [66] R. P. Herrera, V. Sgarzani, L. Bernardi, F. Fini, D. Pettersen, A. Ricci, *J. Org. Chem.* **2006**, *71*, 9869.
- [67] J. Choi, G. C. Fu, *J. Am. Chem. Soc.* **2012**, *134*, 9102.
- [68] M. T. Nelp, V. Bandarian, *Angew. Chem. Int. Ed.* **2015**, *54*, 10627.
- [69] N. Kurono, T. Ohkuma, *ACS Catal.* **2016**, *6*, 989.
- [70] K.-I. Oinuma, Y. Hashimoto, K. Konishi, M. Goda, T. Noguchi, H. Higashibata, M. Kobayashi, *J. Biol. Chem.* **2003**, *278*, 29600.
- [71] Y. Kato, K. Nakamura, H. Sakiyama, S. G. Mayhew, Y. Asano, *Biochemistry* **2000**, *39*, 800.
- [72] K. Kobayashi, S. Yoshioka, Y. Kato, Y. Asano, S. Aono, *J. Biol. Chem.* **2005**, *280*, 5486.
- [73] Y. Kato, Y. Asano, *Biosci. Biotechnol. Biochem* **2005**, *69*, 2254.
- [74] Y. Kato, S. Yoshida, S.-X. Xie, Y. Asano, *J. Biosci. Bioeng.* **2004**, *97*, 250.
- [75] K. Kobayashi, B. Pal, S. Yoshioka, Y. Kato, Y. Asano, T. Kitagawa, S. Aono, *J. Inorg. Biochem.* **2006**, *100*, 1069.
- [76] S.-X. Xie, Y. Kato, H. Komeda, S. Yoshida, Y. Asano, *Biochemistry* **2003**, *42*, 12056.
- [77] Y. Kato, Y. Asano, *Appl. Microbiol. Biotechnol.* **2006**, *70*, 92.
- [78] K. Konishi, T. Ohta, K.-I. Oinuma, Y. Hashimoto, T. Kitagawa, M. Kobayashi, *Proc. Natl. Acad. Sci. U.S.A.* **2006**, *103*, 564.
- [79] X.-L. Pan, F.-C. Cui, W. Liu, J.-Y. Liu, *J. Phys. Chem. B* **2012**, *116*, 5689.
- [80] R.-Z. Liao, W. Thiel, *J. Phys. Chem. B* **2012**, *116*, 9396.
- [81] J.-L. Boucher, M. Delaforge, D. Mansuy, *Biochemistry* **2002**, *33*, 7811.
- [82] J. Hart-Davis, P. Battioni, J.-L. Boucher, D. Mansuy, *J. Am. Chem. Soc.* **1998**, *120*, 12524.
- [83] M. A. Vila, M. Pazos, C. Iglesias, N. Veiga, G. Seoane, I. Carrera, *ChemBioChem* **2016**, *17*, 291.
- [84] K. Oike, *Unpublished results*. Dissertation, Bielefeld, **2018**.
- [85] E. Pinakoulaki, C. Koutsoupakis, H. Sawai, A. Pavlou, Y. Kato, Y. Asano, S. Aono, *J. Phys. Chem. B* **2011**, *115*, 13012.
- [86] Y. Kato, R. Ooi, Y. Asano, *J Mol Catal B Enzym.* **1999**, *6*, 249.
- [87] S. X. Xie, Y. Kato, Y. Asano, *Biosci. Biotechnol. Biochem* **2001**, *65*, 2666.
- [88] A. Piatasi, W. Siegel, K. U. Baldenius, WO2013135601 (A1), **2013**.

- [89] R. Metzner, S. Okazaki, Y. Asano, H. Gröger, *ChemCatChem* **2014**, *6*, 3105.
- [90] R. Metzner, *Chemoenzymatic syntheses for the production of Rosuvastatin and other enantiomerically pure pharmaceutical building blocks*, Bielefeld, **2014**.
- [91] H. Sharghi, M. H. Sarvari, *Synlett* **2001**, *2001*, 99.
- [92] M. Kitamura, M. Yoshida, T. Kikuchi, K. Narasaka, *Synthesis* **2003**, *2003*, 2415.
- [93] T. Uno, B. Gong, P. G. Schultz, *J. Am. Chem. Soc.* **1994**, *116*, 1145.
- [94] J. B. Lambert, R. R. Clikeman, K. M. Taba, D. E. Marko, R. J. Bosch, L. Xue, *Acc. Chem. Res.* **1987**, *20*, 454.
- [95] C. E. Holloway, Vuik, Carol P. J., *Tetrahedron Lett.* **1979**, *20*, 1017.
- [96] G. J. Karabatsos, N. Hsi, *Tetrahedron* **1967**, *23*, 1079.
- [97] C. Czekelius, E. M. Carreira, *Angew. Chem. Int. Ed.* **2005**, *44*, 612.
- [98] S. P. Bhatia, V. T. Politano, A. M. Api, *Food Chem. Toxicol.* **2013**, *59*, 784.
- [99] P. Rommelmann, *Synthese von Lactonen, Dioxinen und Nitrilen unter Verwendung von Bio- und Chemokatalysatoren*. Dissertation, Bielefeld, **2018**.
- [100] D. Enders, M. Backes, *Tetrahedron: Asymmetry* **2004**, *15*, 1813.
- [101] E. Brenna, M. Crotti, F. G. Gatti, A. Manfredi, D. Monti, F. Parmeggiani, S. Santangelo, D. Zampieri, *ChemCatChem* **2014**, *6*, 2425.
- [102] E. Brenna, C. Fuganti, P. Grasselli, S. Serra, *Eur. J. Org. Chem.* **2001**, *2001*, 1349.
- [103] T. Betke, P. Rommelmann, K. Oike, Y. Asano, H. Gröger, *Angew. Chem. Int. Ed.* **2017**, *56*, 12361.
- [104] H. Yavuzer, *Internship - Enantioselektive, biokatalytische Synthese von Brom-Phenylpropannitrilen*, Bielefeld, **2016**.
- [105] I. Brod, *Internship - Biokatalytische, enantioselektive Nitrilsynthese & Kombination aus Bio- und Chemokatalyse zur Synthese von Fettalkoholen*, Bielefeld, **2017**.
- [106] a) J. Neumann, C. Bornschein, H. Jiao, K. Junge, M. Beller, *Eur. J. Org. Chem.* **2015**, *2015*, 5944; b) C. Bornschein, S. Werkmeister, B. Wendt, H. Jiao, E. Alberico, W. Baumann, H. Junge, K. Junge, M. Beller, *Nat. Commun.* **2014**, *5*, 4111.
- [107] a) F. Chen, C. Topf, J. Radnik, C. Kreyenschulte, H. Lund, M. Schneider, A.-E. Surkus, L. He, K. Junge, M. Beller, *J. Am. Chem. Soc.* **2016**, *138*, 8781; b) K. Adam, US3232888 (A), **1959**; c) L. U. Brake, US3773832 (A), **1970**; d) G. I. Bartalini, M. I. Giuggioli, US3821305 (A), **1970**; e) G. Frank, G. Neubauer, US4587228 (A), **1985**; f) G. Frank, G. Neubauer, P. Duffner, H. J. Wilfinger, US4598058 (A), **1985**.
- [108] a) J. R. Johnson, G. M. Whitman, US2477617 (A), **1947**; b) I. D. Webb, G. E. Tabet, US2477672 (A), **1947**; c) G. M. Whitman, US2477674 (A), **1947**.
- [109] M. M. Baizer, *J. Electrochem. Soc.* **1964**, *111*, 215.
- [110] a) C. D. William, V. L. Richard, JR, US3496215 (A), **1965**; b) C. D. William, JR, V. L. Richard, JR, US3536748 (A), **1967**.
- [111] R. V. Jagadeesh, H. Junge, M. Beller, *Nat. Commun.* **2014**, *5*, 4123.
- [112] S. U. Dighe, D. Chowdhury, S. Batra, *Adv. Synth. Catal* **2014**, *356*, 3892.
- [113] Y. Miao, R. Metzner, Y. Asano, *ChemBioChem* **2017**, *18*, 451.
- [114] J. Mormul, J. Breitenfeld, O. Trapp, R. Paciello, T. Schaub, P. Hofmann, *ACS Catal.* **2016**, *6*, 2802.
- [115] S. E. Smith, T. Rosendahl, P. Hofmann, *Organometallics* **2011**, *30*, 3643.
- [116] D. L. Packett, US5312996 (A), **1993**.
- [117] H. J. Nienburg, R. Kummer, DE2317625 (A1), **1973**.
- [118] S. A. Miller, J. M. Bobbitt, N. E. Leadbeater, *Org. Biomol. Chem.* **2017**, *15*, 2817.
- [119] a) J. Barluenga, F. González-Bobes, M. C. Murguía, S. R. Ananthoju, J. M. González, *Chemistry* **2004**, *10*, 4206; b) G. I. Borodkin, I. R. Elanov, M. M. Shakirov, V. G. Shubin, *Russ. J. Org. Chem.* **2003**, *39*, 1144; c) J. Roels, P. Metz, *Synlett* **2001**, *2001*, 789.

- [120] a) R. F. Kleinschmidt, US2560227 (A), **1948**; b) H. Armbrust, DE1643747 (A1), **1968**.
- [121] C. Maurer, E. Pittenauer, M. Puchberger, G. Allmaier, U. Schubert, *ChemPlusChem* **2013**, 78, 343.
- [122] a) P. Chen, J. Hoffner, A. Mueller, R. Fuchs, US5959136 (A), **1999**; b) P. Chen, J. Hoffner, A. Mueller, R. Fuchs, EP0943604 (A1), **1999**; c) U. Arni, A. Faucci, A. Stocker, US4105688 (A), **1971**; d) F. Freeman, *Chem. Rev.* **1969**, 69, 591.
- [123] M. Jochmann, *Bachelor thesis - Biokatalytische Umsetzungen von Aldoximen in Zwei-Phasen-Systemen*, Bielefeld, **2016**.
- [124] H. Gruber-Wölfler, M. Maier, *Unpublished results*, Graz, **2018**.
- [125] C. B. Aakeröy, A. S. Sinha, K. N. Epa, P. D. Chopade, M. M. Smith, J. Desper, *Cryst. Growth Des.* **2013**, 13, 2687.
- [126] A. Behr, D. W. Agar, J. Jörissen, *Einführung in die Technische Chemie*, Spektrum Akademischer Verlag, Heidelberg, **2010**.
- [127] Purolite, can be found under <https://www.purolite.com/life-sciences>, **2018**.
- [128] Resindion, can be found under <https://www.resindion.com/>, **2018**.
- [129] I. Migneault, C. Dartiguenave, M. J. Bertrand, K. C. Waldron, *BioTechniques* **2004**, 37, 790-6, 798-802.
- [130] a) S. Ohlson, P.-O. Larsson, K. Mosbach, *European J. Appl. Microbiol. Biotechnol.* **1979**, 7, 103; b) J. Vaija, Y. Y. Linko, P. Linko, *Appl Biochem Biotechnol.* **1982**, 7, 51; c) J. M. Lee, J. Woodward, *Biotechnol. Bioeng.* **1983**, 25, 2441.
- [131] H. Gröger, E. Capan, A. Barthuber, K.-D. Vorlop, *Org. Lett.* **2001**, 3, 1969.
- [132] M. Heidlindemann, G. Rulli, A. Berkessel, W. Hummel, H. Gröger, *ACS Catal.* **2014**, 4, 1099.
- [133] a) A. Buthe, A. Kapitain, W. Hartmeier, M. B. Ansorge-Schumacher, *J Mol Catal B Enzym.* **2005**, 35, 93; b) M.B. Ansorge-Schumacher, Bentham Science Publisher, *MROC* **2007**, 4, 243; c) P. Hoyos, A. Buthe, M. B. Ansorge-Schumacher, J. V. Sinisterra, A. R. Alcántara, *J Mol Catal B Enzym.* **2008**, 52-53, 133; d) C. Wu, M. Kraume, M. B. Ansorge-Schumacher, *ChemCatChem* **2011**, 3, 1314.
- [134] J. von Langermann, S. Wapenhensch, *Adv. Synth. Catal.* **2014**, 356, 2989.
- [135] S. Martinez Rivadeneira, *Bachelor thesis - Beitrag zur Immobilisierung von Aldoximdehydratasen*, Bielefeld, **2016**.
- [136] D. Uhrich, J. von Langermann, *Front Microbiol.* **2017**, 8, 2111.
- [137] a) van Langen, Luuk M., R. P. Selassa, F. van Rantwijk, R. A. Sheldon, *Org. Lett.* **2005**, 7, 327; b) F. L. Cabirol, U. Hanefeld, R. A. Sheldon, *Adv. Synth. Catal.* **2006**, 348, 1645; c) Sheldon, R. A., *Biochem. Soc. Trans.* **2007**, 35, 1583; d) E. Lanfranchi, B. Grill, Z. Raghoobar, S. van Pelt, R. A. Sheldon, K. Steiner, A. Glieder, M. Winkler, *ChemBioChem* **2017**.
- [138] M. Frese, N. Sewald, *Angew. Chem. Int. Ed.* **2015**, 54, 298.
- [139] M. Frese, C. Schnepel, H. Minges, H. Voß, R. Feiner, N. Sewald, *ChemCatChem* **2016**, 8, 1799.
- [140] A. Hinzmann, *KEMP ELIMINATION of substituted 1,2-Benzisoxazoles by naturally occurring aldoxime dehydratasen*, Toyama, **2017**.
- [141] A. G. Jarvis, L. Obrecht, P. J. Deuss, W. Laan, E. K. Gibson, P. P. Wells, P. C. J. Kamer, *Angew. Chem. Int. Ed.* **2017**, 56, 13596.
- [142] A. N. Khusnutdinova, R. Flick, A. Popovic, G. Brown, A. Tchigvintsev, B. Nocek, K. Correia, J. C. Joo, R. Mahadevan, A. F. Yakunin, *Biotechnol. J.* **2017**, 12.
- [143] T. Haas, R. Krause, R. Weber, M. Demler, G. Schmid, *Nat Catal* **2018**, 1, 32.
- [144] T. Fujii, T. Narikawa, F. Sumisa, A. Arisawa, K. Takeda, J. Kato, *Biosci. Biotechnol. Biochem* **2006**, 70, 1379.
- [145] H. Gröger, *Angew. Chem. Int. Ed.* **2014**, 53, 3067.

- [146] a) C. C. Oliveira, A. Pfaltz, Correia, Carlos Roque Duarte, *Angew. Chem. Int. Ed.* **2015**, *54*, 14036; b) A. H. Mermerian, G. C. Fu, *Angew. Chem. Int. Ed.* **2005**, *44*, 949; c) R. M. Bannister, M. H. Brookes, G. R. Evans, R. B. Katz, N. D. Tyrrell, *Org. Process Res. Dev.* **2000**, *4*, 467; d) O. Ehrmann, H. Nagel **1993**.
- [147] T. H. Ambrosi, A. Scialdone, A. Graja, S. Gohlke, A.-M. Jank, C. Bocian, L. Woelk, H. Fan, D. W. Logan, A. Schürmann et al., *Cell stem cell* **2017**, *20*, 771-784.e6.
- [148] C. K. Savile, J. M. Janey, E. C. Mundorff, J. C. Moore, S. Tam, W. R. Jarvis, J. C. Colbeck, A. Krebber, F. J. Fleitz, J. Brands et al., *Science* **2010**, *329*, 305.
- [149] bionity.com, "Diabetesmedikament könnte die Heilung von Knochenbrüchen verbessern", can be found under [http://www.bionity.com/de/news/162442/diabetesmedikament-koennte-die-heilung-von-knochenbruechen-verbessern.html?WT.mc\\_id=ca0264](http://www.bionity.com/de/news/162442/diabetesmedikament-koennte-die-heilung-von-knochenbruechen-verbessern.html?WT.mc_id=ca0264), **2017**.
- [150] H. Gröger, J. Wilken, *Angew. Chem. Int. Ed.* **2001**, *40*, 529.
- [151] X.-D. An, S. Yu, *Org. Lett.* **2015**, *17*, 5064.
- [152] X.-D. An, S. Yu, *Org. Lett.* **2015**, *17*, 2692.
- [153] C. Fang, M. Li, X. Hu, W. Mo, B. Hu, N. Sun, L. Jin, Z. Shen, *Adv. Synth. Catal.* **2016**, *358*, 1157.
- [154] C. B. Kelly, K. M. Lambert, M. A. Mercadante, J. M. Ovia, W. F. Bailey, N. E. Leadbeater, *Angew. Chem. Int. Ed.* **2015**, *54*, 4241.
- [155] J.-L. Zhu, F.-Y. Lee, J.-D. Wu, C.-W. Kuo, K.-S. Shia, *Synlett* **2007**, *2007*, 1317.
- [156] J. B. Hendrickson, K. W. Bair, P. M. Keehn, *Tetrahedron Lett.* **1976**, *17*, 603.
- [157] G. Yan, Y. Zhang, J. Wang, *Adv. Synth. Catal.* **2017**, *359*, 4068.
- [158] a) V. V. Patil, E. M. Gayakwad, G. S. Shankarling, *J. Org. Chem.* **2016**, *81*, 781; b) S. Cai, S. Zhang, Y. Zhao, D. Wang, *Org. Lett.* **2013**, *15*, 2660; c) A. Dirksen, T. M. Hackeng, P. E. Dawson, *Angew. Chem. Int. Ed.* **2006**, *45*, 7581; d) S. Mangelinckx, N. Giubellina, N. de Kimpe, *Chem. Rev.* **2004**, *104*, 2353; e) J. S. Yadav, Subba Reddy, B. V., R. Srinivas, T. Ramalingam, *Synlett* **2000**, *2000*, 1447; f) A. Hassner, F. Näumann, *Chem. Ber.* **1988**, *121*, 1823; g) W. G. Kofron, M.-K. Yeh, *J. Org. Chem.* **1976**, *41*, 439; h) Narula, A., Rajamony, M., Pawlak, M., Merritt, P., Brooks, C., US2004043916A1.
- [159] A. P. S. Narula, V. J. J. De, C. E. J. Beck, M. R. Hanna, E. J. T. Van, US5274133 (A), **1993**.
- [160] a) S. A. Shipilovskikh, V. Y. Vaganov, E. I. Denisova, A. E. Rubtsov, A. V. Malkov, *Org. Lett.* **2018**, *20*, 728; b) D. Zhang, Y. Huang, E. Zhang, R. Yi, C. Chen, L. Yu, Q. Xu, *Adv. Synth. Catal.* **2018**, *360*, 784; c) X. Fang, P. Yu, B. Morandi, *Science* **2016**, *351*, 832; d) K. M. Lambert, J. M. Bobbitt, S. A. Eldirany, L. E. Kissane, R. K. Sheridan, Z. D. Stempel, F. H. Sternberg, W. F. Bailey, *Chemistry* **2016**, *22*, 5156; e) B. Xu, Q. Jiang, A. Zhao, J. Jia, Q. Liu, W. Luo, C. Guo, *Chem. Commun.* **2015**, *51*, 11264; f) S. Enthaler, *Chemistry* **2011**, *17*, 9316.
- [161] O. Attanasi, P. Palma, F. Serra-Zanetti, *Synthesis* **1983**, *1983*, 741.
- [162] K. Tambara, G. D. Pantoş, *Org. Biomol. Chem.* **2013**, *11*, 2466.
- [163] H. Wagner, R. Luther, T. Mang, *Appl. Catal., A* **2001**, *221*, 429.
- [164] T. Mang, W. Dresel (Eds.) *Lubricants and lubrications*, Wiley-VCH, Weinheim, **2001**.
- [165] U. Biermann, W. Friedt, S. Lang, W. Lühs, G. Machmüller, J. O. Metzger, M. Rüschen. Klaas, H. J. Schäfer, M. P. Schneider, *Angew. Chem. Int. Ed.* **2000**, *39*, 2206.
- [166] S. C. Cermak, G. Biresaw, T. A. Isbell, R. L. Evangelista, S. F. Vaughn, R. Murray, *Ind. Crops Prod.* **2013**, *44*, 232.
- [167] T. A. Isbell, *Grasas Aceites* **2011**, *62*, 8.
- [168] J. A. Zerkowski, *Lipid Technol.* **2008**, *20*, 253.



- [169] S. C. Cermak, J. W. Bredsguard, B. L. John, J. S. McCalvin, T. Thompson, K. N. Isbell, K. A. Feken, T. A. Isbell, R. E. Murray, *Ind. Crops Prod.* **2013**, *46*, 386.
- [170] a) T. A. Isbell, R. Kleiman, B. A. Plattner, *J Am Oil Chem Soc* **1994**, *71*, 169; b) R. E. Harry-O kuru, T. A. Isbell, D. Weisleder, *J Amer Oil Chem Soc* **2001**, *78*, 219; c) S. C. Cermak, T. A. Isbell, *Ind. Crops Prod.* **2003**, *18*, 183; d) S. C. Cermak, T. A. Isbell, *J Amer Oil Chem Soc* **2004**, *81*, 297; e) S. C. Cermak, T. A. Isbell, R. L. Evangelista, B. L. Johnson, *Ind. Crops Prod.* **2011**, *33*, 132; f) S. C. Cermak, J. W. Bredsguard, B. L. John, K. Kirk, T. Thompson, K. N. Isbell, K. A. Feken, T. A. Isbell, R. Murray, *J Am Oil Chem Soc* **2013**, *90*, 1895; g) S. C. Cermak, J. W. Bredsguard, R. O. Dunn, T. Thompson, K. A. Feken, K. L. Roth, J. A. Kenar, T. A. Isbell, R. E. Murray, *J Am Oil Chem Soc* **2014**, *91*, 2101; h) S. C. Cermak, A. L. Durham, T. A. Isbell, R. L. Evangelista, R. E. Murray, *Ind. Crops Prod.* **2015**, *67*, 179; i) S. C. Cermak, T. A. Isbell, US6316649 (B1), **2000**.
- [171] S. C. Cermak, T. A. Isbell, *J Amer Oil Chem Soc* **2001**, *78*, 557.
- [172] S. C. Cermak, T. A. Isbell, *Ind. Crops Prod.* **2002**, *16*, 119.
- [173] S. C. Cermak, G. Biresaw, T. A. Isbell, *J Am Oil Chem Soc* **2008**, *85*, 879.
- [174] K. M. Doll, S. C. Cermak, J. A. Kenar, T. A. Isbell, *J Am Oil Chem Soc* **2016**, *93*, 1149.
- [175] K. M. Doll, T. Isbell, S. C. Cermak, J. A. Kenar, US2017044128 (A1), **2016**.
- [176] S. C. Cermak, K. B. Brandon, T. A. Isbell, *Ind. Crops Prod.* **2006**, *23*, 54.
- [177] H. M. Teeter, L. E. Gast, E. W. Bell, J. C. Cowan, *Ind. Eng. Chem.* **1953**, *45*, 1777.
- [178] T. A. Isbell, M. R. Edgcomb, B. A. Lowery, *Ind. Crops Prod.* **2001**, *13*, 11.
- [179] T. A. Isbell, R. Kleiman, *J Am Oil Chem Soc* **1996**, *73*, 1097.
- [180] B. A. Lowery, B. Andersh, T. A. Isbell, *J Am Oil Chem Soc* **2013**, *90*, 911.
- [181] S. Li, L. Bouzidi, S. S. Narine, *Ind. Eng. Chem. Res.* **2014**, *53*, 12339.
- [182] a) I. Martin-Arjol, M. Busquets, T. A. Isbell, A. Manresa, *Appl. Microbiol. Biotechnol.* **2013**, *97*, 8041; b) K. Myojo, Y. Matsufune, S. Yoshikawa, EP0195311 (A2), **1986**.
- [183] G. Knothe, *J Amer Oil Chem Soc* **2001**, *78*, 537.
- [184] X.-l. He, B.-q. Chen, T.-w. Tan, *J Mol Catal B Enzym.* **2002**, *18*, 333.
- [185] R. Brenneis, B. Baeck, G. Kley, *Eur. J. Lipid Sci. Technol.* **2004**, *106*, 809.
- [186] B. R. Moser, B. K. Sharma, K. M. Doll, S. Z. Erhan, *J Amer Oil Chem Soc* **2007**, *84*, 675.
- [187] A. Sammaiah, K. V. Padmaja, R. B. N. Prasad, *J. Agric. Food Chem.* **2014**, *62*, 4652.
- [188] Y.-H. Kim, J. Han, B. Jung, H. Baek, Y. Yamada, Y. Uozumi, Y.-S. Lee, *Synlett* **2015**, *27*, 29.
- [189] I. Martin-Arjol, T. A. Isbell, A. Manresa, *J Am Oil Chem Soc* **2015**, *92*, 1125.
- [190] a) T. Vanbésien, E. Monflier, F. Hapiot, *Eur. J. Lipid Sci. Technol.* **2016**, *118*, 26; b) A. Behr, A. J. Vorholt, K. A. Ostrowski, T. Seidensticker, *Green Chem* **2014**, *16*, 982; c) L. Wu, Q. Liu, R. Jackstell, M. Beller, *Angew. Chem.* **2014**, *126*, 6426; d) B. Cornils, *Org. Process Res. Dev.* **1998**, *2*, 121; e) M. Beller, B. Cornils, C. D. Frohning, C. W. Kohlpaintner, *J. Mol. Catal. A: Chem.* **1995**, *104*, 17; f) W. A. Herrmann, C. W. Kohlpaintner, *Angew. Chem. Int. Ed. Engl.* **1993**, *32*, 1524.
- [191] E. Benetskiy, S. Lühr, M. Vilches-Herrera, D. Selent, H. Jiao, L. Domke, K. Dyballa, R. Franke, A. Börner, *ACS Catal.* **2014**, *4*, 2130.
- [192] T. Gaide, J. Bianga, K. Schlipköter, A. Behr, A. J. Vorholt, *ACS Catal.* **2017**, *7*, 4163.
- [193] J. Boulanger, A. Ponchel, H. Bricout, F. Hapiot, E. Monflier, *Eur. J. Lipid Sci. Technol.* **2012**, *114*, 1439.

- [194] T. Vanbésien, E. Monflier, F. Hapiot, *ACS Catal.* **2015**, *5*, 4288.
- [195] J. O. Metzger, U. Biermann, *Synthesis* **1992**, 1992, 463.
- [196] U. Biermann, J. O. Metzger, *Fett Wiss. Technol.* **1991**, *93*, 282.
- [197] B. B. Snider, D. J. Rodini, T. C. Kirk, R. Cordova, *J. Am. Chem. Soc.* **1982**, *104*, 555.
- [198] a) U. Biermann, J. O. Metzger, *Fett Wiss. Technol.* **1992**, *94*, 329; b) J. O. Metzger, U. Biermann, *Liebigs Ann. Chem.* **1993**, 1993, 645.
- [199] Klüber Lubrication, *Unpublished results*, München, **2017**.
- [200] J. C. Wong, G. Tang, X. Wu, C. Liang, Z. Zhang, L. Guo, Z. Peng, W. Zhang, X. Lin, Z. Wang et al., *J. Med. Chem.* **2012**, *55*, 8903.
- [201] A. Fryszkowska, K. Fisher, J. M. Gardiner, G. M. Stephens, *J. Org. Chem.* **2008**, *73*, 4295.
- [202] M. Sathish, J. Chetna, N. Hari Krishna, N. Shankaraiah, A. Alarifi, A. Kamal, *J. Org. Chem.* **2016**, *81*, 2159.
- [203] A. Kolarovic, A. Käslin, H. Wennemers, *Org. Lett.* **2014**, *16*, 4236.
- [204] S. Li, K. Huang, J. Zhang, W. Wu, X. Zhang, *Chemistry* **2013**, *19*, 10840.
- [205] D. M. Mampreian, A. H. Hoveyda, *Org. Lett.* **2004**, *6*, 2829.
- [206] B. Ferreira-Silva, I. Lavandera, A. Kern, K. Faber, W. Kroutil, *Tetrahedron* **2010**, *66*, 3410.
- [207] Sigma Aldrich Chemie GmbH, can be found under <http://www.sigmaaldrich.com/spectra/fnmr/FNMR002358.PDF>.
- [208] J. D. Kendall, G. W. Rewcastle, R. Frederick, C. Mawson, W. A. Denny, E. S. Marshall, B. C. Baguley, C. Chaussade, S. P. Jackson, P. R. Shepherd, *Bioorg. Med. Chem.* **2007**, *15*, 7677.
- [209] C. Pascal, J. Dubois, D. Guénard, F. Guéritte, *J. Org. Chem.* **1998**, *63*, 6414.
- [210] Y. Kato, Y. Asano, *Protein Expr. Purif.* **2003**, *28*, 131.
- [211] S. Lopez, F. Fernandez-Trillo, P. Midon, L. Castedo, C. Saa, *J. Org. Chem.* **2005**, *70*, 6346.
- [212] X.-X. Deng, Y. Cui, F.-S. Du, Z.-C. Li, *Polym. Chem.* **2014**, *5*, 3316.
- [213] Y. J. Chung, E. J. Ryu, G. Keum, K. Byeang Hyeon, *Bioorg. Med. Chem.* **1996**, *4*, 209.
- [214] V. V. Sureshababu, S. A. Naik, G. Nagendra, *Synth. Commun.* **2009**, *39*, 395.

## 12 APPENDIX

### 12.1 SEQUENCES AND PLASMIDS CARDS OF THE ALDOXIME DEHYDRATASES (OXDS)

#### 12.1.1 ALDOXIME DEHYDRATASE FROM *PSEUDOMONAS CHLORORAPHIS* B23 (OXDA)

##### Gene sequence

ATGGAAAGCGCAATTGATACCCATCTGAAATGTCCGCGTACCCTGAGCCGTCGTGTTCCGGAAGA  
 ATATCAGCCTCCGTTTCCGATGTGGGTTGCACGTGCCGATGAACAGCTGCAGCAGGTTGTTATGG  
 GTTATCTGGGTGTTCAAGTATCGTGGTGAAGCACAGCGTGAAGCAGCACTGCAGGCAATGCGTCA  
 TATTGTTAGCAGCTTTAGCCTGCCGGATGGTCCGCAGACCCATGATCTGACCCATCATAACCGATA  
 GCAGCGGTTTTGATAATCTGATGGTGTGGGTTATTGGAAAGATCCGGCAGCACATTGTCGTTGG  
 CTGCGTAGTGCCGAAGTTAATGATTGGTGGACCAGCCAGGATCGTCTGGGTGAAGGTCTGGGTT  
 ATTTTCGTGAAATTAGCGCACCGCGTGCAGAACAGTTTGAACCCTGTATGCATTTTCAGGATAATC  
 TGCCTGGTGTGGTGCAGTTATGGATAGCACCAGCGGTGAAATTGAAGAACATGGTTATTGGGG  
 TAGCATGCGTGATCGTTTTCCGATTAGCCAGACCGATTGGATGAAACCGACCAATGAACTGCAGG  
 TTGTTGCCGGTGATCCGGCAAAGGTGGTCGTGTTGTTATTATGGGTGATGATAACATTGCACTG  
 ATTCGTAGCGGTCAGGATTGGGCAGATGCAGAAGCAGAAGAACGTAGCCTGTATCTGGATGAAA  
 TTCTGCCGACCCTGCAGGATGGTATGGATTTTCTGCGTGATAATGGTCAGCCGCTGGGTTGTTAT  
 AGCAATCGTTTTGTTTCGTAATATCGATCTGGATGGCAATTTTCTGGATGTGAGCTATAACATTGGT  
 CATTGGCGTAGCCTGGAAAACTGGAACGTTGGGCAGAAAGCCATCCGACCCATCTGCGTATTTT  
 TGTTACCTTTTTTCGTGTTGCAGCCGGTCTGAAAAACTGCGTCTGTATCATGAAGTTAGCGTGAG  
 TGATGCAAAAAGCCAGGTGTTTGAATATATCAACTGTCATCCGCATACCGGCATGCTGCGTGATG  
 CAGTTGTTGCACCGACCAAGCTTGCGGCCGCACTCGAGCACCACCACCACCACCCTGA

##### Amino acid sequence (352 AS, 40.129 kDa)

MESAIDTHLKCPRTLSRRVPEEYQPPFPMWVARADEQLQVVMGYLGVQYRGEAQREAALQAMRHI  
 VSSFSLPDGPQTHDLTHHTDSSGFDNLMVVGWYKDPAAHCRWLRSAEVNDWWT SQDRLGEGLY  
 FREISAPRAEQFETLYAFQDNLPGVGAVMDSTSGEIEEHGYWGSMDRFPISQTDWMKPTNELQVV  
 AGDPAKGGRRVIMGHDNIALIRSGQDWADAEAEERSLYLDEILPTLQDGMDFLRDNGQPLGCYSNR  
 FVRNIDL DGNFLDVSYNIGHWRSLEKLERWAESHPTHLRIFVTFRVAAGLKKLRLYHEVSVSDAKS  
 QVFEYINCHPHTGMLRDAVVAPT

#### 12.1.2 ALDOXIME DEHYDRATASE FROM *BACILLUS* SP. STRAIN OxB-1 (OXDB) IN PUC18

##### Gene sequence (Changed the start codon from TTG to ATG)<sup>[1b]</sup>

ATGAAAAATATGCCGAAAATCACAATCCACAAGCGAATGCCTGGACTGCCGAATTTCTCCTGA  
 AATGAGCTATGTAGTATTTGCGCAGATTGGGATTCAAAGCAAGTCTTTGGATCACGCAGCGGAAC  
 ATTTGGGAATGATGAAAAAGAGTTTTCGATTTGCGGACAGGCCCCAAACATGTGGATCGAGCCTTG  
 CATCAAGGAGCCGATGGATACCAAGATTCCATCTTTTTAGCCTACTGGGATGAGCCTGAAACATT

TAAATCATGGGTTGCGGATCCTGAAGTACAAAAGTGGTGGTCGGGTAAAAAATCGATGAAAATA  
 GTCCAATCGGGTATTGGAGTGAGGTAACGACCATTCCGATTGATCACTTTGAGACTCTTCATTCC  
 GGAGAAAATTACGATAATGGGGTTTCACACTTTGTACCGATCAAGCATAACAGAAGTCCATGAATA  
 TTGGGGAGCAATGCGCGACCGCATGCCGGTGTCTGCCAGTAGTGATTTGGAAAGCCCCCTTGGC  
 CTTCAATTACCGGAACCCATTGTCCGGGAGTCTTTGCGAAAACGGCTAAAAGTCACGGCGCCGG  
 ATAATATTTGCTTGATTGGAACCGCTCAAATTGGTCTAAATGTGGTAGCGGGGAAAGGGAAACG  
 TATATAGGACTAGTGGAACCGACCCTCATAAAAGCGAATACGTTTCTTCGTGAAAATGCTAGTGA  
 AACAGGCTGTATTAGTTCAAATTAGTCTATGAACAGACCCATGACGGCGAAATAGTAGATAAAT  
 CATGTGTCATCGGATATTATCTCTCCATGGGGCATCTTGAACGCTGGACGCATGATCATCCAACA  
 CATAAAGCGATCTACGGAACCTTTTATGAGATGTTGAAAAGGCATGATTTTAAGACCGAACTTGCT  
 TTATGGCACGAGGTTTCGGTGCTTCAATCAAAGATATCGAGCTTATCTATGTCAACTGCCATCCG  
 AGTACTGGATTTCTCCATTCTTTGAAGTGACAGAAATCAAGAGCCTTTACTGAAAAGCCCTAGC  
 GTCAGGATCCAGTGA

### Amino acid sequence (351 AS, 40.151 kDa)

MKNMPENHNPQANAWTAEFPPMSYVVFQAQIGIQSKSLDHAAEHLGMMKKSFDLRTGPKHVDRAL  
 HQGADGYQDSIFLAYWDEPETFKSWVADPEVQKWWSGKKIDENSPIGYWSEVTTIPIDHFETLHSG  
 ENYDNGVSHFVPIKHTEVHEYWGAMRDRMPVSASSDLEPLGLQLPEPIVRESFGKRLKVTAPDNIC  
 LIRTAQNWSKCGSGERETYIGLVEPTLIKANTFLRENASETGCISSKLVYEQTHDGEIVDKSCVIGYYL  
 SMGHLERWTHDHPHKAIYGTIFYEMLKRHDFKTELALWHEVSVLQSKDIELIYVNCHPSTGFLPFFEV  
 TEIQEPLLKSPSVRIQ

### 12.1.3 ALDOXIME DEHYDRATASE FROM *BACILLUS* SP. STRAIN OXB-1 (OXDB(C<sub>HIS6</sub>), CODON-OPTIMIZED) IN PET-22B

#### Gene sequence

ACAGGGAACGGGGCGGAAATCCCTCTAGAATAATTTGGTTTAACTTTAAGGAAGGAGGATAT  
 ACATATGAAAAATATGCCGAAAATCACAATCCACAAGCGAATGCCTGGACTGCCGAATTTCTC  
 CTGAAATGAGCTATGTAGTATTTGCGCAGATTGGGATTCAAAGCAAGTCTTTGGATCACGCAGCG  
 GAACATTTGGGAATGATGAAAAAGAGTTTCGATTTGCGGACAGGCCCAAACATGTGGATCGAG  
 CCTTGCATCAAGGAGCCGATGGATACCAAGATTCCATCTTTTTAGCCTACTGGGATGAGCCTGAA  
 ACATTTAAATCATGGGTTGCGGATCCTGAAGTACAAAAGTGGTGGTCGGGTAAAAAATCGATGA  
 AAATAGTCCAATCGGGTATTGGAGTGAGGTAACGACCATTCCGATTGATCACTTTGAGACTCTTC  
 ATTCCGGAGAAAATTACGATAATGGGGTTTCACACTTTGTACCGATCAAGCATAACAGAAGTCCAT  
 GAATATTGGGGAGCAATGCGCGACCGCATGCCGGTGTCTGCCAGTAGTGATTTGGAAAGCCCC  
 TTGGCCTTCAATTACCGGAACCCATTGTCCGGGAGTCTTTGCGAAAACGGCTAAAAGTCACGGCG  
 CCGGATAATATTTGCTTGATTGGAACCGCTCAAATTGGTCTAAATGTGGTAGCGGGGAAAGGGA  
 AACGTATATAGGACTAGTGGAACCGACCCTCATAAAAGCGAATACGTTTCTTCGTGAAAATGCTA  
 GTGAAACAGGCTGTATTAGTTCAAATTAGTCTATGAACAGACCCATGACGGCGAAATAGTAGAT  
 AAATCATGTGTCATCGGATATTATCTCTCCATGGGGCATCTTGAACGCTGGACGCATGATCATCCA  
 ACACATAAAGCGATCTACGGAACCTTTTATGAGATGTTGAAAAGGCATGATTTTAAGACCGAACTT  
 GCTTTATGGCACGAGGTTTCGGTGCTTCAATCAAAGATATCGAGCTTATCTATGTCAACTGCCAT  
 CCGAGTACTGGATTTCTCCATTCTTTGAAGTGACAGAAATCAAGAGCCTTTACTGAAAAGCCCT  
 AGCGTCAGGATCCAGCTCGAGCACCACCACCACCACCCTGAGATCCGGCTGCTAACAAAGCCC  
 GAAAGAAGTTTTTT

**Amino acid sequence (359 AS, 41.216 kDa)**

MKNMPENHNPQANAWTAEFPPEMSYVVFQAQIGIQSKSLDHAAEHLGMMKKSFDLRTGPKHVDRAL  
 HQGADGYQDSIFLAYWDEPETFKSWVADPEVQKWWWSGKKIDENSPIGYWSEVTTIPIIDHFETLHSG  
 ENYDNGVSHFVPIKHTEVHEYWGAMRDRMPVSASSDLESPLGLQLPEPIVRESFGKRLKVTAPDNIC  
 LIRTAQNWSKCGSGERETYIGLVEPTLIKANTFLRENASETGCISSKLVYEQTHDGEIVDKSCVIGYYL  
 SMGHLERWTHDHPHKAHYGTFYEMLRHDFKTELALWHEVSVLQSKDIELIYVNCHPSTGFLPFVEV  
 TEIQEPLLKSPSVRIQLEHHHHHH

12.1.4 ALDOXIME DEHYDRATASE FROM *FUSARIUM GRAMINEARUM* MAFF305135  
 (OXDFG(N<sub>HIS6</sub>), CODON-OPTIMIZED) IN PET28A

**Gene sequence**

ATGGGCAGCAGCCATCATCATCATCACAGCAGCGGCCTGGTGCCGCGCGGCAGCCATATGC  
 TCGTAGCCGTTTTCCGGCAAGCCATCATTTACCGTTAGCGTTTTGGTTGTCAGTATCATAGCC  
 AAGCACCGAGCGTTGAAAAACCGAACTGATTGGTCTTTGATAAACTGATTGATAGCGCAGCA  
 ATTCATGTGGAACATCTGGAACAGAATGATGTGCCGAGCAAATTTGGATGAGCTATTGGGAAAG  
 TCCGCAGAAATTCAAACAGTGGTGGGAAAAAGATGATACCGCAAGCTTTTGGGCAAGCCTGCCG  
 GATGATGCAGTTTTTGGCGTGAAACCTTTAGCCTGCCTGCAACCCGTGCAATGTATGAAGGCAC  
 CGGTAAAGATGCCTATGGTTTTGGTCATTGTGGTAGCCTGATTCCGCTGACCACAAAACCGGCT  
 ATTGGGGTGTCATATCGTAGCCGATGACACCGGATTTTGAAGGTGATACCTTTTCAAGCCCGATT  
 CCGACCTATGCAGATCAGAGCGTCCCGGCAGATAAAATTCGTCCGGGTCGTGTTTCGTATTACCGA  
 TTTTCCGATAATCTGTGCATGGTTGTTGAAGGTGAGCATTATGCAGATATGGGTGAACGTGAAC  
 GCGAATATTGGAACGAAAATTTTATGGTCTGACGAAACAGTGGGTTACCAATGTTGTTACCGCA  
 GGTCATGAACAGGGTATGGTTATTGCACGTGCCTGTCATGGTTTTGCCGGTGAAAAAAACTGGG  
 TGCAACCAATGGTCCGGTGAATGGTATTTTTCCGGGTCTGGATTATGTTTCATCAGGCACAGATTC  
 TGATTTGGCAGGATATTAGCAAAATGGAACATATCGGTCTGTTATGATCAGACCCATGTTAACTG  
 CGTCGCGATTTTATGAAAGCCTATGGTCCGGGTGGTGAATGGAAGGTGGTATCTGCTGCTGT  
 GGGTTGATCTGGGTATTCTGAAAAAGACGAAATCGATGCCGAATATGTGGGTTGCTATGAAAGT  
 ACCGGTTTTCTGAAACTGGATAAAGGCCAGTTTTTCAAAGTTGAAAGCACCGCAGGTAGCAA  
 ACTGCCGAGCTTTTTTATGATGAACCGATTGAAAGCAAACCGATCGAATGGTAA

**Amino acid sequence (383 AS, 43.380 kDa)**

MGSSHHHHHHSSGLVPRGSHMLRSRFPASHHFTVSVFGCQYHSEAPSVEKTELIGRFDKLIDSAAIH  
 VEHLEQNDVPSKIWMSYWESPQKFKQWWEKDDTASFWASLPDDAGFWRETFSLPATRAMYEGTG  
 KDAYGFGHCGSLIPLTTKTGYWGAYRSRMTPDFEGDTFSSPIPTYADQSVPADKIRPGRVRITDFPD  
 NLCMVVEGQHYADMGEREREYWNENFDGLTKQWVTNVVTAGHEQGMVIZARACHGFAGEKKGAT  
 NGPVNGIFPLDYVHQAQILIWQDISKMEHIGRYDQTHVKLRDFMKAYGPGGEMEGDLLLWVDL  
 GILKKDEIDAAYVGCYESTGFLKLDKGQFFKVESTAGSKLPSFFDEPIESKPIEW

12.1.5 ALDOXIME DEHYDRATASE FROM *RHODOCOCCSS ERYTHROPOLIS* (*RHODOCOCCSS* SP. N-771, OXDRE(N<sub>HIS6</sub>), CODON-OPTIMIZED) IN PET28A

**Gene sequence**

ATGGGCAGCAGCCATCATCATCATCACAGCAGCGGCCTGGTGCCGCGCGGCAGCCATATGG  
AAAGCGCAATTGGTGAACATCTGCAGTGCCGCGTACCCTGACCCGTCGTGTTCCGGATACCTAT  
ACCCCTCCGTTTCCGATGTGGGTTGGTCGTGCAGATGATGCACTGCAGCAGGTTGTTATGGGTTA  
TCTGGGTGTTTCAGTTTTCGTGATGAAGATCAGCGTCCGGCAGCACTGCAGGCAATGCGTGATATTG  
TTGCAGGTTTTGATCTGCCGGATGGTCCGGCACATCATGATCTGACCCATCATATTGATAATCAG  
GGCTATGAAAACCTGATTGTGGTGGGTTATTGGAAAGATGTTAGCAGCCAGCATCGTTGGAGCA  
CCAGCACCCCGATTGCAAGTTGGTGGGAAAGCGAAGATCGTCTGAGTGATGGTCTGGGTTTTTTTT  
CGTGAAATTGTGGCACCGCGTGCAGAACAGTTTGAACCCTGTATGCATTTCAAGAAGATCTGCC  
TGGCGTTGGTGCAGTTATGGATGGTATTAGCGGTGAAATTAACGAACATGGTTATTGGGGTAGCA  
TGCGTGAACGTTTTCCGATTAGCCAGACCGATTGGATGCAGGCAAGCGGTGAACTGCGTGTTATT  
GCCGGTGATCCGGCAGTTGGTGGTCTGTGTTGTTGTTCTGGTCATGATAACATTGCACTGATTCCG  
TAGCGGTCAGGATTGGGCAGATGCCGAAGCAGATGAACGTAGCCTGTATCTGGATGAAATTCTG  
CCGACCCTGCAGAGCGGTATGGATTTTCTGCGTGATAATGGTCCTGCAGTTGGTTGTTATAGCAA  
TCGTTTTGTGCGCAACATTGATATCGATGGCAATTTTCTGGATCTGAGCTATAACATTGGTCATTG  
GGCAAGCCTGGATCAGCTGGAACGTTGGAGCGAAAGCCATCCGACCCATCTGCGTATTTTTACCA  
CCTTTTTTCGCGTTGCAGCCGGTCTGAGCAAAGTCTGATCATGAAGTTAGCGTTTTTTGATG  
CAGCAGATCAGCTGTATGAATACATTAATTGTCATCCGGGTACAGGTATGCTGCGTGATGCAGTT  
ACCATTGCAGAACATTAA

**Amino acid sequence (373 AS, 42.032 kDa)**

MGSSHHHHHHSSGLVPRGSHMESAIGEHLQCPRTLRRVDPDITYPPFPMWVGRADDALQQVVMGY  
LGVQFRDEDQRPAALQAMRDIVAGFDLPDPAHHDLTHHIDNQGYENLIVVGYWKDVSSQHRWST  
STPIASWWESEDRLSDGLGFFREIVAPRAEQFETLYAFQEDLPVGVAVMDGISGEINEHGYWGS  
MERFISQTDWMQASGELRVIAGDPVAVGGRRVVRGHDNIALIRSGQDWADAEADERSLYLDEILPTL  
QSGMDFLRDNGPAVGCYSNRFVRNIDIDGNFLDSYNIGHWASLDQLERWSESHPTHLRIFTFFR  
AAGLSKLRLYEVSVFDAADQLYEYINCHPGTGMLRDAVTIAEH

12.1.6 ALDOXIME DEHYDRATASE FROM *RHODOCOCCSS GLOBERULUS* A-4 (OXDRG(NHIS6), CODON-OPTIMIZED) IN PET28A

**Gene sequence**

ATGGGCAGCAGCCATCATCATCATCACAGCAGCGGCCTGGTGCCGCGCGGCAGCCATATGG  
AAAGCGCAATTGGTGAACATCTGCAGTGCCGCGTACCCTGACCCGTCGTGTTCCGGATACCTAT  
ACCCCTCCGTTTCCGATGTGGGTTGGTCGTGCAGATGATACCCTGCATCAGGTTGTTATGGGTTA  
TCTGGGTGTTTCAGTTTTCGTGGTGAAGATCAGCGTCCGGCAGCACTGCGTGCAATGCGTGATATT  
GTTGCAGGTTTTGATCTGCCGGATGGTCCGGCACATCATGATCTGACCCATCATATTGATAATCA  
GGGCTATGAAAACCTGATTGTGGTGGGTTATTGGAAAGATGTTAGCAGCCAGCATCGTTGGAGC  
ACCAGCCCTCCGGTTAGCAGTTGGTGGGAAAGCGAAGATCGTCTGAGTGATGGTCTGGGTTTTTT  
TCGTGAAATTGTGGCACCGCGTGCAGAACAGTTTGAACCCTGTATGCATTTCAGGATGATCTGC  
CTGGTGTTGGTGCAGTTATGGATGGTGTAGCGGTGAAATTAATGAACATGGTTATTGGGGTAGC  
ATGCGTGAACGTTTTCCGATTAGCCAGACCGATTGGATGCAGGCAAGCGGTGAACTGCGTGTTG  
TTGCCGGTGATCCGGCAGTTGGCGGTCTGTGTTGTGGTTCGTGGTCATGATAACATTGCACTGATT

CGTAGCGGTCAGGATTGGGCAGATGCCGAAGCAGATGAACGTAGCCTGTATCTGGATGAAATTC  
TGCCGACCCTGCAGAGCGGTATGGATTTTCTGCGTGATAATGGTCCTGCAGTTGGTTGTTATAGC  
AATCGTTTTGTGCGCAACATTGATATCGATGGCAATTTTCTGGATCTGAGCTATAACATTGGTCAT  
TGGGCAAGCCTGGATCAGCTGGAACGTTGGAGCGAAAGCCATCCGACCCATCTGCGTATTTTTAC  
CACCTTTTTTCGCGTTGCAGAAGGTCTGAGCAAACCTGCGTCTGTATCATGAAGTTAGCGTTTTTGA  
TGCAGCAGATCAGCTGTATGAATACATTAATTGTCATCCGGGTACAGGTATGCTGCGTGATGCAG  
TTATTACCGCAGAACATTAA

**Amino acid sequence (373 AS, 42.055 kDa)**

MGSSHHHHHSSGLVPRGSHMESAIGEHLQCPRTLRRVDPDYTPPFPMWVGRADDTLHQVVMGY  
LGVQFRGEDQRPAALRAMRDIVAGFDLPDGPAAHDLTHHIDNQGYENLIVVGYWKDVSSQHRWST  
SPPVSSWWESEDRLSDGLGFFREIVAPRAEQFETLYAFQDDLPGVGAVMDGVSGEINEHGYWGSM  
RERFPISQTDWMQASGELRVVAGDPAVGGRVVVRGHDNIALIRSGQDWADAEADERSLYLDEILPT  
LQSGMDFLRDNGPAVGCYSNRFVRNIDIDGNFLDLSYNIGHWASLDQLERWSESHPTHLRIFTTFFR  
VAEGLSKLRLYHEVSVFDAADQLYEYINCHPGTGMLRDAVITAEH